EPA-650/2-75-027-c

September 1975 Environmental Protection Technology Series

FLUIDIZED BED COMBUSTION PROCESS EVALUATION

PHASE II - PRESSURIZED FLUIDIZED BED COAL COMBUSTION DEVELOPMENT

U.S. Environmental Protection Agency
Office of Research and Development
Washington, DC 20460

EPA-650/2-75-027-c

FLUIDIZED BED COMBUSTION PROCESS EVALUATION

PHASE II - PRESSURIZED FLUIDIZED BED COAL COMBUSTION DEVELOPMENT

by

D.L. Keairns, D.H. Archer, J.R. Hamm, S.A. Jansson, B.W. Lancaster, E.P. O'Neill, C.H. Peterson, C.C. Sun, E.F. Sverdrup, E.I. Vidt, and W.C. Yang

Westinghouse Research Laboratories
Beulah Road, Churchill Borough,
Pittsburgh, Pennsylvania 15235

Contract No. 68-02-0605
ROAP No. 21ADB-009
Program Element No. 1AB013

EPA Project Officer: P.P. Turner

Industrial Environmental Research Laboratory
Office of Energy, Minerals, and Industry
Research Triangle Park, North Carolina 27711

Prepared for

U.S. ENVIRONMENTAL PROTECTION AGENCY
Office of Research and Development
Washington, D. C. 20460

September 1975

EPA REVIEW NOTICE

This report has been reviewed by the U.S. Environmental Protection Agency and approved for publication. Approval does not signify that the contents necessarily reflect the views and policies of the Environmental Protection Agency, nor does mention of trade names or commercial products constitute endorsement or recommendation for use.

RESEARCH REPORTING SERIES

Research reports of the Office of Research and Development, U.S. Environmental Protection Agency, have been grouped into series. These broad categories were established to facilitate further development and application of environmental technology. Elimination of traditional grouping was consciously planned to foster technology transfer and maximum interface in related fields. These series are:

1. ENVIRONMENTAL HEALTH EFFECTS RESEARCH
2. ENVIRONMENTAL PROTECTION TECHNOLOGY
3. ECOLOGICAL RESEARCH
4. ENVIRONMENTAL MONITORING
5. SOCIOECONOMIC ENVIRONMENTAL STUDIES
6. SCIENTIFIC AND TECHNICAL ASSESSMENT REPORTS
9. MISCELLANEOUS

This report has been assigned to the ENVIRONMENTAL PROTECTION TECHNOLOGY series. This series describes research performed to develop and demonstrate instrumentation, equipment and methodology to repair or prevent environmental degradation from point and non-point sources of pollution. This work provides the new or improved technology required for the control and treatment of pollution sources to meet environmental quality standards.

This document is available to the public for sale through the National Technical Information Service, Springfield, Virginia 22161.

Publication No. EPA-650/2-75-027-c

ABSTRACT

Pressurized fluidized bed combustion for electric power generation provides a direct combustion process for coal and low-grade fuels, with the potential for improved thermal conversion efficiency, reduced costs, and acceptable environmental impact. The present work extends the previous studies to include the collection and analysis of data on critical system parameters such as sulfur removal, spent sorbent disposition, and trace element release; development of process options such as particulate control equipment; assessment of power plant cycles and component designs such as low-temperature gas cleaning, alternative cycles and turbine corrosion/erosion; and updated commercial plant design and cost estimates. No problems have been identified which preclude commercialization. Available data support the basic pressurized fluidized bed combustion boiler and adiabatic combustor design and operating parameters previously selected. Updated system economics show energy costs for first-generation plants ranging from 7 to 20 percent less than a conventional plant with stack-gas cleaning. Westinghouse recommends that the development effort be accelerated; a commercial-scale integrated test facility be constructed; and experimental studies on gas-turbine tolerance to particulates and trace contaminants, gas-cleaning technology, and environmental control be expedited.

PREFACE

The Office of Energy, Minerals, and Industry (OEMI) of the United States Environmental Protection Agency (EPA) is sponsoring work on fluidized bed fuel processing, the purpose of which is to develop and demonstrate new methods for utilizing fossil fuels to produce electrical energy from utility power plants, to produce process steam, or to produce process heat that meets environmental standards. These methods should:

- Meet environmental goals for sulfur dioxide (SO_2), nitrogen oxide (NO_x), ash smoke emissions, trace element emissions, and wastes
- Utilize fuel resources efficiently
- Compete economically with alternative means for meeting environmental goals.

Westinghouse Research Laboratories, under contract to OEMI, have carried out a program to evaluate, develop, and demonstrate fluidized bed combustion. This report describes work, performed from June 1973 through December 1974 under contract No. 68-02-0605, based on tasks set forth by EPA which Westinghouse has completed under previous contracts and on work completed by other investigators and government contractors.

The results from the prior tasks carried out by Westinghouse on fluidized bed combustion were published in a three-volume report, "Evaluation of the Fluidized Bed Combustion Process," in November 1971 under contract No. CPA 70-9 and as three volumes of a four-volume report published in December 1973 under contract No. 68-02-0217: Volumes I and II, "Pressurized Fluidized-Bed Combustion Process Development and Evaluation," and Volume III, "Pressurized Fluid Bed Boiler Development Plant Design." This previous work includes:

- Assimilation of available data on fluidized bed combustion, including sulfur dioxide removal, sorbent regeneration, nitrogen oxide minimization, combustion efficiency, heat transfer, particle carry-over, boiler tube corrosion/erosion fouling, and gas-turbine erosion/corrosion
- Assessment of markets for industrial boilers and utility power systems
- Development of designs for fluidized bed industrial boilers
- Development of designs for fluidized bed combustion utility power systems: atmospheric-pressure fluidized bed combustion boilers, pressurized fluidized bed combustion boiler-combined cycle power systems, adiabatic fluidized bed combustion-combined cycle power systems—including first- and second-generation concepts
- Preparation of a preliminary design and cost estimate for a 30 MW (equivalent) pressurized fluidized bed combustion boiler development plant
- Assessment of the sensitivity of operating and design parameters selected for the base power plant design on plant economics
- Preparation of cost and performance estimates for once-through and regenerative sulfur removal systems
- Development of a plant operation and control philosophy
- Collection of experimental data on sulfur removal and sorbent regeneration using limestone and dolomites
- Provision of technical consultation and assistance on the ORD fluidized bed fuel processing program.

The results of these surveys, designs, evaluations,and experimental programs provided the basis for the work presented in this

report. The scope of this work is directed toward the development of pressurized fluidized bed combustion systems and includes:

- Collection and analysis of additional data on the calcium-based sulfur removal system—sorbent selection, high utilization, regeneration
- Collection and analysis of data on spent sorbent disposition—utilization and environmental impact of disposal
- Projection and analysis of trace emissions from fluidized bed combustion systems and their impact on gas-turbine performance
- Analysis of particulate removal requirements and development of a particulate control system for high-temperature, high-pressure fluidized bed combustion systems
- Assessment of gas-turbine design and operating constraints
- Construction of a corrosion/erosion test facility for the 0.63 MW Exxon miniplant
- Continued assessment of fluidized bed combustion power plant cycles and component designs.

A summary of the work is presented here, with details and supplemental information in the appendices.

TABLE OF CONTENTS

Table of Contents (Continued)

LIST OF FIGURES

List of Figures (Continued)

List of Figures (Continued)

List of Figures (Continued)

List of Figures (Continued)

List of Figures (Continued)

List of Figures (Continued)

LIST OF TABLES

List of Tables (Continued)

List of Tables (Continued)

List of Tables (Continued)

LIST OF ABBREVIATIONS

A/F	- air/fuel ratio
$Al(SO_4)_3$	- aluminum sulfate
ANL	- Argonne National Laboratory
BCURA	- British Coal Utilization Research Association
$CaCO_3$	- calcium carbonate
CAFB	- chemically active fluidized bed
CaO	- calcium oxide
$Ca(OH_2)$	- calcium hydroxide
CaS	- calcium sulfide
Ca/S	- calcium/sulfur ratio
$CaSO_4$	- calcium sulfate
CH_4	- methane
CO_2	- carbon dioxide
CuO	- copper oxide
$CuSO_4$	- copper sulfate
EPA	- Environmental Protection Agency
EPRI	- Electrical Power Research Institute
ERDA	- Energy Research and Development Agency
Esso	- Esso Research Centre, Abingdon, England
Exxon	- Exxon Engineering Corporation, Linden, N.J.
GJ	- giga joule (10^9) S.I. unit of energy
HPFBB	- high-pressure fluidized bed boiler
J	- joule, S.I. unit of energy, 1055 J = 1 Btu
K_2SO_4	- potassium sulfate
kg	- kilogram, S.I. unit of weight
kJ	- kilojoule
kPa	- kilopascal, S.I. unit of pressure, 101.3 kPa = 1 atm.
kw	- kilowatt
kWh	- kilowatt hour

m	- meter
Mg	- megagram, S.I. unit of weight, 0.972 Mg = 1 short ton
$MgCO_3$	- magnesium carbonate
MgO	- magnesium oxide
ml	- milliliter
mm	- millimeter
μm	- micron
$MnSO_4$	- manganese sulfate
m/s	- meters per second
MW	- megawatt
Na	- sodium
NALCO	- alumina-based copper oxide catalyst
NAPCA	- National Air Pollution Control Administration (now EPA)
$NaSO_4$	- sodium sulfate
NLLS	- nonlinear least squares
$NiSO_4$	- nickel sulfate
NCB	- National Coal Board, U.K.
NO_2	- nitrogen dioxide
NO_x	- nitrogen oxide
O_2	- oxygen
OEMI	- Office of Energy, Minerals and Industry, EPA
ORNL	- Oak Ridge National Laboratory
ppb	- parts per billion
ppm	- parts per million
PER	- Pope, Evans and Robbins
PFBB	- pressurized fluidized bed boiler
rms	- root mean square
SO_2	- sulfur dioxide
SO_3	- sulfur trioxide
TG	- thermogravimetric
TVA	- Tennessee Valley Authority

LIST OF ABBREVIATIONS

A/F	- air/fuel ratio
$Al(SO_4)_3$	- aluminum sulfate
ANL	- Argonne National Laboratory
BCURA	- British Coal Utilization Research Association
$CaCO_3$	- calcium carbonate
CAFB	- chemically active fluidized bed
CaO	- calcium oxide
$Ca(OH_2)$	- calcium hydroxide
CaS	- calcium sulfide
Ca/S	- calcium/sulfur ratio
$CaSO_4$	- calcium sulfate
CH_4	- methane
CO_2	- carbon dioxide
CuO	- copper oxide
$CuSO_4$	- copper sulfate
EPA	- Environmental Protection Agency
EPRI	- Electrical Power Research Institute
ERDA	- Energy Research and Development Agency
Esso	- Esso Research Centre, Abingdon, England
Exxon	- Exxon Engineering Corporation, Linden, N.J.
GJ	- giga joule (10^9) S.I. unit of energy
HPFBB	- high-pressure fluidized bed boiler
J	- joule, S.I. unit of energy, 1055 J = 1 Btu
K_2SO_4	- potassium sulfate
kg	- kilogram, S.I. unit of weight
kJ	- kilojoule
kPa	- kilopascal, S.I. unit of pressure, 101.3 kPa = 1 atm.
kw	- kilowatt
kWh	- kilowatt hour

m	- meter
Mg	- megagram, S.I. unit of weight, 0.972 Mg = 1 short ton
$MgCO_3$	- magnesium carbonate
MgO	- magnesium oxide
ml	- milliliter
mm	- millimeter
μm	- micron
$MnSO_4$	- manganese sulfate
m/s	- meters per second
MW	- megawatt
Na	- sodium
NALCO	- alumina-based copper oxide catalyst
NAPCA	- National Air Pollution Control Administration (now EPA)
$NaSO_4$	- sodium sulfate
NLLS	- nonlinear least squares
$NiSO_4$	- nickel sulfate
NCB	- National Coal Board, U.K.
NO_2	- nitrogen dioxide
NO_x	- nitrogen oxide
O_2	- oxygen
OEMI	- Office of Energy, Minerals and Industry, EPA
ORNL	- Oak Ridge National Laboratory
ppb	- parts per billion
ppm	- parts per million
PER	- Pope, Evans and Robbins
PFBB	- pressurized fluidized bed boiler
rms	- root mean square
SO_2	- sulfur dioxide
SO_3	- sulfur trioxide
TG	- thermogravimetric
TVA	- Tennessee Valley Authority

ACKNOWLEDGMENTS

The results, conclusions, and recommendations presented in this report represent the combined work and thought of many persons at Westinghouse and OEMI. Other government contractors have freely shared with us the results of their research and development effort.

In particular, we want here to express our high regard for and acknowledge the contribution of personnel at Westinghouse Research Laboratories and at OEMI who have directed the fluidized bed combustion program and who have defined, monitored, and supported the efforts of Westinghouse and others on the program. Mr. P. P. Turner, Chief of Advanced Processes Branch, has served as EPA project officer on our work. Numerous enlightening and helpful discussions have been held with Mr. Turner; with branch members D. B. Henschel and S. L. Rakes; and with R. P. Hangebrauck, director Energy Assessment and Control Division. Personnel from the Westinghouse Research Laboratories have made significant contributions. Drs. M. Menguturk and R. W. Hornbeck participated in the gas turbine assessment work. Dr. L. N. Yannopoulos, Dr. C. Y. Lin, and M. A. Alvin contributed to the work on trace element release and gas turbine tolerance to trace elements. Messrs. R. E. Brinza, W. F. Kittle, W. J. Petlevich, H. W. Sherwin, and L. Toth participated in the collection of data. Westinghouse division personnel were consulted and participated in the evaluation. Steam Turbine Division personnel contributed to the assessment of advanced steam conditions.

I. INTRODUCTION

Coal represents approximately 85 percent of the U. S. fossil fuel resources and will play an important role in achieving greater energy independence. Pressurized fluidized bed combustion for electric power generation provides a direct combustion process for coal, with the potential for improved thermal conversion efficiency, reduced costs, and acceptable environmental impact. This technology can be used to substitute coal and other low-grade fuels for oil and gas and to provide an improved option for conventional coal-fired systems. Contributions from this technology to the energy system have been projected to be up to 40,000 MW of installed capacity by the year 2000, if the development is successful. The basic pressurized fluidized bed combustion technology is available from laboratory- and pilot-plant scale systems. Further engineering and development is required, however, to demonstrate pressurized fluidized bed combustion concepts on a commercial scale.

Westinghouse,under contract to EPA, has carried out a program to evaluate and develop fluidized bed combustion processes.[1,2] The historical, technical, and economic aspects of fluidized bed combustion systems have been reviewed, systems analyses performed, commercial plant design and cost estimates prepared, and experimental data on the sulfur removal system obtained. Two pressurized fluidized bed combustion power plant systems, shown in Figures 1 and 2, have provided the basis for the work on system design, performance, economics, and development. The reference designs and related plant designs have been reported previously.[1,2] The basic design and performance parameters for these two systems are presented in Table 1. Current work extends the previous work to include collection and analysis of data on critical system parameters (sulfur removal, spent sorbent disposition, trace element release);development of process options (particulate control); assessment of power plant cycles

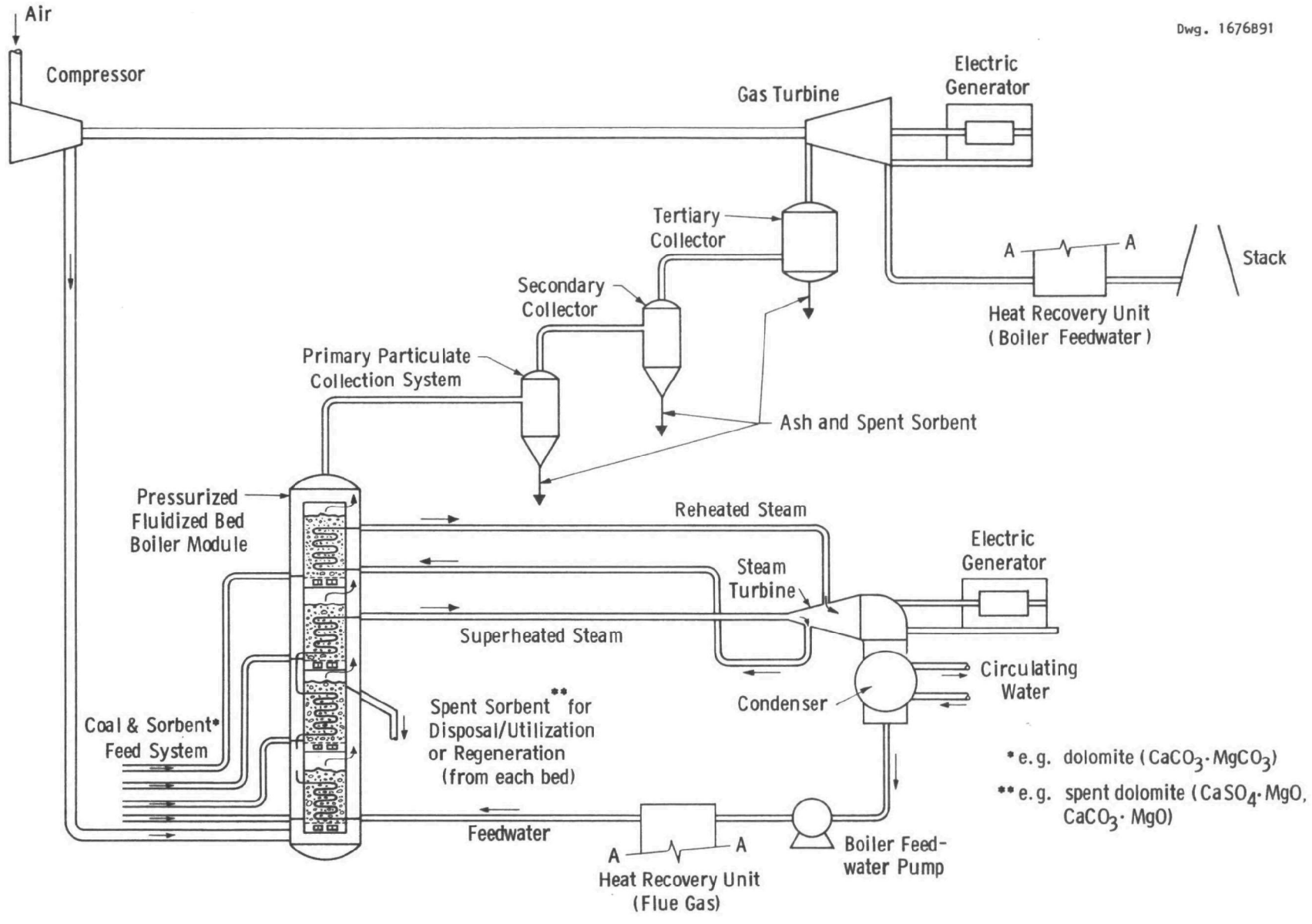

Figure 1—Pressurized fluidized bed boiler - power plant schematic

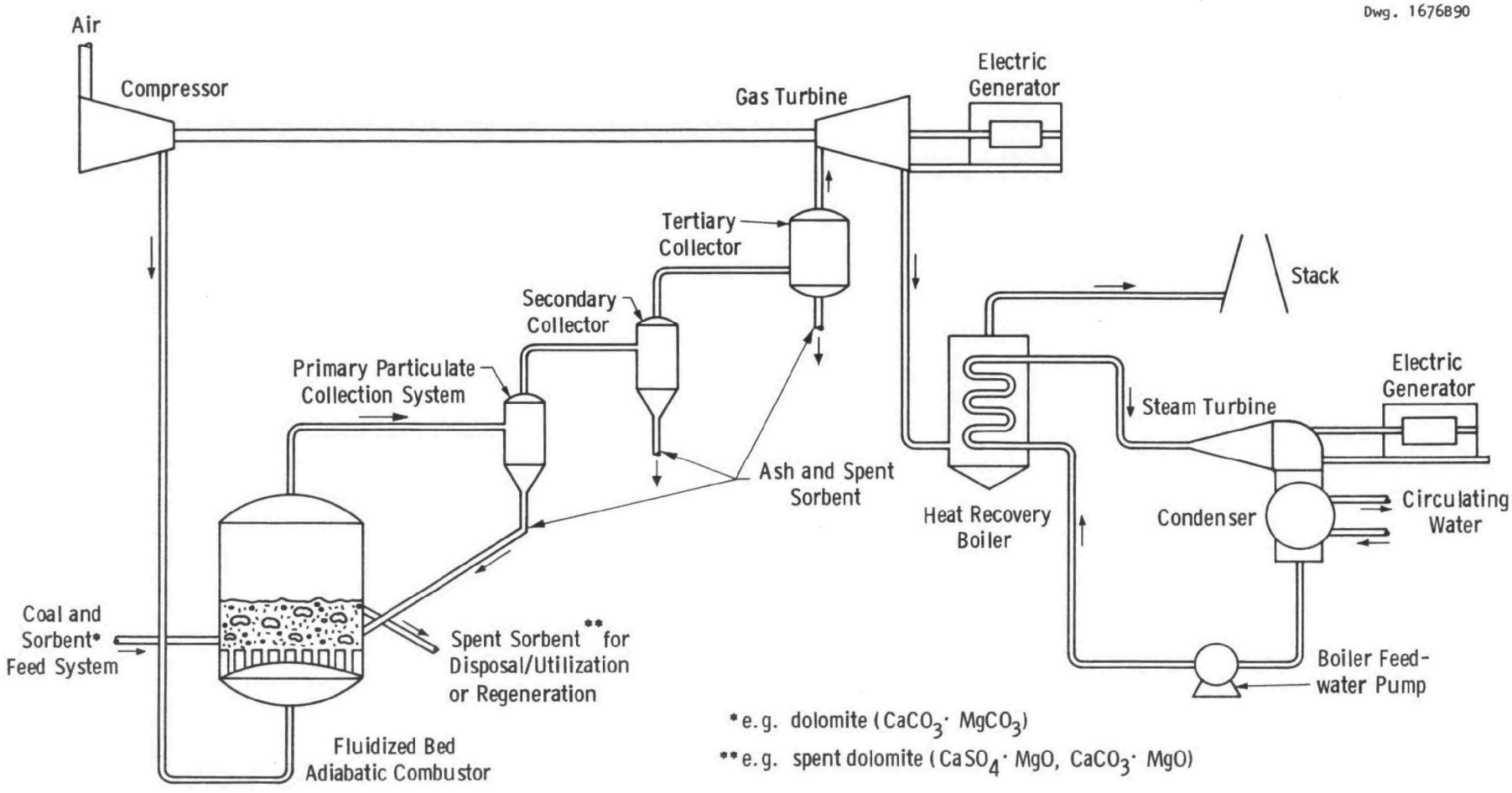

Figure 2—Pressurized fluidized bed adiabatic combustor - combined-cycle power plant schematic

Table 1

PRESSURIZED FLUIDIZED BED COMBUSTION SYSTEMS
REFERENCE DESIGN PARAMETERS AND PERFORMANCE

	Pressurized & fluidized bed boiler power plant	Adiabatic combustor combined-cycle power plant
Plant Capacity (nominal)	300 MW	200 MW
Cycle Parameters		
Steam Conditions	16.547 MPa/538°C/538°C (2400 psi/1000°F/1000°F)	4.823 MPa/427°C (700 psi/800°F)
Condenser Pressure	5.07 kPa (1-1/2 in Hg)	8.45 kPa (2-1/2 in Hg)
Gas-Turbine Expander		
Pressure ratio (100% load)	10:1	10:1
Inlet temperature (100% load)	871°C(1600°F)	927°C(1700°F)
Compressor Expander Pressure Loss (through fuel processing system), % compressor outlet	7.5	7.5
Number of Combustor Modules	4	2
Combustor Modules/Gas-Turbine Module	2	1
Excess Air (range for 100% load and turndown)	10 to 100%	300 to 360%
Fluidized Bed Combustor Design		
Fluid Bed Units/Combustor Module	4	1
Vessel Diameter, m(ft)	3.7 (12)	9.15 (30)
Bed Area	1.5 x 2.1 m; 3.26 m^2 (5 x 7 ft; 35 ft^2)	64.64 m^2 (695 ft^2)
Heat Transfer Surface	(a)	None
Vessel Height, m(ft)	32.94 (108)	4.88 (16)
Fluidized Bed Combustor Operating Conditions		
Bed Temperature 100% load	954°C (1750°F)	954°C (1750°F)
Range for turndown	760-983°C (1400-1800°F)	760-983°C (1400-1800°F)
Gas Velocity (100% load), m/s (ft/sec)	1.71-2.74 (5.6-9.0)	1.8 (6)

Table 1 (Continued)

	Pressurized & fluidized bed boiler power plant	Adiabatic combustor combined-cycle power plant
Bed Depth, m(ft)	3.35-4.36 (11.0-14.3)	2.0 (6.5)
Freeboard, m(ft)	1.53-2.31 (5-7.6)	2.44 (8)
Particle Size (coal & sorbent), mm(in)	up to 6.35 (1/4)	up to 6.35 (1/4)
Ca/S Molar Feed Ratio for Once-through Operation	2[b]	2[b]
Sorbent	Dolomite	Dolomite
Performance		
Power Generation Split (100% load)		
% Gas turbine	18%[c]	70%
% Steam turbine	82%[c]	30%
Plant Heat Rate (HHV)	9040 kJ/kWh (8570)Btu/kWh)[c]	9600 kJ/kWh (9100 Btu/kWh
Turndown Capability (% of full load)	12-1/2%	<10%
Rate	5%/minute	5%/minute
Environmental Impact		
SO_2, kg/GJ (lb/10^6 Btu)	<0.5(<1.2)	<0.5(<1.2)[d]
NO_x, kg/GJ (lb/10^6 Btu)	<0.3(<0.7)[d]	<0.3(<0.7)[d]
Particulate kg/GJ (lb/10^6 Btu)	<0.04(<0.1)	<0.04(<0.1)
Minor and trace element release	To be determined	To be determined
Heat rejection (% less than conventional steam plant)	∿15%[c]	∿60%
Waste liquids	None	None
Waste solids		
Characteristics	Dry, granular, sulfated limestone/dolomite	Dry, granular, sulfated limestone/dolomite
Quantity Mg/hr/MW (tons/hr/MW)	0.18[b] (∿0.2)	0.18[b] (∿0.2)
Resources (multifuel capability)	Yes	Yes

[a] 2 in O.D. tubes on 3-1/2 in welded wall spacing. 1-1/2 in O.D. tubes in preevaporator and superheater; 2 in O.D. in reheater; heat transfer coefficient. 283.5 W/m^2-°K (50 Btu/hr-ft^2-°F); tubes represent 17 to 22.5% of the bed volume.

[b] Subsequent data indicate that Ca/S ratios from 1.0 to 1.2 can be used to achieve 90% sulfur removal. This reduces the waste solids production to ∿0.07 Mg/hr/MW or ∿0.067 ton/hr/MW.

[c] Parameters for the 100% excess air base case are: power generation: 29% gas turbine, 71% steam turbine; plant heat rate 8940 kJ/kWh (8470 Btu/kWh); ∿25% less heat rejection.

[d] Available data indicate NO_2 emissions <0.17 kg/GJ (0.4 lb/10^6 Btu).

and component designs (use of low-temperature gas cleaning, alternative cycles); and provision of support to other contractors (gas-turbine corrosion/erosion test rig design and construction).

II. ASSESSMENT

The results from experimental pressurized fluidized bed combustion test facilities (units operated by Exxon, Argonne National Laboratories[ANL], Combustion Power, and British Coal Utilization Research Association [BCURA]) during the past 18 months confirm the projected performance for the reference power plant designs previously carried out by Westinghouse under contract to EPA. The results support the pressurized fluidized bed combustor and power plant reference design parameters previously utilized. However, these tests have not been carried out under all of the proposed operating conditions, have not investigated all the plant components under projected operating conditions, and have not been carried out on commercial-scale equipment, additional work is required to confirm commercial plant designs. The results indicate:

- High sorbent utilization can be achieved in a once-through system. A calcium/sulfur molar ratio less than 2, with dolomite, will achieve 90 percent removal. This is consistent with the projections reported in 1973 on the basis of thermogravimetric (TG) data[2] and lower than the original projections of 3 to 6.[1]
- Nitrogen oxide emission standards can be met. The mechanism for the nitrogen oxide emissions, however, is not yet understood. Data are typically less than half the emission standard of 0.3 kg/GJ (0.7 lb/10^6 Btu). For example, 0.13 to 0.17 kg/GJ (0.3 to 0.4 lb/10^6 Btu) have been reported for tests with excess air from 15 to 100 percent.[3]
- Combustion efficiency greater than 98 percent at 100 percent excess air can be achieved. The data at 100 percent excess air, with bed depths significantly less than the commercial

design values, indicate that the complete combustion loss of 1.5 percent assumed in the reference design with 100% excess air will be achieved without requiring further processing of the ash carry-over.

- Heat transfer coefficients of 284 $W/m^2-°K$ (50 $Btu/hr-ft^2-°F$) or greater can be achieved.
- Bed temperatures can be used over the range projected -- 760 to 954°C (1400 to 1750°F) -- and still meet environmental standards.

Experimental and analytical studies performed under this contract show that critical parameters in the reference design concepts are:

- Selection criteria for calcium-based sorbents
- Control of alkali-metal compounds to prevent corrosion/ deposition damage to gas turbines.
- Specification for particulate removal equipment to prevent erosion damage to gas turbines
- Disposition of spent sorbent.

The available results from experimental and analytical studies indicate that no problems have been identified which preclude either commercialization or meeting environmental standards. The results also indicate the processes are less sensitive to fuel variations, further advanced in development, less demanding of the gas turbine (as the result of lower turbine inlet temperatures), and superior to or comparable in cost and efficiency with any competitive, advanced fossil fuel processing system under development utilizing state-of-the-art power generation equipment.

The work reported in this contract report focuses on providing additional support data and analyses to understand specific process components — sulfur removal, particulate control, and gas turbine systems: on evaluating the current development status of pressurized fluidized bed

combustion systems; and on providing support to on-going development work being carried out by other contractors.

An assessment of the system economics, system design and performance, and system development follows.

SYSTEM ECONOMICS

Energy costs for pressurized fluidized bed combustion combined-cycle power plant systems are estimated to be up to 20 percent less than those for a conventional plant with stack-gas cleaning at around $100/kw. These savings are based on a 3 percent sulfur fuel cost of 80¢/GJ(10^6 Btu). An energy cost reduction of 17 percent is projected for a pressurized fluidized bed boiler (PFBB) operating at 17.5 percent excess air, with three stages of high-temperature particulate removal utilizing a calcium/sulfur ratio of 1.2 for a once-through sulfur removal system. The same system with low-temperature particulate removal (e.g., water scrubbing) would be approximately 15 percent lower in energy costs than the conventional plant. This is a particularly significant result of the present analysis since it indicates that low-temperature particulate control, which may offer improved power plant reliability, is also economically attractive. The pressurized fluidized bed boiler system, operating at 100 percent excess air to achieve higher carbon utilization in the primary combustors and greater turndown flexibility, is approximately 13 percent lower in cost but must utilize high-temperature particulate removal to be economical. Energy costs for a pressurized fluidized bed adiabatic combustor combined-cycle power plant with a once-through sulfur removal system using a calcium/sulfur ratio of 1.2 and three stages of particulate control are estimated to be approximately 7 percent lower than those of a conventional plant. Plant costs projected for regenerative fluidized bed combustion systems indicate regeneration is not cost competitive with the conventional plant until sorbent costs (including disposal) exceed $10 to 20/Mg. Since the regenerative calcium-based sorbent processes proposed are not yet well defined, however, a definitive conclusion is not possible. A regenerative process is clearly attractive environmentally and, perhaps, will be economically if a

regenerative process can be developed to operate with calcium/sulfur makeup ratios significantly less than 1.

SYSTEM DESIGN AND PERFORMANCE

Cycle Evaluation

The national average heat rates for fossil fuel steam electric plants have leveled off at 11.1 MJ/kWh (10,500 Btu/kWh). The most efficient plants average around 9.4 MJ/kWh (8900 Btu/kWh) and do not include sulfur removal or nitrogen oxide minimization. Conventional plants which meet environmental standards have heat rates near 9.6 MJ/kWh (9100 Btu/kWh). Coal-fired units now being built or on order are all 12.411 MPa/538°C/538°C (1800 psi/1000°F/1000°F), 16.547 MPa/538°C/538°C (2400 psi/1000°F/1000°F), and 24.132 MPa/538°C/538°C (3500 psi/1000°F/1000°F). The first-generation pressurized fluidized bed boiler or adiabatic combustor combined-cycle power plants utilizing state-of-the-art power generation equipment are projected to match the most efficient current plants at reduced cost and to achieve environmental control requirements at the same time. Plant heat rates for the base designs are 8.94 MJ/kWh (8470 Btu/kWh) and 9.04 MJ/kWh (8570 Btu/kWh) for the pressurized fluidized bed boiler plant operating at 100 percent and 17.5 percent excess air,respectively. The adiabatic combustor base plant heat rate is 9.6 MJ/kWh (9100 Btu/kWh).

The two base systems (the pressurized boiler and adiabatic combustor) remain the most attractive. Closed-cycle gas-turbine, air-cooled heat transfer surface and related applications offer potential advantages by avoiding or minimizing possible problem areas in the reference designs and should thus be investigated. However, they do not offer reduced capital cost or improved energy efficiency when compared with the reference systems. The performance and energy cost of a pressurized fluidized bed boiler power plant operating at low excess air (e.g., 17.5 percent) with a low-temperature particulate removal system is competitive with the low excess air pressurized boiler with three stages of high-temperature particulate removal. This concept offers the potential for improved plant reliability by achieving higher

particulate removal efficiencies and condensing alkali metals prior to entering the gas turbine. The gas heat exchanger performance and life must be demonstrated to achieve these advantages. The use of advanced steam conditions is not attractive because of the projected cost increase which would be required for the steam turbine.

Combustor Design

The available data do not indicate any problems which preclude the development of pressurized fluidized bed combustors. Further development work is required in a number of key areas, however, including performance with large-scale heat transfer surface, testing boiler tube life, and operation over the full range of commercial plant conditions.

The results from the Exxon experimental test unit have indicated one area of concern, the potential for nonuniform temperature gradient in a deep fluidized bed combustion boiler. Further tests on this unit and data from large-scale combustors operating at the design pressure, temperature, velocity, and bed height are required to verify this aspect of the reference boiler design. Modifications of the base designs, such as alteration of the tube packing arrangement, may be desired.

Sulfur Removal System

The sulfur removal system must be compatible with the total process. In order to achieve this compatibility, factors such as trace element release and spent sorbent disposition must be investigated along with the sulfur removal characteristics. The work on sulfur removal shows that the conditions under which the calcium-based sorbent is calcined is critical in establishing the calcium utilization. The results show that calcium/sulfur ratios from 1.0 to 1.2 can be achieved. Pilot-scale tests at ANL have demonstrated these results. A model of the desulfurization process was developed which successfully predicts sorbent performance on fluidized bed combustors,using TG data. Investigation of the poor regenerability of calcium sulfide during regeneration continues; analysis of the results to date has not revealed the mechanism for deactivation. Tests on sorbent attrition show that attrition

resistance will be a primary factor in selecting sorbents. Sorbent attrition rates from laboratory screening tests show variations from 1 to 40 percent of the initial bed inventory and indicate that most of the attrition occurs during calcination. Direct disposal and utilization of the spent sorbent were investigated, and both leaching experiments and activity tests indicate that direct disposal of the spent sorbent will not cause water or heat pollution. Process options for alternative disposition of the spent sorbent are identified. There is no indication at this time that the sorbent will contribute a significant or hazardous concentration of trace elements to the environment. The release of sodium and potassium, however, is a primary concern because of gas-turbine corrosion. This aspect will be addressed further.

Nitrogen Oxide Emissions

Nitrogen oxide emissions from fluidized bed combustion processes result from the bound nitrogen in the fuel. Experimental investigations show that the conversion of bound nitrogen is substantially less than 100 percent. Data from pressurized fluidized bed boiler test units and adiabatic combustor test units using coal show that the nitrogen oxide emissions are less than approximately 0.173 kg nitrogen oxide/GJ (0.4 lb/10^6 Btu) for excess air values up to around 300 percent. This is approximately half the EPA standard of 0.302 kg NO_2/GJ (0.7 lb NO_2/ 10^6 Btu).

The mechanism which produces the low nitrogen oxide emission is not yet understood. Those parameters which have been identified as having a significant effect on nitrogen oxide emissions are pressure level, excess air, calcium/sulfur feed ratio, carbon monoxide, and bed hydrodynamics. Sufficient data are not available to assess the effect of the nitrogen content and character of the fuel. Some or all of these factors may determine the nitrogen oxide emission level. Further work is required to understand nitrogen oxide emissions from pressurized fluidized bed combustion systems and to assure selection of design and operating parameters to such emissions. The nitrogen oxide emissions, however, are well within the current emission standard.

Particulate Control

Particulate removal is critical for the successful operation of pressurized fluidized bed combustion combined-cycle power plants. Criteria for particulate control are ill defined, and there is a need for more definitive data. The allowable limit for gas-turbine operation is expected to be lower than the present allowable emissions (0.043 gm/MJ (0.1 lb/10^6 Btu) equivalent to 0.115 gm/m^3 (0.05 gr/scf)).

Simple mechanical collectors, such as cyclones, are inadequate for meeting the dust collection requirements. Instead, three stages of cleaning are projected for particulate control:

- Primary collectors to collect coarse material
- Secondary collectors to remove the bulk of the remaining fine material
- Tertiary collectors to reduce the level of ultrafine particles to acceptable levels.

The use of three stages of particulate removal equipment represents a significant change in the original reference designs,[1,2] which assumed two stages. This change is the result of a further assessment of the gas-turbine tolerance to particulates, which projects a lower dust-loading criteria, and of recent experimental tests on tornado cyclones, which indicate the efficiency will not be as high as originally projected. Experimental testing on large-scale, hot, pressurized equipment is required to establish the operating performance of the dust collection equipment. A test facility capable of handling 14 to 28 actual m^3/min (500 to 1000 acfm) of gas flow is envisioned.

Minor Element and Trace Element Release

Trace emissions are important because of their effect on the environment and on the operability of the plant. Preliminary experiments to investigate the fate of potential environmental pollutants have been initiated in pilot-scale combustors by ANL and by Exxon. This work is still in the early stages and does not yet provide a basis for assessing

the potential environmental impact. The experimental data on alkali-metal emissions from pilot-scale combustors are also limited. The work carried out under this contract was directed toward developing an understanding of the alkali-metal emission chemistry of the gas turbine and its tolerance of alkali metals, relating this understanding to available data and identifying critical concerns. The results indicate:

- That, on the basis of the release of sodium and potassium into the gaseous effluent from the fluidized bed combustor, the equilibrium turbine tolerance for alkali metals may be exceeded in normal operation without some control. It must be noted that the available data are not sufficient to permit a definitive conclusion, and further tests are required.
- That, control options to prevent damage to turbine hardware are available. These include the use of high-purity sorbents; selection of combustor operating conditions to reduce release; prevention of sulfate deposition by controlling chlorine concentration or increasing the sulfur dioxide removal (<<200 ppm); selection of the low-temperature particulate removal option which would condense the alkali metals; use of additives to trap alkali and trace elements.

Gas-Turbine Operation

Erosion, corrosion, and deposition in the gas turbine were investigated, and design features needed to duct the hot gas into the turbine and to protect the turbine from localized contaminants were assessed. Blade erosion data are extrapolated to indicate permissible particulate loading. This projection shows that particulate loadings of 0.012 to 0.093 gm/m^3 (5×10^{-3} to 4×10^{-2} gr/scf) will yield about 25,000 hr blade life when the particle size distribution has a mean size between 4 and 8 μm in diameter (see Appendix J). These estimates must be considered preliminary until data on the erosivity of particulates from fluidized bed combustors are available. The estimated tolerance

expansion gas. The tolerance for the fluidized bed boiler system is significantly higher, since the chlorine concentration is greater with the coal-fired system. If the alkali-metal compound tolerances are met, deposits cemented by alkali-metal compounds should not form when the gas turbine is operating at the temperatures specified. Deposits resulting from the impaction and dry sintering of fine particles can occur. Tolerances required to limit these deposits are not yet established. The turbine tolerance model must be modified to allow for the presence of calcium oxide fines which will increase the turbine tolerance to alkalis. Further turbine design work is required to develop reliable gas transfer pipe designs and to investigate design alternatives to increase turbine life.

SYSTEM DEVELOPMENT

Experimental and systems work is required to investigate potential problem areas, establish commercial-scale design criteria, develop operation and control procedures, test plant components, and investigate environmental impact. Various test facilities have been proposed by different organizations to advance the development of pressurized fluidized bed combustion systems. Three development aspects are critical for the expeditious application of pressurized fluidized bed combustion systems:

- Experimental tests on a commercial-scale pressurized fluidized bed combustor test facility with integrated auxiliary components
- Experimental and analytical studies to establish gas-turbine performance
- Experimental and analytical programs to ensure compliance with environmental regulations (air emissions and spent solids disposition).

A commercial-scale fluidized bed combustion test facility was proposed in 1971 and a preliminary design completed in 1973. An extension of the previous concept is presented in this report. The experimental and analytical work to establish gas-turbine performance must include work

on combustor emissions (particulates and trace elements), particulate control, and gas-turbine unit analysis and tests. Three types of facilities are envisioned to obtain the necessary information:

- Test passages and supporting data from pilot-scale pressurized fluidized bed combustion units
- Operation of an integrated commercial-scale fluidized bed combustor, particulate collection system, and gas-turbine test equipment
- Operation of independent test facilities to study gas cleaning and turbine tolerance.

Under this contract Westinghouse designed and constructed a gas-turbine corrosion/erosion pilot-plant test rig constructed by Westinghouse for the Exxon miniplant and established a test program. Gas-turbine test equipment is also identified for incorporation in a flexible pressurized fluidized bed combustion test facility. Environmental studies should be continued on the laboratory- and pilot-plant scale, and the commercial-scale facility used to determine the environmental impact of pressurized fluidized bed combustion systems.

Additional support studies are recommended to supplement these critical program tests. These support studies should include, but not be limited to, work on boiler tube wastage, instrumentation, operation and control procedures, and solids feeding. Work should also be directed toward the development of regenerative sulfur removal systems--utilizing both calcium-based and alternative sorbents--for second-generation pressurized fluidized bed combustion processes.

III. CONCLUSIONS AND RECOMMENDATIONS

CONCLUSIONS

The primary conclusions from this work are that:

- Pressurized fluidized bed boiler and adiabatic combustor combined-cycle power plants represent an opportunity to improve fuel economy and reduce energy costs within environmental constraints.
- No problems have been identified which preclude commercialization; no problems have been identified which preclude meeting environmental standards. The processes are less sensitive to fuel variations and further advanced in development than competitive advanced fossil fuel processing technology using state-of-the-art power generation equipment, and they are comparable in cost and efficiency.
- Available experimental data support the basic commercial fluidized bed combustion boiler and adiabatic combustor design and operating parameters previously selected.
- Updated system economics show energy costs for first-generation pressurized fluidized bed combustion combined-cycle power plants ranging from 7 to 20 percent less than a conventional plant with stack-gas cleaning.
- Development priorities for pressurized fluidized bed combustion systems are:
  1. Operation of a commercial-scale pressurized fluidized bed combustion test facility with integrated auxiliary components (in other words, solids feed, combustor, particulate control, gas-turbine test system)

2. Experimental and analytical studies to establish gas-turbine tolerance to particulates and trace elements
3. Investigation of high-temperature and low-temperature particulate control systems
4. Experimental and analytical programs to assure compliance with environmental regulations.

Specific conclusions from the experimental and analytical studies are:

- The pressurized fluidized bed boiler power plant operating at low excess air has the lowest projected energy cost for first-generation pressurized fluidized bed combustion systems.
- A pressurized fluidized bed combustion boiler power plant operating at low excess air (e.g. 17.5 percent) is economically attractive(energy cost 15 percent lower than in a conventional plant with stack-gas cleaning) with low-temperature (e.g. water scrubbing) particulate control equipment before the gas turbine.
- Limestone/dolomite sorbent (or alternate sorbent) selection criteria must consider attrition characteristics, trace element content and release characteristics, and spent sorbent disposition factors in addition to the sulfur removal behavior and regenerability.
- Calcination of calcium-based sorbents is critical in establishing high sorbent utilization. Calcium/sulfur ratios from 1.0 to 1.2 can be achieved with dolomite.
- Sorbent performance for sulfur removal in the fluidized bed combustion processes can be successfully predicted from thermogravimetric data.
- The technical or economical feasibility of sorbent regeneration has yet to be demonstrated. A regenerative system with makeup calcium/sulfur ratios significantly less than one would be advantageous to minimize the environmental impact from sorbent procurement and disposition.

- Direct disposal of spent dolomite from a once-through sulfur removal system can be achieved without water or thermal pollution.
- Sufficient data are not yet available to assess the environmental impact from minor and trace element release.
- Available data and modeling of the alkali-metal emission chemistry and gas-turbine tolerance to alkali-metal corrosion/deposition indicate sodium and potassium release may exceed the turbine tolerance unless control techniques are applied. This is based on pilot-plant data indicating sodium-plus-potassium levels greater than 1000 ppb using calcium-based sorbents and on projected criteria for sodium plus potassium in the expansion gas less than 300 ppb.
- Control techniques to prevent turbine damage from alkali-metal compounds are available; preferred options include establishing high purity requirements for the sulfur sorbent, selecting combustor operating conditions to reduce release, preventing sulfate deposition by controlling chlorine concentration utilizing low-temperature particulate removal, or increasing sulfur dioxide removal to achieve << 200 ppm.
- Particulate control requirements for the gas turbine are more restrictive than environmental regulations of 0.043 gm/MJ (0.1 lb/10^6 Btu) equivalent to 0.115 gm/m^3 (0.05 gr/scf).
- Particulate loading permissible for gas turbine operation is projected to be less than 0.012 to 0.093 gm/m^3 (0.005 to 0.04 gr/scf), based on turbine modeling studies (> 25,000 hr life).
- Three stages of high-temperature particulate removal will be required to achieve the allowable limits projected for gas-turbine operation.
- Energy costs can be reduced an additional 8 percent if turbine particulate tolerance is such that only two stages of high-temperature particulate removal equipment are required.

RECOMMENDATIONS

On the basis of the experimental, analytical, and economic studies, and on assessments carried out, Westinghouse recommends that:

- Development of pressurized fluidized bed combustion and adiabatic combustor combined-cycle power plants be accelerated
- A commercial-scale, pressurized fluidized bed combustion test facility with integrated auxiliary components be constructed
- Experimental studies to establish gas-turbine tolerance to particulates and trace contaminants be expedited
- Large-scale [14 to 28 m^3/min (500 to 1000 acfm) gas flow], separate test facilities be operated to develop gas-cleaning technology - particularly particulate removal components
- Environmental control studies be continued to assure that processes meet environmental impact requirements.

Recommendations for specific investigations include:

- Extending analyses of modified power plant cycles, particularly the use of low-temperature particulate removal with the low excess air pressurized boiler concept
- Establishing sorbent selection criteria for sulfur removal, attrition, trace element content, and spent sorbent disposition
- Initiating work to assess the potential of achieving very low sulfur dioxide concentrations in the product gas (1 to 200 ppm) as a means to control gas-turbine corrosion from alkali metals
- Continuing laboratory and pilot-scale work to further understanding of sorbent calcination requirements to achieve high utilization

- Reassessing the use of fine particle calcium-based sorbents to achieve high utilization
- Continuing laboratory-scale work to develop regenerative calcium-based sorbent process(es) and regenerative sulfur removal processes utilizing alternative sorbent materials
- Continuing experimental studies to investigate utilization of spent sorbent and ash from once-through operation
- Continuing work to determine the environmental impact of minor and trace elements
- Extending analyses and continuing experimental studies on alkali-metal emission chemistry and gas-turbine tolerance
- Developing control techniques to prevent damage to gas turbines from alkali-metal compounds
- Carrying out large-scale tests to demonstrate alternative secondary and tertiary particulate control equipment
- Carrying out support work to further understand basic component phenomena such as boiler tube wastage, nitrogen oxide minimization, bed mixing, and heat transfer; and to develop auxiliary systems such as coal feeding and instrumentation.

IV. SYSTEM ECONOMICS

Based on the economic comparison presented in the December 1973 report[2] and on the cost updating discussed in Appendix A of this report, the late-1974 minimum cost for a 600 MW steam power plant with limestone scrubbing is about $465/kw and could range up to $530/kw. Similarly, the late-1974 minimum cost for a once-through dolomite pressurized fluidized bed boiler (PFBB) with 17.5 percent excess air and two stages of particulate removal is $355/kw. The cost with three stages of particulate removal is $394/kw. The adiabatic combustor system cost with three particulate removal stages is $468/kw. The PFBB system operating at 100 percent excess air to provide greater operating flexibility and simplicity costs $426/kw. The capital cost of the low excess air PFBB system using water scrubbing for particulate removal is $395/kw -- essentially the same as the cost estimated with three stages of hot gas particulate control. The PFBB and adiabatic combustion system costs are predicated on a calcium/sulfur molar ratio of 2.0. The limestone scrubbing costs are based on a calcium/sulfur molar ratio of 1.27.

Figure 3 and Tables 2 and 3 are used to illustrate the energy costs for the PFBB with 100 percent excess air and adiabatic combustor plants compared to those of conventional plants. Variations in energy cost are shown for various calcium/sulfur ratios and for a range of conventional plant stack-scrubber costs of $50 to 115/kw ($465 to 530/kw total plant cost).

It is evident from Figure 3 that the PFBB system with 100 percent excess air can cost from 1 to 3 mills less than steam power plants with stack-gas scrubbing, depending on the calcium/sulfur molar ratio used for the once-through PFBB design and the cost of the scrubbing system. The adiabatic combustion system is competitive on a once-through sorbent design with a steam power plant plus a limestone stack-gas scrubbing system costing more than about $60/kw. If the mode of PFBB operation

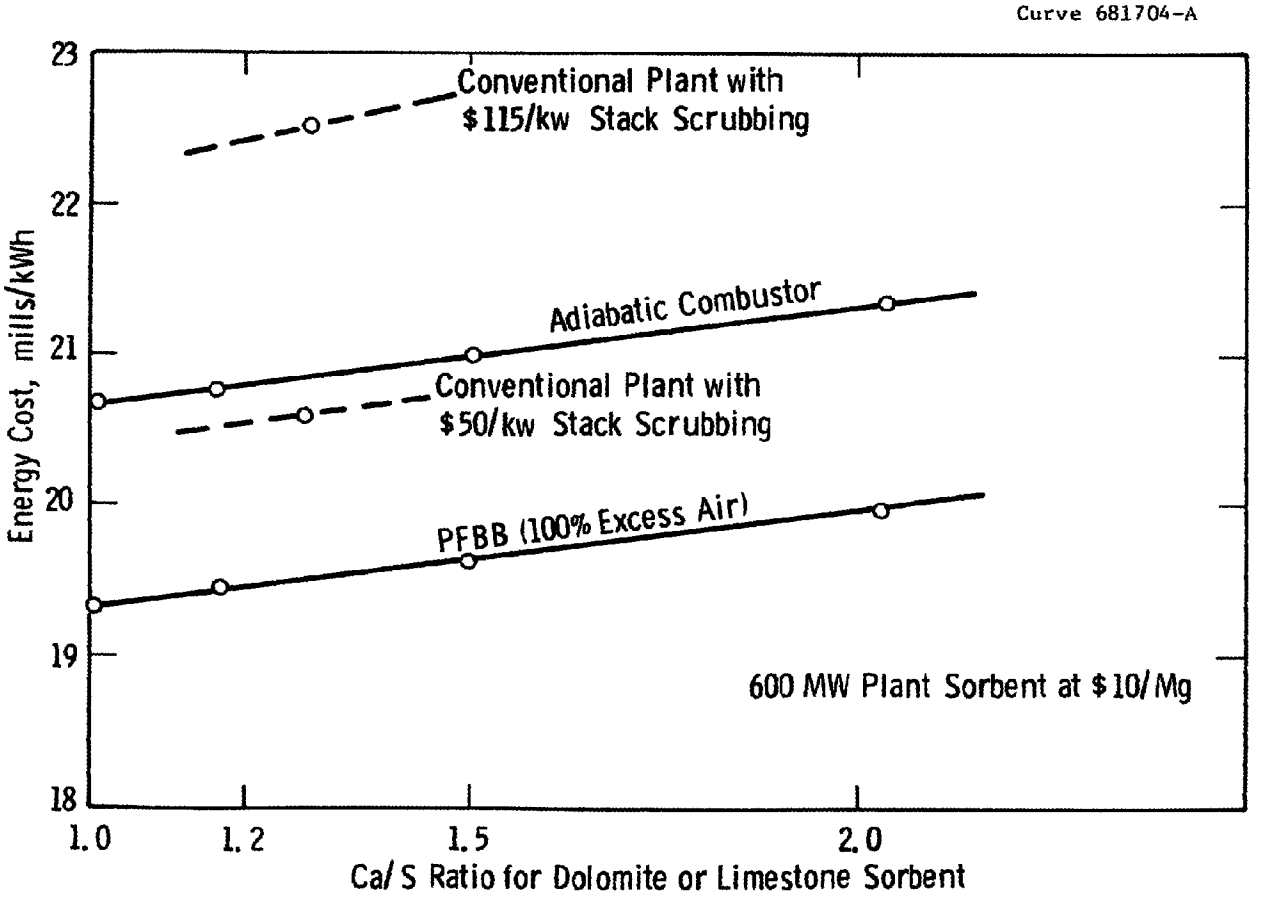

Figure 3—Electrical energy costs

Table 2

ECONOMIC COMPARISON OF 600 MW PLANTS

(3% Sulfur Coal, 90% Sulfur Removal) [a]

	Pressurized fluid bed boiler combined-cycle once-through dolomite sulfur removal system [b]	Adiabatic combustor combined-cycle once-through dolomite sulfur removal system	Conventional steam power plant with limestone scrubbing	
Plant Cost, $/kw [c]	426	468	465 [d]	530 [e]
Dolomite or Limestone Supply & Disposal Cost, $/Mg	10	10	10	10
Energy Cost, mills/kWh				
Fixed charges	10.42	11.45	11.37	12.96
O&M	1.15	1.26	1.39	1.58
Fuel	7.07	7.35	7.42	7.42
S sorbent	1.26	1.31	0.45	0.45
Total Cost Base Ca/S Ratios	19.90 [f]	21.37	20.63	22.41

[a] 15%/year
70% capacity factor
Coal @ 80¢/GJ (10^6 Btu)
1977 operation of PFBB and adiabatic combustor
1978 operation of conventional plant.

[b] 100% excess air, three stages particulate removal.

[c] Based on total costs for November 1974 start of project, and including allowances for 6% contingency, 7.5% interest rate during construction, 7.5% escalation during construction, all plus 2% G&A.

[d] $50/kw for limestone scrubbing.

[e] $115/kw for limestone scrubbing.

[f] The energy cost estimate with two stages of high-temperature particulate removal is 18.30 mills/kWh. The energy cost for the low excess air case with two stages of particulate removal is 17.90 mills/kWh.

Table 3

600 MW PLANT ECONOMICS FOR VARIOUS Ca/S RATIOS[a]

[PFBB (100% excess air) and Adiabatic Combustor]

	Ca/S Ratio			
	1	1.2	1.5	2
Sorbent Cost, mills/kWh				
PFBB	0.63	0.76	0.94	1.26
Adiabatic combustor	0.66	0.79	0.98	1.31
Total Energy Cost, mills/kWh				
PFBB	19.27	19.4	19.58	19.90
Adiabatic combustor	20.72	20.85	21.04	21.37

[a]Based on economics developed for PFBB in Table 2.

were to be changed from once-through to regenerative, the operating cost addition for the regeneration system could approach 3 mills/kWh and still maintain a total cost competitive with that of a conventional steam power plant with $100/kw limestone scrubbing. Further consideration would indicate that the regenerative PFBB system could be preferable to a conventional plant with a once-through scrubber, even at the same energy cost, since both longer construction time and slurry discharge are inherent intangible detriments for the conventional plant installation. The comparison of regeneration processes made in Volume I of the 1973 report,[2] Table 36, showed that the most expensive regeneration system added 2.37 mills/kWh to $10/Mg once-through dolomite system energy costs. Adjusting the 2.37 mills/kWh differential for today's inflated investment costs and for the 80¢/GJ (10^6 Btu) coal cost raises it to 3.14 mills/kWh. Thus, at $10/Mg for dolomite supply and disposal, the use of the most expensive two-step regeneration scheme is a break-even proposition when compared with a conventional plant plus $100/kw limestone scrubbing. At $20/Mg for dolomite, the 3.14 mills/kWh differential drops to 2.78 mills/kWh, and regeneration could be a competitive addition to a PFBB plant installation. Regeneration system technology and costs are not known with sufficient precision to permit a firm conclusion regarding system selection or economics at this time.[4]

Finally, Figure 4 presents the variation in the cost of power produced with the plant-load factor from a 600 MW conventional plant with a $100/kw scrubber, two PFBB plants, a PFBB plant with regeneration, and an adiabatic combustor plant with once-through sorbent. Figure 4 has been based on 3 percent su'fur coal, 90 percent sulfur removal, limestone/dolomite at $10/Mg, coal at 80¢/GJ ($10^6$ Btu), and capital charges as noted for Figure 3.

In summary, the most flexible pressurized fluidized bed boiler power plant (100 percent excess air) is capable of electric power generation at up to 3 mills/kWh less than a conventional steam power plant with a limestone stack-gas scrubber. This system with regeneration can be competitive with a conventional plant/scrubber combination if dolomite

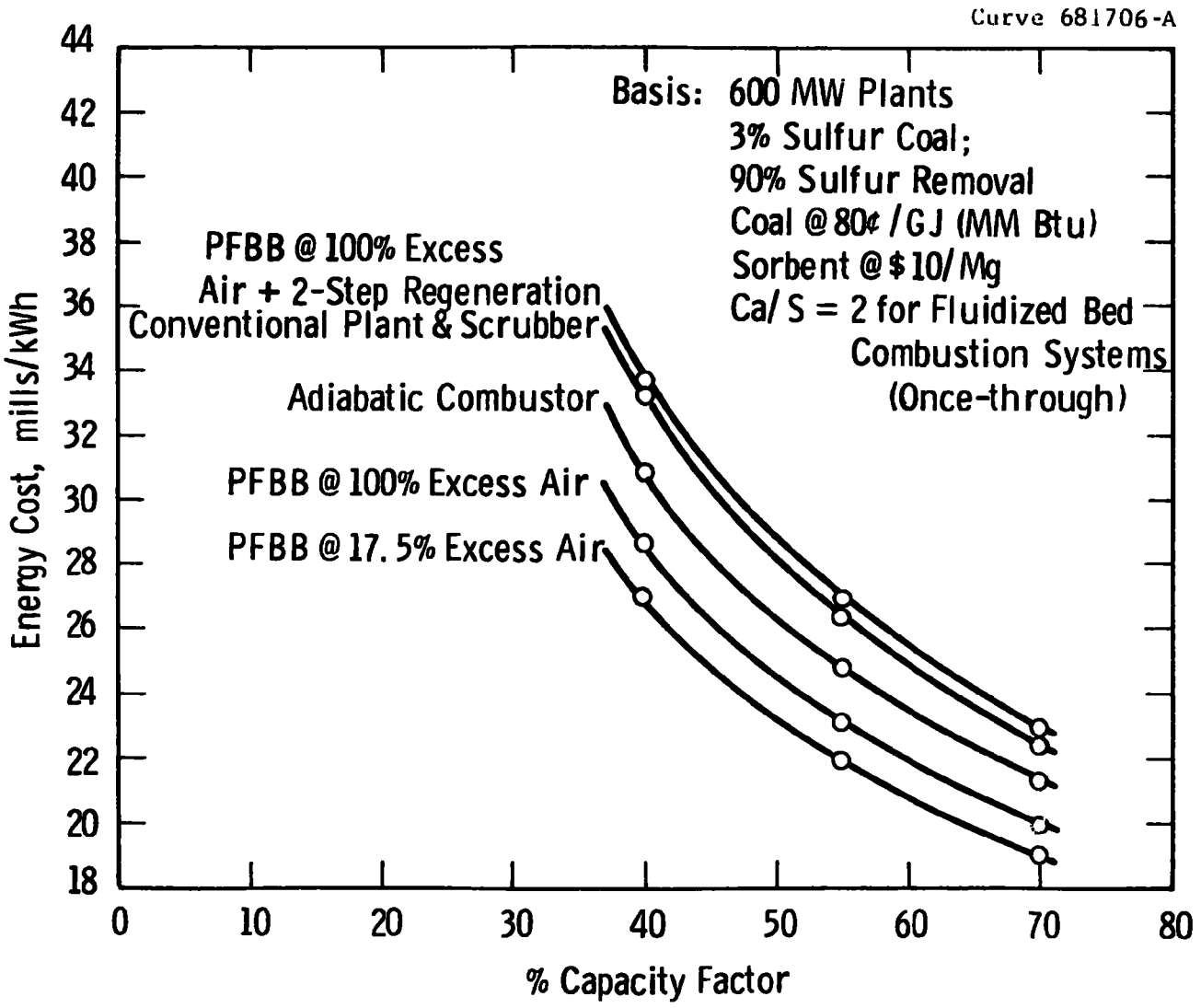

Figure 4—Energy cost vs capacity factor

total costs for supply and disposal are $20/Mg or higher. The adiabatic combustor once-through sorbent system can be competitive with a steam power plant with a stack-gas scrubber system costing over $60/kw. Both the dry and the wet designs of particulate removal applied to a low excess air PFBB system can save about $30/kw compared to the 100 percent excess air PFBB system.

This savings must be balanced against the higher carbon utilization achieved in the primary beds and the flexibility in turndown achieved with the 100 percent excess air case. If the three-stage particulate removal system projected is required, however, then the low excess air, low-temperature particulate removal system offers economic advantages and may offer greater gas-turbine reliability. Also, the fuel cost assumed is lower than typical costs projected for future coal contracts, and the once-through sorbent requirement used for the base case (calcium/sulfur = 2) is expected to be conservative since lower calcium/sulfur ratios (Ca/S = 1.2 to 1.5) have been demonstrated on laboratory- and pilot-scale equipment to achieve the specified sulfur removal. These factors favor the pressurized fluidized bed combustion systems and increase the energy cost differential with conventional plants.

V. SYSTEM DESIGN AND PERFORMANCE

CYCLE EVALUATION

Fluidized bed combustion technology can be applied with many different configurations and can be utilized in many different power cycles. A brief summary is presented here of the proposed pressurized fluidized bed combustion boiler and adiabatic combustor designs. Alternative pressurized fluidized bed combustion power plant cycles are reviewed and their status assessed. Operation, control, and performance of these systems are evaluated.

Base Systems

Pressurized Fluidized Bed Boilers

Under EPA Contract No. CPA 70-9,[1] and on the basis of an evaluation of available data, Westinghouse prepared a preliminary design for a commercial-scale, pressurized fluidized bed boiler power plant. A 320 MW plant required four modules of 3.7 m (12 ft) diameter, and a 635 MW plant required four modules of 5.2 m (17 ft) diameter. Each pressure vessel housed four separate fluidized beds of cross section 1.5 by 2.1 m (5 by 7 ft). The bottom bed was for preevaporation, the top bed for reheating, and the other two beds for superheating. Evaporation of water was accomplished in the water walls which enclosed the beds. The design was characterized by vertical modular components, horizontal steam tubes immersed in the bed, bed depths of 3.3 to 4.3 m (11 to 14 ft), gas velocities of 1.8 to 2.7 m/sec (6 to 9 ft/sec), pressure of 1013 kPa (10 atm), and limestone/dolomite for sulfur removal. The effect of the change in fluidized bed operating conditions and design parameters on economics and performance was analyzed[5] and found to be essentially invariant with the projected design basis. The effects of steam pressure and gas-turbine pressure ratio were also evaluated.

A pressurized fluid bed combustion boiler combined-cycle power plant using state-of-the-art power generation equipment with steam conditions of 16,548 kPa/538°C/538°C (2400 psi/1000°F/1000°F), gas-turbine pressure ratio of 10:1, and gas-turbine temperature of 871°C (1600°F) was the preferred design. This plant has a calculated heat rate of about 9040 kJ/kWh (8570 Btu/kWh). (See Appendix A.)

British Coal Utilization Research Association (BCURA) developed a 140 MW pressurized fluidized bed boiler design for a combined-cycle power plant.[6] The design was characterized by a horizontal 4.3 m (14 ft) diameter, 30.5 m (100 ft) long pressure shell, horizontal steam tubes immersed in the bed, gas velocity of 0.6 m (2 ft)/sec, bed depth of 1.2 m (4 ft), pressure of 810 kPa (8 atm), and no provision for sulfur removal. Subsequent to this initial design, a 70 MW design was proposed. Design features of the 70 MW plant are similar to the Westinghouse-Foster Wheeler design except that the BCURA design operates at a lower fluidizing velocity, 0.8 m/s (2.5 ft/sec), and at a higher pressure, 1611 kPa (16 atm). A pressurized fluid bed combustor pilot plant has been successfully operated at BCURA to obtain process data.[7-9]

Pressurized Fluidized Bed Adiabatic Combustors

The requirement for an internal heat transfer surface in fluidized bed combustion can be eliminated by increasing the excess air to a bed operating at 927°C (1700°F) to approximately 300 percent. An adiabatic coal-fired fluidized bed combustor is applicable to gas-turbine or combined gas-turbine/steam-turbine cycles. Combustion Power Company has operated a pilot plant of a gas turbine with a fluidized bed combustor on prepared solid waste. The unit has been modified, under contract to OCR, to test coal.[10] The pilot plant combustor is 2.7 m (9 ft) in diameter operating at 414 kPa (60 psi) with gas velocities up to 2.1 m (7 ft)/sec and 0.6 m (2 ft) bed depths. The product gas goes to a Rustin TA 1500 gas turbine. Westinghouse, under contract to EPA, previously carried out conceptual designs and performance and economic

studies on adiabatic fluidized bed combustion systems for coal-fired combined-cycle power plants. Two combustor design concepts were studied - a single fluid bed module and a stacked fluid bed module. The fluidized bed combustors were designed to operate at gas velocities of about 1.8 m (6 ft)/sec, bed depths of 1.8 to 2.1 m (6 to 7 ft), and bed temperature of 954°C (1750°F). With a turbine inlet temperature of 927°C (1700°F), the calculated plant heat rate is about 9600 kJ/kWh (9100 Btu/kWh).

Alternative Pressurized Fluidized Bed Combustion Power Cycles

Advanced Steam Conditions

In the late 1950s, the trend toward higher power plant efficiency with little regard for economics culminated in the building of the Eddystone Unit No. 1, with throttle steam conditions of 34,475 kPa /649°C/566°C/566°C (5000 psi/1200°F/1050°F/1050°F).[11] Because of serious operating problems with this unit, and with American Electric Power's Philo No. 6, designed for 31,028 kPa (4500 psi), subsequent supercritical units have been limited to pressures of 24,133 kPa (3500 psi). More recently, the trend has been away from supercritical cycles because they were relatively unreliable and uneconomical, and unable to attain their predicted performance in practice.

During the early 1960s, a number of steam plants were constructed with superheat temperatures of 593°C (1100°F). Operating experience with these plants showed that there was no economic advantage in using steam temperatures above 538°C (1000°F), and since that time most new units have been designed for 538°C (1000°F) superheat and reheat.

A description of the typical coal-fired power plant of the early 1970s is as follows:

- 800 MWe, 3600 rpm, tandem compound, four 31-in low-pressure ends
- Seven feed heaters plus gland, generator, and oil coolers, 5 degree approach

- 16,548 kPa/538°C/538°C (2400 psi/1000°F/1000°F)
- Condensing at 8.4 kPa (2.5 in Hg), natural draft wet towers
- Turbine cycle heat efficiency of 44 percent [8271 kJ/kWh (7840 Btu/kWh)]
- Unit net heat rate 9622 kJ/kWh (9120 Btu/kWh)
- Pulverized coal fired
- Consumptive water use 1.7 kg/kWh/50,006 m^3 per day (3.75 lb/kWh/11,000,000 gpd)

During the initial phases of the preliminary design of the high-pressure fluidized bed boiler for utility applications under Contract No. CPA 70-9,[1] a parametric study was made to compare the estimated performance and energy costs of high-pressure fluidized bed boilers operating at 16,548 (2400) and 24,133 kPa (3500 psi). For both pressure levels the superheat and reheat temperatures were 538°C (1000°F). The results of this parametric study indicated that there was no economic advantage in using supercritical steam conditions in the high-pressure fluidized bed boiler with superheat and reheat temperatures of 538°C (1000°F). Experience with conventional pulverized-coal plants has shown that there is little economic advantage to using 24,133 kPa (3500 psi) steam pressure instead of 16,548 kPa (2400 psi).

There is reason to think that the hot-side corrosion problems in the fluidized bed boiler will be less severe than in the conventional pulverized-coal boilers and, therefore, that superheat and reheat temperatures greater than 538°C (1000°F) would be technically feasible. In view of this a series of cycle performance calculations was made to see how much the heat rate of a plant with high-pressure fluidized bed boilers could be improved with higher steam superheat and reheat temperatures (and correspondingly higher pressures). The results of these calculations for a gas turbine with a pressure ratio of 10, a turbine inlet temperature of 871°C (1600°F), and an air equivalence ratio of 1.1 are shown in Table 4.[2]

Table 4

PLANT HEAT RATE AS A FUNCTION OF STEAM CONDITIONS

Throttle pressure, kPa,(psi)	Superheat temperature, °C(°F)	Reheat temperature, °C(°F)	No. of heaters	Heat rate kJ/kWh (Btu/kWh)	Ratio of heat rate to base case
16,548 (2400)	538 (1000)	538 (1000)	7	9040 (8570)	1.000
24,133 (3500)	538 (1000)	538 (1000)	7	8900 (8440)	0.985
31,028 (4500)	649 (1200)	649 (1200)	8	8190 (7770)	0.907
34,475 (5000)	760 (1400)	760 (1400)	8	7840 (7430)	0.868

Cost estimates of high-pressure fluidized bed boiler systems with advanced steam conditions made under NASA Contract NAS 3-19404 gave the results shown in Table 5 for a gas turbine with a pressure ratio of 10:1, a turbine inlet temperature of 871°C (1600°F), and an air equivalence of 1.1. The increased cost of the high-pressure steam turbine for steam temperatures higher than 538°C (1000°F) with corresponding pressures more than offsets the effect of the improved heat rate on the cost of energy.

Table 5

ENERGY COST AS A FUNCTION OF STEAM CONDITIONS

PLANT HEAT RATE AS A FUNCTION OF PRESSURE RATIO

Throttle pressure, kPa (psi)	Superheat temperature, °C(°F)	Reheat temperature, °C(°F)	Specific cost, $/kw	Cost of energy, $/kw
24,133 (3500)	538 (1000)	538 (1000)	374	21.28
31,028 (4500)	649 (1200)	649 (1200)	474	23.70
34,475 (5000)	960 (1400)	760 (1400)	534	25.19

Oxygen-Blown System

Westinghouse has made an evaluation of an oxygen-blown atmospheric-pressure fluidized bed boiler[12,13] under EPA Contract 68-02-0605, which led to the conclusion that the high cost of oxygen prohibits the use of an oxygen-blown atmospheric-pressure fluidized bed combustion system for economical steam or power generation. The bare cost of 95 percent oxygen, using depreciation rates allowable for utilities, and direct costs only for fuel and labor, is $6.81/Mg. The additional charges incurred by an industrial producer of oxygen such as Linde or Air Products add at least $7 or $8 more per Mg of oxygen and give over-the-fence costs of about $14. Since there would be no significant cost reduction associated with an oxygen-fired plant, an increase in energy costs of up to 10 mills/kWh would result.

Low-Temperature Cleanup Techniques for High-Pressure Fluidized Bed Boilers

A study has been carried out to determine the performance penalty which accompanies reduced-temperature techniques for removing particulates from the combustion products of a high-pressure fluidized bed boiler.

Two alternatives have been investigated:

- Cooling the combustion products by the use of a convection-type boiler and removing particulates by cyclone separators, tornado separators, electrostatic precipitators, or combinations thereof, at intermediate temperatures
- Cooling the combustion products with a recuperator followed by a scrubber-cooler.

The arrangement for the high-pressure fluidized bed boiler system with intermediate temperature particulate removal is shown in Figure 5. The convection-type boiler for cooling the products of combustion to a temperature well below the bed operating temperature is in series/parallel* with the fluidized bed boiler. This permits the

*Series for combustion products-parallel for working fluid.

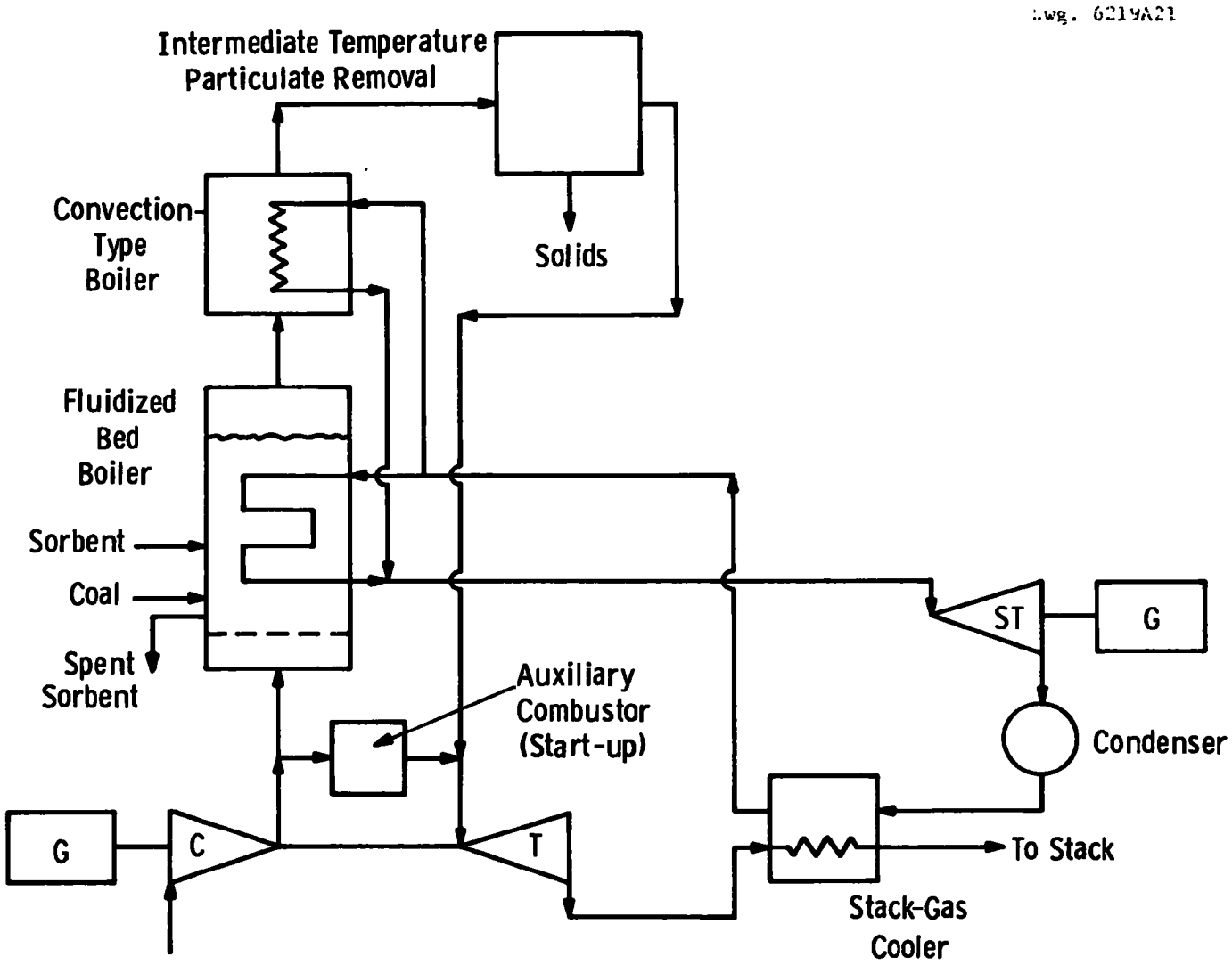

Figure 5 —High-pressure fluidized bed boiler power system with intermediate temperature particulate removal

temperature of the combustion products to be reduced from 870°C (1600°F) to the gas-turbine idle temperature which is in the range of 482 to 538°C (900 to 1000°F). Analysis of the performance of this system shows that the plant capacity decreases about 1.8 percent, and the plant heat rate increases about 158 kJ/kWh (150 Btu/kWh) for each 38°C (100°F) drop in temperature.

The arrangement of the high-pressure fluidized bed boiler with low-temperature particulate removal is shown in Figure 6. The hot combustion products are passed through one stage of cyclone separation to recover the larger fraction of the char particles which are elutriated from the bed so that the carbon losses will be reduced to a minimum value. The effluent from the char separator will retain the finer ash particles with relatively low carbon content. This stream will be cooled to a temperature in the range of from 93 to 204°C (200 to 400°F), depending on the recuperator effectiveness and the temperature of the cold products of combustion out of the scrubber-cooler. In the scrubber-cooler the products are evaporatively cooled to the saturation line and then further cooled along the saturation line until the water vapor content of the gas mixture is equal to the initial value out of the fluidized bed boiler.

Performance calculations were made to determine the effects of air equivalence ratio, boiler outlet temperature, system pressure ratio, and recuperator effectiveness. The results of this parametric analysis were as follows:

- The plant heat rate increases about six percentage points for each ten percentage points decrease in recuperator effectiveness.
- Plant heat is a rather weak function of the pressure ratio, and the optimum pressure ratio is about 8.5:1.
- The plant heat rate varies only about one percent over the range of boiler outlet temperatures from 704 to 926°C (1300 to 1700°F).

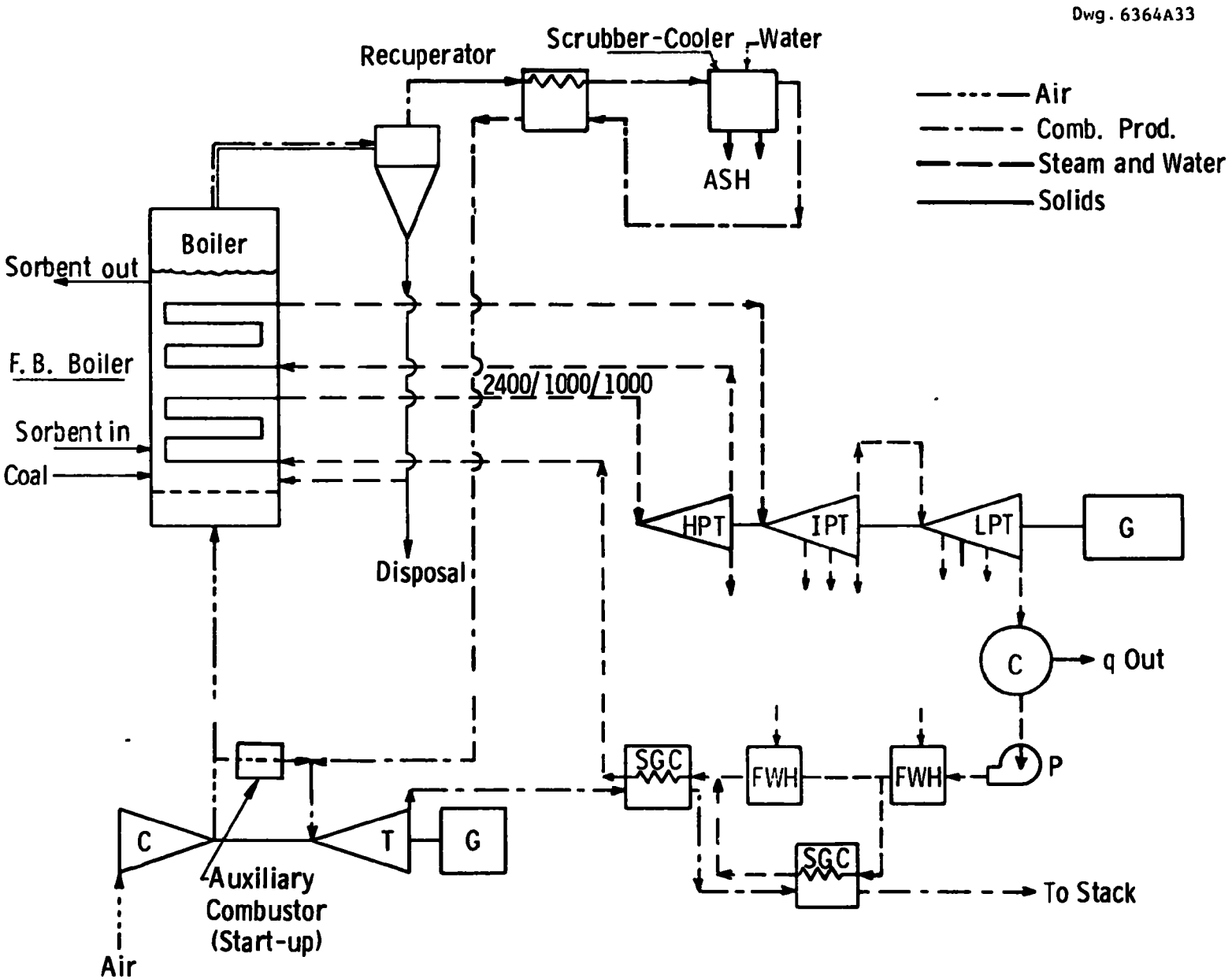

Figure 6—Pressurized fluidized bed combustion power plant with cold cleanup of combustion products

- Plant heat rate is a rather strong function of the air equivalence ratio, with the heat rate increasing as the air equivalance ratio increases.

Economics for the options considered for the PFBB include the use of hot pressurized electrostatic precipitators for gas cleanup ahead of the turbine, and heat exchange of the boiler off-gases down to water-scrubbing temperature prior to injection into the turbine. The results of these studies are presented in Appendix A and are reviewed in Section IV.

Gas Turbine Cycle with Indirect Air-Cooled Fluidized Bed Combustor

One variation of the adiabatic combustor concept is the utilization of the excess air required to maintain the bed temperature in air-cooled heat transfer surface in the bed. This open-cycle gas turbine with a pressurized fluidized bed combustor/air heater has been described by Harboe.[14] This permits part of the air (about 70%) from the compressor to by-pass the combustor gas flow, pass through the heat transfer surface immersed in the fluidized bed, where it approaches the bed temperature, and be mixed with the products of combustion after they have been cleaned of particulates. This alternative is less demanding of the particulate control system than the pressurized boiler and adiabatic combustor base designs. The cycle performance will be slightly lower than the adiabatic combustor system for a given bed temperature, since the excess air will only approach the bed temperature and result in a slightly lower gas-turbine inlet temperature. The capital cost, compared with the adiabatic combustor, will depend on a trade-off between an increase in the combustor cost due to the air-cooled heat transfer surface and a decrease in the particulate removal system cost due to reduced volumetric gas flow. The plant reliability may be increased if the particulate loading to the gas turbine can be significantly reduced over that achieved with the adiabatic combustor. This may result in a lower development risk.

Balance Pressure Reheater Cycle

Progress in the art of steam power generation depends on innovation as well as on an analysis and extension of existing concepts.

Westinghouse Research Laboratories has conceived a new, improved, combined cycle. This cycle is called "superreheat with vapor phase recuperation." As shown in Figure 7, this cycle consists of:

1. High subcritical or supercritical vapor generation in a boiler which has been fired with gas-turbine exhaust and fuel which need not be "clean"
2. Superheating the vapor to the 538°C (1000°F) range in an orthodox superheater
3. Turbine expansion to reheat pressure near the saturation line
4. Reheating in a steam-steam recuperator to the 538°C (1000°F) range
5. Reheat in "Balanced Pressure Superreheater" to 816°C (1500°F) or higher
6. Turbine expansion of steam from 816°C (1500°F) to First Law balance point
7. Expanded hot reheat steam recuperating Item 4 above to pinch point
8. Pinch point steam expanding to condenser.

This apparatus includes a reheat exchange and a high-pressure ratio gas turbine in "Velox" arrangement. The reheat exchanger is a carbon-steel, refractory-lined drum containing a radiant-convection steam reheat exchanger made of thin-walled, high-alloy tubes. Gas-side pressure is approximately equated to steam-side pressure. Clean fuel is fired to the drum and again at the drum exit. Reheated gas is expanded in the gas turbine. Gas-turbine exhaust is cooled against feed heating, steam generation, and (possibly) steam generation at cold reheat pressure. The gas turbine may beneficially consist of a free gas generator and a reheated power turbine.

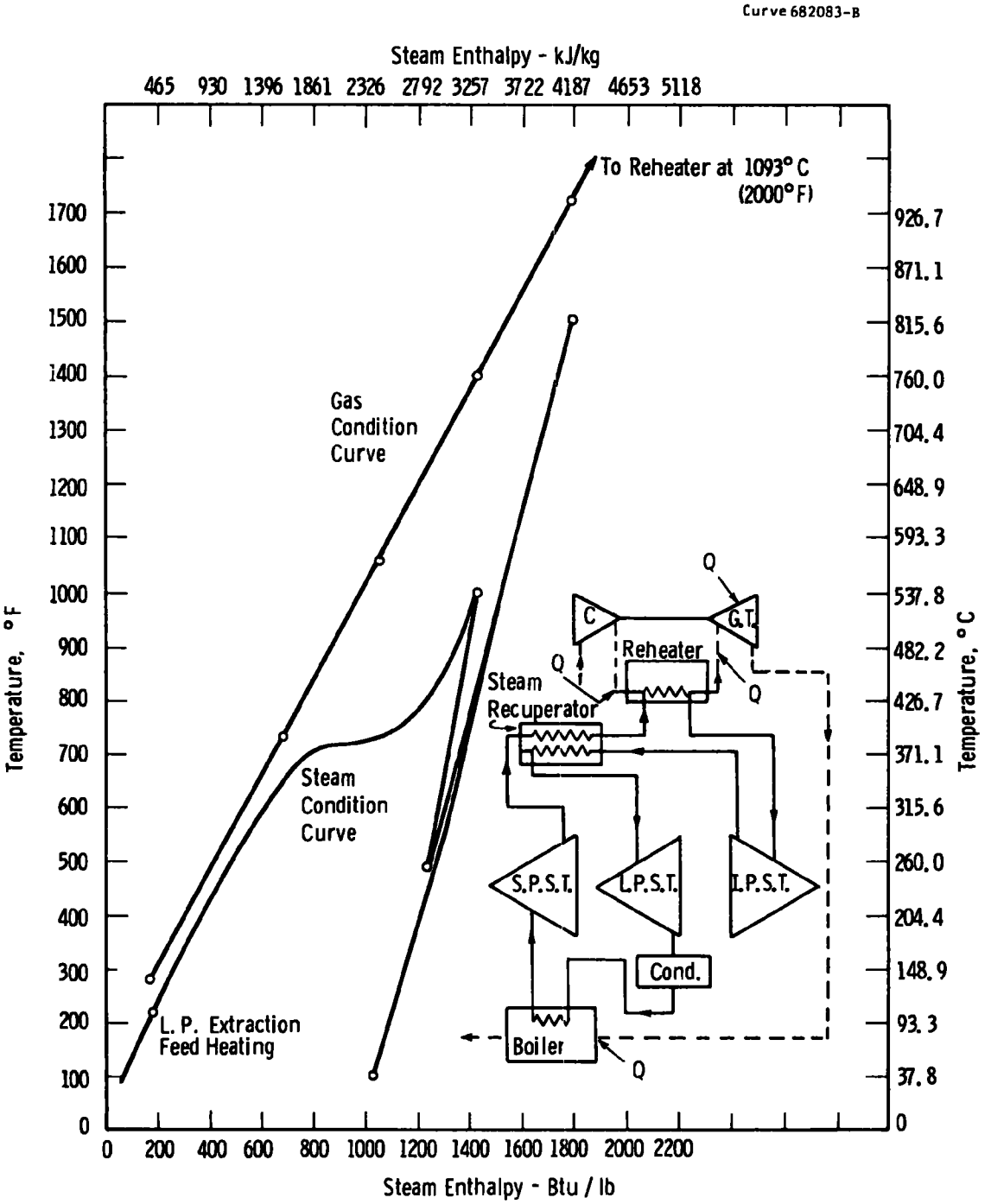

Figure 7 – Recuperative supercharged reheater cycle

The strategy of this unusual arrangement is to maximize the temperature of heat addition by means which do not require material breakthroughs in terms of cost, corrosion resistance, and stress-rupture properties. The superreheat turbine is at reasonable pressure for thermal stress minimization, and its steam path may be cooled with saturated (or near) cold reheat steam.

The main features are:

- Use of gas-turbine cycle compressed air to permit a very high-temperature, unstressed steam reheater
- Use of steam-steam recuperator to suppress the addition of low-temperature heat in the steam reheater
- Use of gas-turbine reject heat for feed heating to maximize the steam flow in the high-temperature reheater
- Optimization of gas-turbine compressor intercooler pressure to emphasize either (a) the minimum heat rate by raising the compressor outlet temperature or (b) the maximum gas-turbine net power by reducing the compressor work
- Minimization of steam extraction by maximizing the gas-turbine/boiler-exhaust feed heating. This step results in a power split which leans toward the gas-turbine shaft. Optionally, boiler exhaust heat may be used for additional steam generation at cold reheat pressure.

The cycle chosen for a rough test of these principles used 24,133 kPa/538°C/816°C (3500 psi/1000°F/1500°F) steam coupled to a 34/1 pressure ratio, 941°C (1725°F) reheated gas turbine. A unit heat rate of approximately 6858 kJ/kWh (6500 Btu/kWh) appears to be possible for gas firing. This relationship implies about 7913 kJ/kWh (7500 Btu/kWh).

The superreheat cycle with vapor-phase recuperation appears to be a good opportunity for application of high-pressure fluidized bed boiler technology to an advanced steam system.

Figure 8 shows the superreheat with vapor-phase recuperation cycle modified to operate with high-pressure fluidized bed combustion. There are two high-pressure fluidized bed combustors. The first generates and superheats steam at supercritical pressure and operates at an intermediate pressure level. The second fluidized bed combustor is used to reheat the steam up to a temperature of about 816°C (1500°F) with the boiler pressure level approximately equal to that of the reheat steam pressure. The bed temperatures and, consequently, the gas-turbine inlet temperatures would most likely be equal.

Liquid-Metal Topping Cycles with Fluidized Bed Combustion

Investigations of liquid-metal topping cycles coupled with pressurized fluidized bed fired heaters (see Figure 9) have been made by Oak Ridge National Laboratory[15] and by General Electric under joint NASA/OCR funding.[16] The conclusions of these studies were that overall plant efficiencies of 50 to 60 percent were attainable with this system.

A recent evaluation of this system made by Westinghouse under NASA Contract NAS 3-19404 concluded that maximum overall plant efficiency would be in the order of 48 percent and that the cost of energy would be about 20 percent greater than that for the pressurized fluidized bed boiler steam plant with 24,133 kPa/538°C/538°C (3500 psi/1000°F/1000°F) steam conditions.

Closed-Cycle Gas-Turbine Applications

Recently Westinghouse carried out an evaluation of closed cycle gas-turbine systems under NASA Contract NAS 3-19404 in which fluidized bed fired heaters were applied. Figure 10 shows a pressurized fired heater with fluidized bed combustion. When applied to the helium, closed-cycle, gas-turbine system with steam bottoming shown on Figure 11, the calculated plant heat rate is about 8750 and the estimated capital cost for a plant with construction starting in mid-1974 is about $635/kW. This gives an estimated energy cost which is approximately 33 percent greater than that for a pressurized fluidized

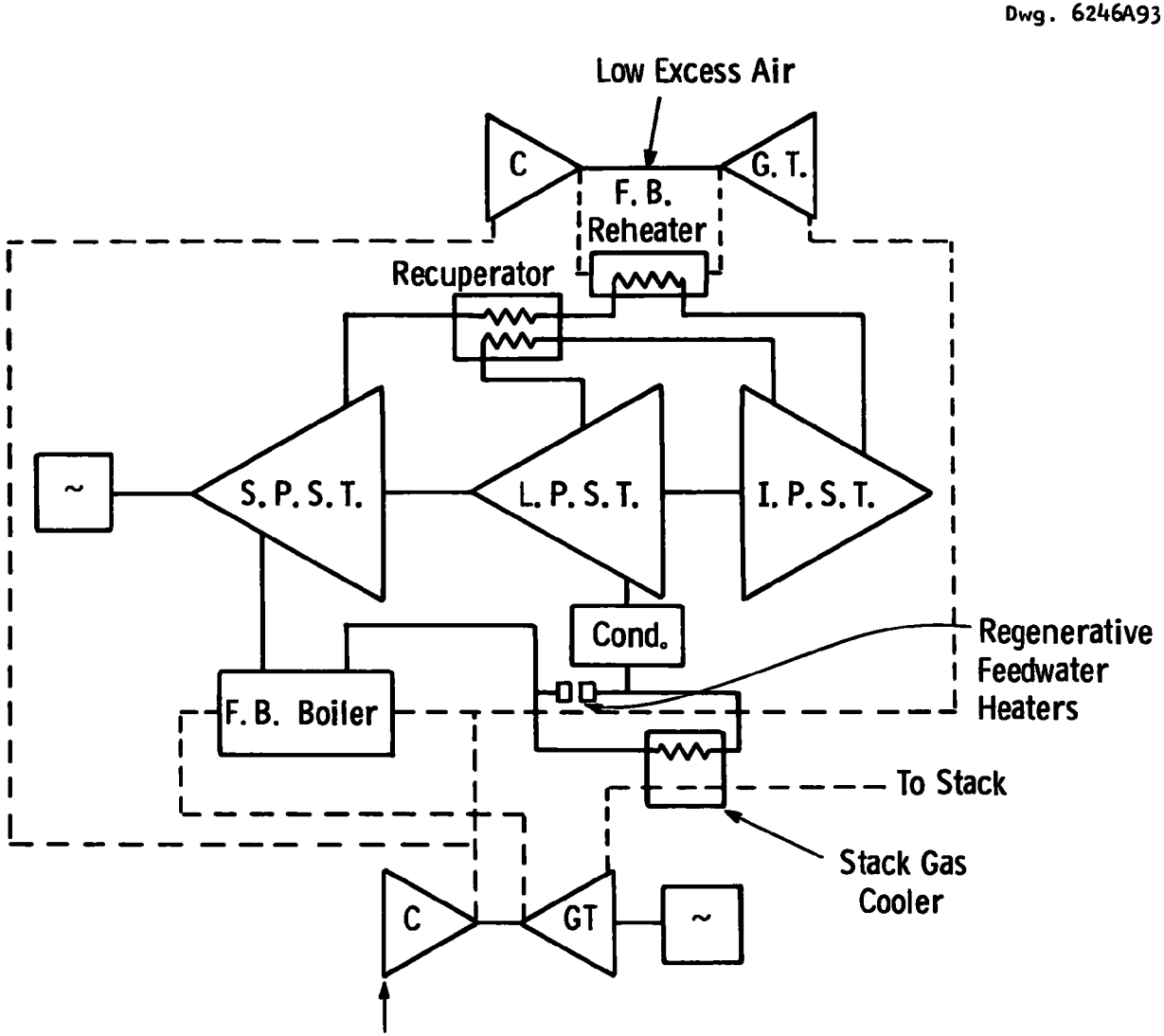

Figure 8 – Superreheat with vapor phase recuperative cycle with high pressure fluidized bed boilers added

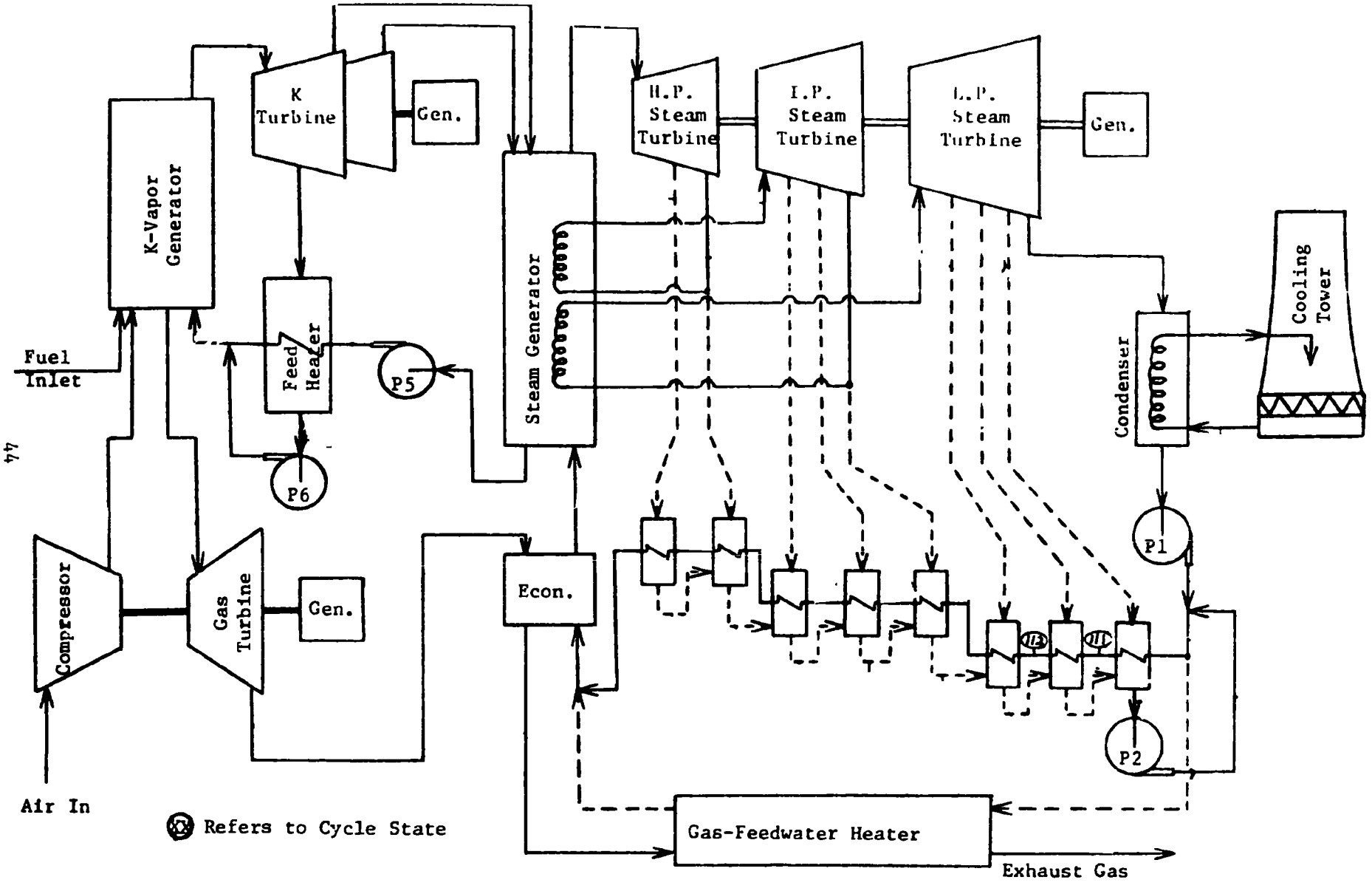

Figure 9 - Schematic for Pressurized Furnace Potassium Topping Cycle

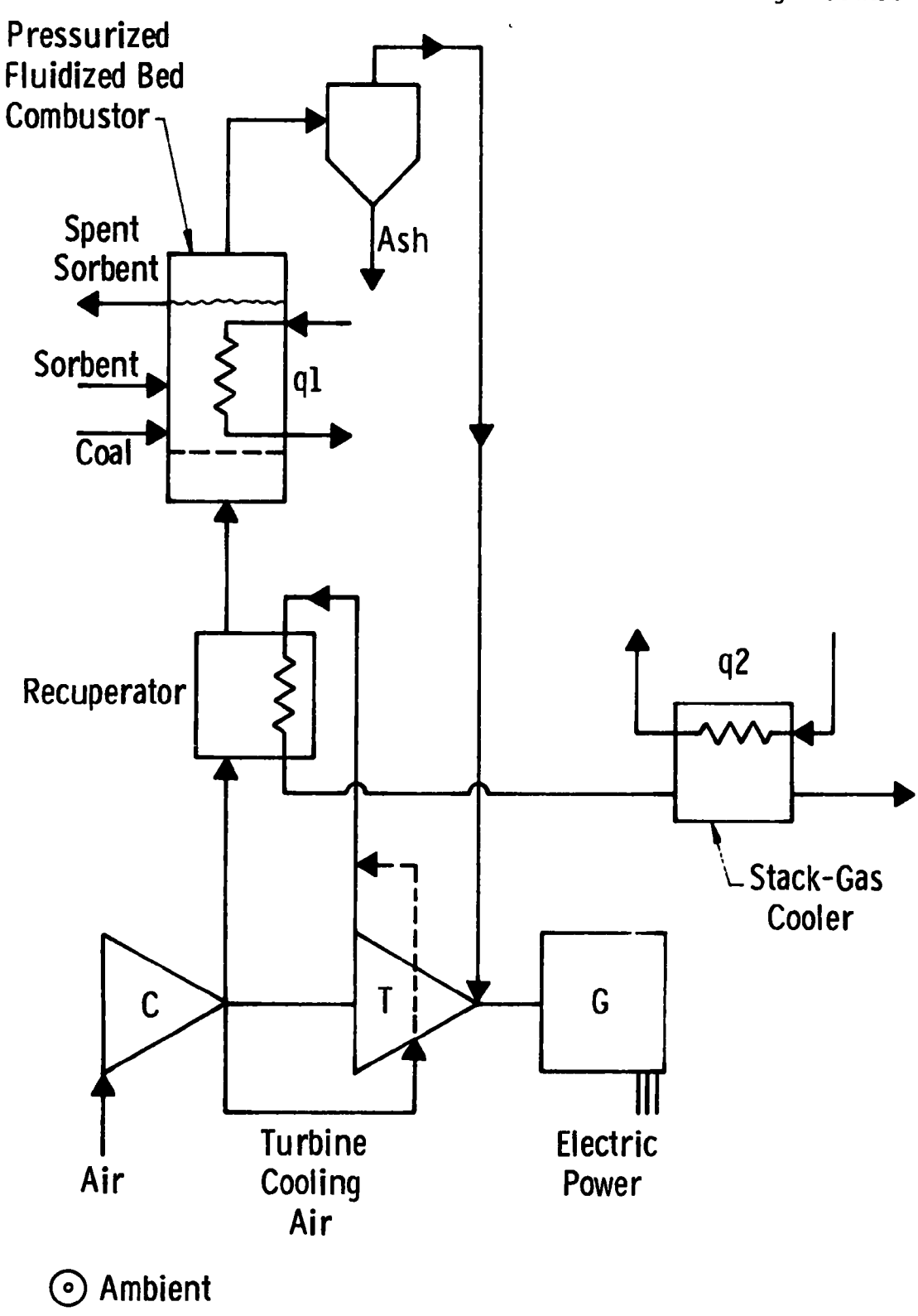

Figure 10 -Pressurized fired heater subsystem

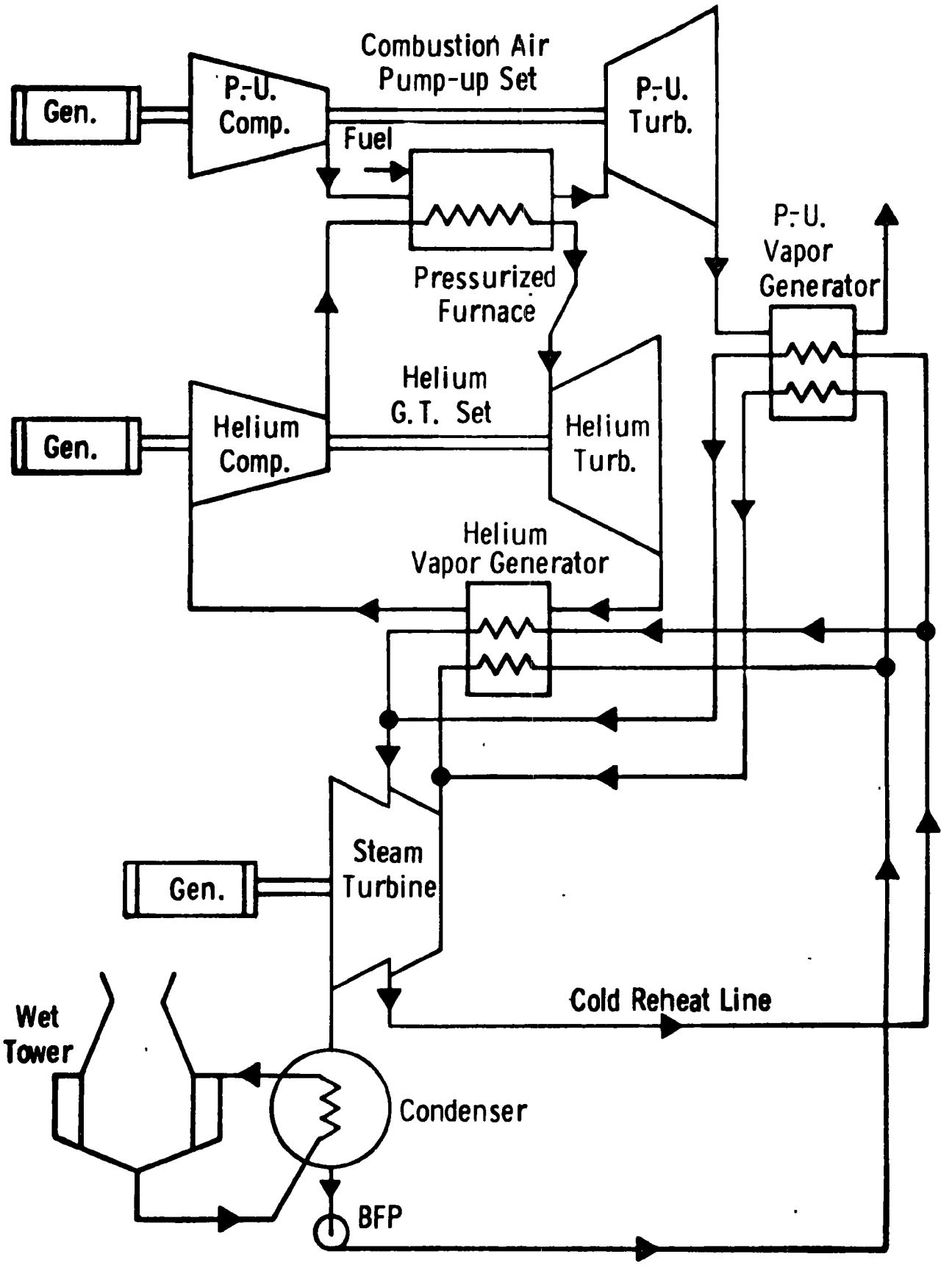

Figure 11 – Closed-cycle combined flow diagram

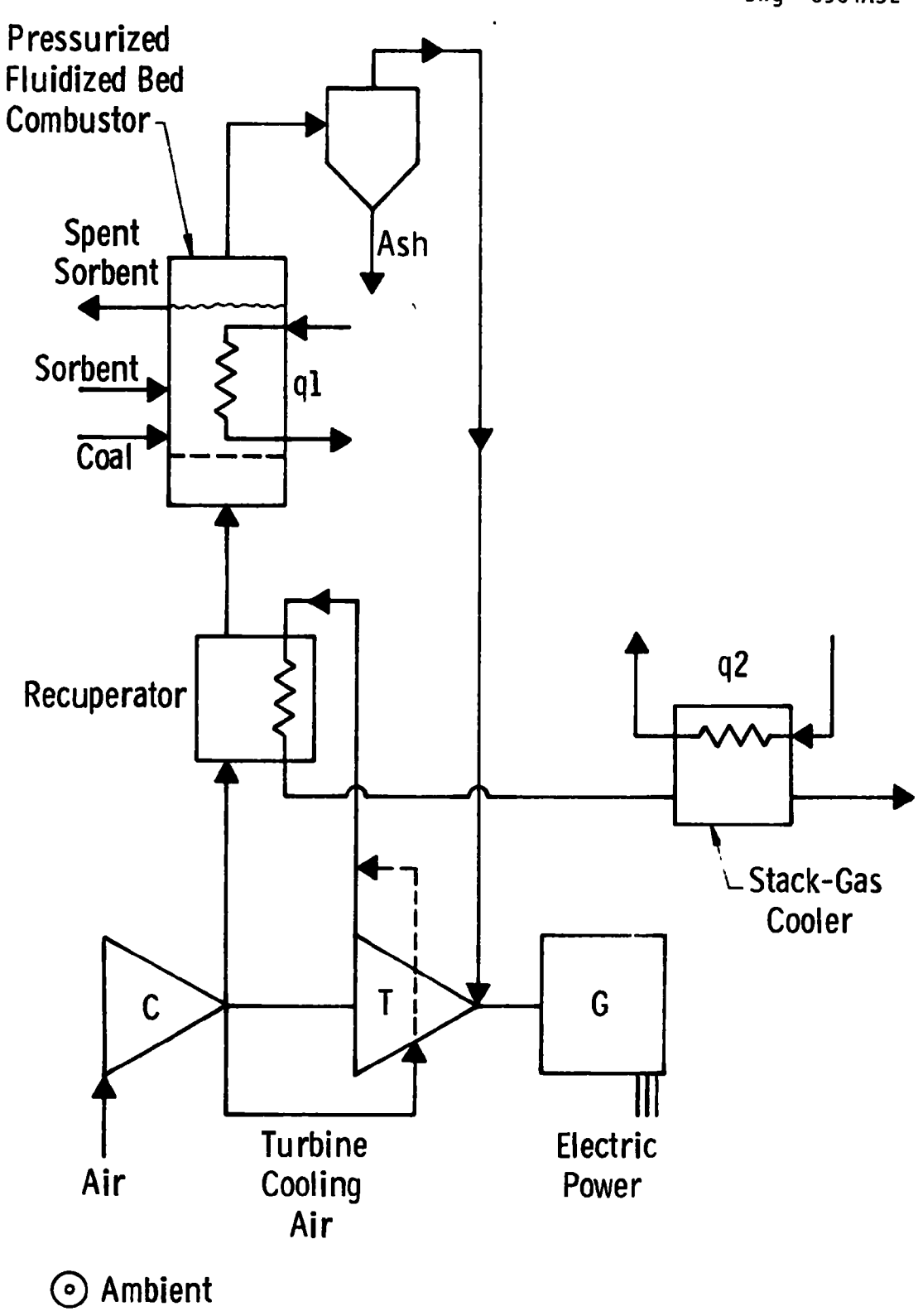

Figure 10 -Pressurized fired heater subsystem

Dwg. 6251A08

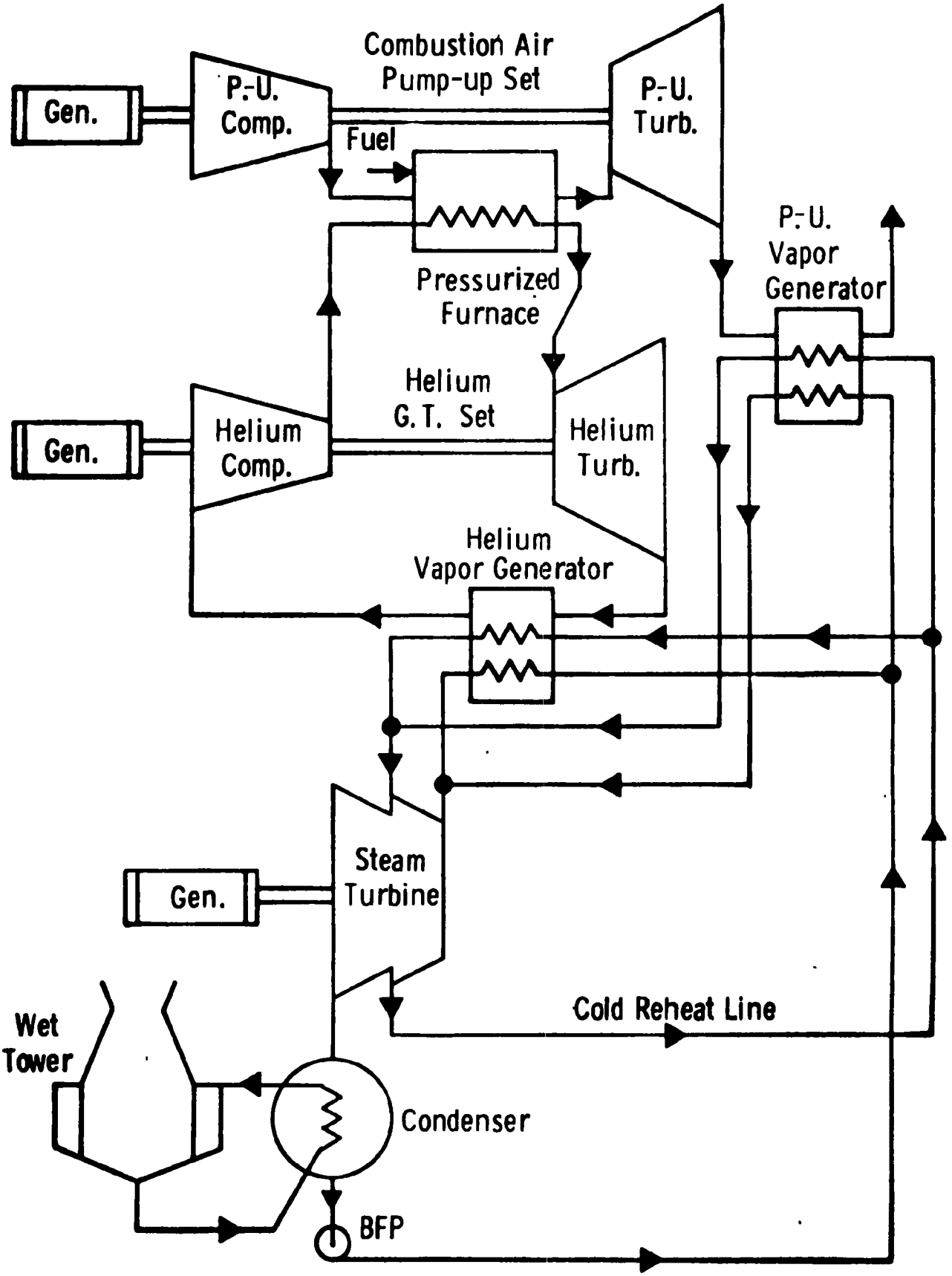

Figure 11 — Closed-cycle combined flow diagram

bed boiler with steam conditions of 24,133 kPa/538°C/538°C (3500 psi/1000°F/1000°F).

Technique for Increasing Turbine Inlet Temperature in High-Pressure Fluidized Bed Boilers

Turbine inlet temperatures for industrial and commercial gas turbines have historically increased about 14°C (25°F) per year over the past two decades. Current levels are 1038 to 1093°C (1900 to 2000°F) for intermediate load units and 1093 to 1149°C (2000 to 2100°F) for peaking units. These levels significantly exceed the value of 871 to 927°C (1600 to 1700°F) imposed on the gas turbine in the high-pressure fluidized bed boilers by the sulfur sorbent. The maximum allowable bed temperature for effective, in-bed desulfurization is thought to be in the range of 954 to 1010°C (1750 to 1850°F), and the turbine inlet temperature is estimated to be about 66°C (150°F) lower than the bed temperature.

Westinghouse has made cycle calculations to determine the effect of turbine temperature on the performance of the high-pressure fluidized bed boiler.[2] The results of these calculations indicate that the heat rate of this system improves about 0.5 percent for every 56°C (100°F) increase in turbine inlet temperature.

One possible technique for obtaining turbine inlet temperatures which exceed the limits imposed by in-bed desulfurization is shown in Figure 12. Here char which is elutriated from the primary beds is used as a feedstock for a gasifier. The fuel gas produced in the gasifier is burned in a separate combustor to give state-of-the-art gas-turbine inlet temperatures.

The separate gas-turbine combustor for burning the fuel gas from the gasifier would probably be a conventional, integrated type, which has a definite design and cost advantage over an external combustor, especially for high turbine inlet temperatures.

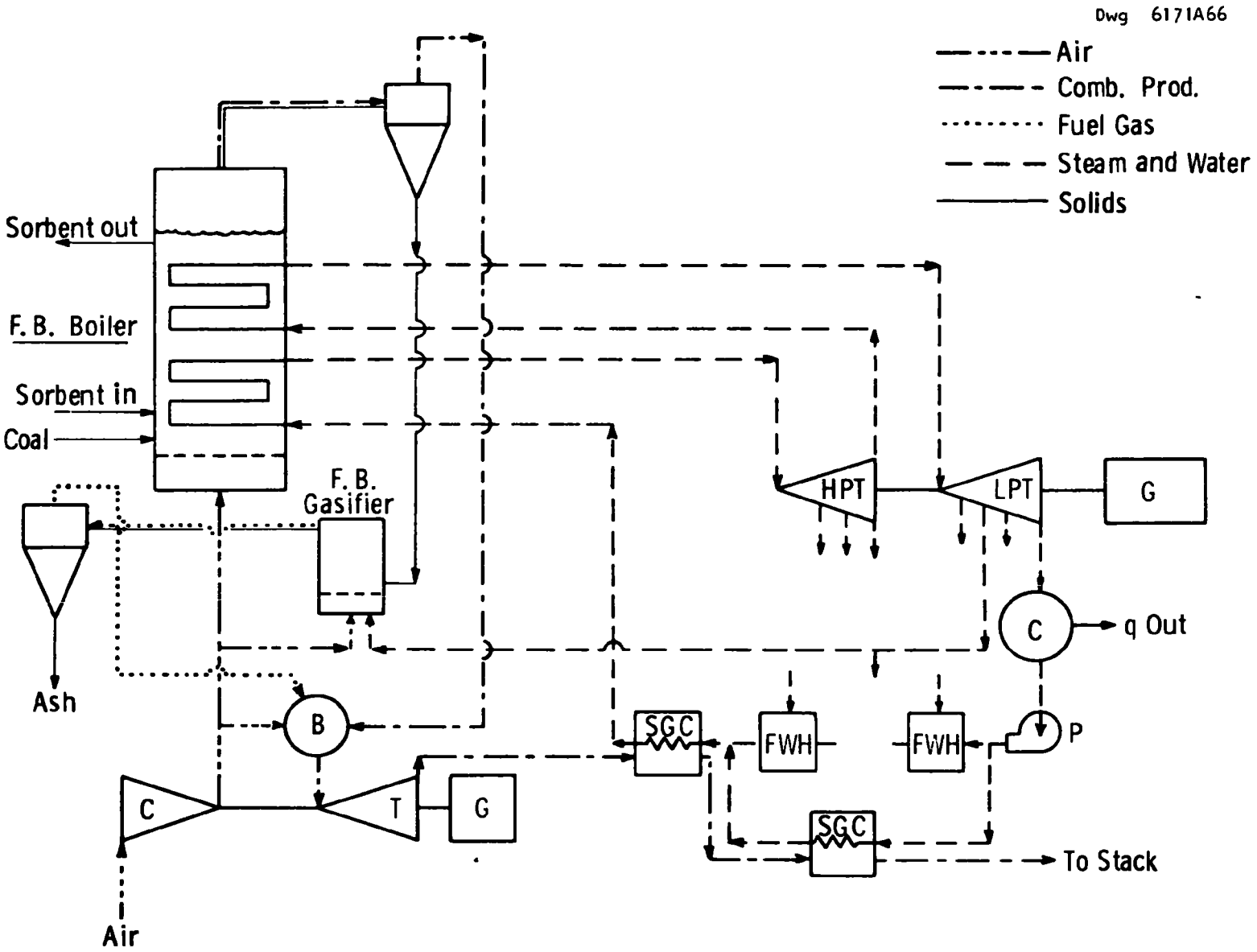

Figure 12– Pressurized Fluidized Bed Combustion Power Plant with Secondary C·

Modular Integrated Utility System

Oak Ridge National Laboratory (ORNL), under funding from the Departments of Housing and Urban Development and Interior, has made an evaluation of small coal-burning gas turbines with fluidized bed combustion.[17] This modular integrated utility system would use a small on-site utility plant located adjacent to a new housing development to provide electricity, hot water for building heating, domestic hot water, and chilled water for air conditioning. Solid waste from the housing complex would be used as a supplemental fuel in the energy system.

These fundamental gas-turbine cycle configurations were considered in this study:

- Direct-fired open cycle
- Exhaust-fired open cycle
- Indirect-fired closed cycle

An indirect-fired closed cycle with an air preheater was selected as the preferred system for this application because of its superior part-load performance. The distribution of input energy in the preferred system was 30 percent converted into electricity and 60 percent into steam at 120°C (250°F) and 202.6 kPa (2 atm) or hot water at 65°C (150°F). It was estimated that the overall installed cost of the coal-fired fluidized bed combustion system and gas turbine would be $350 to 400/kw(e) for production units.

FLUIDIZED BED COMBUSTOR

Atmospheric and pressurized fluidized bed combustion boilers and adiabatic fluidized bed combustors have been demonstrated on pilot-scale units. Atmospheric and pressurized fluidized bed combustor tests[3,7,9,18-27] have demonstrated control of sulfur dioxide, nitrogen oxide, and particulates; acceptable combustion efficiency; boiler tube materials; and coal-feed systems.

Economic studies[2,5] on operating and design parameters show that the uncertainties for successful application of the pressurized boiler are minimized, since cost and performance are essentially

invariant with the projected design basis. Back-up design and operating alternatives, however, have been specified in those problem areas which have been identified. An illustration of the problem areas, proposed solutions, and back-up alternatives has been presented. The proposed design for a pressurized fluidized bed combustion boiler may be conservative in some areas. If deep beds are practical, for example, the number of fluid bed units can be reduced; and the carbon burn-up cell, which is desirable in an atmospheric pressure system, may not be required with deep beds and high excess air.

Results from operating units can be used to construct first-generation prototype plants. In order to take advantage of the full potential of fluidized bed combustors, large-scale tests will also be required with advanced designs at advanced operating conditions, for example, deep bed [(4.57 to 9.14 m [15 to 30 ft)] and high velocity (> 3.04 m/sec [10 ft]) operation for pressurized combustors, heat transfer surface material, and configuration tests at advanced steam conditions [31,028 kPa, 649°C (4,500 psi, 1200°F)], advanced combustor designs (for example, circulating bed), and advanced control systems to achieve improved load-follow capabilities (circulating beds, use of excess air).

Assessment

The operational conditions and the design parameters used for the basic design[2,5] were evaluated on the basis of recent data available from the pressurized BCURA pilot-scale unit and the Exxon mini-plant (Appendix B). High combustion efficiencies were obtained with excess air from 10 to 17 percent. This may allow the carbon burn-up cell in the basic design to be eliminated and considerably simplify the operation and control of a pressurized fluid bed combustor. Operation with excess air up to 100 percent offers additional operating advantages and would assure high combustion efficiency. Based on the data available so far, the assumption of a bed-tube heat transfer coefficient of 284 W/m^2-°K (50 Btu/ft^2-hr-°F) in the basic design appeared to be reasonably conservative.

Long-term boiler tube wastages were estimated from the available experimental data. Weight loss usually reached a reliable, steady state after long duration. The steady-state weight loss was considerably lower than the initial weight-loss rate. The preliminary evaluation with the available data indicated that conventional boiler tube materials could be used in the fluidized bed boiler application if the long-duration runs showed that the rate of weight loss did, indeed, level off with an increase in operation time. Higher alloy materials can be used with minimum cost penalty (a cost increase of less than one percent of the total plant cost). A final assessment can be carried out only after more data are accumulated at higher fluidized velocity, higher operating pressure, high temperature, and longer duration. The effect of adding limestone and of burning different coals with different impurities, especially the high-sulfur coals, should also be studied.

Conflicting observations have been made with regard to temperature distribution in a deep pressurized coal combustor. The difference was due to the operating conditions and the design parameters. From the existing evidence it was clear that a reasonably uniform temperature profile could be obtained in a pressurized fluidized bed combustor if the operating conditions and the design parameters were properly set. More data from large combustors operating at high pressure, high temperature, high velocity, and large bed height are required to verify the basic design conditions. These appear still reasonable on the basis of available data.

No particular difficulty was experienced in multiple feeding of coal. Since in a commercial unit coal will be fed at more points and at higher rates, more experience in these respects is required. No general operational problems were encountered. No data, however, are yet available on controllability of a pressurized fluidized bed boiler. The response of the boiler to load-follow and the turndown capability are important in plant operation and cannot be effectively studied in smaller combustors.

SULFUR REMOVAL SYSTEM

The sulfur removal system in fluidized bed combustion is based on the principle that a solid sorbent can trap the fuel sulfur in solid form as the coal is burned and prevent its release to the environment as gaseous sulfur dioxide (SO_2). Thermodynamic analysis shows which solids will react with sulfur dioxide under process conditions and, therefore, defines those sorbents which must be considered for use. The calcium-based sulfur removal process has been developed more extensively than have those using alternative sorbents. Experimental work to date has used limestone or dolomite sorbents as sources of calcium carbonate ($CaCO_3$) or calcium oxide (CaO) in the processes outlined in Figure 13. Primary consideration has been given to optimizing operation of the fuel processing/sulfur removal system module.

More than 90 percent of sulfur dioxide emissions can be prevented and the fuel sulfur captured in a dry solid using limestone or dolomite as sorbents. The environmental standard of 0.54 kg (1.2 lb) sulfur dioxide/1.055 GJ (10^6 Btu) can be readily obtained. Maintenance of this standard of sulfur dioxide pollution abatement for the combustor operating conditions, while minimizing solid waste accumulation, has required excess sorbent or calcium/sulfur molar feed ratios of about 2/1 for dolomite and 3/1 for limestone.

The TG analysis studies reported here and in previous reports may be used to project the calcium/sulfur feed ratios necessary for adequate desulfurization. The projections are summarized in Table 6. The reduction of these ratios is a major goal in the development of the fluidized bed combustion system.

The primary objectives of experimental programs carried out thus far have been to determine sulfur dioxide removal capability with calcium-based sorbents and to investigate the effect of operating conditions and choice of sorbent on sulfur removal. To a limited extent models have been proposed to represent the available data.

The most important results established, which include those performed in parallel with those reported here, related to the effects

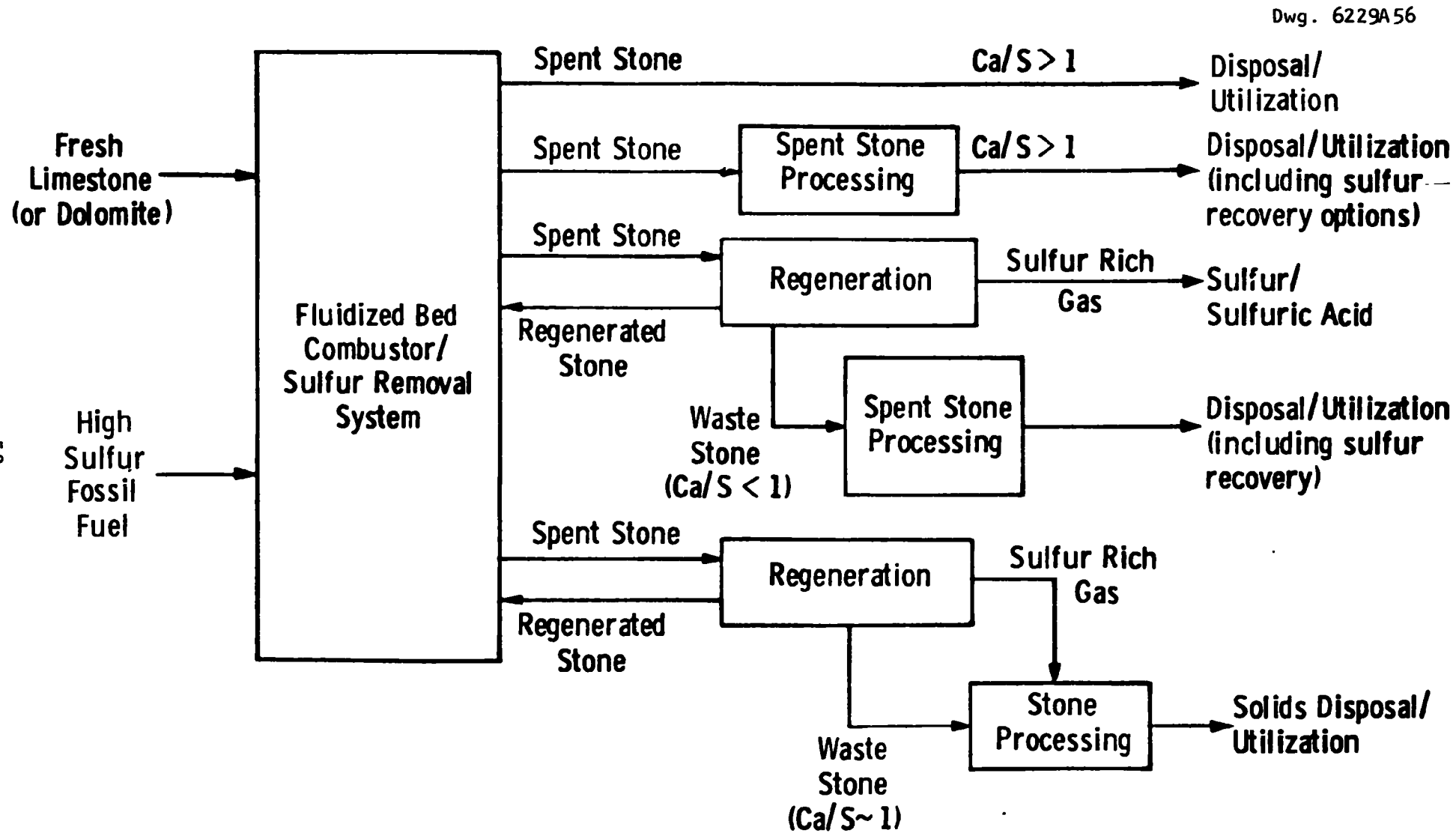

Figure 13–Sulfur removal system process concepts

Table 6

PROJECTIONS OF THE CALCIUM TO SULFUR FEED RATIOS[a]

Sorbent	Pressure, 101.3 kPa (atm)		Pressurized, 1013 kPa (10 atm)	
	816°C (1500°F)	954°C (1750°F)	816°C (1500°F)	954°C (1750°F)
Limestone				
Uncalcined	---	---	---	---
Calcined	2.8/1	>5/1	2.2/1	2/1
Dolomite				
Half-calcined	---	---	1.6/1	1.6/1
Calcined	2.2/1	∿4/1	1.2/1	1.2/1

[a]Mean particle size of 500 μm,
Gas residence time = 1 second
>80% sulfur removal efficiency.

of calcium/sulfur molar feed ratio, pressure, temperature, and gas velocity on sulfur removal. The data have been reviewed previously.[1]

The calcium/sulfur feed ratio at atmospheric pressure, which achieved over 90 percent sulfur dioxide removal, was found by several groups of investigators to be 2.5/1 for dolomite, and about 3/1 for limestone.[28,29] At temperatures above 843°C (1550°F), however, sulfur removal efficiency was drastically reduced.[30] Reduction of the sorbent particle size from 600 μm to 40 μm did not improve desulfurization efficiency or calcium utilization,[28] largely because of reduced stone residence times. Fines recycling, however, made an important contribution in improving desulfurization efficiency.[9] The effect of gas velocity was to reduce desulfurization efficiency drastically where desulfurization efficiency was already low; but when desulfurization efficiency was high, doubling the gas velocity had a minor effect in reducing the fraction of sulfur dioxide captured in the fluidized bed.[1]

The initial results on pressure at 506.5 kPa (5 atm) showed that limestone was marginally less efficient in desulfurization than at atmospheric pressure.[9] (This effect has been confirmed; it is in agreement with projections from TG data). Later fluidized bed results with dolomite showed that TG analysis results demonstrating high calcium utilization (90 percent) were reflected in calcium sulfur molar feed ratios of 1/1 at high desulfurization efficiency.[31] The decline in desulfurizing performance noted at atmospheric pressure above 843°C (1550°F) was not noted at 1013 kPa (10 atm) pressure, and excellent sulfur removal performance was noted up to 954°C (1750°F).[31,8]

Laboratory studies in support of the sulfur removal system development were carried out under this contract in three areas:

- Development of techniques for lowering the calcium/sulfur molar ratio required for desulfurization, thereby reducing sorbent requirements and spent sorbent disposal problems (Appendix D).
- Development of a model to predict quantitatively the sulfur removal in a fluidized bed combustor, (Appendix E), and

- Development of sorbent selection criteria (Appendices C and E).[32]

In addition, work has continued on the low-temperature regeneration step of converting calcium sulfide to calcium carbonate under contract to Energy Research and Development Administration (ERDA). A brief summary of this work as it pertains to fluidized bed combustion is given below.

Sulfur Removal

Experimental work to develop an understanding of the processes which limit the calcium/sulfur molar ratio has continued, using the thermogravimetric apparatus described previously[1,2] over a range of temperatures, 750 to 950°C (1382 to 1742°F); pressure, 101.3 to 1013 kPa (1 to 10 atm); stone particle sizes (2,000 to 500 μm diameter); stone sorbents (limestone, dolomite, alumina-based copper oxide); and calcination conditions (half-calcined dolomites, limestone and dolomite calcined in atmospheres containing variable partial pressures of carbon dioxide). The thermogravimetric data suitably interpreted provide a record of the extent of sulfation which can be achieved and the rate of reaction as a function of sulfur loading on the stone.

The conditions under which the calcium-based sorbent has been calcined was shown to be a critical factor in establishing the calcium oxide utilization in subsequent sulfation of the stone, both at 101.3 (atmospheric pressure) and at 1013 kPa (10 atm), as shown in Figure 14.[33] The change from rapid to slow reaction can occur at 5 percent or 30 percent utilization of the calcium in the stone. For dolomite, calcination under a relatively high partial pressure of carbon dioxide (60 percent of the equilibrium partial pressure over calcium carbonate/calcium oxide) increases the utilization achievable in fast sulfation from ∿40 percent of the calcium reacted to 90 percent reacted. This effect is independent of total system pressure. The importance of this finding is evident when the desulfurization process takes place in a pressurized fluidized bed combustor where the carbon dioxide partial

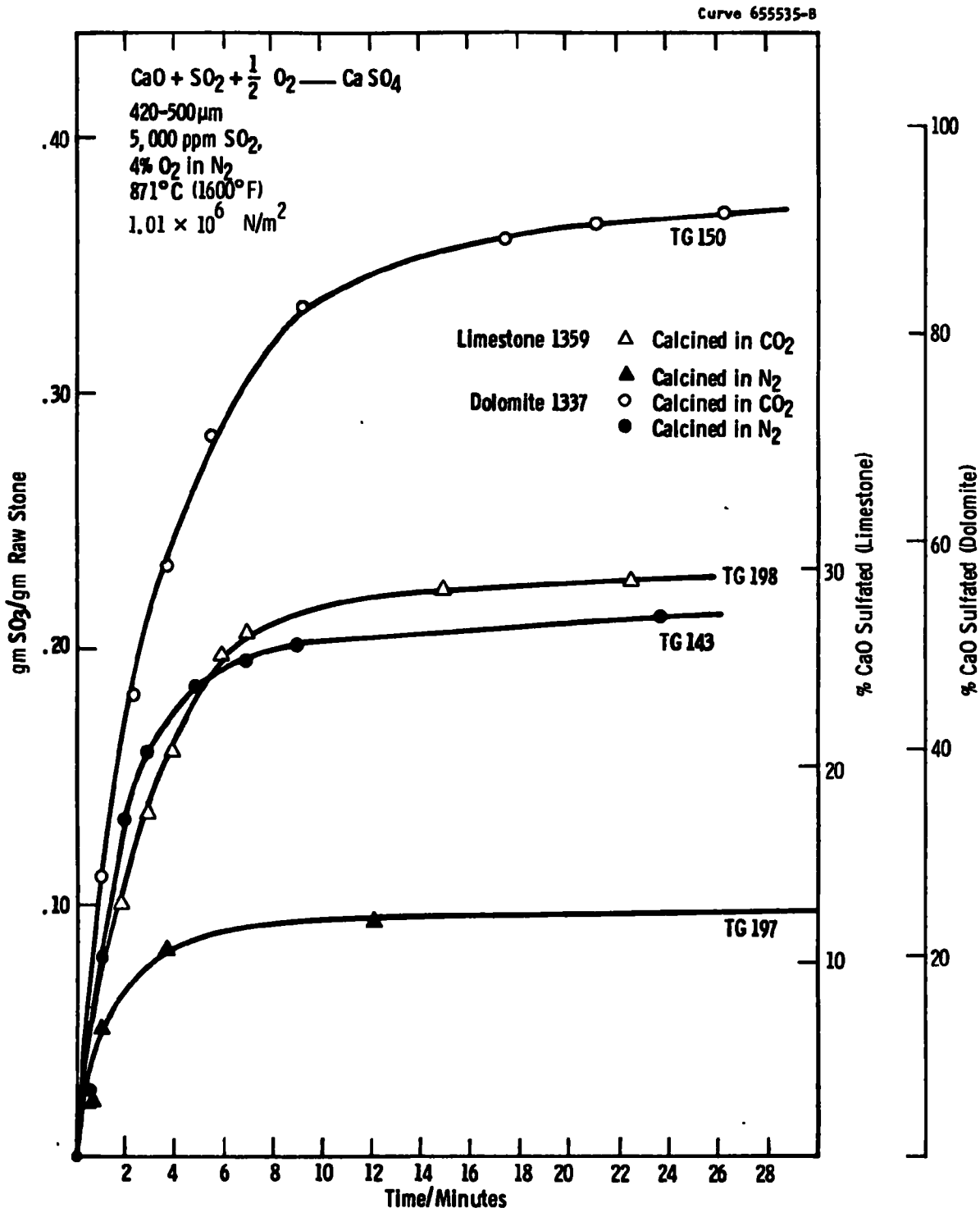

Figure 14 4–Comparison of pressurized sulfation of limestone and dolomite

pressure may rise to 152 kPa (1.5 atm) at the freeboard as a result of fuel combustion. This creates the correct conditions for forming a calcined dolomite which may be 90 percent sulfated at a fast rate of reaction. This, in turn, should result in excellent sulfur removal at calcium/sulfur molar ratios close to 1.2 to 1.0 - performance which has been demonstrated by Argonne National Laboratories (ANL) in their pressurized fluidized bed combustor.[31] Additional evidence for the impact of calcination is presented in Appendix D.

In combination with the effect of temperature on the sulfation, the effect of prior calcination conditions was shown to reproduce the maximum in calcium utilization at 843°C (1550°F) at atmospheric pressure which has been noted in fluidized bed combustion, as shown in Figure 15. At 1013 kPa (10 atm) the results were not as clean, but it was shown that high calcium utilization (35 percent sulfated) in limestone can be attained at 950°C (1742°F) and 1013 kPa (10 atm) pressure. This extends the upper limit for desulfurization with calcium oxide from limestone at pressures to temperatures above the atmospheric pressure limit of 850°C (1560°F). (It had previously been demonstrated that Tymochtee dolomite remained active at temperatures up to 1010°C [1850°F]).[2]

For conditions under which calcium carbonate is the stable form of the unsulfated sorbent, it was confirmed that limestone 1359 cannot be directly sulfated and that no activation of the sorbent by calcination and recarbonation occurs. As previously noted, however, half-calcined dolomite is an excellent sulfur dioxide sorbent in general (dolomite 1337, Tymochtee dolomite, Salamonie dolomite); a half-calcined mountain dolomite (large grains) (Canaan dolomite), however, did not show kinetic activity in sulfation and, like limestone, it could not be activated by calcination and recarbonation. Previous results were extended to show that over 50 percent sulfation by large particles (2,000 μm) of half-calcined dolomite could be attained. Half-calcined dolomite should be utilized at calcium/sulfur molar ratios intermediate between those for activated calcined dolomite (1/1) and normally calcined dolomite (2.5/1).

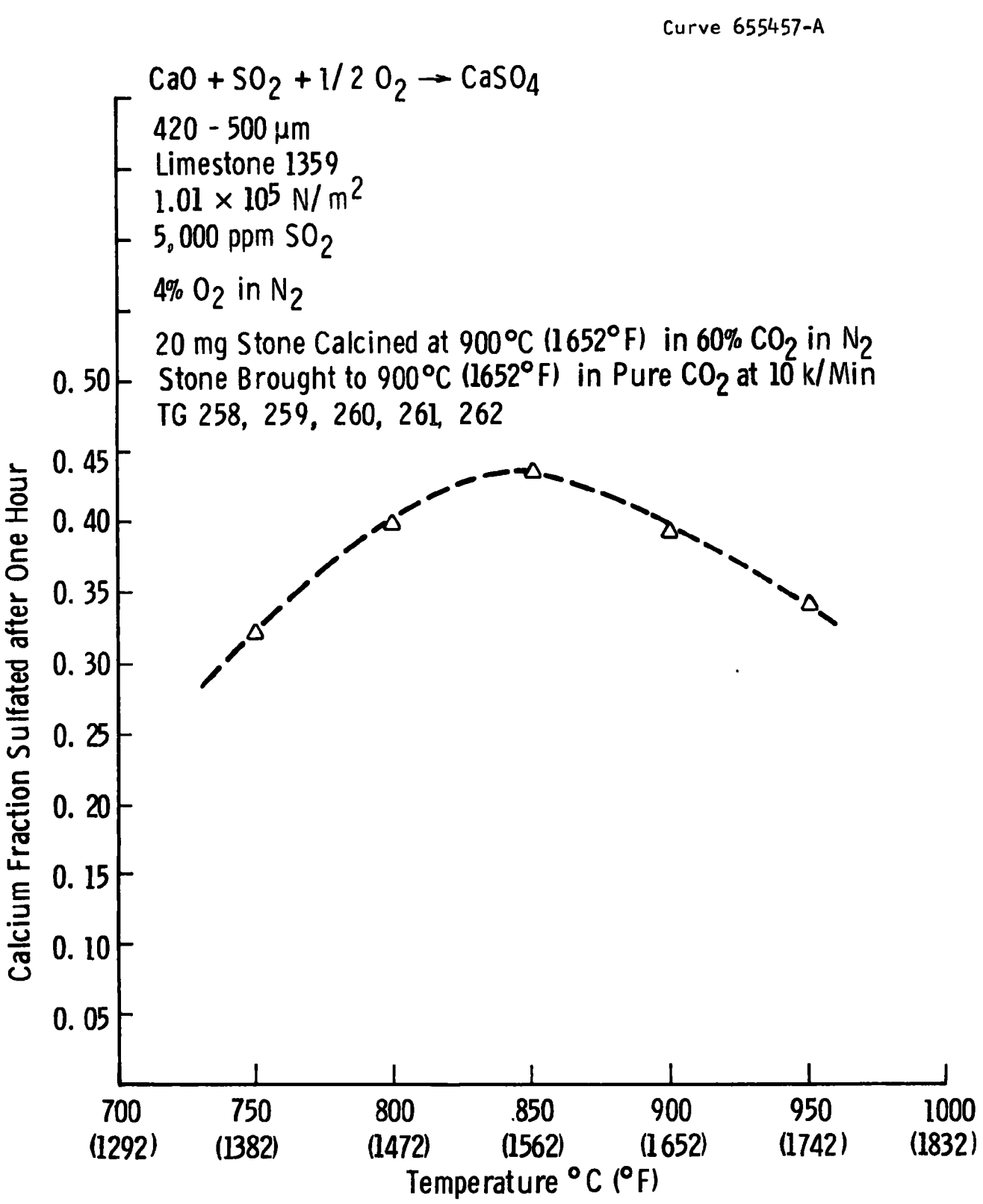

Figure 15 -The effect of temperature on CaO utilization in sulfation

Process Modeling

In order to apply thermogravimetric data to the prediction of sorbent performance in fluidized bed combustion, a first-order model of the desulfurization process was developed. In the model described in Appendix E_1, it is assumed that sulfur dioxide is liberated from coal uniformly throughout the bed and the fraction of sulfur dioxide available for capture in each element of bed height is calculated. The fraction of sulfur dioxide captured is then computed for a mean first-order reaction rate between sulfur dioxide and lime in the bed. The result is plotted in the form of mean reaction rate as a function of calcium/sulfur molar ratio fed to the bed, or calcium utilization of the stone. Experimental thermogravimetric data on the rate of reaction as a function of calcium utilization intersects this curve to produce a steady-state value for the calcium utilization and, hence, the degree of sulfur dioxide removal. If a functional relationship (empirical or theoretical) describes the rate of reaction as a function of calcium utilization, then the sulfur retention can be solved directly at a given calcium/sulfur molar feed ratio, calcium density, and gas residence time in the combustor. Agreement between the predictions of the model using Westinghouse thermogravimetric data and experimental data from fluidized bed combustors was excellent.

In addition to overcoming anomalies resulting from previous modeling studies, the modeling results correctly showed:

- The maximum temperature for sulfur dioxide removal at atmospheric pressure
- The variation in sulfur dioxide removal with calcium/sulfur molar ratio in the feedstock, as shown in Figure 16
- The effects of superficial gas velocity on sulfur dioxide retention at two different calcium/sulfur molar ratios.

The model can be used to specify the rate of reaction required in a given fluidized bed combustor design to achieve a desulfurization

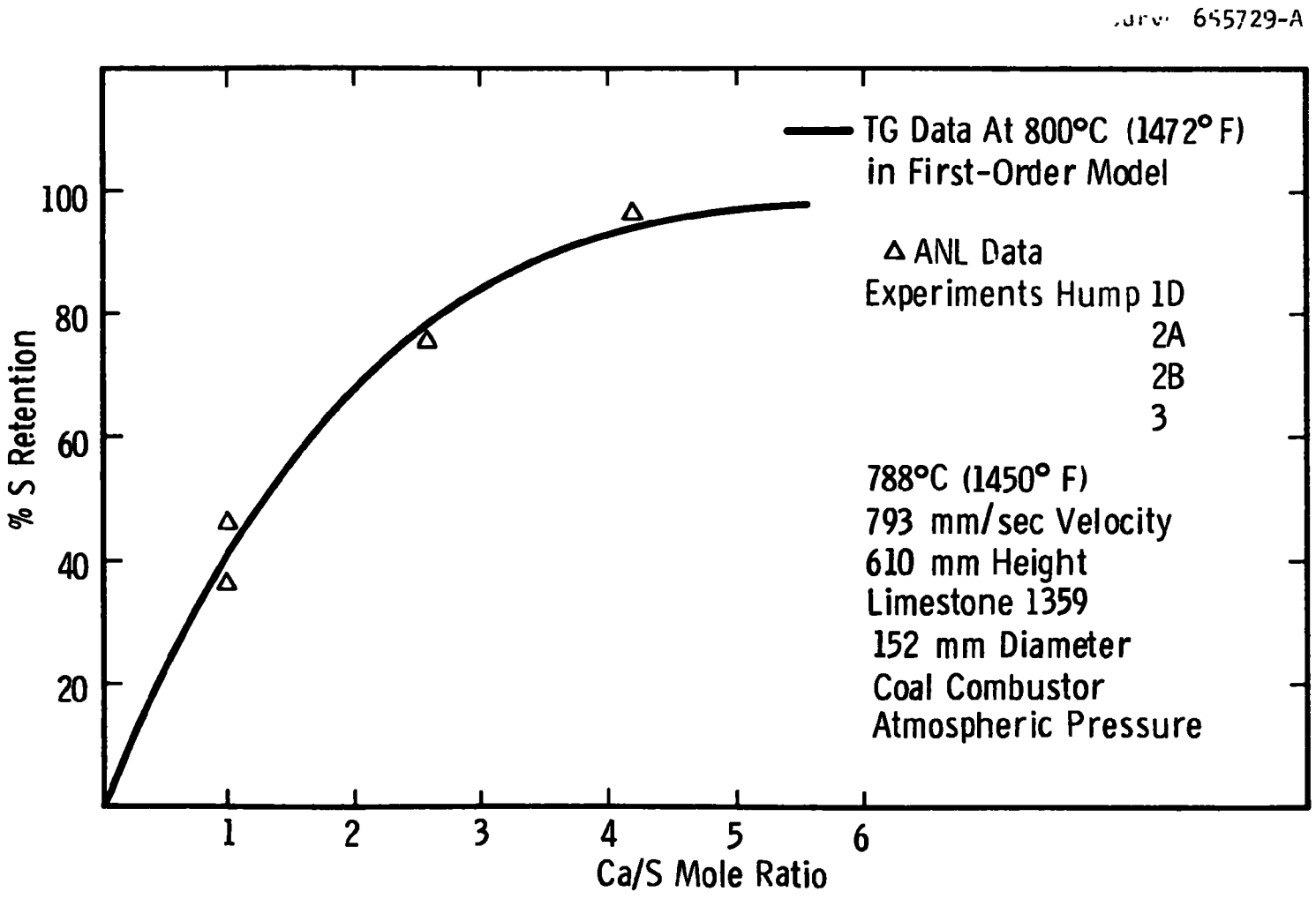

Figure 16—The effect of Ca/S mole ratio on sulfur retention

target. The thermogravimetric apparatus may then be used, under the appropriate conditions (with particular emphasis on carbon dioxide pressure), to establish the stone utilization at which the sulfation rate falls below that specified by the model. The required operating conditions of calcium/sulfur feed rate is thus established for the particular sorbent.

Further investigation of the use of limestones and dolomites for fluidized bed desulfurization can be carried out within the framework of the model developed. The use of thermogravimetric experiments coupled with application of the model should be extended beyond the range of sorbents so far tested (one limestone, four dolomites). The selection criteria for reaction rate at a given utilization should be most useful in comparative evaluations of different sorbents available at a particular plant location.

Additional work should be carried out on the extension of the temperature interval for desulfurization above 950°C (1742°F) at 1013 kPa (10 atm) pressure. Results previously published showed that sulfation of Tymochtee dolomite at pressure is rapid up to temperatures of 1010°C (1850°F) (depending on the calcium/sulfur feed ratio required).

Sorbent Regeneration

Regeneration of the sulfur sorbent is a potentially attractive option for fluidized bed combustion systems because it will:

- Reduce the sorbent requirements
- Reduce the spent sorbent to be handled by a disposal system
- Recover the fuel sulfur
- Perhaps reduce the contribution to trace-element emission from the sulfur-removal system (while this might be an important advantage of regeneration over once-through systems, it is only a postulate at this time).

The disadvantages of regeneration arise from:

- The increased plant costs of the regeneration system
- The energy penalty associated with reduction of the stable compound calcium sulfate
- The additional complexity introduced into plant operations.

The increased costs of regenerative as opposed to once-through systems have been evaluated,[2] and an overall economic assessment is presented in Section IV. For high-temperature reduction of calcium sulfate, the one-step regenerative process energy costs were approximately 13 percent higher than those for the once-through system. The optimum case for once-through sulfur removal considered by Newby[2] (Ca/S = 1.2), which was based on projections from TG data, is now reasonably established by fluidized bed combustion experiments. The status of calcium/sulfur feed ratio for the regenerative system, however, remains at 1/1:[34] the advantages of using a regenerative system in this instance are extremely dubious.

For the two-step regenerative process, in which calcium sulfate is first reduced to calcium sulfide and then reacted with steam and carbon dioxide, according to the equation:

$$CaS + H_2O + CO_2 \rightarrow CaCO_3 + H_2S \ ,$$

energy cost was found to be similar to that of one-step, high-temperature regeneration; and the capital investment, assuming a constant load design, was also similar.

In this case there is experimental evidence that the calcium/sulfur makeup ratio assumed (1/1) can be lowered. Laboratory work at Westinghouse[35] has shown that the reaction cycle

$$CaCO_3 + H_2S \rightleftarrows CaS + H_2O + CO_2$$

can be continued for thirty cycles. For a dolomite which is fully sulfided after each regeneration, the extent of regeneration decreases after each cycle, as shown in Figure 17. These results agree with those reported by Conoco Coal Development Co.[36] for the decline in regenerability of calcium sulfide. If similar results can be obtained for the two-stage process in which the calcium sulfide is produced by direct reduction of calcium sulfate, then the calcium/sulfur makeup rate would fall to 1/3 for the 20 percent sulfur differential between combustor and regenerator taken as the base case.

Thermogravimetric experiments to probe the decline in regenerability of calcium sulfide on repeated cycling have been continued.[37] In these experiments dolomites from a five-state area - Ohio, Indiana, Illinois, Kentucky, and Michigan - have been tested. None of the stones tested gave more efficient regeneration than did the dolomite 1337 shown. Variation in the partial pressure of steam and carbon dioxide in the regeneration case altered the initial rates of regeneration but not the cut-off value at which regeneration virtually ceases.

A structural study of the formation of crystallites of sulfide and carbonate in regenerated and sulfided dolomite is continuing. To date, none of the results indicate the mechanism of deactivation. The sole means of achieving complete conversion of calcium sulfide to calcium carbonate is to raise the temperature of the regeneration reaction; at 870°C (1600°F) it was found that total regeneration is possible. The equilibrium concentration of recovered hydrogen sulfide, however, decreases rapidly with increasing temperatures. Temperatures close to 650°C (1200°F) must be maintained if hydrogen sulfide yields more than 3 percent are to be expected. Since detailed economic studies of this regeneration scheme are being prepared, the potential for improving the overall economics by adjusting reaction kinetics should become clear, and further experimental work can be focused on the sensitive areas.

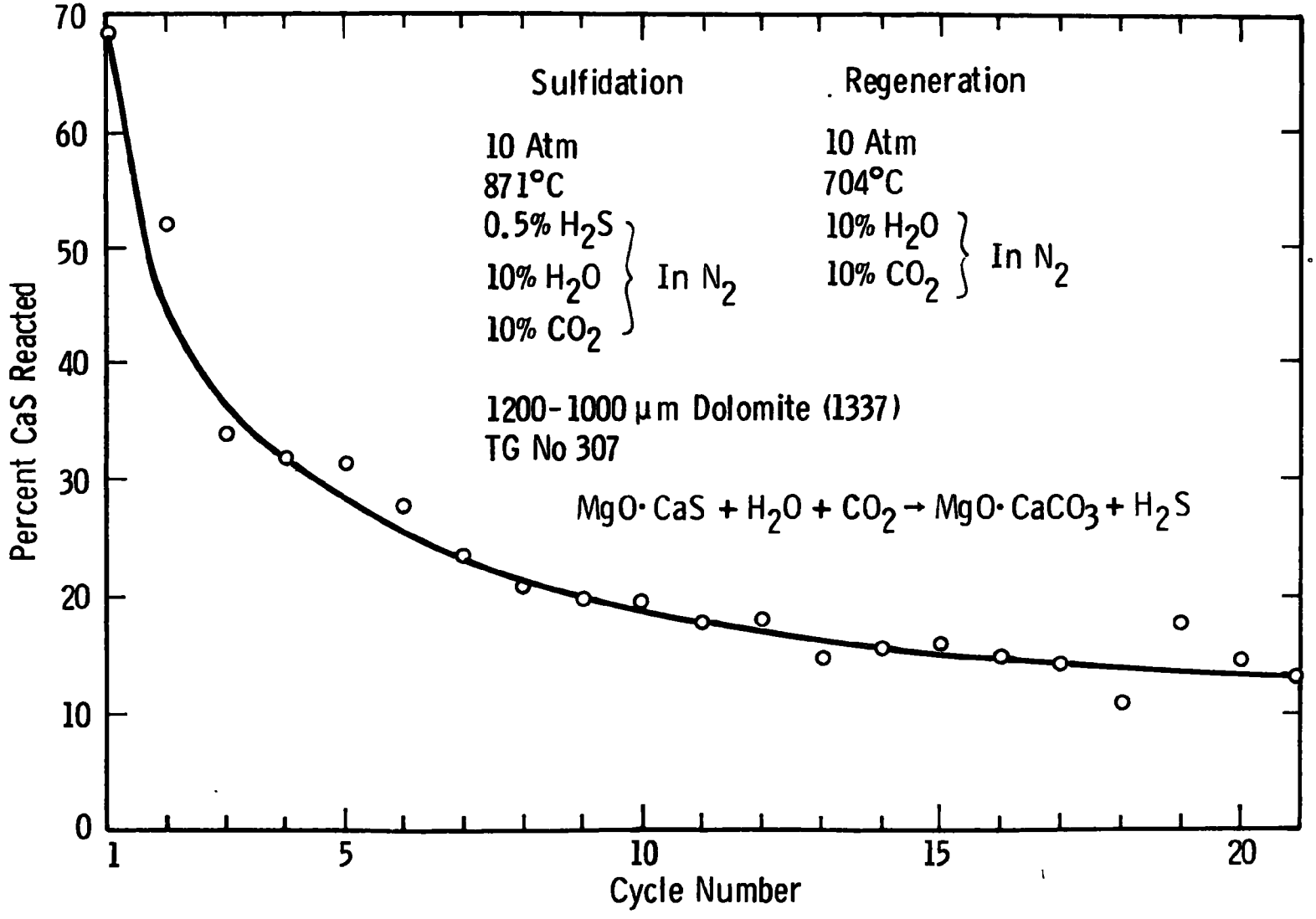

Figure 17 – Cyclic regeneration of $CaCO_3$ in sulfided dolomite

Sorbent Attrition

Sorbent attrition is discussed in Appendix C, and in more detail in Volume II of Fluidized Bed Combustion Process Evaluation: Phase 1 - Residual Oil Gasification/Desulfurization Demonstration at Atmospheric Pressure (March 1975).

The results available from fluidized bed combustors show a wide range of sorbent attrition rates and indicate that attrition resistance will be a primary factor in selecting sorbents for the fluidized bed combustor. For regenerative systems the loss rate by attrition, rather than the decline in kinetic activity on regeneration, may limit the lifetime of the sorbent in the system, particularly at high sorbent recirculation rates between a combustor and regenerator with a low-sulfur differential. These are some results which suggest that sorbent attrition is process dependent: the rate of fines production depends on whether the chemical environment is that of calcination, combustion, or sulfur removal in a reducing atmosphere. Work[38] to date on attrition resistance has consisted of comparative bed weight-loss measurements for a series of limestones and dolomites during calcination and half-calcination in a 2 cm (1.3 in) fluidized bed. Comparison of the data with results obtained on the Esso[39] 1 MW pilot-plant oil gasifier showed that stones suffering high attrition or very low attrition behaved similarly on both units. The attrition loss from some stones with intermediate loss rates is not predictable.

Additional work has demonstrated that the water content in some dolomites contributes appreciably to sorbent decrepitation.[37] Further work on identifying the properties of sorbents, and the process conditions to which they can be subjected to make them attrition resistant, is necessary.

Trace Element Emission Characteristics

The emission of trace elements from the sorbent into the effluent gas from the combustor raises environmental and corrosion questions (as discussed in Appendix H).

From the process viewpoint the major concern is that sufficient sodium and potassium will be liberated into the gas stream to induce hot corrosion in the turbine. The best approach is to use the dolomite with the lowest alkali content: samples of dolomite from different deposits contain from 100 to 6000 ppm (by weight) of potassium.

One alternative for preventing the deposition of sulfates is to increase the efficiency of the sulfur removal system. If the sulfur dioxide level in the gas is sufficiently reduced, the deposition of liquid sodium and potassium sulfate films in the turbine can be prevented. The projected sulfur dioxide concentration required to achieve this goal is less than 200 ppm. This option is discussed in greater detail in the section on minor-element and trace-element emissions and in Appendix H.

There is no indication as yet that the sorbent will contribute a significant, environmentally hazardous concentration of trace elements to the atmosphere.

Spent Sorbent Disposition

The pressurized fluidized bed combustion process, as presently conceived, results in the production of dry, partially utilized dolomite or limestone particles up to 6 mm in size. In addition, fine particles of sorbent and ash will be collected in the particle removal system. The sorbent material may be either regenerated for recycling to the fluid bed boiler for repeated sulfur dioxide removal or disposed of in its partially utilized form in a once-through system. The former process has the potential advantage of producing less solid waste for disposition, but much uncertainty still exists about the regenerative processes. Conceptually, it is possible in a regenerative process to recycle all of the sorbent. This might involve a synthetic calcium-based material, reconstitution of the spent sorbent, or an alternative sorbent material. The composition of the spent sorbent depends on the characteristics of the original stone, the coal feed, the variation in operating temperature and pressure, as well as on once-through or

regenerative modes of operation. The major compounds in the waste stone to be disposed of are calcium sulfate ($CaSO_4$), calcium oxide (or calcium carbonate), and magnesium oxide (MgO when dolomite is used, and calcium sulfate and calcium oxide or calcium carbonate when limestone is used. Trace elements arising from impurities in the coal and dolomite will also be present.

A summary of the general process options for disposition of the spent sorbent is presented in Figure 18. Two methods of dealing with the spent sorbent are being considered:

- Disposition of the spent stone being discharged directly from the fluidized bed combustion process (once-through or regenerative, Options 1 and 3)
- Disposition of the spent stone after further processing (Options 2 and 4).

Disposition without processing includes direct disposal or utilization of the material in soil stabilization, for example. This is the preferred option,since it does not require additional processing. Disposition of the spent stone after further processing is being considered in order to develop methods for rendering the stone environmentally acceptable for disposal, if direct disposal is not universally permitted, and to investigate alternative markets for the spent stone, such as in the form of refractory brick.

Recovery of sulfur from the spent stone for disposal or utilization has not been considered attractive, although the waste stone could be processed to recover the sulfur. Sulfur or sulfuric acid (H_2SO_4) would be recovered from the sulfur-rich gas (SO_2 or H_2S) from the regeneration processes. A third general option for processing the waste stone (Option 5) would be to react the off-gas from the regenerator with the waste sorbent to produce a solid material for disposal or utilization. This option does not appear to offer advantages over the once-through process options.

Among the factors that will affect the disposition of the spent sorbent are, for example, the quantity of spent sorbent, its

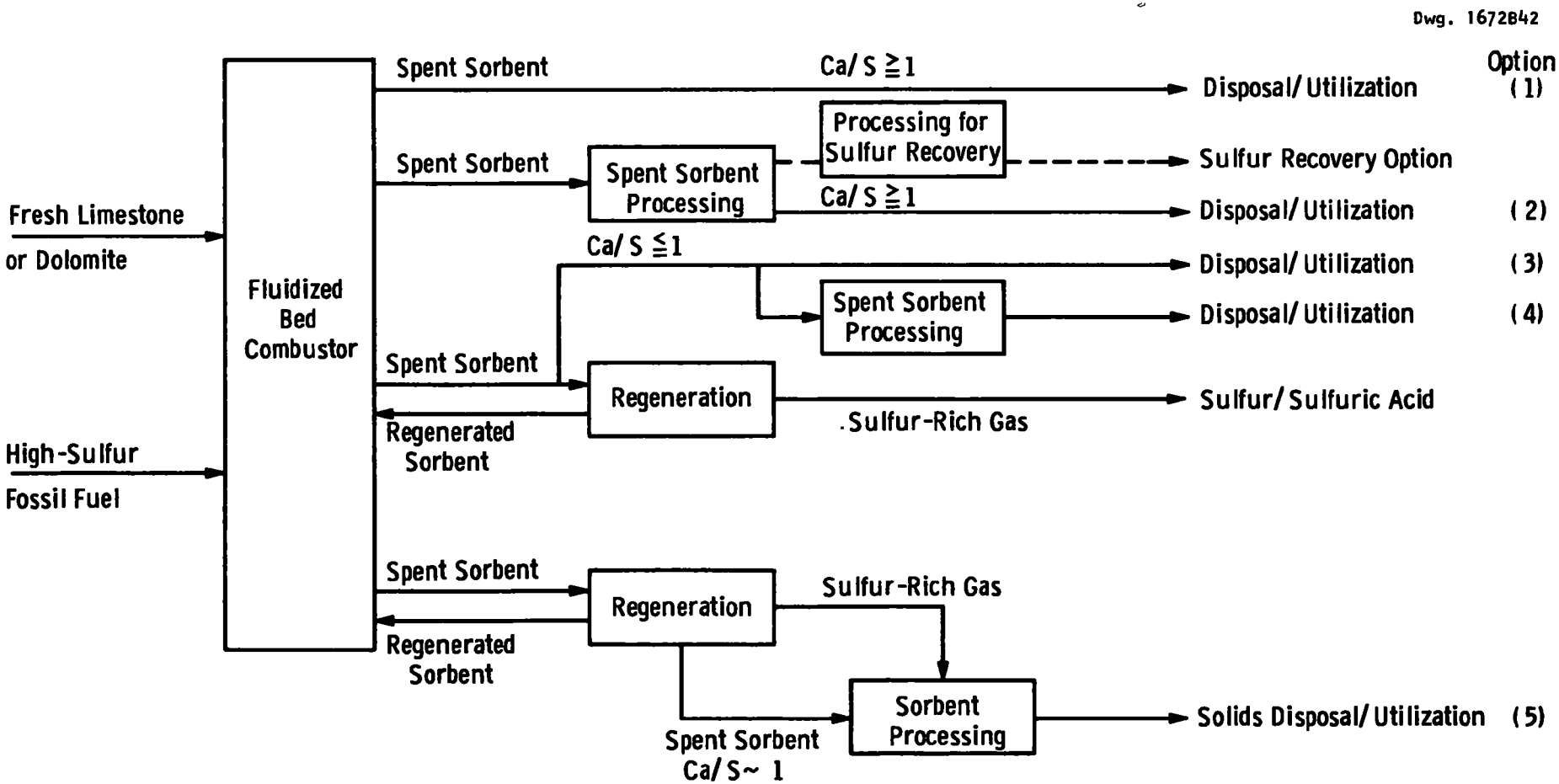

Figure 18 –Sulfur removal system process alternatives

chemical characteristics, regulations, geographical location, and the size of the market for respective applications. These factors are discussed in Appendix F.

Typical quantities of spent sorbent projected for disposal from a 500 MW power plant burning a 3 wt % sulfur fuel with 95 percent removal would range from approximately 41 Mg/hr (45 tons/hr) for a once-through system using dolomite (Ca/S = 1.5) to approximately 19 Mg/hr (21 tons/hr) for a regenerative system utilizing a calcium/sulfur makeup rate of 0.75. Specific quantities will depend on operating conditions and sorbent characteristics.

The disposition of unprocessed spent sorbent is represented by Options 1 and 3 in Figure 18. Westinghouse obtained samples of spent dolomite from the Argonne and Exxon pressurized fluidized bed combustion pilot plants and carried out preliminary leaching experiments and activity tests.

Results from these preliminary tests indicate:

- Natural gypsum leachates contain approximately the same amounts of dissolved calcium and sulfate ions as the fluidized bed combustion spent sorbent leachates. Both agreed relatively well with the calcium sulfate solubility, and both exceeded the water quality standards, 75 mg/l for calcium and 250 mg/l for sulfate.
- There was negligible dissolution of magnesium ions.
- Insignificant amounts of heavy metal ions were found in the leachates.
- Fluidized bed combustion spent sorbent leachates were alkaline, with pH = 10.6 to 12.1. It is interesting to note, however, that the run-off leachates showed a gradual decrease in pH with the amount of leachates passing through.
- Temperature increase of the spent sorbent will be negligible when subjected to the environment.

The experimental data and an assessment of the environmental impact of direct disposal are presented in Appendix G. The chemical composition of the spent sorbent from once-through and regenerative processes and its likely environmental impact require additional comprehensive leaching tests and activity tests to determine the chemical fate of the constituent compounds (calcium, magnesium, sulfate ion, and so on) and trace elements which may occur in the raw sorbent or which may accumulate during the combustion of the coal.

The direct disposal or utilization of spent sorbent may not be possible or permitted in all cases. Thus, alternatives for spent stone disposition must be developed to permit utilization of the fluidized bed combustion process. It may also be possible to develop a more attractive use for the spent sorbent through some processing technology. Several proposed processes are presented in Appendix F.

Several potential applications for the processed spent sorbent and for the unprocessed spent sorbent were identified:

- Soil stabilization
- Landfill
- Concrete
- Refractory brick
- Gypsum
- Municipal waste treatment
- Acid mine drainage.

Both high-temperature stone processing, including spent sorbent/fly ash and spent sorbent/clay sintering, and low-temperature pozzolanic activity require further study. Materials to be tested should include the spent stone from the once-through process, spent stone from pilot plant and prototype plant tests, and blends of these materials with fly ash, clay, and soil. The soil stabilization tests will require determination of unconfined compressive strength, Atterberg limits, and direct and triaxial shear strengths. The influence on agricultural soils of surface dumping of the spent sorbent should also be investigated. Spent sorbent should be evaluated for suitability as aggregate material

by testing it in concrete mixes for compressive strength, splitting tensile strength, flexural strength, and modulus of elasticity. The interfacial behavior of the concrete and foundation soil should be examined.

In summary, environmental problems associated with disposal of the spent sorbents from fluidized bed combustion systems differ favorably from those associated with disposal of lime sludges, in that they are solids and they do not possess great water solubility. Data indicate the spent dolomite (or limestone) can be used as dry landfill with known civil engineering practices for controlling structural rigidity and ground water flows. Alternatives are also available for utilization of the spent stone. In addition, the advanced sulfur removal systems being developed would minimize the quantity of spent stone available and, thus, could minimize the problem.

NITROGEN OXIDE EMISSIONS

In the fluidized bed combustion of coal with in-bed desulfurization using limestone and dolomite sorbents, the operating temperature range for the bed is from 704 to 1010°C (1300 to 1850°F). Since 1010°C (1850°F) is well below the temperature level at which fixation of free nitrogen (thermal nitric oxide) through the Zeldovich mechanism[40] becomes negligible [about 1538°C (2800°F)], the only significant source of nitric oxide is from bound nitrogen in the coal.

In diffusion flames the conversion of bound nitrogen to nitric oxide which takes place during the carbon-hydrogen-oxygen reactions, has been found to be nearly 100 percent. At flame temperatures greater than about 1538°C (2800°F), where thermal nitric oxide formation occurs, the net conversion of bound nitrogen is less than 100 percent, since the presence of nitric oxide from bound nitrogen suppresses the formation of thermal nitric oxide. This indicates that the conversion of bound nitrogen in fluidized bed combustion at bed temperatures less than 1010°C (1850°F) should be nearly 100 percent. Experimental investigations, however, have shown that, on the contrary,

the conversion of bound nitrogen in fluidized bed combustion is substantially less.[8,31,41]

Various investigators have attempted to determine the effect of the fluidized bed combustion design parameters on nitrogen oxide emission. Those parameters which have been identified as having a significant effect on nitrogen oxide emissions are pressure level, excess air, calcium-sulfur ratio, water vapor, carbon monoxide concentration, and constraint on mixing in the bed.

Argonne National Laboratories (ANL) have measured nitrogen oxide emissions levels at 810.4 kPa (8 atm),[31] considerably less than those previously measured by them at atmospheric pressure.[42] Combustion power test data show that emissions at 405.2 kPa (4 atm) are substantially lower than those at low pressures.[10] Similar effects of pressure on nitrogen oxide emissions were reported at the Third International Conference on Fluidized Bed Combustion.[43]

Test results obtained by Exxon from both their batch unit[44] and their miniplant[41] show that nitrogen oxide emissions are a strong function of the percent excess air for excess air levels up to about 50 percent. Above 50 percent excess air, the nitrogen oxide emissions are indicated to be nearly independent of excess air. The National Research Development Corporation (NRDC) data agree well with the Exxon data.[41]

ANL has conducted tests to determine the effect of calcium sulfur ratio on the nitric oxide concentration in flue gas.[31] The results of these tests show that increasing the calcium sulfur ratio above a value of 1 causes a substantial increase in the nitrogen oxide emissions from fluidized combustion of coal when operating at 810.4 kPa (8 atm), 15 percent excess air, and 788 to 899°C (1450 to 1650°F) bed temperature. The explanation for this effect is that the presence of sulfur dioxide in the bed either suppresses the formation or promotes the decomposition of nitric oxide. The reduction of nitrogen oxide to elemental nitrogen by carbon monoxide has also been postulated.[27] Water vapor may have a catalytic effect.

Results of tests conducted by Exxon in their batch unit indicate that constraints on mixing within the bed tend to increase the nitrogen oxide emissions.[44] When horizontal coils were replaced by vertical ones which were more open, the nitrogen oxide emission decreased significantly.

No data were found in the literature from which could be discerned the effect of the nitrogen content of the coal on the nitrogen oxide emission level. Tests in gas-turbine combustors using simulated bound nitrogen showed that the nitrogen oxide concentration in the products of combustion are less than proportional to the nitrogen content of the No. 2 distillate.[45]

Figure 19 is a composite plot of the nitrogen oxide emission data from Exxon and NRDC, which shows that the nitrogen oxide emissions from fluidized bed combustion of coal is well below the current EPA emission standard over a range of excess air levels up to about 50 percent.

Extrapolation of the Exxon and NRDC data indicates that the nitrogen oxide emissions for adiabatic fluidized bed combustion would also be below the EPA emission standard of 0.302 kg NO_2/GJ (0.7 lb NO_2/10^6 Btu) input. Data from the Combustion Power Company's process development unit[10] indicate that the nitrogen oxide emission level from an adiabatic combustor (excess air 200 to 300 percent) is in the order of 0.173 kg NO_2/GJ (0.4 lb NO_2/10^6 Btu) input.

In summary, the data indicate that nitrogen oxide emissions from pressurized fluidized bed boilers and adiabatic combustors will be well below the EPA emission standards.

PARTICULATE CONTROL

Particulate removal is critical for the successful operation of pressurized combined-cycle fluidized bed combustion power plants. The particulate removal system must be capable of reducing the particulate loading in the combustion off-gas to levels compatible with gas-turbine operating conditions and environmental standards. Analyses of

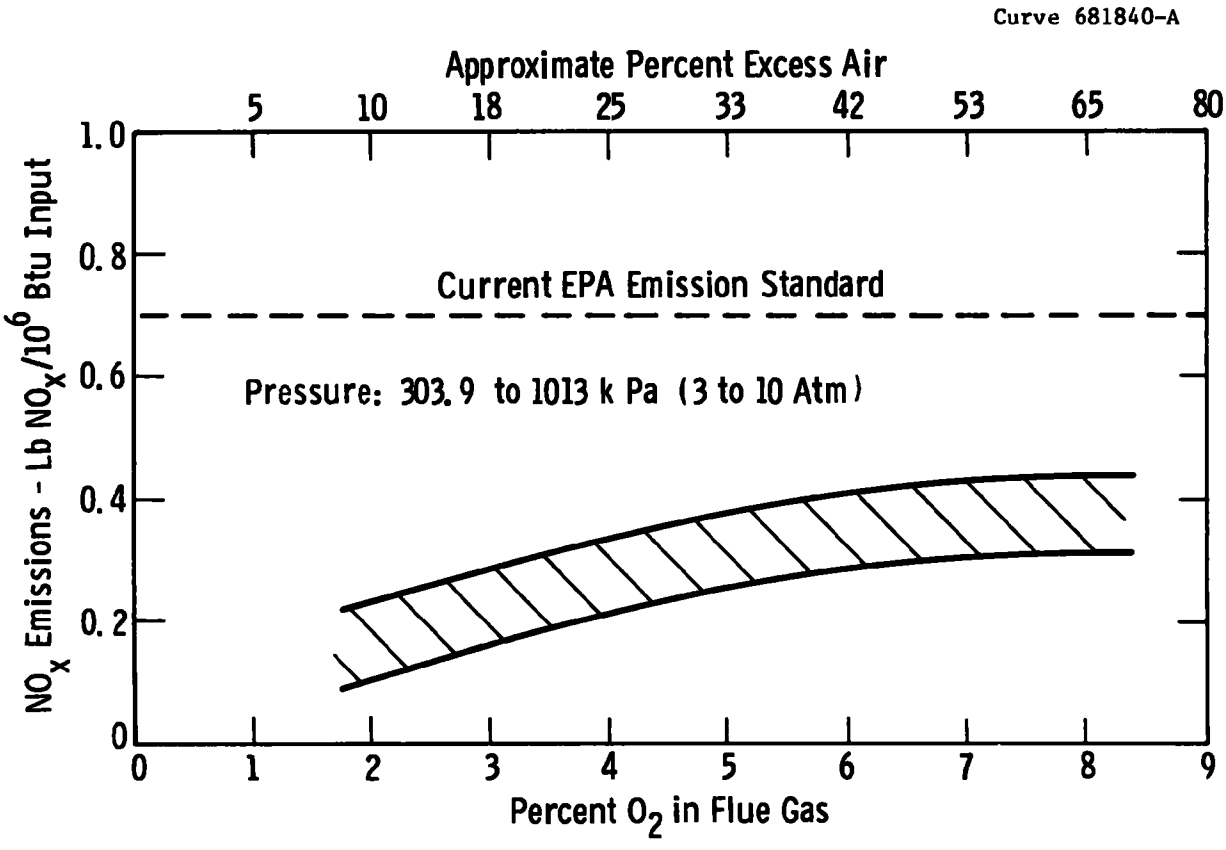

Figure 19–Composite plot of data for NO_x emissions from fluidized combustion of coal

particulate control systems have been based on estimates of carry-over from fluidized beds, of turbine tolerance for particulates, and of dust collector performance. Unfortunately, there is no reliable estimate of turbine tolerance for particulates or the dust loading from a commercial-scale fluidized bed combustor. As a result, criteria for the particulate removal system are ill defined, and more definitive experimental data are needed.

Fluid Bed Boiler Carry-over

Estimates of carry-over have been published in earlier reports.[2,46] The basic design assumes a carry-over of 15 gm/m^3 (6.7 gr/scf), with particle size distributions as indicated in Figure 20. Dust loadings of up to 67 gm/m^3 (30 gr/scf) have been assumed in parametric studies. Particulate emissions will include fuel ash, unburned carbon, and sulfur sorbent. The dust loading from the combustor will depend on the fluidized bed combustion design (e.g. bed internals, freeboard) and operating conditions (e.g. gas velocity, bed depth, temperature); the solids feed preparation (e.g. washed and unwashed coal, fresh or regenerated sorbent); the solids feed characteristics (e.g. coal size and ash content, sulfur sorbent size and attrition characteristics); and sulfur removal system (e.g. sorbent makeup rate).

Gas-Turbine Specifications

The turbine tolerance will depend on particle size, particle physical properties, impact velocity, impact angles, and turbine materials. Thus, the turbine tolerance will depend on the particles, the gas-turbine design, and the operating conditions. Current estimates, based on model studies and on extrapolation of experimental data, indicate that gas turbines will tolerate dust loadings two to one hundred times greater than present specifications allow. [Presently allowed are 4.6×10^{-4} gm/m^3 (2×10^{-4} gr/scf) in the turbine expansion gas.] Thus, the allowable limit may be estimated to be somewhere

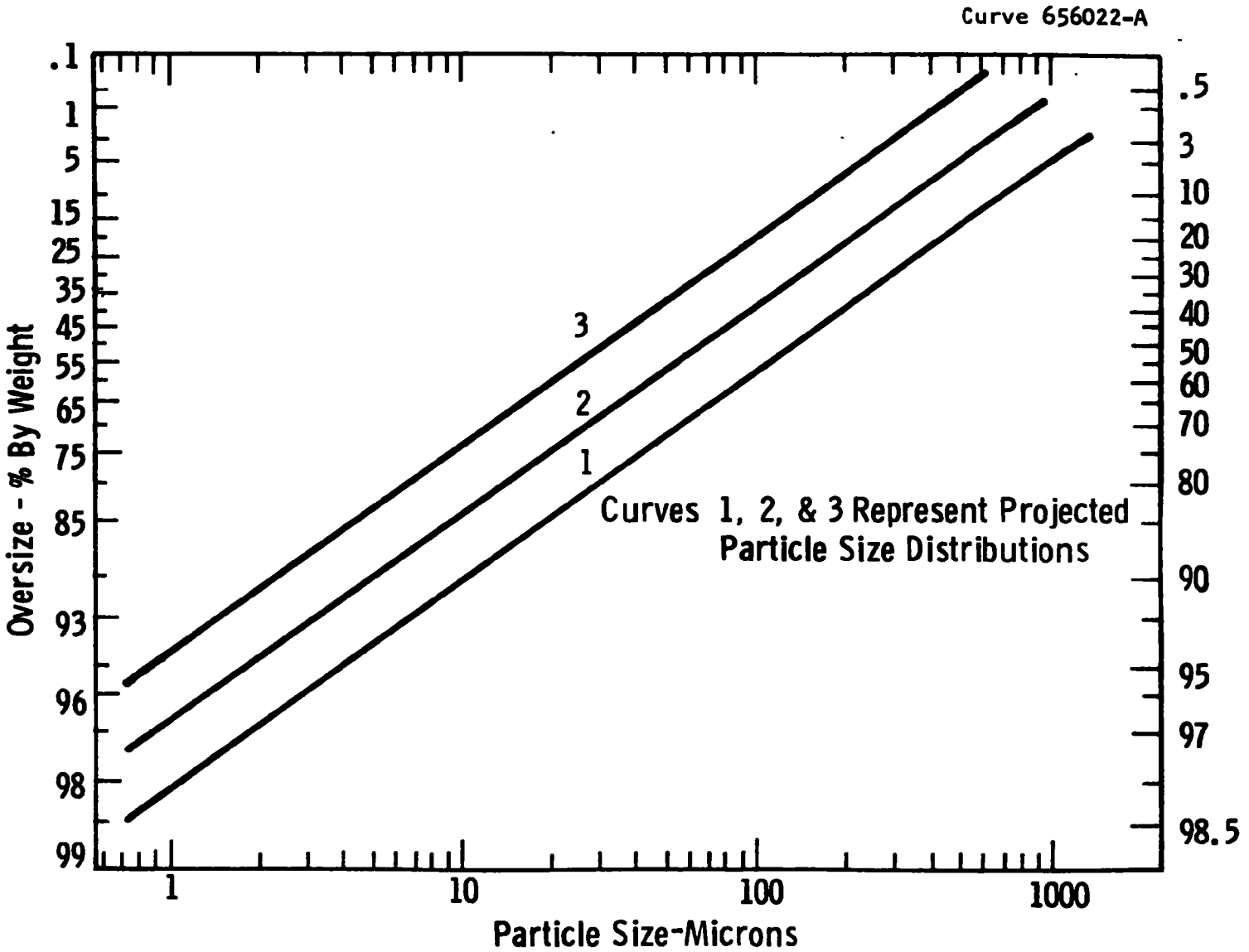

Figure 20 —Particle size distribution assumed for dust elutriated from gasifier

between 9.2×10^{-4} and 4.6×10^{-2} gm/m^3 (4×10^{-4} and 2×10^{-2} gr/scf). A preliminary estimate of the turbine tolerance for particulates is presented in Appendix J. This estimate projects a tolerance from 0.012 to 0.093 gm/m^3 (5×10^{-3} to 4×10^{-2} gr/scf). Further work is required to establish more precise specifications. For the present assessment of particulate control requirements, however, it has been assumed that 4.6×10^{-3} gm/m^3 (2×10^{-3} gr/scf) is the allowable limit.

This limit must be associated with an allowable particle size distribution. Using current specifications, an acceptable size distribution has been projected (Table 7). Clearly, smaller particles will be less erosive than large particles; and, consequently, heavier loadings than these allowable limits may be accommodated, provided the size distribution is finer.

A technique for estimating the erosive power of various size fractions (Appendix I) has been used to produce particle loading/particle size distribution combinations which are considered to have erosive characteristics equivalent to those of the allowable one. It can be shown that a fine particle size distribution may have a loading ten times higher than the allowable specification yet have the same erosive characteristics (Table 7).

Environmental Standards

Allowable emission levels, 0.042 gm/MJ (0.1 lb/10^6 Btu-equivalent to 0.115 gm/m^3 [0.05 gr/scf] for the pressurized boiler with 15 percent excess air) from fossil fuel plants are higher than the limit of 2×10^{-3} gr/scf imposed by gas-turbine erosion. Consequently, in meeting these turbine demands the legislative requirements on particulates will also be met.

It has been found that health hazards and haze problems are most acute with submicron particles which contribute little to the mass of emissions and cause no turbine problems. Future legislation may require better control of these emissions -- and this could require a revision of the particulate control system design. On the basis of

Table 7

ACCEPTABLE DUST LOADINGS IN EXPANSION GAS BASED ON CURRENT WESTINGHOUSE SPECIFICATIONS

Allowable particle loading and size distribution estimated from current gas-turbine specifications		Particle loading with fine size distribution equivalent in erosive nature to allowable case	
Size (μm)	Expansion gas gm/m^3 (gr/scf)	Size (μm)	Expansion gas gm/m^3 (gr/scf)
0-2	0.0018 (0.0008)	0-2	0.045 (0.20)
2-3	0.00045 (0.0002)	2-3	0.016 (0.007)
3-4	0.00036 (0.00016)	3-4	0.0036 (0.0016)
4-5	0.00022 (0.0001)	4-5	0.0009 (0.0004)
5-6	0.00018 (0.00008)	5-6	0.0003 (0.00012)
6-10	0.00055 (0.00024)	6-10	0.0002 (0.00006)
10-20	0.00045 (0.00020)	10-20	--
20 +	0.00050 (0.00022)	20 +	--
TOTAL	0.00451 (0.00200)	TOTAL	0.066 (0.0292)

current technology, however, collectors for these ultrafine particles could be operated more effectively at low temperature and pressure. Consequently, major revision of the high-pressure equipment design to meet such emission requirements is not anticipated.

Process Operating Range

Gas cleaning equipment employed in fluid bed boiler facilities will probably rely on inertial mechanisms for dust collection. Equipment of this nature shows a decline in operating performance when gas velocity through the apparatus is reduced. As a consequence, it is necessary to examine how start-up, shutdown, and turndown will affect gas-flow rates and, hence, dust collector performance.

The current concept for turndown involves an adjustment of gas temperature and pressure which only slightly alters the volumetric gas flow through the collectors. Thus, turndown is unlikely to have a significant affect on collector performance.

Shutdown procedures will involve slumping the bed. While a reduced gas flow may be maintained during this period, particle elutriation rates would be low, and collector efficiency, although reduced, will be adequate.

Start-up may involve a significant period during which gas-flow rates are reduced to minimize heat loss from the bed. Reduced collector performance may be anticipated during this period. If this is not matched by an equivalent drop in elutriation, the gas cleaning system must be installed in a modular arrangement which would allow individual units to be shut down, maintaining design flows to the remaining equipment.

Alternative Particulate Removal Systems

An initial stage of conventional high-temperature cyclones will be used to collect coarse material carried over from the fluidized beds. This will be followed by one or more stages of high-efficiency dust collection which will reduce particulate loadings to levels compatible with the requirements of the expansion turbines.

Several alternative collectors have been considered for this duty (Table 8). In all cases, however, the available operating data cannot be directly related to fluid bed combustion processes. As a consequence, various systems have been selected for further experimental evaluation. This selection is based on availability, operability, and performance potential.

System Selection

The gas cleaning system consists of three stages:

- Primary cyclones to collect coarse material and return material to the beds if the carbon content is high
- Secondary collectors to remove the bulk of the remaining fine material
- A tertiary collector to reduce the level of ultrafine particulates to acceptable limits.

Primary Collectors

Primary collectors will be cyclones of conventional design.

Secondary Collectors

The gas stream passing to the secondary collectors will contain approximately 2.3 gm/m^3 (1 gr/scf) of dust. Most of the dust particles will be smaller than 5 μm. Consequently, the collector must be able to handle large quantities of dust routinely and still have useful efficiency down to 2 μm.

Of the equipment considered, cyclones offer the most appropriate characteristics. Cyclones of conventional design, manifolded as multicyclone units, are preferred,as they do not require clean secondary gas streams to maintain efficiency.

Table 9 lists the estimated dust loading and particle size distribution at the inlet and outlet of this collector. The overall efficiency is approximately 50 percent with 80 percent collection of the +2 μm fraction.

Table 8

ALTERNATIVE PARTICULATE REMOVAL SYSTEMS

Item	Type	Comments
Cyclones	Conventional	Commercially available, performance available
	Aerodyne	Commercially available, under test
	Shell	Commercially available, performance available
	Donaldson	Commercially available
Filters	Granular bed	Pilot-plant testing complete
	Porous metal	Commercially available
	Porous ceramic	
Electrostatic	Research Cottrell	Laboratory investigations show feasibility

Table 9

ESTIMATED DUST COLLECTION HIGH-EFFICIENCY MULTI-CYCLONE SECONDARY COLLECTOR (Stairmand Design)

Dust size (μm)	Inlet Loading gm/m^3 (gr/scf)	Outlet Loading gm/m^3 (gr/scf)
0-2	0.500 (0.220)	0.363 (0.16)
2-3	0.114 (0.050)	0.045 (0.02)
3-4	0.079 (0.035)	0.018 (0.008)
4-5	0.054 (0.024)	0.009 (0.004)
5-6	0.041 (0.018)	0.007 (0.003)
6-10	0.057 (0.025)	0.007 (0.003)
10-20	0.045 (0.020)	0.0015 (0.0007)
20 +	0.014 (0.006)	0.0005 (0.0002)
TOTAL	0.904 (0.398)	0.451 (0.1989)

Tertiary Collector

The final filter stage must reduce the loading of dust from 0.46 gm/m^3 (0.2 gr/scf) to a level acceptable in turbine expansion gas. Westinghouse projections show that this will require a collection efficiency of at least 90 percent and possibly as high as 99 percent on a particle size distribution which is essentially all below 10 μm.

Granular bed filters show the greatest potential for meeting this requirement, and experimental development of these filter systems is recommended. Preliminary testing in the laboratory has shown adequate efficiency, but more data are required.

Assessment

Simple mechanical collectors, such as cyclones, are inadequate for meeting the dust collection requirements. Specialized high-efficiency cyclones which require clean flows of high-pressure secondary gas are difficult to incorporate into a power plant scheme without seriously reducing cycle performance.

Granular bed filters have shown acceptable efficiency. A more detailed study of mechanical design, however, and of cleanup cycles is required to establish their utility.

The requirement for particulate removal equipment primarily remains dependent on the gas turbine tolerance. This tolerance depends, in turn, on particle characteristics as size distribution and density; on the turbine operating conditions; and on the turbine design. The function of each particulate removal stage must also be assessed; for example, a first-stage cyclone may not be required if solids are not returned to the combustor. Thus, simplifying the particulate removal system may be achieved by increasing turbine tolerance, improving particulate removal capability, or combining component functions to reduce the number of stages , and may result in significant cost reductions and improved reliability.

Intensive experimental testing on large-scale, hot, pressurized equipment is required to establish more effectively the operating performance of dust collection equipment.

MINOR-ELEMENT AND TRACE-ELEMENT EMISSIONS

Trace emissions from the fluid bed combustion process are important from two standpoints:

- Their effect upon the environment
- Their effect on the operability of the power plant.

The primary environmental concern is with the toxic effects of the compounds of beryllium, mercury, fluorine, lead, cadmium, arsenic, nickel, copper, zinc, barium, tin, phosphorous, lithium, vanadium, manganese, chromium, and selenium. The primary technical concern is with the corrosion of turbine metal induced by the deposition of liquid films of minor elements such as alkali-metal sulfates.

In order to predict the impact of trace element emissions on the operability and environmental acceptability of the fluidized bed combustion process, it is necessary to know:

- The quantity and chemical form in which each trace element of concern enters the fluidized bed combustion process
- The chemistry of the processes by which the elements are partitioned between the solid and gaseous effluents from the process
- The tolerance of the system operations to the release of trace elements within the plant
- The release of trace elements within the plant
- The emission levels acceptable for environmental protection
- The control measures which can be taken to alter the chemistry of the release process or the quantities of trace elements released, and the tolerance to trace elements.

The chemistry of occurrence and release of minor and trace elements could develop into an interminable task; a prudent approach, however, will require reference to experimental data obtained on fluidized bed combustion and analysis of the behavior of those elements which clearly raise environmental or technical questions.

Trace Element Quantities Input to the System

The distribution of trace elements in U.S. coals has been explored by the Illinois State Geological Survey.[47] Studies at Westinghouse on the quantities of trace elements present in some western coals agreed very closely with Gluskoter's work. The form in which these elements occur is not well characterized, so that, at present, estimates of their ultimate form are best obtained from analysis of the solid residues and gaseous effluents from the fuel processing system. For the dolomitic sorbent, the trace element data are sparse and of unknown value. Initial studies of the distribution of trace elements in dolomites are in progress at the Ohio Geological Survey,[48] and work on the distribution of alkali metals in dolomites

is in progress at Westinghouse under contract to the Energy Research and Development Administration.[49] An acceleration of effort in this area is essential in order to define sorbent selection criteria and to assess spent sorbent and ash disposal processes.

Experimental Data on Emissions.

Preliminary experiments on the fate of mercury, lead, beryllium, and fluorine in a fluidized bed combustor have been reported by the Argonne National Laboratory.[50] This work is still in the developmental stage, but it indicates that fluorine and lead were retained by the solid products, but the quantities of mercury and beryllium recovered were about one-third and two-thirds of the input. The estimation of trace element emissions is also in progress at Exxon.[44] Their experimental results indicate an 86 percent retention of arsenic and 96 percent retention of manganese. The uncertainties involved in the analyses indicate that trace element analyses will be necessary on condensate obtained from flue gas.

The experimental data on alkali-metal emissions are sparse but consistent. The BCURA-NRDC[8] report indicates that ∿1.5 ppm sodium and potassium are liberated into the gas phase beyond the test cascade from a continuous fluid bed combustor at 607.8 kPa (6 atm) pressure and 899°C (1650°F). The Exxon data obtained by material balance after solids analysis indicate that 10 percent of the sodium and 20 percent of the potassium input to their pressurized combustor escaped from the bed in the gas phase. Even at the low sulfur dioxide levels (<25 ppm) achieved in the BCURA combustor, the sodium concentration in the off-gas exceeds the calculated turbine tolerance for sodium as given by the pure sodium sulfate melt model or by the assumption that a eutectic melt of potassium and sodium sulfate forms.[48] The chlorine content of the coal used was about one-third of the mean value for U.S. coals, but even had there been a three-fold increase in chlorine content, the turbine tolerance for pure sodium sulfate would have been exceeded.

Emission Chemistry and Turbine Tolerance

The components of gas turbines exposed to the hot gas stream are made of materials that form oxide scales to protect themselves from oxidation. High-strength nickel-based superalloys are used for the highly stressed rotating components. More oxidation-resistant, but lower-strength, cobalt-based alloys are used for the stationary components. Inlet gas temperatures over 1093°C (2000°F) are currently used in industrial turbines. Air cooling is used to maintain metal temperatures lower than 899°C (1650°F) so that the alloys retain sufficient mechanical strength.

Metal recession rates due to oxidation alone are of the order of 0.10 mm (0.004 in) per year on the hottest components of current Westinghouse turbines. In the presence of alkali-metal compounds, which react with sulfur dioxide and sulfur trioxide from the combusted fuel gas, liquid films of sulfate and sulfate-chloride mixtures can be deposited on the turbine hardware. In the sodium-potassium-sulfur-oxygen-chlorine (Na-K-S-O-Cl) system, liquid films are possible over the temperature range of 514 to 1069°C (957 to 1956°F), which coincides with the range of temperatures encountered in the turbine flow path. (Gases are exhausted from turbines at about 400°C [752°F].)

Molten alkali-metal compound films are dangerous because under some conditions they attack the protective oxide scale, allowing accelerated or catastrophic oxidation (hot corrosion) of the turbine components. The films can also accumulate particulates that allow the build-up of thick deposits on the metal surfaces. Aerodynamic performance of the turbine can thus be seriously impaired.

Sodium and potassium compounds emitted into the gas stream are potentially hazardous to the operation of the gas turbine. Chlorides and hydroxides are volatile species and can transport sodium and potassium from the combustor to the turbine. At hydrogen chloride (HCl) levels exceeding 0.4 ppm by volume in the combustor gas, solid or liquid sodium sulfate (Na_2SO_4) will convert to gaseous sodium

chloride (NaCl). The hydrogen chloride level in the combustion gas resulting from the complete release of chlorine from a low-chlorine coal (100 ppm chlorine) exceeds this level by over a factor of ten and is 5 ppm. In a fluid bed combustion process the predominant transport should be by the chlorides, as discussed in Appendix H.

In the gas turbine, reactions between the chloride and the sulfur oxides in the combustion gas will form liquid sulfate-chloride melts on the turbine hardware if the sodium and potassium levels are sufficiently high. These melts must be prevented because they initiate hot-corrosion and deposit formation. The gaseous concentrations of sodium, chlorine, sulfur, oxygen, and steam in the turbine at the turbine tolerance level are interrelated and may not be considered independently of one another. Hydrogen chloride in the turbine acts to prevent sulfate deposits from forming or, once formed, acts to remove them. A hydrogen chloride level of 40 ppm by volume in the combustion gas is sufficient to prevent a liquid sodium sulfate melt from being stable at sodium concentrations in the gas up to 0.2 ppm by volume when present in 100 percent excess air. (Forty ppm hydrogen chloride corresponds to complete release of chlorine from coal containing 800 ppm by weight of chlorine; 0.2 ppm of sodium corresponds to a one percent release of sodium from a coal containing 130 ppm by weight of sodium.) The concentration both of hydrogen chloride and of sulfur oxides (SO_2 and SO_3) have a strong influence on the stability of the melt. If the sulfur dioxide level in the gas is dropped from 200 ppm to 100 ppm by volume, the concentration of hydrogen chloride required to prevent deposition of a liquid sodium sulfate film would drop to about 25 ppm by volume. Three additional factors must be understood before it will be possible to define the sodium and potassium tolerances which will prevent hot-corrosion attack in the turbine. These are:

- The influence of the interaction between sodium and potassium to form complex melts on the hardware. In such melts the activities of the sodium and

potassium are reduced, and the equilibrium concentrations of sodium and potassium species that can exist in gas above the melt are also lowered. Interaction tends to reduce the tolerable concentrations of sodium and potassium in the turbine expansion gas. Westinghouse is working to establish the magnitude of this effect and also to establish the influence of the relative sodium and potassium levels on the composition and melting point of stable deposits.

- The ability of turbine stator vane and rotor blade alloys to withstand a combustion gas containing up to 200 ppm sulfur dioxide and up to 40 ppm hydrogen chloride
- The shifts in the turbine tolerance which will occur if equilibrium levels of sulfur trioxide are not achieved and the degree to which kinetic factors such as these influence the tolerable concentration of sodium and potassium chlorides.

Control

Our present knowledge of the system suggests that control of the impact of trace element release may be achieved in four ways:

- The concentrations of minor elements input to the combustor may be controlled by using high-purity dolomites.
- The concentration of trace elements may be minimized by selecting combustor operating conditions which prohibit or reduce release from the coals and sorbents.
- The deposition of sulfates may be prevented by
  - Removing chlorine in coal during pretreatment (to minimize formation of sodium chloride during fuel processing)

- Using high-chlorine concentration coals (to minimize sodium sulfate formation on turbine components)
- Addition of hydrogen chloride to the turbine inlet gas
- Improving the efficiency of the sulfur removal system
- Combinations of the above.

- Additives may be introduced into the fluidized bed to trap the alkali and trace elements as they are released from coal and dolomite.
- Additives may be introduced into the turbine combustor to retain the alkalis in the gas phase as they pass through the turbine.

Assessment

- Current data on the release of sodium and potassium into the gaseous effluent from the fluidized bed combustor (>1000 ppb sodium plus potassium) indicate that the projected turbine tolerance for alkali metals (<300 ppb sodium plus potassium) may be exceeded in normal operation without some control techniques.
- The equilibrium turbine tolerance model currently in use overestimates the turbine tolerance to alkali metals because it does not account for the lowered activities which result from eutectic melt formation. The model, however, may underestimate the turbine tolerance because the kinetics of the conversion to sodium sulfate on the turbine hardware may not permit the reactions to proceed to equilibrium within the relevant gas residence times. The presence of calcium oxide fines has not been considered:

their effect would be to increase the tolerance to alkalis by lowering the sulfur dioxide partial pressure (Appendix H).

- A variety of control options to prevent damage to turbine hardware is available.

GAS-TURBINE OPERATION

There are four areas of concern for reliable gas-turbine performance with pressurized fluidized bed combustion systems:

- Blade erosion
- Blade corrosion
- Relation of deposits in the turbines
- Special design features needed to duct air out and hot gas into the turbine and to protect the turbine from localized containment concentration.

Blade Erosion

In turbine stages in which all particulates may be safely considered to act as solids and where low-melting liquid films cannot form, turbine vane and blade erosion may limit turbine life. Empirically, turbines operated at turbine inlet temperatures below 680°C (1250°F) experienced erosion (as opposed to corrosion) damage.

Several gas turbines have been built and tested which utilize dust-laden gases. These results are summarized in Table 10.

Table 10 does not permit a design correlation of erosion with dust loading for the fluidized bed system. The tolerance of the turbine from the standpoint of erosion depends on:

- The physical characteristics of the particles - which depend heavily on the fuel processing system involved
- The velocities of particulate impact - which depend on turbine size and design
- The size distribution of the particles escaping the particulate cleanup system.

Table 10

EROSION OF TURBINE BLADES

Facility	Dust Loading, gm/m^3 ($gr/10^3\ ft^3$)	Comment
Locomotive Gas Turbine	>2.8 (>120)	Bad erosion-4000 hr of operation with 3 sets of blades
USBM Tests, Locomotive GT	2.8 (120)	Erosion-limited blade life estimated to be 5000 to 7000 hr
Australian Joint Coal Board-Ruston Hornsby GT	0.042 (18)	Some erosion-several thousand hr of HP blade life estimated
German Blast-Furnace GT	0.0016 (0.7)	No erosion
Westinghouse/USS(Steel) Blast-Furnace GT	0.0028 (1.2)	No erosion
Donaldson Air Cleaners fit to small GT		
Helicopters	0.0023 to 0.012[a] (1 to 5)	No erosion
Hovercraft	0.016 to 0.069[a] (7 to 30)	No erosion
Trucks	<0.0037 (<1.6)	No erosion
BCURA Fluid Bed Combustor Test	0.16 to 3.7 (70 to 160)	No erosion

[a]With 99% particulate removal of predominantly large particles, 30 to 170 μm.

Both the locomotive gas turbine and the BCURA fluidized bed tests had about the same average particle size - the locomotive gas turbine had particles somewhat smaller than 5 μm diameter, and the average particle size of the BCURA particles ran between 6 and 8 μm. With respect to particle structure, the fly ash in the locomotive tests was a fused glassy particle resulting from exposure of ash with about a 1204°C (2200°F) softening temperature to a fire zone in the combustor of 2204°C (4000°F), and the particles in the BCURA tests were somewhat friable platelets that were exposed to peak temperatures well below the softening point of the fly ash [a 816°C (1500°F) bed temperature compared to a 1204°C (2200°F) softening temperature]. The BCURA particles contained both coal-ash mineral matter and denser sulfated dolomite particles, the comparative erosivity of which is not yet well known. Particle velocities at impact differ between the turbines tested and what would be expected in large machines installed in a fluid bed combustion power plant. Modern gas turbines in electrical utility services have gas velocities leaving first-stage stator vanes in excess of 609.6 m/s (2000 ft/sec). In the older or smaller machines gas velocities less than 457.2 m/s (1500 ft/sec) are more typical. The particle velocities on impact depend on both the gas velocity and the turbine flow-path design, which influences the ability of the particulates to follow the changes in gas velocity. The lag of particle velocities behind the gas velocity variation gives rise to large particle velocities with respect to blading in the later stages of the turbine.

In Appendix J blade erosion data from the Australian Direct Coal-Fired Turbine Project are extrapolated to indicate permissible particulate loadings to prevent excessive erosion damage. A rule of thumb dependence of erosion damage on gas velocity exiting from the stator vanes is used to account for the differences in gas velocities. The results of a geometric scaling study are employed to account for the decrease in the number of impacting particles, the increase of impact velocity, and the grazing angles of particulate impact that occur in a large-sized machine. No allowance for the differences in the erosivity

of the particulates is made to provide a safety factor in these estimates. In other words, particulates from a pressurized fluidized bed combustor system are projected to be less erosive than the fused ash from the Australian experience. The estimates show that a modern 60 MW turbine should be able to operate with an acceptable level of erosion damage on turbine expansion gas containing particulate loadings between 9×10^{-6} and 6×10^{-5} kg dust/kg of expansion gas. This corresponds to a particulate loading of 0.012 to 0.093 gm/m^3 (5×10^{-3} to 4×10^{-2} gr/scf) of expansion gas. These particulate levels are 10 to 100 times the current Westinghouse standard for particulate matter when the fuel gas particulate standard is converted to the exhaust gas by including the diluting effect of the excess air used to obtain a satisfactory turbine inlet temperature. The allowable particulate loadings are less than the air pollution environmental protection particulate limits, 0.043 kg dust/GJ fuel (0.1 lb dust/10^6 Btu of fuel input to a stationary power source) which for a fluid bed combustion system is equivalent to a particulate loading of 0.115 gm/m^3 (5×10^{-2} gr/scf) of particulate matter . A turbine erosion-deposition damage model using calculated particle impact velocities and angles and measured particle impact data is being developed to define better the turbine particulate tolerance.

Blade Corrosion

The first tests (1951 through 1959) on coal-fired gas turbines were on small rating turbines aimed at locomotive usage. The problem of blade erosion dominates these investigations. The gas-turbine temperatures were considerably below those of today's machines, and corrosion was of secondary consequence.

Work on corrosion directly applicable to fluidized bed combustion is in progress at BCURA on pressurized fluidized bed combustion operating at 788 to 949°C (1450 to 1740°F). BCURA cites an exhaust gas with contaminant levels of 0.4 to 0.7 ppm of sodium-potassium alkali at bed temperatures of 788 to 816°C (1450 to 1500°F) and contrasts this with levels of 10 to 40 ppm of sodium-potassium alkali in the exhaust gas from conventional pulverized-coal burning plants operating with

flame temperatures in excess of 1649°C (3000°F). The large difference in alkali vapor present in the exhaust gases from the fluidized bed and from the pulverized-coal burning is attributable to the much lower release of alkali at the lower temperatures in the fluidized bed.

Hot corrosion is essentially prevented if liquid sulfate-chloride melts are prevented from forming on the components so that reactions to penetrate and remove the protective oxide or to prevent the oxide from reforming cannot occur.

Appendix J reports the results of chemical equilibrium and calculations to establish the maximum concentrations of sodium compounds that can exist in the turbine expansion gas without forming liquid sodium sulfate films. The tolerable concentrations are shown to be strong functions of the sulfur dioxide and hydrogen chloride levels in the gas stream. If sodium were the only alkali-metal compound present, the turbine expansion gas could contain between 0.05 and 0.2 ppm of sodium compounds by volume with 90 percent sulfur removal, depending on the hydrogen chloride level in the gas. The higher tolerance could correspond to a hydrogen chloride concentration in the coal gas of about 40 ppm by volume that obtained by burning a high (0.8 percent) chlorine content U.S. coal.

The presence of potassium compounds in the turbine expansion gas lowers the allowable tolerance further, as discussed in Appendix H. The formation of the eutectic melt between potassium and sodium sulfate [melting point 832°C (153°F)] would reduce the tolerance for sodium by a factor of four to between 0.01 and 0.05 ppm with 90 percent sulfur removal. The addition of chlorides to the melt further depresses the melting point and the allowable sodium compound concentrations. Further work is required to establish:

- The range of melt composition that can exist in each turbine stage and the corresponding gas phase composition tolerances
- The degree of supersaturation that can exist in the turbine and the effect of supersaturation on the turbine tolerance

- The effect of process residence time and process temperatures on the alkali-metal content of the gases leaving fluid bed combustion processes in order to design a process capable of meeting the turbine tolerance
- The technical feasibility of limiting alkali release in the fluid bed combustors through hydrogen chloride level control
- The technical and economic feasibility of using higher hydrogen chloride levels and lower sulfur dioxide levels in the turbine to enable the turbine tolerance to meet process capability.

Deposition

If the alkali-metal compound tolerances are met, one is reasonably assured, because of the low-combustion temperatures in a fluid bed combustion system, that liquid films will not be present on either the turbine hardware or on the surface of the particles. Deposits cemented by alkali-metal compounds should not form. Sintering of deposits will not be accelerated by the presence of the liquid.

Deposits resulting from the impaction and dry sintering of the mix of fine particulates can still occur, especially in the first stages of the turbine where blade-metal temperatures may exceed 870°C (1600°F) in some places. We are not yet in a position to define particulate tolerances to limit deposit growth to acceptable rates. We need to understand the influence of blade temperature and particulate arrival rates on the growth and sintering of deposits and to establish rates of erosion of deposits so that deposit formation and removal processes are quantified.

Deposit formation is less of a problem at low-turbine inlet temperatures. Turbine operating experience had indicated that below 677°C (1250°F) erosion rather than deposition may become the factor that limits turbine life.

Turbine Design

To preserve high efficiency in a pressurized fluid bed combustor system, hot gases [1013 to 1520° kPa (10 to 15 atm), 871 to 927°C (1600 to 1700°F)] leaving the dust collection system must be transferred directly to the gas turbine for expansion. Various design configurations to accommodate thermal expansion, to control leakage, and to provide a uniform distribution of particles over the flow channel of the turbine have been suggested. Operating experience is available from European compound-cycle power plants utilizing one of two high-pressure connections to the turbine. These installations have generally delivered hot gas at turbine inlet temperatures between 700 and 760°C (1300 and 1400°F); in other words, about 300°C (500°F) below the turbine inlet temperatures currently used in electrical utility gas turbines.

Further work is needed to develop reliable and economical transfer pipe designs. Tests on an integrated fluid bed combustor-turbine system at an appropriately large scale will be needed.

A turbine design is needed that:

- Provides for uniform distribution of the dust-laden gas over the inlet flow channel
- Directs particle flows in blade and vane wakes to avoid raising the erosion and deposition potential of dust at blade and vane roots
- Uses stepped sidewalls, carbide wear-resisting inserts, and/or cooling air injection as appropriate to protect blade and vane roots from erosion damage
- Appropriately thickens and hard-faces blade tips to resist erosion damage
- Incorporates spray systems and drains, and provides for injection and removal of milled nut shells (or equivalent) for washing and cleaning of blade and vane surfaces without the need to open the turbine

- Lowers the velocity of gases in the turbine, if required, to achieve satisfactory erosion life.

In order to realize the full potential of pressurized fluidized bed combustion systems, work must continue to:

- Develop commercial gas-turbine designs
- Carry out analytical and laboratory tests to understand turbine tolerance to corrosion, erosion, and deposition
- Obtain data on large-scale integrated fluidized bed combustor, particulate control, and turbine test systems.

VI. SYSTEM DEVELOPMENT

Pressurized fluidized bed combustion systems have the potential to meet environmental requirements at energy costs lower than any other competitive system. This assessment is based on the available experimental data and on systems studies which have been carried out by Westinghouse and other investigators in the U.S. and abroad. In order to realize this potential further experimental work is required to:

- Investigate potential problem areas
- Establish design criteria for commercial fluidized bed combustion plants
- Develop operation and control procedures
- Test plant components - for example, fluidized bed combustor designs, coal feeding, particulate removal, gas turbine, instrumentation, materials
- Investigate environmental impact.

A variety of test facilities has been proposed by different organizations to advance the development of pressurized fluidized bed combustion systems. Development work is required in three primary areas: commercial-scale fluidized bed combustor/component test facility, gas-turbine tolerance and performance, and environmental impact. A fluidized bed combustion test facility and a gas-turbine corrosion/erosion pilot-plant test rig and program are addressed in this report.

FLUIDIZED BED COMBUSTION TEST FACILITY

A pressurized fluidized bed boiler development plant was conceived to demonstrate pressurized fluidized bed boiler operation under a previous contract to the EPA.[2] Preliminary designs, cost estimates, experimental programs, schedule, and program alternatives were reported. During the period of this contract, Westinghouse was invited to submit

a proposal for a program to design, construct, and operate a multi-purpose environmental test facility. A proposal was submitted in November 1974. The work in this proposal to extend the original development plant concept was not carried out as part of this Westinghouse-EPA contract; since such a facility is considered important for the efficient development of pressurized fluidized bed combustion, the basic philosophy and plant concept is presented in Appendix M.

The test facility includes two pressurized fluidized bed combustor modules served by one common set of auxiliaries. One module is designed as a fluidized bed boiler, and one is designed to operate as a recirculating bed boiler or an adiabatic combustor. The utilization of two modules permits the real-time test capability to be increased, with only an incremental increase in plant cost, and the added capability of simulating multibed operation.

The size of a test facility is always a critical decision, both from a technical and an economic view. The size of a test facility should be determined on the basis of the problems to be investigated, an assessment of what phenomena are critical to understanding the problem areas, and the risk permitted, before proceeding to the next stage of development. The philosophy behind building the test facility is to provide information which will permit direct application of pressurized fluidized bed combustion systems on a commercial scale. The primary problems identified include performance of a commercial-size fluid bed unit (e.g., assure resolution of tube configuration to avoid operating problems such as temperature distribution and tube vibration), performance of the gas turbine (e.g., understand particle erosion and alkali-metal deposition phenomena), and performance of particulate removal equipment (particularly the final stage of cleanup). The size selected for the proposed test facility is a commercial size fluidized bed, with a coal feed rate up to 10,000 kg/hr (approximately 22,000 lb/hr). The basis for this selection is discussed in Appendix M. The fluidized bed combustor operating conditions for the proposed facility, the prior development plant, and a commercial-scale pressurized boiler and adiabatic combustor are summarized in Table 11.

Table 11

FLUIDIZED BED COMBUSTION SYSTEM DESIGN PARAMETERS

	Commercial bed designs			Fluidized bed combustion test facility	
	Pressurized fluid bed boiler[a,b]	Adiabatic combustor[b]	Development plant design[c]	Boiler module	Adiabatic combustor module
Operating Conditions					
Pressure, kPa(atm)	1013(10)	1013(10)	101.3-2026(1-20)	101.3-2026(1-20)	1013(10)
Temperature, °C(°F)	760-954(1400-1750)	760-954(1400-1750)	704-1093(1300-2000)	704-1093(1300-2000)	704-954(1300-1750)
Gas Velocity, m/s(ft/s)	1.71-2.74(5.6-9.0)	1.8(6)	(6-15)	1.8-4.6(6-15)	1.8(6.0)
Excess Air, % of stoichiometric	10-100	300-360	up to 100	up to 160	300-360
Bed Depth, m(ft)	3.35-4.36(11.0-14.3)	2.0(6.6)	1.22-9.15(4-30)	1.22-9.15(4-30)	2.0(6.6)
Freeboard, m(ft)	1.53-2.31(5-7.6)	2.44(8)	1.22-12.80(4-42)	1.22-12.80(4-42)	up to 7.3(24)
Coal Size, mm (in)	6.35 x 0(1/4 x 0)	3.18 x 0(1/8 x 0)	6.35 x 0(1/4 x 0).	6.35 x 0(1/4 x 0)	3.18 x 0(1/8 x 0)
Sorbent Size, mm (in)	up to 6.35(1/4) top size	up to 3.18(1/8) top size	up to 6.35(1/4) top size	up to 6.35(1/4) top size	up to 3.18(1/8) top size
Ca/S Molar Feed	3-6	3	up to 6	up to 6	1-6
Coal Feed Rate kg/hr (lb/hr)	9.78×10^4 (2.16×10^5) (300 MW plant)	6.36×10^4 (1.40×10^5) (200 MW plant)	1.0×10^4 (2.2×10^4)	up to 1.0×10^4 (2.2×10^4)	4.8×10^3 (1.06×10^4)
Design Parameters					
Bed Area, m^2(ft^2)	3.25(35)	10.5-64.5(113-695)	3.25(35)	3.25(35)	10.5(113)
Bed Height/Diameter, m(ft)	2-2.5(6.6-8.2)	0.2-0.5(0.65-1.6)	1.5-3.0(4.9-9.8)	1.5-3.0(4.9-9.8)	0.5(1.6)
Heat Transfer Coefficient, W/m^2-°K(Btu/ft^2-hr-°F)	283.5(50)		2.83.5(50)	283.5(50)	
Tube Packing, % bed volume	17-22.5		17-22.5	10-30	

[a] Archer, D. H., et al. Evaluation of the Fluidized Bed Combustion Process. Office of Air Program. Westinghouse Research Laboratories. Pittsburgh, Pa. NTIS PB 211-494, PB 212-916, PB 213-152. November 1971. (318 MW_e plant capacity).

[b] Keairns, D. L., et al. Evaluation of the Fluidized Bed Combustion Process. Office of Research and Development. Environmental Protection Agency. Westinghouse Research Laboratories. Pittsburgh, Pa. EPA-650/2-3-73-048a. Contract 68-02-0217. December 1973. Vol. I. (200 MW_e plant capacity).

[c] Ibid. Vol. III. (10 to 30 MW_e equivalent capacity).

The test facility also provides for tests on:

- Commercial-scale regenerative processes, once-through processes, and waste sorbent processing for by-product utilization or disposal with limestone/dolomite sorbents or alternative sorbents
- Primary, secondary, and tertiary particulate removal equipment
- Gas-turbine performance, utilizing a rotating, multi-stage turbine and several stationary test passages
- Auxiliary systems such as solids feeding, on-line gas composition monitoring, etc.
- Operation and control philosophies
- Advanced system and component concepts.

The estimated installed cost (December 1974) for the facility is $21 million.

GAS TURBINE CORROSION/EROSION PILOT-PLANT TEST RIG

Exxon Research and Engineering is under contract to EPA for the design, construction, and operation of a high-pressure, fluidized bed boiler, 0.63 MW-equivalent miniplant to obtain information for the design of a high-pressure fluidized bed boiler demonstration plant. Westinghouse was responsible for designing and constructing an erosion/corrosion test rig for installation in the discharge line from the miniplant. The test rig has been constructed and shipped to Exxon and a test program developed. The technical basis for the design of the erosion/corrosion test rig, the detailed design of the test rig, the apparatus and procedures for sampling particulates, a plan for tests to be conducted in the test rig, and an analytical procedure for interpreting the test results are presented in Appendix K.

The plant operates at 1010 kPa (10 atm) pressure with a product gas flow rate of 0.739 kg/s (1.63 lb/sec). Two stages of cyclone separators are located in the discharge line from the combustor.

This is not expected to give dust loadings as low as the projected turbine requirements. Another final particulate collection stage is scheduled to be included which should provide an improved simulation of the expected particle loading.

Two concepts were considered for the test rig: a cascade-type unit patterned after the design used by BCURA and a straight-through test unit (see Figure 21). Since the results obtained on a cascade rig for the Exxon miniplant would be of questionable value because of the reduced scale, and simultaneous testing of several vane and blade materials would not be possible, it was concluded that a cascade-type erosion test rig was not feasible for this application. A straight-through erosion/corrosion test rig, therefore, was designed for the Exxon miniplant conditions.

The straight-through erosion test rig consists of a bell-mouth nozzle followed by a length of straight duct to provide adequate time for the particles to accelerate to near gas-stream velocity ahead of the target. Here, again, a 6.35 mm (1/4 in) diameter cylinder is considered to be the minimum practical size for the erosion target. A 6.35 mm (1/4 in) diameter target located in the straight section would limit the velocity to less than 457 m/s (1500 ft/sec) because of choking in the plane of the target. Since this velocity is too low, the erosion target is located in the diffuser section, where the gas stream velocity will reach about 579 m/s (1900 ft/sec) at the design conditions for the Exxon miniplant.

Two types of erosion targets will be utilized -- the cylindrical rod and the wedge target. The cylindrical target has the advantage, theoretically, of giving erosion as a function of impact angle over a full spectrum of impact angles (from 0 to 90 degrees), whereas the wedge-type target will give erosion data for a relatively narrow range of impact angles. This is particularly significant since it is anticipated that erosion will be taking place in the oxide layer, and there is no information available on the impact angle for the maximum erosion rate of the oxide layer. With the wedge-type probe, tests with a minimum of

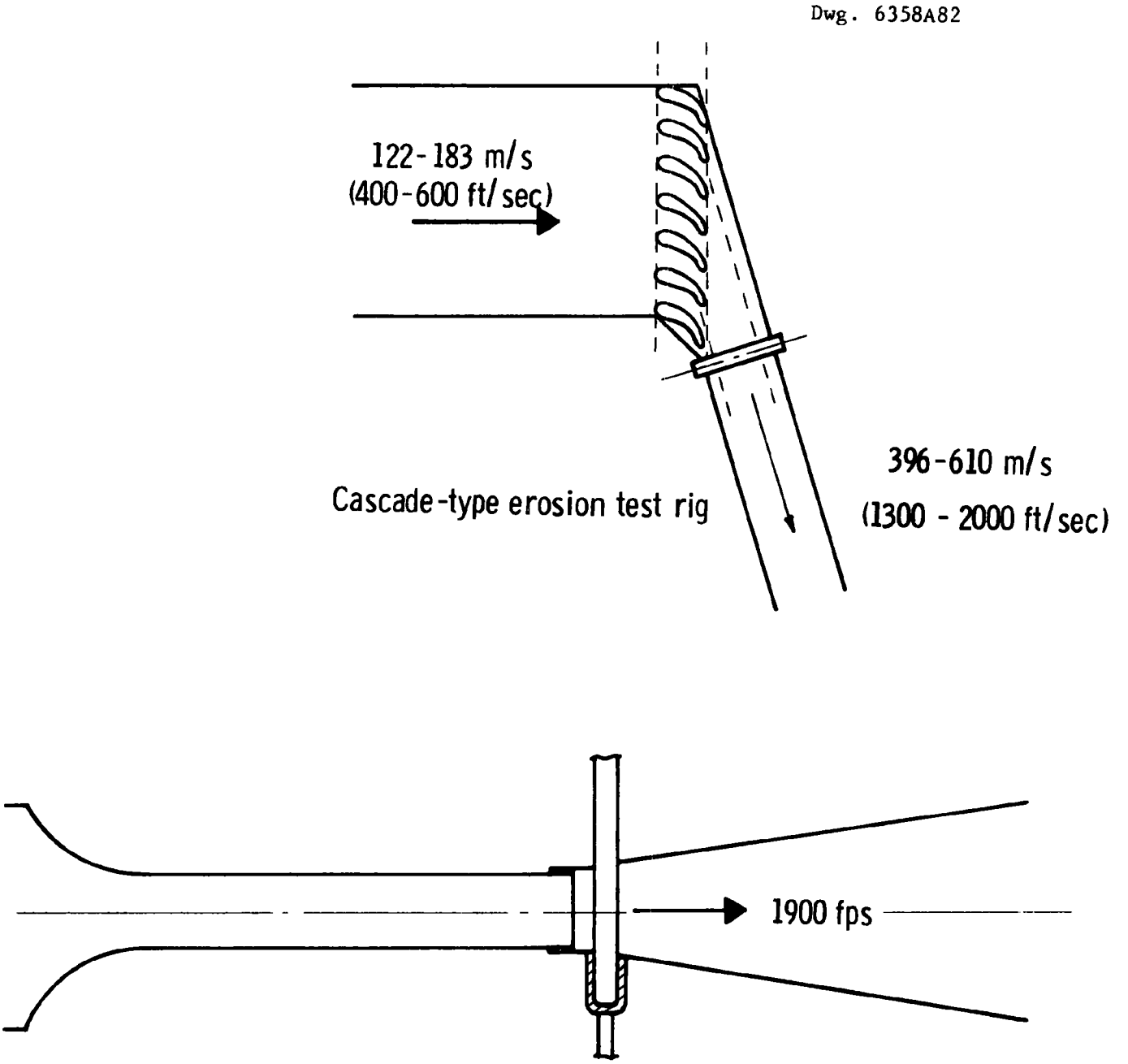

Figure 21 —Erosion test rig concept

three angles would be necessary to determine the impact angle for the maximum erosion rate. An advantage of the wedge target is that it gives a more precise measurement of the erosion rate at the impact angle of maximum erosion rate. Measurement techniques are reviewed in Appendix K.

A high-pressure, high-temperature particulate sampling system for use in the Exxon miniplant erosion/corrosion tests has been designed and constructed. A sampling probe and sampling system were designed and shipped to Exxon for use in the erosion test program.

The proposed test plan utilizes both cylindrical and wedge targets, cooled and uncooled target specimens, and four different materials. The initial test plan is for 12 test runs. A procedure was also developed to analyze results from these tests.

In summary, the straight-through erosion/corrosion test rig designed for installation in the Exxon Research and Engineering high-pressure fluidized bed boiler miniplant will simulate the most severe conditions of impact velocity, impact angle, and temperature to be found in a gas turbine in the first generation high-pressure fluidized bed boiler. However, the predicted volumetric concentration of particulates in the discharge stream from the miniplant may be more than 25 times greater than the level anticipated in the fuel-scale plant with the present particle collection system. Current plans to add another collection unit will help alleviate this problem.

VII. REFERENCES

1. Archer, D. H., et al. Evaluation of the Fluidized Bed Combustion Process. Vols. I-III. Final Report. Office of Air Pollution. Westinghouse Research Laboratories. Pittsburgh, Pennsylvania. November, 1971. Contract 70-7. NTIS PB 211-494, PB 212-916, PB 213-152.
2. Keairns, D. L. et al. Evaluation of the Fluidized Bed Combustion Process -- Vol. I and II: Pressurized Fluidized Bed Combustion Process Development and Evaluation, and Volume III: Pressurized Fluidized Bed Boiler Development Plant Design. Environmental Protection Agency. Westinghouse Research Laboratories. Pittsburgh, Pennsylvania. December, 1973. Publication No. EPA-650/2-73-048a, b and c. NTIS PB 231-162, PB 231-163, and PB 232-433.
3. Miniplant Tests. Under contract to Environmental Protection Agency. Exxon Research and Engineering Company. Linden, N.J. Contracts 68-02-1451 and 68-02-1312. 1975.
4. Keairns, D.L., R.A. Newby, B.W. Lancaster, and D.H. Archer. Sulfur and Particulate Emissions Control from Pressurized Fluidized Bed Combustion Systems. Proceedings of Fluidized Combustion Conference. Vol. I. Institute of Fuel Symposium Series No.1. 1975.
5. Keairns, D. L., W. C. Yang, J. R. Hamm, and D. H. Archer. Fluidized Bed Combustion Utility Power Plants - Effect of Operating and Design Parameters on Performance and Economics. Proceedings of the Third International Conference on Fluidized Bed Combustion. Hueston Woods, Ohio. 1972.
6. National Air Pollution Control Assocation - National Coal Board. Information Exchange Meeting in United Kingdom. April 20-24, 1970.
7. Hoy, H. R., and J. E. Stantan. Amer. Chem. Soc. Div., Fuel Chem. Prepr. 14(2):59, 1970.

8. Pressurized Fluidized Bed Combustion. Report No. 85. Interim No. 1. Office of Coal Research. National Research Development Corporation. London, England. 1974.

9. Reduction of Atmospheric Pollution. Final Report. Vols. 1-3. Office of Air Programs. National Coal Board. London, England. September 1971. PB 210-673, PB 210-674, PB 210-675.

10. Energy Conversion from Coal Utilizing CPU 400 Technology. Interim Report No. 1. Office of Coal Research. Combustion Power Company. November 1974.

11. Rincliffe, R. G. The Eddystone Story. Electrical World. March 11, 1963.

12. Keairns, D. L. Private Communication to P. P. Turner. July 15, 1974.

13. Keairns, D. L. Private Communication to R. R. Hangebrauck. July 31, 1974.

14. Harboe, H. Coal for Peak Power. Stal-Laval, Ltd. (Presented at ACS National Meeting, Chicago, August 1973). Div. of Fuel Chem. Preprints. 18 (4).

15. Fraas, A. P. Potassium-Steam Binary Vapor Cycle with Fluidized-Bed Combustion. (Presented at Annual AIChE Meeting, New York, November 1972).

16. Rossbach, R. S. Final Report of Joint NASA/OCR Study of Potassium Topping Cycles for Stationary Power. GESP 741. NASA Lewis. General Electric Company. Cincinnati, Ohio. November 13, 1973.

17. Fraas, A. P. Concept Preliminary Evaluation of Small Coal-Burning Gas Turbine for Modular Integrated Utility System. Atomic Energy Commission. Oak Ridge National Laboratory. Department of Housing and Urban Development; Office of Coal Research. May-Sept. 1974. NTIS PB 239-109.

18. Bagnulo, A. H. et al. Development of Coal-Fired Fluidized Bed Boilers. Final Report 14-01-0001-478. Office of Coal Research. Pope, Evans and Robbins. Alexandria, Virginia. 1970.

19. Multi-Cell Fluidized-Bed Boiler. Contract No. 14-32-0001-1237. Office of Coal Research, Department of the Interior. Pope, Evans and Robbins. Alexandria, Virginia.

20. Reduction of Atmospheric Pollution by the Application of Fluidized Bed Combustion and Reduction of Sulfur-Containing Additives. Annual Report. Environmental Protection Agency. Argonne National Laboratory. June, 1973. Publication No. EPA-R2-73-253. Interagency Agreement EPA-1AG-0020.

21. Robison, E. G. et al. Study of Characterization and Control of Air Pollutants from a Fluidized-Bed Combustion Unit. Environmental Protection Agency. Pope, Evans and Robbins. Contract No. CPA 70-10. 1972.

22. Gordon, J. S. et al. Study of Characterization and Control of Air Pollutants from a Fluidized-Bed Boiler -- The SO_2 Acceptor Process. Final Report. Environmental Protection Agency. Pope, Evans and Robbins. Alexandria, Virginia. Contract No. CPA 70-10. July 1972. NTIS PB 229-242.

23. Jonke, A. A. et al. Reduction of Atmospheric Pollution by the Application of Fluidized-Bed Combustion. Argonne National Laboratory Annual Report ANL-ES-CEM-1001. July 1968 to June 1969.

24. Jonke, A. A., et al. Reduction of Atmospheric Pollution by the Application of Fluidized Bed Combustion. Report ANL/ES-CEN-1004. Environmental Protection Agency. Argonne National Laboratory. June 1971.

25. Skopp, A. et al. Studies of the Fluidized Lime-Bed Coal Combustion Desulfurization System. Final Report. Environmental Protection Agency. Esso Research and Engineering. Linden, N.J. 1971. NTIS PB 210-246.

26. Hammons, G. A., and A. Skopp. A Regenerative Limestone Process for Fluidized-Bed Coal Combustion and Desulfurization. Final Report. Environmental Protection Agency. Esso Research and Engineering. Linden, N.J. February 28, 1971. PB 198-822.

27. Hoke, R. C. et al. A Regenerative Limestone Process for Fluidized Bed Coal Combustion and Desulfurization. Environmental Protection Agency. Esso Research and Engineering. Linden, N.J. EPA-650/2-74-001. January 1974.

28. Jonke, A. A. et al. Reduction of Atmospheric Pollution by the Application of Fluidized Bed Combustion. Environmental Protection Agency. Argonne National Laboratory. ANL/ES-CEN-1002, 1970.
29. Skopp, A. et al. Fluid Bed Studies of the Limestone Based Flue Gas Desulfurization Process. Final Report to NAPCA. Esso Research and Engineering. Linden, N.J. PH 86-67-130. 1969.
30. Moss, G. The Fluidized Bed Desulfurizing Gasifier. Proceedings of the 2nd International Conference on Fluidized Bed Combustion. Hueston Woods, Ohio. 1970. Published by EPA as AP-109.
31. Vogel, G. J. et al. Reduction of Atmospheric Pollution by the Application of Fluidized-Bed Combustion. Environmental Protection Agency. Argonne National Laboratories. EPA-650/2-74-057. 1974.
32. O'Neill, E. P. and D. L. Keairns. Selection of Calcium-Based Sorbents for High-Temperature Fossil Fuel Desulfurization. Westinghouse Research Laboratories. (Paper presented at 80th National AIChE Meeting, Boston, September 7-10, 1975).
33. O'Neill, E. P., D. L. Keairns and W. F. Kittle. A Thermogravimetric Study of the Sulfation of Limestone and Dolomite - The Effect of Calcination Conditions. Proceedings of the annual meeting of the North American Thermal Analysis Society. Trent University. Peterborough, Ontario. June 8-12, 1975.
34. Robinson, E. B. et al. Characterization and Control of Gaseous Emissions from Coal-Fired Fluidized Bed Boilers. Interim Report. NAPCA. Pope, Evans and Robbins. October 1970.
35. Keairns, D. L., E. P. O'Neill, D. H. Archer. Sulfur Emission Control with Limestone/Dolomite in Advanced Fossil Fuel Processing Systems. Proceedings of Symposium: Environmental Aspects of Fuel Conversion Technology. May 1974. St. Louis. EPA 650/2-74-118. 1974.
36. Curran, G. P. et al. Production of Clean Fuel Gas From Bituminous Coal. Environmental Protection Agency. Consolidation Coal Co. EPA 650/2-73-049. December 1973.
37. Advanced Coal Gasification System for Electric Power Generation. R&D Report No. 81. Interim Report No. 2. Energy Research and Development Administration. Westinghouse Electric Corporation. July 1, 1973 - June 30, 1974.

38. Keairns, D. L. et al. Fluidized Bed Residual Oil Gasification/ Desulfurization at Atmospheric Pressure. Vols. I and II. Environmental Protection Agency. Pittsburgh, Pa. Westinghouse Research Laboratories. EPA 650/2-75-027a and b. March 1975. NTIS PB 241-834 and PB 241-835.

39. Craig, J.W.T. et al. Chemically Active Fluid Bed Process for Sulfur Removal during Gasification of Heavy Fuel Oil -- Second Phase. Environmental Protection Agency. Esso Research Centre. Abingdon, England. EPA 650/2-73-039. November 1973.

40. Zeldovich, J. The Oxidation of Nitrogen in Combustion and Explosions. Acta Physicochim. URSS, 21(4) 577 (1946).

41. Nutkis, M. P. Pressurized Fluidized Bed Coal Combustion. Proceedings of International Fluidization Conference, (Engineering Foundation Conference). Asilomar Conference Grounds. California. June 15-20, 1975.

42. Jonke, A. A. et al. Reduction of Atmospheric Pollution by the Application of Fluidized-Bed Combustion. Annual Report. July 1971-June 1972, ANL/ES/CEN-1004 (1972).

43. Proceedings of Third International Conference on Fluidized Bed Combustion. Environmental Protection Agency. EPA 650/2-73-053. December 1973.

44. Ruth, L. A. Combustion and Desulfurization of Coal in a Fluidized Bed of Limestone. Exxon Research and Engineering Co. Proceedings of International Fluidization Conference (Engineering Foundation Conference). Asilomar Conference Grounds. California. June 15-20, 1975.

45. Dilmore, J. A. Nitric Oxide Formation in the Combustion of Fuels Containing Nitrogen in a Gas Turbine Combustor. ASME Paper 74-GT-37.

46. Clean Power Generation from Coal. Final Technical Report. Office of Coal Research. Westinghouse Research Laboratories. Pittsburgh, Pa. Contract 14-32-0001-1223. April 1974. NTIS PB 234-188-1.

47. Ruch, R. R., H. J. Gluskoter, et al. Occurrence and Distribution of Potentially Volatile Trace Elements from Coal. Environmental Protection Agency. Illinois State Geological Survey. EPA 650/2-74-054. July 1974.

48. Streib, D. Ohio Geological Survey. Private Communication.

49. Advanced Coal Gasification System for Electric Power Generation. Interim Report No. 3. Energy Research and Development Administration. Westinghouse Electric Corporation. July 1, 1974 - June 30, 1975.

50. Vogel, G. J., A. A. Jonke et al. Reduction of Atmospheric Pollution by the Application of Fluidized Bed Combustion and Regeneration of Sulfur-Containing Additives. Environmental Protection Agency. Argonne National Laboratories. EPA 650/2-74-104. 1975.

APPENDIX A

PERFORMANCE ANALYSIS OF HIGH-PRESSURE FLUIDIZED BED BOILER SYSTEMS

APPENDIX A

PERFORMANCE ANALYSIS OF HIGH-PRESSURE FLUIDIZED BED BOILER SYSTEMS

MODIFICATION IN PERFORMANCE CALCULATION PROCEDURES

The procedure used for calculating the performance of high-pressure fluidized bed boiler systems as reported in References 1 and 2 has been revised. The heat rates given in these references were calculated using the conventional boiler efficiency expression. For the parametric studies reported in Reference 1, an assumed boiler efficiency value of 89.6 percent was used.

The conventional loss factors for Ohio Pittsburgh No. 8 seam coal with 3 percent moisture, a stack-gas temperature of 135°C (275°F) and 17.5 percent excess air, and regenerative desulfurization were calculated to be as follows:

• Sensible heat loss of dry stack gas	3.88%
• Sensible and latent heat losses of moisture in coal and water from hydrogen in fuel	4.14
• Sensible heat loss of moisture in air	0.08
• Radiation loss	0.15
• Incomplete combustion	1.50
• Sensible heat loss of solids	0.11
• Unaccounted-for losses and manufacturer's margin	1.50
TOTAL	11.36%

This gives a boiler efficiency of 88.6 percent,which was used to calculate the heat rates used for energy cost estimates in Reference 1 and all of the heat rates in Reference 2.

It has been determined that the conventional definition of boiler efficiency is not applicable to the high-pressure fluidized bed

boiler system, and a corrected boiler efficiency has been developed for use instead. The correct procedure for calculating the plant heat rate for a high-pressure fluidized bed boiler system with in-bed desulfurization is as follows:

- Ideal fuel rate:

(W_f) ideal = (heat to steam + heat to gas turbine)/LHV

- Plant heat rate (HHV):

Plant heat rate = $((W_f)$ ideal x HHV)/[(net plant power)(combustion efficiency)]

$$= \left(\frac{\text{heat to steam + heat to gas turbine}}{\text{net plant power}}\right)\left(\frac{\text{(HHV/LHV)}}{\text{combustion efficiency}}\right)$$

The loss factors for Ohio Pittsburgh seam No. 8 coal with 3 percent moisture and once-through desulfurization are as follows:

• Incomplete combustion	1.50%
• Radiation losses	0.04
• Sensible heat in solid wastes	1.50
• Heat absorbed by desulfurization reactions	(-0.80)
• Unaccounted-for losses and manufacturer's margin	1.50
TOTAL	4.10%

If the difference between the higher and lower heating values of this coal is included as a boiler loss factor (as it is in the conventional boiler efficiency expression), there is an additional loss factor of 3.9 percent and the total losses are 8.0 percent. The combustion efficiency for the high-pressure fluidized bed boiler is, therefore, 92.0 percent rather than the calculated conventional boiler efficiency value of 88.6 percent.

Those heat rates calculated using a boiler efficiency of 88.6 percent are 3.8 percent higher than they should have been; and the heat rates for the parametric studies in Reference 1, which were based

*In this case the ratio HHV/LHV becomes part of the boiler efficiency.

on an assumed boiler efficiency of 89.6 percent, were 2.7 percent higher than they should have been. The corrected heat rate for the base case wherein the condenser pressure is 1-1/2 in Hg,the boiler efficiency is 92.0 percent, and the gas-turbine pressure loss is 7.5 percent is, therefore, 9040 (8568) rather than 9381 kJ/kWh (8892 Btu/kWh).

EFFECT OF GAS-TURBINE DISCHARGE TEMPERATURE LIMIT ON OPERATION

The Westinghouse Gas Turbine Engine Division limits the discharge temperature of the gas turbines which it manufacturers to 538°C (1000°F). This limit imposes constraints on the operation of the high-pressure fluidized bed boiler systems which use these gas turbines. These constraints can be defined in terms of minimum allowable pressure ratios for given values of turbine inlet temperature and air equivalence ratios.* Minimum allowable cycle pressure ratios for turbine inlet temperatures of 871, 927, and 982°C (1600, 1700, and 1800°F) and for an air equivalence ratio of 1.1 are shown on Figure A-1 to be 5.7, 7.2, and 8.9 respectively.

Figure A-2 shows that the minimum allowable cycle pressure ratio imposed by the 538°C (1000°F) limit on turbine discharge temperature is a weak function of the air equivalence ratio.

The cycle pressure ratio at which the plant heat rates of high-pressure fluidized bed boilers are minimum is about 8:1 (see Figure A-3). For the range of turbine inlet temperatures which are of interest in fluidized bed combustion, the minimum allowable cycle pressure ratio imposed by the 538°C (1000°F) limit on gas-turbine discharge temperature is, therefore, generally lower than the value for minimum plant heat rate. It can be concluded, therefore, that a 538°C (1000°F) limit on the discharge temperature of gas turbines used in high-pressure fluidized bed boilers does not impose a significant constraint on the operation of the boiler system unless the turbine inlet temperature exceeds 982°C (1800°F).

For a gas-turbine cycle with an adiabatic combustor, the optimum pressure ratio is greater than for that of the pressurized boiler cycle. The gas-turbine discharge temperature limit, therefore, imposes even less of a constraint on its operation.

* Ratio of actual to stoichiometric air/fuel ratios.

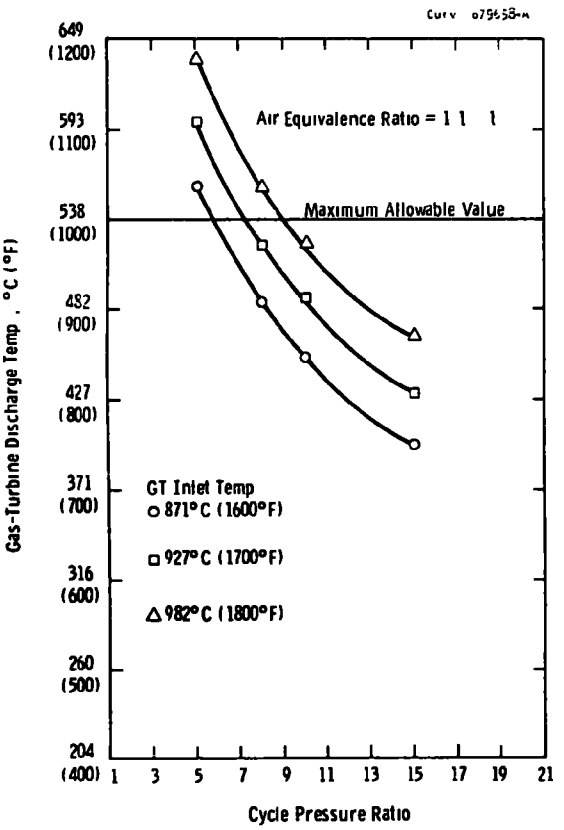

Figure A-1—Performance of pressurized fluidized bed power plant

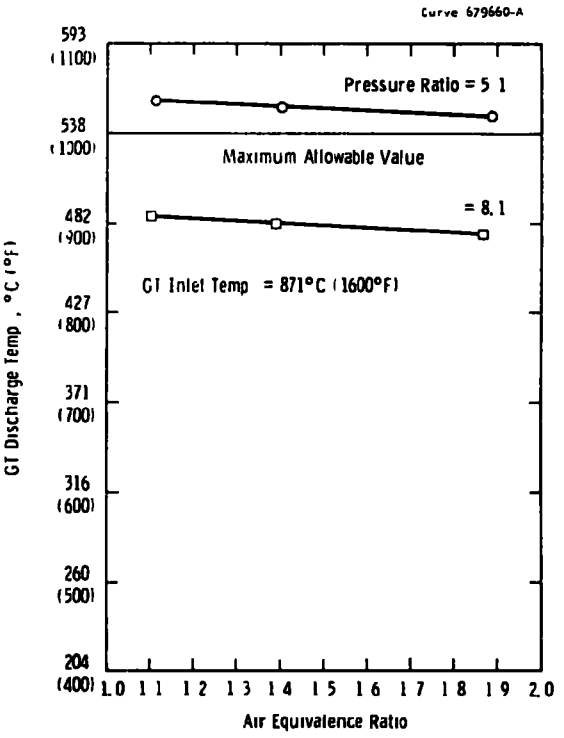

Figure A-2—Performance of pressurized fluidized bed power plant

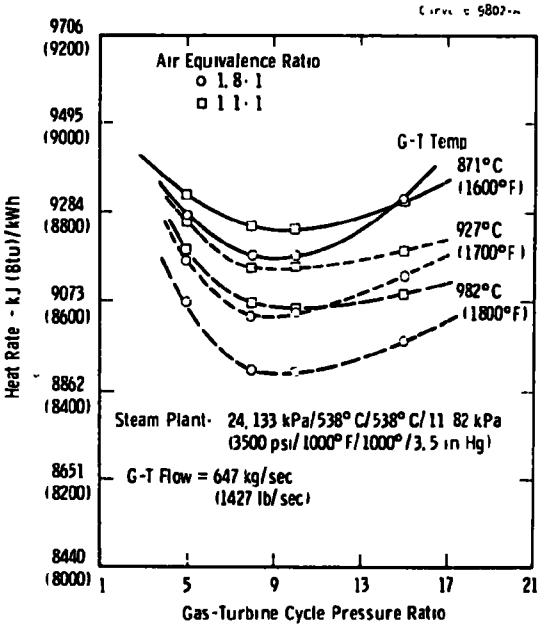

Figure A-3—Performance of pressurized fluidized bed power plant vs cycle pressure ratio

EVALUATION OF LOW-TEMPERATURE CLEANUP OF COMBUSTION PRODUCTS

One of the design premises for the high-pressure fluidized bed boiler design concept has been particulate removal at boiler outlet temperature. Since the cost of particulate removal equipment is a rather strong function of operating temperature level, there is a possibility that the minimum cost for energy produced by the high-pressure fluidized bed boiler would occur when particulate removal is carried out at a reduced temperature level. There is also a possibility that the only practical technique for particulate removal which would give the required degree of removal for reasonable turbine life is scrubbing. A study has been carried out, therefore, to determine the performance penalty which accompanies reduced temperature techniques for removing particulates from the combustion products of a high-pressure fluidized bed boiler.

Two alternatives have been investigated:

- Cooling the combustion products by the use of a convection-type boiler and removing particulates by cyclone separators, tornado separators, electrostatic precipitators, or combinations thereof at intermediate temperatures
- Cooling the combustion products with a recuperator followed by a scrubber-cooler.

The arrangement for the high-pressure fluidized bed boiler system with intermediate temperature particulate removal is shown in Figure A-4. The convection-type boiler for cooling the products of combustion to a temperature well below the bed operating temperature is in series/parallel* with the fluidized bed boiler. This permits the temperature of the combustion products to be reduced from 871°C (1600°F) to the gas-turbine idle temperature which is in the range of 482 to 538°C (900 to 1000°F) and independent of air equivalence ratio.

If the plant were operated with the gas-turbine inlet temperature at or near the idle valve, plant turndown (by reducing bed temperature)

---

* Series for combustion products-parallel for working fluid.

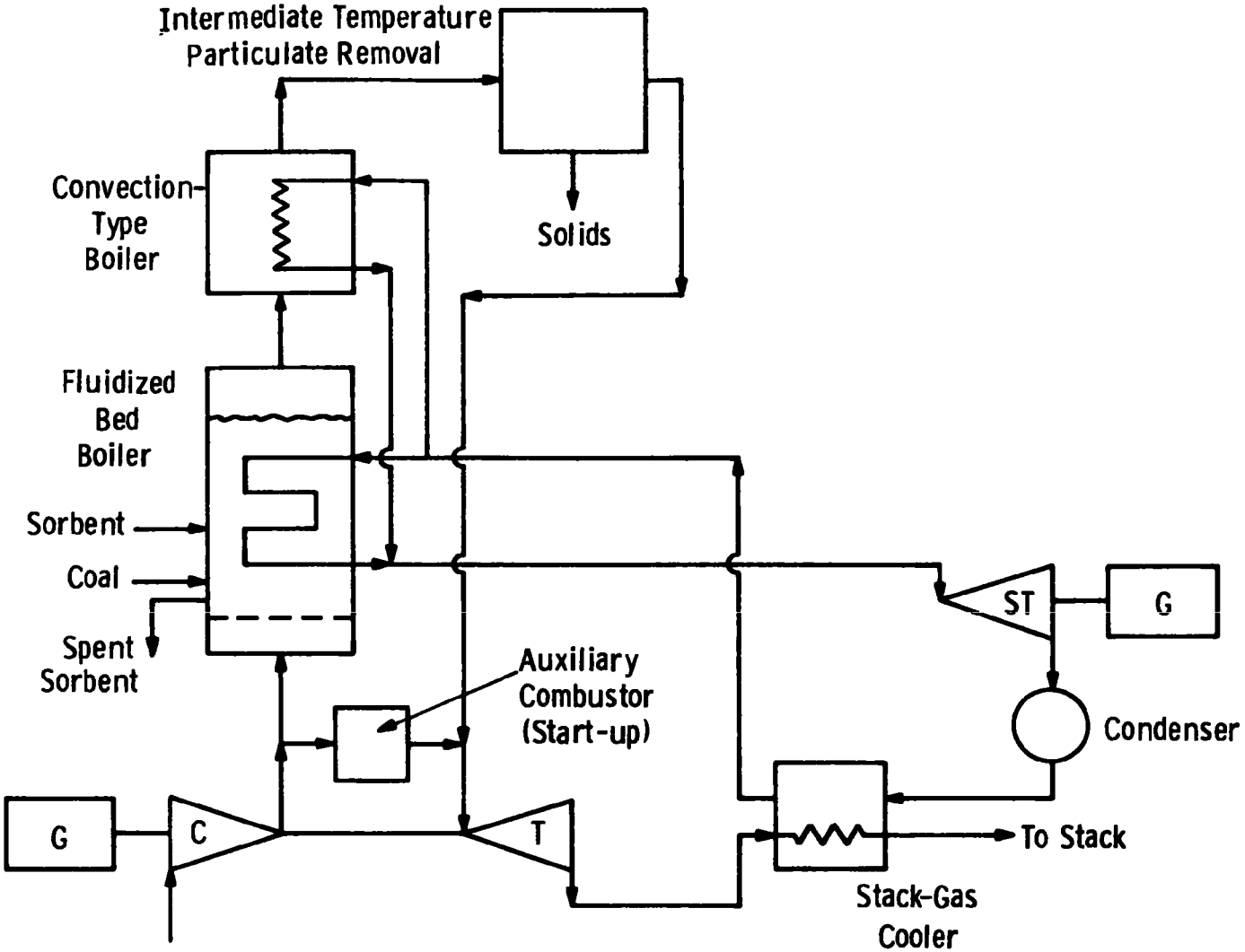

Figure A-4 —High-pressure fluidized bed boiler power system with intermediate temperature particulate removal

would require by-passing of a fraction of the products of combustion around the convection boiler in order to maintain the turbine inlet temperature at or above the minimum value. This minimum value will increase as bed temperature decreases, because of the reduction in the quantity of combustion products to the turbine.

The effect of gas-cleaning temperature on plant capacity is shown in Figure A-5. This shows that plant capacity decreases about 8 MW per 56°C (100°F) drop in temperature.

The effect of the gas-cleaning temperature on the plant heat rate is shown in Figure A-6. This indicates that the plant heat rate increases about 158 kJ (150 Btu)/kWh for each 56°C(100°F) drop in temperature.

The arrangement of the high-pressure fluidized bed boiler with low-temperature particulate removal is shown in Figure A-7. The hot combustion products are passed through one stage of cyclone separation to recover the larger fraction of the char particles which are elutriated from the bed so that the carbon losses will be reduced to a minimum value. The effluent from the char separator will retain the finer ash particles with relatively low carbon content. This stream will be cooled to a temperature in the range of from 93 to 204°C (200 to 400°F), depending on the recuperator effectiveness and the temperature of the cold products of combustion out of the scrubber-cooler.

In the scrubber-cooler the products are evaporatively cooled to the saturation line and then further cooled along the saturation line until the water vapor content of the gas mixture is equal to the initial value out of the fluidized bed boiler. The initial water vapor content of the combustion products is a function of the coal composition and the percent excess air in the fluidized bed combustor, and the final temperature of the products out of the scrubber-cooler is a function of the water vapor content and the system pressure ratio. The temperature of the clean fuel gas leaving the scrubber-cooler and entering the recuperator is, therefore, a function of the excess air in the combustion process and the system pressure ratio.

Westinghouse made performance calculations for the parametric combinations shown in Table A-1 to determine the effect of air equivalence ratio, boiler outlet temperature, system pressure ratio, and recuperator effectiveness.

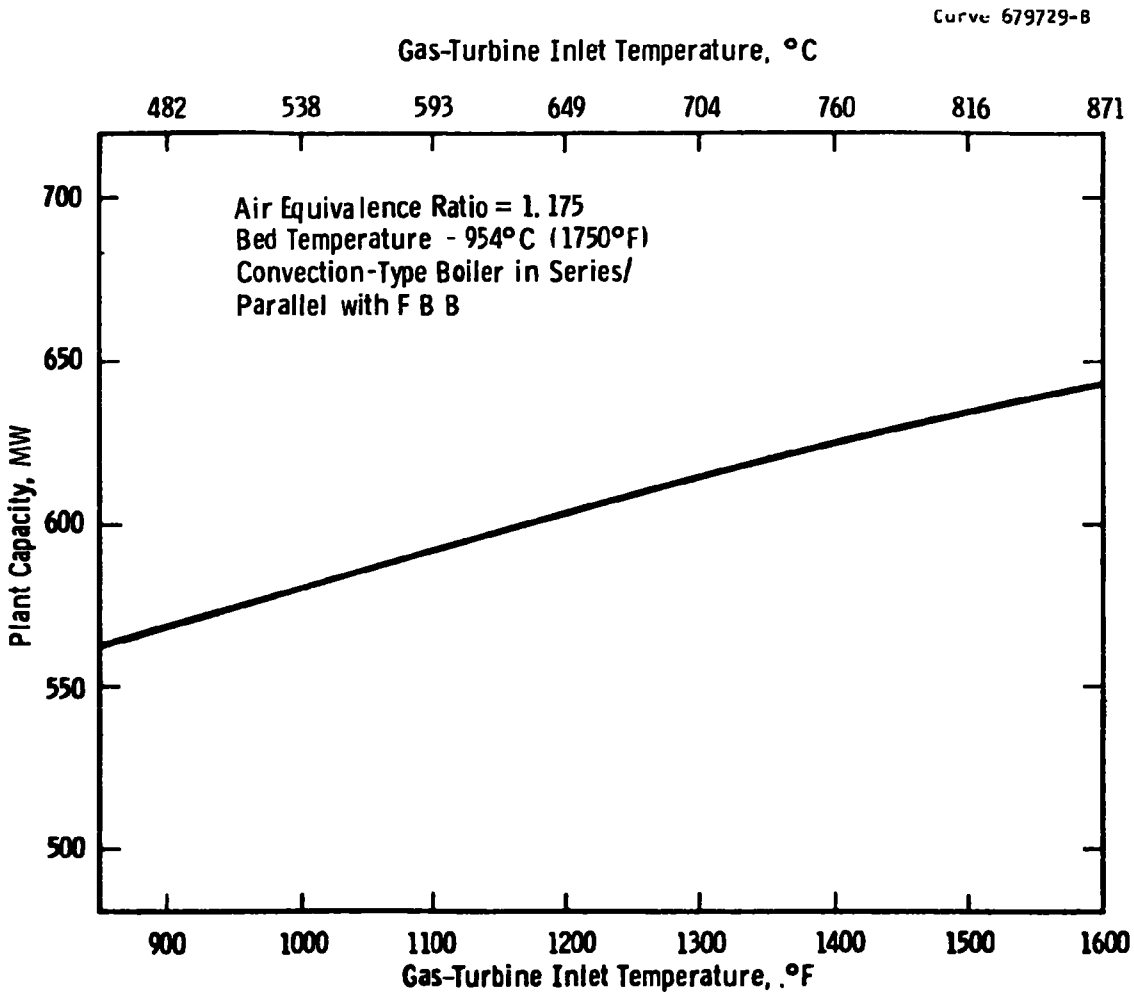

Figure A-5—Plant capacity vs gas-turbine inlet temperature for high-pressure fluidized bed boiler with intermediate temperature particulate removal

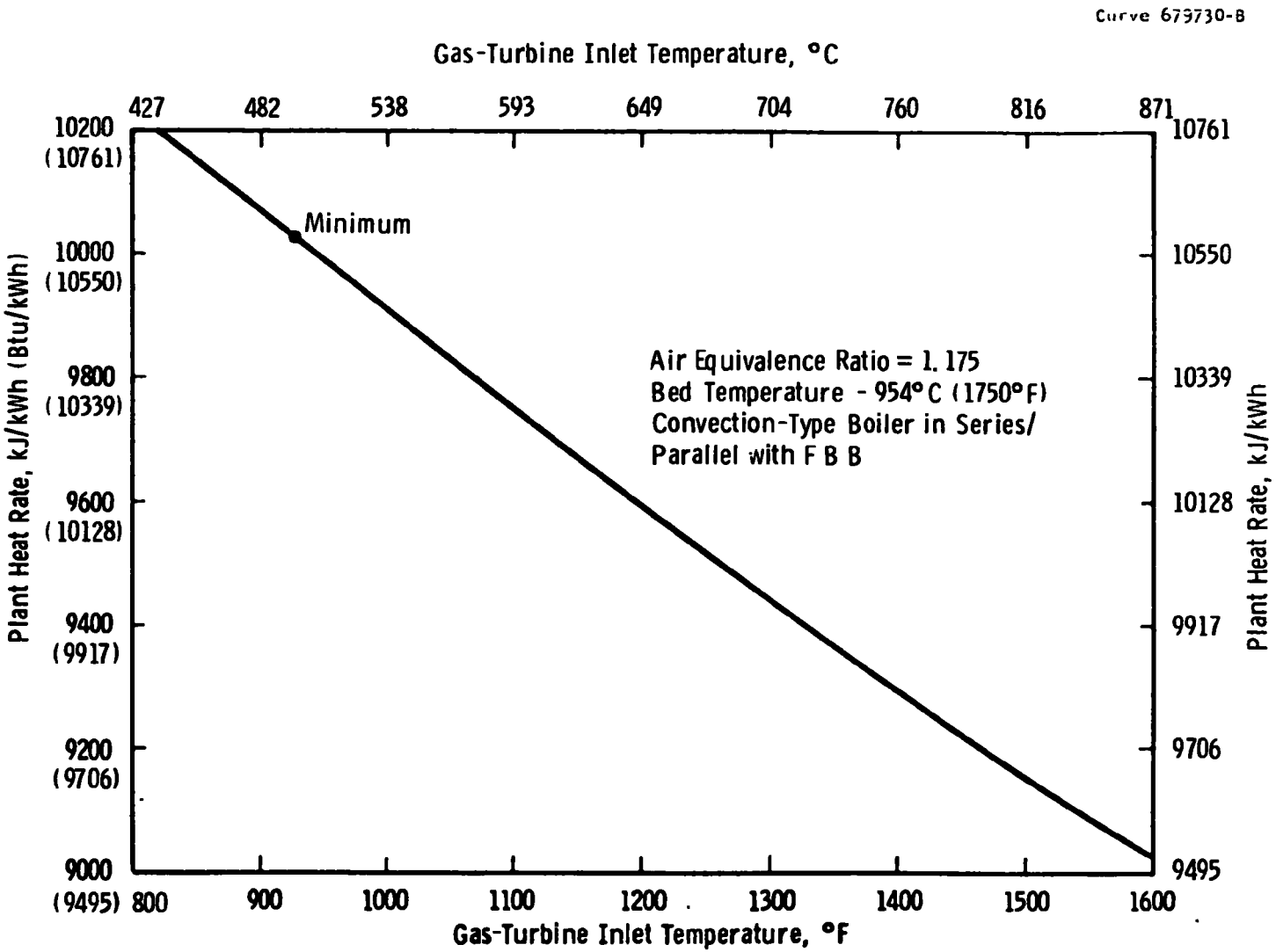

Figure A-6—Plant heat rate vs gas-turbine inlet temperature for high-pressure fluidized bed boiler with intermediate temperature particulate removal

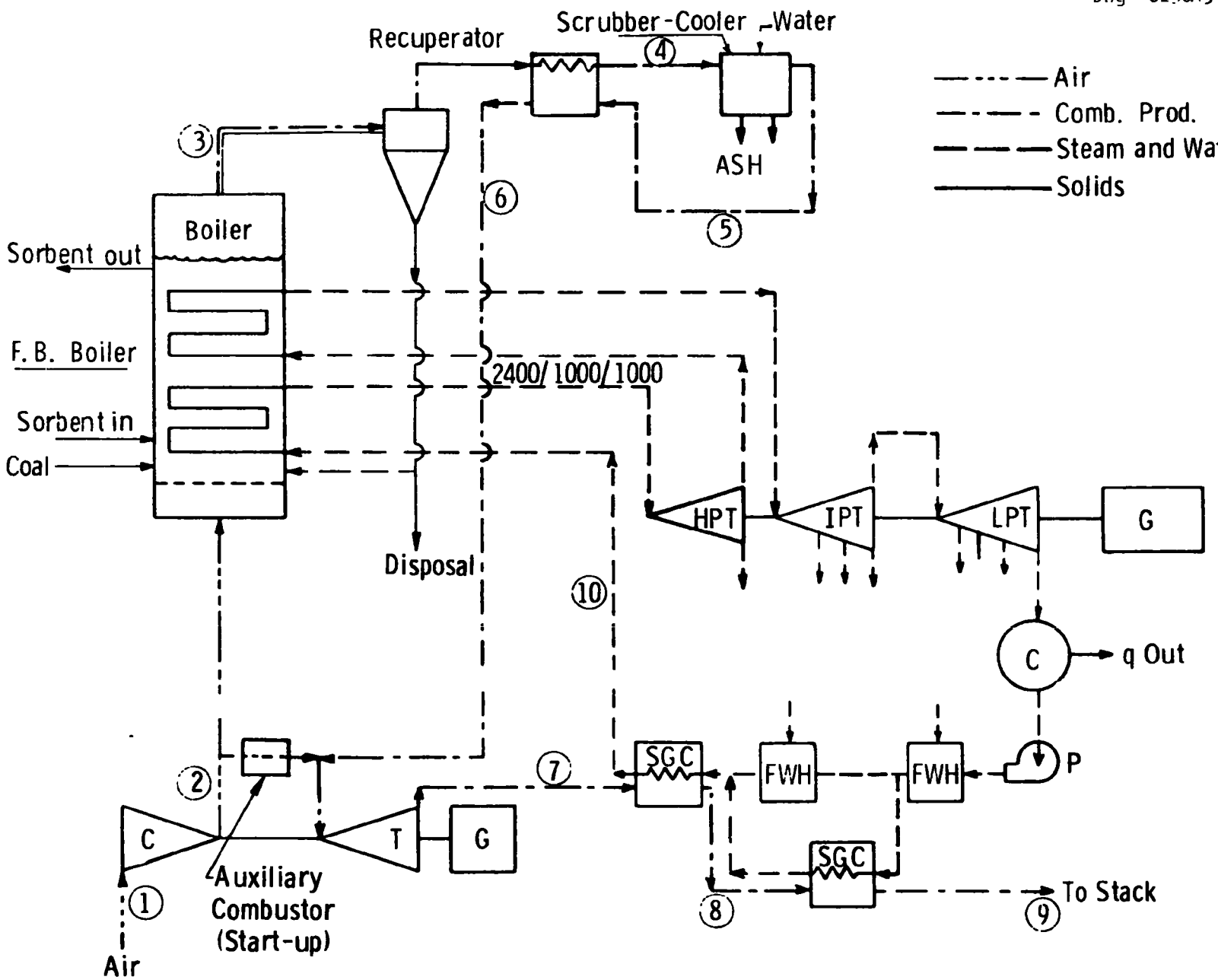

Figure A-7—Pressurized fluidized bed combustion power plant with cold cleanup of combustion products

Table A-1

PARAMETRIC COMBINATIONS USED IN PERFORMANCE CALCULATIONS[a]

Case	Φ_{air} [b]	Boiler outlet temp., °C (°F)	System press. ratio	Recuperator effectiveness [c]
1	1.175	871 (1600)	10	0.860
2	1.175	871 (1600)	10	0.930
3	1.175	871 (1600)	10	0.789
4	1.50	871 (1600)	10	0.860
5	2.00	871 (1600)	10	0.860
6	1.175	927 (1700)	10	0.860
7	1.175	816 (1500)	10	0.860
8	1.175	871 (1600)	15	0.860
9	1.175	871 (1600)	5	0.860

[a] A gas-turbine compressor air flow of 635 kg/s (1400 lb/sec) was used for all cases.

[b] Air equivalence ratio.

[c] Recuperative effectiveness = $(t_3 - t_4)/(t_3/t_5)$. See Figure A-7.

The temperatures at each of the ten stations shown in Figure A-7 for the nine cases are shown in Table A-2:

Table A-2

TEMPERATURES FOR TEN STATIONS

Station number	Temperature °C (°F)								
	Case 1	Case 2	Case 3	Case 4	Case 5	Case 6	Case 7	Case 8	Case 9
1	15 (59)	15 (59)	15 (59)	15 (59)	15 (59)	15 (59)	15 (59)	15 (59)	15 (59)
2	313 (596)	313 (596)	313 (596)	313 (596)	313 (596)	313 (596)	313 (596)	387 (728)	204 (400)
3	871 (1600)	871 (1600)	871 (1600)	871 (1600)	871 (1600)	927 (1700)	816 (1500)	871 (1600)	871 (1600)
4	191 (376)	136 (276)	247 (476)	189 (372)	183 (362)	198 (389)	182.5 (361)	200 (392)	177 (350)
5	90 (176)	80 (176)	80 (176)	77 (171)	71 (160)	80 (176)	80 (176)	90 (195)	64 (147)
6	760 (1400)	816 (1500)	704 (1300)	759.5 (1399)	759 (1398)	808 (1487)	713 (1315)	762 (1403)	758 (1397)
7	376 (709)	412 (773)	340 (644)	371 (700)	365 (689)	407 (764)	345 (653)	326 (618)	474 (885)
8	274 (525)	274 (525)	274 (525)	274 (525)	274 (525)	274 (525)	274 (525)	274 (525)	274 (525)
9	135 (275)	135 (275)	135 (275)	135 (275)	135 (275)	135 (275)	135 (275)	135 (275)	135 (275)
10	286 (547)	298 (568)	274 (525)	296 (565)	314 (598)	298 (569)	274.5 (526)	268 (515)	318 (604)

The calculated plant power outputs and plant heat ratio are shown in Table A-3:

Table A-3
PLANT POWER OUTPUTS AND HEAT RATES

Case	Plant power - kw	Plant heat rate kJ/kWh (Btu/kWh)
1	612410	10058 (9534)
2	630150	9650 (9147)
3	596594	10485 (9938)
4	469945	10254 (9719)
5	343700	10553 (10003)
6	606535	10007 (9485)
7	626762	10078 (9553)
8	608780	10139 (9610)
9	610404	10113 (9586)

Plant heat rate as a function of recuperator effectiveness is shown plotted on Figure A-8. The heat rate is shown to increase about six percentage points for each ten percentage points decrease in recuperator effectiveness.

Plant heat rate is plotted as a function of gas-turbine pressure ratio on Figure A-9. This shows that plant heat rate is a rather weak function of pressure ratio and that the optimum pressure ratio is about 8.5:1.

Plant heat rate is plotted as a function of boiler outlet temperature on Figure A-10. This indicates that over the range of boiler outlet temperatures which correspond to upper and lower limits on fluidized bed temperatures with in-bed desulfurization, in other words, 926

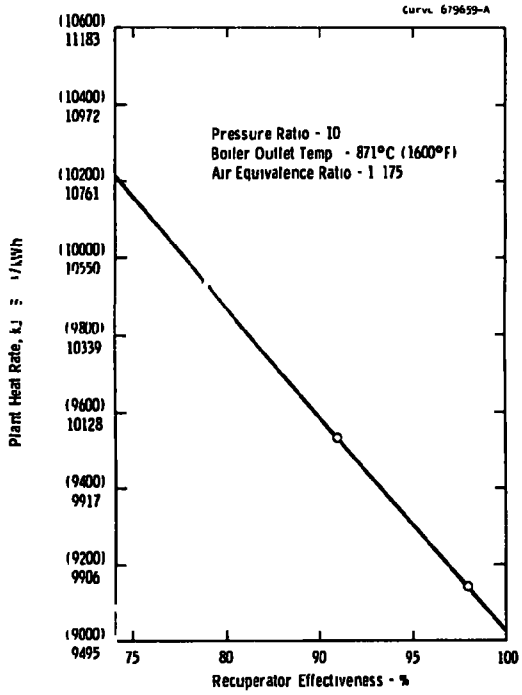

Figure A-8—Plant heat rate vs recuperator effectiveness

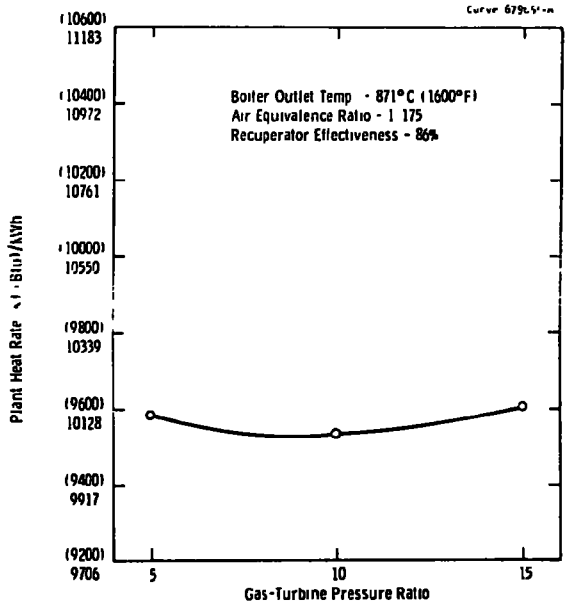

Figure A-9—Plant heat rate vs gas-turbine pressure ratio

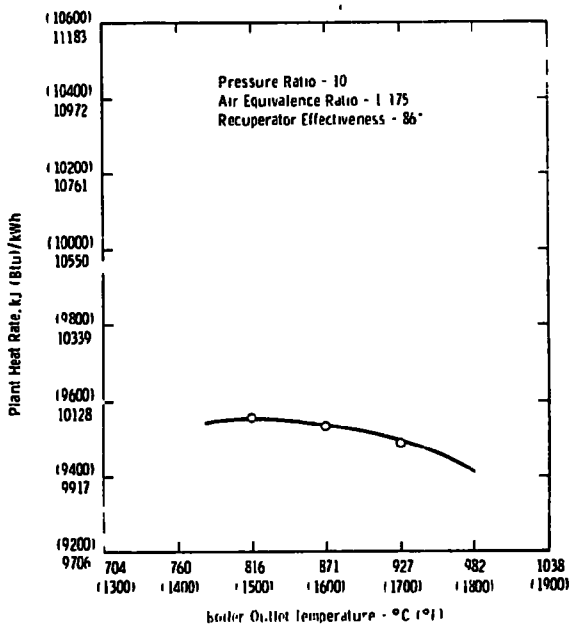

Figure A-10 -Plant heat rate vs boiler outlet temperature

and 704°C (1700 and 1300°F) respectively, the heat rate varies only about one percent.

Plant heat rate is plotted as a function of air equivalence ratio on Figure A-11 This shows that the heat rate is a rather strong function of air equivalence ratio, with the heat rate increasing with an increasing air equivalence ratio. This results from the increase in the fraction of gas-turbine power as the air equivalence ratio increases and indicates that the optimum air equivalence ratio is the minimum level which will give good carbon burn-up—in other words, 1.15 to 1.20.

COST ESTIMATE

Order of magnitude cost estimates have been made to evaluate the intermediate temperature and water scrubbing options for gas cleaning. First, the PFBB investment cost of $265/kw[3] for a 635 MW installation was escalated to late 1974, using the Chemical Engineering construction cost index for process facilities, to give a November 1974 cost of $355/kw. Then, the cost for a third stage of granular bed filter particulate removal was added to the PFBB investment. The installed subcontract cost for the eight pairs of granular bed filters required to clean up the effluent from the eight tornado cyclones constituting the second particulate removal stage in a 600 MW unit in late-1974 is $16,128,000. When interest during construction, escalation during construction, and so on are added to this, the total installed cost of the granular bed filtration third-stage particulate removal is $23,452,000, or $39/kw. Thus $355 plus $39,or $394/kw,represents the late 1974 cost of a PFBB installation based on 17.5 percent excess air. If 100 percent excess air is used in the PFBB, the boiler effluent gas quantity increases and so does the cost of removing particles from it. The $39/kw derived above, plus $25/kw for the first two stages of particulate removal, total $64/kw. This, when increased to accommodate the larger gas volume at 100 percent excess air design, becomes $96/kw. The total PFBB cost, therefore, becomes $355-25+96 = $426/kw. This amount does not account for the incremental change in the boiler and power generation equipment cost which will result from higher excess

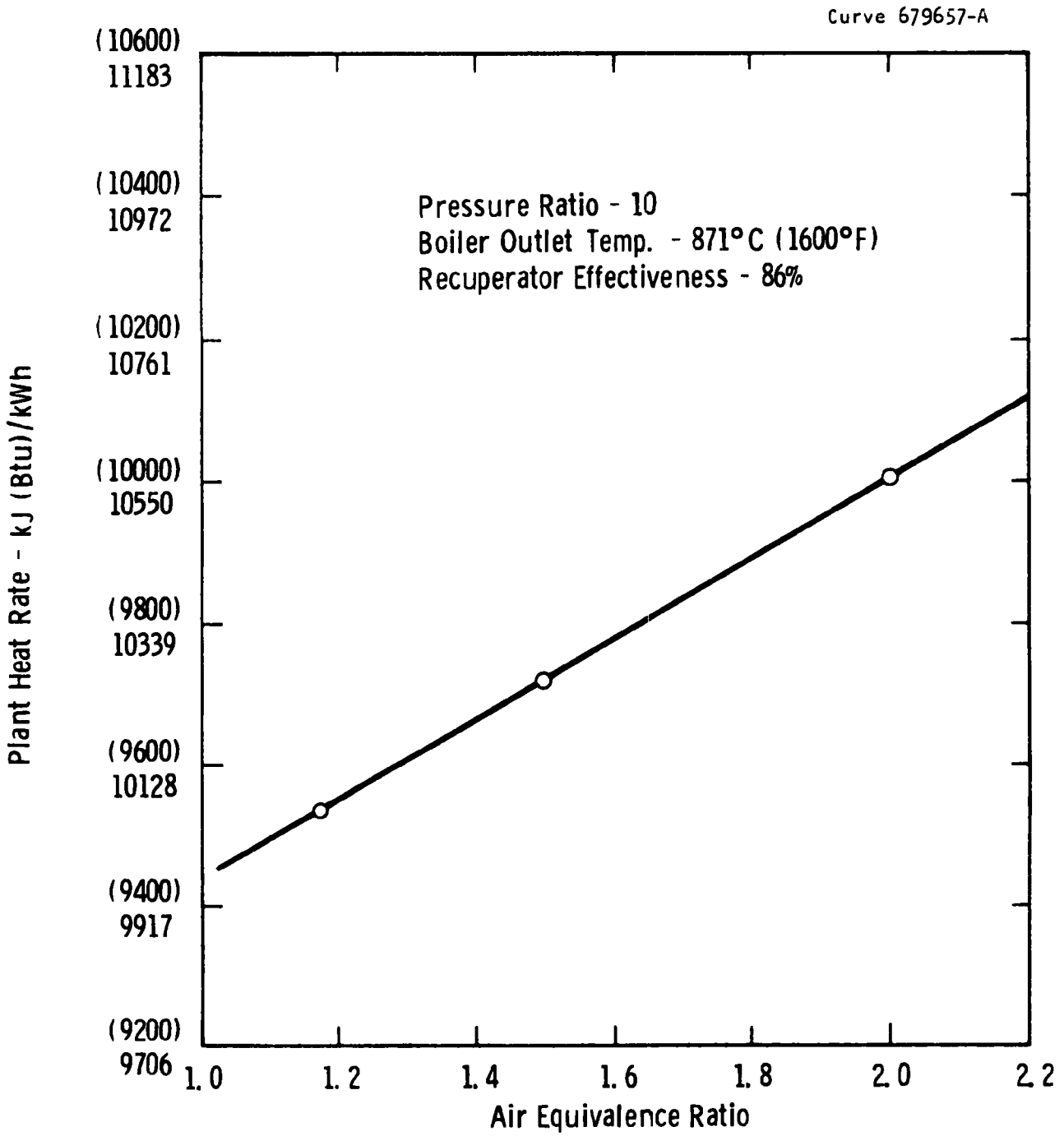

Figure A-11—Plant heat rate vs. air equivalence ratio

air. The boiler cost is reduced as the result of changes in the shell and heat transfer surface costs and elimination of a carbon burn-up cell. The power generation equipment cost increases slightly due to the shift in the percentage of gas turbine power generated. Finally, the $340/kw cost for a conventional stream power plant with a stack-gas scrubber was updated. Removing $30/kw for the scrubbing unit, and escalating by the above referenced cost index to late 1974, gives $415/kw. If the recent TVA-evaluated [4] limestone scrubbing system minimum costs of $50/kw are added, the minimum cost for a steam power plant with limestone scrubbing is $465/kw, and that cost, according to TVA, could range as high as $530/kw.

With cooling of the 871°C (1600°F) PFBB products of combustion in a waste heat boiler to 482°C (900°F) so as to permit metal such as low chrome-molybdenum steel alloy to be substituted for refractory lining, it can be seen from Figure A-12 that total costs rise (for a PFBB with conventional cyclones in series with tornado cyclones and granular bed filters) so that the plant cost at 427°C (800°F) gas cleanup temperature is $458/kw. Most of the rise in cost is due to decreased plant output. Investment costs for refractory-lined and low-alloy steel particulate removal equipment goes down as temperature (and gas volume) go down, while waste heat boiler cost goes up as cleaning temperature goes down. These two cost trends tend to cancel each other. The net $/kw increase, then, is due entirely to the loss in plant output shown earlier in Figure A-5.

If an electrostatic precipitator could replace the tornado cyclones and granular bed filters at 538°C (1000°F), approximately $65/kw or $39 million would be saved in particulate removal installed-system costs. The cost of a pressurized, 538°C (1000°F), low-sulfur-content gas precipitator has been investigated to determine if cost savings would be possible from its use. A precipitator design based on 1.5 m (3.5 ft)/sec velocity adds roughly $25/kw for installed-system costs. Thus, it is apparent that precipitators may be substantially

Curve 681705-A

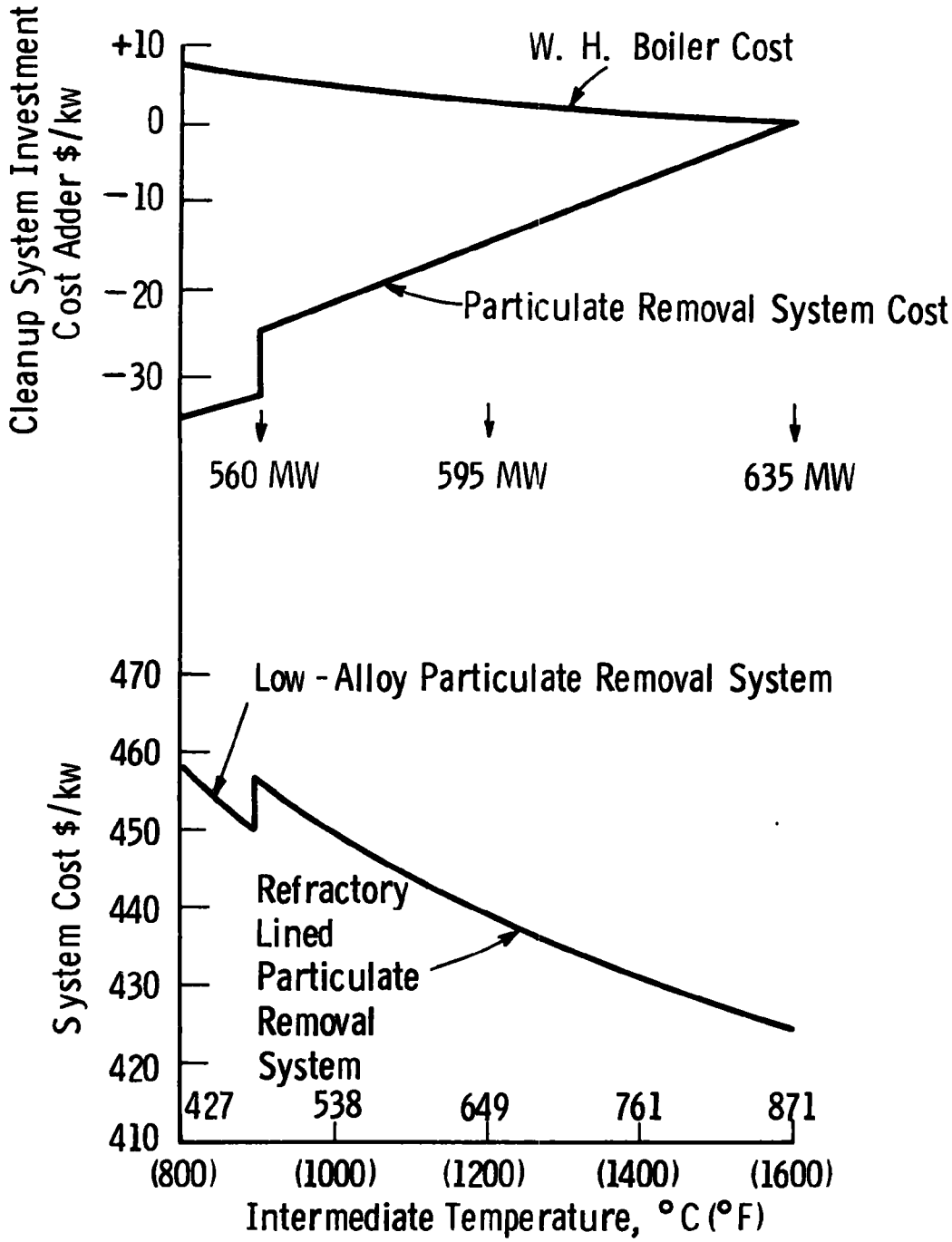

Figure A-12—Intermediate temperature gas cleaning for PFBB (Nominal 635 MW size)

less expensive than tornado cyclone and granular bed filter combinations at 538°C (1000°F).

An inquiry to the EPA staff at Research Triangle Park revealed that Mr. J. Abbott at that location is instigating work on hot pressurized electrostatic precipitators. Mr. Abbott explained during a subsequent phone conservation that Research Cottrell will soon receive an EPA contract to study pressurized precipitators. Mr. Abbott pointed out, though, that present indications are not very optimistic regarding the performance of the pressurized units. Collection efficiency, gas density, charge potential, and other factors indicate that pressurized precipitation will be difficult. Also, 538°C (1000°F) is possibly too high a temperature for effective precipitator operation. A 316°C (600°F) temperature level may be much better for electrostatic precipitators at 1013 kPa (10 atm). In any case, Research Cottrell will quantify the problems involved in hot pressurized electrostatic precipitation in their forthcoming contract.

Costs were obtained for the cases in Table A-2 dealing with wet-scrubbing alternative systems. It immediately became apparent that for Case 4 (50 percent excess air) and Case 5 (100 percent excess ari) wet scrubbing was uneconomical. The losses in cycle efficiency, plus the larger size wet scrubbers and recuperators required, added more than $150/kw for Case 4 and $350/kw for Case 5, making total plant costs $505/kw and $705/kw respectively. They are both costs that exceed the conservatively estimated dry particulate removal cost of $426/kw for a 100 percent excess air PFBB installation.

It is apparent from the cost increases incurred by Cases 4 and 5 that a wet-scrubbing gas cleanup system would also be much too costly for use with adiabatic combustion to be competitive with conventional boiler/scrubber power systems.

Order-of-magnitude costs for the 17.5 percent excess air cases showed Case 7 to have the least added cost for wet scrubbing, and Case 2 to have the highest added cost. All of these eight cases showed between

$40 and $75/kw added costs for wet scrubbing, with about $55/kw a representative average added cost. Considering the very approximate type of cost estimating used, and until more becomes known about actual costs for the Incoloy 617 heat exchange material assumed for the very large (46,450 to 139,350 m^2/500,000 to 1,500,000 ft^2 of surface) recuperative heat exchangers used in the cost estimates, no firm conclusions can be drawn regarding the relative costs of the seven cases studied with 17.5 percent excess air.

It may be of future interest to compare cold sulfur dioxide removal, once the gas was cooled for particulate removal in a 17.5% excess air design, with the cost of hot limestone pickup of sulfur dioxide. The pressurized low-temperature sulfur dioxide scrubber may possibly be less costly than once-through limestone for sulfur dioxide removal.

PERFORMANCE OF THE HIGH-PRESSURE FLUIDIZED BED BOILER WITH ADVANCED STEAM CONDITIONS

Reference 5 contains performance data on high-pressure fluidized bed boiler systems with steam conditions of 22,754 kPa/593°C/593°C (3300 psi/1100°F/1100°F) and 31,028 kPa/649°C/593°C (4500 psi/1200°F/1100°F). Performance calculations have now been extended to even higher steam conditions of 31,028 kPa/649°C/649°C (4500 psi/1200°F/1200°F) and 34,475 kPa/760°C/760°C (5000 psi/1400°F/1400°F). Figure A-13 is a plot of the plant heat rate as a function of the air equivalence ratio with steam condition parameters for a gas-turbine inlet temperature of 871°C (1600°F), 10:1 pressure ratio, and a steam condenser pressure of 11.82 kPa (3-1/2 in. Hg). This shows that the plant heat rate is a weak function of the air equivalence ratio for all supercritical steam conditions.

Steam conditions of 31,028 kPa/649°C/649°C (4500 psi/1200°F/1200°F) have a potential for plant heat rates which are 8 to 10 percent better than for those steam conditions which currently predominate in conventional steam plants—in other words, 16,548 kPa/538°C/538°C (2400 psi/1000°F/1000°F) and 24,133 kPa/538°C/538°C (3500 psi/1000°F/1000°F). These steam conditions are similar to the design conditions for Eddystone No. 1,

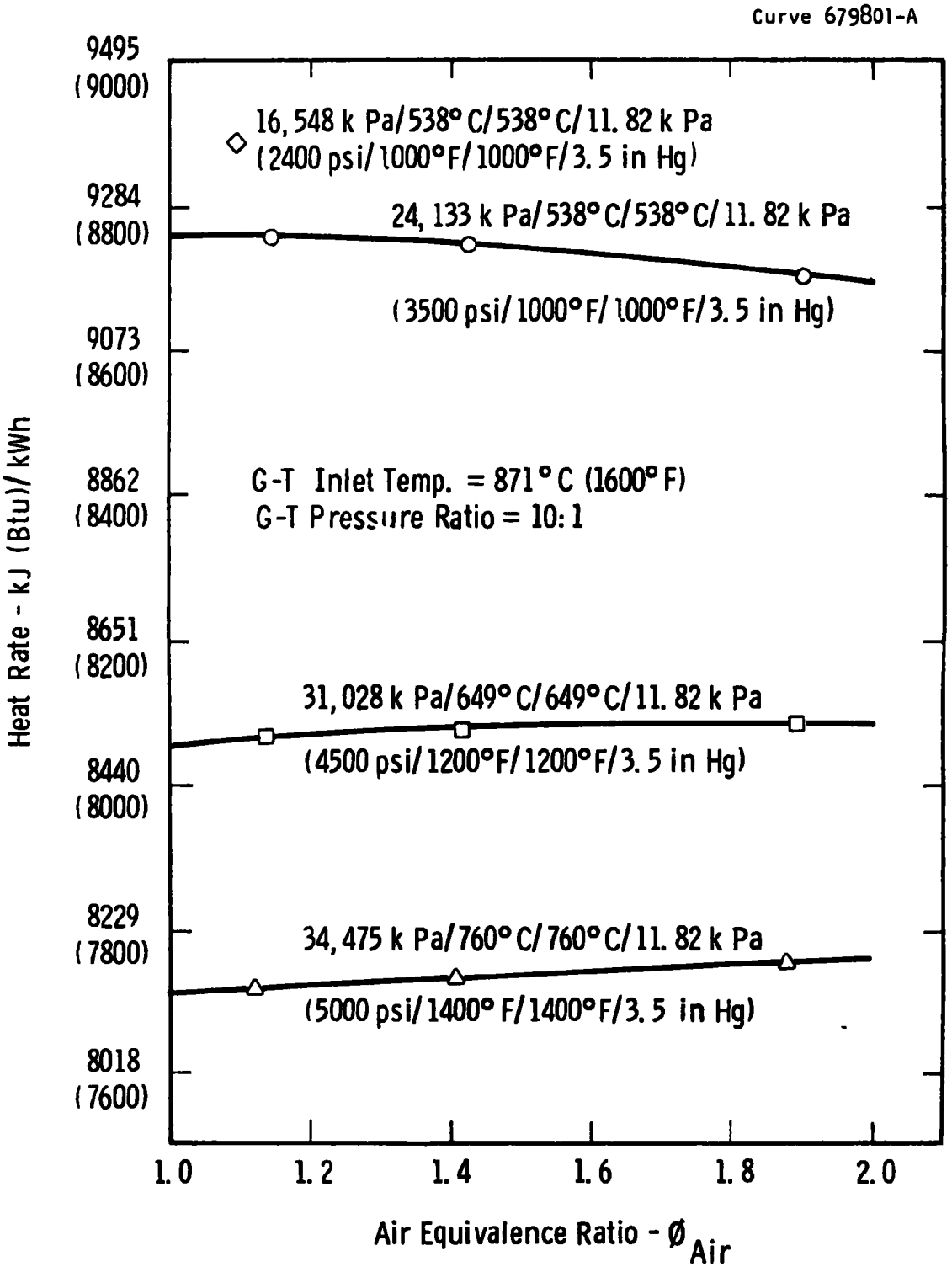

Figure A-13—Performance of pressurized fluidized bed power plant with advanced steam conditions

34,475 kPa/649°C/566°C/566°C (5000 psi/1200°F/1050°F/1050°F). The Eddystone plant has had only limited operation at design conditions but extensive operation at a superheat temperature of 613°C (1135°F). Operation is limited to superheat temperatures less than 649°C (1200°F) by low-cycle fatigue problems on turbine control and stop valves. The operation of the boiler and steam turbine at 649°C (1200°F) superheat temperature is reported to be technically and economically feasible. The equivalent plant efficiency level for these steam conditions is about 44 percent.

Steam conditions of 34,475 kPa/760°C/760°C (5000 psi/1400°F/1400°F) can potentially further improve plant heat rate by 4 to 5 percent. These steam conditions, however, are well beyond the state-of-the-art technology for steam superheaters and steam turbines. (See discussion of advanced steam cycles technology in Appendix L.)

REFERENCES

1. Archer, D. H. et al. Evaluation of the Fluidized Bed Combustion Process. Office of Air Programs. Environmental Protection Agency. Westinghouse Research Laboratories. Pittsburgh, Pennsylvania. Contract 70-9. NTIS PB 211494 and PB 212916. November 1971. Vols. I and II.
2. Keairns, D. L., et al. Evaluation of the Fluidized Bed Combustion Process. Office of Research and Development. Environmental Protection Agency. Westinghouse Research Laboratories. Pittsburgh, Pennsylvania. EPA-650/2-3-73-048 a, b, c, d. Contract 68-02-0217. December 1973. Volumes I to IV. NTIS PB 231 162/9, 231 163/7, 232 439/3, and 233 101/5.
3. Ibid. Volume I. p. 25.
4. McGlamery, G. G., et al. Detailed Cost Estimates for Advanced Effluent Desulfurization Processes. Tennessee Valley Authority. Muscle Shoals, Alabama. January 1975. TVA-Bull-Y-90, EPA/600/2-75-006. PB-242 541/1WP 429p.
5. Reference 2. Volume I. p. 97.

APPENDIX B

BOILER DESIGN EVALUATION

APPENDIX B

BOILER DESIGN EVALUATION

Problems are invariably associated with a new development such as fluidized bed combustion boilers. The potential technical uncertainties have been discussed previously.[1] The evaluation here will be confined to those problems pertaining to the fluidized bed boiler design alone.

In order to optimize boiler design, deep fluidized beds on the order of 3.35 to 4.27 m (11 to 14 ft) deep were selected. Fluidizing velocities of 1.83 to 2.74 m/sec (6 to 9 ft/sec) were proposed in the basic design. Both the bed depth and the operating velocity are outside the range of experimental conditions employed in the pilot-scale units of other contractors. The recent completion of a pressurized fluidized bed combustion experimental series in the British Coal Utilization Research Association (BCURA) pilot unit and the start-up of the Exxon Research and Engineering Company, Linden, New Jersey (Exxon) miniplant have contributed significantly to the understanding of coal combustion in a pressurized fluidized bed combustor. We are now in a better position to assess the operating conditions and design parameters set for the basic boiler design.

REVIEW OF EXPERIMENTAL DATA

BCURA Pilot-Scale Unit

Combustor Design[2]

The pressurized combustor was a 0.91 m by 0.61 m (3 ft by 2 ft) fluidized bed housed in a refractory-lined pressure shell of 1.83 m (6 ft) diameter. Heat transfer surfaces in the form of tube bundles were located at different levels. The lowest tube bundle, which was always immersed

in the fluidized bed during normal operation, was referred to as the "bed cooling coils." In the freeboard there were two sets of uncooled baffle tubes which helped to reduce solids carry-over. The top tube bundle, situated above the baffle tubes, was referred to as the "freeboard cooling coils." The bed cooling coils were of 25.4 mm (1 in) outside diameter, stainless steel tubing. There were 25 rows of tubes linked into 10 separate cooling circuits located between 394 mm (15.5 in) and 1410 mm (55.5 in) from the distributor plate. The 25 rows were arranged on a staggered configuration with 152 mm (6 in) horizontal pitch and 38 mm (1.5 in) vertical pitch.

Air to fluidize the bed was supplied through a distributor plate with 185 stainless steel tubes on a 52.4 mm by 95.3 mm (2-1/16 by 3-3/4 in) square pitch. The tubes were closed off at the upper ends. Four holes were drilled through the tube walls 25.4 mm (1 in) above the upper surface of the supporting mild-steel plate. The unfluidized bed below the holes acted as an insulating layer between the hot fluidized bed and the supporting mild-steel plate.

Four coal-feed nozzles, two on each side of the casing along the 0.91 m (3 ft) dimension, were situated 88.9 mm (3.5 in) above the distributor plate. The water-cooled nozzles were 19.1 mm (3/4 in) inside diameter and extended 10.2 mm (4 in) horizontally into the bed.

Two natural-gas-fired burners with a nominal maximum heat output of 422 million J/hr (0.4 million Btu/hr) each were provided for initial bed heating and for igniting propane vapor supplied via the distributor plate.

Experimental Conditions[2]

The operating conditions are compared with those of the basic design in Table B-1. The main changes in operating variables during the experiments were:

- Bed temperature - 899°C and 954°C (1650°F and 1750°F)
- Coal source - Pittsburgh and Illinois coals
- Type of additive - Dolomite and limestone
- Ratio of calcium/sulfur input - 1.4 to 2.2 mole/mole.

Table B-1

COMPARISON OF OPERATING CONDITIONS

	Basic design	BCURA unit	Exxon miniplant	
			Test conditions to date	Design conditions
Fluidizing velocity, m/sec (ft/sec)	1.83-2.74 (6-9)	0.67-0.76 (2.2-2.5)	1.83-3.05 (6-10)	3.05 (10)
Bed depth (expanded) m (ft)	3.35-4.27 (11-14)	1.22-1.43 (4.0-4.7)	0.91-4.57 (3-15)	up to 4.57 (up to 15)
Combustor pressure, kPa (atm)	1013 (10)	456 (4.5-5.0)	405-1013 (4-10)	1013 (10)
Excess air, %	17.5	14-20	25-130	---
Bed temperature, °C (°F)	954 (1750)	884-952 (1630-1745)	815-982 (1500-1800)	982 (1800)

Experimental Results[2]

The experimental results are discussed below. Only results relevant to the boiler design are included here.

Combustion Efficiency. The combustion efficiency increased significantly with an increase in bed temperature. The results from these experiments at bed temperatures of 899°C (1650°F) and 954°C (1750°F) are compared with earlier data obtained at 799°C (1470°F) and 17 percent excess air in Figure B-1. There was no detectable combustion in the freeboard at either 899°C (1650°F) or 954°C(1750°F) bed temperatures, while 2 to 3 percent heat input was released in the freeboard during combustion at 799°C (1470°F). At a 799°C (1470°F) bed temperature, the combustion efficiency was also sensitive to the amount of excess air, increasing from about 96 percent at 10 percent excess air to 97.5 percent at 17 percent and 99 percent at 25 percent.

Heat Transfer Coefficient. The average bed-tube heat transfer coefficients were 380 W/m^2-°K (67 Btu/ft^2-hr-°F) at 899°C (1650°F) bed temperature and 403 W/m^2-°K (71 Btu/ft^2-hr-°F) at 954°C (1750°F). The presence of the tube bank did not affect the heat transfer coefficient significantly. The heat transfer coefficients in the lower 3048 mm (12 in) of the bed where there was no tube bank present were only about five percent higher.

Corrosion of Metal Specimens in the Bed. Metal specimens were examined metallographically after 100 hours' exposure. The duration of exposure was too short to make any generalized conclusion regarding the corrosion. For 1 percent, 2-1/4 percent, and 12 percent chrome steel specimens, the attack was slight, with no evidence of intergranular penetration at temperatures up to their respective recommended maximum operating limits for use in steam boilers. The weight losses are summarized in Table B-2. Comparison with the previously longer duration runs is shown graphically in Figure B-2. Apparently, weight loss reaches a reliable, steady

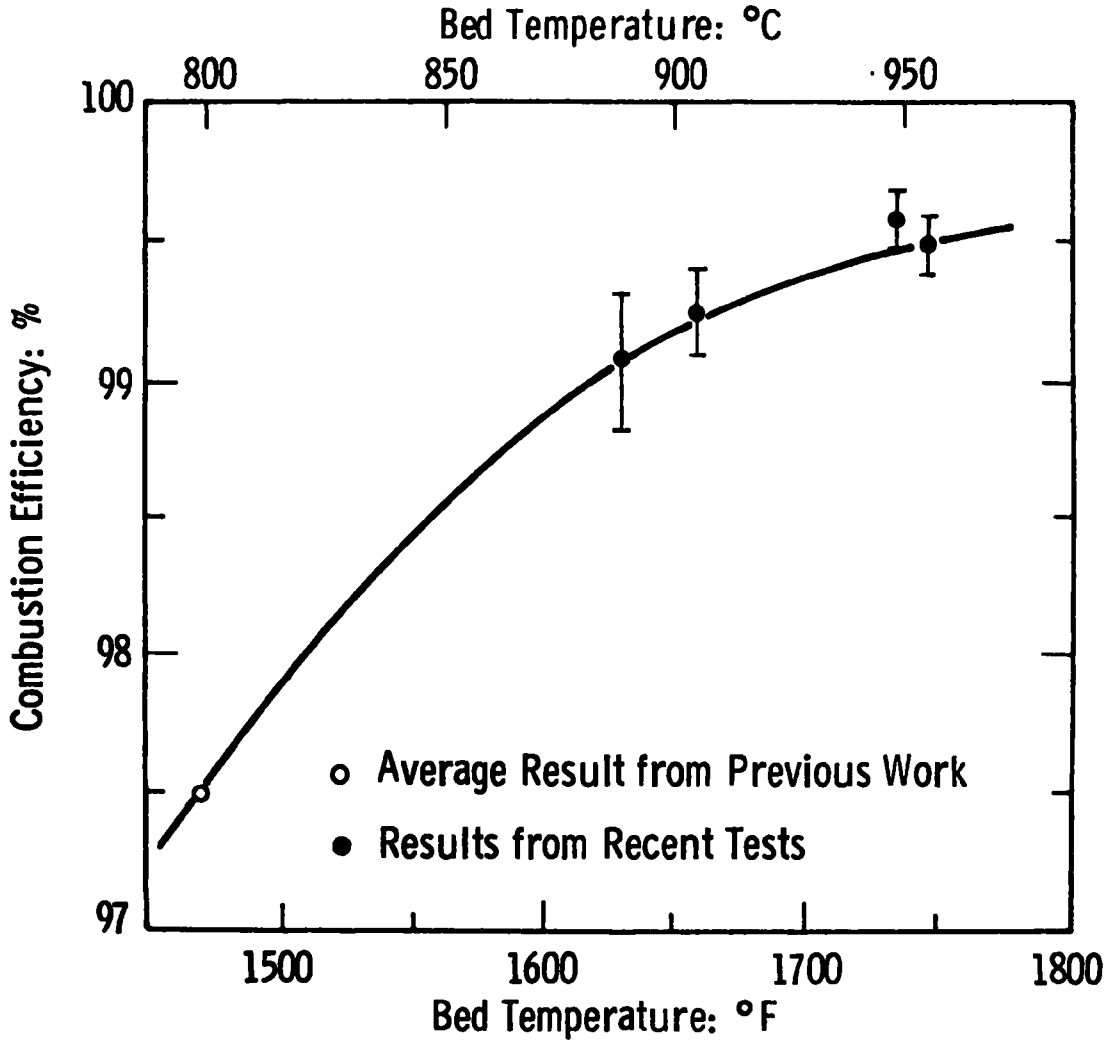

Figure B-1—Effect of bed temperature on combustion efficiency with 17% excess air

Table B-2

SUMMARY OF WEIGHT LOSS MEASUREMENTS
(100 hours' duration)

Alloy		Tube temperature, °C (°F)	Weight loss $\mu g/cm^2h$	Previous measurements in fluidized beds[a] (500 hours & 1000 hours' duration)
1% Chrome		199-371 (390-700)	100	No data
2—1/4% Chrome	(a)	371-538 (700-1000)	260	180 to 230 $\mu g/cm^2h$ @ 499°C [930°F]
	(b)	260-677 (500-1250)	400	570 to 970 $\mu g/cm^2h$ @ 599°C [1110°F]
12% Chrome	(a)	521-660 (970-1220)	160	7 to 14 $\mu g/cm^2h$ @ 699°C [1290°F]
	(b)	671-777 (1240-1430)	170	790 to 1000 $\mu g/cm^2h$ @ 840°C [1560°F]
18% Chrome (AISI 321)	(a)	621-749 (1150-1380)	70	10 - 20 $\mu g/cm^2h$ @ 699°C [1290°F] For AISI
	(b)	777-832 (1430-1530)	40	10 - 70 $\mu g/cm^2h$ @ 840°C [1560°F] 316
21% Chrome (Incoloy 800)		749-827 (1380-1520)	45	No data

[a] National Coal Board. Reduction of Atmospheric Pollution. Final Report. Environmental Protection Agency. September 1971.

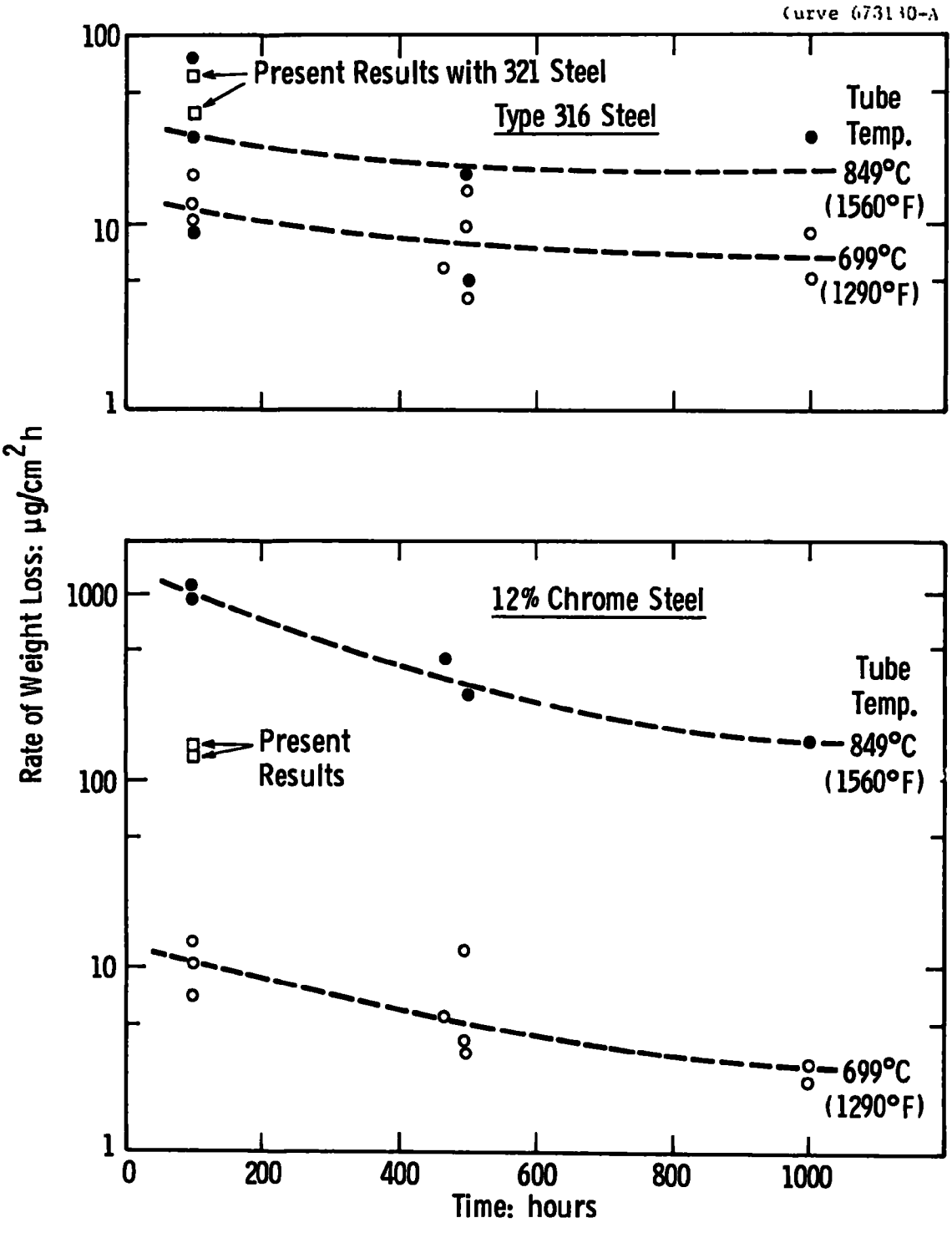

Figure B-2—Effect of time on corrosion (previous results in fluidized beds)[2]

state only after long duration -- a few hundred hours for high-alloy materials and at least 1000 hours for low-alloy materials. On the basis of experimental results, the wastage was not excessive for alloys operating up to their recommended maximum design temperatures for use in steam boilers. With Incoloy 800, which is a possible material for air heater applications, attacks at 816°C (1500°F) appeared to be minimal.

Temperature Distribution in the Bed. Temperature distribution throughout the bed was reasonably uniform. In tests at 899°C (1650°F) the bed temperature measured by 14 thermocouples from a point 76 mm (3 in) above the distributor air nozzles to the top of the bed varied only by about 5.5°C (10°F). The corresponding variation at 954°C (1750°F) bed temperature was 19°C (66°F).

General Operation. No difficulty was experienced in feeding coal into the bed at any of the operating conditions. No substantial operational difference was observed between Pittsburgh and Illinois coals. Although no clinker or accumulation formed in the bed or on the tubes in the bed, extensive accumulations formed on the cooling coils in the freeboard at 954°C (1750°F) bed temperature, but not at 899°C (1650°F). The deposits were extremely powdery and crumbled away on touching.

A refractorylike deposit accumulated on the walls of the primary cyclone but not on the secondary cyclone and interconnecting ducts. The dense and hard deposit contained mainly calcium and magnesium compounds. The deposit was more prevalent at 954°C (1750°F) than at 899°C (1650°F). The deposit did not affect the cyclone efficiency. A refractory-lined cyclone with hotter inside-wall temperature may prevent this condensation.

Exxon Miniplant

Combustor Design[3,4]

The combustor was a 610 mm (24 in) steel sheet lined with refractory to an actual internal diameter of 318 mm (12.5 in). The

reactor was constructed in flanged sections with an overall height of 9.76 m (32 ft). The heat transfer surface in the bed was provided with 19 mm (3/4 in) outside diameter stainless steel serpentine tubes on a 57 mm (2-1/4 in) horizontal pitch. Each loop occupied 457 mm (18 in) of bed height, and approximately 0.7 m^2 (7.5 ft^2) of surface area. Altogether, ten individual loops were available for controlling the bed temperature. The bottom of the first coil was located 686 mm (27 in) above the grid, and the top of the last coil, 5 m (16.5 ft) above the grid. The overall heat transfer coefficients were determined during experiments by measuring the cooling-water flow and temperature. The coolant (demineralized water) entered and left the combustor through five coolant distributor plates between flanges at 0.9 m (3 ft) vertical intervals.

Fluidizing air was supplied by a stationary compressor at operating pressure up to 862 kPa (125 psig). The air passed through the distributor plate and out through two stages of cyclones for solids removal before it was cooled in a heat exchanger. The distributor plate was a 10 mm (3/8 in) stainless steel plate with 137 air nozzles on a 23.8 mm (15/16 in) square pitch. The nozzles were 16 mm (5/8 in) in diameter and contained eight equally spaced horizontal holes of 2.0 mm (5/64 in) diameter. The nominal pressure drop through the grid was 483 mm (19 in) of water. One coal feedpoint was provided at about 279 mm (11 in) above the grid.

Experimental Conditions[4]

The miniplant is in the shakedown phase of operation. The test conditions to date are summarized and compared with those of the basic design in Table B-1. The design conditions of the miniplant are similar to those of the basic design.

Experimental Results

No comprehensive experimental results are available so far; some important preliminary results, however, can be briefly discussed here.

Temperature Distribution in the Bed. Contrary to the observation in the BCURA unit, where a small temperature gradient 19°C (66°F) was observed in a 1.3 m (4.4 ft) bed depth at 927°C (1700°F) bed temperature, the temperature gradient in the miniplant during shakedown runs (curves 1 and 2, Figure B-3) was 56 to 83°C (100 to 150°F) for a 0.9 m (3 ft) static bed and 167 to 222°C (300 to 400°F) for a 1.5 m (5 ft) static bed at 927°C (1700°F) bed temperature. The highest temperature invariably occurred at the vicinity of the coal feedpoint.

Substantial improvements in fluidization and heat dispersion throughout the fluidized bed combustor have been accomplished recently by modifications to the coil configuration, orientation, and distribution along the bed height.[5] The bed temperature variations are currently less than 67°C (120°F) within the first 3 m (10 ft) of the expanded bed at a combustor operating temperature of 927°C (1700°F) (see curves 3 and 4 in Figure B-3.) Vertical tube orientation was found to be superior to horizontal tube orientation in smoothing out the temperature gradient in the combustor.

Corrosion of Boiler Tubes in the Bed. Samples from the bottom-most cooling coil were examined after exposure to the high-temperature coal combustion conditions for approximately 50 hours. The temperature in the combustion zone near this coil ranged from 816 to 1010°C (1500 to 1850°F). Short intervals of temperatures exceeding 1066°C (1950°F) were also experienced. The water temperature inside the coil tube varied from 138 to 160°C (280 to 320°F). The results of the metallurgical analysis showed no evidence of corrosion or deterioration of the coil.

A section of the 3 mm (1/8 in) stainless steel supporting rod was also subjected to metallurgical analysis. The rod was not cooled and, therefore, was exposed to the high-temperature environment existing in the combustor. The results showed carbide precipitation in the grain boundaries and signs of corrosion.

General Operation. No great difficulty was encountered in operating the combustor. The pressurized coal-feeding system was

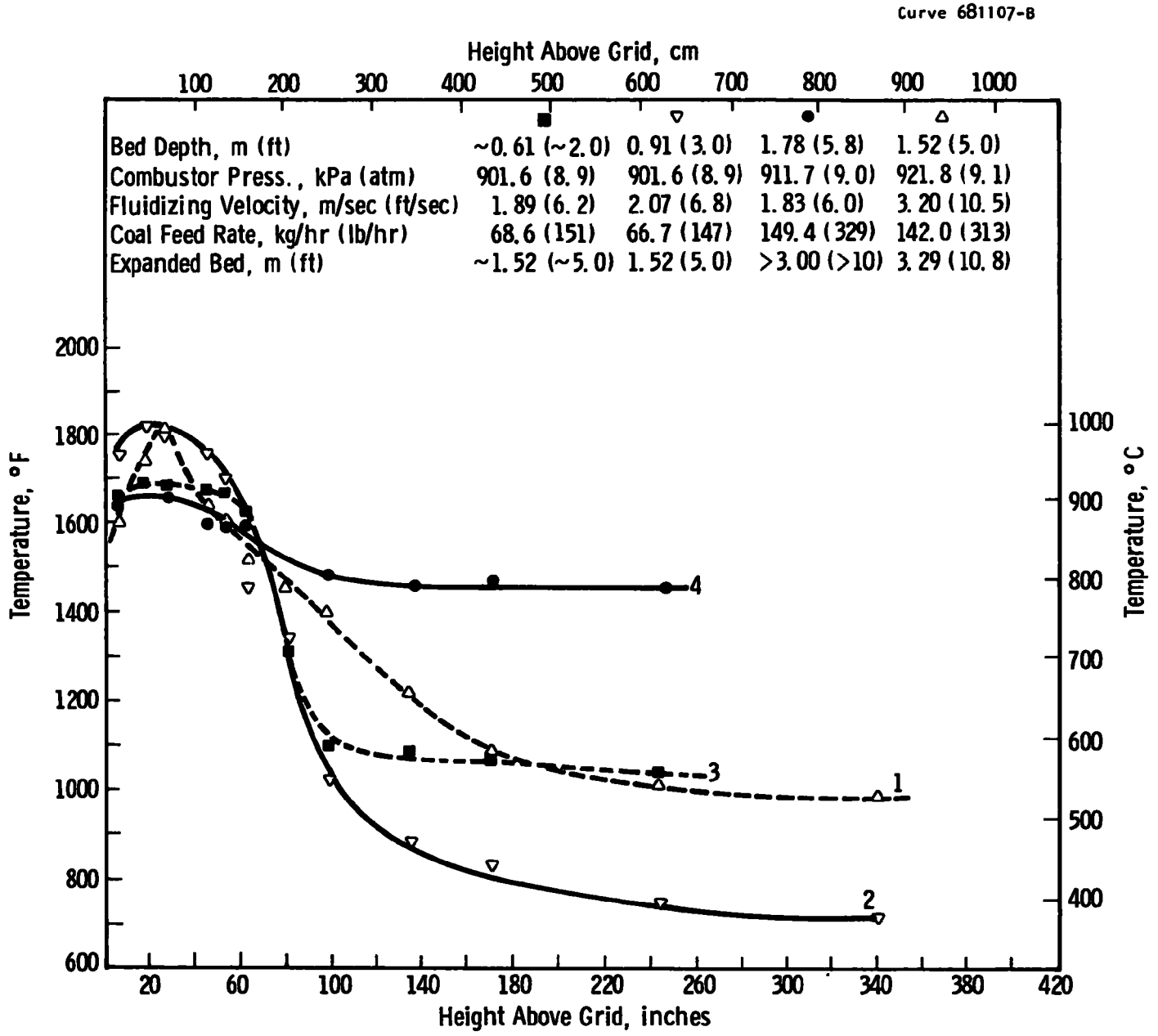

Figure B-3—Fluidized bed combustion miniplant combustor temperature

adequate but still could be improved to provide more reliable service. Distortion of the bottom-most cooling coil was extensive, but all other coils were in satisfactory condition. The bottom coil was compressed and pushed to one side. Two vertical bends were flattened, and most of the 3.0 mm (1/8 in) stainless steel supporting rods were either bent or broken loose. The cause of this distortion is still unknown.

Evaluation of the Basic Design

The most comprehensive pressurized fluidized bed coal combustion data were obtained from the BCURA unit. Unfortunately, the operating conditions were at considerably lower fluidizing velocities and lower bed depths. Even with this handicap extrapolation of the results to higher fluidizing velocities and higher bed depths may be possible with a minimum of error. Exxon's miniplant, which was designed to operate at essentially the basic design conditions, will provide data directly applicable to the basic design. The basic design conditions are reevaluated below on the basis of information presently available.

Combustion Efficiency

At low velocities (∿ 0.76 m/sec/∿ 2.5 ft/sec) and low bed depths (∿ 1.37 m/∿ 4.5 ft), the BCURA unit obtained a combustion efficiency of 96 percent at 10 percent excess air, 97.5 percent at 17 percent, and 99 percent at 25 percent. The BCURA unit also operated at a lower pressure (506.5 kPa/5 atm). Increasing the fluidizing velocity to 3.0 m (10 ft/sec), bed depth to 3 to 3.7 m (10 to 12 ft), and pressure to 1013 kPa (10 atm) may give similar combustion efficiency or higher because an increase in both the bed height and the operating pressure will increase the combustion efficiency; the coal residence time in the bed increases with increasing bed height and decreases with increasing fluidizing velocity. In a 114 mm (4.5 in) inside diameter pressurized batch combustor, Exxon observed a 98.1 percent combustion efficiency operating at 628 kPa (6.2 atm), 927°C (1700°F), 58 percent excess air, 1.9 m/sec (6.2 ft/sec), and 0.6 m (2 ft) bed depth without carbon recycle. If the observed

combustion efficiencies are typical, a carbon burn-up cell may not be needed in the basic boiler design. This will considerably simplify the operation and control of a pressurized fluid bed combustor, although the corresponding saving in reactor cost is small.

Heat Transfer Coefficient

The basic design assumed an average bed-tube heat transfer coefficient of 284 W/m^2-°K (50 Btu/ft^2-hr-°F). The bed-tube heat transfer coefficient depends on physical properties of the bed material and fluidizing gas--such as particle size, thermal conductivity--and on operating conditions--such as temperature, pressure, and fluidizing velocity. The BCURA unit attained an average bed-tube heat transfer coefficient of 380 W/m^2-°K (67 Btu/ft^2-hr-°F) at 899°C (1650°F) bed temperature and 403 W/m^2-°K (71 Btu/ft^2-hr-°F) at 954°C (1750°F). The presence of the tube bank did not affect the heat transfer coefficient significantly. The overall heat transfer coefficient with Exxon miniplant have been measured to be 284 to 312 W/m^2-°K (50 to 55 Btu/ft^2-hr-°F) with the bed temperature at 927°C (1700°F) velocity at 1.83 m/s (6 ft/sec), and pressures at 911.7 kPa (9 atm).

Corrosion/Erosion Heat Transfer Tubes in the Bed

Again, the most comprehensive data were from the BCURA unit. The corrosion/erosion data for the boiler tubes in the bed were reviewed earlier.[6] The more recent data are reviewed here. The boiler tube materials proposed for use in the basic design and the conditions they will be subjected to are summarized in Table B-3. Chemical compositions of the selected boiler tube materials are presented in Table B-4. The chemical composition of the material tested in the BCURA unit is presented in Table B-5 and the corrosion results in Table B-2 and Figure B-2. Note that the current tests are of short duration. Weight loss usually reached a reliable, steady state after long duration (see Figure B-2 and Reference 7). The steady-stage weight loss was considerably lower than the initial weight loss. On the basis of these experimental results, the wastage was not excessive for alloys operating up to their recommended maximum design temperatures for use in steam boilers.

Table B-3

BOILER TUBE MATERIALS

Tube locations	Pressurized Boiler	
	Proposed material	Design temp. °C (°F)
Water Walls	SA-213-T22	524 (975)
Preevaporator	SA-210-A1	389 (732)
Evaporator	--	--
Superheater	SA-213-T2	482 (900)
	SA-213-T22	570 (1058)
	SA-213-TP-304H	621 (1150)
Reheater	SA-213-T22	606 (1122)

A cost study was performed on the assumption that higher alloys were required for the boiler tubes. The originally proposed tube materials and the assumed tube materials for cost study are compared in Table B-5. The metal wastages due to corrosion/erosion projected for 30 years are included. Weight losses were calculated on the basis of long-duration tests performed in the BCURA unit on comparable tube materials. The average weight losses in 500 hours' operation were taken to be typical wastages for long-term projection. This was a conservative assumption because weight losses level off considerably after about 100 hours' operation. If the steady-state weight losses after 500 hours' operation are taken to be the typical long-term wastages, the wastages in Table B-5 could presumably be reduced by about a factor of three. At these weight losses, the proposed 2-1/4 percent chromium steel (SA-213-T22) for reheater and upper-superheater in the basic design was probably a little bit too optimistic. A new cost study was performed by assuming that the 18 percent chromium alloy (SA-213-TP304H) would be used for all beds except the boiler tubes in the preevaporator, where the 2-1/4 percent chromium

Table B-4

CHEMICAL COMPOSITIONS OF SELECTED BOILER TUBE MATERIALS

(in wt %)

	Carbon	Manganese	Phosphorus	Sulfur	Silicon	Chromium	Molybdenum	Nickel
SA-210-A1	0.27 max	0.93 max	0.048 max	0.058 max	0.10 min	-	-	-
SA-213-T2	0.10-0.20	0.30-0.61	0.045 max	0.045 max	0.10-0.30	0.50-0.81	0.44-0.65	-
SA-213-T22	0.15 max	0.30-0.60	0.030 max	0.030 max	0.50 max	1.90-2.60	0.87-1.13	-
SA-213-TP304H	0.04-0.10	2.00 max	0.04 max	0.03 max	0.75 max	18.00-20.00	-	8.00-11.00
Welded SA-178-A tubing (low-carbon steel)	0.06-0.18	0.27-0.63	0.05 max	0.06 max	-	-	-	-
Seamless SA-192 tubing	0.06-0.18	0.27-0.63	0.048 max	0.058 max	0.25 max	-	-	-

steel would be sufficient. The cost for the boiler tubes (including fabrication) increased from the original $1.3/kw to about $4.1/kw, a sizable increase for boiler tube cost; however, it represented less than a one percent increase in total plant cost. This cost estimation was conducted with 1972 dollars so that a comparison with cost figures in the earlier reports[1,7] would be valid.

Table B-5

TYPICAL ANALYSES OF METAL SPECIMENS

Designation	Nominal composition %							
	Cr	Ni	Mo	Mn	Ti	Al	Nb	Fe
12% Cr	12							88
Rf 36	18	12					1	69
SF 316	17	12	2.5	2				66.5
Esshete 1250	15	10	1	6			1	67
P.E. 16	18	37	5		1.2	1.2		37
1% Cr 1/2% Mo	1		0.5	0.5				98
2-1/4% Cr 1% Mo	2.25		1	0.5				96.25

To evaluate the present fluidized bed boiler designs critically, longer-duration runs of up to 2000 hours should be performed at a higher velocity (up to 4.57 m/sec/15 ft/sec), and a higher pressure (up to 1013 kPa/10 atm). The effect of adding limestone and of burning different coals with different impurities, especially high-sulfur coals, should be studied.

The preliminary evaluation with the available data indicates that conventional boiler tube materials may be used in the fluidized bed boiler if the long-duration runs show that the rate of weight loss does, indeed, level off with an increase in operation time. Otherwise, higher alloy materials can be used with minimal cost penalty. Final assessment can be carried out only after more data are accumulated at higher velocity, higher pressure, high temperature, and longer duration.

Temperature Distribution in the Bed

There were two conflicting observations on temperature distribution in two different pressurized fluidized bed combustors. BCURA obtained a reasonably uniform temperature profile in experiments -- 6°C at 899°C (10°F at 1650°F) bed temperature and 19°C at 954°C (35°F at 1750°F). Exxon, however, had difficulty in reducing the bed temperature gradients to less than 56°C (100°F) at 0.9 m (3 ft) static bed depth and to less than 167°C (300°F) at 1.5 m (5 ft) static bed depth in the miniplant. This difference in observation probably stems from the difference in operating conditions and in design parameters. A few factors can be elaborated here.

- The miniplant was operated at higher pressure--911.7 kPa (9 atm) versus 506.5 kPa (5 atm) for the BCURA unit. Higher pressure resulted in a higher combustion rate. This tended to promote combustion in the vicinity of the coal-feeding nozzles. The dissipation of heat was then dependent on the solid mixing rate in the bed, which is slow when compared to the combustion rate.
- Coal-particle size distribution will also affect the temperature distribution. Too large a quantity of fines will promote rapid combustion near the coal-feeding nozzles and increase the temperature gradient in the bed. The fines in the coal fed to the BCURA unit were screened out, which helped the temperature distribution.
- The designs of the BCURA unit and the Exxon miniplant are different in bed area, cooling coils arrangement, and coal feed-rate. The design parameters for the basic design, the BCURA unit, and the Exxon miniplant are compared in Table B-6. Heat release rates per unit bed area and per unit bed volume are essentially similar for the basic design and the Exxon miniplant. These heat release rates are five times larger than those in the BCURA unit, based on unit bed area, and about twice as large, based on unit bed volume.

Table B-6

COMPARISON OF DESIGN PARAMETERS BETWEEN THE BASIC DESIGN AND THE PILOT-SCALE EXPERIMENTAL UNITS

	Basic design[b]	BCURA unit	Exxon miniplant
Bed Cross-Section	1.52 m x 2.13 m (3.25 m^2) (5 ft x 7 ft [35 ft^2])	0.61 m x 0.91 m (0.56 m^2) (2 ft x 3 ft [6 ft^2])	0.3175 m I.D. (0.08 m^2) (12.5 in I.D. [0.85 ft^2])
Bed Height	3.35 m-4.27 m (11-14 ft)	1.37 m (4.5 ft)	3.05 m-4.6 m (10-15 ft)
Bed Height/Diameter Ratio[a]	2-2.5	2	9.5-14.5
Tube Packing, % bed cross-section	21.5-28.5	17	28
% bed volume	17-22.5	8	9
Heat Release Rate/Bed Area	1.2-2.0 x 10^7 J/m^2-sec (3.8-6.3 x 10^6 Btu/ft^2-hr)	3.2 x 10^6 J/m^2-sec (1.0 x 10^6 Btu/ft^2-hr)	1.46 x 10^7 J/m^2-sec (4.6 x 10^6 Btu/ft^2-hr)
Volume Heat Release Rate	3.6-4.7 x 10^6 J/m^3-sec (3.5-4.5 x 10^5 Btu/ft^3-hr)	2.3 x 10^6 J/m^3-sec (2.2 x 10^5 Btu/ft^3-hr)	3.7 x 10^6 J/m^3-sec (3.6 x 10^5 Btu/ft^3-hr)
Bed Area/Coal Feeding Nozzle	0.81 m^2 (8.75 ft^2)	0.14 m^2 (1.5 ft^2)	0.08 m^2 (0.85 ft^2)

[a] For beds of rectangular cross-section, the hydraulic diameters are used.

[b] Basic design has four fluidized beds of slightly different designs per module for preevaporation, superheating, and reheating.

These differences in design are primarily due to differences in bed depth. The high heat release rate will certainly contribute to the poor temperature distribution. The poor temperature profile may also result from the size difference. It is significant that the bed height/diameter ratio for the BCURA unit and the basic design is around 2 while that for the miniplant is 10 to 15. The solid mixing rate has been found to depend strongly on the bed depth/bed diameter ratio.[8] Thus, it is dangerous to extrapolate the result of the bed-temperature profile obtained in the miniplant directly to that of the basic design.

Other factors which will affect the temperature distribution are the tube arrangement and bed area per unit coal-feeding nozzle. The tube packings are compared in terms of percentage bed volume in Table B-6. The tube packing will affect the rate of solid mixing and the rate of heat removal from the bed. The effect of tube packing on the bed temperature profile is not clearly known. The effect of bed area on the coal-feeding nozzle is also not known at this moment. These all point to the necessity of a large, flexible, fluidized bed combustion facility to study the factors identified here.

From the existing evidence it is clear that a reasonably uniform temperature profile can be obtained in a pressurized fluidized bed combustor if the operating conditions and the design parameters are properly set. More data from large combustors operating at high pressure, high temperature, high velocity, and large bed height are required to verify the basic design conditions. The conditions still appear reasonable on the basis of available data.

Coal Feeding

No difficulty was experienced in multiple feeding of coal into the pressurized BCURA unit at any operating conditions up to 506.5 kPa (5 atm) pressure. Exxon did encounter some difficulties in trying to maintain a steady flow of coal to the combustor. In view of the shakedown

nature of the miniplant, this difficulty should not constitute a major problem. In fact, in some more recent runs coal up to more than 136 kg/hr (300 lb/hr) was successfully fed into the combustor. In a commercial unit coal will be fed at more points and at higher rates. On the basis of current experience, no serious trouble is anticipated.

General Operation

Pittsburgh and Illinois coals were combusted in the BCURA unit without substantial difficulty. No clinker or accumulation formed in the bed or on the tubes in the bed. Exxon's miniplant shakedown operation also uncovered no serious flaws. BCURA did observe extensive accumulations on the cooling coils in the freeboard at 954°C (1750°F) bed temperature, but not at 899°C (1650°F); the deposits were extremely powdery and crumbled away on touching. The accumulations may also relate to the particular coal used. Thus, it does not seem to be a serious problem.

A refractory-like deposit, mainly of calcium and magnesium compounds, also appeared on the walls of the primary cyclone primarily due to condensation. A refractory-lined cyclone with hotter inside-wall temperature may avoid this problem.

Another important facet which cannot be studied in smaller combustors is the controllability of a pressurized fluidized bed boiler. The response of the boiler to load-follow and the turndown capability are important in plant operation. No data are yet available.

REFERENCES

1. Keairns, D. L. et al. Evaluation of the Fluidized-Bed Combustion Process - Vol. I, Pressurized Fluidized-Bed Combustion Process Development and Evaluation. Environmental Protection Agency. Westinghouse Research Laboratories. Pittsburgh, Pennsylvania. December 1973. Publication No. EPA 650/2-73-048a. NTIS PB 23] 162/9.
2. Pressurized Fluidized Bed Combustion. Final report. Contract 14-32-0001-1511. The Office of Coal Research, Department of the Interior. National Research Development Corporation. London, England. November 1973.
3. Nutkis, M. S. and A. Skopp. Design of Fluidized Bed Miniplant. Proceedings of the Third International Conference on Fluidized Bed Combustion. Hueston Woods Lodge, Ohio. October 29 - November 1, 1972.
4. Exxon Research and Engineering Program. (Presented at FBC Contractors Meeting. Argonne National Laboratories. September 11-12, 1974.)
5. Nutkis, M. S. Pressurized Fluidized Bed Coal Combustion. Proceedings of the International Fluidization Conference. Asilomen Conference Grounds. Pacific Grove, California. June 15-20, 1975.
6. National Coal Board. Reduction of Atmospheric Pollution. Final Report. Environmental Protection Agency. September 1971.
7. Archer, D. H. et al. Evaluation of the Fluidized Bed Combustion Process-Vol. II, Technical Evaluation. Environmental Agency. Westinghouse Research Laboratories. Pittsburgh, Pennsylvania. November 1971. NTIS PB 212 960/9.
8. Kunii, D. and O. Levenspiel. Fluidization Engineering. New York. John Wiley & Sons, Inc., 1969.

APPENDIX C

SORBENT SELECTION AND ALTERNATIVE SORBENTS

APPENDIX C

SORBENT SELECTION AND ALTERNATIVE SORBENTS

SORBENT SELECTION

The use of calcium-based sorbents (limestone or dolomite) to trap in solid form the sulfur released from "dirty" fuels during combustion is based on the thermodynamic stability of calcium sulfate under fluidized bed combustion conditions;and on the kinetic efficiency, structural integrity, and economical availability of the sorbent, which permit application of the basic idea in a technically sound process.

Calcium carbonate is found as both limestone and dolomite in the eastern and midwestern states which produce high-sulfur coal. Both pure and impure limestones and dolomites have been tested as sorbents: the sulfur removal efficiency has generally been well within EPA limits. In order to select the best available material as sorbent, sorbent selection criteria must be developed. Establishing selection criteria will minimize the cost and time involved in assessing the usefulness of rock quarried near a particular plant site.

The criteria (which require further development) for choosing a stone are based on:

- Acceptor properties of the stone for sulfur removal
- Attrition resistance of the stone
- Trace element emission characteristics
- Regeneration characteristics
- Suitability of spent sorbent for final processing for disposal
- Economic availability of the stone.

Acceptor Properties of the Stone for Sulfur Removal

The acceptor properties of the stone depend on the stable form of the sorbent in the particular process, and on the kinetics of the sulfation reaction.

Both limestone and dolomite may be used as sorbents at atmospheric pressure. At higher pressures and under exit gas conditions as Figure C-1 shows,[1] calcium carbonate is the stable form of the sorbent. Calcium carbonate in limestone does not react rapidly with sulfur dioxide: the sorbent probably depends for its desulfurizing action on the extent of calcination which occurs at or near the bed air inlet. Both sulfur dioxide and carbon dioxide will then compete for the calcined lime. Although Exxon[2] Research and Engineering (Exxon) has been successful in using limestone as a sorbent at pressure, it is uncertain if there are high-pressure and low-temperature limits to its use. Dolomite, on the other hand, is normally reactive in the half-calcined state and may be used as sorbent, irrespective of the carbon dioxide pressure in the system. The calcium-to-sulfur molar ratio fed to the bed, however, will be higher with half-calcined than with fully-calcined dolomite.

The kinetics of the sulfation reaction are discussed in Appendix D; the application of the data to estimating fluidized bed desulfurization performance is described in Appendix E. To date, most of the data have been concerned with the effects of process variables on a few stones. For those stones for which thermogravimetric (TG) data are available, an estimate of performance can be made, given the proposed operating conditions. For any proposed system it is also possible to carry out TG tests on a particular stone to estimate its suitability as a sorbent under the system operating conditions. Extension of the data base on the kinetics of dolomite and limestone sulfation to cover the major variations in stone type encountered in the eastern United States is desirable.

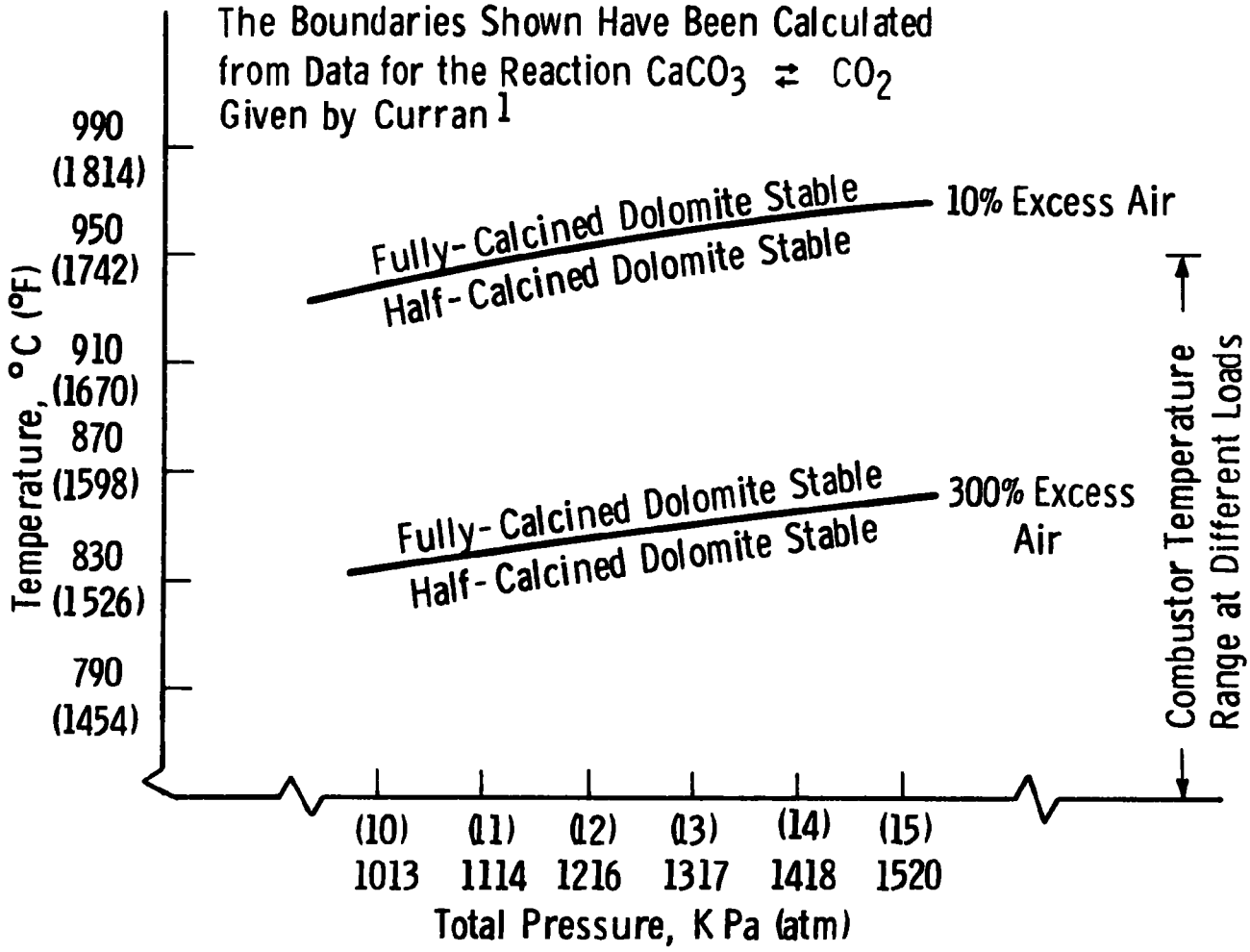

Figure C-1 — Temperature and pressure conditions for stability of the sulfur sorbent as half-calcined or fully-calcined dolomite at projected combustor outlet gas compositions.

Attrition Resistance

The term attrition is used to cover all aspects of loss of sorbent from the fluidized bed by elutriation, irrespective of the mechanism. Decrepitation, thermal shock shattering, bursting apart during calcination, fragmentation during sulfation, abrasion between sorbent and ash and sorbent and refractory or internals, distributor jet impingement, and sorbent circulation through ducts may all contribute to loss of sorbent from the bed. It is impossible to establish criteria for attrition resistance which must be met without reference to the system design, since the system design itself may take into account the attrition loss expected from available sorbents. In general, however, a minimal amount of attrition loss is desirable, if only to reduce the load on dust removal equipment. Additionally, for regenerative systems where long cumulative residence times in the desulfurizing system are required, the rate of calcium makeup feed to the bed may be governed by attrition losses. At the other end of the scale, continuous recirculation of fines assists in attaining higher stone utilization in once-through systems, or in systems with a high calcium-to-sulfur molar feed rate.

The prediction of attrition losses a priori for any particular stone is not yet possible. In stone selection tests for the chemically active fluidized bed (CAFB) oil gasification process, initial laboratory tests screening candidate stones met with some success. The extremes of high attrition rate and low attrition rate correlated well with results obtained on Esso Research Centre, Abingdon, England (Esso) batch units.[3] An intermediate range of attrition loss in the laboratory unit, however, yielded no information on the suitability of the stone as a sorbent in that particular process. At the moment, laboratory tests can give a relative listing of the expected order of attrition losses from a series of stones. The evidence, however, is that suitable adjustment of the process variables may alter attrition loss sufficiently to accommodate a particular stone to a particular process. For example, Pope, Evans and Robbins (PER)[4] successfully modified initial calcination conditions in their fluidized bed combustor to permit operation with a local, impure limestone.

The original conditions, standardized for operation with a high-purity limestone, had resulted in such a high loss rate that the bed could not be maintained. Another approach is evident in the work of Pell et al.[5] at Conoco Coal Development Company. Their procedure for hardening the stone sorbent has increased the number of cycles for which the sorbent can be circulated between desulfurization (under reducing conditions) and regenerator, permitting a low sulfur differential between the two vessels.

The development of relative measures of attrition rates depends on further research into the mechanism of particle fracture, in addition to laboratory measurements of decrepitation and fluidized bed attrition during calcination and sulfation. Experiments to generate sufficient data,under identical process conditions, which compare attrition losses for a range of dolomites and limestones of different grain structure to permit empirical evaluation of stone sorbents should proceed in order to assist in the screening of candidate stones.

Trace Element Emission Characteristics

The possibility of the emission of trace elements from the sorbent into the effluent gas from the fluidized bed combustor raises environmental and corrosion questions. These considerations are discussed in Appendix H. The present state of knowledge as it affects stone selection is summarized here.

The major concern is that sodium and potassium liberated into the gas stream will form liquid deposits on turbine components, thereby inducing hot corrosion. Preliminary results to date indicate that a very small fraction of the alkali-metal content will be liberated from dolomites during fluidized bed combustion. The major alkali-metal species emitted are potassium compounds. Since it is not yet known what potassium species in the original sorbent liberates its potassium to the gas stream, the best approach is to use the dolomite with the lowest alkali-metal content. Analysis of a range of dolomites from Ohio, Indiana, Illinois, and Michigan indicates that the potassium content varies from 100 to 6000 ppm (by weight), while the sodium content

varies from 150 to 350 ppm (by weight). Occasional large deviations from these values may be encountered: for example, a Bahaman aragonite dredged from the sea contains 4,000 ppm sodium. To date, no correlation of alkali-metal content with geological formation has been found. The sparse data available show that the alkali content may vary significantly through a series of rock strata, and within one stratum from quarry to quarry. It is extremely doubtful whether reported values in the older literature should be used,other than for internal comparison with other reported data: details of the analytical procedures adopted have rarely been reported.

In the current state of knowledge, the best recommendation is to choose as sorbent from those available the dolomite or limestone which is lowest in potassium content.

Regeneration Characteristics

Data at the moment are insufficient to distinguish between different stones on the basis of regenerability. Optimization of regenerability will in all likelihood include a study of the influence of stone structural type on the loss of kinetic activity in desulfurization, both for the high-temperature and low-temperature (two-step) regeneration schemes.

Suitability of Spent Sorbent for Final Processing for Disposal

Any final processing of the spent sorbent required before disposal will probably be a local problem—dependent on the particular fluidized bed combustion system operated,on regulations governing disposal of solid wastes, or on local marketing opportunities. The major influence these factors may have is in requiring a choice between limestone or dolomite. Investigation of this aspect of stone selection is dependent on the production of tonnage quantities of spent sorbent so that its properties may be characterized. (See Appendices F and G.)

Economic Availability of the Stone

The cost of dolomite in the eastern and midwestern states was in the range of $2.30 to 5.00/Mg (ton) at the plant (late 1974). Significant transport costs are likely if the sorbent must be hauled for long distances. For this reason, operation with local sources of stones will be preferable. While systems studies can reveal the impact of sorbent cost on plant economics, additional work to determine the design conditions needed to operate (desulfurize) with a wide variety of stone types is equally important. Successful operation of the Rivesville plant with a local, impure limestone indicates the potential for this approach. TG work to modify the properties of the stone sorbents by special calcination treatment in order to develop suitable stone porosity for desulfurization was successful with pure and impure dolomites and with a pure limestone.

Conclusion

The establishment of stone selection criteria for choosing limestones and dolomites suitable for use as fluidized bed desulfurizing agents is an important part of the technical support studies needed to optimize the fluidized bed combustion process.

The stone selection criteria developed will not be rigid specifications but will depend on the particular system design. The availability of particular sorbents will influence optimization of a particular design with respect to local conditions.

ALTERNATIVE SORBENTS

Because of the low cost and widespread geographical availability of calcium carbonate as limestone or dolomite rocks and its excellent performance as a sorbent in preventing sulfur dioxide emission, a compelling reason must exist before an alternative sorbent is considered as a substitute. Apart from cases where an alternative to calcium carbonate might be considered because of local availability, the most general ground for assessing alternative sorbents is that of regenerability.

Calcium sulfate is extremely stable and requires the expenditure of considerable energy before it will release sulfur, either as sulfur dioxide or as hydrogen sulfide, in concentrated form. The desirability of regeneration rests on two factors—the recovery of sulfur as a valuable resource and a reduction in both the material requirements for sulfur sorption and the quantities of spent sorbent solid which are produced as a by-product of the sulfur removal process. The ideal alternative sorbent is one which is mechanically resistant to attrition in the solids circulation system of the fluidized bed process; is an efficient sulfur getter over the range of coal combustion conditions in the fluidized bed process; can be regenerated under mild reducing conditions (or by thermal decomposition alone); and yields a solid oxide which retains the capacity and kinetic activity of the original sorbent on repeated recycling. In addition, it should contribute no fine particulate matter or trace elements to the effluent gases and should trap these materials as they are released from coal and coal ash during combustion.

A large number of metal oxides have been screened for their suitability in removing sulfur dioxide from flu gases. The thermodynamic data tabulated for the stability of metal sulfates rule out most of these oxides for consideration as sorbents in the fluidized bed combustion process.

The free-energy diagram for metal sulfate stability shown by Bartlett,[6] indicates that at 727°C (1341°F), the order of thermal stability of the common metal sulfates is:

- Potassium sulfate (K_2SO_4)
- Sodium sulfate ($NaSO_4$)
- Calcium sulfate ($CaSO_4$)
- Manganese sulfate ($MnSO_4$)
- Nickel sulfate ($NiSO_4$)
- Copper sulfate ($CuSO_4$)
- Aluminum sulfate ($Al_2[SO_4]_3$).

Calcium sulfate requires severe treatment in reducing gas (in other words, high temperature) to release the sulfur, indicating that the more stable alkali-metal sulfates may be excluded.

At the request of EPA, a special alumina-based copper oxide catalyst, NALCO 471, was evaluated as a potential sulfur removal sorbent. Both the thermodynamics and kinetics of the reaction of sulfur dioxide with the catalyst were examined.

Thermodynamic Evaluation

Copper sulfate ($CuSO_4$) decomposes thermally in two stages as shown by the equations:

$$2\ CuSO_4 \rightleftarrows CuO \cdot CuSO_4 + SO_2 + \frac{1}{2}\ O_2 \qquad (C\text{-}1)$$

$$CuO \cdot CuSO_4 \rightleftarrows 2\ CuO + SO_2 + \frac{1}{2}\ O_2 \qquad (C\text{-}2)$$

At a given temperature in the range of interest for fluidized bed combustion the equilibrium pressure of sulfur dioxide is lower for reaction 2 than for reaction 1. Therefore, reaction 2 should be considered as the process which will thermodynamically limit the sulfur retention in a fluidized bed of copper oxide. The degree of dispersion of copper oxide on the alumina base, however, may either prevent formation of the oxysulfate or, indeed, stabilize it. Mixtures of sodium sulfate and copper oxide are more effective sulfur dioxide sorbents than copper oxide alone; the sulfation reaction is faster than with copper oxide; and thermal decomposition requires heating to a higher temperature.[7]

The limitations which reaction 2 places on sulfur dioxide removal are shown in Figure C-2 for: (A) the 101.3 kPa (1 atm) pressure combustor, (B) the 1013 kPa (10 atm) combustor with 10 percent excess air, (C) the 1520 kPa (15 atm) with 10 percent excess air, and (D) the 1520 kPa (15 atm) adiabatic combustor. Table C-1 shows the assumed exit gas conditions.

Exxon[8] reported that their calculations indicated that sulfur retention would fall off from more than 90 percent to 20 percent in the range 627 to 727°C (1161 to 1341°F).

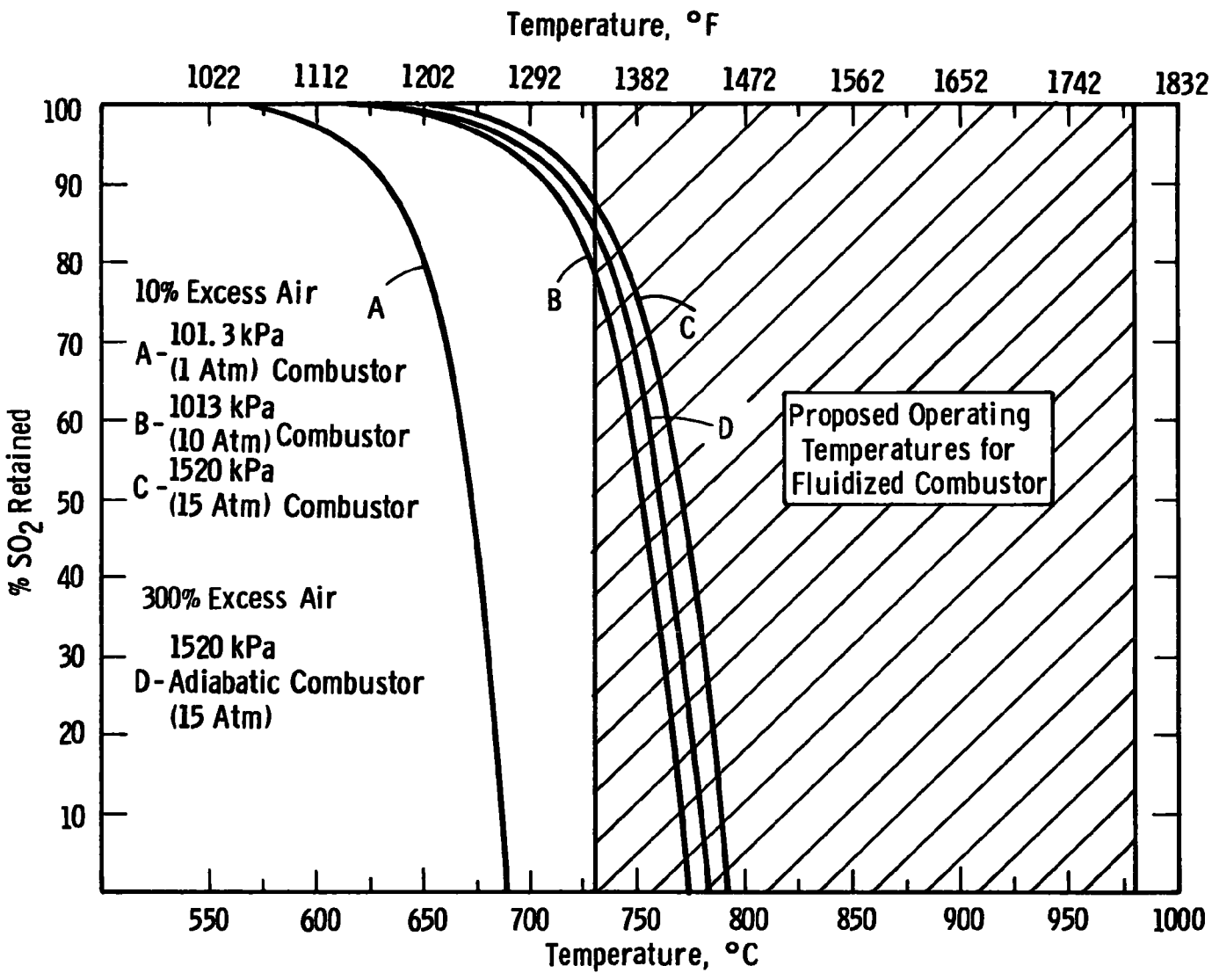

Figure C-2—Maximum SO_2 retention in fluidized beds of $CuO \cdot Cu\ SO_4$ (thermodynamic limit)

Table C-1

EXIT GAS CONDITIONS FOR FLUID BED COMBUSTORS

System	P_{SO_2} with no sorbent (atm)	P_{O_2} (atm)
A. 101.3 kPa (1 atm) fluidized bed with 10 percent excess air	.005	.04
B. 1013 kPa (10 atm) pressure with 10 percent excess air	.05	.17
C. 1520 kPa (15 atm) pressure with 10 percent excess air	.075	.255
D. Adiabatic combustor 1520 kPa (15 atm) pressure	.0188	2.265

Experimental Results

TG experiments were carried out at atmospheric pressure using the copper-impregnated alumina catalyst and an oxide prepared by thermal decomposition of copper sulfate pentahydrate.

The copper sulfate pentahydrate decomposed to yield a 32.1 percent weight loss for dehydration (theoretical value = 32.3 percent)and a 36.1 percent weight loss for decomposition of sulfate to oxide (theoretical value = 36.1 percent). The oxide was then exposed to 12 percent sulfur dioxide/nitrogen/4 percent oxygen and the temperature varied in the range 600 to 800°C (1112 to 1472°F). Equilibrium temperatures were noted at the transition from weight gain to weight loss.

As expected, two equilibrium temperatures were noted,and the temperatures were in relatively good agreement with those predicted from the experimental thermodynamic data in the literature,[9] as shown in Table C-2.

This is not to suggest that the data were taken under the precisely-controlled conditions Ingraham reported: his values are noted to indicate that the TG values are fairly close to the true values and are a guide in interpreting the behavior of the sorbent.

Table C-2

DECOMPOSITION TEMPERATURES OF COPPER SULFATE AND COPPER OXYSULFATE: COMPARISON OF (W) TG DATA AND THERMODYNAMIC PREDICTIONS FROM INGRAHAM'S STUDY[a]

TG temperature °C (°F)	I&M temperature °C (°F)	Reaction
720 (1328)	740 (1364)	$2\ CuSO_4 \rightarrow CuO \cdot CuSO_4 + SO_2 + \frac{1}{2}\ O_2$
773 (1422) 782 (1438) } 778 (1432)	795 (1463)	$CuO \cdot CuSO_4 \rightarrow 2\ CuO + SO_2 + \frac{1}{2}\ O_2$

[a] T.R. Ingraham. Thermodynamics of the Thermal Decomposition of Cupric Sulfate and Cupric Oxysulfate. Trans. Met. AIME 233: 359, 1965.

The NALCO 471 catalyst, impregnated with copper oxide (as supplied by Exxon) was then tested in the same sulfur dioxide/nitrogen/oxygen mixture. For runs with two samples, only one equilibrium temperature was found at 684°C ± 5°C (1263°F ± 41°F) (9 readings). This apparently anomalous behavior results from the reaction

$$Al_2(SO_4)_3 \rightleftarrows Al_2O_3 + 3\ SO_2 + \frac{3}{2}\ O_2.$$

Calculation of the temperature for equilibrium at the experimental gas pressures, using the thermodynamic tabulation of Stern and Weise,[10] gave 680.5°C (1257°F). In addition, the total quantity of sulfur trioxide (SO_3) reacted was about three times stoichiometric for formation of copper sulfate (on a 5 wt % copper basis). It was decided to reverse the experimental procedure and start the absorption/temperature run at high temperatures, cool the solid, and determine the temperature for formation of either copper sulfate or copper oxysulfate free from interference from the alumina.

Copper Oxide Sorbent

Pressurized sulfation runs (1013 kPa/10 atm) were carried out on the NALCO catalyst. A trace reaction was noted at 900°C (1652°F). On cooling the sample in the gas flow (0.5 percent sulfur dioxide; 4 percent oxygen in nitrogen), the sorbent gained weight at the temperature where aluminum sulfate becomes thermodynamically stable. The sample lost weight on recycling through this temperature (650°C [1202°F]). A blank run on colloidal alumina showed a trace reaction at 900°C (1652°F), similar to that observed for the NALCO catalyst, a weight gain corresponding to 1 percent of the original sample weight.

It was concluded that the copper-impregnated catalyst is not a suitable sorbent for sulfur dioxide removal in fluidized bed combustion: the sulfur dioxide adsorption step takes place below the practical temperature range for operation of the fluidized bed combustor.

General Assessment

The chief interest in alternative sorbents lies in finding a sorbent which can undergo multiple regeneration. For this reason an analysis of the minimum acceptable performance of a sorbent should be carried out. This analysis would require definition of

1. A range of acceptable hydrogen sulfide or sulfur dioxide concentrations produced in the regenerator
2. Acceptable fuel consumption in the regenerator
3. Minimum sulfur loading on the sorbent and acceptable stone recirculation rates
4. Thermodynamic screening of the sorbents in light of 1 and 2.
5. Kinetic tests for sorbent activity in the light of 4.

The criteria developed would be system dependent: the atmospheric pressure, pressurized boiler, and adiabatic combustor cases would each be treated separately.

REFERENCES

1. Curran, G.P., C.E. Fink, and E. Gorin. CO_2 Acceptor Gasification Process in Fuel Gasification. Consolidation Coal Co. Advances in Chemistry Series 69. American Chemical Society. Washington, D.C. 1967. p. 141.
2. Hoke, R. C., L. A. Ruth, and H. Shaw. Combustion and Desulfurization of Coal in a Fluidized Bed of Limestone. Exxon Research and Engineering Co. Linden, N.J. (Presented at IEEE-ASME Joint Power Generation Conference, Miami Beach, Fla. Sept. 15-19, 1974.)
3. Keairns, D. L., et al. Fluidized Bed Residual Oil Gasification/ Desulfurization at Atmospheric Pressure. Vols. I and II. United State Environmental Protection Agency. Westinghouse Research Laboratories. Pittsburgh, Pennsylvania. Contract No. 68-02-065. December 1974.
4. Mesko, J. E., S. Ehrlich, and R. A. Gamble. Multicell Fluidized-Bed Boiler Design Construction and Test Program. Office of Coal Research. Pope, Evans and Robbins. New York, N.Y. NTIS PB 236-254. August 1974. PB 236-254. August 1974.
5. Pell, M. Conoco Coal Development Co. Private Communication. 1974.
6. Bartlett, R. W. Sulfation Kinetics in SO_2 Absorption from Stack Gases. Environmental Protection Agency. Stanford University. Palo Alto, California. Grant No. AP00876. June 1972.
7. Bumazhmov, F. T. Sulfation of Copper Oxide by Mixtures of Air and Sulfur Dioxide. Izv. Vyssh. Ucheb. Zaved., Tsvet. Met. 22-6, 1973. (Chemical Asbtracts 79, 55489C).
8. Exxon Research and Engineering. Private Communication. 1974.
9. Ingraham, T. R. Thermodynamics of the Thermal Decomposition of Cupric Sulfate and Cupric Oxysulfate. Trans. Met. AIME 233: 359, 1965.
10. Stern, K. H. and E. L. Weise. High Temperature Properties and Decomposition of Inorganic Salts. Part 1 - Sulfates. NSRDS-NBS7. National Bureau of Standards. Washington, D. C. 1966.

APPENDIX D

THERMOGRAVIMETRIC STUDIES OF THE SULFATION OF LIMESTONES AND DOLOMITES

APPENDIX D

THERMOGRAVIMETRIC STUDIES OF THE SULFATION OF LIMESTONES AND DOLOMITES

SUMMARY

- The sulfation of limestone proceeds to higher calcium utilization at a fast rate of reaction at atmospheric pressure and at 1013 kPa (10 atm) if the pressure of carbon dioxide (CO_2) has been high ($\sim$ 0.6 x Peq) during the limestone calcination step (where Peq is the equilibrium pressure of carbon dioxide over calcium carbonate at the reaction temperature).
- The effect of temperature on sulfur dioxide (SO_2) retention in fluidized beds of limestone is governed by the above calcination effect and by the effect of temperature on the reaction of lime with sulfur dioxide and oxygen—not primarily by the oxidation/reduction cycle in the fluidized bed.
- Pressurized reaction may require the use of half-calcined dolomite or uncalcined limestone. Most half-calcined dolomites are excellent sulfur dioxide sorbents, intermediate in reactivity between dolomite calcined under low carbon dioxide pressure and dolomite calcined at high carbon dioxide pressure. Uncalcined limestone is an extremely poor sorbent for sulfur dioxide; calcination and recarbonation does not improve its sorbent properties.

INTRODUCTION

The use of limestone and dolomite to maintain sulfur dioxide emissions below the levels required by the Environmental Protection Agency (EPA) during the fluidized bed combustion of coals has been successfully demonstrated by several teams of investigators whose work has been summarized in previous contract reports.[1] Because of the enormous range of conditions which must be considered in designing fluidized bed combustors for electric power generation, there is an urgent need for models of the desulfurization process which will permit simulation of the effects of changes in operating conditions on the efficiency of sulfur removal. Such models require data on the kinetics of lime and dolomite sulfation taken under conditions which isolate the important rate-influencing variables in the fluidized bed combustion process. The field of operation of proposed systems—excess oxygen, total pressure, combustion, conditions, and temperature—dictates the form in which the dolomite sorbent will be used, as shown in Figure D-1. (The variation in carbon dioxide pressure along the bed height means that parts of the bed may exist in a different stability area, a complication which will be considered later.) The same stability field applies to limestone, where half-calcined dolomite and uncalcined limestone exist under the same conditions, as do fully-calcined dolomite and calcined lime. Desulfurization may be affected using any of these four forms of calcium sorbent either singly or in combination.

The thermodynamics of the reactions

$$CaO + SO_2 + \frac{1}{2} O_2 \rightarrow CaSO_4$$

$$CaCO_3 + SO_2 + \frac{1}{2} O_2 \rightarrow CaSO_4 + CO_2$$

show a strong driving force for desulfurization by removal of sulfur dioxide from the gas stream. The kinetics which govern the rate of sulfur dioxide removal dictate the size of the fluidized bed reactor (gas and solid residence times), the excess calcium required (extent of reaction),

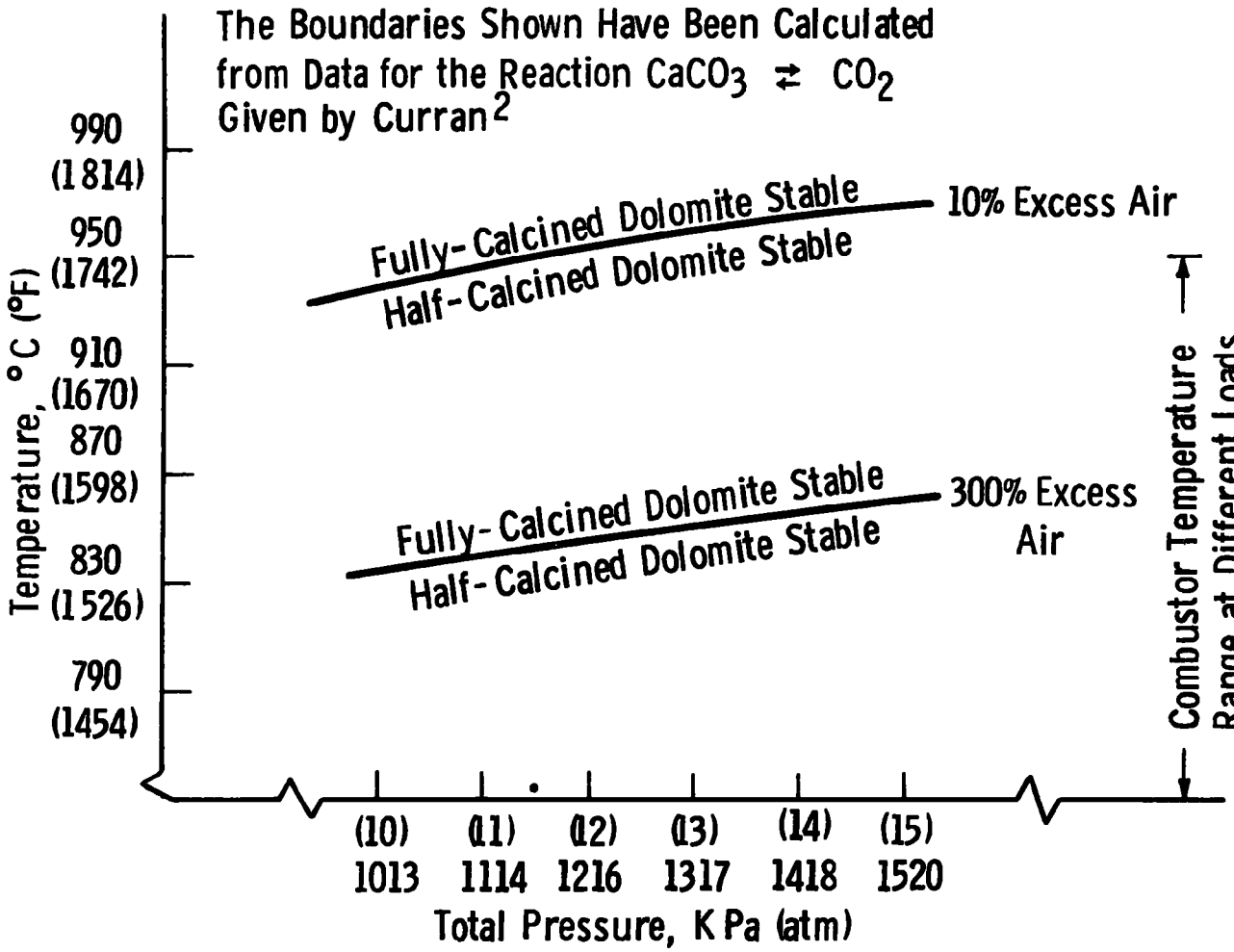

Figure D-1—Temperature and pressure conditions for stability of the sulfur sorbent as half-calcined or fully-calcined dolomite at projected combustor outlet gas compositions.

particle size of the sorbent, the temperature and pressure of the process, and the stone pretreatment. The ranges of these variables which have been considered are shown in Table D-1, which illustrates the scope of the investigation of kinetics of sulfation. It should be noted that factors not directly concerned with the desulfurization reaction may limit the choice of sorbent. These may be listed as:

- The economic availability of limestone or dolomite at a power plant site
- The attrition behavior of the sorbent in the fluidized bed
- The emission of trace elements from the sorbent into the effluent gas (or turbine feed streams)
- The method chosen for disposal of spent sorbent
- The requirements of a regeneration process.

The work described here is a continuation of investigations described in an earlier report, in which thermogravimetric (TG) studies of the sulfation of calcium-based sorbents showed a close correspondence with fluidized bed work.

In particular, the work showed that calcium utilization in the sulfation of dolomite at pressure was highly dependent on the conditions of carbon dioxide partial pressure which prevail during stone calcination. This work was extended to consider both the sulfation of limestone and dolomite at atmospheric pressure, and the sulfation of half-calcined dolomite at pressure.

Summary of Previous Laboratory Studies

The results of several laboratory studies on the sulfation of lime and calcined dolomite are summarized here.[3-9]

- Sulfation is first order with respect to sulfur dioxide.
- Sulfation is zero order with respect to oxygen.
- The rate of reaction increases with temperature. Various values of activation energy have been derived, but there is no unambiguous determination of activation energy.

Table D-1

SORBENT STABILITY IN THE PRESSURIZED FLUIDIZED BED COMBUSTOR

% Excess Air	10		300	
Pressure, kPa (atm)	1013 (10)		1013 (10)	
$CaO/CaCO_3$ Boundary Temperature	C < 950 F < 1740	> 950 > 1740	< 850 < 1562	> 850 > 1562
Sorbent	Dolomite	Dolomite Limestone	Dolomite	Dolomite Limestone
Reaction[a]	1	2	1	1, 2
Relevant TG Data[b]	A, B	A, B	A	A, B

[a] Reaction 1 $MgO \cdot CaCO_3 + SO_2 + \frac{1}{2} O_2 \rightarrow MgO \cdot CaSO_4 + CO_2$

Reaction 2 $MgO \cdot CaO + SO_2 + \frac{1}{2} O_2 \rightarrow MgO \cdot CaSO_4$

[b] A - This report.

B - Keairns, D.L., et al. Evaluation of the Fluidized Bed Combustion Process. Environmental Protection Agency. Westinghouse Research Laboratories. Pittsburgh, Pa. Vol. 1. NTIS PB-231 162/9. December 1973.

- Reactivity depends upon the pore volume formed during calcination:
  - Small pores give a high initial reaction rate but, if the particles are large, a low overall capacity results.
  - Large pores give lower rates but increased capacities.
  - For small particles, capacity is determined by the pore volume available for product accumulation.
  - Other properties which influence the pore structure formed on calcination may serve as general indices to the capacity, in other words, temperature and conditions of calcination, sodium content of the stone.
  - The distribution of sulfur through a sulfated stone depends on the stone: a coarse limestone shows total permeation of the stone by sulfate, while Iceland spar forms a rim of sulfate.

EXPERIMENTAL RESULTS

The Sulfation of Limestone and Dolomite

Experiments were carried out in the following areas:

- The effect of calcination conditions on the sulfation of limestone and dolomite
- The effect of temperature on limestone sulfation
- The effect of pressure and temperature on limestone sulfation
- The effect of temperature on the reaction between sulfur dioxide and calcium oxide.

The materials used in the experiments and their composition are listed in Table D-2. The thermogravimetric equipment used has been described in an earlier contract report.[1]

Table D-2

SORBENTS USED TO STUDY THE SULFATION REACTION

Sorbent	Ca	Mg	Ignition wt. loss	Principal impurities
Limestone 1359 Stephens City, Va.	38.4	.04	43.4	Silica
Tymochtee Dolomite Huntsville, Oh.	20.5	11.9	44.4	Silica, pyrites, alumino silicates
Glasshouse Dolomite (Dolomite 1337) Gibsonberg, Oh.	21.5	12.5	47.7	Silica, pyrites, alumino silicates
Salamonie Dolomite Portland, Ind.	21.7	12.9	47.9	
Canaan Dolomite New Canaan, Conn.	22.2	12.8	46.0	Traces of amphibole

The Effect of Calcination Conditions

Experimental runs aimed at determining the effect of calcination conditions on the sulfation of limestone 1359 are listed in Table D-3.

In the first set of experiments, at 1013 kPa (10 atm) pressure, TG 196-199, the effect of carbon dioxide partial pressure during calcination was probed. By calcining the limestone in nitrogen, either rapidly at 900°C (1814°F), or slowly in the temperature range 680 to 870°C (1256 to 1598°F), a lime was formed which was relatively inert and ceased to sulfate at a rapid rate after 14 percent utilization of the calcium. When calcination was retarded, however, by maintaining 101.3 kPa (1 atm) of carbon dioxide over the solid and heating it to 930°C (1706°F), a more active lime was produced which yielded 32 and 37 percent calcium utilization in successive experiments.

A second set of runs at atmospheric pressure, TG 215, 216, 220, 221, demonstrated that the activation of the lime is not due to pressurized operation: Figure D-2 shows the effect of calcination history on the course of the subsequent sulfation reaction.

Since the carbon dioxide partial pressure during calcination controls the activity of the product lime during sulfation, even at atmospheric pressure, tests were run using dolomite 1337 as sorbent at atmospheric pressure. It was evident that dolomite could be activated at atmospheric pressure by calcining it under a high partial pressure of carbon dioxide. The comparative results for limestone and dolomite are shown in Figures D-3 and D-4, using some TG results reported earlier.[1] At the two pressures studied dolomite is a superior sorbent, both on the basis of the weight of raw sorbent used and on the basis of calcium utilization. The possibility remains, however, of greatly increasing the capacity of the limestone, but over 80 percent of the calcium in the dolomite is sulfated, leaving only a small margin for further improvement.

Fluidized Bed Calcine

A set of experiments, TG 262-265, was run on the sulfation of lime calcined in the 50 mm fluidized bed unit. The calcined sample was

Table D-3

LIMESTONE 1359 SULFATION RUNS

TG no.	Pressure, kPa (atm)	Particle size, μm	Calcination			Sulfation	
			Temperature, °C (°F)	Atmosphere	Time/min.	Temperature, °C (°F)	Utilization, % Ca
196	1013 (10.0)	420-500	900 (1652)	N_2	4.0	871 (1600)	14.0
197	1013 (10.0)	420-500	680-870 (1256-1598)	N_2	∿ 12.0	871 (1600)	14.0
198	1013 (10.0)	420-500	930 (1706)	10% CO_2/N_2	8.0	871 (1600)	32.0
199	1013 (10.0)	420-500	930 (1706)	10% CO_2/N_2	8.0	871 (1600)	∿ 37.0
215	101.3 (1.0)	420-500	900 (1652)	N_2	2.5	871 (1600)	9.0
216	101.3 (1.0)	420-500	900 (1652)	30% CO_2 in N_2	5.0	871 (1600)	14.0
220	101.3 (1.0)	420-500	871 (1600)	55-30% CO_2 in N_2	80.0	871 (1600)	34.5
221	101.3 (1.0)	420-500	900 (1652)	60% CO_2 in N_2	30.0	871 (1600)	42.0
229	101.3 (1.0)	420-500	954 (1749)	15% CO_2 in N_2	∿ 1.2	954 (1749)	12.0
230	101.3 (1.0)	420-500	843 (1549)	15% CO_2 in N_2	34.0	843 (1549)	14.0
231	101.3 (1.0)	420-500	899 (1650)	15% CO_2 in N_2	3.0	900 (1652)	11.0

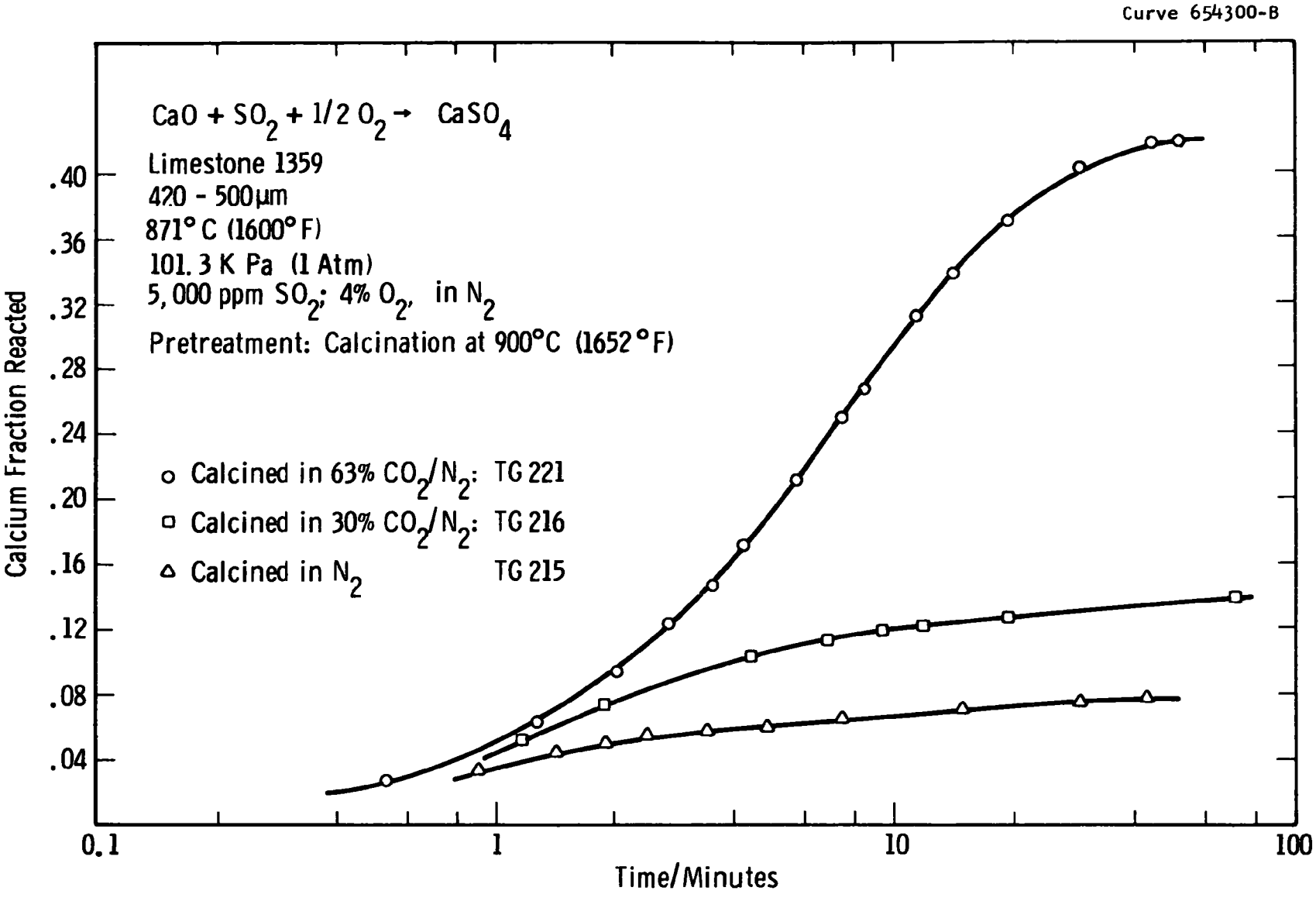

Figure D-2—Atmospheric pressure sulfation of limestone 1359 - the effect of calcination history

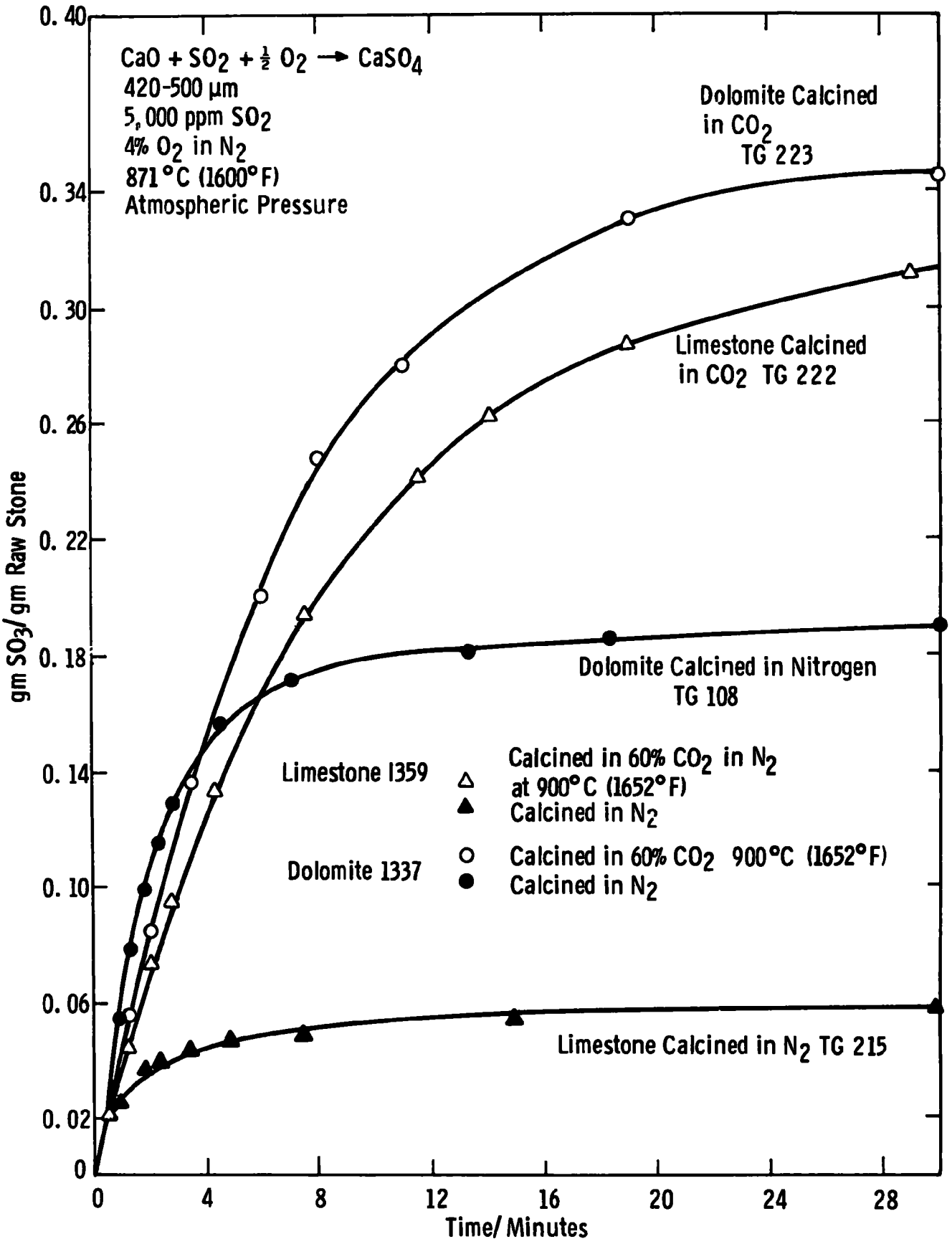

Figure D-3—Sulfation of limestone and dolomite; effect of calcination conditions

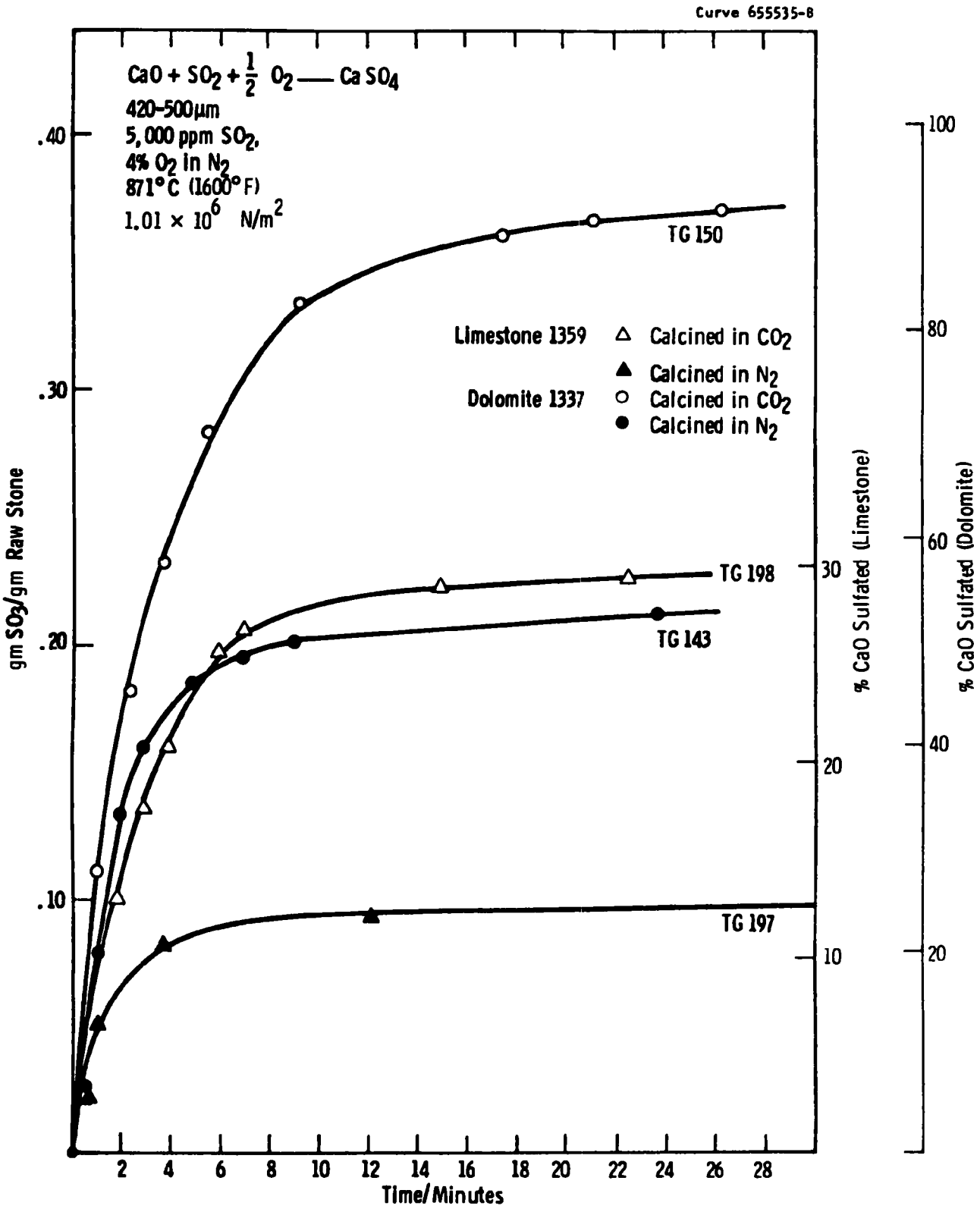

Figure D-4–Comparison of pressurized sulfation of limestone and dolomite

obtained in the test on attrition behavior of limestone 1359 in the screening process for candidate stones for testing in the Esso Research Centre, Abingdon, England (Esso) oil gasification pilot plant. Since the sample was allowed to calcine in a stream of nitrogen in the temperature range 650 to 750°C (1202 to 1382°F), the stone produced have been relatively inactive. The extent of sulfation achieved in TG experiments from 101.3 to 1013 kPa (1 to 10 atm) lay in the range 13.5 to 17.5 percent, as shown in Table D-4. These experiments confirmed that calcination at low partial pressures of carbon dioxide do produce an inactive stone. The experimental schedule on the 50 mm unit has not yet permitted examination of the case where calcination takes place under a relatively high partial pressure of carbon dioxide.

Table D-4

TG SULFATION OF LIMESTONE 1359 CALCINED IN THE 50 MM FLUIDIZED BED[a]

TG no.	$P/(1.03 \times 10^5\ N/m^2)$	% CaO utilization	
		After 5 min	After 1 hr
263	1.0	11.7	17.5
264	10.0	13.9	17.8
265	10.0	11.9	15.1
266	5.0	10.7	13.5

[a]Initial particle size (1,000-420) μm; calcined in nitrogen 650 to 750°C (1202 to 1382°F). Sulfation at 5,000 ppm SO_2, 4 percent O_2 in N_2 at 870°C (1598°F).

Temperature Effect

Previous studies on the sulfation of limestone and dolomite have demonstrated that the effect of temperature on the reaction is a complex phenomenon. Activation energies obtained at low calcium utilization show values in the range of 5 to 15 kcal-mole, 20 to 62 kJ, indicative of a mixture of mass transport and chemical reaction control. In fluidized beds, however, where sulfur dioxide removal is normally

carried out at 30 to 40 percent utilization, a maximum in the extent of sulfur dioxide removal at a fixed calcium utilization is observed at a temperature of about 843°C (1550°F) at atmospheric pressure, implying that the rate of the overall reaction decreases above 843°C (1550°F).

In three experiments, TG 229, 230, and 231 at 843, 899, and 954°C (1550, 1650, and 1749°F), limestone was calcined and sulfated. The stones were inactive, leading to utilization in the range 11 to 14 percent. The results, illustrated in Figure D-5, showed that maximum reactivity was observed at 843°C (1550°F): the calcium utilization, however, was not typical of fluidized bed conditions. It was decided, therefore, to carry out sulfation runs at different temperatures on samples which had all been calcined at the same conditions of temperature and carbon dioxide partial pressure.

Calcination of the samples was effected at 930°C (1706°F) in 60 percent carbon dioxide in nitrogen, and the samples were then sulfated at temperatures from 750 to 950°C (1382 to 1742°F) at 50°C (122°F) intervals, in random order. The results are shown in Figure D-6 and indicate that although the initial rates were scarcely distinguishable, the course of reaction was different for each temperature after 20 percent utilization of the calcium. The importance of these differences becomes clear when the extent of reaction after a fixed time interval, one hour, is plotted as a function of sulfating temperature, Figure D-7. The utilization of the stone peaks at a maximum value of 43 percent at about 860°C (1580°F), reproducing the sulfur dioxide retention efficiency pattern observed in fluidized bed results. The data derived for the rate of reaction as a function of calcium utilization in these experiments are used in Appendix E to project fluidized bed sulfur retention.

The rate of sulfation derived here may be compared with that noted in experiments at TVA. [4] Using limestone 1359, 707 to 595 microns, soft-calcined at 900°C (1652°F) in nitrogen, these experiments were carried out by sulfating 50 mg of calcine in 4 percent sulfur dioxide, 4 percent oxygen isothermally at 930°C (1706°F). The maximum rate of sulfation noted was 3.99 mg/minute, which may be compared with rates of 2.64 and 3.08 mg/minute noted in the Westinghouse experiments. When

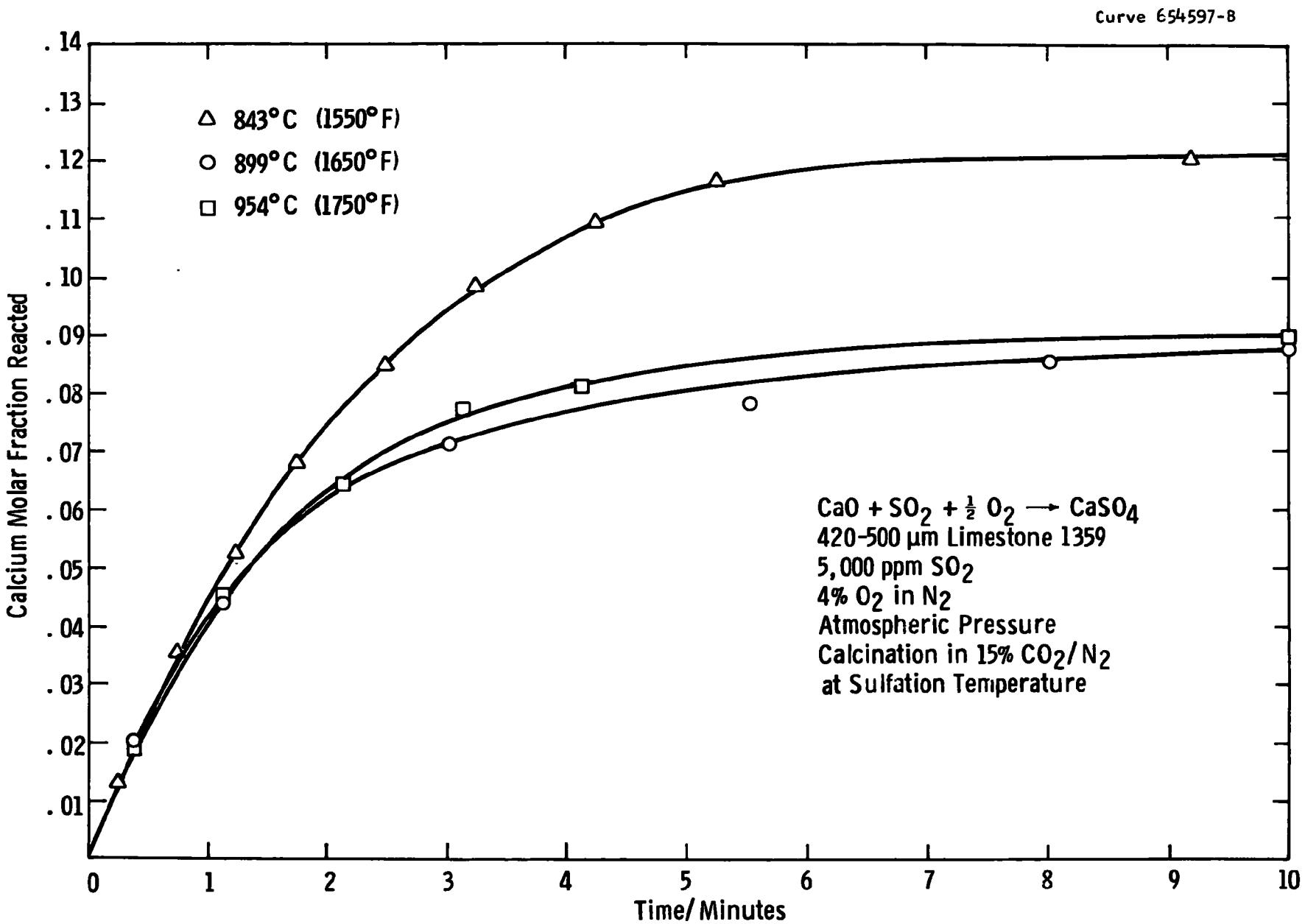

Figure D-5 —Effect of temperature on sulfation of limestone 1359

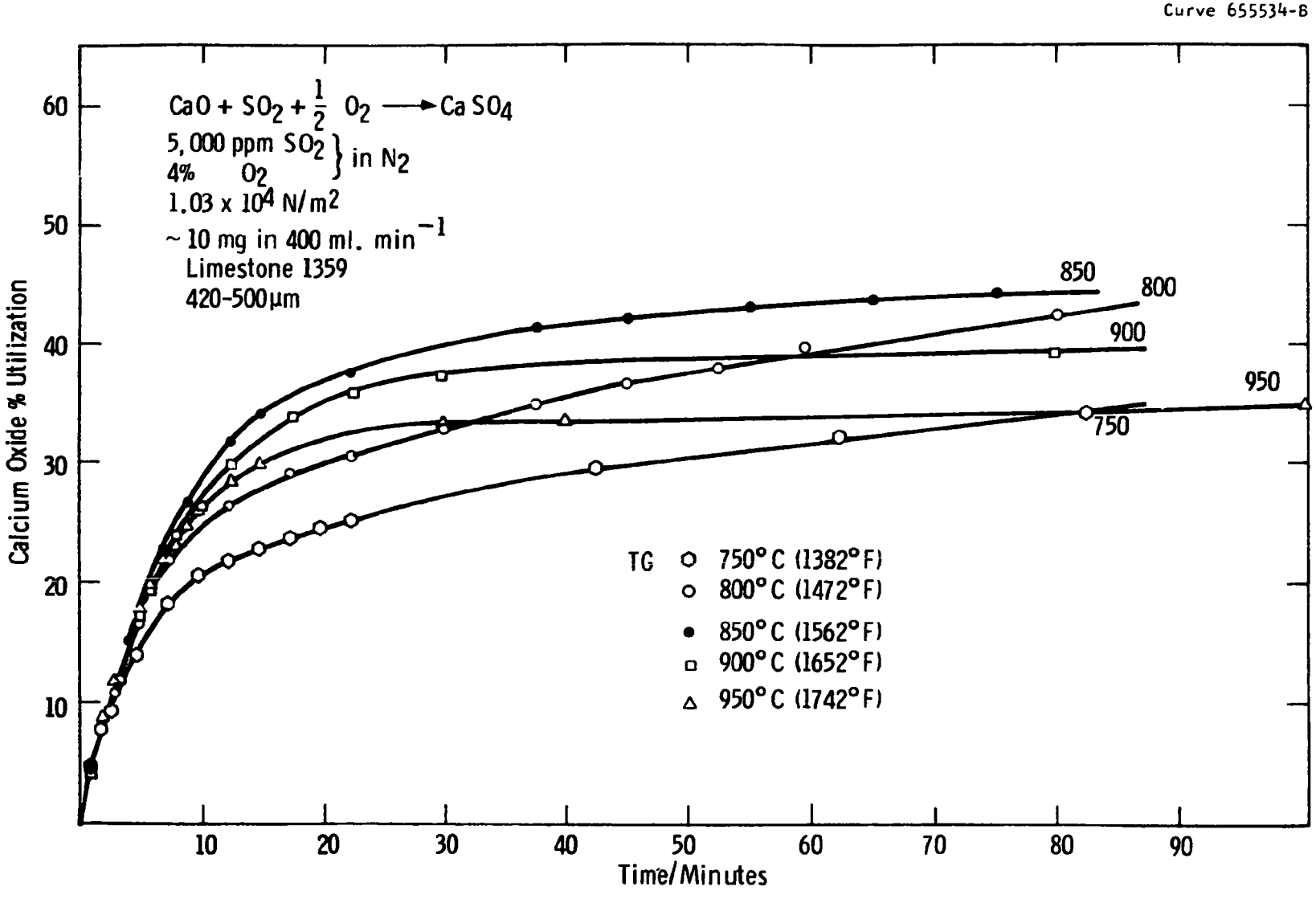

Figure D-6–The effect of temperature on limestone sulfation

Curve 655457-A

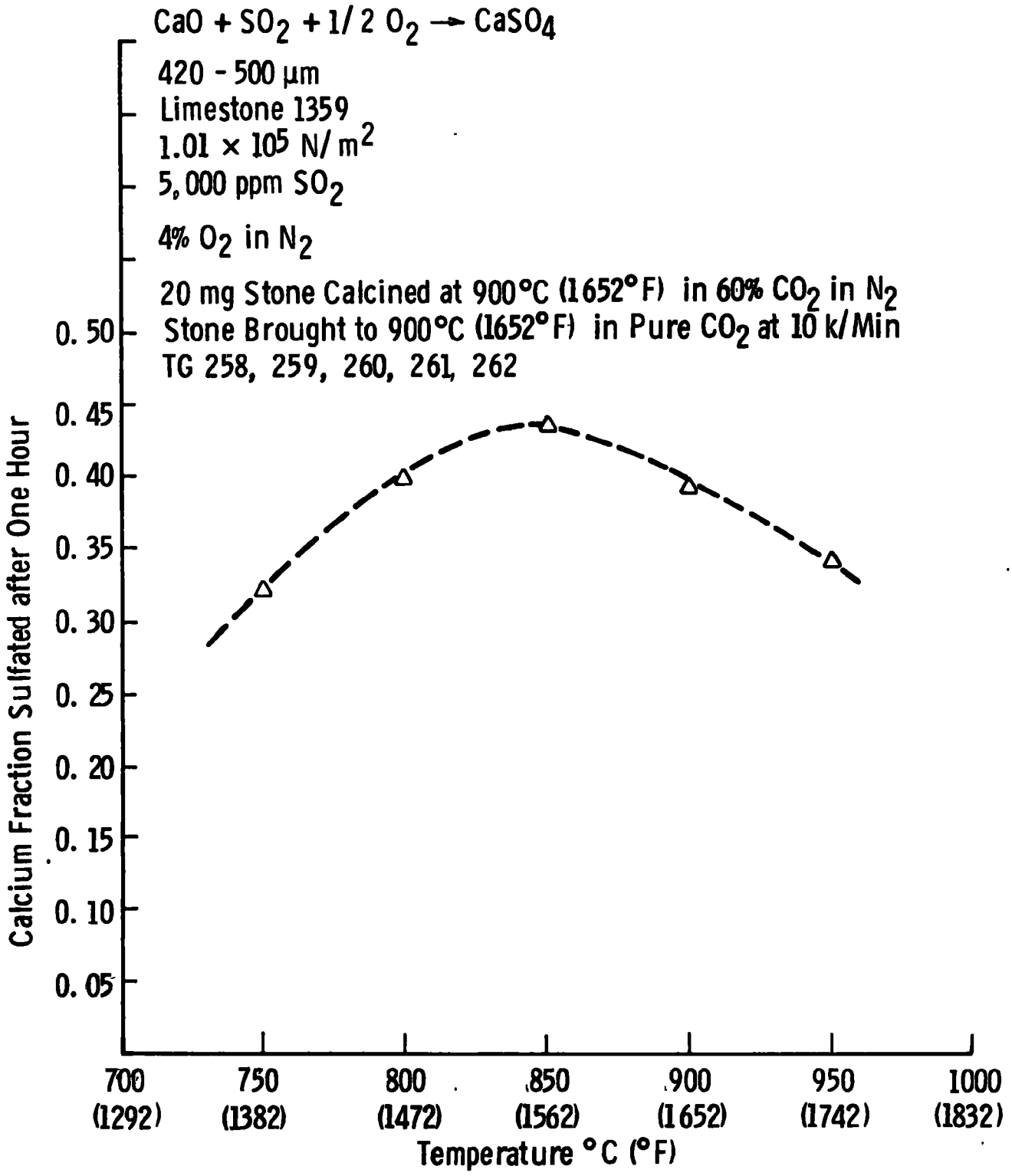

Figure D-7—The effect of temperature on CaO utilization in sulfation

these rates are adjusted to unit gas concentration, the rate noted here is almost six times as rapid as that recorded by TVA. Probably the chief reason for this difference is the small size of the Westinghouse sample (10 mg of calcine). Previous work at Westinghouse has illustrated the effect of sample size on the initial rate of sulfation.[1]

The rate of sulfation was determined for each of the five runs at 10 percent utilization, and an apparent activation energy, Ea, of 5 kcal. $mole^{-1}$ derived using the Arrhenius equation. Such low values of Ea are typical for reactions in regimes where the rate is predominantly mass-transport controlled.

The data obtained in experiments TG 258 through 262 were obtained on samples calcined after heating to the temperature of calcination at 10°C (18°F) per minute. Two runs at a different heating rate, 20°C (36°F) per minute, carried out before and after the above-mentioned runs, gave a reactivity in sulfation different from the 10°C (18°F) per minute experiments, as Figure D-8 shows. The utilization after one hour in each of these experiments was 48 percent calcium, as opposed to 40 percent in the 10°C (18°F) per minute run. The initial rates of sulfation in runs on samples heated at 10°C/min (18°F/min) and 20°C/min (36°F/min) were identical, as Figure D-9 shows: possibly it is during the later phase of sulfation that the structure developed in the stone affects the reaction rate. Application of the data to fluidized bed modeling, however, as described in Appendix E, showed that the latter data, taken at the higher heating rate and indicating higher reactivity, more accurately predicted fluidized bed performance. This suggests that the data in TG 262 was anomalous and that the sample heat-up rate is not important at the level of 10 to 20°C (18 to 36°F)/minute.

The Effect of Temperature on the Sulfation of Limestone 1359 at Pressure

A set of experiments parallel to those described above was carried out at a pressure of 1013 kPa (10 atm). The results obtained were far less clear-cut, principally because of the difficulty in reproducing controlled conditions of calcination. At the higher volumetric

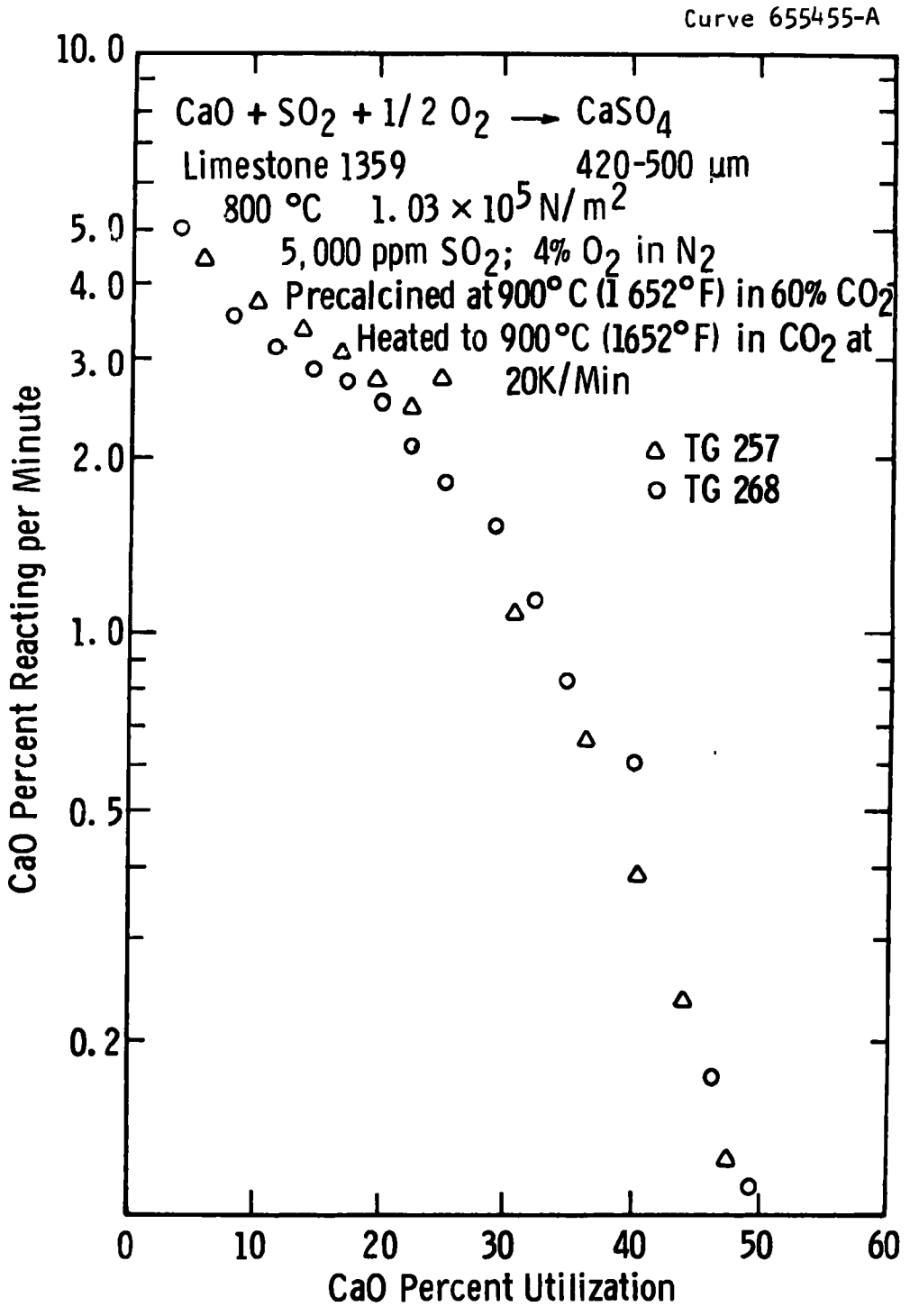

Figure D-8—Comparison of rates for identical sulfation runs

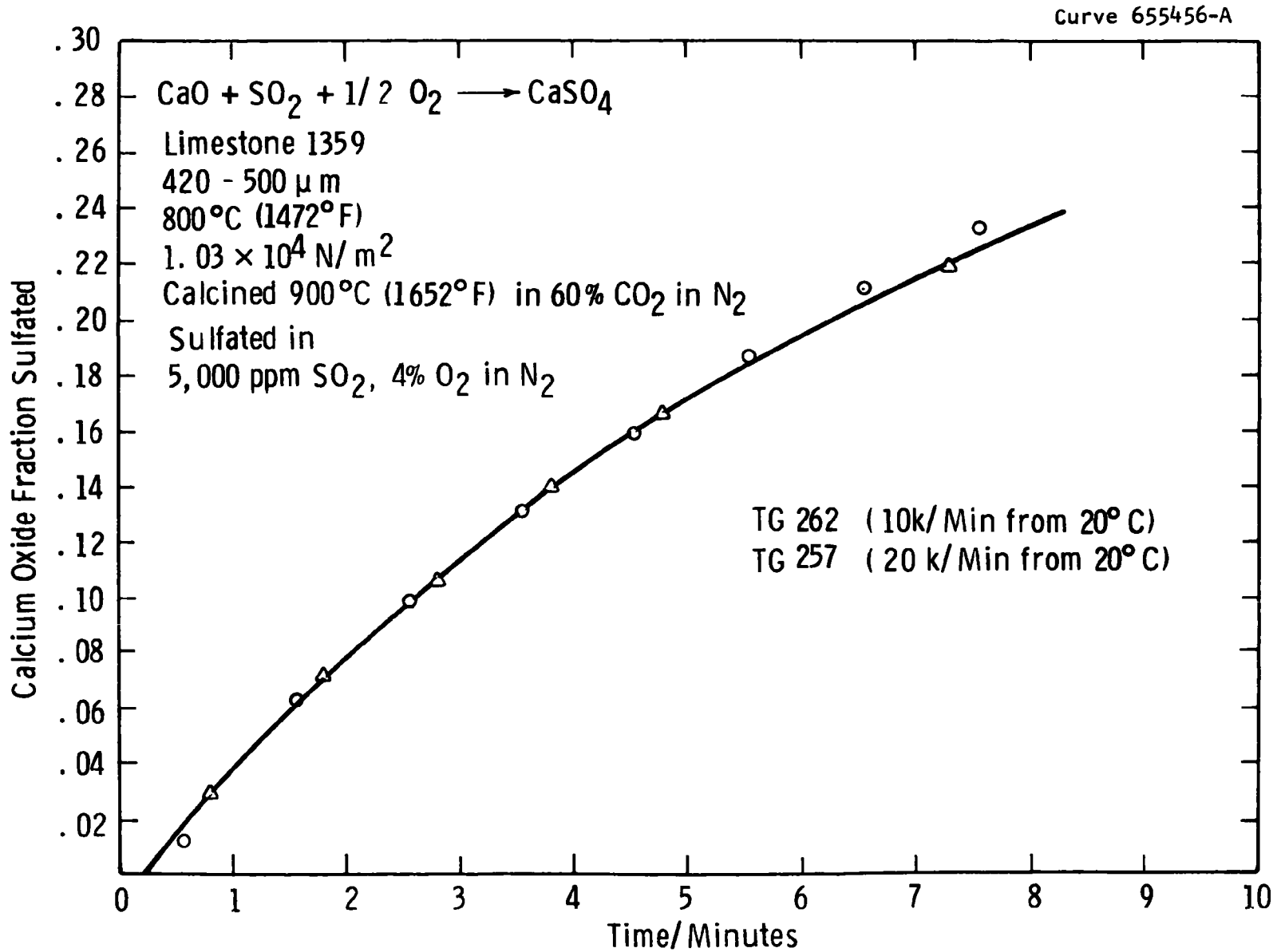

Figure D-9—Comparison of repeat experiments - fast phase of sulfation

flow rates reproduction of the temperature and gas composition was poor, as evidenced by the variation in calcination time recorded.

The extent of sulfation recorded in these experiments after 30 minutes is shown in Figure D-10 as a function of temperature. The extent of sulfation increases up to 900°C (1652°F). At 950°F (1742°F) it has decreased; but, as shown, significant differences in the extent of the decrease were noted. The conclusion that may be drawn is that calcined limestone should be an effective sorbent at pressures up to a temperature between 900 and 950°C (1652 and 1742°F). Reexamination of the sulfation kinetics in the region 900 to 950°C (1652 to 1742°F) at pressure is required.

The Sulfation of Dolomite

The activation process of calcining under a high partial pressure of carbon dioxide yields a dolomite with greater sulfur dioxide sorption capacity at a fast rate of reaction.[1] Since the data reported earlier referred to 420 to 500 μm particles, the effect of an increase in particle size to 1,000 μm particles was studied. In TG 201 1200/1000 μm particles of dolomite 1337 were calcined in 10 percent carbon dioxide in nitrogen at 750°C (1382°F) to calcine the magnesium carbonate fraction. The sample was then heated to 925°C (1695°F) and the carbon dioxide partial pressure dropped to 81.04 kPa (0.8 atm). The sample was calcined and sulfated at 871°C (1600°F) in 0.5 percent sulfur dioxide in 4 percent oxygen in nitrogen. A comparison sample, TG 202, was similarly sulfated after calcination under nitrogen by heating to 880°C (1616°F). Comparison of the rates of reaction showed that the calcination treatment in carbon dioxide had increased the stone capacity. If 2 percent calcium/minute is taken as the criterion for an acceptably fast rate of reaction with sulfur dioxide under the given experimental conditions, then the rate of reaction fell below this value at 50 percent utilization in TG 201 and 35 percent utilization in TG 202. This can be regarded as an improvement of the calcium/sulfur molar feed ratio from 2.6 to 1.8 at a mean particle size of 1100 μm. The activation process for increasing the utilization of dolomite can be used with large particles of sorbent.

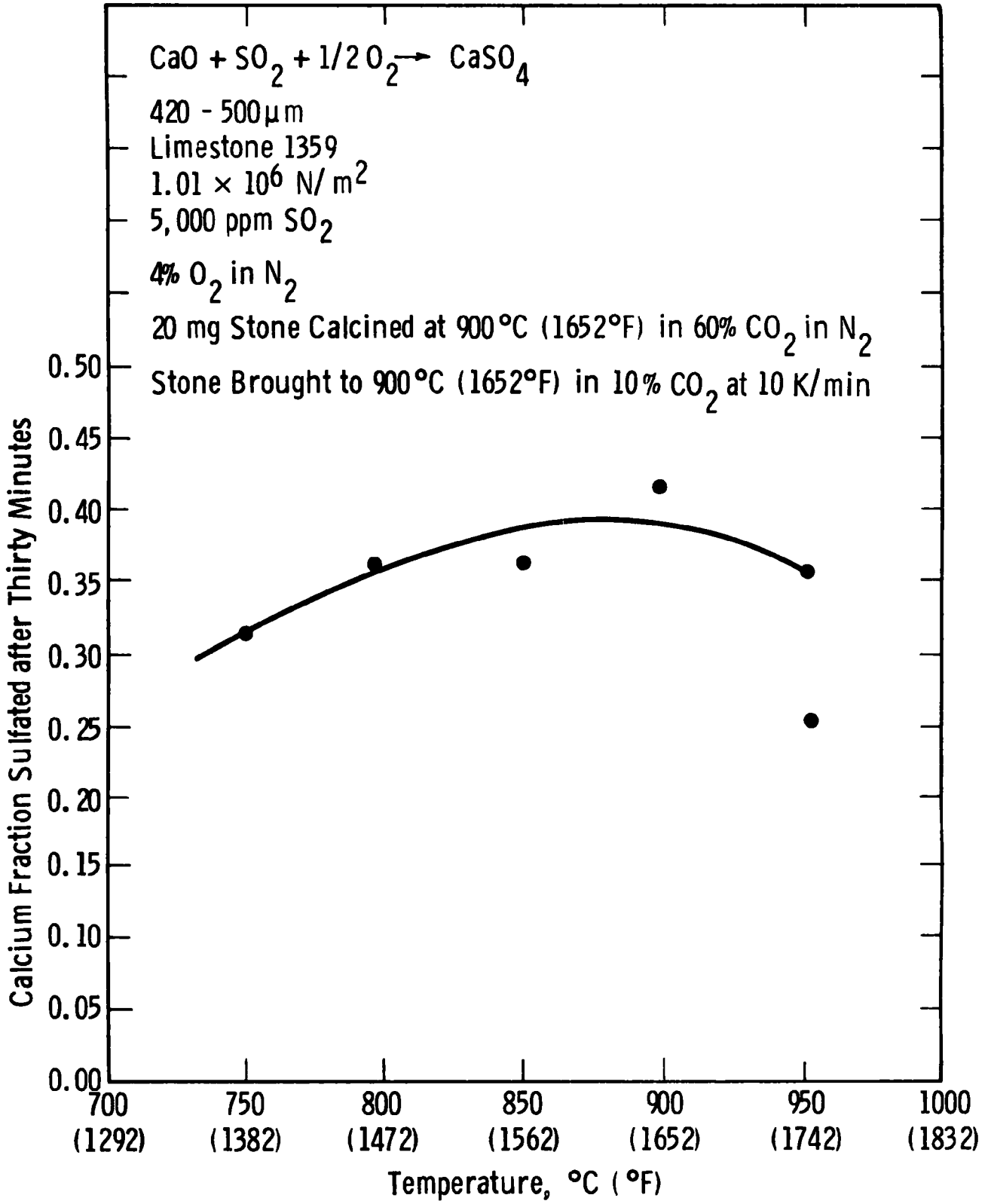

Figure D-10—The effect of temperature on CaO utilization in sulfation at pressure

Attempted Sulfation of Limestone 1359 (Uncalcined)

A 450-to-500 μm sample of limestone 1359 was heated to 850°C (1562°F) under carbon dioxide and sulfated in 0.18 percent sulfur dioxide, 4 percent oxygen, 60 percent carbon dioxide in nitrogen. The total weight gain noted corresponded to sulfation of 3.4 percent of the calcium carbonate content of the stone in 100 minutes. The thermodynamic equilibrium for the reaction

$$CaCO_3 + SO_2 + \frac{1}{2} O_2 \rightarrow CaSO_4 + CO_2$$

lies far to the right: at 816°C (1500°F) and 871°C (1600°F) the equilibrium pressure of sulfur dioxide is less than 1 ppb and 1 ppb in 4 percent oxygen and 10 percent carbon dioxide at 1013 kPa (10 atm). The limitation on desulfurization is kinetic.

In order to test the possibility of activating limestone as a sorbent, a sample was calcined, recarbonated, and exposed to sulfur dioxide and oxygen. A slight weight increase occurred at a slow rate indicating that residual calcium oxide which had not recarbonated was reacting to form the sulfate.

Sulfation of Half-Calcined Dolomite

As Figure D-1 illustrates, half-calcined dolomite is stable over much of the operating range of the low excess-air fluidized bed combustor. The stability line shown in the figure is for the exit gas carbon dioxide composition; at the bed entrance, where the fluidized gas is mainly air, some calcination will take place, yielding fully-calcined dolomite; and sulfur dioxide and carbon dioxide will compete for the calcium oxide generated. Previous work at Westinghouse has shown that half-calcined dolomite is a reactive sorbent for sulfur dioxide removal.[1,5] The runs carried out, however, used larger samples than have been found optimal in subsequent studies, and the kinetics of the reaction could not be assessed relative to the reactivity of calcined dolomite.

Three experiments were carried out on the sulfation of half-

calcined dolomite 1337. The first two experiments (280, 281) were tests with 1680 to 2000 μm diameter particles. (It should be noted that only two particles are used in a run with this size stone.)

In the first experiment the temperature was cycled between 850 and 690°C (1562 and 1274°F) as the reaction proceeded. After 23 minutes 33 percent utilization was noted, during which time the sample had been cooled to 690°C (1274°F) and heated back to 820°C (1508°F). In the following experiment isothermal sulfation at 800°C (1472°F) gave 50 percent utilization in 23 minutes. The decline in reaction was not as abrupt as has been universally noted with calcined dolomite after two hours of reaction; 87 percent utilization was noted in the isothermal experiment.

A third experiment on (420 to 500 μm) 1337 half-calcined dolomite showed greater initial reactivity—61 percent utilization in 23 minutes. The subsequent activity, however, was slow, yielding 68 percent utilization after two hours. (See Figure D-11.)

The reactivity of half-calcined dolomite appears to be intermediate between nitrogen-calcined dolomite and dolomite which has been calcined under a high partial pressure of carbon dioxide relative to the equilibrium pressure. In addition, the slowing down of reaction is less abrupt than with calcined dolomite or limestone. This latter fact means that increased gas residence times in the fluidized bed should improve (lower) the calcium/sulfur molar ratios required for any given sulfur removal criterion.

Discussion of the Temperature Effect

The phenomenon of an optimum temperature for sulfur dioxide absorption has been discussed by Moss.[6] He pointed out that when a fresh bed of limestone was used, absorption efficiency was 90 to 95 percent in the Esso experiments, and the efficiency was unaffected by temperature in the range recorded (presumably around 800 to 925°C/1472 to 1697°F). This phase of reaction corresponds to the initial phase of reaction in the Westinghouse TG data and other kinetic curves: in this range of reaction (5 to 10 percent calcium oxide reacted) a slight increase in reaction rate is noted corresponding to an activation energy of 5 to 15 kcal.

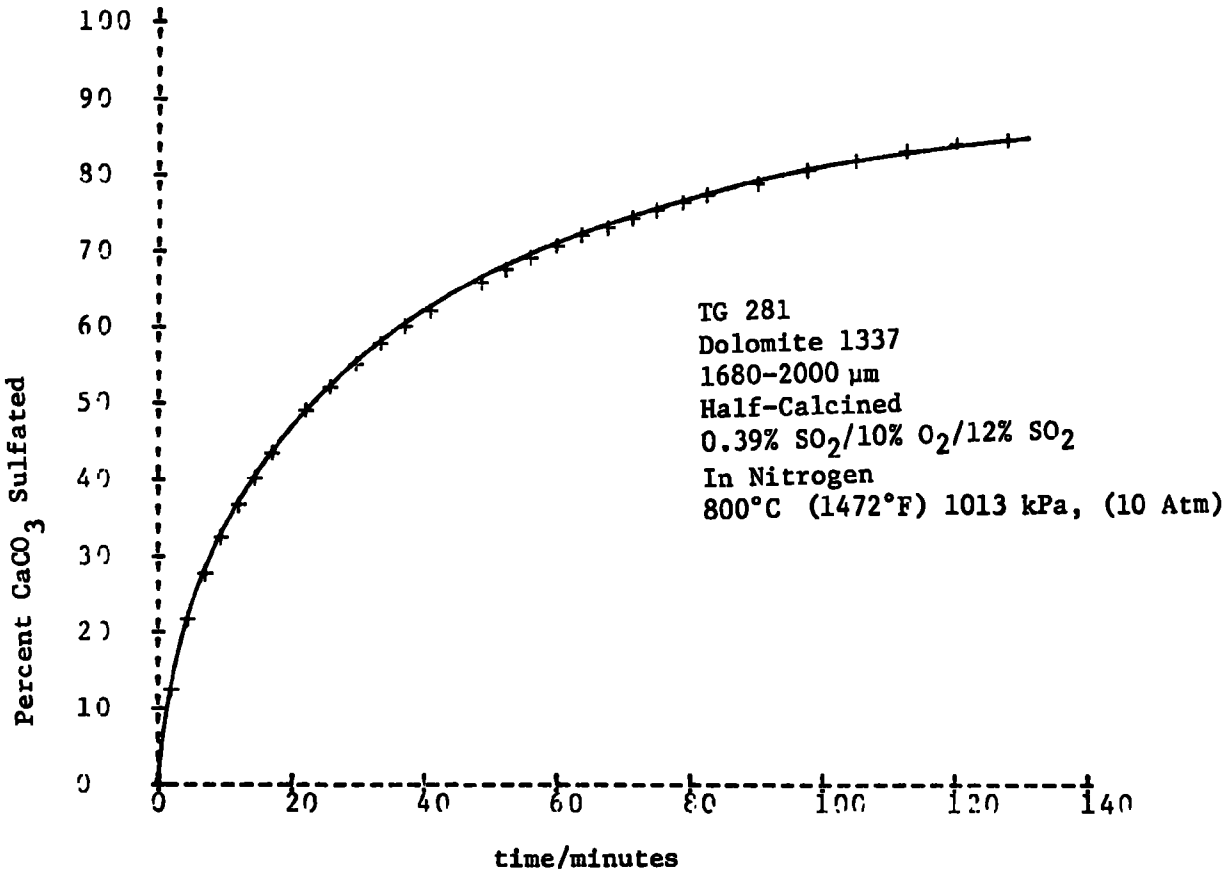

Figure D-11. Sulfation of half-calcined dolomite

mole^{-1}—insufficient to cause any appreciable change in the extent of sulfur dioxide absorption as noted in the fluidized bed experiments.

Moss has noted, however, that when 31 percent of the lime has reacted, absorption efficiency is markedly temperature-dependent with a maximum at 865°C (1589°F). He argues that since this optimum temperature "only becomes apparent after the lime is appreciably reacted, it follows that chemical reaction rate cannot be the controlling factor, it would operate on used and fresh lime alike." This argument is excessively universal—while it could be true it need not be true, and the overall evidence of the TG work reported here weighs against it. The primary flaw in the argument lies in the inherent assumption that if the chemical rate is controlling at 32 percent calcium oxide utilization, then it must also control at lower utilization. A typical TG rate curve, as in Figure D-12, may be conveniently considered as a three-stage process. Initially, region A, the rate of reaction, is controlled by mass transfer to the surface of the solid from the gas stream. The evidence that this is true is provided by

- The insensitivity of the rate to temperature (apparent Ea at 10 percent sulfation of calcium oxide is 5.3 kcal. mole^{-1})
- The insensitivity of the rate to source of calcium oxide—both limestone and dolomite of different calcium content, 40 to 18 percent, have similar rates of reaction.
- The dependence of initial rate on pressure, is accurately predicted by consideration of the mass transfer rate to ideal spherical particles under TG experimental conditions

The final phase of reaction, C, is controlled by the rate of diffusion of the reactant or reactants across the solid product accumulated in the pores of the solid. This interpretation is supported by

- The insensitivity to temperature of final rate of reaction

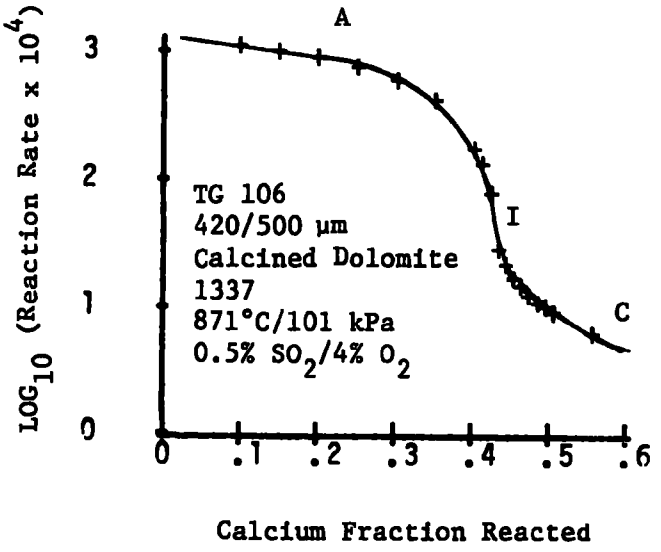

Figure D-12a: The decline in rate of reaction (calcium fraction reacting per minute) as calcined dolomite sulfates

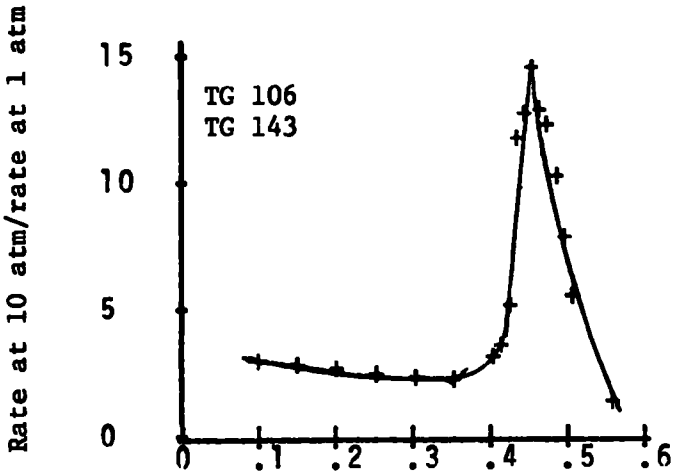

Figure D-12b: The effect of pressure on sulfation of calcined dolomite 1337 (420 µm; 0.5% SO_2/4% O_2; 871°C).

- The insensitivity to system pressure of the final rate of reaction. Since the diffusion coefficient, D, varies inversely with P (the system pressure), the effect of increasing the partial pressure of sulfur dioxide by pressurized operation is negated.
- The successful prediction of the rate of reaction to form calcium carbonate when carbon dioxide is substituted for sulfur dioxide as the reactant because of the different diffusivities of carbon dioxide and sulfur dioxide.

The intermediate range I, in which the rate falls through several orders of magnitude is a region of mixed kinetic control—and it is difficult to devise tests which will separate the controlling factors. The mechanism thought to apply will be described, and the evidence will be discussed qualitatively.

For the initial stages of reaction, the flow of sulfur dioxide gas through the external surface of the solid is immediately reacted with calcium oxide—so that an effective sulfur dioxide sink exists, and flow is governed solely by the diffusional resistance at the surface. As the walls of the pores in the calcium oxide react, however, the rate at which sulfur dioxide is fixed decreases, and the pressure of sulfur dioxide in the pores increases. The calcium oxide available for direct reaction as the gas collides with the solid has decreased; the resistance to reaction rises; and as it becomes rate controlling, the flow of sulfur dioxide into the solid is controlled by

- The constant boundary diffusional resistance at the surface
- The in-series resistance within the stone, which increases as reaction proceeds.

As reaction inside the pores gets slower, owing to the depletion of solid reactant on the internal surface, the available supply of sulfur dioxide increases until the pressure in the pores equals the partial pressure of sulfur dioxide outside the stone. This effect should be noticeable the

slower the overall rate, while there is still unreacted solid which can be reached by the gas without diffusion across the solid product layer on the pore wall (which, of course, makes a continuous minor contribution to the overall reaction rate). The first critical test can now be applied to this model. If the mechanism described is correct, the effect of increasing total pressure at constant sulfur dioxide concentration on the rate of reaction expressed as the ratio of the overall rates should increase from about 2 (the ratio for mass transfer control) to about 10 (the ratio for chemical control) and then fall to 1 (as diffusion through the product layer takes over). Figures D-12 a and b show that the effect is observed for kinetic experiments at 101.3 and 1013 kPa (1 and 10 atm) total system pressure. The comparison was made for calcium oxide sorbents calcined under the same conditions of carbon dioxide partial pressure to ensure as far as possible that the same pore structure exists in both samples. Each of the comparisons made demonstrated the effect noted.

The second indicator of a change from boundary layer mass transfer to chemical control in region D lies in the effect of temperature on the rate of reaction in this region. In TG 303 the rate of reaction was determined as a function of utilization in the range 33 to 44 percent and found to follow closely the relation:

$$\log \text{rate} = -k\,(\text{utilization}) + \text{constant}.$$

The temperature of the sample was then raised to 950°C (1742°F) and cooled again. The rate data (uncorrected for the effect of utilization) showed an activation energy of 60.7 kcal. mole^{-1}. Correction for the increasing stone utilization, however, yielded the value 51 kcal. mole^{-1} over the range 817 to 950°C (1503 to 1742°F). The only value found in the literature which does not reflect diffusional limitations is 57 kcal. mole^{-1} obtained by Jungten and van Heek,[7] in the lower temperature range.

In order to probe further the mechanism of lime sulfation, experiments were carried out on the reaction

$$CaO + SO_2 \rightarrow [CaSO_3] \rightarrow \frac{1}{4} CaS + \frac{3}{4} CaSO_4$$

which may be the first step in the lime sulfation reaction.

Experiments on the Reaction Between Sulfur Dioxide and Calcined Lime

The equilibrium between calcium oxide, sulfur dioxide, and calcium sulfite was briefly examined in order to explore the reaction between calcined limestone and sulfur dioxide and to find the source of the decreasing utilization as temperature is increased.

The ability of the TG apparatus to determine such an equilibrium was checked in a preliminary experiment by determining one equilibrium point for the reaction

$$CaCO_3 \rightleftarrows CaO + CO_2$$

The solid used was obtained by calcining calcium hydroxide ($Ca[OH]_2$) reagent. Pure carbon dioxide was passed over the sample and the temperature raised and lowered. The TG balance output was connected so that weight was recorded as a function of temperature, and the sensitivity of the system adjusted so that a one percent change in the solid weight yielded a 25.4 mm (1 in) deflection on the chart paper. The tracing can be read to within 1.3 mm (1/20 in). The result obtained, averaged over four cycles of decomposition and recarbonation, is compared with some literature values.

	P_{CO_2}, kPa (atm)	T°C (°F)
TG (W)	96.8 (0.956)	892.1 (1638)
Hill[8]	96.8 (0.956)	901.0 (1654)
Curran[2] et al.	96.8 (0.956)	891.3 (1636)
Chemical Rubber Company[9]	96.8 (0.956)	895.0 (1643)

There was a 7°C (13°F) difference between the recarbonation and regeneration temperatures, but this precision and accuracy should be adequate.

A sample of limestone 1359 was then tested. The first calcination temperature under 96.6 kPa (0.954 atm) carbon dioxide was obsured by the decomposition of the magnesium carbonate($MgCO_3$) content of the stone. The recarbonation and subsequent cycling gave equilibrium temperatures of 896.5, 892.0, and 895.5°C (1645, 1637.6, and 1643.9°F), compared with literature values of 900.8°C (1653.3°F) (Hill)[9] and 890.5 (1634.9°F) (Curran).[2]

The sample was heated and cooled in sulfur dioxide (.005 atm) to form calcium sulfite, reheated in nitrogen to drive off residual carbon dioxide, and cooled in sulfur dioxide. The sample was then cycled through weight gain and weight loss, and the average equilibrium temperature was 930.7°C $\pm$ 25°C (1707.1°F $\pm$ 77°F). The temperature span was much greater here than in the case of the calcium carbonate decomposition.

The sample was heated and cooled further, and an interesting anomaly was apparent. The sample was heated in 0.005 atm sulfur dioxide until it lost weight at 938°C (1720.4°F) and on cooling down it gained weight at 968°C (1774.4°F). Reheating caused a weight loss to begin at 956°C (1752.8°F) and further heating caused a weight gain at 1013°C (1855.4°F). On cooling, the sample gained weight continuously. Reheating caused a weight loss at 900°C (1652°F) followed by a reversal to weight gain at 979°C (1794.4°F).

In summary, there was an equilibrium pressure of sulfur dioxide calcium sulfite ($CaSO_3$)/calcium oxide at 900 to 950°C (1652 to 1742°F) and a second equilibrium point at 979 to 1013°C (1794.4 to 1855.4°F). This would require that the solid phase pass through a transformation which lowered its free-energy by about 2800 cal. $mole^{-1}$. Possibly, liquid formation in the system calcium sulfide(CaS)/calcium sulfate caused by disproportionation of the calcium sulfite would suffice to stabilize the calcium sulfite or calcium sulfite/calcium sulfate mixture.

Apart from the possible use of this method to determine the liquid eutectic in the calcium sulfide/calcium sulfate, the apparent equilibrium temperatures observed are surprising. Since calcium sulfite is thermodynamically unstable with respect to disproportionation to calcium sulfide and calcium sulfate, and the latter react to form sulfur dioxide according to the equation

$$\frac{1}{4}\ CaS + \frac{3}{4}\ CaSO_4 \rightarrow CaO + SO_2,$$

the equilibrium pressure of sulfur dioxide should be that noted by Curran.[2] At the partial pressure of sulfur dioxide used, the equilibrium temperature should be ∿840°C (1544°F) according to Curran's data for calcium sulfide/calcium sulfate, and Esso obtained the same equilibrium pressures as Curran starting with calcium oxide and sulfur dioxide. The Radian data[10] calculated using estimated values for the thermodynamic properties of calcium sulfite give 760°C (1400°F) as the temperature for equilibrium by sulfur dioxide over calcium oxide at .005 atm sulfur dioxide. It was thought necessary to repeat the experiments with pure calcium oxide rather than with lime derived from limestone containing impurities such as magnesium oxide (MgO) or ferrous oxide (Fe_2O_3).TG experiments were carried out in which a flow of sulfur dioxide (0.5 percent) in nitrogen over calcined calcium carbonate caused a weight change, as the temperature was varied, at a constant heating rate.

- The rate of sulfur dioxide uptake increases with increasing temperature, up to 815°C (1499°F) at 0.5 percent sulfur dioxide. The rate decreases on heating past 815°C (1499°F).
- At above 890°C (1634°F) the product begins to decompose, as the solid is heated. Complete reversal of the weight gain was never noted.
- No substantial oxidation of calcium sulfide takes place during the experiment, since reaction ceased entirely when 100.8 percent of stoichiometric calcium sulfite (as determined by weight gain) has formed.

- The second equilibrium point was noted at 976°C (1789°F), in other words, readsorption began again on heating through this temperature.
- The samples may have suffered surface melting during the experiments. Figure D-13 shows the weight changes observed during a typical heating run.

It can be concluded from these experiments that

- The rate of reaction between sulfur dioxide and calcium oxide reaches a maximum between 800 and 850°C (1472 and 1562°F) closely corresponding to the optimum temperature for lime sulfation.
- Desorption of sulfur dioxide occurs at 900°C (1652°F), so that formation of calcium sulfate will be a competitive process between oxidation and desorption.
- Complex equilibria involving solid solutions or liquid eutectics occur at temperatures close to 950°C.
- Further work, including differential thermal analysis and microscopic examination of sample structure should be carried out to characterize the effects observed at 950°C (1742°F).

Kinetic data, representative of the experiments represented in Table D-5, are shown in Tables D-6 through D-15.

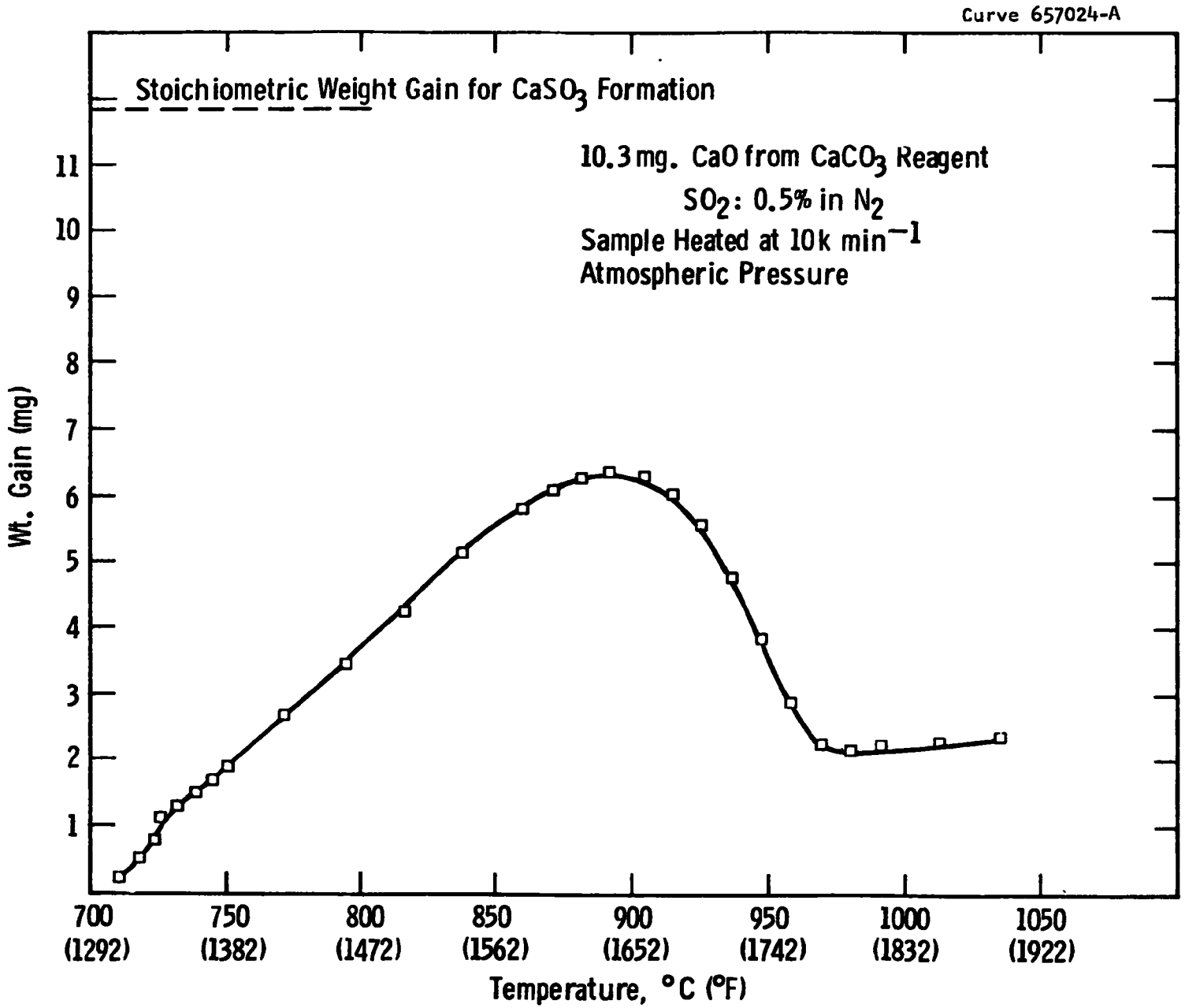

Figure D-13—The effect of temperature on the course of the reaction between SO_2 and CaO

Table D-5

TG RUNS ON SULFATION OF CALCINED LIMESTONE, CALCINED DOLOMITE, AND HALF-CALCINED DOLOMITE

TG no.	Stone	Pretreatment	Sulfation P,kPa(atm)	Sulfation T,°C(°F)	Result molar %SO_4/mins	Comment or purpose
196	L1359 420-500 micron	Calcination at 871°C (1000°F) retarded by CO_2	10^3(10)	871 (1600)	12.7/71	Calcination effect
197	L1359 420-500 micron	Calcination in N_2 at 34°C/min to 871°C (1600°F)	10^3(10)	871 (1600)	12.5/60	Calcination effect
198	L1359	Calcined in 5% CO_2 at 930°C (1706°F)	10^3(10)	871 (1600)	29/60	Calcination effect
199	L1359		10^3(10)	871 (1600)	41.8/220	Calcination effect
200	D1337 420-500 micron	Slow $MgCO_3$ calcination at 730°C(1346°F) slow $CaCO_3$ calcination at 930°C(1706°F)	10^3(10)	871 (1600)	86/10	
201	D1337 1200-1000 micron	"	10^3(10)		69/60	Slow calcium calcination
202	D1337 1200-1000 micron	Calcined in N_2	10^3(10)		62/60	62% utilization in one hour-N_2 calcination has effect
204	D1337 1200-1000 micron	Calcined in two stages using CO_2 suppression	10^3(10)	871 (1600)	69/60	65% utilization in one hour-max. temp. in calcination was 1100°C (2012°F)

Table D-5 (Continued)

TG no.	Stone	Pretreatment	Sulfation P,kPa(atm)	Sulfation T,°C(°F)	Result molar %SO_4/mins	Comments or purpose
210	Tymochtee				80/63	Leaching effect
214	D1337	Calcined in two stages-$CaCO_3$ at 900°C(1652°F)			54/114	Calcination effect
215	L1359	Heated to 900°C(1652°F)-calcined in N_2	10^2(1.0)	871 (1600)	9/114	Calcination effect
216	L1359	Heated to 900°C(1652°F) in CO_2-calcined in 30% CO_2/N_2	10^2(1.0)	871 (1600)	14/72	Calcination effect
220	L1359	Heated to 871°C (1600°F)-calcined in 30% CO_2/N_2	10^2(1.0)	871 (1600)	34/46	Calcination effect
221	L1359	Heated to 901°C(1654°F) in CO_2-calcined in 30% CO_2/N_2	10^2(1.0)	871 (1600)	42/52	Calcination effect at 1 atm
222	D1337	Calcined in two stages	10^2(1.0)	871 (1600)	86/60	High utilization at atmospheric pressure
226	D1337 2000-1680 micron	Two-stage calcination	10^3(10)	871 (1600)	86.9/60	
229	Limestone 1359 420-500 micron	Fast calcination in nitrogen	10^2(1.0)	954 (1749)	13/165	
230	"		10^2(1.0)	843 (1549)	14	
231	"		10^2(1.0)	899 (1650)	11/120	
257	L1359	Procedure A Heated to 900°C (1652°F) in CO_2 at 20°C/min calc. in 60% CO_2	10^2(1.0)	800 (1472)		

Table D-5 (Continued)

TG no.	Stone	Pretreatment	Sulfation P,kPa(atm)	Sulfation T,°C(°F)	Result molar %SO_4/mins	Comments or purpose
258	L1359	Heated to 900°C(1652°F) in CO_2 at 10°C/min calc. in 60% CO_2	10^2(1.0)	950 (1742)	34/60	Effect of temperature on reaction
259	L1359	B	10^2(1.0)	750 (1382)	32/60	"
260	L1359	B	10^2(1.0)	900 (1652)	39/60	"
261	L1359	B	10^2(1.0)	850 (1562)	43.2/60	"
262	L1359	B	10^2(1.0)	800 (1472)	39.7/60	"
268	L1359	A	10^2(1.0)	871 (1600)		"
263	L1359 420-500 micron	Fluid bed calcined in nitrogen	10^2(10)	870 (1598)	17.5/60	Low calcium utilization
264	L1359 420-500 micron	"	10^3(10)	870 (1598)	17.8/60	System pressure does not affect utilization significantly
265	L1359 420-500 micron	"	10^3(10)	870 (1598)	15.1/60	"
266	L1359 420-500 micron	"	507(5)	870 (1598)	13.5/60	"
267	D1337 2000-1680 micron	Half-calcined in 1.5 atm CO_2	10^3(10)	893-903 (1639-1657)	40/60	Rate does not decline abruptly
279	L1359		10^3(10)		5.6/100	
280	D1337 2000-1680 micron	Half-calcination	10^3(10)	900-700-900 (1650-1382-1652)		Temperature scan

Table D-5 (Continued)

TG no.	Stone	Pretreatment	Sulfation P,kPa(atm)	Sulfation T,°C(°F)	Result molar $\%SO_4$/mins	Comments or purpose
281	D1337 2000-1680 micron	Half-calcination	10^3(10)	800 (1472)	87/120	
282	D1337 420-500 micron	Half-calcination	10^3(10)	800 (1472)	68	
283	Tymochtee					
298	L1359		10^3(10)	850 (1562)		Temperature effect at pressure
299	L1359		10^3(10)	950 (1742)	23/	Temperature effect at pressure (utilization low run repeated in TG304)
300	L1359		10^3(10)	750 (1382)		Temperature effect at pressure
301	L1359		10^3(10)	900 (1652)		"
302	L1359		10^3(10)	850 (1562)	34/37	"
303	L1359		10^3(10)	800 (1472)		"
304	L1359		10^3(10)	950 (1742)		"
305	L1359		10^3(10)		37/60	"
320	Powdered $CaCO_3$ (Fisher)	Calcined in nitrogen	10^2(1.0)	scan		
330	Limestone N.B.S. standard	2.0 wt% NaCl added	10^2(1.0)	scan		
331	"	"		scan 750-1000(1382-1832)		

Table D-6

TG DATA FOR RUN 202[a]

(DOL 1337 1200/1000 μm; SULFATION)

% REACTED	TIME/MIN.	% /MIN.	% REACTED	UNIT RATE
5.28	0.38	13.62	2.64	27252.91
9.72	0.63	17.76	7.50	35521.70
13.56	0.88	15.36	11.64	30721.47
17.28	1.13	14.88	15.42	29761.42
20.52	1.38	12.96	18.90	25921.24
23.28	1.63	11.04	21.90	22081.05
25.80	1.88	10.08	24.54	20160.96
27.84	2.13	8.16	26.82	16320.78
29.76	2.38	7.68	28.80	15360.73
31.80	2.63	8.16	30.78	16320.78
36.48	3.38	6.24	34.14	12480.59
41.52	4.38	5.04	39.00	10080.48
47.04	5.88	3.68	44.28	7360.35
52.92	8.38	2.35	49.98	4704.22
56.64	10.88	1.48	54.78	2976.14
59.52	14.38	0.82	58.08	1645.79
61.56	18.38	0.51	60.54	1020.04
63.84	25.88	0.30	62.70	608.02
66.12	40.88	0.15	64.98	304.01
68.16	55.88	0.13	67.14	272.01
69.12	70.88	0.06	68.64	128.00
69.48	80.66	0.03	69.30	73.66

[a]Conditions on Table D-5.

Table D-7

TG DATA FOR RUN 215[a]

(LIMESTONE 1359; SULFATION)

% REACTED	TIME/MIN.	%/MIN.	% REACTED	UNIT RATE
2.00	0.41	4.88	1.00	9760.42
2.73	0.66	2.93	2.36	5869.26
3.33	0.91	2.40	3.03	4802.12
3.73	1.16	1.60	3.53	3201.41
4.20	1.41	1.86	3.96	3734.98
5.06	2.41	0.86	4.63	1734.10
5.73	3.91	0.44	5.40	889.28
6.00	4.91	0.26	5.86	533.56
6.40	7.41	0.16	6.20	320.14
7.00	14.91	0.08	6.70	160.07
7.33	22.41	0.04	7.16	88.92
7.50	29.91	0.02	7.41	44.46
7.67	37.41	0.02	7.58	44.46
8.20	74.36	0.01	7.93	28.88
8.33	94.36	0.00	8.27	13.33
8.50	114.36	0.00	8.42	16.67

[a]Conditions on Table D-5.

Table D-8

TG DATA FOR RUN 221 [a]

(LIMESTONE 1359 420/500 μm; SULFATION)

% REACTED	TIME/MIN.	%/MIN.	% REACTED	UNIT RATE
1.44	0.27	5.24	0.72	10487.68
2.75	0.52	5.24	2.09	10487.68
3.93	0.77	4.71	3.34	9438.91
5.11	1.02	4.71	4.52	9438.91
6.35	1.27	4.98	5.73	9963.30
9.43	2.02	4.10	7.89	8215.35
12.19	2.77	3.67	10.81	7341.37
14.74	3.52	3.40	13.47	6816.99
16.97	4.27	2.97	15.86	5943.02
19.14	5.02	2.88	18.05	5768.22
20.97	5.77	2.44	20.05	4894.25
22.35	6.52	1.83	21.66	3670.68
24.71	7.52	2.35	23.53	4719.45
27.33	9.02	1.74	26.02	3495.89
29.82	10.52	1.66	28.57	3321.10
30.80	11.52	0.98	30.31	1966.44
33.42	14.02	1.04	32.11	2097.53
35.13	16.52	0.68	34.28	1363.39
36.64	19.02	0.60	35.88	1206.08
37.75	21.52	0.44	37.19	891.45
38.41	24.02	0.26	38.08	524.38
39.72	29.02	0.26	39.06	524.38
40.70	36.52	0.13	40.21	262.19
41.29	44.02	0.07	41.00	157.31
41.49	51.97	0.02	41.39	40.47

[a] Conditions on Table D-5.

Table D-9

TG DATA FOR RUN 257[a]

(LIMESTONE 1359 SULFATION)

% REACTED	TIME/MIN.	%/MIN.	% REACTED	UNIT RATE
2.30	0.55	4.18	1.15	8363.65
3.81	1.05	3.02	3.05	6045.72
6.30	1.55	4.99	5.06	9988.58
8.14	2.05	3.68	7.22	7360.01
11.43	3.05	3.28	9.79	6571.43
13.01	3.55	3.15	12.22	6308.58
14.58	4.05	3.15	13.80	6308.58
15.90	4.55	2.62	15.24	5257.15
18.59	5.55	2.69	17.25	5388.58
21.02	6.55	2.43	19.81	4862.86
23.19	7.55	2.16	22.11	4337.15
25.16	8.55	1.97	24.18	3942.86
26.94	9.55	1.77	26.05	3548.57
28.45	10.55	1.51	27.69	3022.86
30.75	12.05	1.53	29.60	3066.67
32.59	13.55	1.22	31.67	2453.33
34.82	15.55	1.11	33.71	2234.28
35.88	17.05	0.70	35.35	1401.90
39.16	21.76	0.69	37.52	1393.73
41.40	26.76	0.44	40.28	893.71
44.68	36.76	0.32	43.04	657.14
46.78	46.76	0.21	45.73	420.57
48.23	56.76	0.14	47.51	289.14
49.54	66.76	0.13	48.89	262.85
50.07	74.26	0.07	49.81	140.19

[a]Conditions on Table D-5.

Table D-10

TG DATA FOR RUN 258[a]

(LIMESTONE 1359 SULFATION)

% REACTED	TIME/MIN.	%/MIN.	% REACTED	UNIT RATE
1.30	0.25	5.23	0.65	10466.48
4.05	0.75	5.49	2.68	10989.81
6.41	1.25	4.70	5.23	9419.83
8.50	1.75	4.18	7.45	8373.18
10.20	2.25	3.40	9.35	6803.21
11.90	2.75	3.40	11.05	6803.21
13.60	3.25	3.40	12.75	6803.21
14.91	3.75	2.61	14.26	5233.24
16.35	4.25	2.87	15.63	5756.56
17.53	4.75	2.35	16.94	4709.91
19.88	5.75	2.35	18.70	4709.91
21.71	6.75	1.83	20.80	3663.27
23.28	7.75	1.56	22.50	3139.94
25.25	9.75	0.98	24.26	1962.46
26.82	10.75	1.56	26.03	3139.94
28.65	12.75	0.91	27.73	1831.63
29.96	14.75	0.65	29.30	1308.31
30.74	17.25	0.31	30.35	627.98
31.66	19.75	0.36	31.20	732.65
32.18	22.25	0.20	31.92	418.65
33.23	29.75	0.13	32.70	279.10
33.42	37.25	0.02	33.32	52.33
34.01	57.45	0.02	33.72	58.29
34.80	107.45	0.01	34.40	31.39
35.12	147.45	0.01	34.96	16.35

[a]Conditions on Table D-5.

Table D-11

TG DATA FOR RUN 259[a]

(LIMESTONE 1359 SULFATION)

% REACTED	TIME/MIN.	%/MIN.	% REACTED	UNIT RATE
1.05	0.27	3.85	0.52	7705.43
2.91	0.77	3.70	1.98	7416.48
4.63	1.27	3.44	3.77	6886.73
6.22	1.77	3.17	5.42	6356.98
7.81	2.27	3.17	7.01	6356.98
9.27	2.77	2.91	8.54	5827.23
10.46	3.27	2.38	9.86	4767.73
11.65	3.77	2.38	11.05	4767.73
12.84	4.27	2.38	12.25	4767.73
13.97	4.77	2.25	13.40	4502.86
15.89	5.77	1.92	14.93	3840.67
17.48	6.77	1.58	16.68	3178.49
19.73	8.77	1.12	18.60	2251.43
20.52	9.77	0.79	20.13	1589.24
21.85	12.27	0.52	21.18	1059.49
23.04	14.77	0.47	22.44	953.54
23.83	17.27	0.31	23.44	635.69
24.50	19.77	0.26	24.16	529.74
25.16	22.27	0.26	24.83	529.74
27.54	32.27	0.23	26.35	476.77
29.40	42.27	0.18	28.47	370.82
30.99	52.27	0.15	30.19	317.84
32.18	62.27	0.11	31.58	238.38
33.37	72.27	0.11	32.77	238.38
35.22	92.27	0.09	34.30	185.41
37.08	112.27	0.09	36.15	185.41
37.81	123.77	0.06	37.44	126.67

[a]Conditions on Table D-5.

Table D-12

TG DATA FOR RUN 260[a]

(LIMESTONE 1359 SULFATION)

% REACTED	TIME/MIN.	%/MIN.	% REACTED	UNIT RATE
2.11	0.43	4.91	1.05	9824.18
4.36	0.93	4.49	3.23	8993.88
6.33	1.43	3.95	5.34	7903.71
8.44	1.93	4.22	7.39	8448.79
10.01	2.43	3.13	9.23	6268.46
11.65	2.93	3.27	10.83	6541.00
13.08	3.43	2.86	12.36	5723.37
14.58	3.93	2.99	13.83	5995.92
17.23	4.93	2.65	15.90	5314.56
19.75	5.93	2.52	18.49	5042.02
21.87	6.93	2.11	20.81	4224.39
23.84	7.93	1.97	22.85	3951.85
25.27	8.93	1.43	24.56	2861.68
26.77	9.93	1.49	26.02	2997.96
29.97	12.43	1.28	28.37	2561.89
32.15	14.93	0.87	31.06	1744.26
33.79	17.43	0.65	32.97	1308.20
34.88	19.93	0.43	34.34	872.13
35.97	22.43	0.43	35.43	872.13
36.52	24.93	0.21	36.24	436.06
38.15	39.51	0.11	37.33	224.23
38.83	59.51	0.03	38.49	68.13
39.51	99.51	0.01	39.17	34.06
39.72	122.01	0.01	39.62	18.16

[a]Conditions on Table D-5.

Table D-13

TG DATA FOR RUN 261[a]

(LIMESTONE 1359 SULFATION)

% REACTED	TIME/MIN.	%/MIN.	% REACTED	UNIT RATE
2.18	0.40	5.47	1.09	10941.98
4.65	0.90	4.92	3.41	9847.78
6.56	1.40	3.82	5.60	7659.38
9.71	1.90	6.29	8.13	12583.28
10.25	2.40	1.09	9.98	2188.39
11.89	2.90	3.28	11.07	6565.19
14.97	3.90	3.07	13.43	6154.86
17.78	4.90	2.80	16.37	5607.76
20.51	5.90	2.73	19.14	5470.99
23.79	7.40	2.18	22.15	4376.79
28.31	9.90	1.80	26.05	3610.85
31.18	11.90	1.43	29.74	2872.27
33.23	13.90	1.02	32.21	2051.62
34.74	15.90	0.75	33.98	1504.52
36.45	18.90	0.56	35.59	1139.79
37.74	22.40	0.37	37.10	742.49
39.25	27.40	0.30	38.50	601.80
39.93	29.90	0.27	39.59	547.09
41.30	37.40	0.18	40.62	364.73
42.12	44.90	0.10	41.71	218.83
43.08	54.90	0.09	42.60	191.48
43.76	64.90	0.06	43.42	136.77
44.86	94.90	0.03	44.31	72.94
45.81	144.90	0.01	45.34	38.29
46.16	164.90	0.01	45.99	34.19

[a]Conditions on Table D-5.

Table D-14

TG DATA FOR RUN 300[a]

(LIMESTONE 1359 SULFATION)

% REACTED	TIME/MIN.	%/MIN.	% REACTED	UNIT RATE
3.75	0.41	9.09	1.87	18193.39
6.03	0.66	9.11	4.89	18225.88
8.04	0.91	8.04	7.03	16081.66
9.91	1.16	7.50	8.97	15009.54
14.07	1.91	5.53	11.99	11078.47
17.15	2.66	4.10	15.61	8219.51
20.37	4.16	2.14	18.76	4288.44
21.71	5.66	0.89	21.04	1786.85
22.78	7.16	0.71	22.24	1429.48
24.45	10.16	0.55	23.61	1116.78
27.40	17.66	0.39	25.93	786.21
29.48	25.16	0.27	28.44	553.92
31.09	32.66	0.21	30.28	428.84
32.49	40.16	0.18	31.79	375.23
33.63	47.66	0.15	33.06	303.76
35.64	62.66	0.13	34.64	268.02
38.19	77.66	0.16	36.92	339.50
38.72	92.66	0.03	38.46	71.47
39.66	97.53	0.19	39.19	384.86

[a]Conditions on Table D-5.

Table D-15

TG DATA FOR RUN 301[a]

(LIMESTONE 1359)

% REACTED	TIME/MIN.	%/MIN.	% REACTED	UNIT RATE
1.27	0.12	10.16	0.63	20329.18
2.25	0.22	9.88	1.76	19764.48
3.52	0.32	12.70	2.89	25411.47
4.94	0.47	9.41	4.23	18823.31
7.05	0.72	8.47	5.99	16940.98
9.17	0.97	8.47	8.11	16940.98
10.65	1.22	5.92	9.91	11858.68
12.28	1.47	6.49	11.47	12988.08
15.52	1.97	6.49	13.90	12988.08
19.05	2.72	4.70	17.29	9411.65
21.17	3.22	4.23	20.11	8470.49
24.42	4.22	3.24	22.79	6494.04
27.10	5.22	2.68	25.76	5364.64
30.14	6.72	2.02	28.62	4047.01
32.32	8.22	1.45	31.23	2917.61
34.30	10.22	0.98	33.31	1976.44
35.29	12.22	0.49	34.79	988.22
36.98	18.39	0.27	36.14	549.58
37.76	23.39	0.15	37.37	310.58
38.47	33.39	0.07	38.11	141.17
38.82	43.39	0.03	38.64	70.58
39.38	59.39	0.03	39.10	70.58

[a]Conditions on Table D-5.

The Calcination of Limestone and Dolomite

The TG curves for the calcination of limestone and dolomite obtained in preparing the samples for sulfation tests generated enormous quantities of data. For the most part the detailed kinetics have not been analyzed; when the data acquisition/data reduction system has been commissioned, these data will be reduced as a matter of course. Several features of the curves were examined, however, as time permitted.

Sample Consistency. The normal sample weight for limestone 1359 was approximately 19 mg. It is possible that the choice of a small sample (essential if the maximum rates of reaction are to be recorded) may lead to gross variations in sample content and give results unrepresentative of the particular stone. One check on this possibility is to examine the variation in carbon dioxide loss on calcination in the TG apparatus.

For samples calcined in nitrogen the carbon dioxide weight loss corresponded to 43.59 ± 0.20 percent (16 samples). This may be compared to the weight loss noted on ignition to 1000°C (1932°F): 43.32 percent, (Westinghouse), 43.6 percent (TVA).[4] For samples on the TG apparatus which were calcined after annealing in carbon dioxide the weight loss was 44.15 percent ± 0.15 percent (seven samples). It seems unlikely that errors were introduced by wide impurity variations in the small samples.

The Rate of Limestone Calcination

For TG 215, in which 420-to-500 micron limestone 1359 was held in carbon dioxide, heated to 901°C(1652°F) and then calcined in nitrogen, the contracting cube equation

$$1-(1-\alpha)^{1/3} = 3kt$$

adequately described the course of reaction, yielding a k value of 2.2×10^{-2} sec^{-1} (-calcination completed in 3.9 minutes). This value

can be compared with a value obtained by extrapolating k values for isothermal experiments at different temperatures (550 to 870°C/ 1022 to 1598°F)which is 1.2×10^{-2} sec^{-1}. The rate constant obtained from nonisothermal TG measurements, however, using the nonlinear least squares (NLLS) method is 2.6×10^{-2} sec^{-1}, in excellent agreement with the observed value.[11] Since the isothermal experiments were carried out by plunging the sample into the furnace at the temperature of the experiment (probably fracturing some of the particles), it is not surprising that the nonisothermal method in which the sample was heated slowly (10 K/min) yields the closest value. The NLLS data should be valuable as a predictor of the calcination behavior of limestone.

The Rate of Dolomite Calcination

The nonisothermal data for the calcination of dolomite 1337 (1200 to 1000 micron) in nitrogen in TG 205 was analyzed by the method of Coates and Redfern.[12] The data yielded an activation energy of 214.9 kJ/mole (51.4 kcal/mole) which is close to the value of 54.5 for an Ohian dolomite (of almost identical analysis) given by Jungten and van Heek in their monograph on nonisothermal kinetics.[7]

REFERENCES

1. Keairns, D. L., D. H. Archer, R. A. Newby, E. P. O'Neill, E. J. Vidt. Evaluation of the Fluidized Bed Combustion Process. Vol. I. Environmental Protection Agency. Westinghouse Research Laboratories. Pittsburgh, PA. EPA-650/2-73-048 a. NTIS PB-231 162/9. December 1973.
2. Curran, G. P., C. E. Fink, and E. Gorin. CO_2 Acceptor Gasification Process in Fuel Gasification. Consolidation Coal Co. Advances in Chemistry Series 69. American Chemical Society. Washington, D.C. 1967. p. 141.
3. Hartman, M. and R. W. Coughlin. Reaction of Sulfur Dioxide with Limestone and the Influence of Pore Structure. Ind. Eng. Chem. Process Des. Develop. 13: 248, 1974.
4. Hatfield, J. D., Y. K. Kim, R. C. Mullins, and G. H. McClellan. Investigation of the Reactivities of Limestone to Remove Sulfur Dioxide from Flue Gas. Office of Air Pollution. Tennessee Valley Authority. 1971.
5. O'Neill, E. P., D. L. Keairns, and W. F. Kittle. (Proceedings of the Third International Conference on Fluidized Bed Combustion. Hueston Woods, Ohio, 1972). EPA 650/2-73-053. December 1973.
6. Moss, G. Sulphur Removal During Fluidized Bed Combustion. Esso Research Center. Abington, England. The Chemical Engineer (Birmingham University) 23: 24, 1972.
7. Jungten, H. and K. H. van Heek. Topics in Current Chemistry. 13, 3/4, 601-699, Springer-Verlag, Berlin, 1970.
8. Hills, A. W. D. Transactions/Section C of the Institution of Mining and Metallurgy, 76: C241, 1967.
9. Chemical Rubber Co. Handbook. ed. Weast. 53rd Edition, F66, 1972.

10. Schwitzgebel, K. and P. S. Lowell. Thermodynamic Basis for Existing Experimental Data in MgO-SO_2-O_2 and Ca-SO_2-O_2 Systems. (Radian Corporation, Texas). Env. Sci. Technol. 7: 1147, 1973.

11. Handman, L. M. and E. P. O'Neill. Unpublished. Westinghouse Research Laboratories. Pittsburgh, Pa. 1972.

12. Coats, A. W. and J. P. Redfern. Kinetic Parameters from Thermogravimetric Data. Nature, 201: 68, 1964.

APPENDIX E

PROJECTIONS OF SORBENT UTILIZATION AND SULFUR REMOVAL EFFICIENCY USING THERMOGRAVIMETRIC DATA

APPENDIX E_1

DERIVATION OF THE MODEL EQUATIONS

APPENDIX E

PROJECTIONS OF SORBENT UTILIZATION AND SULFUR REMOVAL EFFICIENCY USING THERMOGRAVIMETRIC DATA

INTRODUCTION

The object of the thermogravimetric (TG) studies on the sulfation of limestone and dolomite is to obtain design parameters for fluidized bed desulfurization systems. At the outset of this study it was postulated that the rate of sulfur sorption by particles of limestone or dolomite by the overall Reaction 1:

$$CaO + SO_2 + 1/2\ O_2 \rightarrow CaSO_4$$

and the total capacity of the stone to absorb sulfur are primary factors in determining the usefulness of a particular sorbent, granted the thermodynamic conditions for sulfur dioxide (SO_2) removal are favorable. TG studies can be assumed, a priori, to provide an estimate of the relative impact of particle size, temperature, pressure, gas composition, and choice of sorbent on desulfurization in a fluidized bed. The TG data should, therefore, permit a qualitative assessment of the effect of these parameters on the design and operation of fluidized beds. The possibility of enhancing the value of TG data, however, by using it to make quantitative predictions of sulfur removal in fluidized beds, is worth analysis because it would:

- Permit a critical assessment of advanced designs
- Permit optimization of a given system
- Permit development of a meaningful laboratory screening technique for choosing particular sorbents
- Provide a valuable tool for trouble-shooting in cases where poor desulfurization may be the result of a number of factors
- Justify development work by TG analysis to improve the sulfur removal system, as opposed to total reliance on more expensive fluidized bed tests as the sole experimental tool.

LABORATORY STUDIES OF THE KINETICS OF REACTION

Numerous studies of the kinetics of Reaction 1 have been published. Justification for further work on the system rests on the need for data under closer simulation of proposed fluidized bed operating conditions (1013 to 1520 kPa; 10 to 15 atm pressure) and also on the failure of currently available data to explain fluidized bed results. As examples of the latter, work at Exxon Research and Engineering,[1*] Tennessee Valley Authority (TVA),[2] and the National Coal Board, U.K. (NCB),[3] may be cited.

In the TVA study kinetic measurements on a particular limestone (limestone 1359), the maximum degree of sulfation observed was 18 percent.[2] Using the same type of stone, Exxon workers found that 32 percent of the stone was sulfated in fluidized beds before significant escape of sulfur dioxide from the bed was observed.[1] Similar particle sizes and oxygen pressures were used at atmospheric pressure in both tests. The results are significant because Borgwardt[4] has established that the limit on fast sulfation kinetics is determined by the space available in the stone pores to accommodate the bulky sulfate ion. This limit should not depend on whether the reaction takes place in a TG apparatus or a fluidized bed. In the NCB study[3,5] laboratory results from a differential reactor were used to model extensive fluid bed results. Excellent agreement was obtained for one limestone and for one dolomite, but with a second limestone (limestone 1359) significantly better retention was observed in the fluid bed than predicted by the model.[5] A successful resolution of these apparent anomalies will be necessary before the utility of models can be accepted.

Projections of Fluidized Bed Performance

Application of kinetic studies to projections of fluidized bed desulfurization has been carried out by at least two groups working at

---

*At the time this report was written, the corporation was named Esso. To avoid confusion with Esso (U.K.) the current name, Exxon, will be used.

Argonne National Laboratory (ANL)[6] and NCB.[5] The results these workers obtained represent important milestones, but they were not carried through to the point of assessing what performance projections could be made using laboratory kinetic data, and they did not have data at pressure, a parameter of considerable importance to the practical application of fluidized bed desulfurization.

In addition to providing a resolution of the anomalies noted, a successful model which uses laboratory kinetic data should predict the effect of:

- Calcium/sulfur (Ca/S) ratio on desulfurization
- Temperature on desulfurization
- Bed height and gas velocity on desulfurization
- Pressure on desulfurization.

Fluidized Bed Predictions

The model developed at ANL simulates the sulfation process as a first-order reaction which proceeds to an equilibrium loading on the stone, Ye, which is less than stoichiometric, as experiments show. Sulfur retention in the bed is calculated by mass balancing this stone reaction rate with the removal of sulfur dioxide as it passes through the bed and the generation of sulfur dioxide in the bed by coal combustion. While application and development of the model was clearly hampered by the dearth of suitable kinetic data, estimated data from experiments conducted by the National Air Pollution Control Administration (NAPCA)* were used to illustrate the model. The predictions of 90 to 99 percent sulfur removal compared with the value of 80 percent observed in a fluidized bed test (BCR-8). In order to apply the model the equilibrium loading and the calcium/sulfur molar ratio in the feed are specified. This model has not undergone subsequent development but was used by Westinghouse to apply TG data to predicting a fluidized bed test result.[7] The chief difficulty lay in defining Ye, the equilibrium loading, on the sorbent, and arbitrary

*Now the EPA.

allocation of Ye (by inspection of the TG kinetic curve) for a representative TG result predicted a sulfur removal efficiency of 87 percent as opposed to 81 percent in a fluidized bed test. Had the equilibrium sulfur loading been chosen as 37 percent (the actual stone loading) in the experiment the model would have yielded the correct answer, 81 percent, since the reaction rate of the stone up to 37 percent was sufficiently high.

A more recent model has been published by the NCB investigators,[5] who were, once again, hampered by the lack of appropriate kinetic data to use in their model. They achieved excellent agreement between laboratory kinetic data and their fluidized bed results, with the conspicuous exception of fluidized bed sorbent tests with the widely used fluidized bed sorbent, limestone 1359,* which did not agree with the model predictions. The reasons for this disagreement are essential to an understanding of the processes controlling fluidized bed desulfurization.

It is accepted that the pore structure formed in the sorbent during calcination controls the kinetics of sulfation.[4] The Westinghouse work on calcination under different partial pressures of carbon dioxide (see Appendix J) shows that when calcination occurs under carbon dioxide with $P_{CO_2}/Pe \geq 0.6$ (where Pe = equilibrium partial pressure of CO_2 over $CaCO_3/CaO$ at the temperature of calcination), the capacity of the stone for sulfation at a high rate of reaction is increased; inspection of the fluidized bed literature on sulfur dioxide retention shows powerful evidence confirming this phenomenon.

In the course of experiments designed to determine the optimum temperature for sulfur dioxide capture by limestone, the NCB workers operated a fluidized bed of coal and limestone at a series of temperatures and recorded the steady-state sulfur dioxide retention as a function of temperature. They determined that the optimum temperature for sulfur dioxide removal was approximately 830°C (1526°F). Their data, however, can

---

*Not stated in their paper[5] but can be inferred from this paper and the overall project report.[3]

be examined from the point of view of the carbon dioxide particle pressure condition in the bed. (The carbon dioxide is contributed both by limestone and by coal combustion.) The sulfur dioxide escaping from the bed has been plotted here as a function of P_{CO_2}/Pe, and, as illustrated in Figure E-1, it shows that maximum sulfur dioxide retention in the bed occurs when P_{CO_2}/Pe is about 0.6.

In order to see if the TG results for sulfation after calcination under high relative partial pressures of carbon dioxide explained the relatively high utilization obtained by the NCB, the data for a typical run TG 199 were approximated by first-order equation. The data were then used to predict fluidized bed experimental results as NCB noted. A comparison of predicted and observed results is shown in Figure E-2. Since the NCB investigators found about 11 percent utilization in their laboratory tests, it is clear that their data could not predict 80 percent sulfur retention at a calcium/sulfur molar ratio of 3/1 within any imaginable gas residence time in the fluidized bed. It can be concluded that the carbon dioxide partial pressure during calcination is a factor of crucial importance for fluidized bed desulfurization. Accordingly, a simple model of fluidized bed desulfurization, which permits direct use of the TG data without arbitrary allocation of an equilibrium sulfur loading, was developed. A set of sulfation experiments using limestone 1359 was carried out under carefully monitored calcination conditions, the data were applied to the model, and the results were compared with fluidized bed experimental results.

Experimental

Limestone 1359 (M. J. Grove Lime Co., Stephens City, Va.) containing 96.7 percent calcium carbonate was ground and the fraction 420 to 500 μm used in the experiments. Calcination and sulfation were effected using 20 mg samples of limestone in a Pt gauze basket in a DuPont 951 thermobalance modified for work with corrosive gases.[7,8] The samples were brought to 900°C (1652°F) in pure carbon dioxide, then calcined in 60 percent carbon dioxide in nitrogen at 900°C (1652°F). Sulfation at

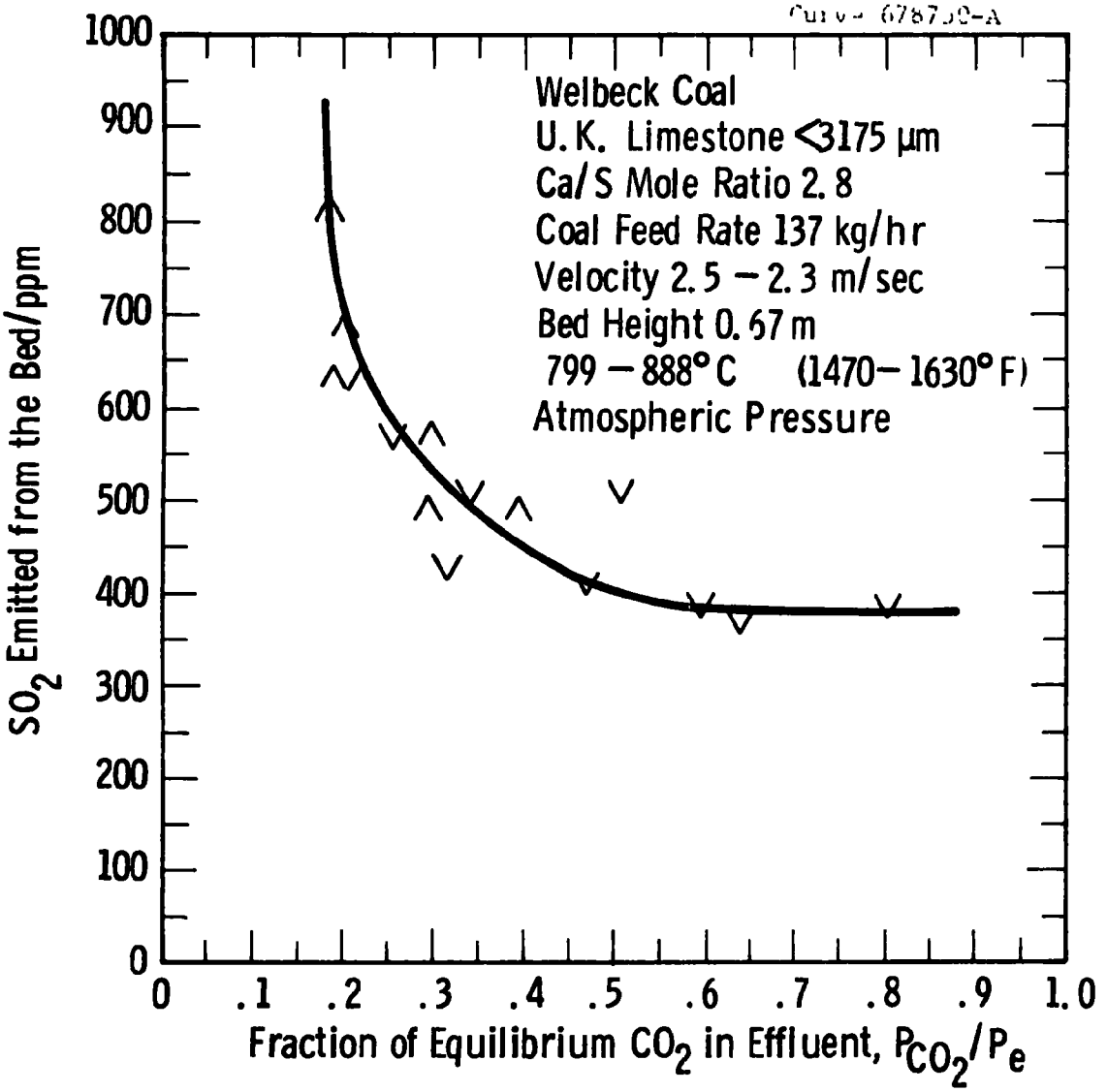

Figure E-1—The effect of CO_2 pressure during calcination on SO_2 emissions from a fluid bed. (Data taken from National Coal Board (U.K.) Study - Temperature Survey – Table A. 1. 3.19, Page Al. 95)

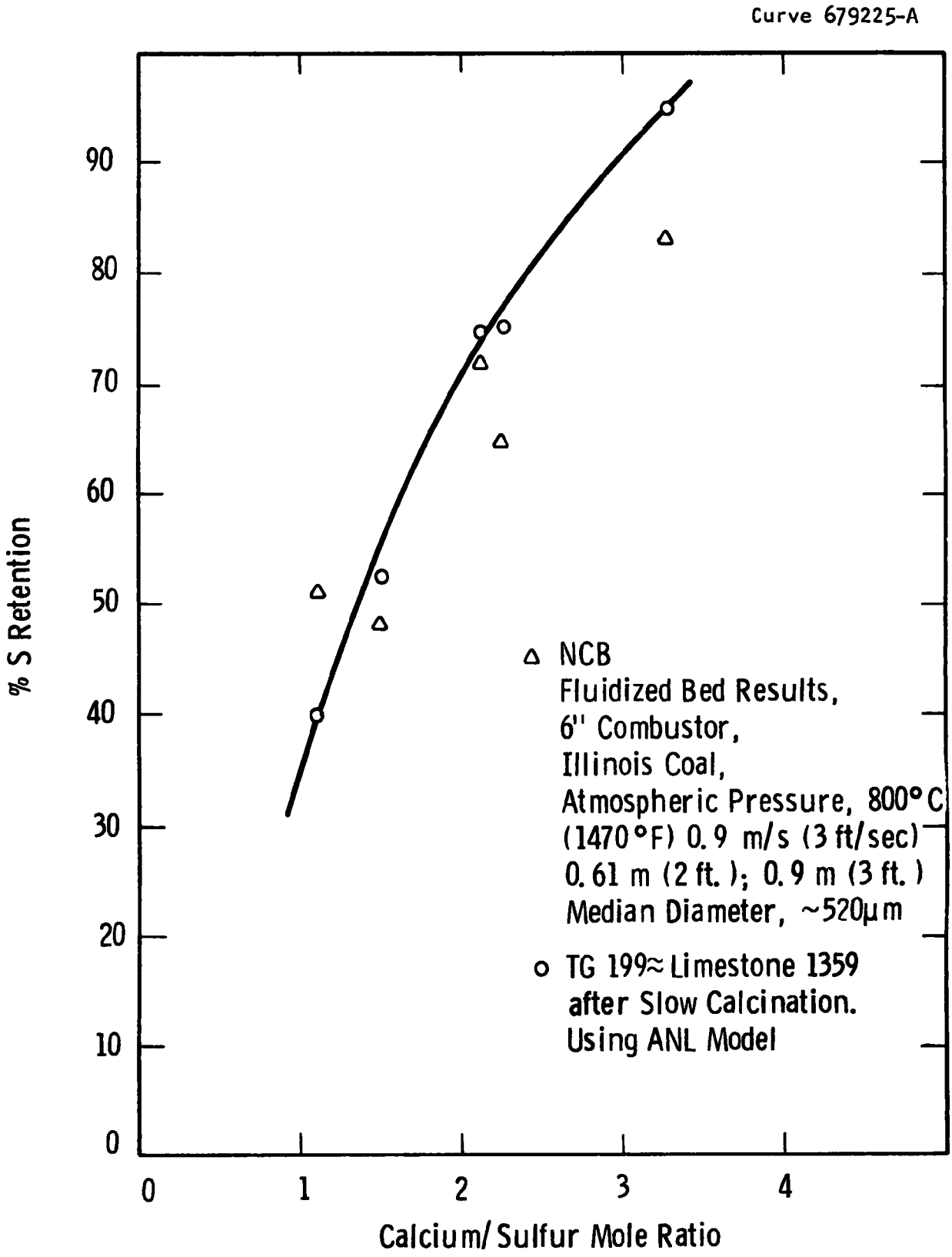

Figure E-2—TG data predictions compared to fluidized bed data atmospheric pressure limestone 1359

each temperature was in 5,000 ppm sulfur dioxide, 4 percent oxygen in nitrogen, flowing at 400 ml min^{-1} through the 20 mm diameter reactor, at atmospheric pressure. The primary data recorded, weight as a function of time, indicate the course of sulfation, as shown in Figure E-3. The derived rate of reaction is shown as a function of the extent of reaction or calcium oxide utilization in Figure E-4 for two temperatures. Analytic expressions for these data can only be written in terms of coupled reaction and diffusion rates requiring arbitrary parameters.[9,10] The data, however, can be used in the graphic form shown to project fluidized bed performance.

Calculation of Kinetic Limits to Sulfur Retention

To apply the data from the TG runs (257 to 262) to "predictions" of fluidized bed sulfur retention, the following procedure was adopted:

- The fluidized bed conditions were those described by ANL[6] in their tests AR-1 and HUMP as shown in Tables E-1 and E-2.
- A first-order model with respect to gas concentration was assumed, and uniform generation of sulfur dioxide in the bed was considered, according to the equations which follow.

Table E-1

PHYSICAL PARAMETERS OF THE TG SYSTEM

	ANL/fluid bed	Westinghouse/TG
Stone	Limestone 1359 (98 wt % $CaCO_3$)	Limestone 1359 (96.75% $CaCO_3$)
Particle Size	615 μm	460 μm
Temperature Range	788 to 871°C (1450 to 1560°F)	750 to 950°C (1382 to 1742°F)
Oxygen	3.5%	4%
SO_2	3,000 to 420 ppm	5,000 ppm

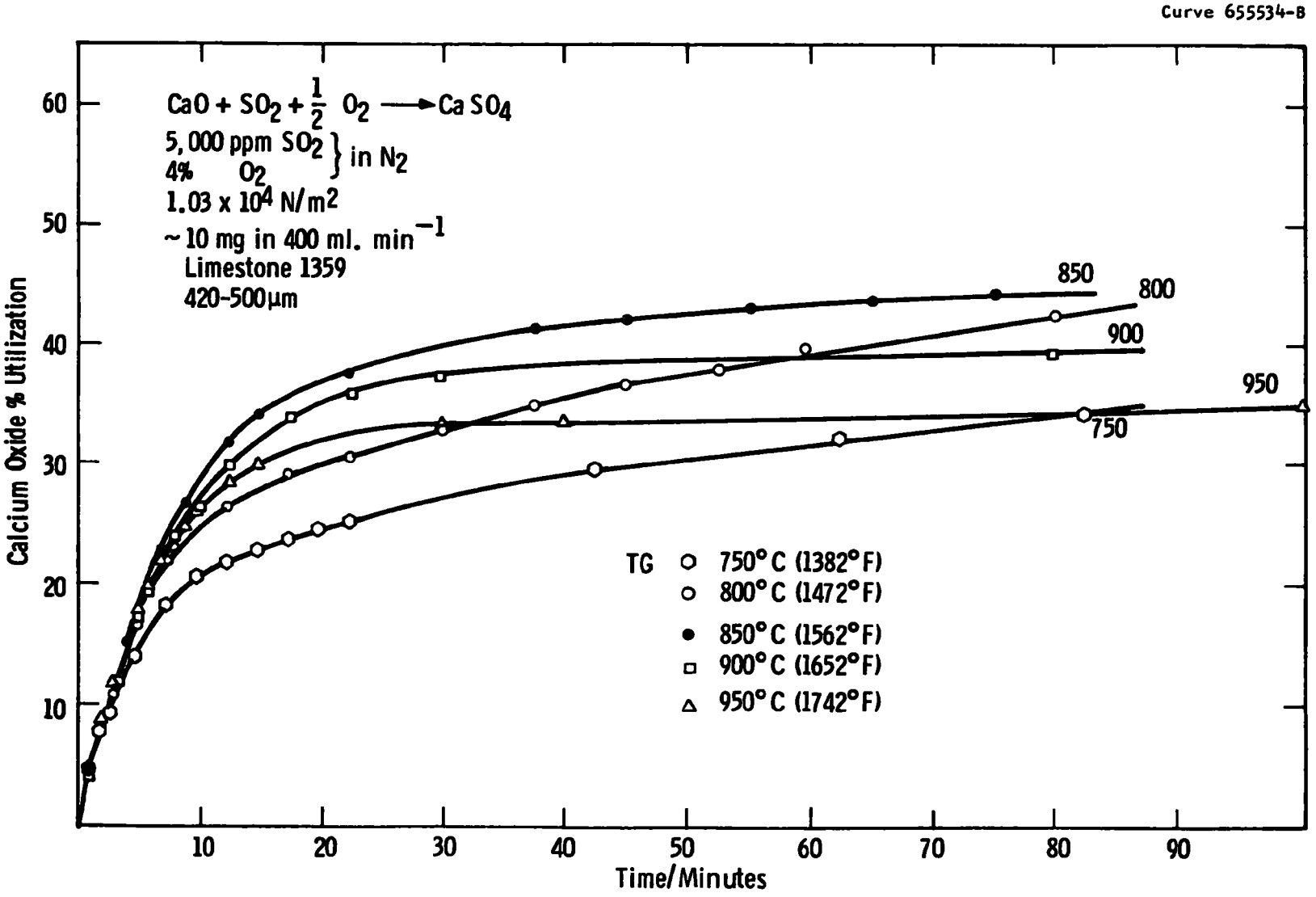

Figure E-3—The effect of temperature on limestone sulfation

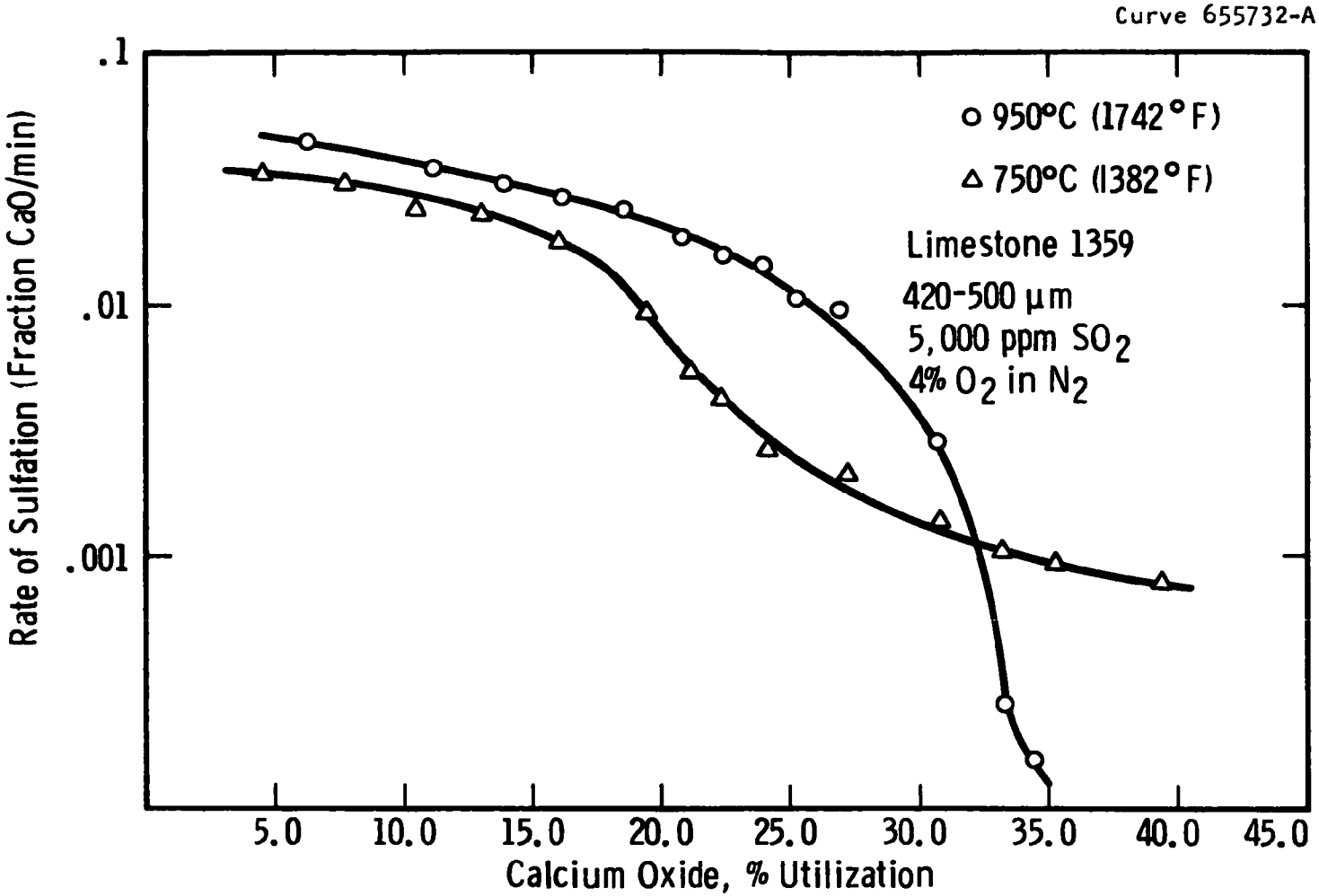

Figure E-4—The rate of sulfation of limestone 1359

Table E-2

SULFUR RETENTION PROJECTIONS COMPARED
WITH EXPERIMENTAL DATA (ANL-AR1)

Experiment	Temperature °C (°F)	Utilization,%	% sulfur retention
TG/W	750 (1382)	14.7	36.3
FB/ANL	760 (1400)	18	44
FB/ANL	787 (1448.6)	26	65
TG/W	800 (1472)	23.6	59
FB/ANL	816 (1500.8)	36	91
FB/ANL	843 (1549.4)	36	91
TG/W	850 (1562)	33.2	83
FB/ANL	871 (1599.8)	34	86
TG/W	900 (1652)	32.4	80
TG/W	950 (1742)	26.2	65.5

$$U = \frac{1}{F}\left\{1 - \frac{v}{kH}\left(1 - e^{-\frac{kH}{v}}\right)\right\} \qquad \text{(E-1)}$$

$$R = 100\left\{1 - \frac{v}{kH}\left(1 - e^{\frac{-kH}{v}}\right)\right\} \qquad \text{(E-2)}$$

where

U = CaO fraction sulfated ("the utilization")

R = % sulfur retained in the fluidized bed

v = actual gas velocity in fluidized bed, mm/sec

H = bed height, mm

k = first-order rate constant for the reaction

$$CaO + SO_2 + 1/2\ O_2 \longrightarrow CaSO_4$$

where $k = f(U, \rho)$

F = Ca/S mole ratio as supplied to the bed

ρ = molar density of calcium in the fluid bed.

(Equations E-1 and E-2 are derived in Appendix E_1.)

- The values of F (Ca/S mole ratio), v (gas velocity), H (bed height) are taken from the ANL description of their experiments. The value of v was corrected for the effect of solid volume in the bed. The value of ρ, the molar density of calcium in the bed, was estimated.
- The values of k, the rate constant, necessary to achieve the sulfur retention implicit in fixed Ca/S feed rate ratios and stone utilization were calculated as a function of U, the utilization.
- The values of k were converted into the rate, k', as usually expressed for the TG data where $\rho k'/C_i = k$ (described in Appendix E_1).

- The values of k = f (u) from the model equations were compared with graphic plots of the experimental data. The coincidence of k and the experimental rate gives the utilization U and, hence, the sulfur retention, as shown in Figure E-5.

Results

A comparison of the limits predicted by the TG results and fluidized bed experimental results for sulfur retention with limestone 1359 is shown in Figures E-6 and E-7. At a calcium/sulfur ratio of 2.5/1, the sulfur retention predicted is within 10 percent of that observed up to 871°C (1600°F) and is predicted to fall off in the range 870 to 950°C (1598 to 1742°F). The apparent temperature for maximum sulfur retention is about 30°C (86°F) higher for the TG data than for the fluidized bed experiments at ANL but is in close agreement with the optimum temperature Esso[11] noted.

The experiments with Humphrey coal, at a calcium/sulfur ratio of 4.5/1, are also relatively well predicted (within 10 percent) by the TG data, up to 850°C (1562°F). The 900°C (1652°F) temperature result at this calcium/sulfur ratio shows that in practice the sulfur retention is much poorer than the predicted value.

The good agreement at the lower temperatures is further demonstrated by the comparison of TG projections and experiments in which the calcium/sulfur ratio was varied (from 1 to 4) at 788°C (1450°F), as shown in Figure E-8. This agreement covers a range of sulfur retention in the bed from 38 to 95 percent.

The model equations were used to project the effect of superficial gas velocity on sulfur retention at two calcium/sulfur ratios; 4/1 and 1/1, as shown in Figure E-9. Qualitatively, the projections are in agreement with the experimental data from fluidized beds, which show:[12]

- Increasing the velocity four-fold (up to about 2.5 m/sec [8 ft/sec]) decreases sulfur retention from over 90 percent to about 80 percent.

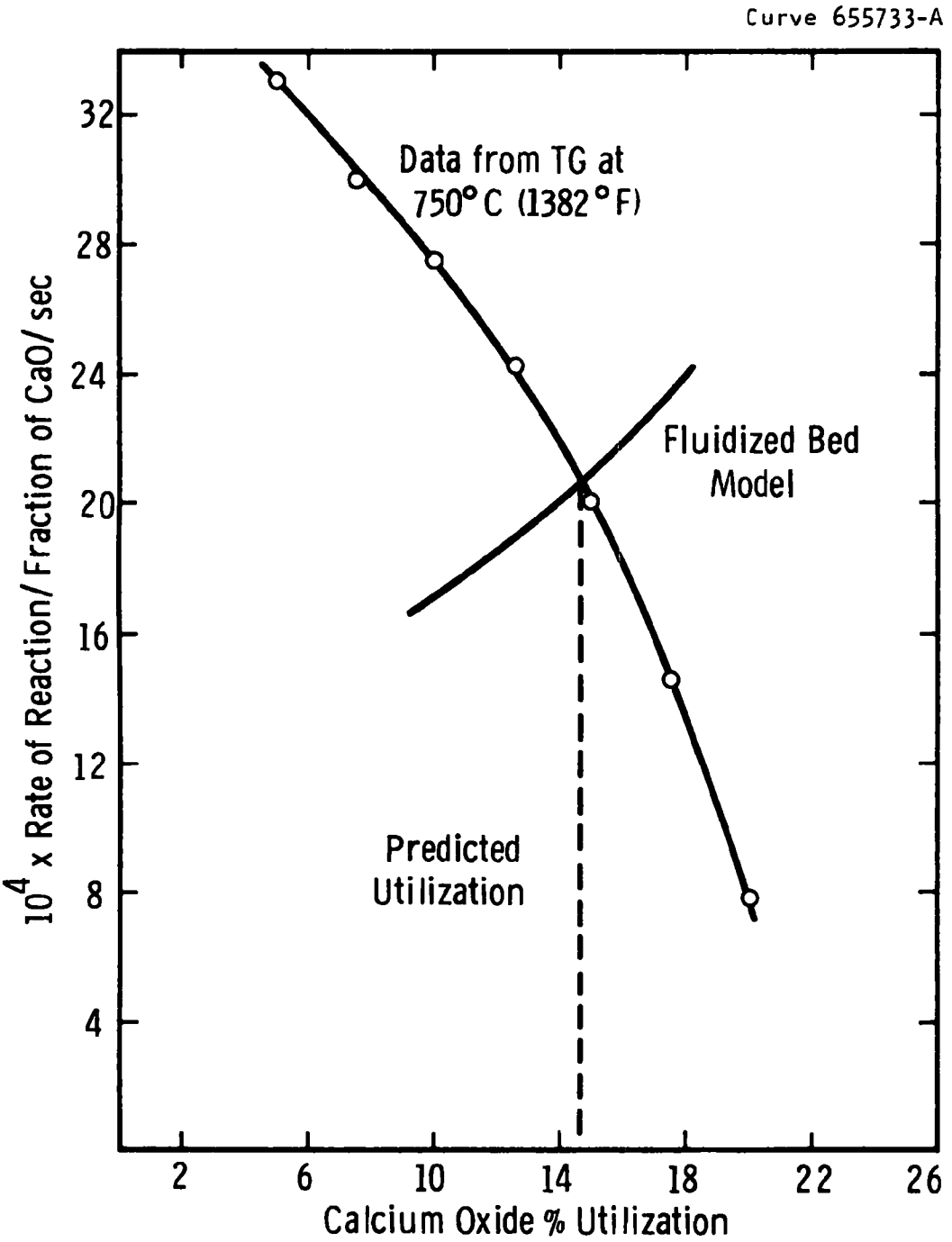

Figure E-5— Determination of the stone utilization atwhich the rate of reaction satisfies the fluidized bed rate criteria

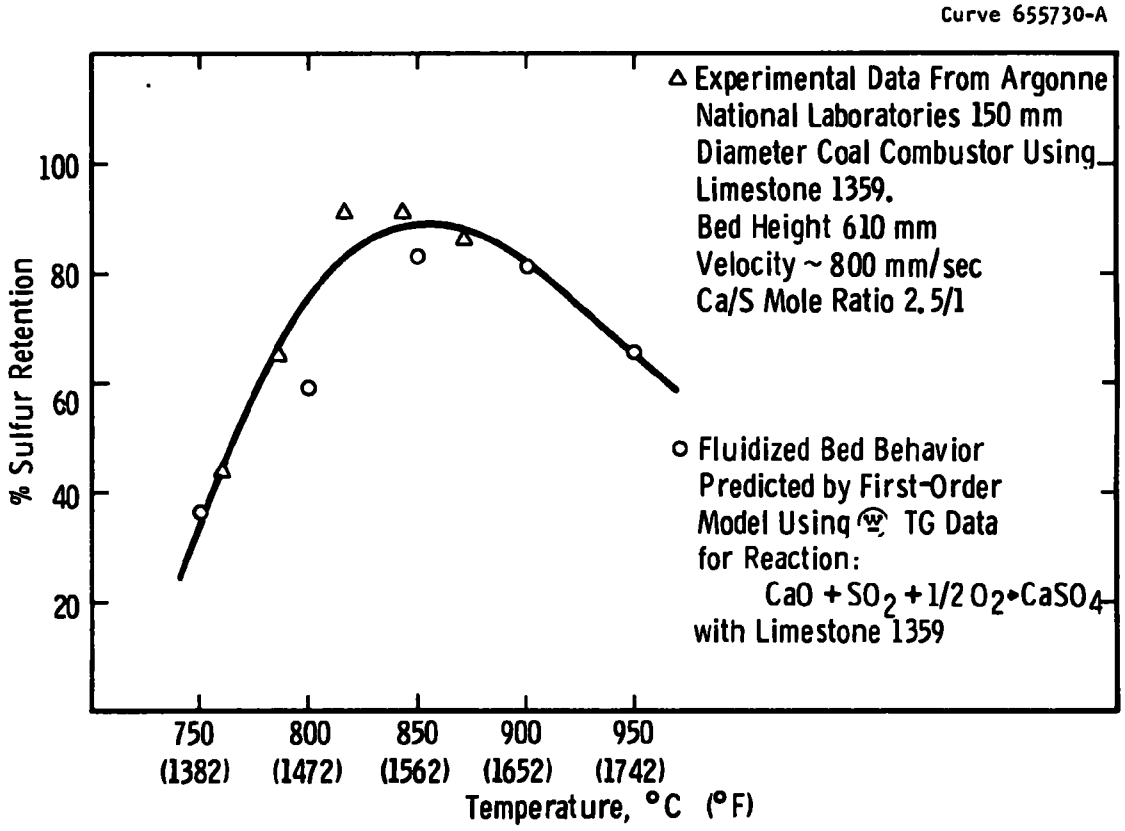

Figure E-6—The effect of temperature on sulfur retention in a fluidized bed of limestone 1359

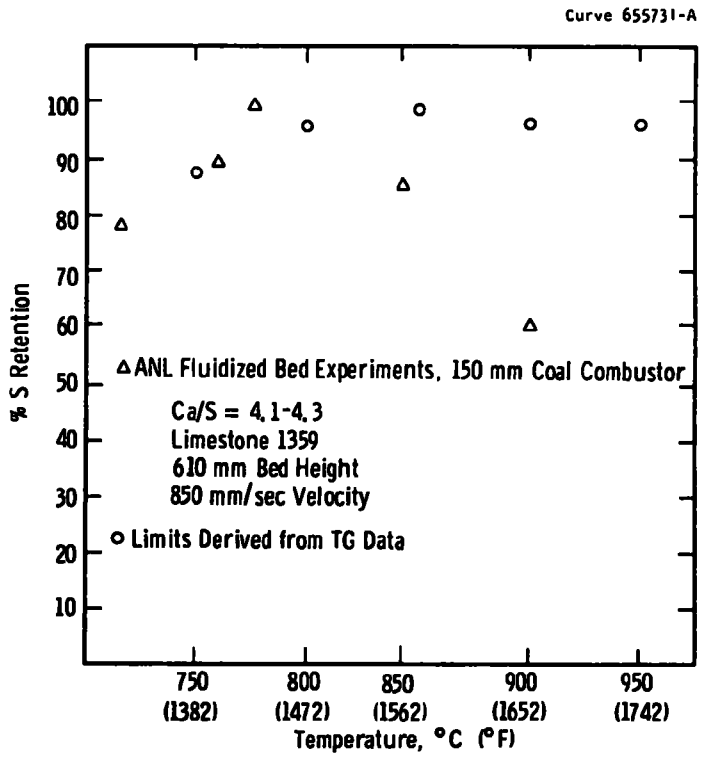

Figure E-7—Comparison of TG data with fluidized bed results

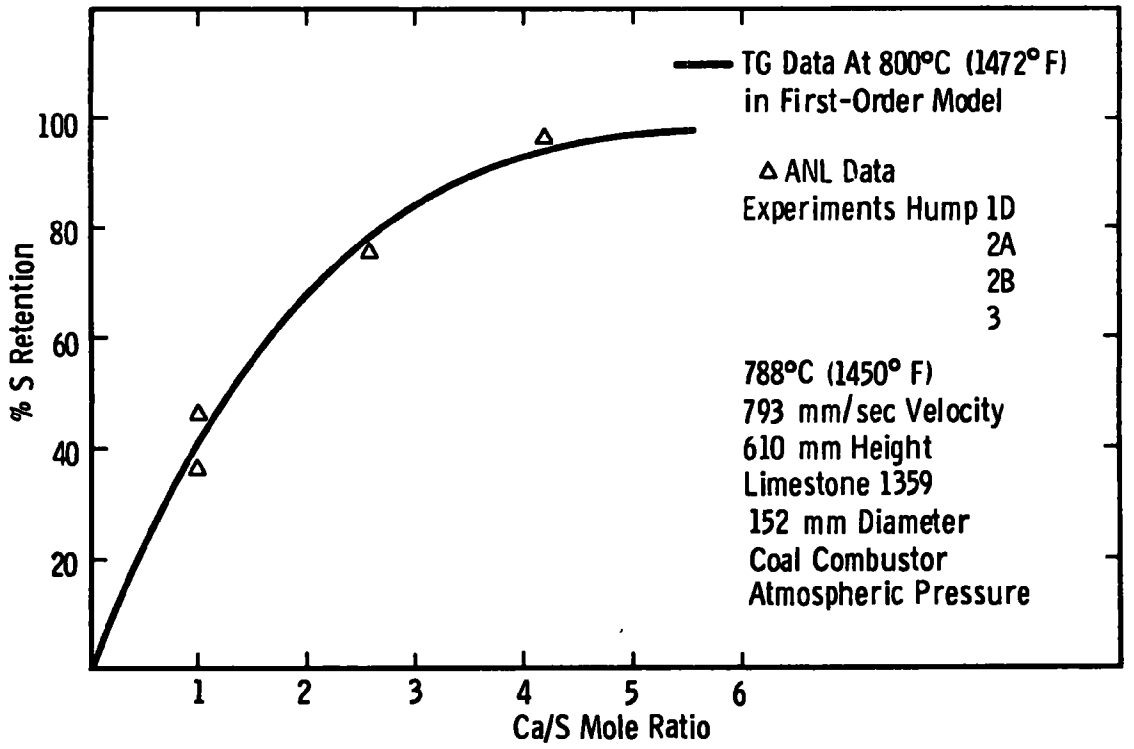

Figure E-8—The effect of Ca/S mole ratio on sulfur retention

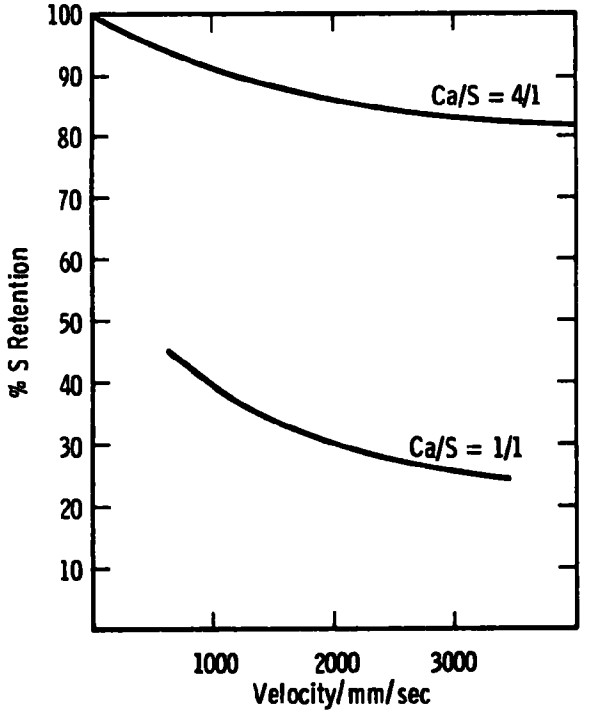

Figure E-9—Model predictions of the effect of superficial velocity on sulfur retention

- The decrease in sulfur retention follows a steeper curve at low calcium/sulfur ratios (1/1).

Both of these features are predicted by the model, as shown in Figure E-9.

The decrease in sulfur retention at temperatures above 870°C (1598°F) is more severe in practice than the simple first-order model predicts. The TG data used here, however, do not faithfully reproduce the conditions of the fluidized bed experiments; calcination in the fluidized bed will be much more rapid in this temperature range than occurred in the TG experiments, since the equilibrium pressure of carbon dioxide rises rapidly in this temperature range. Thermogravimetric experiments show that the time/temperature history during calcination affects the capacity of the calcined stone for reaction with sulfur dioxide.[7,13]

Projections Using the First-Order Model

Because the model shows a satisfactory relation between sulfur removal in fluidized beds and the TG data obtained under careful simulation of fluidized bed conditions, a number of general curves were generated from Equation E-2 to show the average reaction rate required to desulfurize the gases generated in the fluidized bed combustion of coal.

The curves in Figure E-10 illustrate the effect of gas residence time (actual) in the bed on sulfur removal. For 80 percent sulfur removal with a residence time of one second, a rate of reaction in the TG tests at (0.5 percent sulfur dioxide, 101.3 kPa [1 atm]) of 2.2×10^{-2} calcium reacting per minute is required.

Table E-3 shows the utilization of sorbent at which the reaction rate has fallen to the critical value for maintenance of the 80 percent sulfur dioxide retention level.

While the parametric plot of Figure E-10 can be used to estimate the performance of a sorbent in a given configuration of fluidized bed combustor using TG data from Appendix D, the data used must be selected to reflect the calcination conditions in the fluidized bed.

Table E-3

FLUID BED SORBENT UTILIZATION PREDICTED
FROM THERMOGRAVIMETRIC DATA

TG	Sorbent	Calcination	Pressure kPa,(atm)	% Ca utilization for 80% SO_2 removal at 1.0 sec gas residence time
215	Limestone 1359 (420-500 μm)	Calcined in N_2	101.3(1)	7
221	"	Calcined in CO_2	"	37
257	"	"	"	50
258	"	"	"	33
259	"	"	"	34
260	"	"	"	38
261	"	"	"	42
300	"	"	1013(10)	21
301	"	"	1013(10)	34
202	Dolomite 1337 (1200-1000 μm)		1013(10)	54

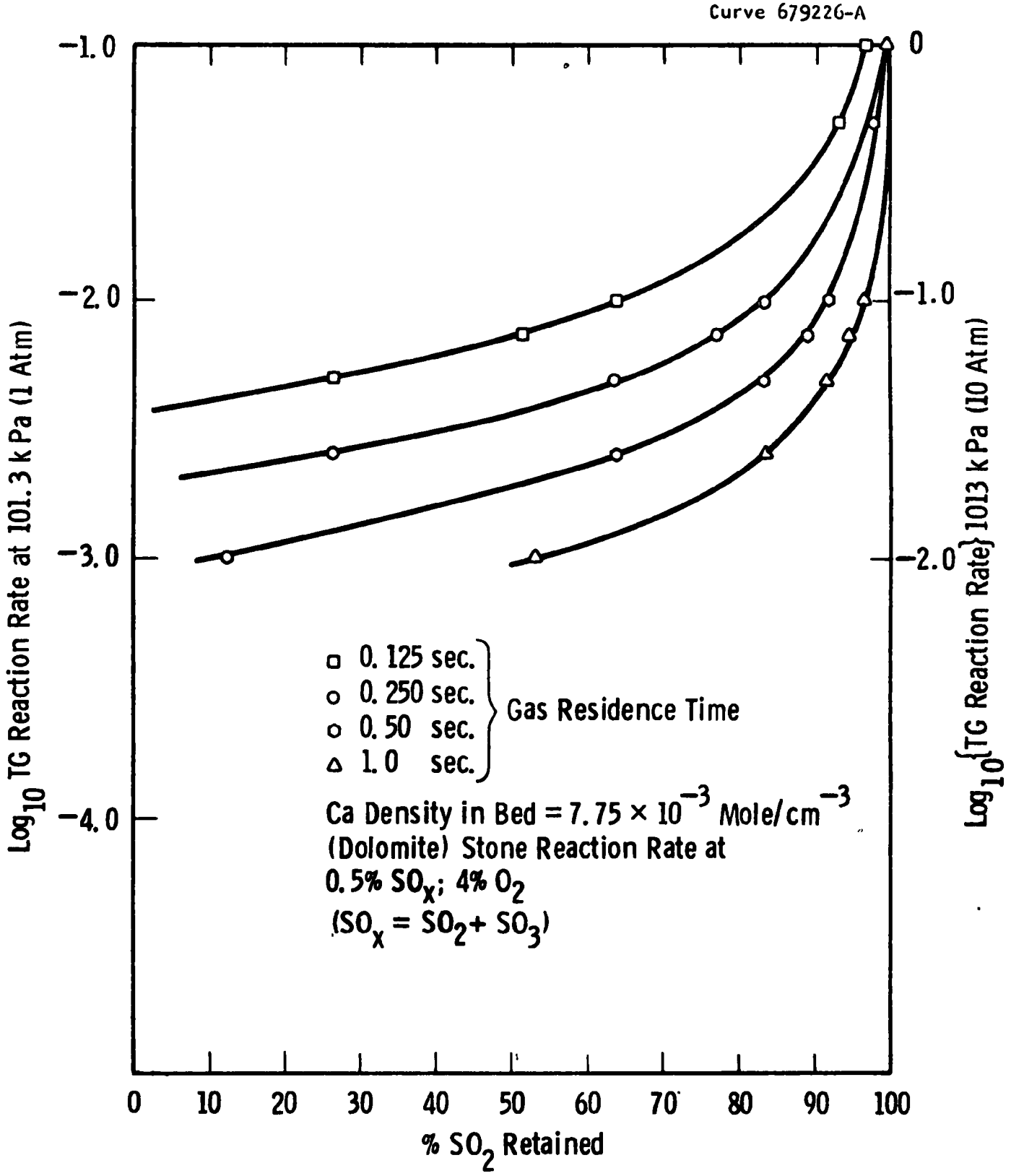

Figure E-10—The reaction rate criteria for desulfurization

The model developed, in spite of its simple approach, shows that fluidized bed results on desulfurization are accurately paralleled by TG data and that quantitative conclusions can be drawn from TG data. Specifically, the model showed:

- A temperature maximum for desulfurization at atmospheric pressure
- The effect of calcium/sulfur molar ratio on desulfurization
- The effect of gas velocity on desulfurization
- The effect of the ambient carbon dioxide partial pressure on desulfurization by virtue of the effect of P_{CO_2} on calcination
- The effect of pressure which raises the partial pressure of carbon dioxide thereby causing higher utilization through increased stone capacity rather than by directly influencing the rate of reaction.

The overall conclusion from the application of TG data to the model is that:

- Ca/S mole ratios of $\sim$ 1/1 can achieve 90 percent desulfurization if the dolomite is not calcined under low partial pressures of carbon dioxide. Pressurized operation, therefore, which maintains a high P_{CO_2} in the bed should tend towards the 1/1 calcium/sulfur molar ratio.
- Half-calcined dolomite should be used as a sorbent in the range intermediate between 1/1 and 2.5/1 calcium/sulfur molar feed ratio. Improvement in desulfurization can be affected by modest increases in bed height or gas residence time.
- Further experimental and theoretical development of the model should consider
  - The effect of particle size distribution
  - The effect of high-temperature operation above 1750°C (3182°F)

- The effect of grain structure of the raw dolomite on its capability to be calcined so that it can be used at low calcium/sulfur molar ratios.

REFERENCES

1. Hammons, G. A. and A. Skopp. A Regenerative Limestone Process for Fluidized Bed Coal Combustion and Desulfurization. Environmental Protection Agency. Report to A.P.C.O. Exxon Research and Engineering Co. Linden, N.J. February 1971.
2. Hatfield, J. D., Y. K. Kim, R. C. Mullins, and G. H. McClellan. Investigation of the Reactivities of Limestone to Remove Sulfur Dioxide from Flue Gas. Air Pollution Control Office. Tennessee Valley Authority. 1971.
3. Cox, D. G., J. Highley, et al. Reduction of Atmospheric Pollution. Environmental Protection Agency. National Coal Board. London, England. September 1971.
4. Borgwardt, R. H. and R. D. Harvey. Env. Sci. Tech. 6: 350, 1972.
5. Bethell, F. V.,D. W. Gill, and B. B. Morgan. Mathematical Modeling of the Limestone-Sulfur Dioxide Reaction in a Fluidized Bed Combustor. Fuel. 52, 1973.
6. Jonke, A. A., G. J. Vogel, et al. Reduction of Atmospheric Pollution by the Application of Fluidized Bed Combustion. Environmental Protection Agency. Argonne National Laboratory. Argonne, Illinois. ANL/ES-CEN-1002. June 1970.
7. Keairns, D. L., D. H. Archer, et al. Evaluation of the Fluidized Bed Combustion Process, Volume 1. Environmental Protection Agency. Westinghouse Research Laboratories. Pittsburgh, Pennsylvania. EPA-650/2-73-048a. December 1973. NTIS PB 231 162/9.
8. Ruth, L. A. Ph.D. Dissertation. The Reaction of Hydrogen Sulfide with Half-Calcined Dolomite. City University of New York. New York. N.Y. (1972).
9. Wen, C. Y. and M. Ishida. Reaction Rate of Sulfur Dioxide with Particles Containing Calcium Oxide. Env. Sci. Technol. 1: 703, 1973.

10. Pigford, R. L. and G. Sliger. Ind. Eng. Chem. Process Des. Develop. 12: 85, 1973.
11. Moss, G. The Fluidized Bed Desulfurizing Gasifier. (Proceedings of the 2nd International Conference on Fluidized Bed Combustion. Hueston Woods. 1970.)
12. Archer, D. H., D. L. Keairns, et al. Evaluation of the Fluidized Bed Combustion Process. Environmental Protection Agency. Westinghouse Research Laboratories. Pittsburgh, Pennsylvania. Contract CPA 70-9. November 1971. NTIS PB 211 494, 212 968/9, 213 152/2.
13. Appendix D—this report.

APPENDIX E_1

DERIVATION OF THE MODEL EQUATIONS

The fluidized bed is assumed to behave as a series of plug-flow reactors in each of which a first-order reaction with respect to gas concentration reduces the concentration of sulfur dioxide from C_o to C, so that

$$C = C_o e^{-k'\tau}$$

where

C_o = SO_2 concentration entering an element of bed height
C = SO_2 concentration leaving an element of bed height
τ = residence time of the gas in the bed element
k' = first-order rate constant for the reaction
$CaO + SO_2 + 1/2\ O_2 = CaSO_4$; $k' = f(u, \rho, C)$
u = mean utilization of the stone in the bed
ρ = molar density of CaO in the bed
v = gas velocity through the bed

If the sulfur is liberated from the coal uniformly throughout the bed, the fraction of the total sulfur released in the element of bed height, db, is given by db/H.

Since this sulfur travels through a bed height, b, the fraction of the sulfur released in the element db which is reacted and retained in the bed is $1 - e^{-k'\tau'}$, where τ' is the residence time of the gas in the bed height b above the element db. The sulfur retention due to sulfur generation in the element db is

$$\frac{1}{H}\left(1 - e^{\frac{-k-(H-b)}{v}}\right)db$$

The fraction of the total sulfur retained in the bed is given by

$$\frac{1}{H} \int_0^H \left[1 - e^{\frac{-k'(H-b)}{v}}\right] db$$

$$= 1 - \frac{v}{k'H} \left(1 - e^{\frac{-k'H}{v}}\right)$$

$$R = 100 \left[1 - \frac{v}{k'H} \left(1 - e^{\frac{-k'H}{v}}\right)\right].$$

Using the definitions

$$R = \frac{\text{moles of sulfur reacted with CaO}}{\text{moles of sulfur input}} \times 100$$

$$F = \frac{\text{moles of calcium input}}{\text{moles of sulfur input}}$$

$$U = \frac{\text{moles of sulfur reacted with CaO}}{\text{moles of Ca input}} \times \frac{100}{1}$$

$$R = FU$$

$$U = \frac{1}{F} \left\{1 - \frac{v}{k'H} \left(1 - e^{\frac{-k'H}{v}}\right)\right\}$$

k' is obtained from TG data as follows: At any given utilization of the calcium oxide in the stone, the rate of reaction of the stone at sulfur dioxide concentration C_i is

$$\frac{d\alpha}{dt} = k; \qquad \alpha = \text{molar fraction}$$

If ρ = molar density of the stone in the fluidized bed, the rate of reaction (moles m^{-3} sec^{-1}) is

$$\rho \frac{d\alpha}{dt} = k\rho.$$

At unit gas concentration, the rate of reaction (sec^{-1}) is

$$\frac{\rho}{C_i}\frac{d\alpha}{dt} = \frac{k\rho}{C_i} = k'.$$

APPENDIX F

SPENT STONE DISPOSITION

APPENDIX F
SPENT STONE DISPOSITION

INTRODUCTION

The pressurized fluidized bed combustion process, as presently conceived, results in the production of dry, partially utilized dolomite or limestone particles from 0 to 6 mm in size. In addition, fine particles of sorbent and ash will be collected in the particle removal system. The sorbent material may be either regenerated for recycling to the fluid bed boiler for repeated sulfur dioxide (SO_2) removal[1,2] or disposed of in its partially utilized form in a once-through system.[1] The former process has the potential advantage of producing less solid waste for disposition, but much uncertainty still exists about the regenerative processes.[3] Conceptually, it is possible in a regenerative process to recycle all of the sorbent. This might involve a synthetic calcium-based material, reconstitution of the spent sorbent, or an alternative sorbent material. The composition of the spent sorbent depends on the characteristics of the original stone, the coal feed, the variation in operating temperature and pressure, as well as on once-through or regenerative modes of operation. The major compounds in the waste stone to be disposed of are calcium sulfate ($CaSO_4$), calcium oxide (CaO)(or calcium carbonate [$CaCO_3$]), and magnesium oxide (MgO) when dolomite is used, and calcium sulfate and calcium oxide or calcium carbonate when limestone is used. Trace elements arising from impurities in the coal and dolomite will also be present.

A summary of the general process options for disposition of the spent sorbent is presented in Figure F-1. Two methods of dealing with the spent sorbent are being considered:

- Disposition of the spent stone being discharged directly from the fluidized bed combustion process (once-through or regenerative, Options 1 and 3)

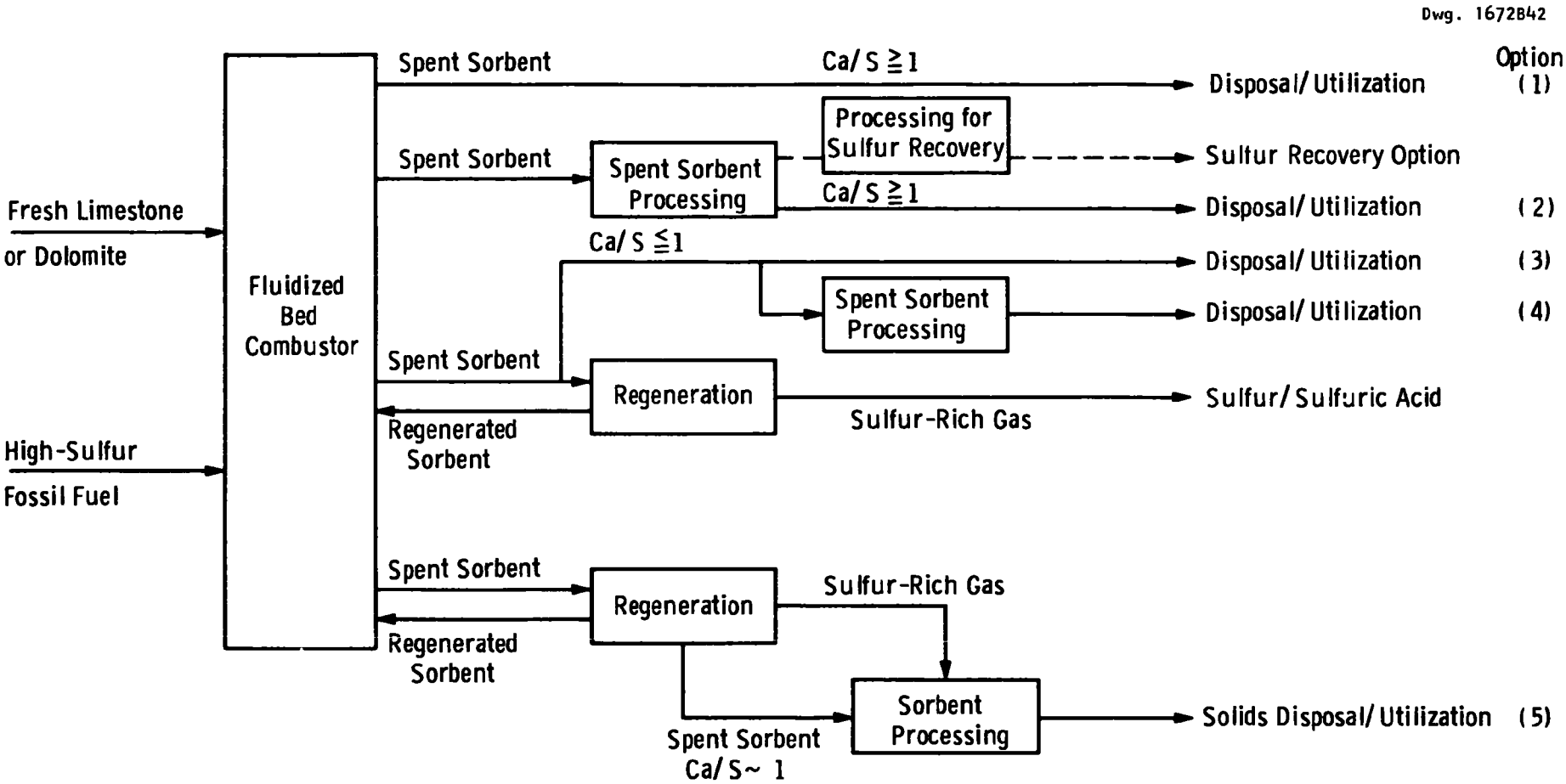

Figure F-1—Sulfur removal system process alternatives

Figure 18

- Disposition of the spent stone after further processing (Options 2 and 4).

Disposition without processing includes direct disposal or utilization of the material in soil stabilization, for example. This is the preferred option since it does not require additional processing. Disposition of the spent stone after further processing is being considered in order to develop methods for rendering the stone environmentally acceptable for disposal, if direct disposal is not universally permitted, and to investigate alternative markets for the spent stone, such as in the form of refractory brick.

Recovery of sulfur from the spent stone for disposal or utilization has not been considered attractive, although the waste stone could be processed to recover the sulfur. Sulfur or sulfuric acid (H_2SO_4) would be recovered from the sulfur-rich gas (SO_2 or H_2S) from the regeneration processes. A third general option for processing the waste stone (Option 5) would be to react the off-gas from the regenerator with the waste sorbent to produce a solid material for disposal or utilization. This option does not appear to offer advantages over the once-through process options.

FACTORS AFFECTING SPENT STONE DISPOSITION

Among the factors that will affect the disposition of the spent sorbent are, for example, the quantity of spent sorbent, its chemical characteristics, regulations, geographical location, and the size of the market for respective applications.

Quantity

Representative quantities of spent material are illustrated in Table F-1 for application in fluidized bed combustion systems. Comparisons with regenerative systems and stack-gas cleaning effluents were prepared by Westinghouse and presented in previous reports.[1] Typical quantities of spent sorbent projected for disposal from a 500 MW power plant burning a 3 wt % sulfur fuel with 95 percent removal would range

Table F-1

SPENT STONE DISPOSITION

	1970	1975	1985	2000
Total Utility Consumption				
Coal, Tg (10^6 ton)	296 (326)	369 (407)	485 (535)	708 (780)
Sulfur[a], Tg (10^6 ton)	8.9 (9.8)	11 (12.2)	14.6 (16.1)	21.2 (23.4)
Fluidized Bed Installation Factor[b]	0.0	0.0	0.09 (0.10)	0.41 (0.45)
Spent Dolomite[c], Tg (10^6 ton)				
• Once-through	0.0	0.0	9.5 (10.5)	62.6 (69.0)
• Regenerative	0.0	0.0	4.9 (5.4)	31.8 (35.0)
Landfill, (acre-ft)				
• Once-through	0.0	0.0	4,560	30,000
• Regenerative	0.0	0.0	2,350	15,200

[a]Sulfur in coal at 3 percent.

[b]Ratio of electrical energy produced in coal-fired plants with fluid-bed units to electrical energy produced in coal-fired plants with other combustion units.

[c]Assumes dolomite Ca/S molar ratio of 1.5 for once-through and 0.75 for regeneration.

from approximately 41 Mg/hr (45 tons/hr) for a once-through system using dolomite to approximately 19 Mg/hr. (21 tons/hr) for a regenerative system utilizing a calcium/sulfur makeup rate of 0.75. Specific quantities will depend on operating conditions and sorbent characteristics.

Chemical Characteristics

The chemical characteristics of the spent sorbent will depend on a number of operating and design parameters—for example:

- The operating conditions
- The specific stone utilized in the process
- The location of the effluent stream from the process (for example, in a regenerative process the stone for disposal can be removed before or after the regeneration process).

The primary constituents are calcium sulfate, calcium oxide (or calcium carbonate), and magnesium oxide when dolomite is used; and calcium sulfate and calcium oxide (or calcium carbonate) when limestone is used. The amount of magnesium oxide present is determined by the magnesium carbonate ($MgCO_3$) composition of the fresh stone. The distribution of the calcium-based compounds in the spent sorbent is summarized in Table F-2. The chemical characteristic of the spent sorbent are assessed in Appendix G, Spent Stone Disposal—Assessment of Environmental Impact.

The solubility of calcium and magnesium compounds are of particular importance in determining chemical activity. A compilation of readily available solubility data on calcium and magnesium compounds was made. The solubility data are presented in Tables F-3 and F-4 in order of decreasing solubility. The oxide form, as well as carbonates, phosphates, and silicates, of magnesium have minimal environmental impact. Magnesium sulfites and sulfates would not be inert. The concentration of these compounds, however, is negligible in the spent sorbents tested (Appendix G). This raises the possibility, however, of achieving a separation of dolomitic sorbents into calcium and magnesium compounds which

separately might have market potential. One problem with phosphate end forms is that phosphoric acid is relatively expensive, and there does not appear to be a cheap source of the phosphate ion for spent stone processing.

Table F-2

TYPICAL COMPOSITION OF CALCIUM COMPOUNDS IN SPENT SORBENT

	CaO or $CaCO_3$[a] mole %	$CaSO_4$ mole %
Once-through		
Dolomite	10	90
Limestone	50	50
Regenerative		
Dolomite/limestone	10-70	30-90[b]

[a]The oxide or carbonate form is determined by the fluidized bed combustor operating temperature, pressure, and excess air.

[b]The $CaSO_4$ composition is determined by the sulfur loading for the sorbent to the regenerator.

Regulations

An important aspect in the development of a viable stone disposal process is the constraint of existing regulations relative to environmental impact. Each site will require examination of both local and federal regulations.

The Solid Waste Disposal Act was set forth as Title II of Public Law 89-272 of the 89th Congress, S. 306, approved October 20, 1965. This was amended by Public Law 91-512, H.R. 11833, approved October 26, 1970. In essence, these laws recognized that the problems of waste disposal had become national in scope and required federal action to promote the development of solid waste management and resource recovery systems and, also, an overall national research and development program. Legal documents and technical investigations which have been reported to carry out the provisions of these acts will provide background information and criteria for disposition of spent sorbent from the fluidized bed combustion process.

Table F-3

SOLUBILITY OF CALCIUM COMPOUNDS IN WATER

Formula	Form or natural mineral	Solubility, ppm	Temperature, °C(°F)
$Ca(HCO_3)_2$		166,000	20 (68)
$Ca(HSO_3)_2$		sol.	
$Ca(HS)_2 \cdot 6H_2O$		70,000-250,000	20 (68)
$CaSO_4 \cdot 1/2\ H_2O$	α (stable form)	3,000-8,000	20 (68)
	β (unstable form)	6,600	30 (86)
$CaSO_4$ III	Soluble anhydrite	7,000	20 (68)
II	Insoluble anhydrite	2,100-3,000	20 (68)
$Ca(OH)_2$		1,300-1,400	0 (32)
$CaO + 2SiO_2$		236[a]	30 (86)
$2CaO + SiO_2$		212[b]	30 (86)
$CaO \cdot SiO_2$	Pseudowollastonite	95	17 (63)
		212[c]	
CaS	Oldhamite	120-210[d]	15 (59)
$CaSO_3 \cdot 2H_2O$		43	18 (64)
$Ca_3(PO_4)_2$		25	
$CaCO_3$	Calcite	13-14	25 (77)
	Aragonite	12-15	25 (77)

[a]Hydrolysis studies; 164 ppm free SiO_2 also in solution at equilibrium with solid containing 0.103 moles CaO/mole SiO_2.

[b]Hydrolysis studies; 83 ppm free CaO also in solution at equilibrium with solid containing 1.13 moles CaO/mole SiO_2.

[c]Hydrolysis studies; solid phase 1.07 moles CaO/mole SiO_2.

[d]Decomposes.

Table F-4

SOLUBILITY OF MAGNESIUM COMPOUNDS IN WATER

Formula	Natural Mineral	Solubility, ppm	Temperature, °C (°F)
$MgSO_4 \cdot 7H_2O$	Epsomite	710,000	20 (68)
$MgSO_3 \cdot 6H_2O$		660,000	25 (77)
$MgHPO_4 \cdot 7H_2O$		3,100	
$MgCO_3 \cdot 3H_2O$	Nesquehonite	1,790	16 (61)
$MgCO_3 \cdot 5H_2O$	Landsfordite	1,760	7 (45)
$3MgCO_3 \cdot Mg(OH)_2 \cdot 3H_2O$	Hydromagnesite	400	
$MgCO_3 \cdot Mg(OH)_2 \cdot 3H_2O$	Artinite	---	
$CaO \cdot MgO \cdot 2CO_2$	Dolomite	260-440	25 (77)
$MgHPO_4 \cdot 3H_2O$	Newberyite	250	
$Mg_3(PO_4)_2 \cdot 4H_2O$		200	
$MgCO_3$	Magnesite	106	
$Mg(OH)_2$	Brucite	9	18 (64)
MgO	Periclase	6.2	
MgS		Dec.[a]	
$Mg_3(PO_4)_2 \cdot 8H_2O$	Bobierite	200	
$Mg_2P_2O_7$		200	
$MgO \cdot SiO_2$	Clinoenstatite	I[b]	
$7MgO \cdot 8SiO_2 \cdot H_2O$	Anthophyllite	---	
$3MgO \cdot 4SiO_2 \cdot H_2O$	Talc	---	
$3MgO \cdot 2SiO_2 \cdot 2H_2O$	Serpentine	---	
$2MgO \cdot SiO_2$	Forsterite	I	
$CaO \cdot MgO \cdot SiO_2$	Monticellite	---	
$CaO \cdot MgO \cdot 2SiO_2$	Diopside	I	
$2CaO \cdot MgO \cdot 2SiO_2$	Akermanite	---	
$3CaO \cdot MgO \cdot SiO_2$	Nervinite	---	
$3CaO \cdot MgO \cdot 2SiO_2$	Merwinite	---	
$CaO \cdot 3MgO \cdot 4CO_2$	Huntite	---	
$2CaO \cdot 5MgO \cdot 8SiO_2 \cdot H_2O$	Tremolite	---	

[a] Dec. = decomposes.

[b] I = insoluble.

Location and Market

The geographical location of each plant will determine the sorbent utilized and the disposal options. Limestones and/or dolomites vary geographically. Factors which affect sorbent selection and will be dependent on location are discussed in Appendix C. The question of market compatibility with by-products must be considered for each case. Illustrations of possible applications are presented in the following sections. One aspect of the market picture is to assess the total market available. For example, the domestic consumption of magnesium compounds is of interest. Domestic usage of magnesium compounds in 1968 is presented in Table F-5.

The two largest uses were high-temperature refractory applications--dead-burned dolomite and refractory magnesia. This is not a likely market for the spent stone sorbent from the fluidized bed combustion process in the nonregenerative versions. The effluent sorbent would in these cases have a high sulfate content which could not be retained at refractory use-temperatures. The regenerative versions with low calcium sulfate loading, however, might be able to supply stone to this market. At 330 on-stream days per year, a 500 MW plant would produce on the order of 25,000 Mg (27,557 tons) of magnesium per year in various forms (fully-calcined dolomite, half-calcined dolomite, and so on) in the regenerative process, and twice that quantity in the nonregenerative versions. It appears that the potential market for refractory forms of magnesia and dolomite could be large enough to accommodate the output from a substantial number of 500 MW plants.

If the spent sorbent cannot be used as dead-burned dolomite, the market size shrinks substantially. In this case new, large-scale uses would have to be developed.

Other potential markets exist for the spent sorbent. A comprehensive assessment of the alternatives is required, followed by tests with actual spent sorbent for the preferred options.

TABLE F-5

DOMESTIC USAGE OF MAGNESIUM COMPOUNDS, 1968[a]

	End use/%	Mg	M$	$/Mg
Dead-burned Dolomite		1,664,000	31.63	19
Refractory Magnesia		600,000	44.54	74
Other Magnesia		122,000	12.23	100
Pulp and paper	12			
Chemical processing	11			
Oxychloride and oxysulfate cement	10			
Rayon	10			
Rubber	8			
Fertilizer	6			
Insulation - 80% MgO	1			
Other[b]	42			
	100			
Magnesium Hydroxide		60,800	2.48	41
Magnesium Chlorides		357,000	27.5	76

[a]U. S. Bureau of Mines. Minerals Yearbook. 1968. p. 667-681.

[b]Including electrical and medicinal uses; and in flux, ceramic, glass, sugar, animal feed, fuel additives, water treatment, and uranium processing.

DISPOSITION OF UNPROCESSED SPENT SORBENT

The disposition of unprocessed spent sorbent is represented by options 1 and 3 in Figure F-1. Westinghouse recently obtained samples of spent dolomite from the Argonne and Exxon fluidized bed combustion pilot plants and carried out preliminary leaching experiments and activity tests.

Results from these preliminary tests indicate:

- In both the leaching-time experiment and the stone-loading experiment calcium and sulfate dissolution plateaued at concentrations limited to the calcium sulfate solubility.
- The equilibrium calcium and sulfate concentrations were high, exceeding the water quality criteria. Since calcium sulfate occurs abundantly in nature as gypsum, leachates induced from a natural gypsum offers a good reference for its calcium and sulfate concentrations. Iowa ground gypsum No. 114 was selected to undergo parallel leaching tests with the ANL waste stone. Results indicated that gypsum leachates contained approximately the same amounts of dissolved calcium and sulfate ions as the ANL leachates. Both agreed relatively well with the calcium sulfate solubility, and both exceeded the water quality standards, 75 mg/l for calcium and 250 mg/l for sulfate.
- There was negligible dissolution of magnesium ions.
- Insignificant amounts of heavy metal ions were found in the leachates.
- ANL leachates were alkaline, with pH = 10.6 to 12.1. It is interesting to note, however, that the run-off leachates showed a gradual decrease in pH with the amount of leachates passing through.

The experimental data and an assessment of the environmental impact of direct disposal are presented in Appendix G.

The spent sorbent characteristics (size and composition) may make the stone attractive for utilization. Areas of particular interest include soil stabilization and landfill. In a general sense, soil stabilization includes any treatment of soil whereby it is made more stable. It is well established for conventional soils that such properties as strength, stiffness, compressibility, permeability, workability, susceptibility to frost and sensitivity to changes in moisture content may be altered by various methods. Such methods range from simple compaction to expansive techniques for grouting, drainage, waterproofing, and strengthening of material by thermal means. Locally available road-bed soils are stabilized commonly by the addition of agents such as Portland cement, lime, and lime/fly ash mixtures. They act by forming cementitious compounds that more or less permanently bond together individual particles or aggregates of soil.

Tests are required to determine what the characteristics of various types of soils are when they are blended with the spent sorbent. Specifically, tests to determine the unconfined compressive strength, the Atterberg limits, and direct and triaxial shear strength of soils blended with various amounts of the waste materials should be performed. These tests would provide sufficient information to enable specification of soil-waste material mixtures which can be used as load-bearing materials in highway foundation and embankment structures. Wherever necessary, these mixtures of soil and waste material may be further blended with conventional cementitious materials such as Type I Portland cement.

DISPOSITION OF PROCESSED SPENT SORBENT

The direct disposal or utilization of spent sorbent may not be possible or permitted in all cases. Thus, alternatives for spent stone disposition must be developed to permit utilization of the fluidized bed combustion process. It may also be possible to develop a more attractive use for the spent sorbent through some processing technology.

Several processes are proposed, as summarized in Figure F-2. The direct disposal options discussed in the previous section and the final disposition of the sulfur in the regenerative processes are also

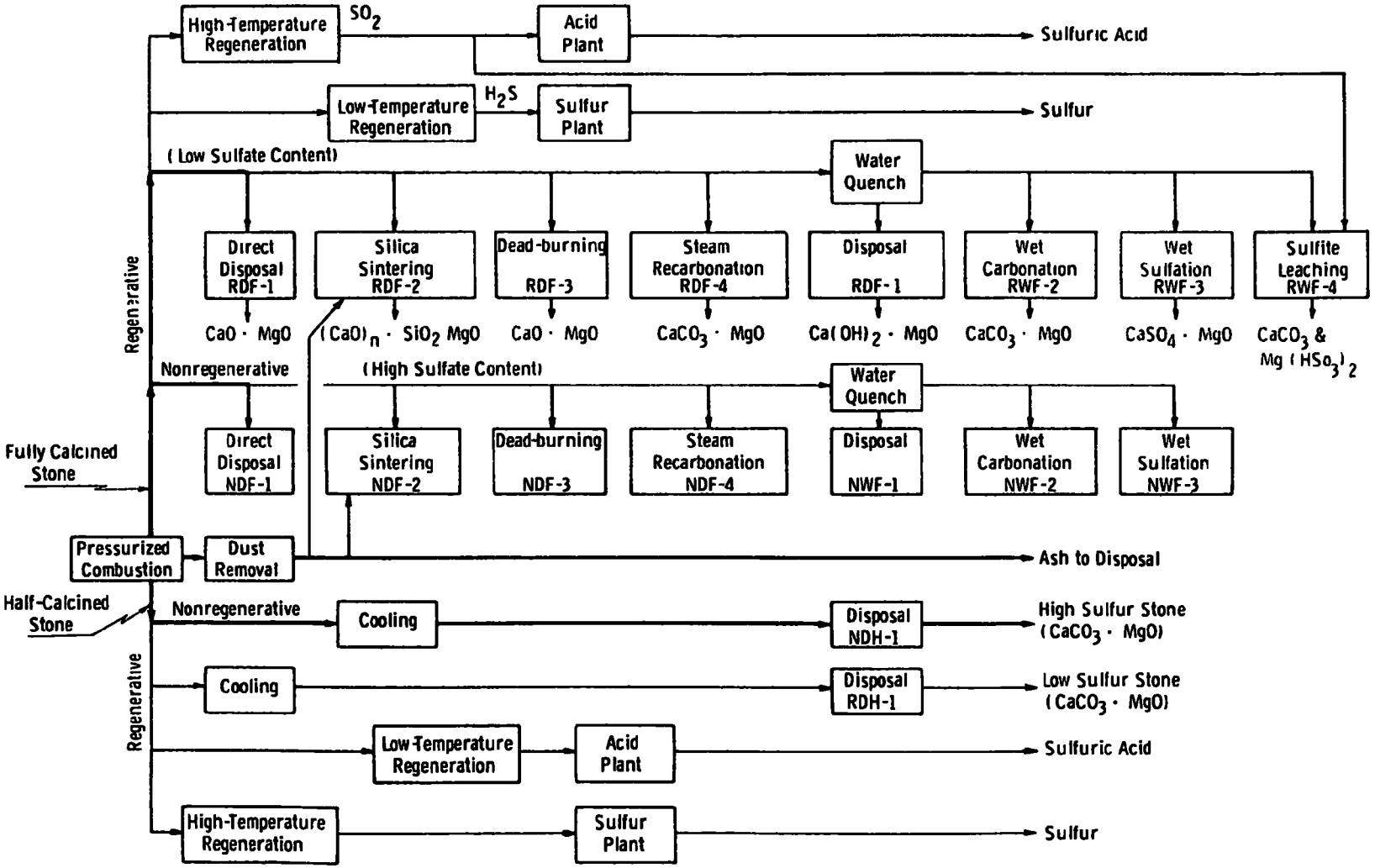

Figure F-2—Pressurized fluidized bed combustion: spent stone disposal processes

shown. The basic option for dolomite is to operate either half-calcined or fully-calcined. In each of these modes it is possible to operate regeneratively or nonregeneratively. Further, there are two options on regeneration: a one-step, high-temperature process, and a two-step, low-temperature process. The former leads to sulfur dioxide, which is probably best routed to an acid plant but can be converted to sulfur. The latter releases hydrogen sulfide, which is convertible to elemental sulfur or acid. In reading the figure, for each of the options on the respective regenerative branches one must include one of the two sulfur processing alternatives.

The figure is expressed in terms of dolomite, but similar considerations apply if limestone is used. This figure focuses on the processing of the unsulfated fraction of the stone.

In all cases coal ash is assumed to be taken overhead and removed from the pressurized hot flue gas stream by particulate removal system before sending the gas on to power recovery turbines. The various process options shown on Figure F-2 are given a letter code for convenience.

First letter - R for regenerative
N for nonregenerative (once-through)
Second letter - D for dry process
W for wet process
Third letter - H for half-calcination (retention of $CaCO_3$)
F for full-calcination (formation of CaO)

Where compositions are shown, only the form of the residual excess calcium compound is given. In every case calcium sulfate is also present as calcium sulfate/magnesium oxide. Brief descriptions of the process options follow.

Disposal: Option NDH-1

This is a simple method for stone disposal, involving only cooling of the stone, since the composition calcium sulfate, calcium carbonate, and inerts is expected to be environmentally inert. While landfill is the most likely end use, it is possible that special cements may be made from

it. As a nonregenerative process, all the sulfur captured is removed from the process as calcium sulfate. No sulfur recovery facilities are required.

Disposal: Option RDH-1

This is also a simple stone disposal process, needing only stone cooling. Sulfur processing facilities are needed since it is a regenerative process. The type depends on which regeneration process is used. The final spent stone may have a low sulfur content. This depends on the concentration of calcium sulfate specified for the regeneration process. Spent stone having a low calcium sulfate/magnesium oxide concentration, say 5 wt %, may be a better candidate for use in the cement industry than the stone from NDH-1.

Direct Disposal: Options RDF-1 and NDF-1

The bulk of the processes proposed deal with fully calcined stone. They fall into two groups according to whether they are regenerative or once-through. It is convenient to discuss the counterparts together.

Both RDF-1 and NDF-1 will have stone cooling. The ability to use this material as landfill will depend on the content and the reactivity of the stone. RDF-1 product might be marketable where an inexpensive alkali is needed, as in municipal waste treatment or acid mine drainage treatment. NDF-1 product has only 33 percent calcium oxide/magnesium oxide, which probably makes this process less attractive than RDF-1.

Silica Sintering: Options RDF-2 and NDF-2

To take advantage of the free calcium oxide in the spent stone, recovered coal ash, which is expected to be high in silica, is blended with the stone and sintered at temperatures perhaps as high as 1500°C (2732°F). The conditions would be a compromise between what is required for sintering and what must be avoided to prevent loss of sulfur dioxide

from the sulfate present. It is likely that a cooling and a grinding step for the spent stone prior to blending will be required.

If cements cannot be prepared from the spent stone, it would appear that whatever pozzolanic activity is present would result in a material that would behave as a stable soil in a landfill operation.

Dead-Burning: Options RDF-3 and NDF-3

Exposure of materials like calcium oxide and calcium sulfate for sufficient lengths of time to elevated temperatures reduces their surface area and, hence, their general chemical reactivity. Because of the presence of calcium sulfate, the dead-burned product probably could not be used as a refractory. The material, however, is expected to have a minimal impact on the environment if used for landfill because of the reduced activity of calcium and magnesium compounds.

Steam Recarbonation: Options RDF-4 and NDF-4

In both processes the stone is cooled to an intermediate temperature, say 500 to 700°C (932 to 1292°F), pulverized with air in a jet mill, and then contacted with flue gas and steam to convert calcium oxide to calcium carbonate. The steam increases the reaction rate. This provides a method for rending the sorbent inactive if the calcium oxide activity prohibits direct disposal.

Disposal: Options RWF-1 and NWF-1

These are simple wet processes in which the calcium oxide is merely hydrated to calcium hydroxide to eliminate any problems in handling calcium oxide. The treated stone may be usable as an inexpensive alkali.

Wet Carbonation: Options RWF-2 and NWF-2

Spent stone is quenched with water and subjected to a three-stage carbonation using recycled flue gas. The object is to convert the free calcium oxide to the less active carbonate form to facilitate disposal.

Wet Sulfation: Options RWF-3 and NWF-3

An alternative to carbonation is to use sulfuric acid to convert the free calcium oxide to calcium sulfate. Since magnesium oxide is soluble in acids, it may not be possible to avoid forming magnesium sulfate. Gypsum and epsom salts are possible end products.

Sulfite Leaching: Option RWF-4

A Canadian patent (639,443) covers a process being used by the Aluminum Company of Canada to recover magnesium from dolomitic ores. It features the use of carbon dioxide as well as sulfur dioxide to achieve a 92 percent recovery of magnesia, while holding the solution of calcium to less than 3 percent in the magnesium solution. Sulfur dioxide from the regenerator, fortified with carbon dioxide, might be used to produce magnesium bisulfite, usable in the paper industry. Alternatively, the bisulfite could be calcined to recycle the sulfur dioxide and produce pure magnesia. Here, sulfur recovery facilities would also be required. A nonregenerative version is not included because a ready source of sulfur dioxide is lacking.

SUMMARY

Solids from fluidized bed combustion plants will vary, depending on how the system is operated. Spent solids include fuel ash and dry, granular, spent sulfur sorbent. Spent sorbent composition with limestone or dolomite may consist of

- $CaSO_4$ and $CaCO_3$
- $CaSO_4$ and CaO
- $MgO \cdot CaSO_4$ and $MgO \cdot CaCO_3$
- $MgO \cdot CaSO_4$ and $MgO \cdot CaO$.

The sorbent material may be disposed of in its partially utilized form in a once-through sorbent system or regenerated for reuse in the fluidized bed combustor. Available pilot-plant test data show that calcium to sulfur (Ca/S) ratios of approximately 2 or greater are required

to achieve 90 percent sulfur removal for a once-through dolomite system. Recent tests carried out at Westinghouse indicate the stone requirement for a once-through system can be significantly reduced—1.2 Ca/S ratio for 90 percent sulfur removal. Regeneration of the spent stone has the potential to reduce stone requirements further and, if the stone (or alternate sorbent) can be reconstituted, virtually to eliminate the need for makeup sorbent.

Direct disposal of the spent sorbent is attractive for first-generation plants. Results from preliminary tests indicate the disposition of the spent sorbent from fluidized bed combustors will not cause water pollution problems. Preliminary activity tests indicate the temperature increase of the spent stone will be negligible when subjected to the environment. Extensive tests must be carried out, however. The chemical composition of the spent sorbent from once-through and regenerative processes and its likely environmental impact require comprehensive leaching tests and activity tests to determine the chemical fate of the constituent compounds (calcium, magnesium, sulfate ion, and so on) and trace elements which may occur in the raw sorbent or which may accumulate during the combustion of the coal.

Several potential applications for the processed spent sorbent were identified:

- Soil stabilization
- Landfill
- Concrete
- Refractory brick
- Gypsum
- Minicipal waste treatment
- Acid mine drainage.

Both high-temperature stone processing, including spent sorbent/fly ash and spent sorbent/clay sintering, and low-temperature pozzolanic*

*A pozzolan is defined as a siliceous or siliceous and aluminous material which in itself possesses little or no cementitious value but which will, in the finely divided form and in the presence of moisture, chemically react with calcium hydroxide (lime) at ordinary temperature to form compounds possessing cementitious properties.

activity require further study. Materials to be tested should include the spent stone from the once-through process, spent stone from pilot plant and prototype plant tests, and blends of these materials with fly ash, clay, and soil. The soil stabilization tests will require determination of unconfined compressive strength, Atterberg limits, and direct and triaxial shear strengths. The influence on agricultural soils of surface dumping of the spent sorbent should also be investigated. For suitability as aggregate material, spent sorbent should be evaluated by testing it in concrete mixes for compressive strength, splitting tensile strength, flexural strength, and modulus of elasticity. The interfacial behavior of the concrete and foundation soil should be examined.

In summary, environmental problems associated with disposal of the spent sorbents from fluidized bed combustion systems differ favorably from those associated with disposal of lime sludges, in that they are solids and they do not possess great water solubility. Data indicate the spent dolomite (or limestone) can be used as dry landfill with known civil engineering practices for controlling structural rigidity and ground water flows. Alternatives are also available for utilization of the spent stone. In addition, the advanced sulfur removal systems being developed would minimize the quantity of spent stone available and, thus, could minimize the problem.

REFERENCES

1. Keairns, D. L. et al. Evaluation of the Fluidized Bed Combustion Process, Vols. I and II. Environmental Protection Agency. Westinghouse Research Laboratories. Pittsburgh, Pennsylvania. EPA-650/2-73-048a and b. December 1973. NTIS PB 231 162/9, 231 163/70.
2. Archer, D. H. et al. Evaluation of the Fluidized Bed Combustion Process. Office of Air Pollution. Westinghouse Research Laboratories. Pittsburgh, Pennsylvania. NTIS PB 211-494, 212-916, 213-152. November 1971.
3. Consolidated Coal Company.
4. Brunner, D. R.,and D. J. Keller. Sanitary Landfill Design and Operation. Environmental Protection Agency. 1972.
5. U. S. Bureau of Mines. Minerals Yearbook. Vols. I and II. 1968. p. 669-681.
6. Pressurized Fluidized Bed Combustion. Office of Coal Research. National Research Development Corporation. England. Report No. 85, Interim No. 1. 1974.

APPENDIX G

SPENT STONE DISPOSAL -

ASSESSMENT OF ENVIRONMENTAL IMPACT

G

APPENDIX G

SPENT STONE DISPOSAL-ASSESSMENT OF ENVIRONMENTAL IMPACT

The pressurized fluid bed combustion process results in the production of partially utilized dolomite or limestone material in the form of calcium sulfate ($CaSO_4$). This sorbent material may be regenerated for recycling to the fluid bed boiler for repeated sulfur dioxide (SO_2) removal or disposed of in its partially utilized form in a once-through system. Although the regenerative process has the advantage of decreased solid waste for disposition,[1] there is still much uncertainty about it. In either case, the spent stone is composed of magnesium oxide (MgO), calcium sulfate, calcium oxide (CaO) (or calcium carbonate [$CaCO_3$]) when dolomite is used, and calcium sulfate, calcium oxide (or calcium carbonate) when limestone is used. The waste stone has particle size ranges of 6.4 mm (1/4 in) and down. Factors affecting the final composition include composition of the fuel, composition of the limestone or dolomite, and operating conditions. The spent sorbent may be utilized as road-base aggregates, concrete and block fillers, neutralizing agents for acid mine drainage, and so on; or marketed for chemical recovery -- sulfur recovery or magnesium oxide extraction. Appendix F deals more extensively with this subject. In this section, the environmental impact of the spent stone when it is dumped or used as a landfill is assessed.

CHEMICAL STABILITY[2,3]

Of the above compounds, calcium sulfate and calcium carbonate are most likely to be environmentally stable and suitable for direct disposal without further processing, as the abundance of naturally occurring limestone and gypsum deposits will attest. Calcium oxide will hydrate readily to form calcium hydroxide ($Ca[OH]_2$) with release of heat (64.041 J/gm-mole [15,300 cal/gm-mole]) on contact with water unless it

is dead-burned. Recarbonation of calcium oxide will also occur with carbon dioxide in the ambient air in the presence of water or water vapor.

Magnesium oxide is virtually insoluble (0.0086 gm) and does not hydrate under atmospheric pressure except in the case of commercially prepared reactive grades. When most types of dolomite quicklimes are hydrated under atmospheric conditions, all calcium oxide components readily hydrate, but very little of magnesium oxide slakes. As a result, high-calcium quicklime slakes much more readily than does dolomitic, which usually requires pressure or long retention periods for complete hydration because of its hard-burned magnesium oxide component.

Magnesium oxide occurs infrequently in nature as the mineral periclase; it is also the end product of the thermal decomposition of numerous magnesium compounds. The physical and chemical properties of magnesium oxides vary greatly with the nature of the initial material, time and temperature of calcination, and trace impurities. The increase in density which results from increasing calcination temperature is paralleled by a decrease in reactivity. Magnesium oxide, prepared in the temperature range of 400 to 900°C (752 to 1652°F) from magnesium hydroxide or basic magnesium carbonate, is readily soluble in dilute acids and hydrates rapidly, even in cold water. Fused magnesium oxides are virtually insoluble in concentrated acids and are indifferent to water unless very finely pulverized. The oxides prepared below 900°C (1652°F), which are easily hydrated with water, are known as caustic-burned magnesias. The unreactive magnesias, prepared at higher temperatures, are called dead-burned or sintered magnesias. The hydration rate of various magnesium oxides is determined by the active surface area and may vary from a few hours, in the case of the reactive oxides obtained at low temperatures, to months or even years for the dead-burned grades.

It is generally recognized that the dissociation temperature for calcite is 898°C (1648°F) under atmospheric pressure in a 100 percent carbon dioxide atmosphere. The temperature of dolomite, however, is not nearly as explicit. Magnesium carbonate ($MgCO_3$) dissociates at a much lower temperature -- 402 to 480°C (756 to 896°F). Since the proportion

of magnesium carbonate to calcium carbonate differs in the many species of dolomites, the dissociation temperature also varies. Differences in the crystallinity of stone also appear to add to the disparity of data. The magnesium carbonate component of dolomite decomposes at higher temperatures than do natural magnesites. A good average value for complete dissociation of magnesium carbonate in dolomite at 760 mm pressure in a 100 percent carbon dioxide atmosphere is 725°C (1337°F); the calcium carbonate component of dolomite would, of course, adhere to the above higher value representing dual-stage decomposition. As a result of these differences in dissociation points, the magnesium oxide is usually hard-burned before the calcium oxide is formed.

From the above discussion it follows that there may be some question about the environmental stability of the magnesium oxide component of the spent sorbent mixtures calcium carbonate/calcium sulfate/magnesium oxide. With the fluid bed boiler conditions approaching 955°C (1750°F) and 1013 kPa (10 atm), it is expected that the magnesium oxide component is hard-burned and, therefore, suitable for disposal without further processing. Activity and leaching tests have been performed on the waste stone from the Argonne National Laboratory (ANL) 152.4 mm (6 in) fluid bed boiler and the Exxon Research and Engineering (Exxon) batch unit and miniplant and will be discussed in a later section of this appendix.

ENVIRONMENTAL IMPACT

The environmental impact of any disposed material is a function of its physical and chemical properties and of the quantity involved. Potential water pollution problems can, in many cases, be predicted by chemical properties such as solubility, the presence of toxic metals, and the pH of leachates. Disposal of the spent stone from the fluid bed combustion system may create air pollution or an odor nuisance such as hydrogen sulfide, depending on the amount of calcium sulfide present, although it is not expected in significant quantities. Heat may be

released on hydration of calcium oxide when the calcium in the spent stone exists in the calcined state if the combustion temperature is high enough to produce fully calcined dolomite.

The first consideration when looking at potential water pollution from the solid waste disposal is the volume of leachate that will be produced. This is a direct function of the amount of water reaching the landfill. There are two possible sources of this water: rainfall and naturally occurring subsurface flow through the landfill site. Subsurface flow is a natural phenomenon which can seriously interfere with safe operation of landfills in two ways. First, it is a source of additional, potentially harmful leachate. Second, it can serve as a direct means of groundwater contamination. Prevention can be effected by a thorough geological study of the site beforehand and, if needed, installation of rerouting devices for the groundwater flow. In a similar vein, coverage of the landfill area when complete will greatly reduce, if not eliminate, the amount of leachate produced.

In order to predict leachate characteristics of a landfill, it is first necessary to describe the general features of water movement and geological considerations for this disposal method. Due to the recent surge of ecological interest in sanitary landfills for solid waste disposal, there is an abundance of information available. Emrich's review of research in this field presents an overall perspective of progress on this subject.[4,5] Research is being conducted to define and solve this problem, but results available to date are not sufficient to assess it fully.[6]

EXPERIMENTS

Leaching experiments and activity tests were performed in order to assess the potential environmental impact of the spent stone from the pressurized fluid bed combustion process and its suitability for disposal as a landfill material. The samples used in these experiments were the spent sorbents from the ANL and Exxon pressurized fluid bed combustion pilot plants (partially sulfated Tymochtee dolomite from ANL run C2 and C3[7] and partially sulfated Grove limestone 1359 from Exxon run 8.4[8]). As calcium

sulfate was a major constituent of the waste stone from the pressurized fluid bed combustion processes, a naturally occurring calcium sulfate (ground gypsum 114 of -20 mesh from Fort Dodge, Iowa) was selected to undergo similar leaching conditions for comparative purposes. Table G-1 summarizes the chemical compositions of the ANL and Exxon spent stones as well as the Iowa gypsum.

Table G-1

CHEMICAL COMPOSITIONS OF SPENT STONE FROM ANL AND EXXON PRESSURIZED FLUID BED COMBUSTION PILOT PLANTS AND IOWA GROUND GYPSUM 114

Composition, %	ANL spent stone	Exxon spent stone	Gypsum 114
$CaSO_4$	57	26	74.0
$CaCO_3$	9	58	1.8
CaO	2	7.6	--
CaS	<0.05	<0.05	--
MgO	20	0.8	0.2
H_2O (combined)	--	--	19.0
Others	12	7.6	5.0

Leaching Tests

Procedures

A series of leaching experiments was designed to study leachate characteristics as functions of the varying parameters and procedures to induce leachates, as follows:

1. Mixing time - 250 ml of deionized water was mixed with 25 gm of waste stone in a 500 ml Erlenmeyer flask. The mixture was agitated for various lengths of time using an automatic shaker (Eberback) at 70 excursions per minute and room temperature. The supernatant resulting from this operation was passed through a Whatman No. 42 filter. The filtrate was used for determination of pH, specific

conductance, calcium, magnesium, sulfate, sulfide, and trace metal concentrations.

2. Stone load - 250 ml of deionized water was mixed with different amounts of spent stone and shaken for 24 hours. The supernatant was filtered and analyzed.
3. Mixing mode - shaking versus nonshaking: 250 ml of deionized water was mixed with 25 gm of waste stone. The mixture was allowed to sit for 24 hours at room temperature with and without shaking. The supernatant was filtered and analyzed.
4. Sample compaction - 25 gm of sample stone, either in its original size or ground to fine powder, was isostatically pressed at 68,950 to 344,750 kPa (10,000 to 50,000 psi) into pellet form and then immersed in 250 ml for 24 hours for nonshaking leaching time. The supernatant was filtered and analyzed.
5. Run-off tests - Deionized water was dripped at a constant rate onto 25 gm ANL waste stone which was packed manually in a cylindrical column of 11 mm (0.43 in) diameter and 213 mm (8.375 in) height. Successive 250 ml leachates were collected and monitored for pH, specific conductance, calcium, magnesium, and sulfate.

Results

Table G-2 summarizes the chemical characteristics (pH, specific conductance, calcium, magnesium, sulfate, sulfide, and trace metal concentrations) of leachates induced from the ANL waste stone under conditions corresponding to the severest cases and compares them with leachates from a natural gypsum and with water quality standards set by the Commonwealth of Pennsylvania,[9] the U. S. Public Health Service, and the World Health Organization.[10]

Table G-3 presents results from leaching tests on the ANL waste stone and Iowa gypsum No. 114 using the procedures described previously.

Table G-2

SUMMARY OF LEACHATE CHARACTERISTICS

Species[a]	Stone composition (%)		Leachates (mg/l)		Water standards (mg/l)		
	ANL waste stone	Iowa gypsum No. 114	ANL waste stone 50 gm/250 ml/24 hr	Iowa gypsum No. 114 50 gm/250 ml/24 hr	U. S. Public Health Service Drinking Water Standards[b]	World Health Organization Standards for Potable Water[b]	Commonwealth of Pennsylvania Water Quality Standards[c]
pH			12.1	7.4		7.0 to 8.5	6.0 to 8.5
Specific Conductance micromhos/cm			3850	2140			
$SO_4^=$	40	52	1280	1465	250	200	250
$S^=$	< 0.05						
$CO_3^=$	5.1	1.1					
Ca	22.5	22.2	744	607		75	
Mg	11.7	0.14	0.03	0.5		50	
Al	5	0.1	ND[d] < 0.1	ND < 0.1			
Ag	< 0.001	< 0.01	ND < 0.05	ND < 0.05	0.05		
B	0.03	< 0.03	0.03	< 0.3			
Bi	< 0.002	< 0.01	ND < 0.1	ND < 0.1			
Be		< 0.001	ND < 0.01	ND < 0.01	1.0		
Co		< 0.01	ND < 0.1	ND < 0.1			
Cr	0.005	< 0.01	ND < 0.1	ND < 0.1	1.0		
Cu	0.001	< 0.01	ND < 0.1	< 0.1	1.0	1.0	0.1
Fe	3	0.3	< 0.1	< 0.1	0.3	0.3	0.3
K	0.2	0.1	0.3	0.5			
Li	0.01	< 0.01	0.2	< 0.1			
Mn	0.05	< 0.01	ND < 0.05	< 0.05	0.05	0.1	1.0
Mo	0.002	< 0.01	ND < 0.03	ND < 0.1			
Na	0.1	0.1	6	0.5			
Ni	0.002	< 0.01	ND < 0.1	ND < 0.1	2.0		
Pb	< 0.01	< 0.03	ND < 0.1	ND < 0.2	0.05	0.1	
Sb	< 0.005		ND < 0.3				
Si	> 10	3	0.2	0.4			
Sn	< 0.005	< 0.01	ND < 0.1	ND < 0.1	1.0		
Ti	0.08	0.03	ND < 0.05	ND < 0.1			
V	0.002	< 0.01	ND < 0.05	ND < 0.05			
Zn	< 0.02	< 0.01	ND < 0.4	ND < 0.4	5.0	5.0	0.05
Zr	< 0.01	< 0.03	ND < 0.05	ND < 0.05			
Sr		0.1	0.3	1			

[a] All cations except Ca and Mg are determined by emission spectrochemical method, 1/3 to 3x estimates.

[b] Lund, H. F. Ed. Industrial Pollution Control Handbook. New York. McGraw-Hill Book Co. 1971.

[c] Pennsylvania Department of Environmental Resources. Water Quality Standards Summary. Harrisburg, Pennsylvania 17120. Document No. 42-006.

[d] ND - Not detected.

Table G-3

SUMMARY OF LEACHATE CHARACTERISTICS

Experimental parameters					Leachate results									
					ANL spent stone					Iowa gypsum No. 114				
Stone weight (gm)	H_2O volume (ml)	Mixing time (hr)	Shaking	Procedure (referred to text description)	pH	Specific conductance (micromho/cm)	Ca (mg/l)	Mg (mg/l)	SO_4 (mg/l)	pH	Specific conductance (micromho/cm)	Ca (mg/l)	Mg (mg/l)	SO_4 (mg/l)
1	250	24	Yes	2	11.2	1260	304	< 0.2	690	---	---	---	---	---
2.5	250	24	Yes	2	11.4	1590	397	< 0.2	883	---	---	---	---	---
5	250	24	Yes	2	---	---	---	---	---	7.4	2000	570	---	1380
10	250	24	Yes	2	11.8	2210	508	< 0.2	1048	7.4	2100	603	---	1450
25	250	24	Yes	2	11.9	3100	870	< 0.2	1725	7.4	2150	615	---	1470
50	250	24	Yes	2	12.1	3850	744	< 0.2	1280	7.4	2140	607	---	1465
25	250	1	Yes	1	11.8	1290	226	---	422	---	---	---	---	---
25	250	3	Yes	1	11.9	1810	326	---	576	---	---	---	---	---
25	250	6	Yes	1	11.9	1860	330	---	576	7.3	2040	590	---	1500
25	250	17	Yes	1	12.0	2280	456	---	865	---	---	---	---	---
25	250	24	Yes	1	11.9	3100	870	---	1725	7.4	2150	615	---	1470
25	250	48	Yes	1	11.9	3475	908	---	1840	7.4	2150	610	---	1470
25	250	96	Yes	1	11.9	3980	916	---	1830	7.4	2150	615	---	1470
25	250	24	Yes	3	11.9	3100	870	---	1725	7.4	2150	615	---	1470
25	250	24	No	3	12.1	1940	306	---	480	7.3	1910	530	---	1270
25[a]	250	24	No	4	11.9	2300	---	---	---	---	---	---	---	---
25	250	1st run-off	Rate 5 ml/min	5	11.8	2180	305	---	1055	---	---	---	---	---
---	250	2nd run-off	5 ml/min	5	11.5	1960	491	---	1130	---	---	---	---	---
---	250	3rd run-off	5 ml/min	5	11.3	1920	510	---	1240	---	---	---	---	---
---	250	4th run-off	5 ml/min	5	11.3	1980	545	---	1240	---	---	---	---	---
---	250	5th run-off	5 ml/min	5	11.2	1870	500	---	1130	---	---	---	---	---
---	250	6th run-off	5 ml/min	5	11.2	1780	483	---	1110	---	---	---	---	---
---	250	7th run-off	5 ml/min	5	11.2	1760	463	---	1110	---	---	---	---	---
---	250	8th run-off	5 ml/min	5	10.6	1640	460	---	1055	---	---	---	---	---
25	50	1st run-off	0.24 ml/min	5	---	---	---	---	---	7.4	2250	620	---	1490
---	50	2nd run-off	0.24 ml/min	5	---	---	---	---	---	7.1	2160	615	---	1440

[a] Pellet pressed at 10,000 psi.

Calcium and sulfate concentration, pH, and specific conductance of the leachates were shown as functions of batch mixing time, between 1 and 96 hours, in Figure G-1. Leaching Procedure 1 was used for inducing the leachates. In Figure G-2 calcium, sulfate, pH, and specific conductance were plotted as functions of stone loading from 1 to 50 gm of sample stone in 250 ml deionized water using Procedure 2. Characteristics of leachates from a natural gypsum induced under identical conditions are also shown in Figures G-1 and G-2 for comparison. A shaking versus non-shaking mode of leaching was studied using Procedure 3 and results summarized in Table G-3. Procedure 4 was used in an attempt to compact sample stone into dense pellets so that water permeability might be reduced, but the pellets crumbled on contact with water and resulted in leachates similar to those from the unpressed samples. Finally, a run-off test was carried out on ANL waste stone using Procedure 5. Figure G-3 shows the calcium concentration, sulfate, pH, and specific conductance for successive 250 ml leachates collected. Such data would be useful in cases where stone washing before disposal or leachate treatment was needed.

Conclusions

Results from leaching tests on ANL spent stone from the pressurized fluid bed combustion process indicated that:

- In both the leaching-time experiment (Figure G-1) and the stone-loading experiment (Figure G-2), calcium and sulfate dissolution plateaued at concentrations limited by the calcium sulfate solubility.
- The equilibrium calcium and sulfate concentrations were high, exceeding the water quality criteria. Since calcium sulfate occurs abundantly in nature as gypsum, leachates induced from a natural gypsum offers a good reference for its calcium and sulfate concentrations. Iowa ground gypsum No. 114 was selected to undergo parallel leaching tests with the ANL waste stone. Results

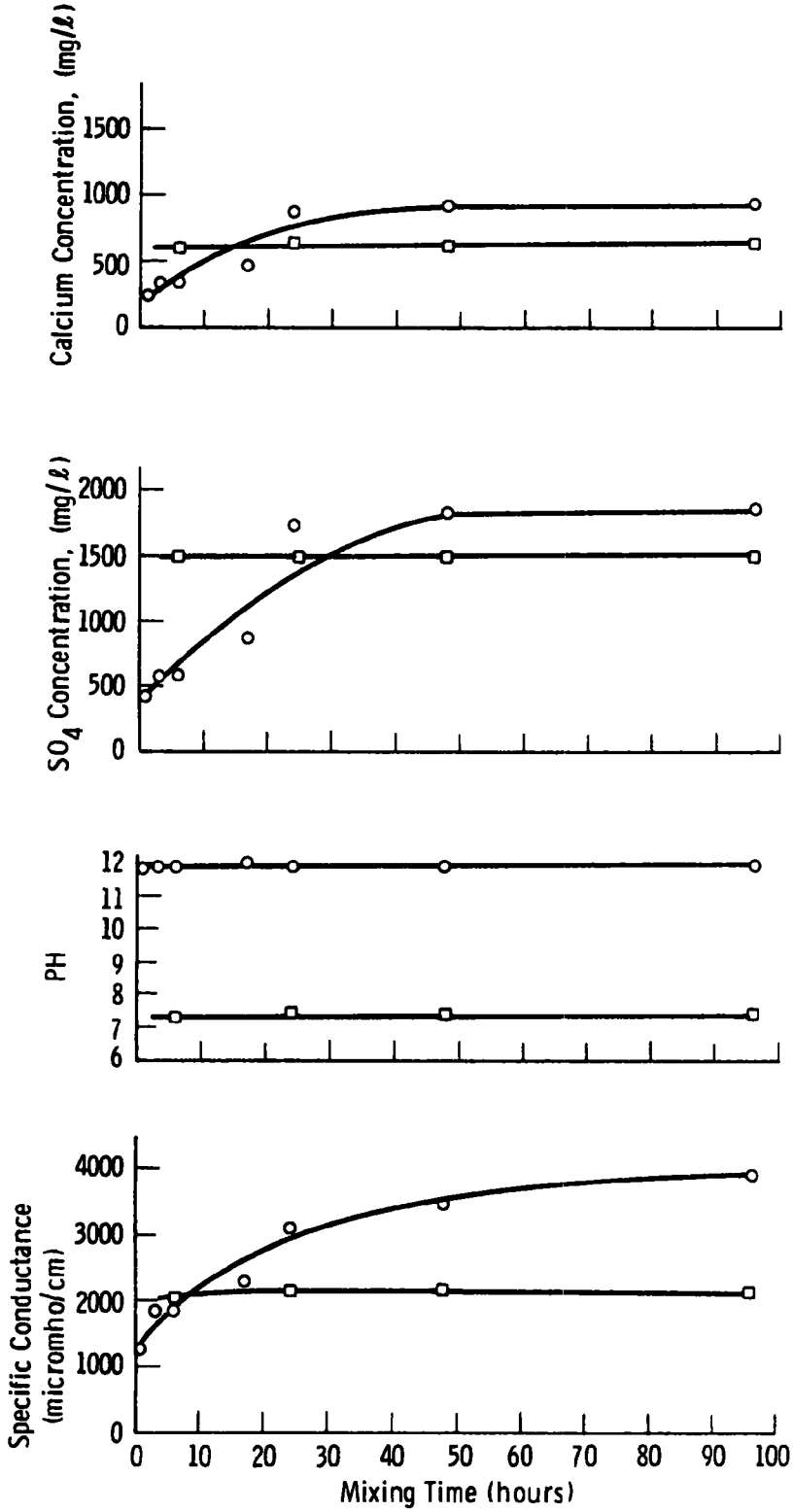

Figure G-1—Leachate characteristics as functions of batch mixing time for
- o Argonne spent stone
- □ Iowa gypsum #114

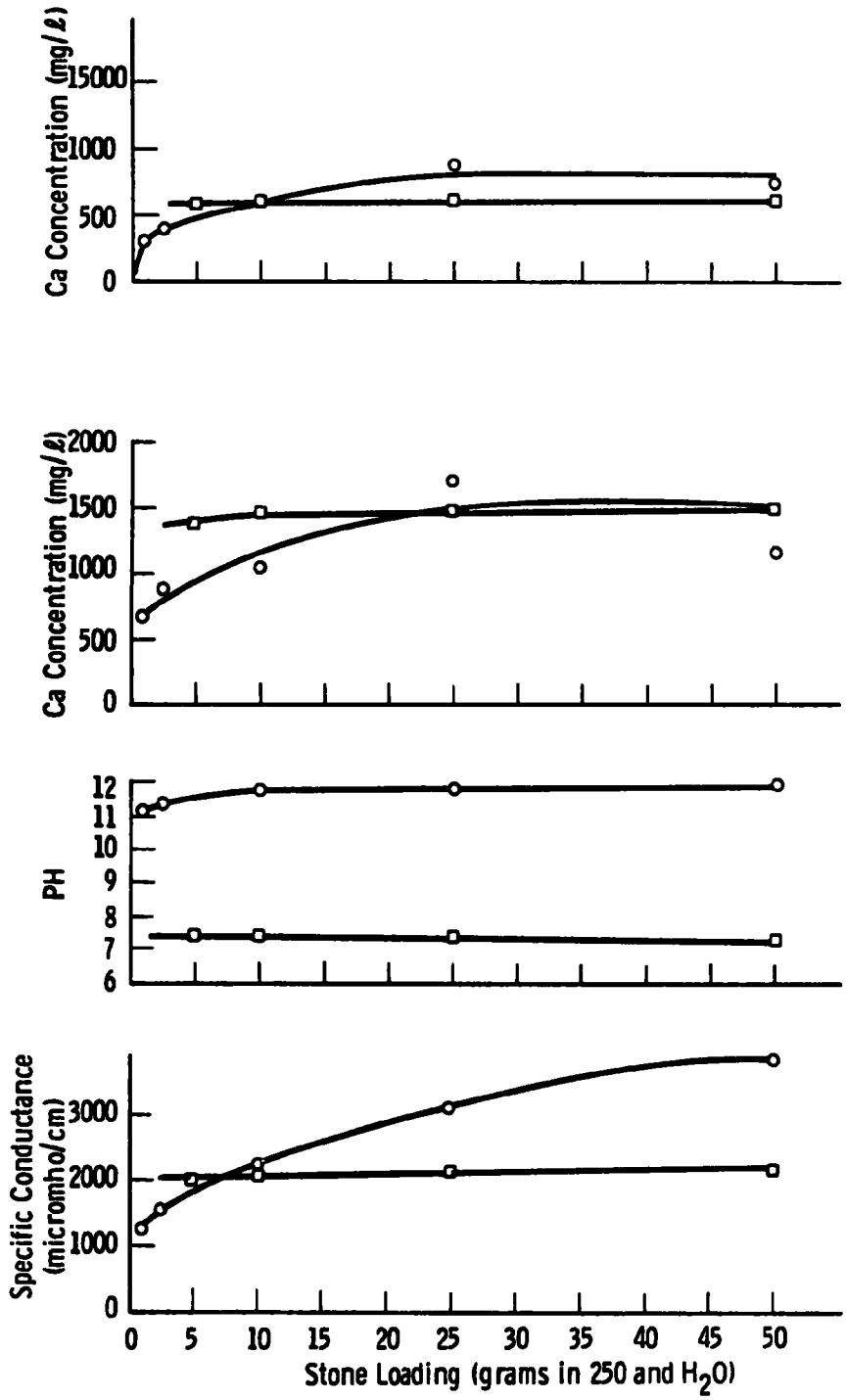

Figure G-2—Leachate characteristics as functions of stone loading for
- o Argonne spent stone
- □ Iowa gypsum #114

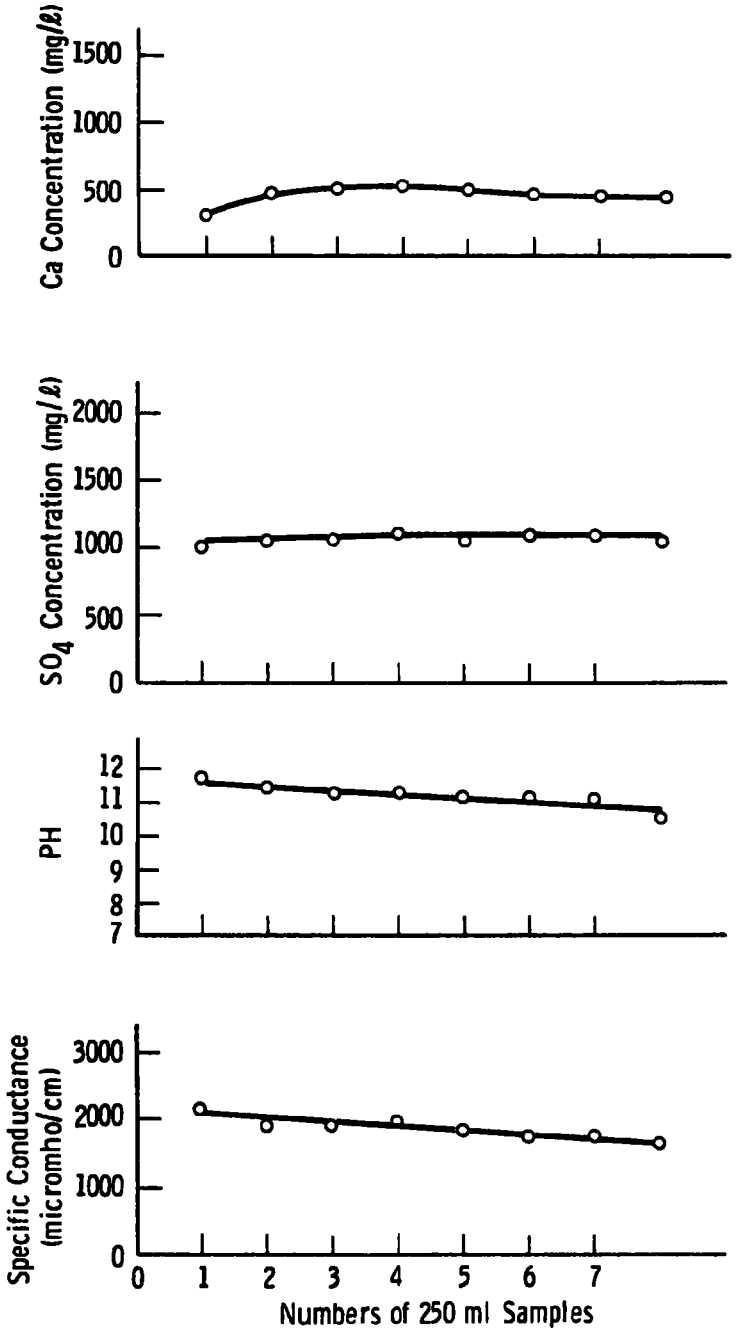

Figure G-3—Leachate characteristics of the Argonne spent stone leachates induced by the run-off tests

indicated that gypsum leachates contained approximately the same amounts of dissolved calcium and sulfate ions as the ANL leachates. Both agreed relatively well with the calcium sulfate solubility,and both exceeded the water quality standards, 75 mg/l for calcium and 250 mg/l for sulfate.

- There was negligible dissolution of magnesium ions.
- Insignificant amounts of heavy metal ions were found in the leachates.
- ANL leachates were alkaline, with pH = 10.6 to 12.1. It is interesting to note, however, that the run-off leachates showed a gradual decrease in pH with the amount of leachates passing through.

Results from the leaching experiments on ANL spent stone agreed well with those reported by the British Coal Utilization Research Association (BCURA)[11] and Pope, Evans and Robbins (PER)[12] in that the leachates had high pH, calcium, and sulfate, and negligible magnesium ions. The difference between the PER and BCURA findings in the extent of calcium and sulfate extraction was, in the light of the Westinghouse stone-loading and mixing-time studies, largely due to the difference in the stone-to-water ratio and the leaching time of their experiments. The Westinghouse results also indicated that it is unlikely that the heavy metal ions in the leachates from pressurized fluid bed combustion processes will cause water pollution. The solutions were alkaline, but the run-off tests showed a gradual decrease in pH with the amount of water passing through. Superficially, the calcium and sulfate concentrations in the leachates might suggest the possibility of a water pollution hazard from these ions, but it must be emphasized that the conditions in these experiments were much more extreme than those that would exist in actual cases, where water percolation is minimized. The fact that equally high calcium sulfate dissolution was found in gypsum leachates under identical conditions offers a useful comparison. Further tests using much larger quantities of material and taking into consideration geocriteria such as topography, geology, hydrology, and soil conditions

of the actual landfill site are needed to determine fully the environmental impact of spent stone disposal.

Activity Test

Heat release experiments were carried out on the following samples to determine their reactivity toward water:

1. Spent sorbent from ANL pressurized fluidized bed combustion process of run C2/C3[7]—sulfated Tymochtee dolomite, -14 mesh
2. Tymochtee dolomite, -16 +18 mesh
3. Spent sorbent from Exxon pressurized fluidized bed combustion process of run No. 8.4[8]—sulfated limestone 1359, -8 +80 mesh
4. Limestone 1359, -16 +18 mesh
5. Limestone 1359, -18 +35 mesh
6. Calcined limestone 1359 at 960°C (1760°F) -18 +35 mesh.

In each of the above tests, 3 gm of stone was added to 20 ml of deionized water in a Dewar flask which had been thermally equilibrated. Iron-constantan thermoccuples were used to monitor the temperature rise in the stone/water system with an Omega cold junction compensator and a digital voltmeter readout. Table G-4 summarizes the maximum temperature rise and time required for reaching the temperature. Less than 0.2°C (0.36°F) temperature rise was found for the above samples 1 to 5 but a temperature rise of 55°C (99°F) was found for sample 6. The great contrast between the calcined limestone and the other samples indicated the validity of the experiment as well as the lack of reactivity of the ANL and Exxon spent stones with water. Although it can be safely assumed that no heat pollution will result if these particular batches of spent stone are subjected to rainfall after disposal, it must be pointed out that the activity and heat release properties of the spent sorbent are functions of the operating conditions of the fluid bed combustion process.

Table G-4

SUMMARY OF STONE ACTIVITY TESTS

Samples	Stone/H_2O	ΔT_{max}, °C (°F)	t_{max}
ANL spent stone -14 mesh	3 gm/20 ml	0.1 (0.18)	--
Tymochtee Dolomite -16 +18 mesh	3 gm/20 ml	0.1 (0.18)	--
Exxon Spent Stone -8 +80 mesh	3 gm/20 ml	0.2 (0.36)	5 sec
Limestone 1359 -16 +18 mesh	3 gm/20 ml	0.1 (0.18)	--
Limestone 1359 -18 +35 mesh	3 gm/20 ml	0.1 (0.18)	--
Calcined Limestone 1359 -18 +35 mesh	3 gm/20 ml	55 (99)	4 to 20 sec

CONCLUSIONS AND RECOMMENDATIONS

The pressurized fluid bed combustion process results in the production of spent solids in the form of partially sulfated limestone or dolomite. The long-term stability and the suitability for its disposal into the environment have been discussed. Laboratory leaching and activity tests have been initiated. Preliminary results indicate that it would probably not cause water and heat pollution. It must be remembered, however, that the physical and chemical properties of the spent sorbent are functions of the operating conditions of the pressurized fluid bed process and that the physical characteristics of the specific disposal site must be judged individually in evaluating the leaching properties of the spent stone.

To assess fully the environmental impact of spent sorbent, further tests on stone analyses, leaching properties, heat release properties, landfill properties, and air emission should be performed.

REFERENCES

1. Keairns, D. L., et al. Evaluation of the Fluidized Bed Combustion Process. Vol. IV. Office of Research and Development. Environmental Protection Agency. Westinghouse Research Laboratories. Pittsburgh, Pa. EPA-650/2-3-73-048d. Contract 68-02-0217. NTIS PB 233 101/15. December 1973. 322 pages.
2. Standen, A., ed. Kirk-Othmer Encyclopedia of Chemical Technology John Wiley & Sons, Inc. New York 1967.
3. Boynton, R. S. Chemistry and Technology of Lime and Limestone John Wiley and Sons, Inc. New York. 1966.
4. Emrich, G. H. "Guidelines for Sanitary Landfills -- Ground Water and Percolation. Compost Science. May, 1972. pp. 12-15.
5. Emrich, G. H., Merrit, G. L., and Rhindress, R. D. Geocriteria for Solid Waste Disposal Sites (Program for the 5th Annual Meeting, Northeastern Section, Geological Society of America) 2(1), 1970, p. 17.
6. Phillips, N. P. and Wells, R.M. Solid Waste Disposal. Environmental Protection Agency. Radian Corporation EPA-650/2-74-003, May 1974.
7. Argonne National Laboratory. Monthly Progress Reports Nos. 70 and 71 ANL-ES/CEM-FO-70 and 71. August and September, 1974.
8. Exxon Research and Engineering Company. Monthly Progress Report No. 57, Environmental Protection Agency. Contracts 68-02-1451 and 68-02-1312. November 1974.
9. Pennsylvania Department of Environmental Resources. Water Quality Standards Summary. Harrisburg, Pennsylvania, 17120. Document No. 42-006.
10. Lund, H. F., ed. Industrial Pollution Control Handbook McGraw-Hill Book Company. New York. 1971.
11. Pressurized Fluidized Bed Combustion. Office of Coal Research. National Research and Development Corporation. Contract No. 14-32-0001-1511. November 1973.
12. Pope Evans and Robbins, Inc. Multicell Fluidized-Bed Boiler Design Construction and Test Program. Interim Report No. 1. Report PER-570-74. Contract No. 14-32-0001-1237. August 1974.

APPENDIX H

TRACE EMISSIONS AFFECTING GAS-TURBINE PERFORMANCE

APPENDIX H
TRACE EMISSIONS AFFECTING GAS-TURBINE PERFORMANCE

SUMMARY

Sodium and potassium compounds are potentially hazardous to the operation of the gas turbine. Chlorides and hydroxides are volatile species and can transport sodium and potassium from the combustor to the turbine. At hydrogen chloride (HCl) levels exceeding 0.4 ppm by volume in the combustor gas, solid or liquid sodium sulfate (Na_2SO_4) will convert to gaseous sodium chloride (NaCl). The hydrogen chloride level in the combustion gas resulting from the complete release of chlorine from a low-chlorine coal (100 ppm Cl) exceeds this level by over a factor of ten and is 5 ppm. In a fluid bed combustion process the predominant transport should be by the chlorides.

In the gas turbine, reactions between the chloride and the sulfur oxides in the combustion gas will form liquid sulfate-chloride melts on the turbine hardware if the sodium and potassium levels are sufficiently high. These melts must be prevented because they initiate hot-corrosion and deposit formation. Hydrogen chloride in the turbine acts to prevent sulfate deposits from forming or, once formed, acts to remove them. A hydrogen chloride level of 40 ppm by volume in the combustion gas is sufficient to prevent a liquid sodium sulfate melt from being stable at sodium concentrations in the gas up to 0.2 ppm by volume. (Forty ppm hydrogen chloride corresponds to complete release of chlorine from coal containing 800 ppm by weight of chlorine; 0.2 ppm of sodium corresponds to a one percent release of sodium from a coal containing 130 ppm by weight of sodium.) The concentration both of hydrogen chloride and of sulfur oxides (SO_2 and SO_3) have a strong influence on the stability of the melt. If the sulfur dioxide level in the gas is dropped from 200 ppm to 100 ppm by volume, the concentration of hydrogen chloride

required to prevent deposition of a liquid sodium sulfate film would drop to about 25 ppm by volume. Three additional factors must be understood before it will be possible to define the sodium and potassium tolerances which will prevent hot corrosion attack in the turbine. These are:

- The influence of the interaction between sodium and potassium to form complex melts on the hardware. In such melts the activities of the sodium and potassium are reduced,and the equilibrium concentrations of sodium and potassium species that can exist in gas above the melt are also lowered. Interaction tends to reduce the tolerable concentrations of sodium and potassium in the turbine expansion gas. Westinghouse is working to establish the magnitude of this effect and also to establish the influence of the relative sodium and potassium levels on the composition and melting point of stable deposits.
- The ability of turbine stator vane and rotor blade alloys to withstand a combustion gas containing up to 200 ppm sulfur dioxide and up to 40 ppm hydrogen chloride. Careful experimental studies are needed.
- The shifts in the turbine tolerance which will occur if equilibrium levels of sulfur trioxide are not achieved and the degree to which kinetic factors such as these influence the tolerable concentration of sodium and potassium chlorides.

In the combustor itself a competition takes place for the sodium and the potassium. Hydrogen chloride attacks the sodium and potassium compounds attempting to form the volatile chlorides. On the other hand, in the burning char particle, silica reacts with sodium to form stable silicates. Unfortunately, potassium silicates are not stable, and potassium clay mineral compounds are breaking down and converting to either polysulfides or chlorides, depending on the composition of the local atmosphere. In the oxidizing atmospheres outside of combusting particles,

the sulfates are stable at low levels of hydrogen chloride; but at levels above 0.4 ppm, reconversion of condensed sulfates to chlorides will occur. Westinghouse is attempting to establish the feasibility of controlling the alkali-metal content of the gas through:

- Control of the level of hydrogen chloride in the combustor. Reducing hydrogen chloride levels in the combustor below 0.4 ppm by volume would lower the sodium chloride content of the transport gas by slowing or preventing attack of ash minerals and by promoting conversion to low-volatility condensed sulfate.
- Conversion of high-volatility sodium and potassium chlorides (KCl) in coal and dolomites to sulfates or silicates, with simultaneous removal of hydrogen chloride by low-temperature pretreating in the coal and stone dryers and preheaters.

Experimental measurement of the actual release of alkali that can be translated to gas compositions projections for power plants are needed. Because release fractions near one percent are anticipated, measurements of the material released are required for accuracy.

TRACE EMISSIONS

Trace emissions from the fluid bed combustion process are important from two standpoints:

- Their effect upon the environment
- Their effect on the operability of the power plant.

The primary environmental concern is with the toxic effects of the compounds of beryllium, mercury, fluorine, lead; cadmium, arsenic, nickel; copper, zinc, barium, tin, phosphorous, lithium, vanadium, manganese, chromium, and selenium.

From the standpoint of preventing hot corrosion of turbine alloys, growth of deposits within the turbine, and corrosion and heat transfer problems in heat recovery boilers, Westinghouse is concerned with the

compounds of sodium, potassium, lead, vanadium, calcium, and magnesium. The latter are of concern primarily as particulates that can contribute to deposition problems.

Argonne National Laboratory (ANL)[1] working in conjunction with the Office of Coal Research (OCR), has been studying the release during fluid bed combustion of those trace contaminants dangerous to the environment. The Illinois Geological Survey[2] has continued and expanded its extensive work on the mineralogy of coals and the distribution of trace elements in coal. Westinghouse under this contract with OCR[3] has been concerned primarily with the release of contaminants potentially dangerous to the operability of power plants. Other work has been directed initially to sodium and potassium release since these are considered the most hazardous. Vanadium release is potentially dangerous, and the experimentation measuring release studies the composition of deposits to detect all components transported in the combustion gas.

The Turbine-Corrosion/Deposition Problem

The components of gas turbines exposed to the hot gas stream are made of materials that form oxide scales to protect themselves from oxidation. High-strength nickel-based superalloys such as Inconel 738 or Incolloy 700, are used for the highly stressed rotating components. More oxidation-resistant, but lower-strength, cobalt-based alloys, such as X-45 or MAR M509, are used for the stationary components. Air cooling is used to maintain metal temperatures lower than 899°C (1650°F) so that the alloys retain sufficient mechanical strengths. Inlet gas temperatures over 1093°C (2000°F) are currently used.

Metal recession rates due to oxidation alone are of the order of 0.10 mm (0.004 in) per year on the hottest components of current Westinghouse turbines. In the presence of alkali-metal compounds, which react with sulfur dioxide and sulfur trioxide from the combusted fuel gas, liquid films of sulfate and sulfate-chloride mixtures can be deposited on the turbine hardware. Figure H-1[3] shows the temperatures at which liquid deposits form in the sodium-potassium-sulfur-oxygen-chlorine (Na-K-S-O-Cl) system. The figure shows that liquid films are possible

Curve 652781-A

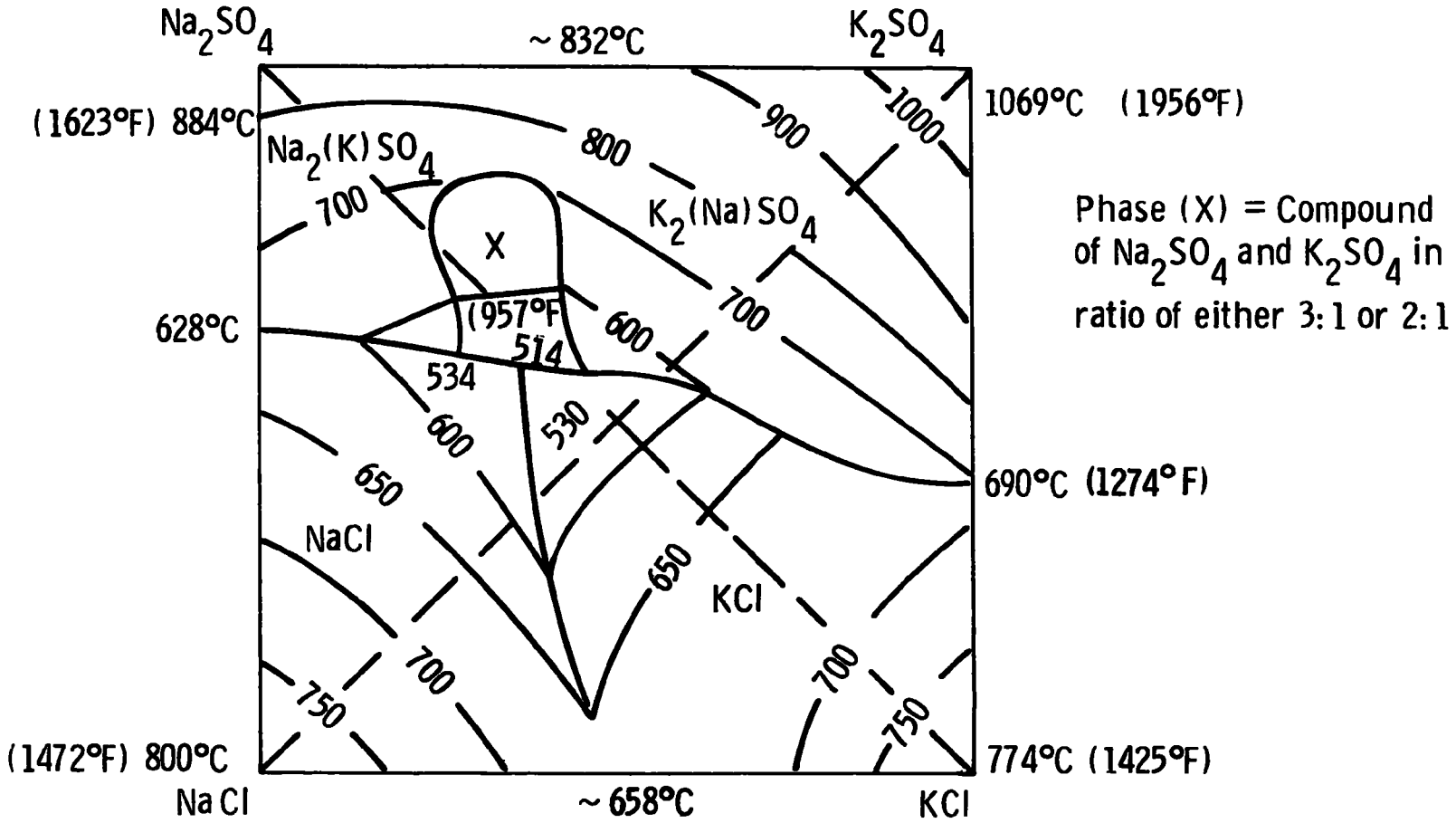

Figure H -1—Projection of liquidus surface of Na_2SO_4—K_2SO_4—KCl—NaCl system showing temperature contours (after E. K. Akopov and A. G. Bergman).[3]

over the temperature range of 1069 to 514°C (1956 to 957°F), which coincides with the range of temperatures encountered in the turbine flow path. (Gases are exhausted from turbines at about 400°C [752°F].)

Molten alkali-metal compound films are dangerous because under some conditions they attack the protective oxide scale, allowing accelerated or catastrophic oxidation (hot corrosion) of the turbine components. The films can also accumulate particulates that allow the build-up of thick deposits on the metal surfaces. Aerodynamic performance of the turbine can be seriously impaired.

Alkali-Metal Components in Coals and Dolomites

Sodium and potassium exist in similar chemical form in coal and in dolomite, as clay minerals (primarily illite and montmorillonite which contain both elements) and as sodium and potassium chlorides in saline ground water filling pores or cracks in coal and rock beds. The proportions of different mineral constituents in coal vary from one site to another. The degree of saline water entrainment and the resulting sodium chloride content of coal and rock depend on the porosity and crack structure of the material and on the depth from which it is mined. The salinity of the ground water increases with depth. As a rule, strip-mined coal and rock will, therefore, have a lower content of sodium chloride than deep-mined material. The high volatility of sodium chloride makes it likely that coal and rock containing entrained saline water will release sodium (as the chloride) to the coal gases. Volatilities of mineral-type alkali compounds are low, lower than those of sodium sulfate. From the point of view of alkali-release, reactions of alkali-containing clay minerals at coal gasification temperatures[4,5] are important. When illite, the principle clay mineral contaminant, is heated in air, dehydration occurs below 600°C (1112°F) and dehydroxylation is complete at about 800°C (1472°F).[6,7] The illite anhydride structure formed by these processes begins to decompose at 850°C (1562°F), forming a spinel-type crystal phase if the illite is not associated with kaolinite. The amount of spinel phase increases with firing temperature

to 1200°C (2192°F) and then disappears gradually above this temperature. This behavior is attributed to the presence of iron and magnesium and to a slightly lowered aluminum content in the unassociated (pure) illite aluminosilicate structure. Mullite ($3\ Al_2O_3 \cdot 2\ SiO_2$) appears as a crystal phase only above 1100°C (2012°F). If the illite is associated with kaolinite (illite fire-clays), mullite begins to crystallize between 900 and 950°C (1652 and 1742°F). Amorphous glassy phases also form. The formation of mullite below 1000°C (1832°F) is attributed to the potassium and other alkali and alkali-earth cations present in the illite structure. The potassium ions are thought to move in to prop the structure open and prevent the reformation of broken silicon-oxygen bonds.

The glasses that form at the highest temperatures should be resistant to attack by hydrogen chloride and retain alkali-metal compounds in the ash.

Factors Affecting Release of Alkali-Metal Compounds to the Expansion Gas

In order to estimate the extent of alkali release from mineral constituents, it is assumed that the glassy phase can be approximated by sodium disilicate ($Na_2Si_2O_5$). This represents a composition in the sodium oxide-silicon dioxide (Na_2O-SiO_2) system which is stable in the presence of an excess of silica, a condition which is typical for coal ash minerals.

During combustion of char in a dolomite/char/ash or limestone/char/ash fluidized bed with an average temperature (and exit gas temperature) of 871°C (1600°F), the temperature of individual burning char particles will exceed the bed temperature by several hundreds of degrees.

As combustion of char particles proceeds, the surface zones of these particles convert to a fine powder of mineral matter and residual carbon which is carried away with the gas stream. This picture is valid for temperatures below the fusion temperature of the ash.

Figure H-2 is a thermochemical phase diagram for the sodium-silicon-oxygen-sulfur system at 1093°C (2000°F). The different scales show interrelated chemical potentials for oxygen and sulfur. Slanted,

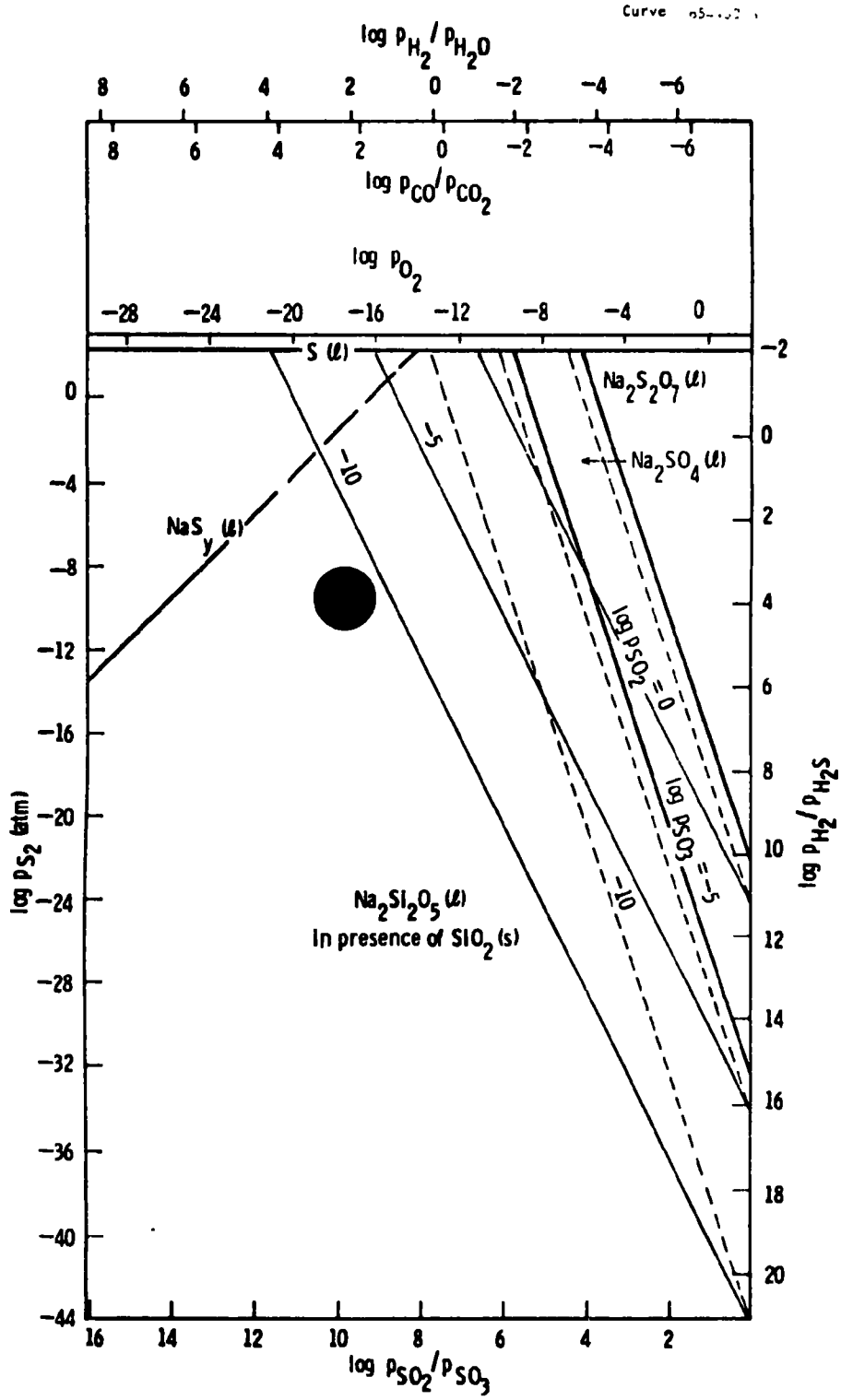

Figure H-2—Thermochemical equilibria in the sodium-silicon-oxygen-sulfur system at 1093°C (2000°F). Filled circle indicates local chemistry at surface of char particle.

thin, solid or broken lines show equilibrium sulfur dioxide and sulfur trioxide pressures. These lines, and the information contained in the different scales, allow immediate definition of the most important gas-pnase components at any point of the diagram. Heavy, solid, and broken lines separate the regions of stability of condensed phases in the system. The large filled circle indicates the estimated chemistry at the surface of a burning char particle. The position of this circle in the diagram corresponds to local equilibrium at a carbon/gas interface. It takes into account a counterflow mass balance in a boundary diffusion layer where oxygen, carbon dioxide, and water vapor move towards the particle to form carbon monoxide and hydrogen at the proper pressures and pressure ratios, and where the latter reaction products diffuse away from the char particle before reacting any further. As shown in the diagram, the filled circle falls in the liquid sodium disilicate field. Thermochemical calculations show that the most important gaseous sodium species that will be released from liquid sodium disilicate in this environment are gaseous sodium hydroxide and sodium chloride. The equilibrium gaseous sodium hydroxide pressure for the reaction

$$Na_2Si_2O_5(\ell) + H_2O(g) \rightleftarrows 2\ NaOH(g) + 2\ SiO_2(s)$$

at relevant water vapor pressure is $\sim 10^{-6.4}$, $\log P_{NaOH} \approx -6.4$. This corresponds to a concentration of 40 ppb by volume. The formation of silica as a reaction product may separate the silicate phase from the gaseous environment. This would tend to slow down the continued reaction and,thus, the release of sodium from the silicates. Gaseous hydrogen chloride can react with liquid sodium disilicate to form gaseous sodium chloride volatile species. The reaction is:

$$Na_2Si_2O_5(\ell) + 2\ HCl(g) \rightarrow 2\ NaCl(g) + 2\ SiO_2(s) + H_2O(g).$$

It is thermochemically strongly favored even at trace levels of gaseous hydrogen chloride and becomes more important as the level increases. The

formation of solid silicon dioxide reaction product may again be an important factor in limiting the extent and rate of this reaction.

As the volatile alkali compounds or species reach the outside of the diffusion layer and enter the main gas stream, and as fine particles are carried in that gas stream, further opportunities for particle/gas interactions occur. Figure H-3 shows a thermochemical phase diagram for the sodium-silicon-oxygen-sulfur system at 871°C (1600°F). The filled circle represents the approximate chemistry of the gas stream that leaves the boiler. The circle is in the sodium sulfate field. Consequently, liquid sodium disilicate from mineral matter is unstable and reacts to form silicon oxides and either sodium sulfate or gaseous sodium compounds or species, if sufficiently volatile and thermochemically favored. For the calculations of alkali reactions under these conditions, which also are valid for gas entering the gas turbine, the boiler gas composition is assumed to be 74 mole % nitrogen, 15 mole % carbon dioxide, 2 mole % oxygen, 9 mole % water, and 1.7×10^{-2} mole % sulfur dioxide/sulfur trioxide. The volatility of sodium sulfate is low, or $\log P_{Na_2SO_4} \sim -7.7$, (see Figure H-4). Figure H-5 shows the equilibrium pressures of gaseous sodium hydroxide and gaseous sodium chloride over solid sodium sulfate under boiler conditions. The figure shows that the reaction of solid sodium sulfate to form volatile gaseous sodium hydroxide is not important, the vapor pressure of sodium sulfate exceeding the equilibrium pressure of gaseous sodium. The critical level of hydrogen chloride above which the driving force for release of sodium by hydrogen chloride attack exceeds the driving force for sodium release by sulfate vaporization is $\log P_{HCl} \sim -5.4$ or $P_{HCl} = 4.05 \times 10^{-4}$ kPa (4×10^{-6} atm). This corresponds to a gaseous hydrogen chloride level of 400 ppb by volume.

Although in gas- or oil-fired gas turbines sodium is the predominant alkali contaminant, coal and dolomite contain both sodium and potassium. Thermochemical equilibrium calculations have been made for several systems containing potassium. Figures H-6 and H-7 show thermochemical diagrams for the potassium-oxygen-sulfur-carbon and potassium-silicon-oxygen-sulfur systems at 1093°C (2000°F), representing the conditions inside or in the diffusion layer around a burning char

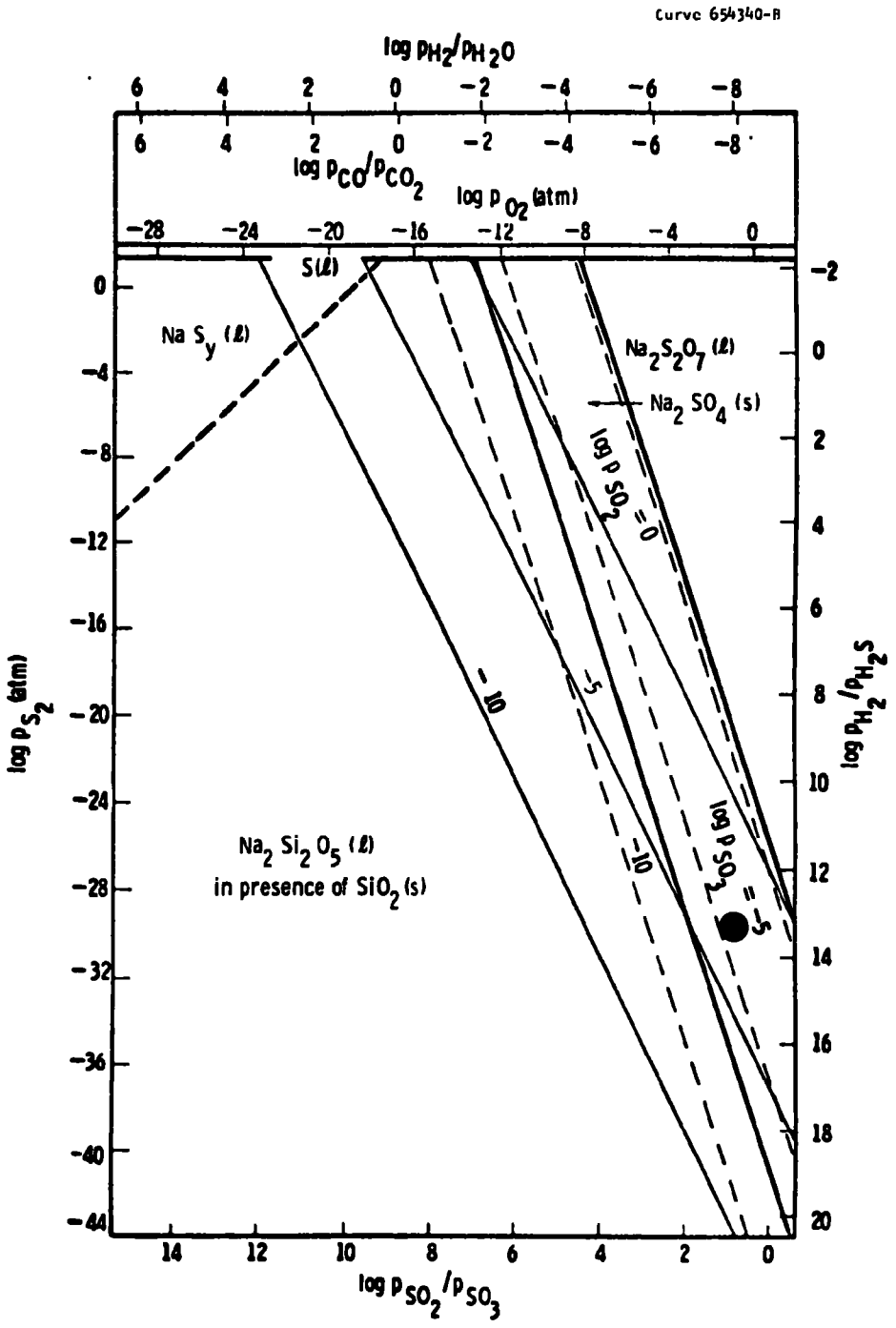

Figure H-3 –Thermochemical equilibria in the sodium-silicon-oxygen-sulfur system at 871°C (1600°F). Filled large circle indicates chemistry of gas phase at exit end of fluidized bed boiler

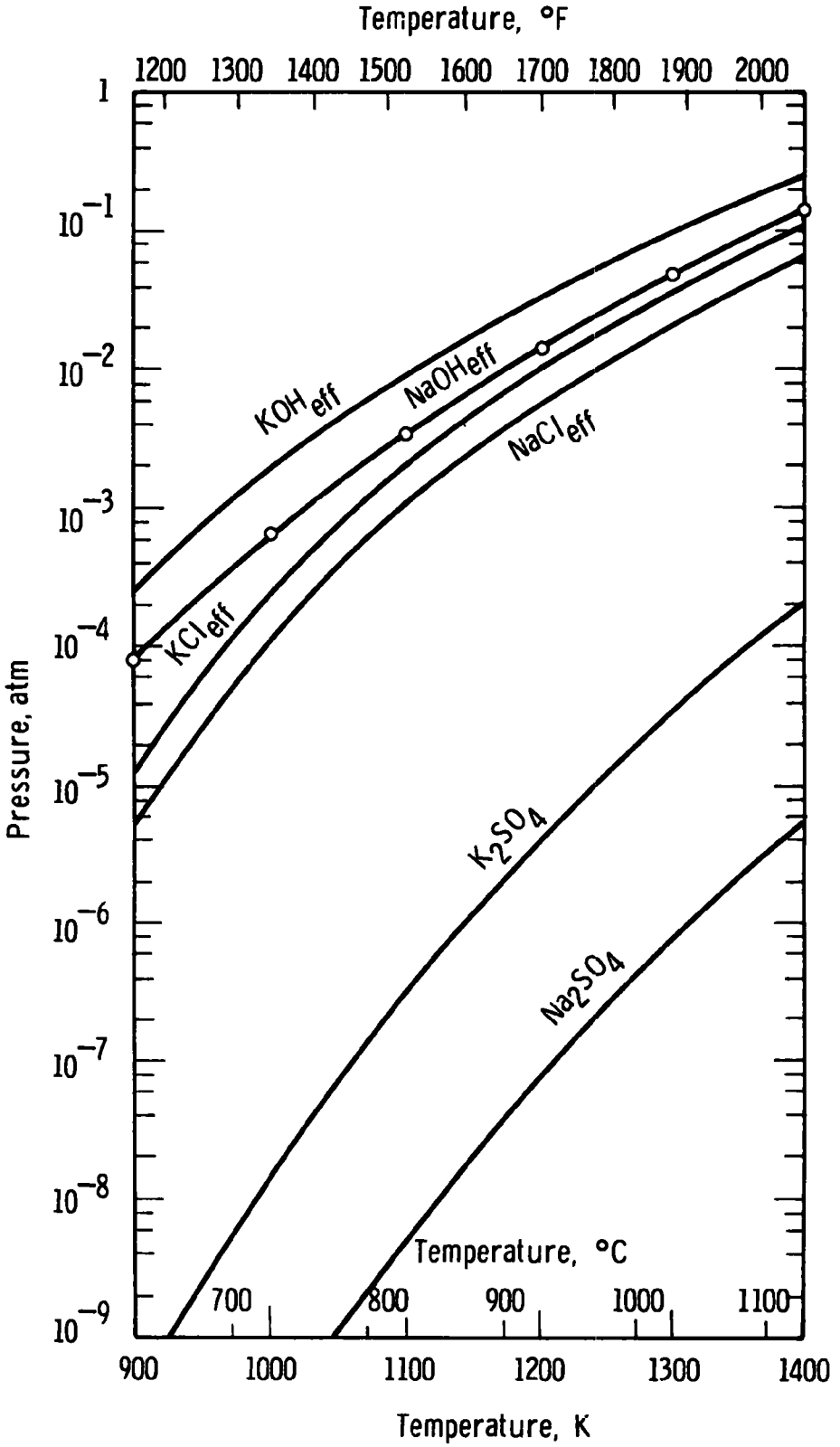

Figure H-4—Vapor pressures of NaOH, KOH, NaCl, KCl, Na_2SO_4 and K_2SO_4. $NaOH_{eff}$, KOH_{eff}, etc., are effective equilibrium pressures which represent the sums of the pressures of monomer and (twice the) dimer species.

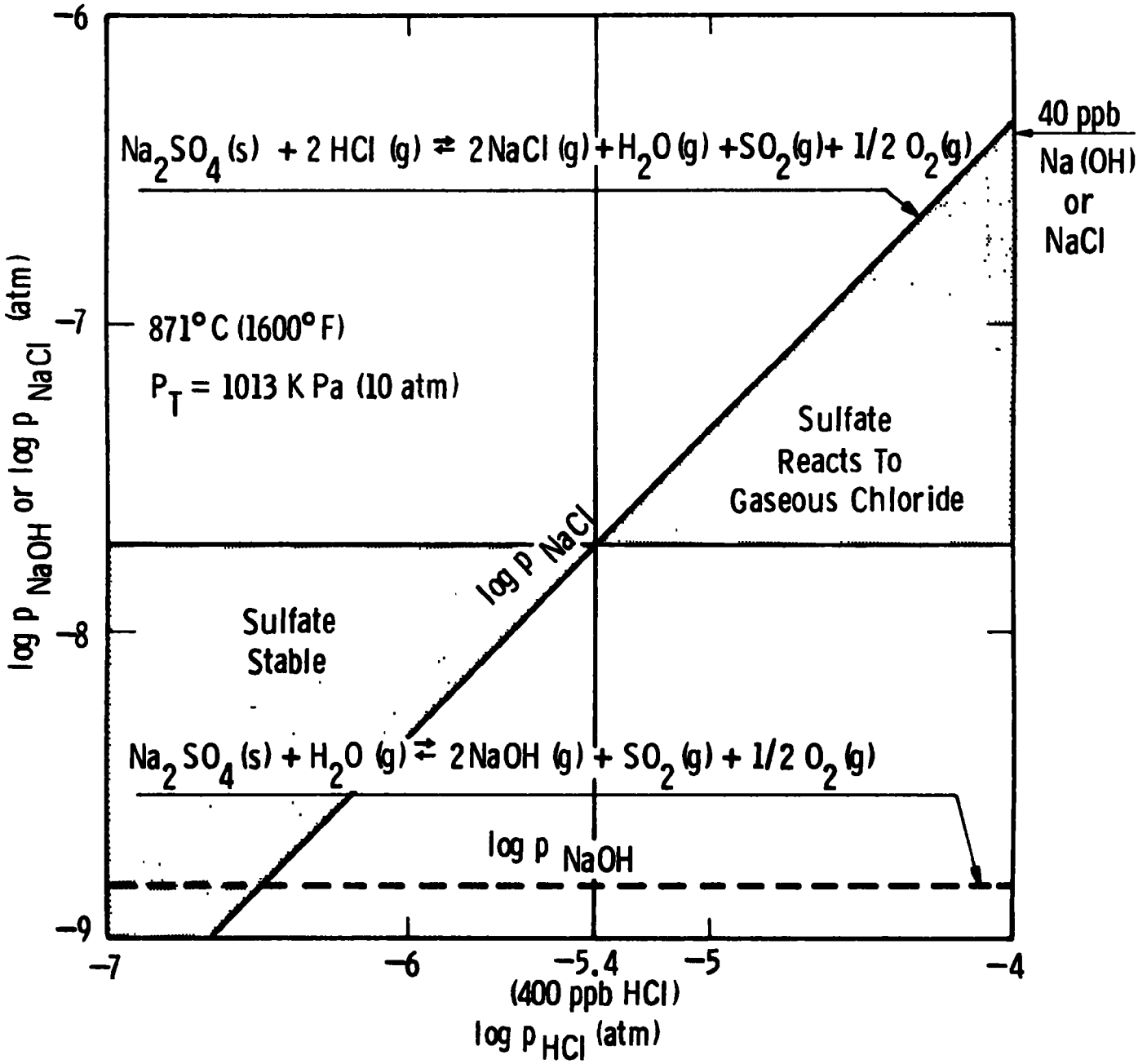

Figure H-5—Equilibrium pressures of NaOH (g) and NaCl (g) over Na_2SO_4 (s) exposed to steam and HCl (g) under fluidized bed boiler gas phase conditions

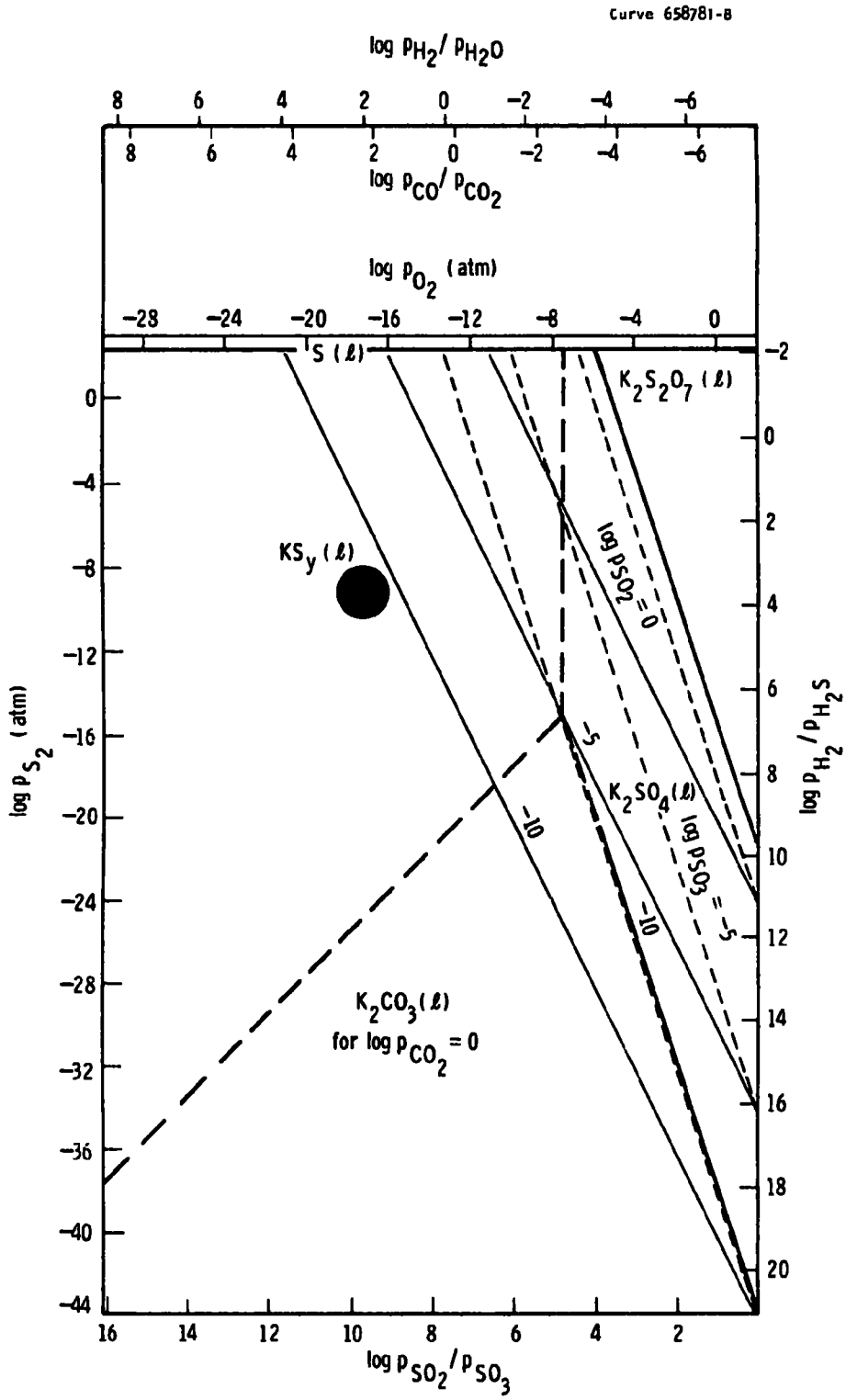

Figure H-6 – Thermochemical equilibria in the potassium-oxygen-sulfur-carbon system at 1093° C (2000° F). Filled circle indicates local chemistry at surface of char particle.

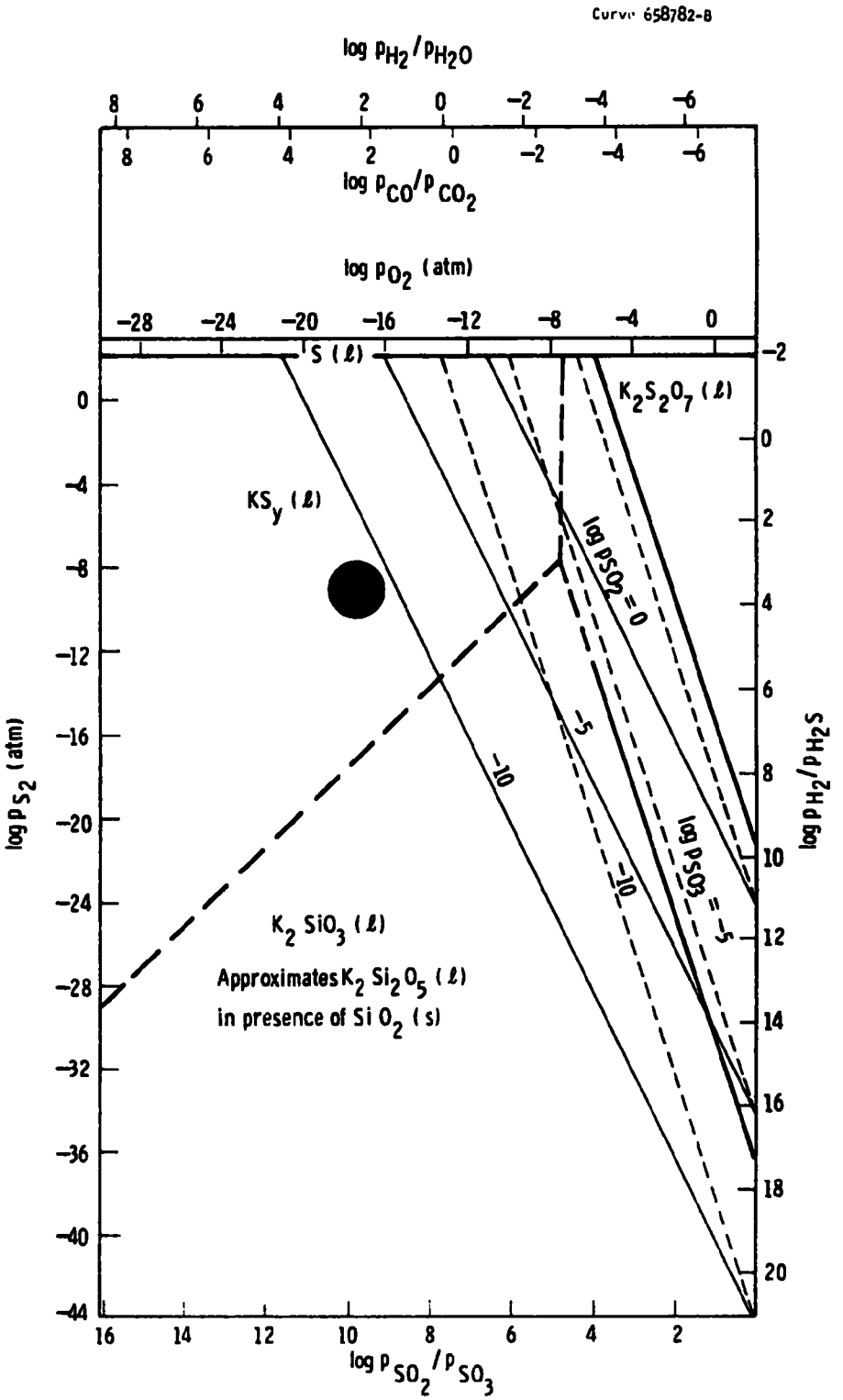

Figure H-7—K—O—Si—C—S system at 1093°C (2000°F)

particle. The large filled circles show the estimated chemical composition of the gas phase at the surface of the particle. The circle falls within the field of stability for liquid potassium sulfide [$KS_y(\ell)$]. Potassium silicate and potassium carbonate formation are not favored.

Estimated of Levels of Chlorine Compounds and Alkali-Metal Compounds Based on Mass Balance Considerations

The concentrations of alkali metals appearing in the gas will be limited by the feed rate of coal and dolomite to the combustion system and the rate at which alkalis can be liberated from the stone and char particles during their stay in the reactors.

Figures H-8 through H-10 summarize material balances and the estimated levels of alkali and chlorine contaminants in one of four fluidized bed boiler modules in a 318 MW power plant equipped with a W 501 gas turbine.

The contaminant estimates are based on assumed release fractions for coal and dolomite. These are at this time strictly working estimates, the validity of which are being examined through laboratory experiments. For the calculations it was assumed that sodium and potassium are released to the gas stream as volatile chlorides and hydroxides at the one percent level. All chlorine that enters the fluidized bed boiler was assumed to be released to the gas stream as hydrogen chloride gas. This assumes that all but one percent of the sodium and potassium entering the system as chlorides converts to silicates or sulfates, most of which are retained in the bed ash. The chlorine is released as hydrogen chloride and finds its way to the turbine. These are oversimplified assumptions, but they provide a starting point.

It should be noted that Pope, Evans and Robbins[8] have measured hydrogen chloride emissions from an atmospheric pressure fluidized bed combustor under conditions where a solution of sodium chloride is added to the bed. They found about three percent of the chlorine as hydrogen chloride in the flue gas. It is important to note differences in the chemical environment experienced by sodium chloride in a burning coal

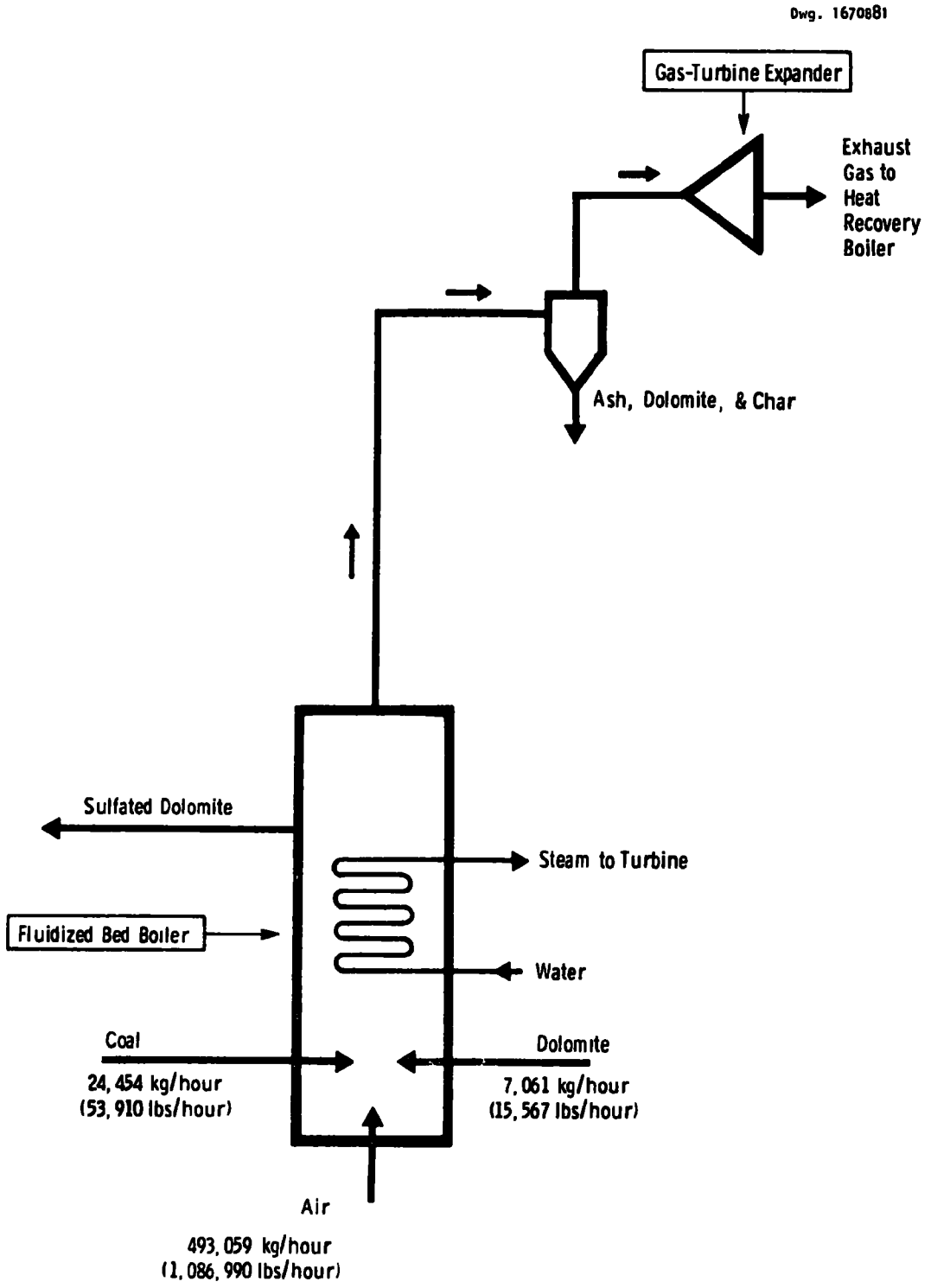

Figure H-8— Schematic flow diagram for important gas and solids streams in one of four fluidized bed boiler modules in a 318 MW power plant

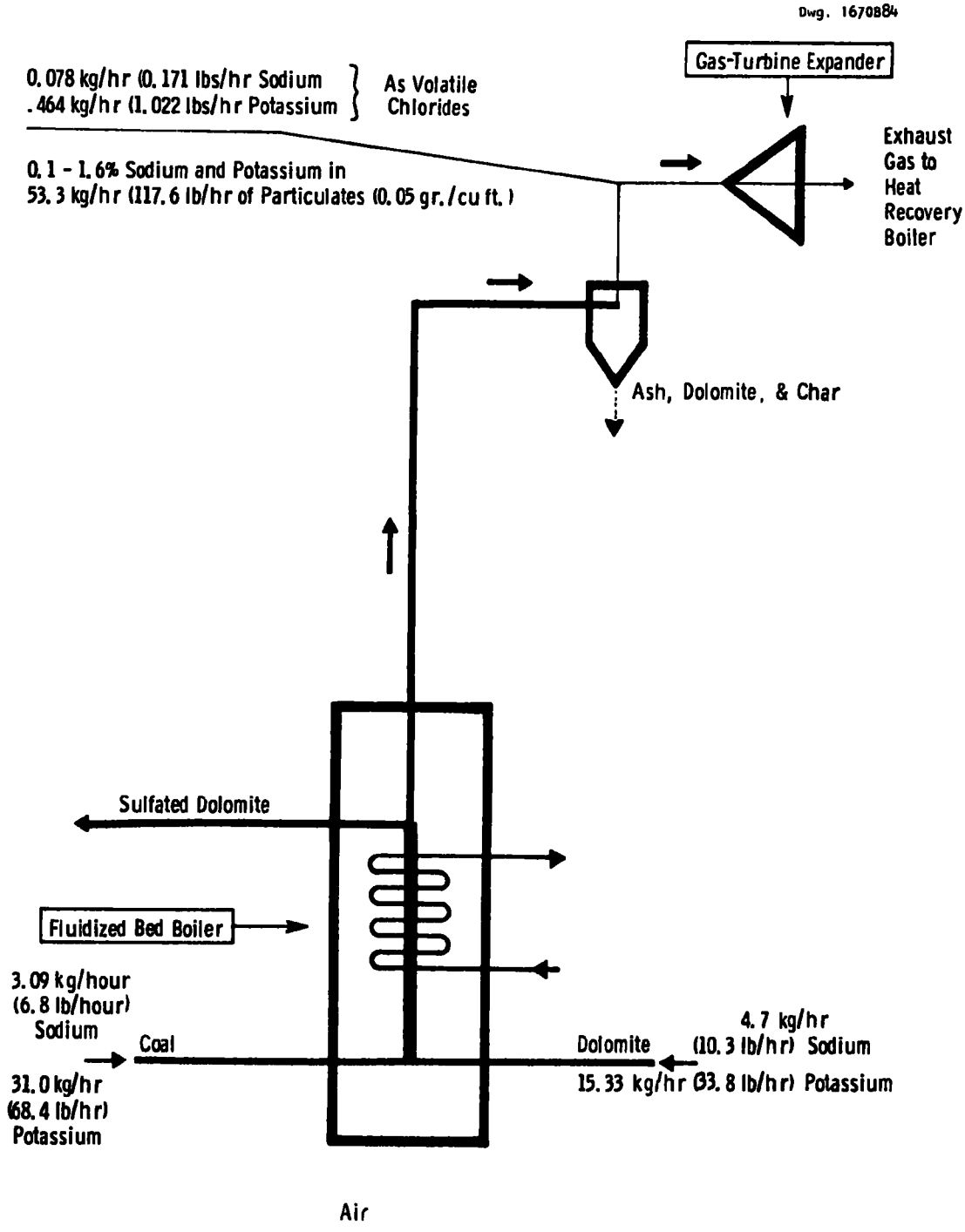

Figure H-9—Flow diagram showing transport of sodium and potassium in one of four fluidized bed boiler modules in a 318 MW power plant. One percent of the alkali content in Pittsburgh No. 8 coal and Tymochtee dolomite was assumed to produce volatile alkali compounds that reach the gas turbine

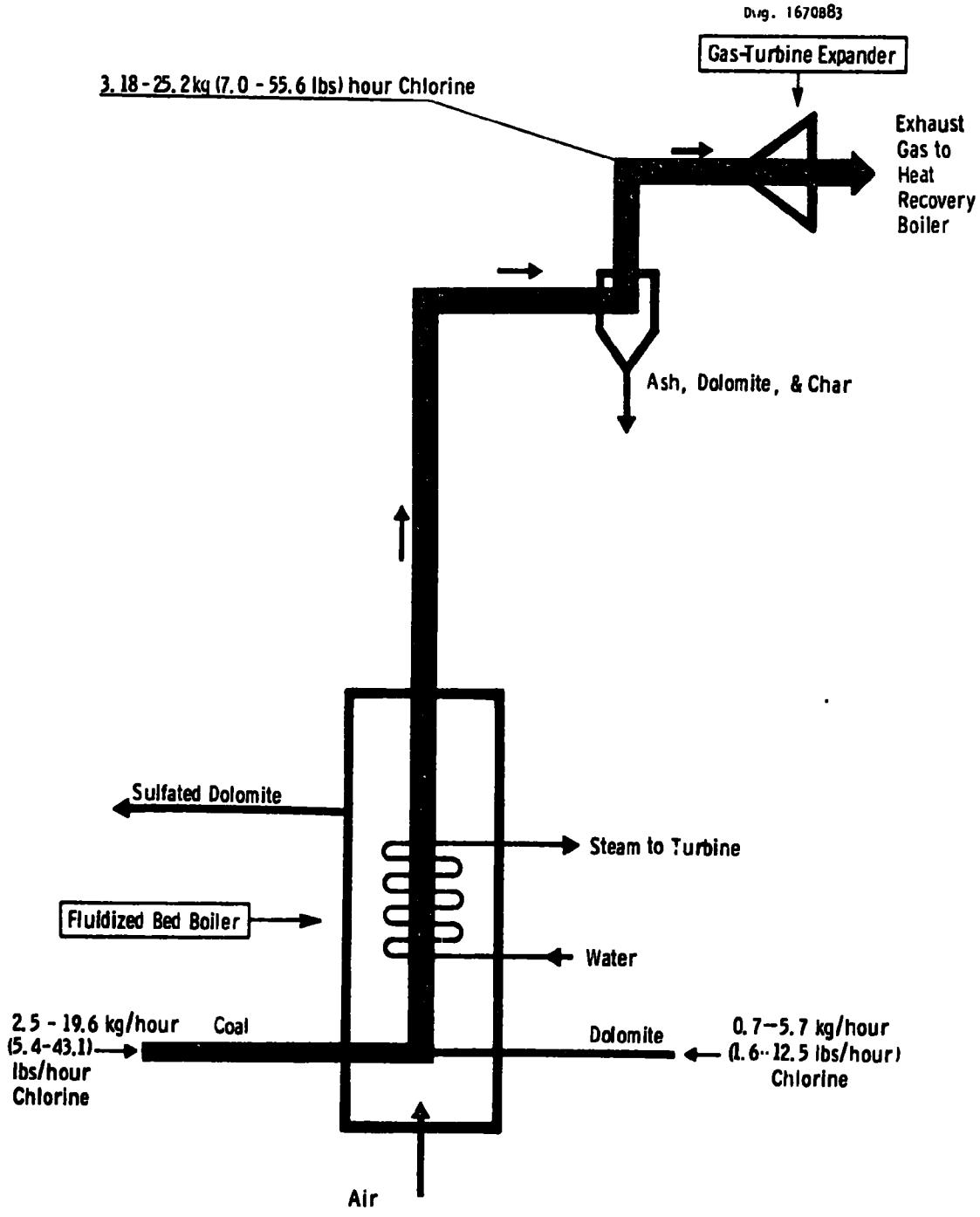

Figure H-10—Flow diagram showing transport of chlorine in one of four fluidized bed boiler modules in a 318 MW power plant. All chlorine, estimated to range between 100 and 800 ppm by weight was assumed to produce hydrochloric acid vapors that reach the gas turbine.

particle as treated here and by sodium chloride injected in a solution. Additionally, the recovery of hydrogen chloride from flue gas depends on the extent to which the gas had equilibrated at the sampling temperature. Typically, there is a lowering of equilibrium gaseous hydrogen chloride concentration greater than one order of magnitude in cooling from 700°K to 300°K: measurement of hydrogen chloride levels at 300°K will then be appropriate for assessment of the environmental impact, but they may be irrelevant as an indication of the hydrogen chlorine concentration in the gas entering the turbine.

The calculations were made for Pittsburgh No. 8 coal and for Tymochtee dolomite. Although the alkali levels of this coal are typical for eastern United States coals, the Tymochtee dolomite has alkali levels which are near the higher end for rock beds. Lower alkali dolomites typically have alkali contents which are three to ten times lower.

These calculations project a turbine expansion gas that could contain as much as 5 to 40 ppm hydrogen chloride with complete chlorine release from coals containing 100 to 800 ppm chlorine. Sodium chloride at the 200 ppb and potassium chloride at the 700 ppb level would result from a one percent release of these species from the mineral constituents.

Stability of Sodium Sulfate Melts on Turbine Hardware

Calculations of the conditions for alkali sulfate stability on first- and second-stage components in a large industrial gas turbine as a function of temperature, system pressure, and gas composition have been made. Figure H-12 shows typical pressure-temperature relations for the first- and second-stage vanes and rotating blades in such a turbine. Sulfate deposit stability is calculated for vaporization and reactive decomposition of sodium sulfate by any of the following reaction processes:

$$Na_2SO_4(s,\ell) \rightleftarrows (Na_2SO_4)g \qquad \text{(H-1)}$$

$$Na_2SO_4(s,\ell) + H_2O(g) \rightleftarrows 2NaOH(g) + SO_2(g) + 1/2O_2(g) \qquad \text{(H-2)}$$

$$Na_2SO_4(s,\ell) + H_2O(g) \rightleftarrows 2NaOH(g) + SO_3(g) \quad \text{(H-3)}$$

$$Na_2SO_4(s,\ell) + 2HCl(g) \rightleftarrows 2NaCl(g) + H_2O(g) + SO_2(g) + 1/2O_2(g) \quad \text{(H-4)}$$

$$Na_2SO_4(s,\ell) + 2HCl(g) \rightleftarrows 2NaCl(g) + H_2O(g) + SO_3(g) \quad \text{(H-5)}$$

Figure H-13 shows the results of such calculations for the overall working estimate gas composition presented in Figure H-11. The figure presented the high chlorine case, in other words, with 40 ppm by volume hydrogen chloride in the gas stream. This, in turn, corresponds to 100 percent release of 800 ppm chlorine in coal and from the dolomite fed to the plant. The location of each of the different concentration curves in the figure shows the pressure and temperature relations that represent absence (to the left of each curve) or presence (to the right of each curve) of sodium sulfate deposit for this particular gas composition and range of sodium in the gas stream.

The working estimate level of volatile sodium components (200 ppb sodium chloride by volume) is also indicated in the figure. The position of this curve suggests that liquid sodium sulfate deposits (melting point is 1157°K) will not form on the turbine components for this gas composition. The calculations of stability for other types of deposits, including potassium sulfate, are incomplete. Preliminary estimates, based on the higher volatilities of potassium compounds, show that liquid potassium sulfate deposits are not stable at working estimate chemistry conditions and at the 40 ppm level of hydrogen chloride. The higher melting point of pure potassium sulfate (melting point is 1342°K)make this compound less important as a corrodant for gas-turbine components.

The role of more complicated sodium and potassium sulfate-chloride melts is now being investigated.

The equilibrium model does not consider the effect of particulate calcium oxide on the stability of alkali-sulfate deposits. At equilibrium, if sufficient calcium oxide were present, the partial pressure of sulfur

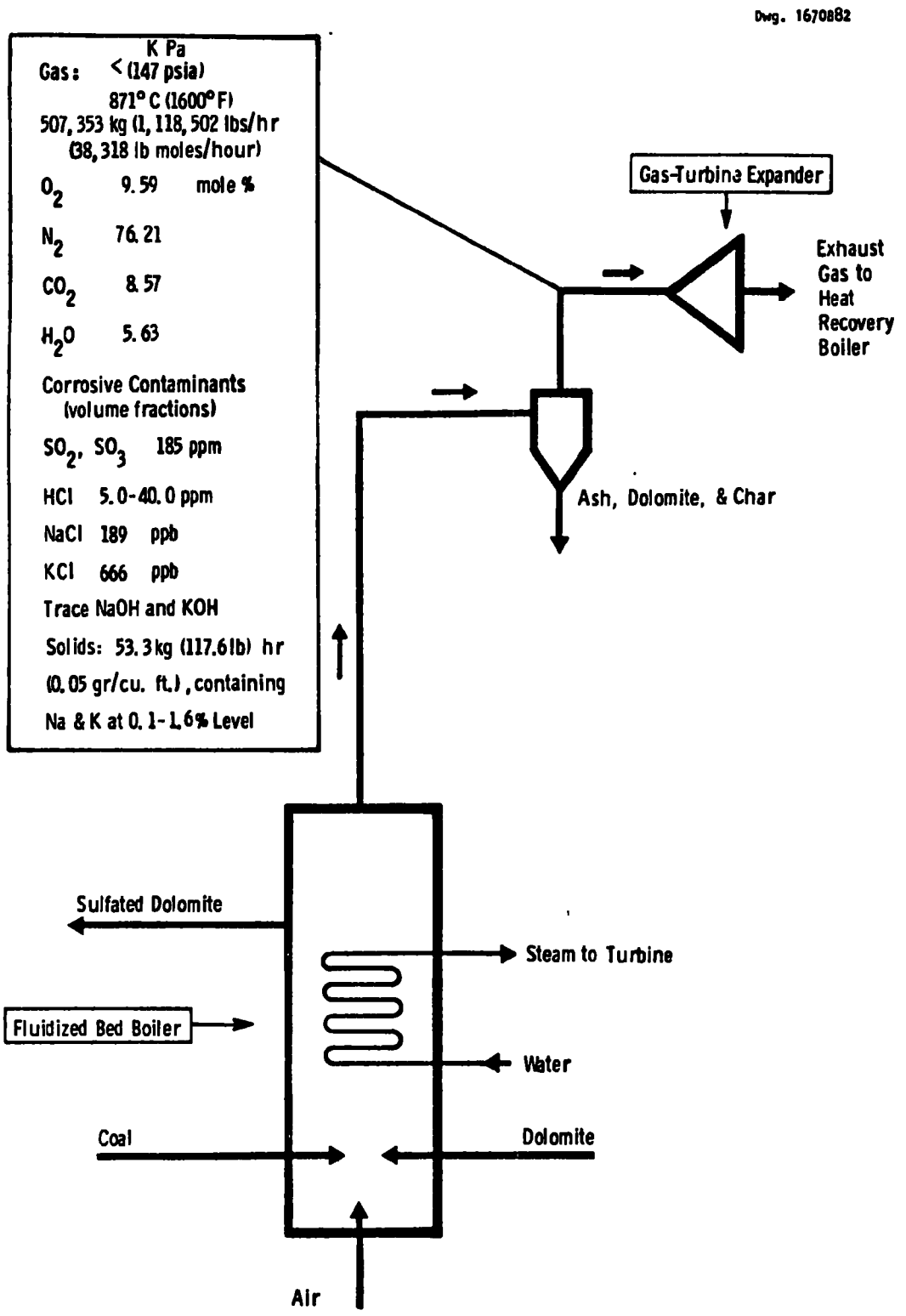

Figure H-11-Summary of gas chemistry and corrosive contaminant levels in the combustion gas stream directed to the gas turbine

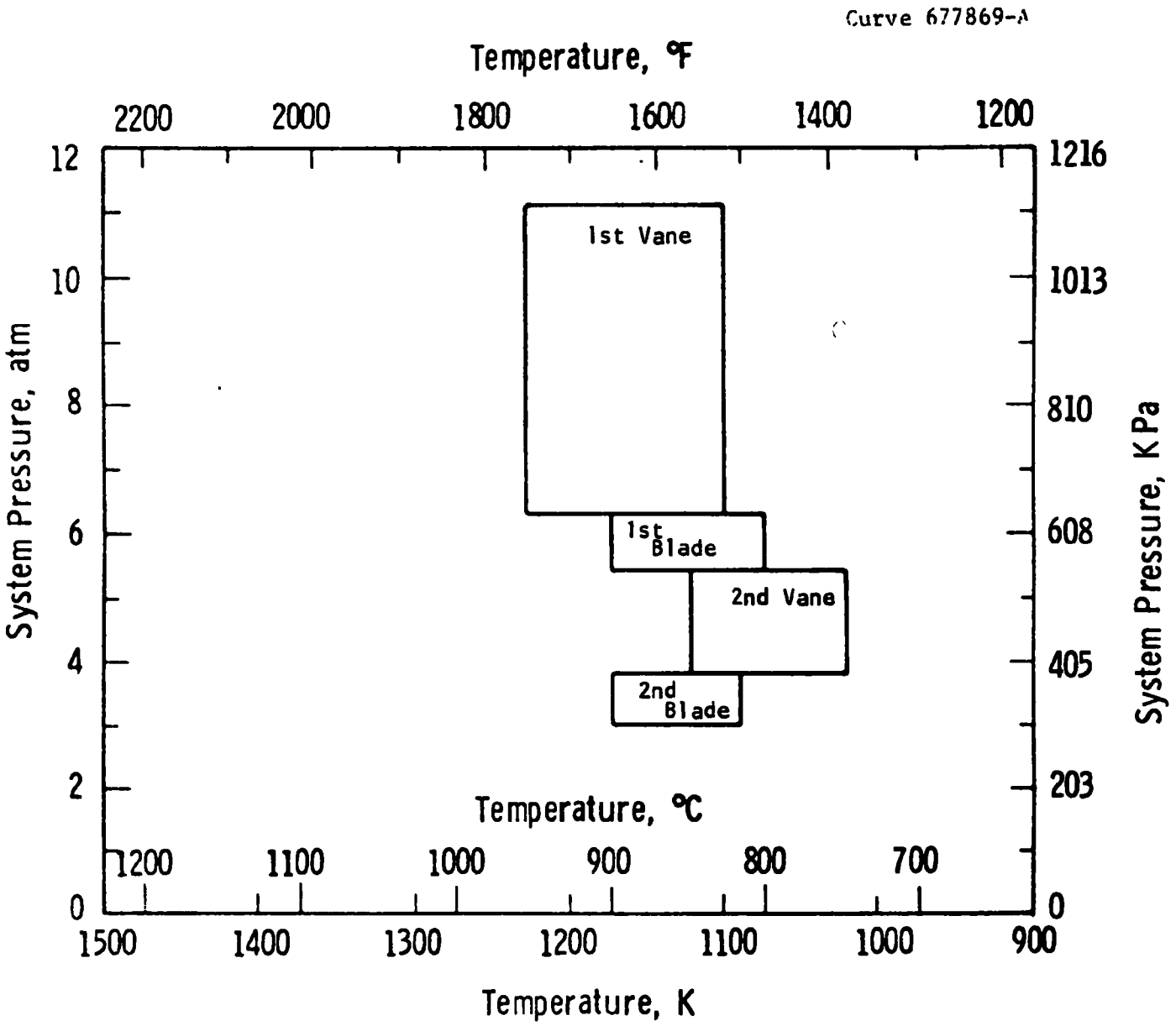

Figure H-12—Pressure-metal temperature relations for first- and second-stage components of a large industrial gas turbine

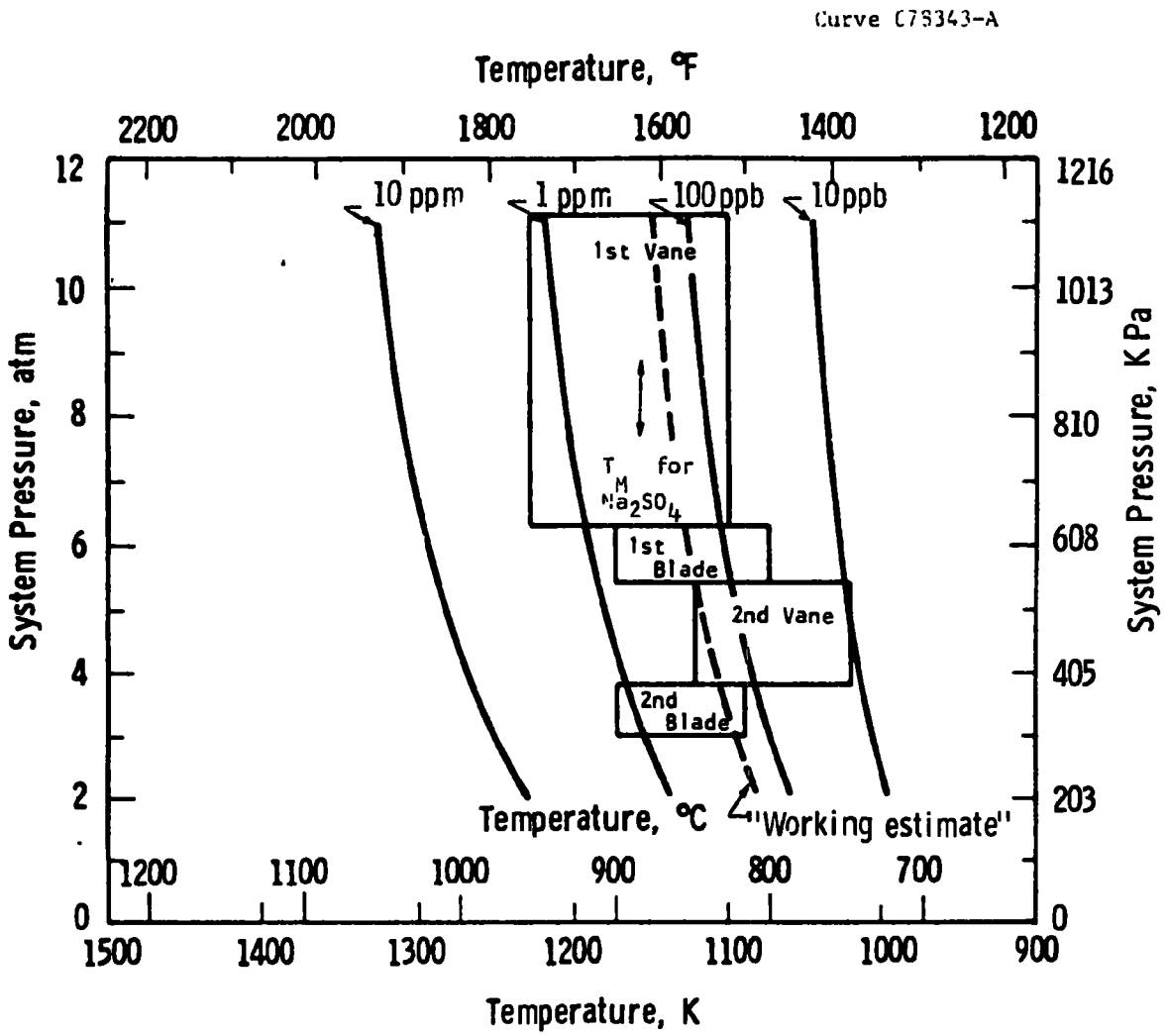

Figure H-13— Conditions of sodium sulfate stability (to the right of the different concentration lines) on the first and second stages of a large industrial gas turbine driven by coal combustion gases from a fluidized bed boiler power plant. These gases contain 40 ppm by volume hydrochloric acid vapor and also sodium chloride at the indicated volume concentration levels. The heavy broken line represents a working estimate for sodium release (1% of that in coal and dolomite).

dioxide would fall because of the formation of calcium sulfate. As the sulfur dioxide concentration falls, the turbine tolerance to alkali metals rises. The extent to which particulate calcium oxide can react with sulfur dioxide is subject to a large number of variables, which means that the turbine tolerance would vary with the number and reactivity of particles with significant residence time in the turbine. At the limit — where reaction of calcium oxide is complete and excess oxide is present — there is about a 30-fold increase in the tolerable concentration of alkali. While it is extremely unlikely that the limit can be approached, the influence of particulates containing calcium oxide will have to be considered in a kinetic model of the turbine tolerance.

CONCLUSIONS

The chemical reaction governing the release of alkali-metal compounds to the gas-turbine expansion gas have been analyzed. Experimental determination of the kinetics of alkali release over the range of hydrogen chloride and sulfur dioxide concentration from 0 to 200 ppm are needed.

Estimates of the tolerance of the turbine to prevent sodium sulfate formation have been made. These show that the tolerable sodium level depends on the hydrogen chloride and the sulfur oxide levels. The predicted sodium tolerance of 0.2 ppm sodium in fuel oil for the case of negligible hydrogen chloride level agrees well with the empirically derived limit of 0.5 ppm sodium in fuel oil. The calculations show that a sodium level of 0.2 ppm in the turbine expansion gas can be tolerated if the hydrogen chloride level in the gas exceeds 40 ppm at a sulfur dioxide level of 180 ppm, provided that turbine materials have a satisfactory life in this atmosphere. Extensions of the turbine tolerance calculations to include the effects of interacting sodium and potassium condensed compounds are needed, along with experimental determination of the sensitivity of the tolerance to kinetic factors.

REFERENCES

1. Jonke, A. A. Reduction of Atmospheric Pollution by the Application of Fluidized Bed Combustion. Office of Coal Research. Environmental Protection Agency. Argonne National Laboratory. Argonne, Illinois. Contracts EPA-1AG-0199 and OCR 14-32-001-1543. 1974.
2. Ruch, R. R., H. J. Gluskoter, and N. F. Shimp. Occurrence and Distribution of Potentially Volatile Trace Elements for Coal. Environmental Protection Agency. Illinois State Geological Survey. EPA-650/2-74-054. July 1974.
3. Akapov, E. K. and A. G. Bergman. Reversible Adiagonal System of Sodium and Potassium Chlorides and Sulfates. Zhur. Obshchei Khim (Moscow) 24: 1524, 1954.
4. Grim, R. E. and W. F. Bradley. J. Am. Cer. Soc. 23: 242-248, 1940.
5. Slaughter, M. and W. D. Keller. Ceramic Bulletin 38: 703-707, 1959.
6. Graf, D. L. The American Mineralogist 37: (162), p. 1-2.
7. Graf, D. L. The American Mineralogist 37: (162), p.706.
8. Mesko, J. E., S. Ehrlich, and R. A. Gamble. Multicell Fluidized Bed Boiler Design Construction and Test Program. Office of Coal Research. Pope, Evans and Robbins. New York, N.Y. NTIS PB-236 254. August 1974.
9. Durgin, G. A. and P. C. Holden. Westinghouse Gas Turbine Systems Division Engineering. Lester, Pa. Private communication. October 1974.

APPENDIX I

PARTICULATE CONTROL

APPENDIX I

PARTICULATE CONTROL

TURBINE TOLERANCE FOR PARTICULATES

Previous estimates of the particle size distribution from combustors have produced the distribution shown in Figure I-1 (curve 1). In addition, two progressively finer distributions (curves 2 and 3) have previously been used in economic sensitivity analyses.

Erosivity

As a first approximation, the turbine erosion damage due to the impact of a single particle is proportional to the kinetic energy of the particle. The erosivity of a dust particle may thus be defined by the product of its kinetic energy and its probability of impacting. To obtain a measure of the erosivity of a dust suspended in a gas stream it is necessary to total the erosivity of all the particles contained in a unit volume of gas. This erosivity may be used to estimate acceptable levels of particulates in gas-turbine expansion gas.

Turbine Specifications

At present, typical specifications for gaseous fuels for gas turbines require that dust loadings be kept below 0.023 gm/m^3(0.01 gr/scf); that 95 percent of the dust be less than 20 μm; and that no particles be greater than 100 μm. These specifications apply to high heating-value fuels and must be adjusted for expansion gas, as the important consideration in turbine operation is the particulate concentration in the expansion gas. The adjustment of specifications must account for the dilution of the fuel gas by excess air during combustion. High heating-value gas requires

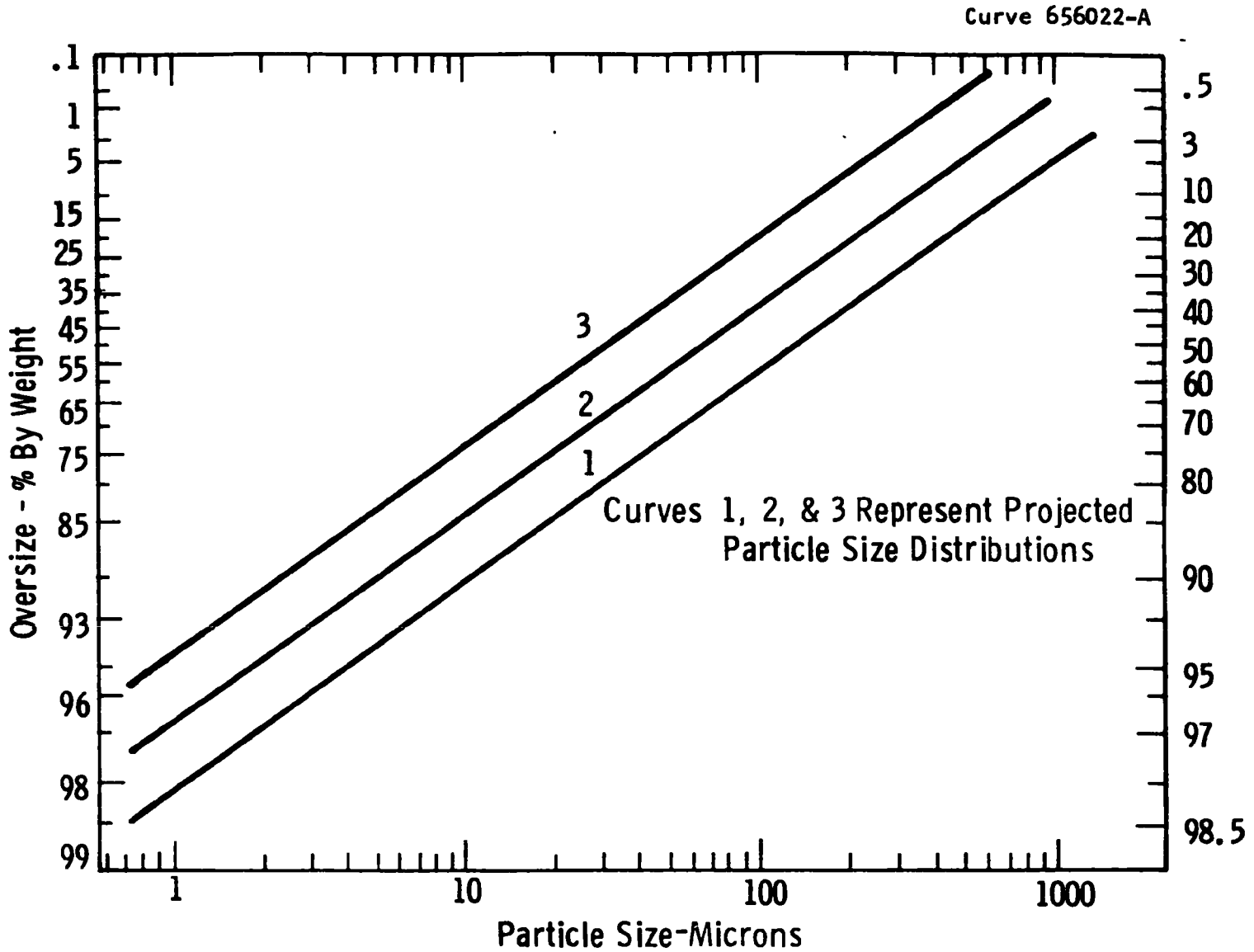

Figure I -1 Particle size distribution assumed for dust elutriated from gasifier

approximately a fifty-times dilution. Consequently, the particulate loading in the expansion gas on this basis should be restricted to one-fiftieth of that specified for high heating-value gas, in other words, 0.0005 gm/m^3 (0.0002 gr/scf).

An estimate of the particle size distribution of a dust which would comply with this specification is shown in Table I-1. The erosive nature of this dust is dependent on the loading, the particle size distribution, and its velocity relative to turbine components.

For example, we might assume that the dust suspension of Table 1.1 is carried by a gas stream which passes over turbine components at 300 m/s (1000 ft/s). If all particles are assumed to travel at the same velocity as the gas stream, then the product of the dust concentration with the probability of impaction (catch efficiency) gives a direct measure of the erosive loading of the dust stream. This is shown to be 133 x 10^{-6} gm/m^3 (58 x 10^{-6} gr/scf) at 300 m/s (1000 ft/s).

Any other dust-laden low-heating-value gas which has an erosive loading of less than 133 x 10^{-6} gm/m^3 (58 x 10^{-6} gr/scf) at 300 m/s would be acceptable as a fuel for gas turbines operating with this gas velocity.

It should be noted that particles below two microns are not considered erosive in this case, as their efficiency of impaction is negligible. These comments illustrate the turbine tolerance considerations and the requirements which the particulate removal system must consider. Turbine blade erosion is discussed further in Appendix J.

REVIEW OF DUST COLLECTION EQUIPMENT

Cyclones

Cyclones are able to handle heavy dust loading and high gas throughput at reasonable cost and low-pressure drop. They are not prone to plugging, but their internal surfaces are subject to erosion.

Cyclones of conventional design lose efficiency as the cyclone diameter is increased. Thus, for high efficiency with high gas flow, banks of small cyclones are manifolded together in a parallel flow arrangement (Figure I-2). If the cyclones are connected directly to a

Table I-1

DATA FOR ESTIMATING TOLERANCE OF GAS TURBINES TOWARDS DUST

Particle size (μm)	Particle loading, gm/m^3 (gr/scf)	Catch efficiency, (@ 300 m/s)	Erosive loading, @ 300 m/s (@ 1000 fps)
0-2	18.2×10^{-5} (8.0×10^{-5})	0	-- (0.6×10^{-6})
2-3	4.5×10^{-5} (2.0×10^{-5})	0.03	1.3×10^{-6} (0.6×10^{-6})
3-4	3.6×10^{-5} (1.6×10^{-5})	0.12	4.3×10^{-6} (1.9×10^{-6})
4-5	2.3×10^{-5} (1.0×10^{-5})	0.21	4.8×10^{-6} (2.0×10^{-6})
5-6	1.8×10^{-5} (0.8×10^{-5})	0.30	5.4×10^{-6} (2.4×10^{-6})
6-10	5.5×10^{-5} (2.4×10^{-5})	0.50	27.5×10^{-6} (12.0×10^{-6})
10-20	4.5×10^{-5} (2.0×10^{-5})	0.90	40.5×10^{-6} (18.0×10^{-6})
20 +	5.0×10^{-5} (2.2×10^{-5})	0.95	47.5×10^{-6} (21.0×10^{-6})
TOTAL	45.4×10^{-5} (20.0×10^{-5})		131.3×10^{-6} (57.9×10^{-6})

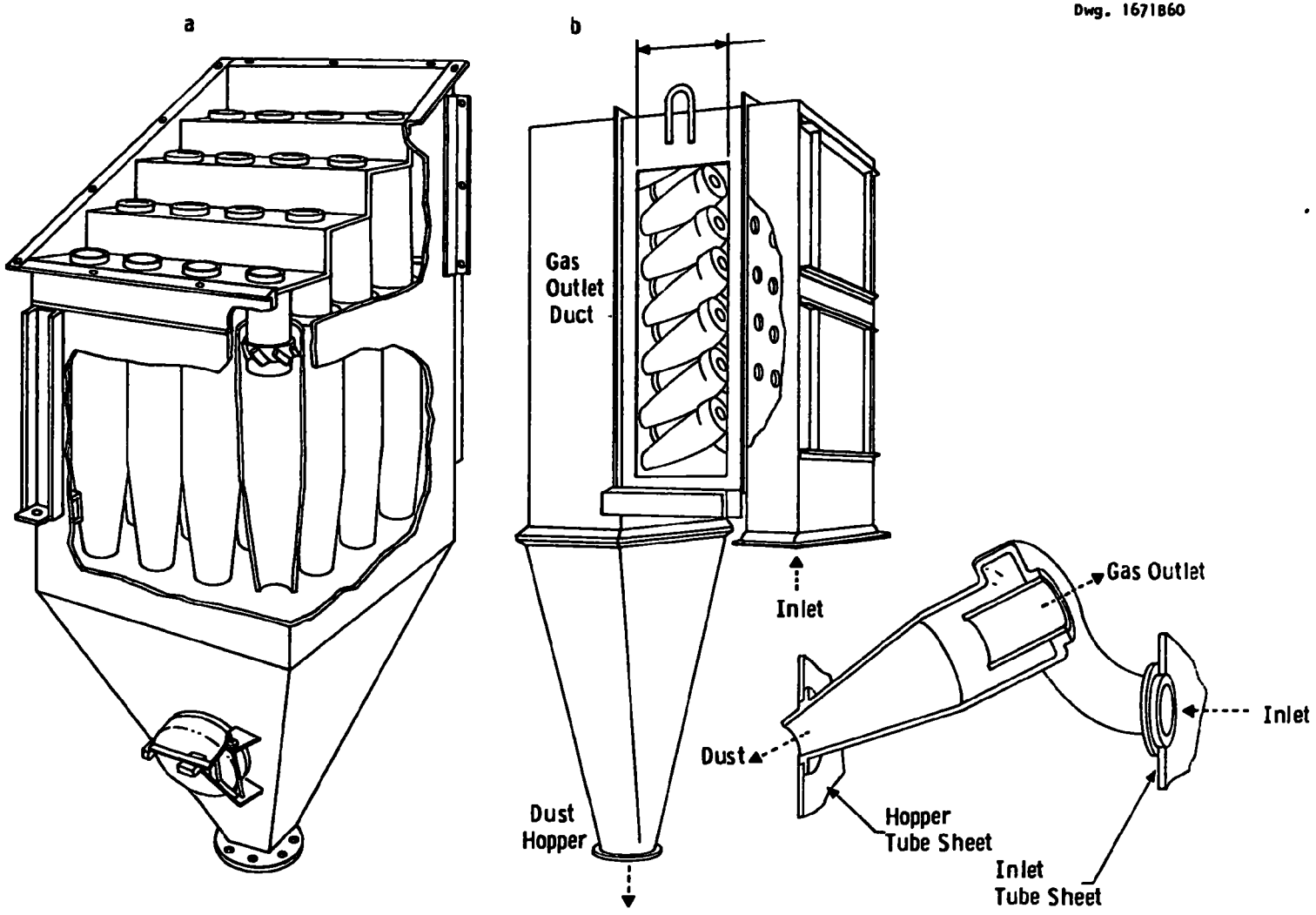

Figure I-2—Multicyclone arrangements
a. Swirl vane inlet
b. Tangential inlet

common dust hopper, secondary flows between individual units reduce the operational efficiency of these units. Consequently, performance may be improved by withdrawing the dust individually from each unit cyclone.

High-efficiency cyclones which employ secondary gas flows to improve collection efficiency are also available both in large individual units and in multicyclone configurations.

Conventional Cyclones

A conventional design high-efficiency cyclone, 203.2 mm (8 in) diameter and with a capacity of 0.07 m^3/s (150 cfm) will have a grade efficiency curve as shown in Figure I-3 (at fluidized bed combustor conditions). Units of this size could be incorporated into a multicyclone design with little loss in efficiency.

Shell Collector

Shell oil uses high-temperature multicyclones to collect particulates from cat cracker off-gases before they are expanded through gas turbines. The performance of these units is similar to that of small conventional cyclones.

Rotational Flow Cyclones (e.g. Aerodyne)

Rotational flow cyclones employ a secondary gas flow as shown in Figure I-4. The vendor's data for fractional efficiency shows extremely high collection efficiency for particles smaller than 5 μm when a clean secondary gas flow is used (Figure I-3). It is difficult, however, to visualize such an arrangement in a fluid bed boiler plant. It has been assumed that in such a plant the secondary gas flow would be provided by using a portion of the dirty gas stream.

Tests of rotational flow cyclones with a dirty secondary gas flow have shown poor collection efficiency for particles 5 μm and smaller. Unless this performance can be radically improved the units could not be considered for use in gas-turbine power plants.

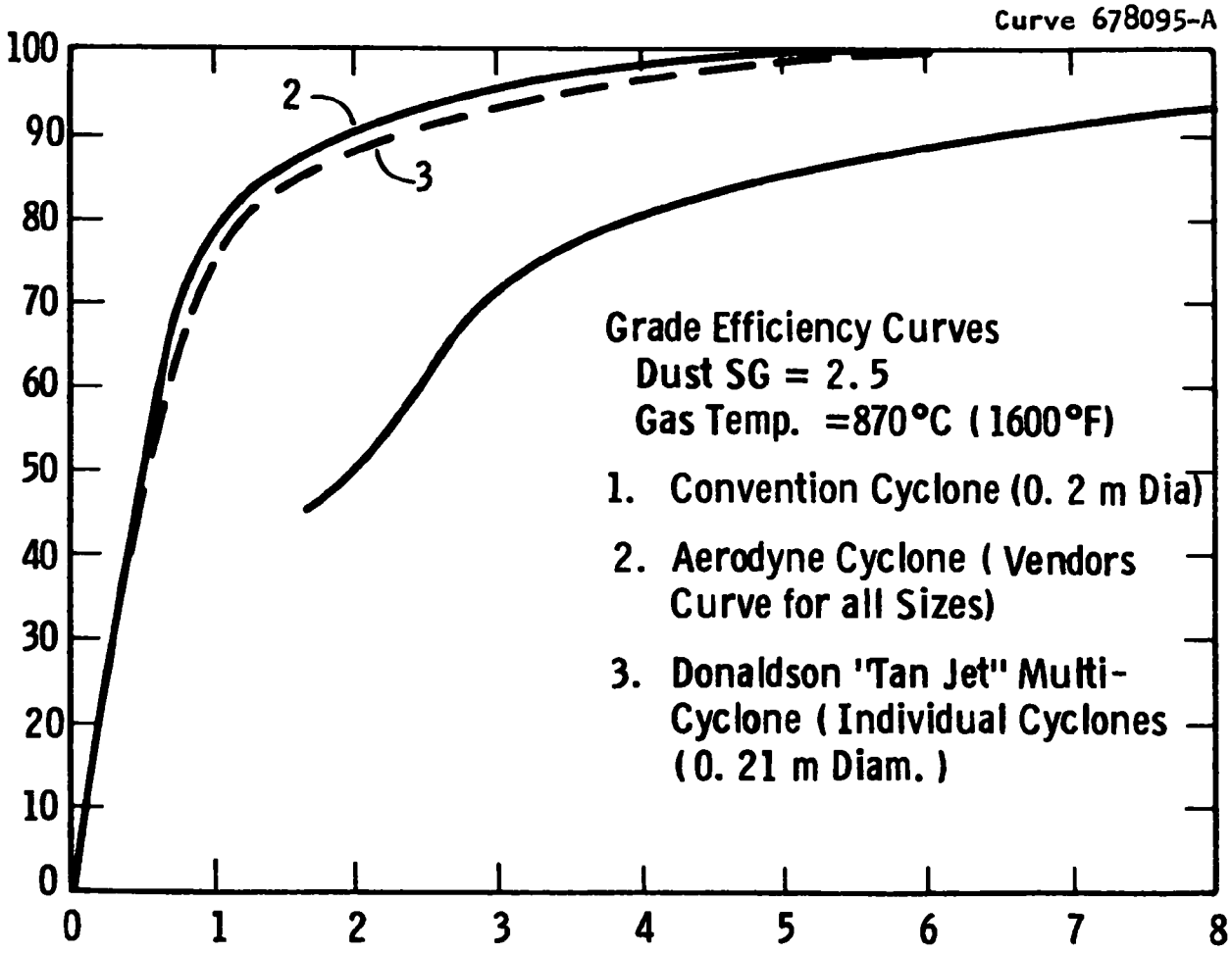

Figure I-3—Cyclone grade efficiency curves

Dwg. 6164A12

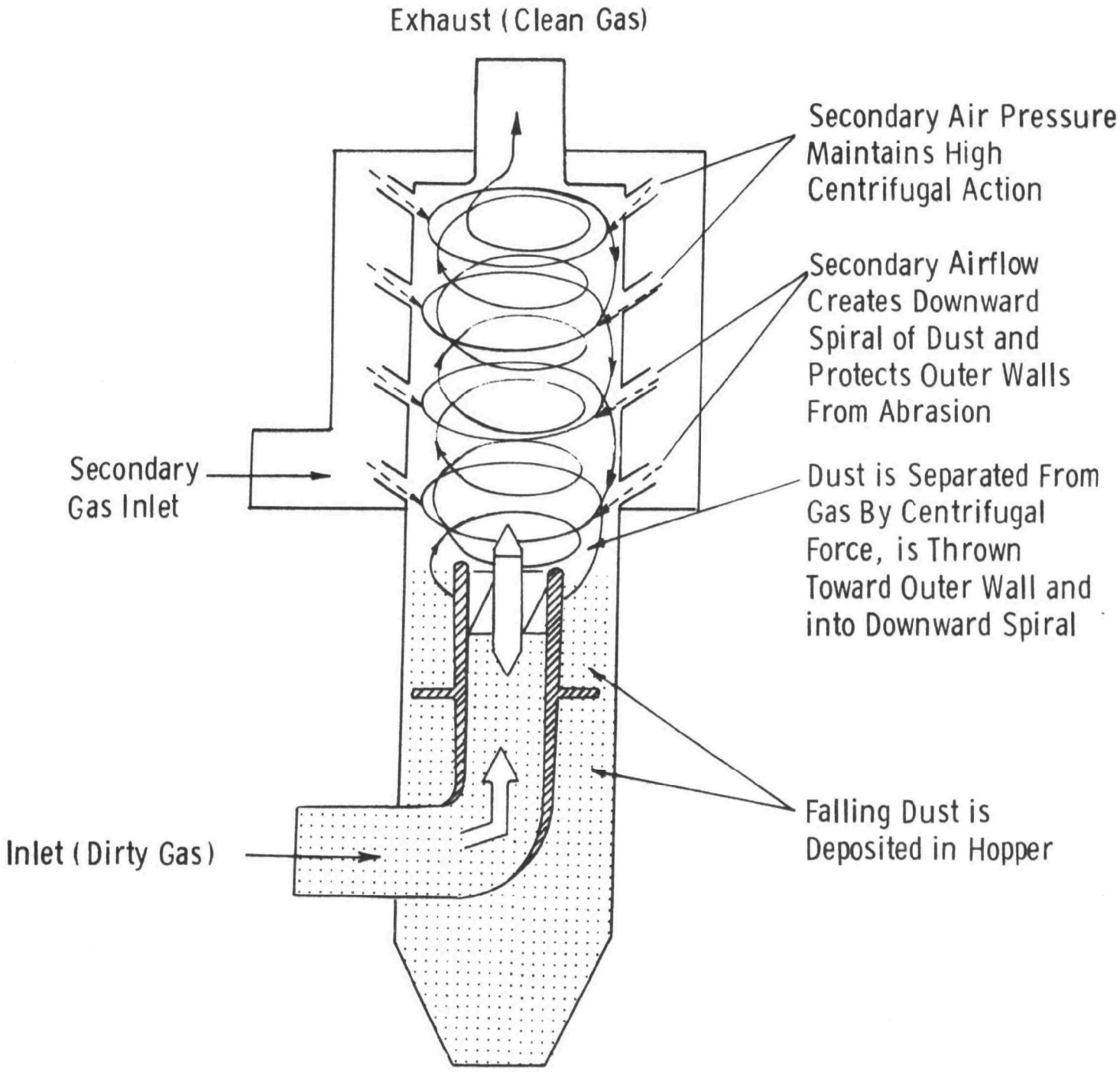

Figure I-4 – Operation of Aerodyne particulate separator

Donaldson "Tan Jet" Cyclone

The Donaldson Company has recently released a new multicyclone system which is significantly more efficient than conventional cyclones in collecting particles in the 0-to-5 μm range (Figure I-3). This unit requires a clean secondary gas flow equivalent to 15 percent of the primary flow. The secondary flow should be at the same temperature as the primary flow to prevent thermal stressing of the assembly and to maintain the flow field at its design condition.

Filters

Three filtration systems have been considered:

- Granular bids
- Porous metals
- Porous ceramics.

Granular Bed Filters

Beds of granules should, in principle, be able to filter dust particles from gas streams in much the same way as do beds of fibers. The literature on fiber filtration is extensive and shows that very high efficiencies can be achieved over a broad range of particle size. Unfortunately, fiber-bed filters cannot easily be cleaned and this limits their utility.

Granular beds are somewhat easier to clean, may be operated at high temperature, and have the potential to achieve the same high efficiencies as fiber filters.

Squires[2] reviewed the literature in 1970. His review indicates that several filters have been operated with collection efficiencies better than 90 percent on dusts down to 2 μm particle size. The data, however, are sparse and inconclusive.

Since 1970, Taub[3] has studied the transient behavior of granular-bed filters while collecting dispersed fly ash. His results show high efficiencies are possible with clean filters, but performance deteriorates

as the dust content of the filter increases. His analysis of the filter performance fails to explain his results adequately; some of them appear spurious.

Ducon has attempted to commercialize a continuously operating granular-bed filter and has published the results of its performance on cat cracker regenerator off-gas.[4] The results are encouraging but are difficult to interpret. The latest information[5] implies that the manufacture of this unit is too costly for it to compete with alternative collectors.

Squires[6] claims encouraging results for his panel-bed filter, but limited data are currently available on its performance.

Mode of Operation. Although it appears that impaction collection will dominate in determining the efficiency of a granular filter, two operating regimes exist: one in which impaction predominates and particles are collected in the interstices of the filter, the second in which the initial collection at the filter surface produces a filter cake. This cake acts as a filter aid, retaining essentially all of the collected solids at the filter surface.

The first operating mode is normally associated with high gas velocities and, consequently, with high-throughput filters. When a filter operates for an extended period under these conditions, the operating efficiency will initially remain constant with time. The bed will become progressively saturated with dust, however, and as the saturation zone extends through the bed, the collection efficiency will decline. Some results of Taub's work[3] show this trend (Figure I-5). Saturation apparently occurs when dust deposits on impaction sites profile the gas flow, avoiding sharp changes in direction and minimizing the effects of inertial deposition. It is most likely that there is also a dynamic equilibrium between deposition and reentrainment in saturated zones.

Analysis of the transient behavior of beds is, thus, complex and is further confused by a lack of fundamental information. The only data available are from Taub and appear to be unreliable. His grade

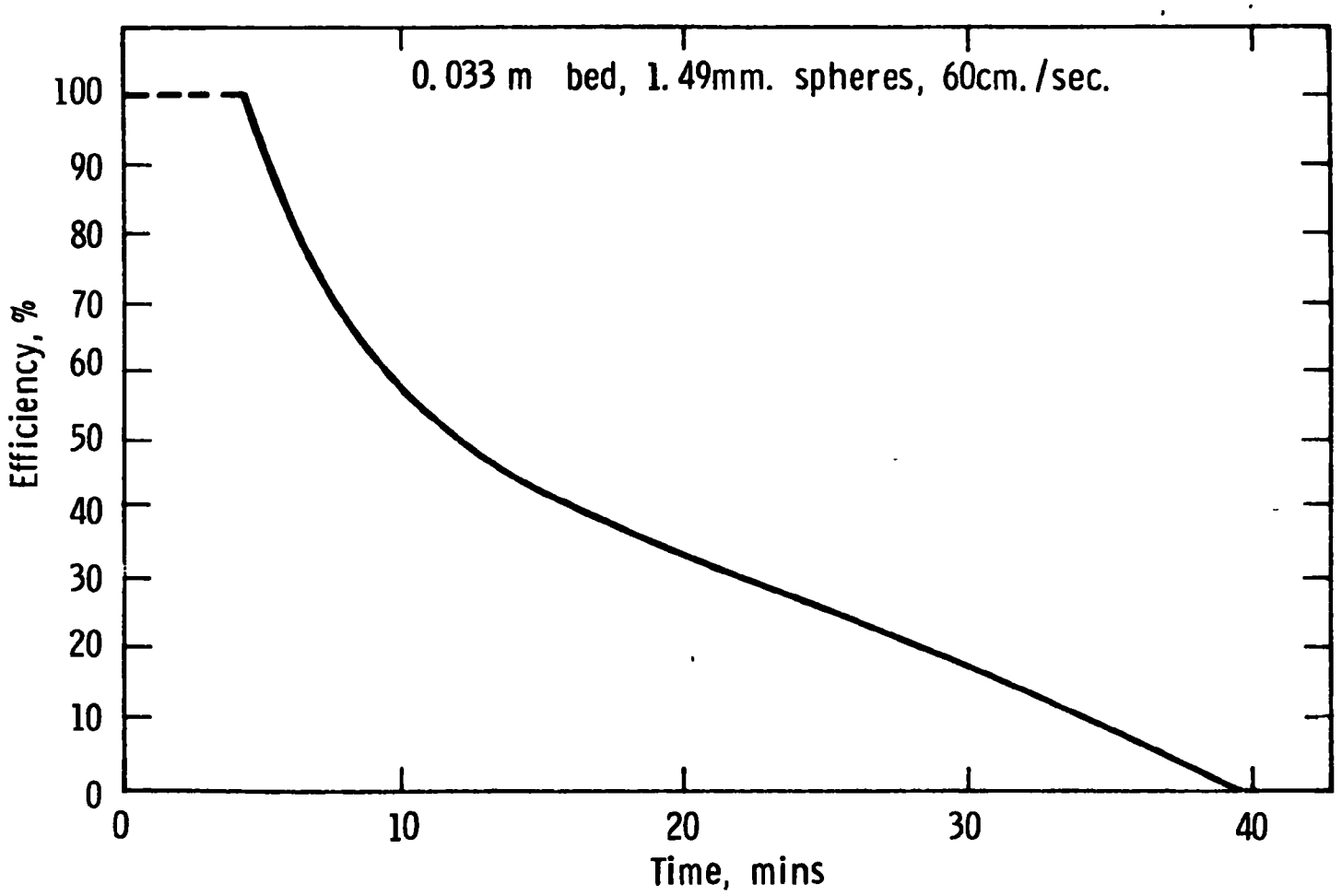

Figure I-5—Time vs efficiency — 0.033 m deep granular bed filtering fly ash

efficiency curves show no significant difference in collection efficiency between particles of 10 μm diameter and particles of 70 μm diameter, which is contrary to general experience. This could result from poor dispersion of the test dust employed. From Taub's description of his equipment, the dust disperser was crude and could not be relied upon for adequate dispersion.

The second operating mode -- formation of a filtering layer -- is essentially the same as is encountered in bag filters and in some porous metal filter installations.[7] Although some dust leakage may be expected through the clean filter, once the filter cake is established filtration is almost absolute. As the cake builds upon the filter surface, there is a consequent increase in pressure drop. At some point, the pressure drop becomes too great; it is necessary to remove the filter cake and repeat the cycle.

Dust Removal. When dust is deposited throughout the filter, it may be removed by one of two methods:

- Fluidizing the bed with a reverse flow of gas. This is limited to horizontal beds and requires some secondary collector for cleaning the flushing gas.
- Removing both the granules and the dust from the filter and repacking the filter with fresh granules. This is normally limited to vertical-panel filters. The packing may be intermittently dumped or continuously removed in a cross-flow arrangement.

When the dust accumulates in a cake on the filter surface, the cake may be removed by a reverse flow of gas. If the filter is a vertical panel, the flushing gas should be supplied as a sharp puff at high pressure. This will lift the cake from the surface and deposit it in a secondary collector. If the filter is arranged horizontally, the reverse flow of gas is used to fluidize the bed and elutriate the dust deposits.

Capacity. The work of Taub[3] shows that a 0.033 m (1.3 in) deep bed of 1500 μm particles has a capacity of approximately 2000 gm/m^2 (3000 gr/ft^2) before the collection efficiency begins to fall. This figure may be used as the safe operating limit for the deeper beds which would be used in a fluidized system.

Ducon Filter

Operation. The Ducon filter employs screens to retain the granular bed while permitting removal of the collected dust by blow-back techniques. The arrangement and operation of the unit are illustrated in Figure I-6.

When being filtered, the dirty gas passes through the outer screen and down through the granular sand bed. When the bed has accumulated sufficient dust, a short blast of high-pressure gas is used to reverse the flow. The bed flexes, is fluidized, and the dust is carried from the bed.

Performance. This unit normally operates with a 0.063 m (2-1/2 in) deep bed of 760 μm sand. The usual superficial gas velocity is between 0.15 and 0.45 m/s (0.5 and 1.5 ft/s).

Performance correlations published by Ducon[4] show that the instantaneous efficiency of the filter improves as the quantity of dust in the bed increases. This implies that collection is enhanced by the formation of a filter cake on the bed surface. The overall efficiency, however, is considerably lower than would be expected if a coherent cake were present. For example, when operating on cat cracker emissions, the efficiency was normally around 95 percent. By using a finer grade of sand, this performance can be improved. Available data on sintered metal filters[7] indicate that 100 percent collection down to 1 μm can be achieved with granules of 100 μm diameter and velocities around 0.03 m/s (1 ft/s).

No grade efficiency curves for the filter have been made available by Ducon.

Dwg. 6224A12

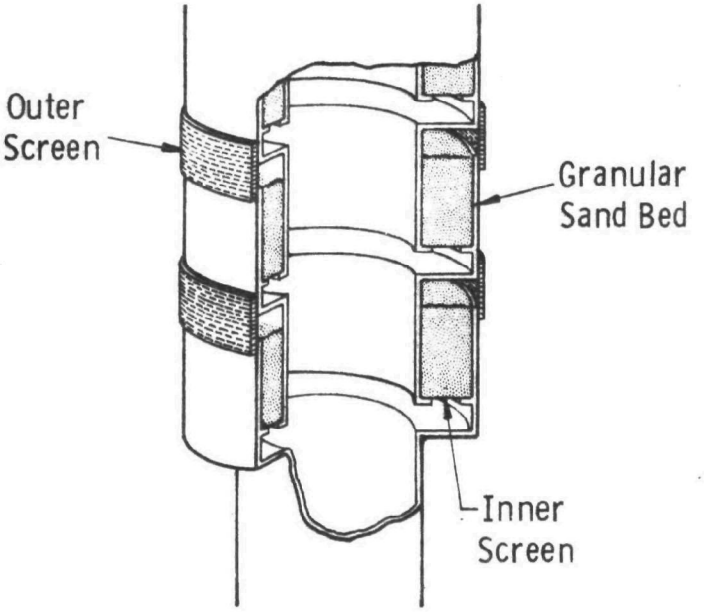

Filter Element Internals

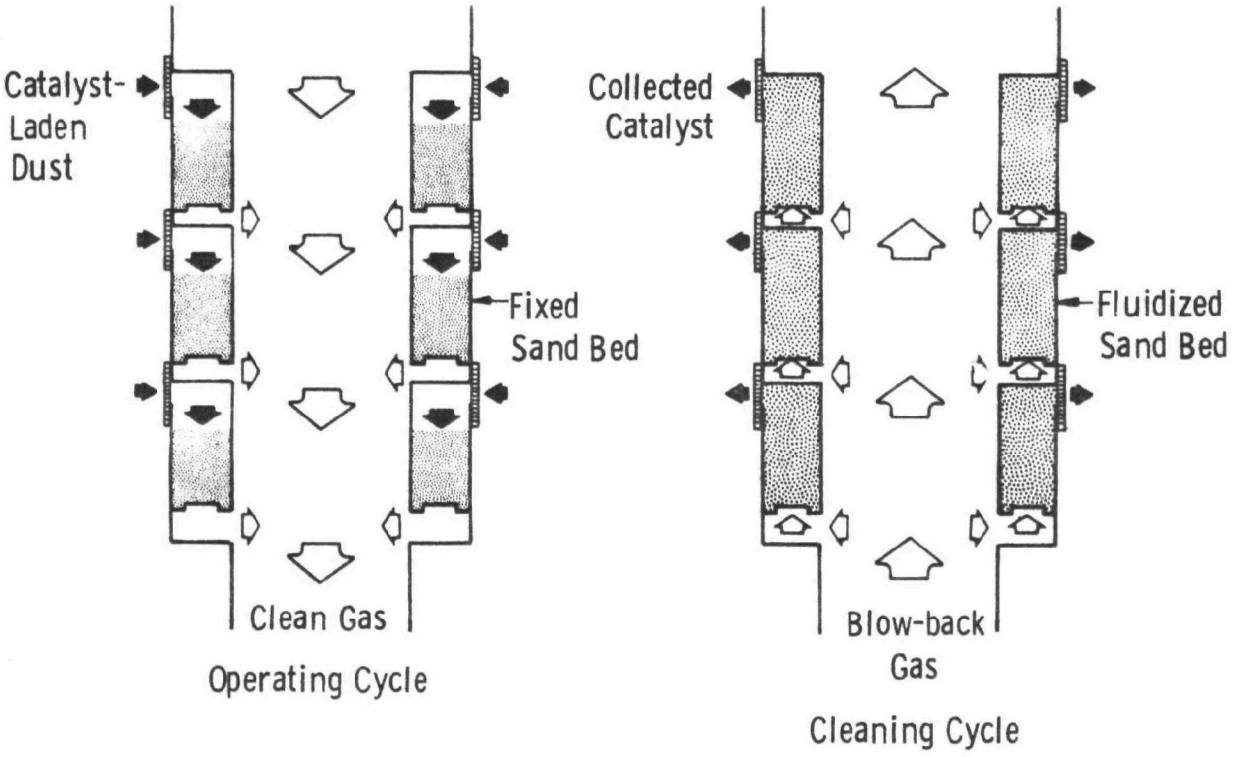

Figure I-6-Ducon sand bed filter

Operating Problems

- Leakage - Ducon has noted that dust leaks through the filter beds during the blow-back phase of the operating cycle. This markedly reduces the efficiency of the unit.
- Plugging - If finer granules are used in the Ducon filter, finer retaining screens will be required. Experience has shown that fine screens have a tendency to accumulate dust deposits and become plugged.

Squires Panel-Bed Filter

Operation. The Squires panel-bed filter consists of a vertical bed of granules held in place by louvered walls which resemble venetian blinds. The unit operates with superficial gas velocities up to 0.15 m/s (0.5 ft/s). Recent information suggests that collection efficiency increases with superficial velocity.

The filter is cleaned intermittently by a sharp puff-back of gas which lifts the filter cake, along with a small quantity of granules, from the surface and deposits it in a collecting hopper. Fresh granules are supplied from the top of the panel to make up for losses during the puff-back.

The operation of the unit is illustrated in Figure I-7.

Performance. There is little data available on the efficiency of the Squires Filter. However, filtration efficiencies of better than 99 percent have been recorded on redispersed fly ash,[2] with a filter consisting of 0.025 m (1 in) sand.

Operating Problems.

- Size - If the equipment operates at low gas velocities, a large filter area is needed for treating commercial quantities of high-temperature gas.
- Solids handling - Distributing and collecting the filter granules will produce mechanical difficulties.

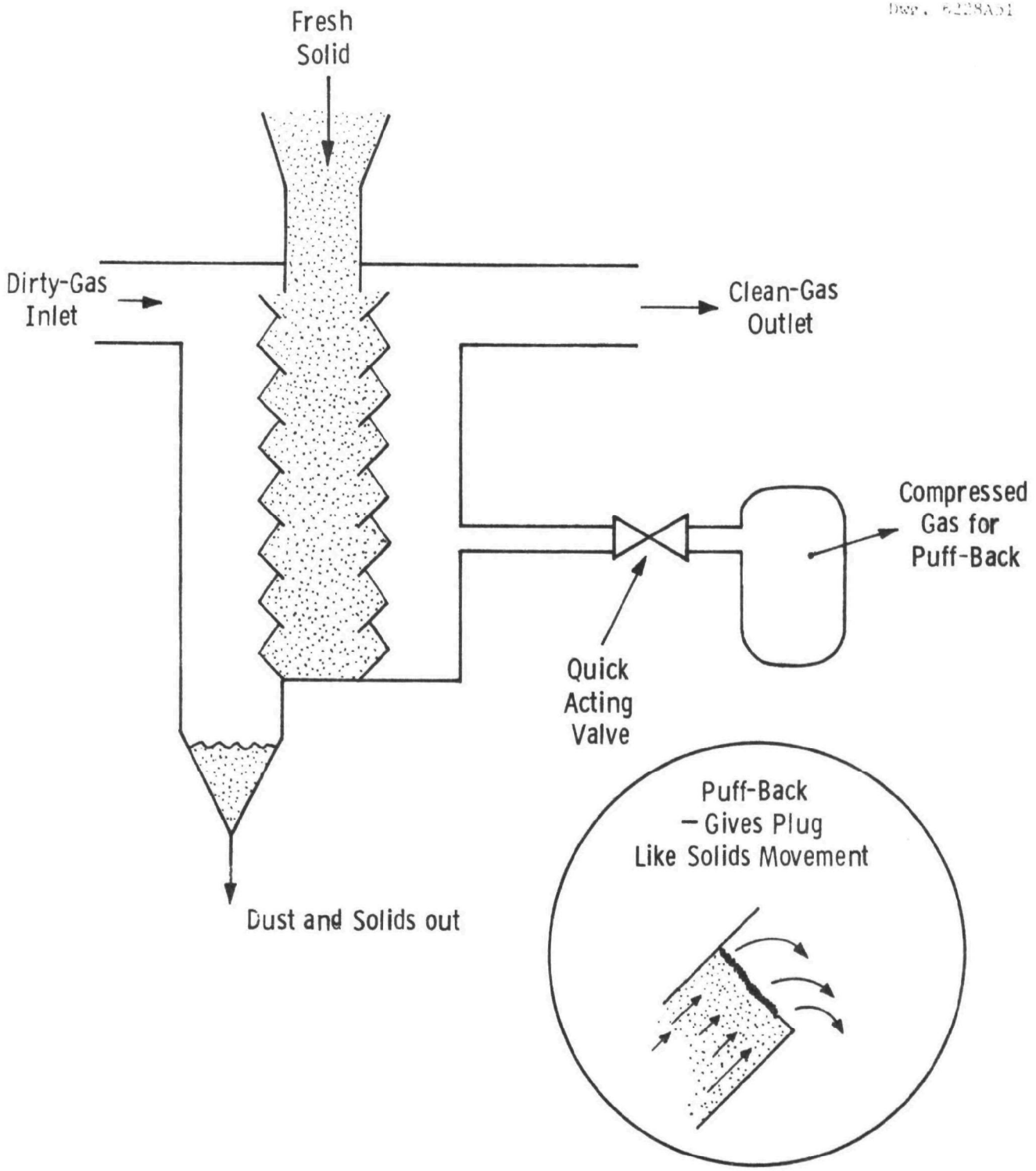

Figure I-7—Squires panel bed filter

- Plugging - The cleanup cycle for this filter will only remove surface accumulations of dust. It is possible that with long operating schedules dust will penetrate the filter panel and block the interstices.

Cross Flow Filters

Operation. Panel bed filters may be operated with a continuous downward movement of the column of solids, clean granules being introduced at the top and a mixture of dust and granules being removed from the bottom. This is consistent with high-gas velocity/impaction collection operation.

For the fluidized bed boiler, the spent limestone granules could be used as the filter medium (Figure I-8), providing a continuous supply of clean, hot, filter granules. As the stone is to be dumped anyway, this arrangement does not produce any secondary disposal problems.

Performance. Dorfan[8] has built cross-flow filters which use 0.013 m (1/2 in) to 0.038 m (1-1/2 in) granules and claim 98 percent collection efficiency for 2 to 10 μm dust carried at superficial velocity of 1.8 m/s (6 ft/s).

Zahradnik et al.[9] report some preliminary results for a cross-flow bed of 1600 μm (1/46 in) alkalized alumina. They show 99 percent collection efficiency for redispersed fly ash carried at 0.15 m/s (0.5 ft/s).

Operating Problems

- Solids flow - Solids flow in a conventional panel bed retained by louvers will create dead zones near the filter surfaces. These zones would eventually saturate with dust and possibly plug (Figure I-9).
- Reentrainment - Relative motion of the filter granules will cause dust reentrainment in the gas stream. Unless the bed is sufficiently wide in the direction of gas flow, poor performance will result.

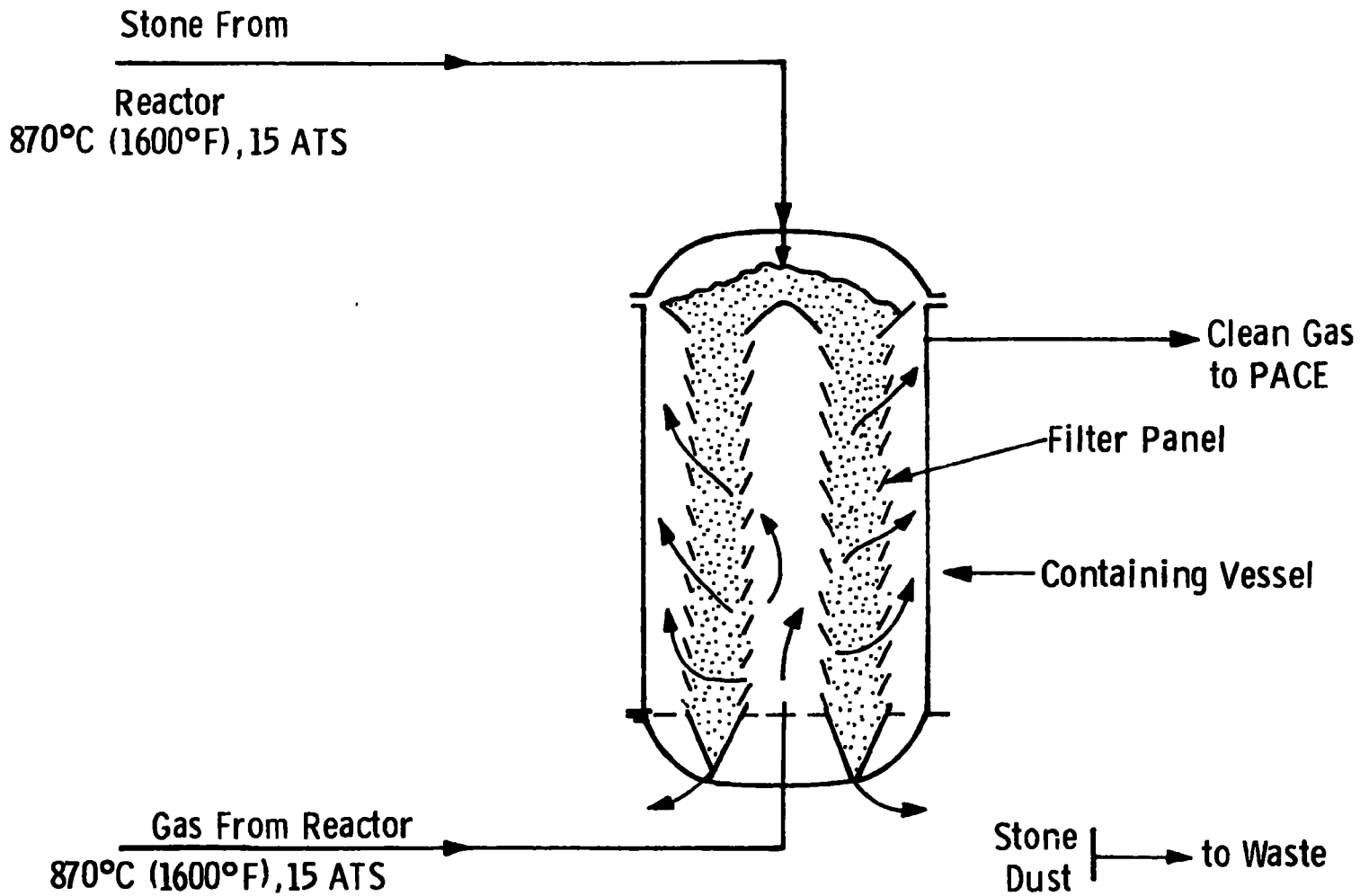

Figure I-8—Cross-flow filter arrangement - Ⓦ gasification plant

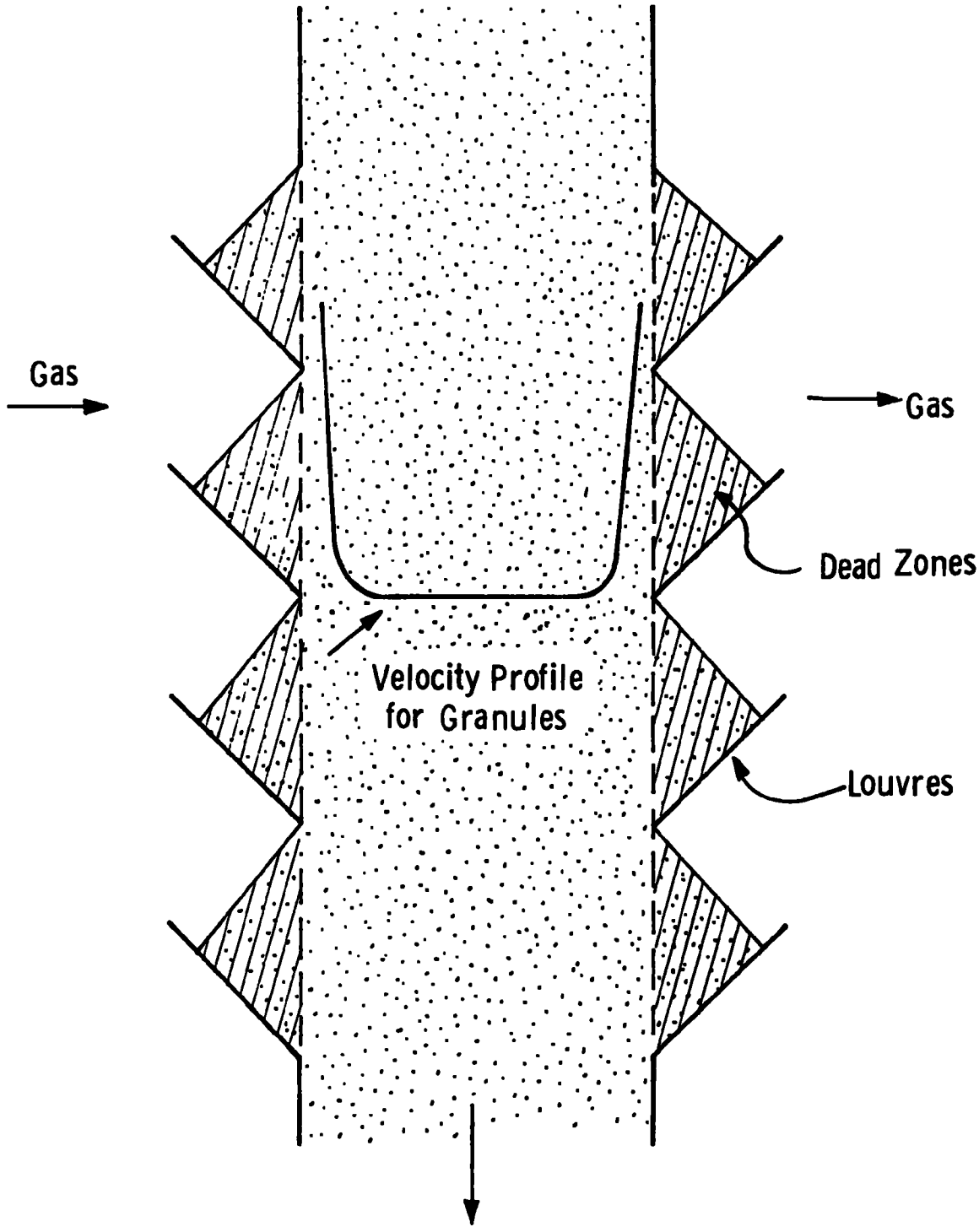

Figure I-9—Anticipated solids flow and "dead" zones for a conventional cross-flow filter

- Solids handling - Solids distribution to the filter panels presents mechanical difficulties.
- Erosion - Solids retaining elements will be subject to erosion by the moving granular bed.

Porous Metal Filters

Porous metal filters have been used commercially for 15 years to filter catalyst fines from effluent gases in fluidized bed reactors. They can be operated with virtually 100 percent efficiency on particles down to one micron on a continual, cyclic basis.

Porous metals have two serious operating problems:

- They are limited to operation at temperatures below 538°C (1000°F)
- They require a clean, high-temperature gas supply for the cleanup portion of the operating cycle.

Porous metals are also costly: a budget estimate is $1000 per square meter of filter surface.

Porous Ceramic Filters

Porous ceramic filters may in principle operate in a way similar to that of porous metal filters. At high gas flows, however, vibrational strains lead to cracking in the ceramic elements. In addition, sealing ceramic elements in a manifold is difficult when high-temperature operation is required.

REFERENCES

1. Keairns, D. L. et al. Evaluation of the Fluidized Bed Combustion Process. Office of Research and Development. Environmental Protection Agency. Westinghouse Research Laboratories. Pittsburgh, Pa. EPA-650-2-3073-048a. Contract 68-02-0217. NTIS PB-231162/9 December 1973.
2. Squires, A. M. and R. Pfeffer. Panel Bed Filters for Simultaneous Removal of Fly Ash and Sulfur Dioxide. J. A. P. C. A. 20: 534, 1970.
3. Taub, R. Filtration Phenomena in a Packed Bed Filter. Ph.D. Dissertation. Carnegie-Mellon University. 1970.
4. Kalen, B. and F. A. Zenz. Pollution Control Operations: Filtering Effluent from a Cat-Cracker. C. E. P. 69: 67, 1973.
5. Tesorio, A., Ducon Company, Inc. Private Communication.
6. Squires, A. M. Private Communication.
7. Pall, D. B. Filtration of Fluid Catalyst Drives from Effluent Gases. I. E. C. 45: 1197, 1953.
8. Perry, R. H., and C. H. Chilton, eds. Chemical Engineering Handbook. Fifth Edition. New York. McGraw-Hill Book Company. 1973.
9. Zahradnik, R. L., J. Anyigbo, R. A. Steinberg, and H. L. Toor. Simultaneous Removal of Fly Ash and Sulfur Dioxide from Gas Streams by Shaft Filter Sorber. Env. Sci. Tech. 4: 665, 1970.

APPENDIX J

GAS-TURBINE DESIGN AND OPERATION

APPENDIX J

GAS-TURBINE OPERATION

To successfully operate a gas turbine on the exit gases of a pressurized fluid bed combustion process, it is necessary to limit the concentration of alkali-metal compounds and of particulates to levels low enough that excessive deposition, hot corrosion, and erosion of turbine components does not occur.

ALKALI-METAL COMPOUND TOLERANCE

Alkali-metal compound concentrations must be low enough so that oxygen-excluding liquid films of sulfates, or mixed sulfates and chlorides do not form to initiate hot corrosion of turbine components. The simplified sodium sulfate deposition model discussed in Appendix H has shown that the tolerance for alkali metals is a strong function of both the sulfur dioxide (SO_2) and the hydrogen chloride (HCl) levels in the expansion gas. If sodium was the only alkali metal present, transport between the fluid bed combustion system would be primarily by sodium chloride (NaCl), and the tolerance of the turbine would vary, as shown by Figure J-1, between 50 and 200 ppb by volume at a sulfur dioxide level of 200 ppm for hydrogen chloride levels between 5 and 40 ppm (those expected in burning low- and high-chlorine coals). Better sulfur removal could increase the sodium tolerance greatly. As indicated in Appendix H, the presence of potassium compounds reduces the allowable alkali-metal concentration.

Figure J-2, which presents the equilibrium case for a deposition model which permits the sodium sulfate-potassium sulfate ($NaSO_4$-K_2SO_4) eutectic melt (melting point 832°C [1530°F])to form on the blading, shows that the maximum alkali-metal tolerance for sodium is reduced by a factor of

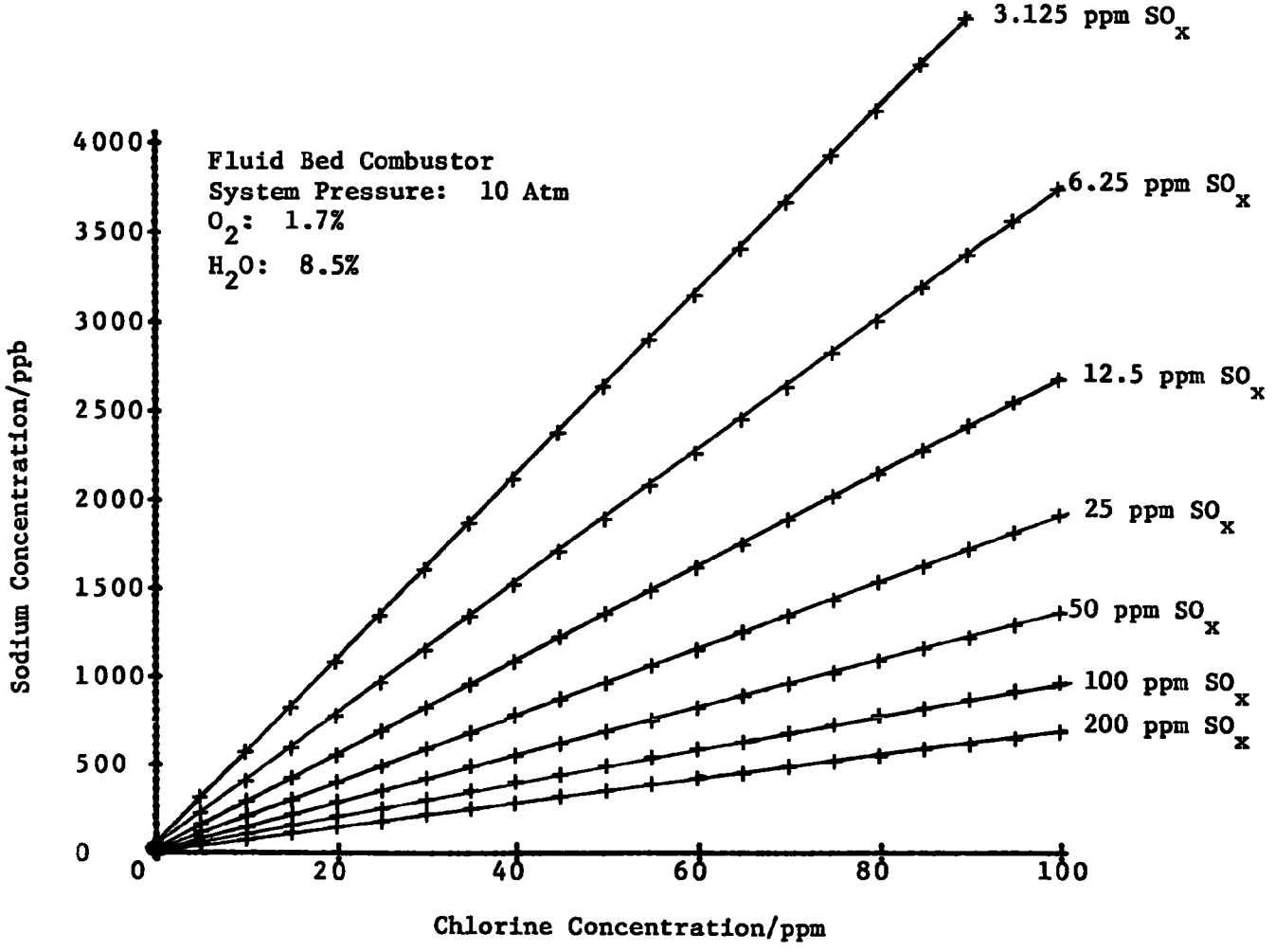

Figure J-1 - Turbine tolerance for sodium as a function of the concentration of chlorine and oxides of sulfur (sodium sulfate melt model)

Basis: $2NaCl + H_2O + SO_2 + 1/2O_2 \rightleftarrows Na_2SO_4 + 2HCl$

Na_2SO_4 melting point, 884°C (1623°F)

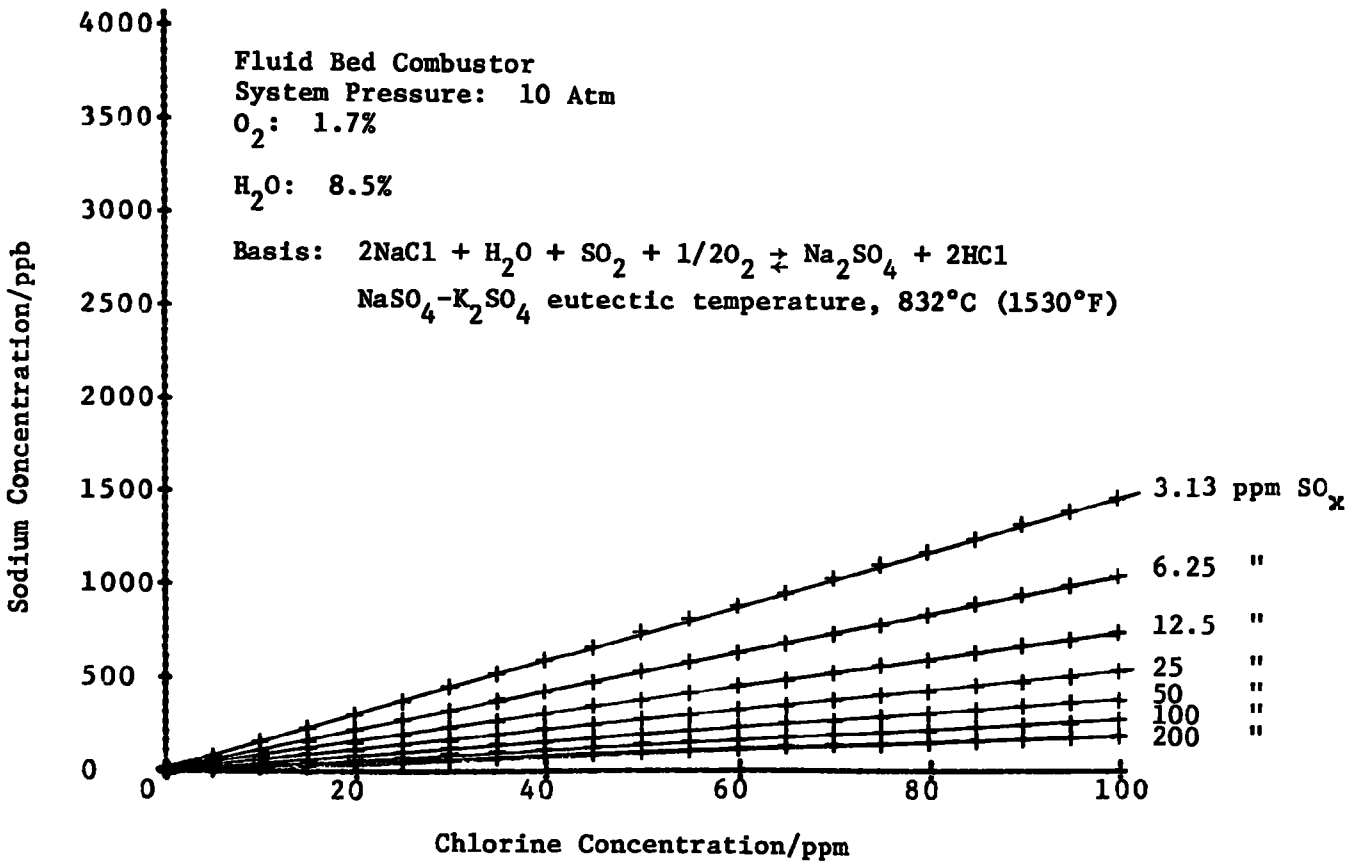

Figure J-2 - Turbine tolerance for sodium as a function of chlorine and oxides of sulfur concentration (Na_2SO_4/K_2SO_4 eutectic melt model)

about 4 by the presence of this melt. This is not the worst case. The addition of potassium and sodium chlorides to the melt permits a four-component eutectic of even lower melting point --514°C (957°F)-- and the permissible concentrations of sodium and potassium to prevent the formation of this liquid will be even lower.

Further work is required to quantify the tolerance for the ranges of sodium and potassium compounds likely to be encountered. In addition to understanding the turbine tolerance, work is needed to understand how best to meet the tolerance. This work includes:

- Developing the effects of bed combustion temperature and residence time on the alkali-metal concentration in the coal gas
- Evaluating the technical and economic effectiveness of additives in the beds or in granular bed filters in lowering concentrations of trace chemical contaminants to the turbine tolerance
- Establishing the technical feasibility of limiting hydrogen chloride concentrations in the combustion systems to minimize alkali release and of increasing hydrogen chloride concentrations in the turbine to prevent deposition
- Evaluating the effectiveness of pretreatment in the coal and stone dryers of the coal and dolomite feed to convert sodium and potassium chlorides to more stable and less volatile compounds before they enter the higher temperature combustion system.

Particulate Tolerances

If the alkali-metal compound tolerances are met, one is reasonably assured, because of the low-combustion temperatures in a fluid bed combustion system, that liquid films will not be present on either the turbine hardware or on the surface of the particules. Deposits

cemented by alkali-metal compounds should not form. Sintering of deposits will not be accelerated by the presence of the liquid phase.

Deposits resulting from the impaction and dry sintering of the mix of fine particles can still occur, especially in the first stages of the turbine where blade-metal temperatures may exceed 870°C (1600°F) in some places. Information is not yet available to define particulate tolerances to limit deposit growth to acceptable rates. We need to understand the influence of blade temperature and particulate arrival rates on the growth and sintering of deposits; we need to establish rates of erosion of deposits so that deposit formation and removal processes are quantified.

Deposit formation is less of a problem at low turbine inlet temperatures. Turbine operating experience has indicated that below 677°C (1250°F) erosion rather than deposition may become the factor that limits turbine life.

A preliminary estimate of the turbine tolerance of particulates for control of erosion damage can be made by utilizing the experimental results of the Australian Direct Coal-Fired Gas Turbine Program.[1] Summarizing their experimental results.

- The turbine inlet temperature was dropped to 677°C (1250°F) so that erosion rather than deposition would limit turbine life.
- Direct firing of pulverized coal through a "can"-type combustor was used so coal ash particulates can experience temperatures above 1650°C (3000°F) in the combustor transit. The melted cenospheres resulting from this flame transit are more erosive than fluid bed combustion ash, which even in the combustion zone does not see temperatures above the softening point of most coal ash; in other words, fluid bed combustor combustion-zone temperatures are near 1100°C (2000°F).

- The turbine was redesigned to lower gas velocities leaving the turbine nozzles from about 370 m/s (1200 ft/sec) to 240 m/s (800 ft/sec) in order to lower erosion damage.
- The redesigned turbine expanded gas contained 7×10^{-4} kg ash/kg gas.
- The mean particle size of the ash entering the turbine ranged between 4 and 8 μm in diameter. The particle size distribution was such that essentially no particles were larger than 22 μm diameter:
  - 10 percent of the particle mass exceeded 10 μm diameter
  - 60 percent of the particle mass exceeded 5 μm diameter
  - 90 percent of the particle mass exceeded 3 μm diameter.

  Figure J-3 shows the measured size distributions.
- The rate of erosion of both stator and rotor blades decreased with time for the first 50 hours of turbine operation and remained stable for the remaining 73 hours of testing.
- Extrapolation of the wear data indicated that rotor blades and stator vanes would require replacement,due to thinning of their trailing edges. (The protection of blade roots from notching afforded by the stepped side-wall construction and trailing edge fences to control dust concentrations appeared to be effective.) Blade life was calculated on the basis of the time required to reduce the trailing edge blade thickness from its design value of 1.47 mm (0.060 in) to zero thickness. Table J-1 shows the life expectancy of the blading in the modified turbine.
- The Australian turbine expanded 9 kg/s (20 lb/sec) of hot gas compared to the nearly 300 kg/s (700 lb/sec) of hot gas expanded by a 60 MW electrical utility gas turbine. The blade height and blade pitch in the first-stage rotor Australian turbine are about half those of a large, 60 MW turbine.

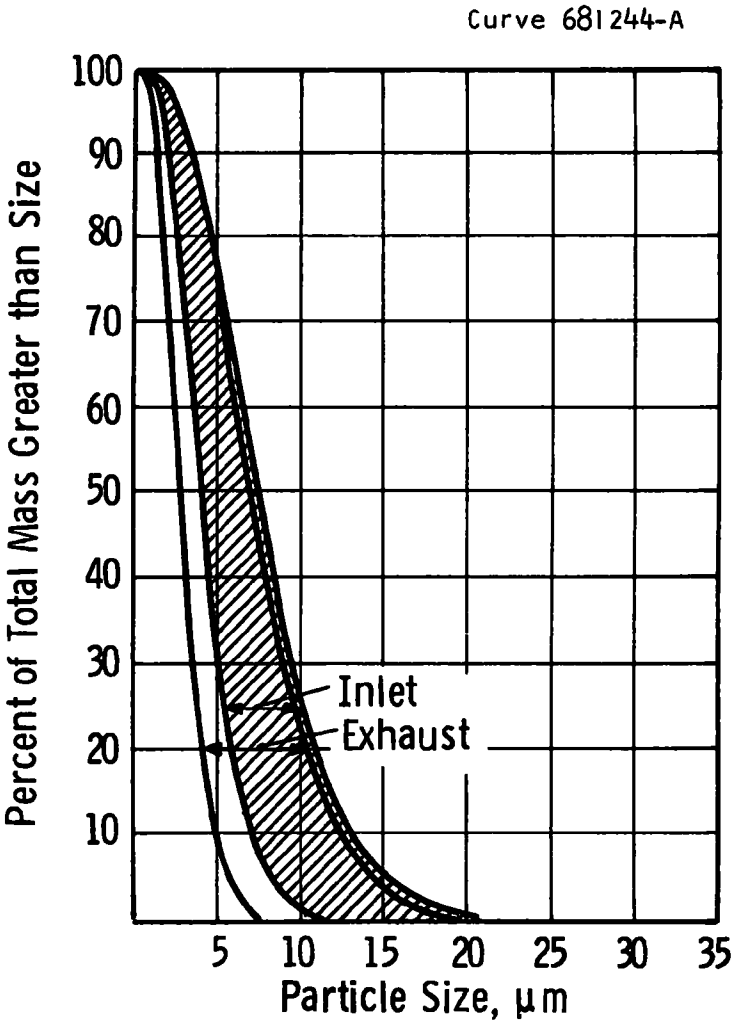

Figure J-3— Particle size distribution measured at entry and exhaust of Australian direct coal-fired gas turbine. Greta Seam Coal Test. Redesigned low gas velocity turbine-(Reference 1, Figure 122)

Table J-1

EXTRAPOLATED LIFE OF BLADING IN REDESIGNED LOW-VELOCITY AUSTRALIAN GAS TURBINE TESTS[a,b,c,d]

	Stators,hr	Rotors,hr
First stage	51,000	31,000
Second stage	25,000	52,000
Third stage	27,000	51,000

[a]Cobalt-based Stellite® Blades HS31.

[b]Design life of original Ruston Hornsby turbine,100,000 hr.

[c]Because of nonuniform ash distribution at entrance to the turbine, blade life is a function of position in the stator row: 5 blades in the second stator row had an estimated life between 10,000 and 15,000 hr; 2 blades in the first-stage stator row, 7 in the second, and 10 in the third had an estimated life between 15,000 and 20,000 hr.

[d]Interdepartmental Steering Committee. The Coal-Burning Gas-Turbine Project. Department of Minerals and Energy. Aeronautical Research Laboratories. Department of Supply. Australian Government Printing Service. Canberra, Australia. 1973. (Table 44).

To a first approximation erosion damage would be expected to be directly proportional to the particulate concentration in the gas being expanded by the turbine, and proportional to some power of the gas velocity leaving the turbine vanes. Empirical evidence has led to estimating this power dependence to be between the gas velocity cubed and the gas velocity to the fifth power. In addition,erosion damage would be expected to be a function of turbine rating because the particle size distribution of the ash is fixed; but as the turbine rating increases, the physical size of the gas passage becomes larger. Figure J-4 and J-5 illustrate this point, showing the trajectories of 9 μm diameter particles through geometrically similar first-stage stator vanes where all linear dimensions have been decreased by the scale factor "k". As the passage size shrinks, the fraction of the particles entering the channel which impact the pressure surface of the passage increases from about 35 percent in the full-scale stator vane to about 60 percent in half-scale passages (see also Figure J-6). The impact velocities and impact angles also change. As Figure J-7 demonstrates, impact velocities drop slightly as the passage is made smaller. This would tend to lower erosion damage in small turbines. Impact angles, however, increase, as seen in Figure J-8. In large turbines, trailing edge impacts tend to occur at grazing angles - about 6 degrees for the 9 μm diameter particles - as shown in Figure J-8. As the passage shrinks, these impact angles become greater, and in half-scale passages, 9 μm particles are now striking at incidence angles near 10 degrees. Erosion damage is a function of impact angle (as the data of Figure J-9 show), and damage rises rapidly as the impact angle changes from 0 toward 20 degrees. The net effect of the larger number of impacts, the slightly lower impact velocities, and the impact at more damaging angles of impact in the smaller passage would be to cause the full-scale machine to erode at about 80 percent of the rate of a half-linear-scale machine (Figure J-10).

To a first-order approximation, the erosion damage yielding acceptable life for the Australian machine was proportional to :

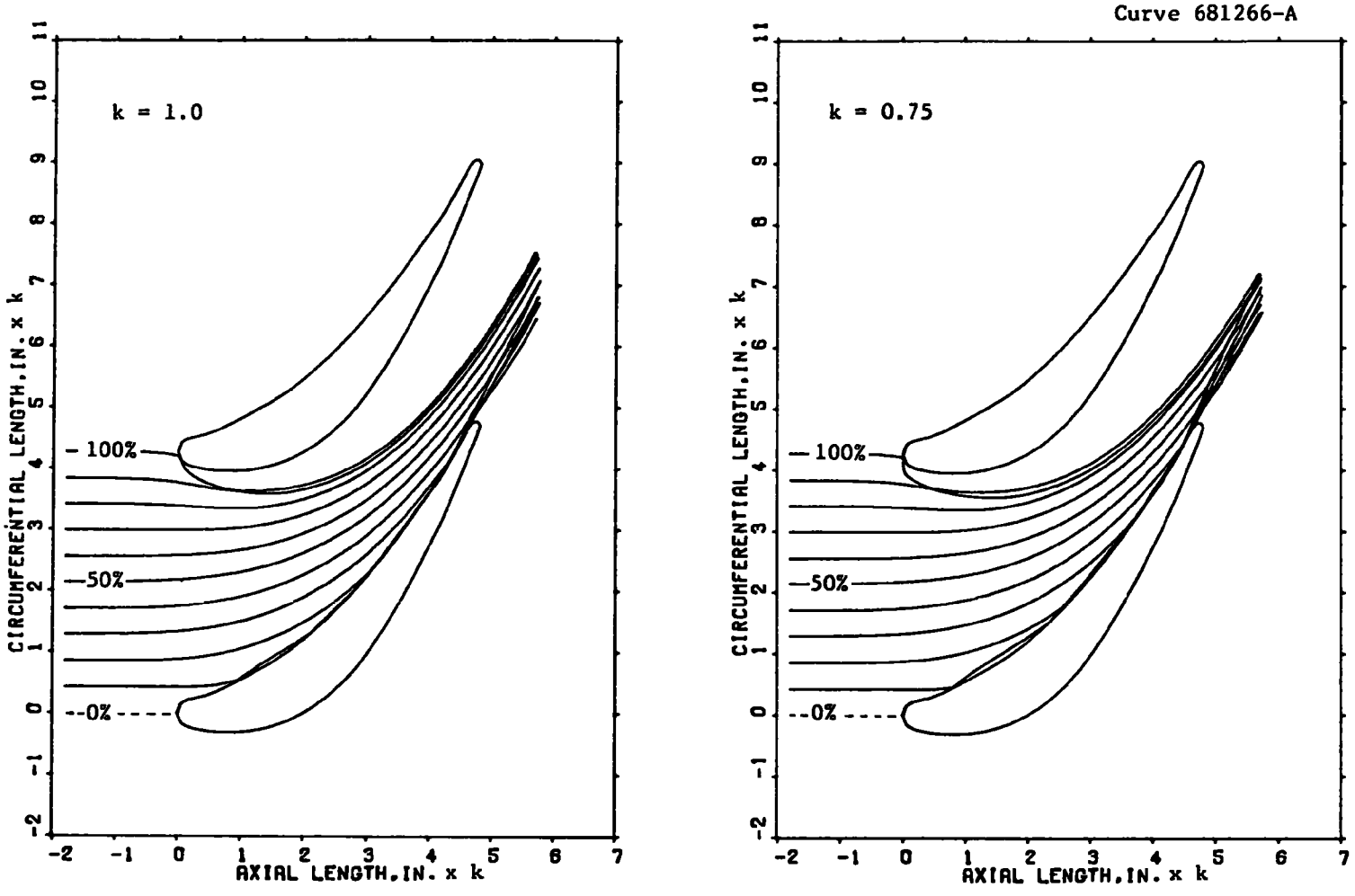

FIGURE J-4- 9 μm particle trajectories in full-scale and 3/4-scale stator passages

Curve 681265-A

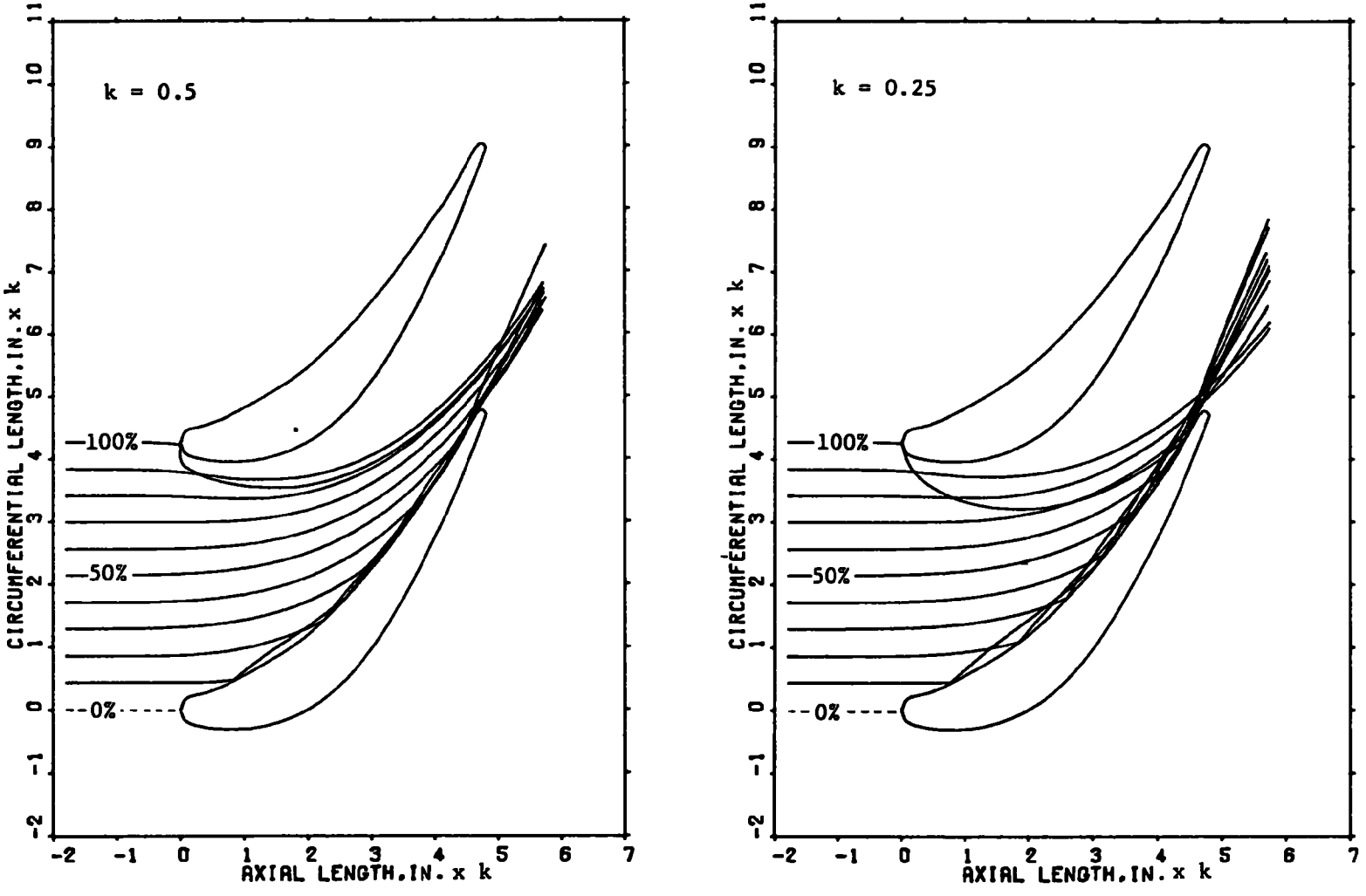

FIGURE J-5 - 9 μm particle trajectories in 1/2-scale and 1/4-scale stator passages

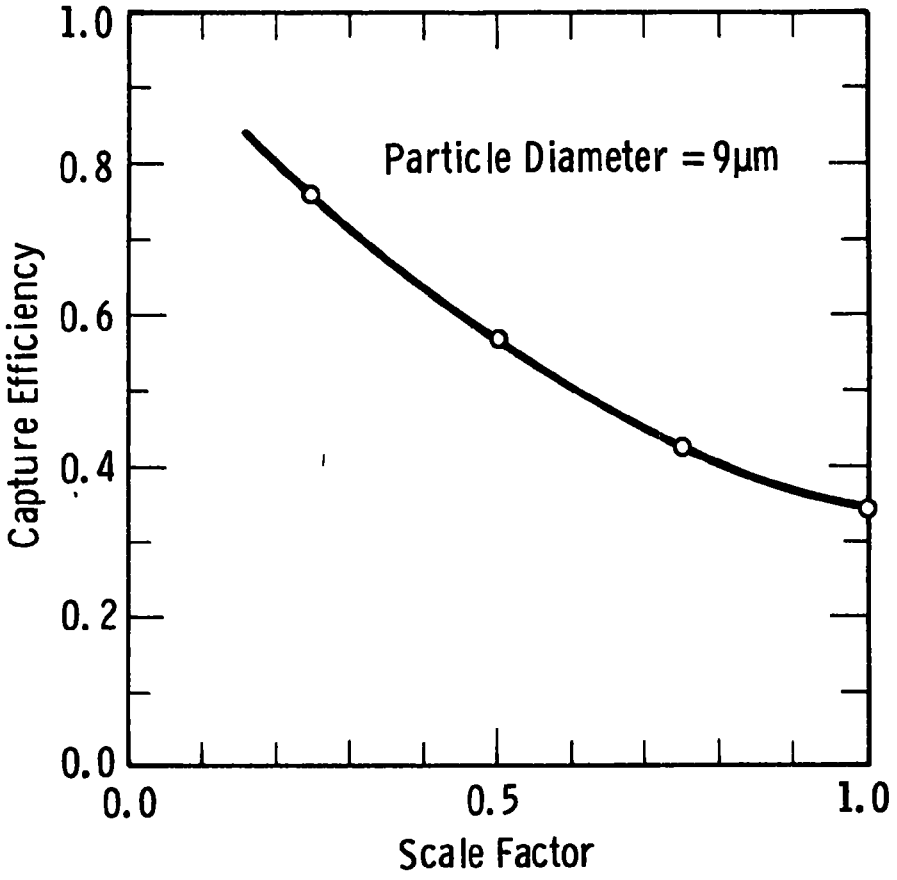

Figure J-6— Effect of scale factor on capture efficiency. (Capture efficiency = number of particles that hit blade surface/ total number of particles at inlet)

Curve 680257-A

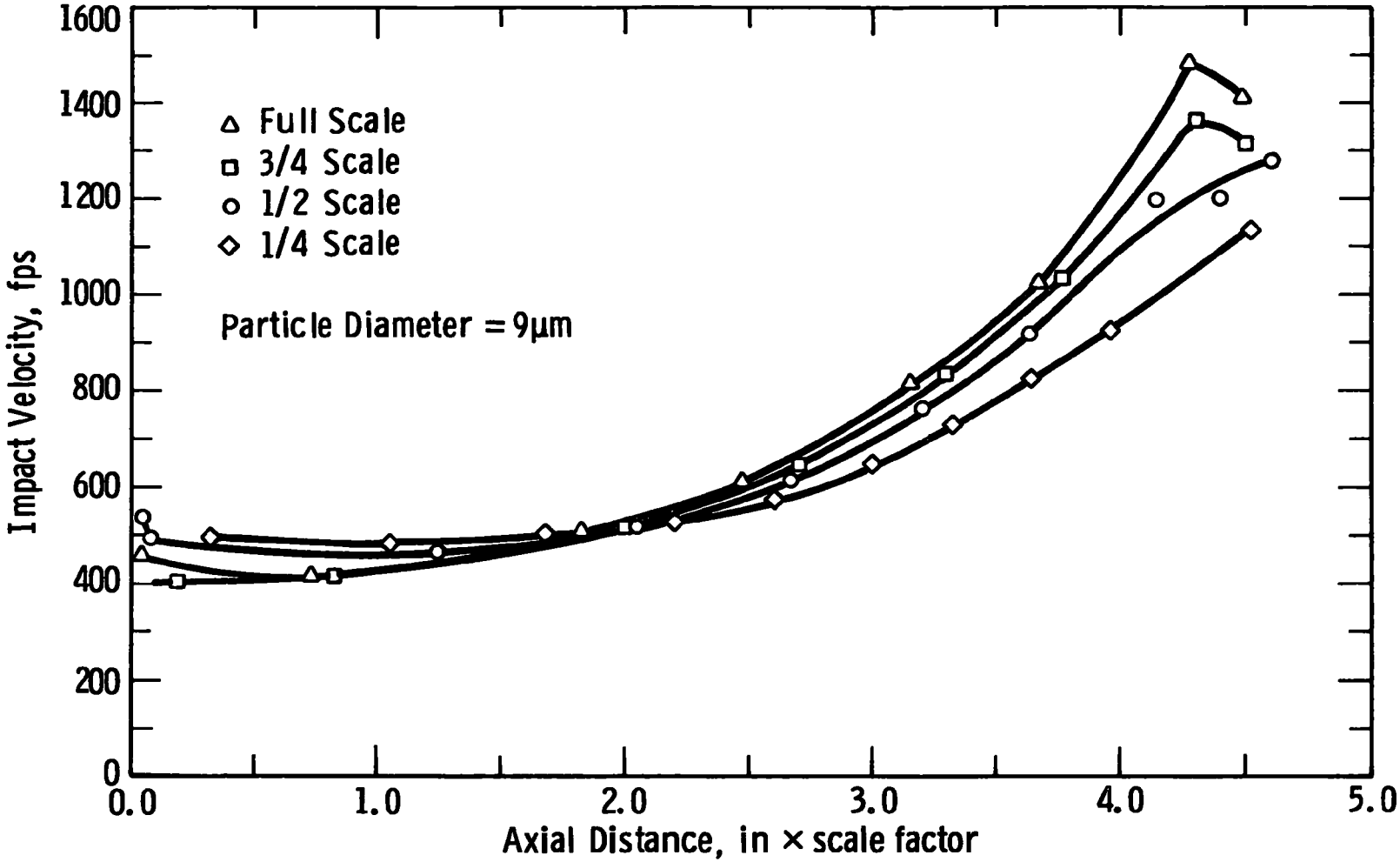

Figure J-7—Effect of scale factor on particle impact velocities

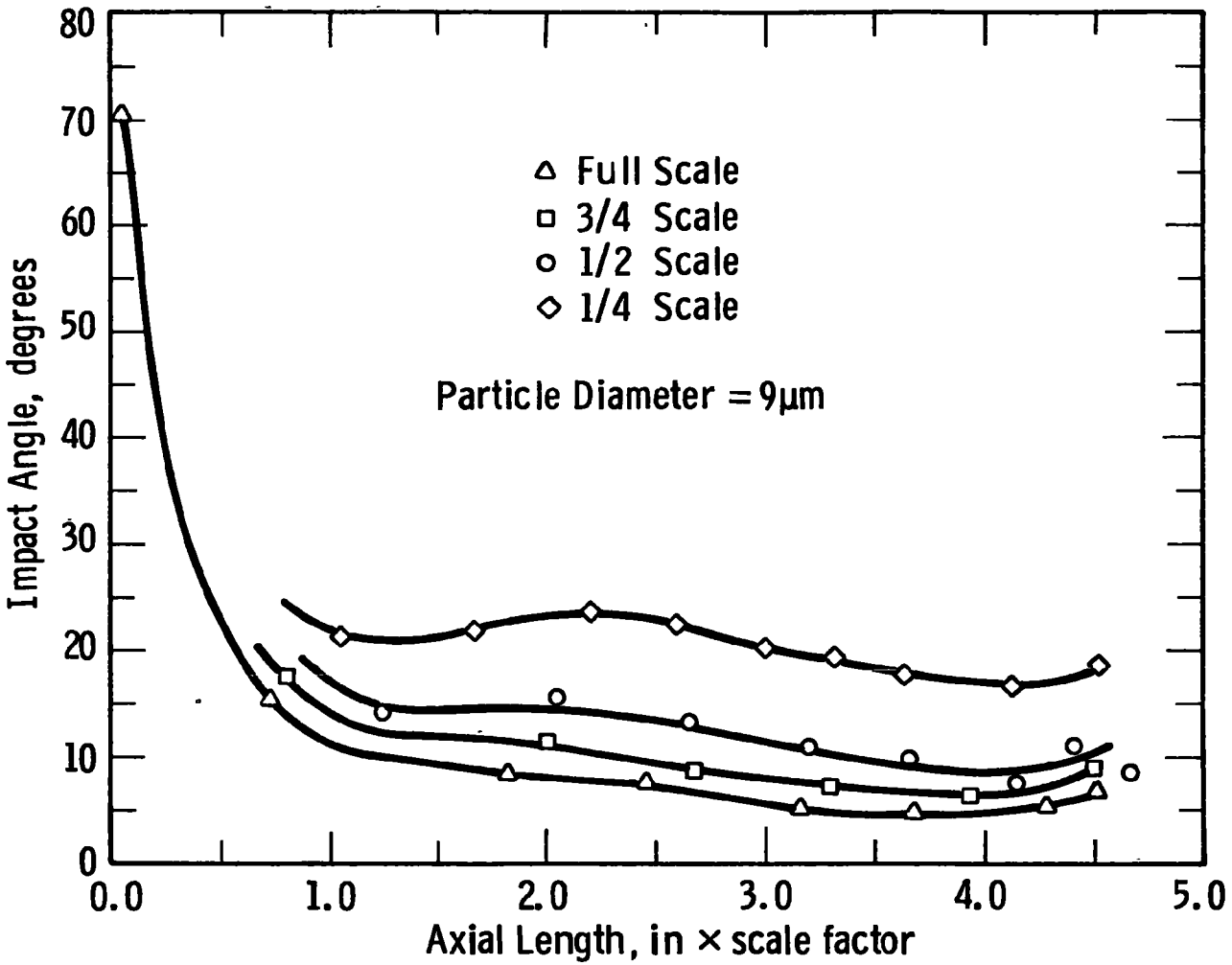

Figure J-8—Effect of scale factor on particle impact angles

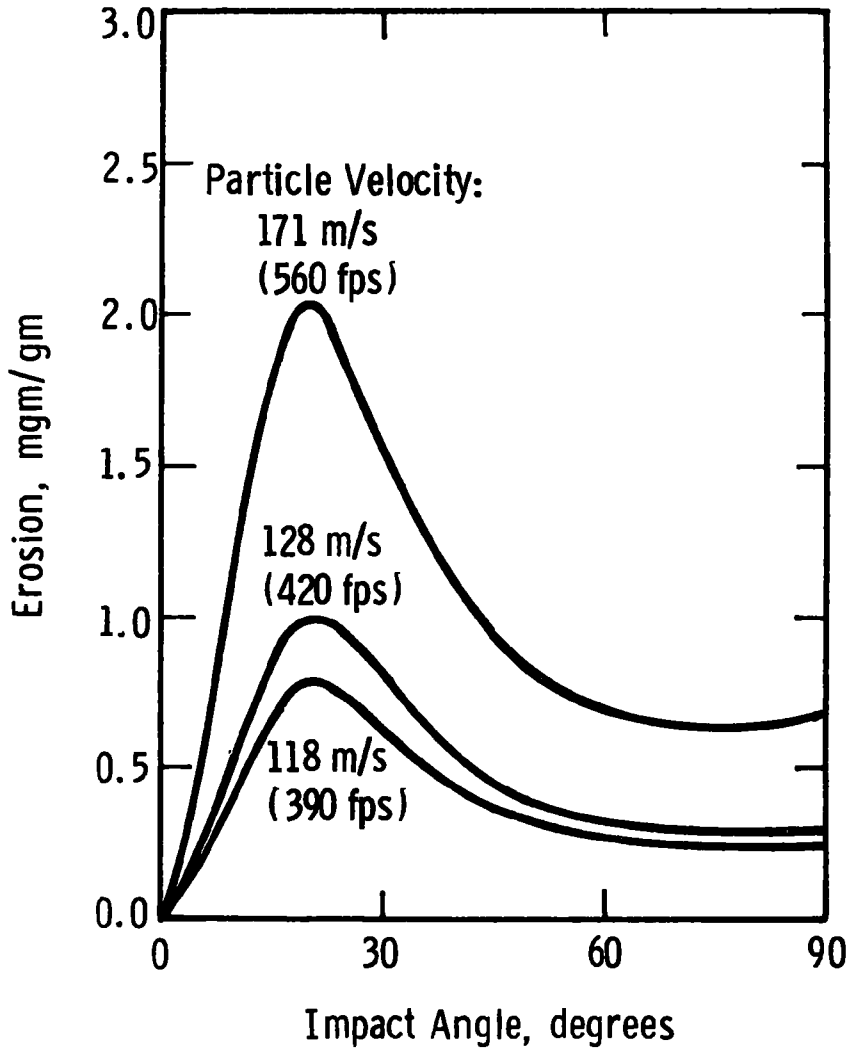

Figure J-9—Erosion results obtained for alumina particles impacting 2024 aluminum alloy [2]

Curve 680606-A

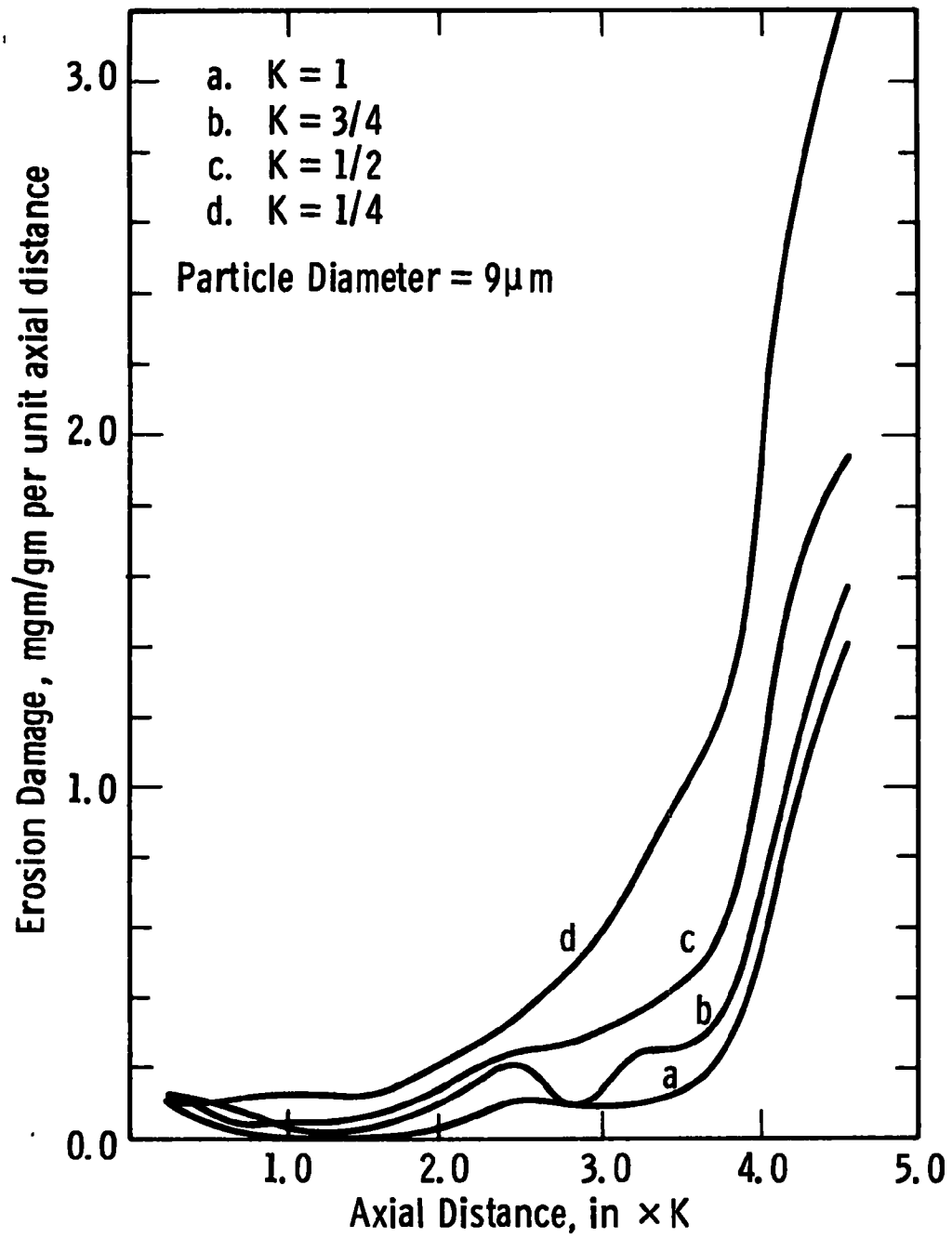

Figure J-10— Effect of scale factor on erosion rate in Ⓦ - 501 first-stage stator

$$\left.\begin{matrix}\text{Turbine Particulate} \\ \text{Erosion Damage}\end{matrix}\right\} \alpha \left(\begin{matrix}\text{Effect of} \\ \text{Machine Scale}\end{matrix}\right) \left(\begin{matrix}\text{Dust} \\ \text{Concentration}\end{matrix}\right)^1 \left(\begin{matrix}\text{Nozzle} \\ \text{Velocity}\end{matrix}\right)^3$$

$$\left.\begin{matrix}\text{Australian Direct Coal-} \\ \text{Fired Turbine Damage}\end{matrix}\right\} \alpha \left(1 \quad \left(7 \times 10^{-4} \frac{\text{kg dust}}{\text{kg gas}}\right)\right) \quad (240 \text{ m/s})^3.$$

And for the same life of blading in a 60 MW turbine:

$$\begin{matrix}\text{Large Electric Utility} \\ \text{Gas-Turbine Damage}\end{matrix} \quad \alpha \quad 0.80 \quad \left(\begin{matrix}\text{Acceptable Particulate} \\ \text{Concentration}\end{matrix}\right)^1 \quad (610 \text{ m/s})^3.$$

So that:

$$\left(\begin{matrix}\text{Acceptable Particulate} \\ \text{Concentration}\end{matrix}\right) = \frac{1 \quad (7 \times 10^{-4}) \quad (240)^3}{0.8 \qquad\qquad (610)^3}$$

$$= \left(1.25\right)\left(7 \times 10^{-4}\right)\left(6.4 \times 10^{-2}\right)$$

$$= 6 \times 10^{-5} \frac{\text{kg of dust}}{\text{kg of expansion gas}} .$$

And since a kilogram of turbine expansion gas occupies about 0.74 m^3, this corresponds to a permissible particulate loading in the turbine expansion gas of $8 \times 10^{-5} \frac{\text{kg}}{\text{sm}^3}$ (4×10^{-2} gr/scf).

If we had considered erosion damage proportional to the fifth power of velocity, the allowable particulate concentration would have been:

$$\left.\begin{matrix}\text{Acceptable Particulate} \\ \text{Concentration}\end{matrix}\right\} \alpha \quad \left(\frac{1}{0.8}\right)\left(7 \times 10^{-4} \frac{\text{kg dust}}{\text{kg gas}}\right) \quad \frac{(240 \text{ m/s})^5}{(610 \text{ m/s})^5}$$

$$= 9 \times 10^{-6} \frac{\text{kg dust}}{\text{kg gas}} .$$

This is almost an order of magnitude lower.

These rule-of-thumb extrapolations have indicated that large electrical utility gas turbines might be operated with acceptable blade life at 10 to 100 times the current allowable particulate loadings in the expansion gas- 5×10^{-4} gm/m^3 (2×10^{-4} gr/scf).

To assess the reliability of these estimates the following factors must be considered:

- Erosivity of the coal ash from the fluid bed combustion process - friable platelets of alumino silicate ash mineral matter - is expected to be much less than that of the direct coal-fired ash. The erosivity of the sulfated, half-calcined, dolomite sulfur sorbent is not known. The first factor would make the estimate conservative. Hard data on the erosivities of the expected particulates impacting turbine materials at the correct particle and metal temperatures are needed.

- The rule of thumb that turbine erosion damage is proportional to gas velocity raised to a power between 3 and 5 is based on limited experience with small turbines. Particle velocities at impact deviate substantially from the gas velocities, and secondary flows in the turbine passage act to change the local particle concentrations in the flow path. To replace this rule-of-thumb estimate with more reliable data, we are calculating erosion damage from a model that calculates the particle trajectories through the turbine, accounting for:

  - The development of the fluid boundary layers on the vane and blade surfaces and on the hub and outer casing end-walls of the turbine

  - The development of the passage vortices

  - The radial flows which occur in the wakes of the vane and blades due to the higher gas pressures at the outer casing wall as compared to the hub of the machine

- The decrease in gas velocity in the blade and vane wakes.

Figure J-11 shows a typical trajectory produced by the program. Top and side views of a 60 MW turbine first-stage stator and rotor are given. In addition to the hardware boundaries, the computer has printed out the boundaries of the regions in which boundary-layer models and blade-wake models are used to calculate the gas flow. The passage vortex flow, which is a function of the turning of the gas flow in the blade passages and the thickness of the end-wall boundary layers, is acting on the particles in both the vane and blade passage. The particle trajectory is shown both in fixed and rotating coordinate systems. Printed program output (not shown) provides the angle and velocity of the particles before and after impact. The program is written to accept experimental data on impact characteristics. Figures J-12 and J-13 show the trajectories of a 6 μm particle through the first stage of the turbine for two differing inlet positions of the particle. These trajectories show the effect of the radially inward gas flow in the blade wakes on the particles. Westinghouse is now adding an erosion damage prediction subroutine and is improving its main gas-flow models to provide a particle trajectory model capable of predicting erosion and deposition damage rates. This model will be used to establish more reliable specifications for the turbine particulate tolerance. It should also be useful in investigating the effectiveness of deposition and erosion control techniques.

TURBINE DESIGN

To preserve high efficiency in a pressurized fluid bed combustor system it is necessary to transfer the 1013 to 1520° kPa (10 to 15 atm), 871 to 927°C (1600 to 1700°F) hot gases leaving the dust collection system directly to the gas turbine for expansion. Various design configurations to accommodate thermal expansion, to control leakage, and to provide a uniform distribution of particulates over the flow channel of the turbine have been suggested. Operating experience is available from European compound-cycle power plants utilizing one or

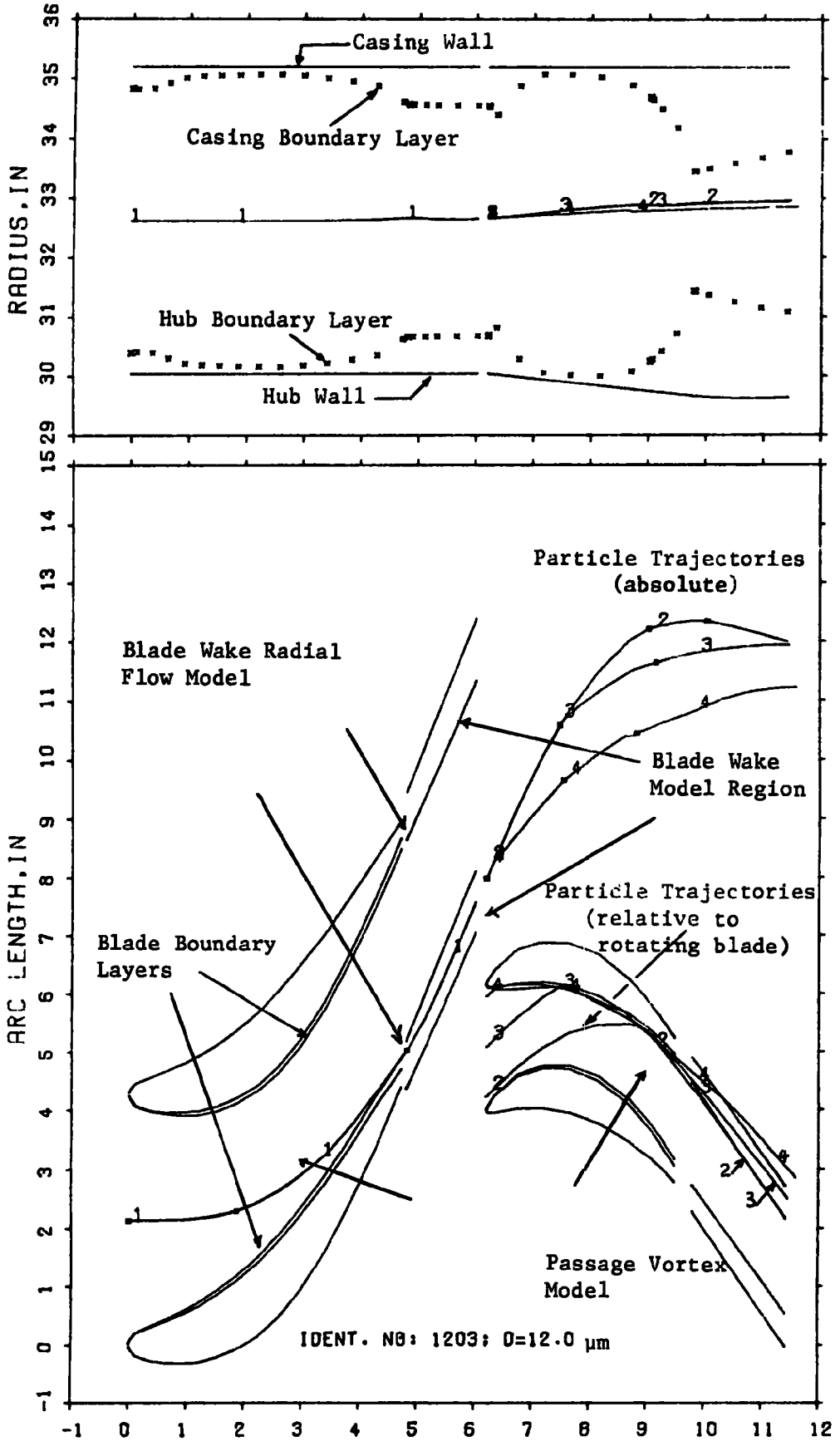

Figure J-11 - Trajectory of a 12 μm diameter particle through first-turbine stage

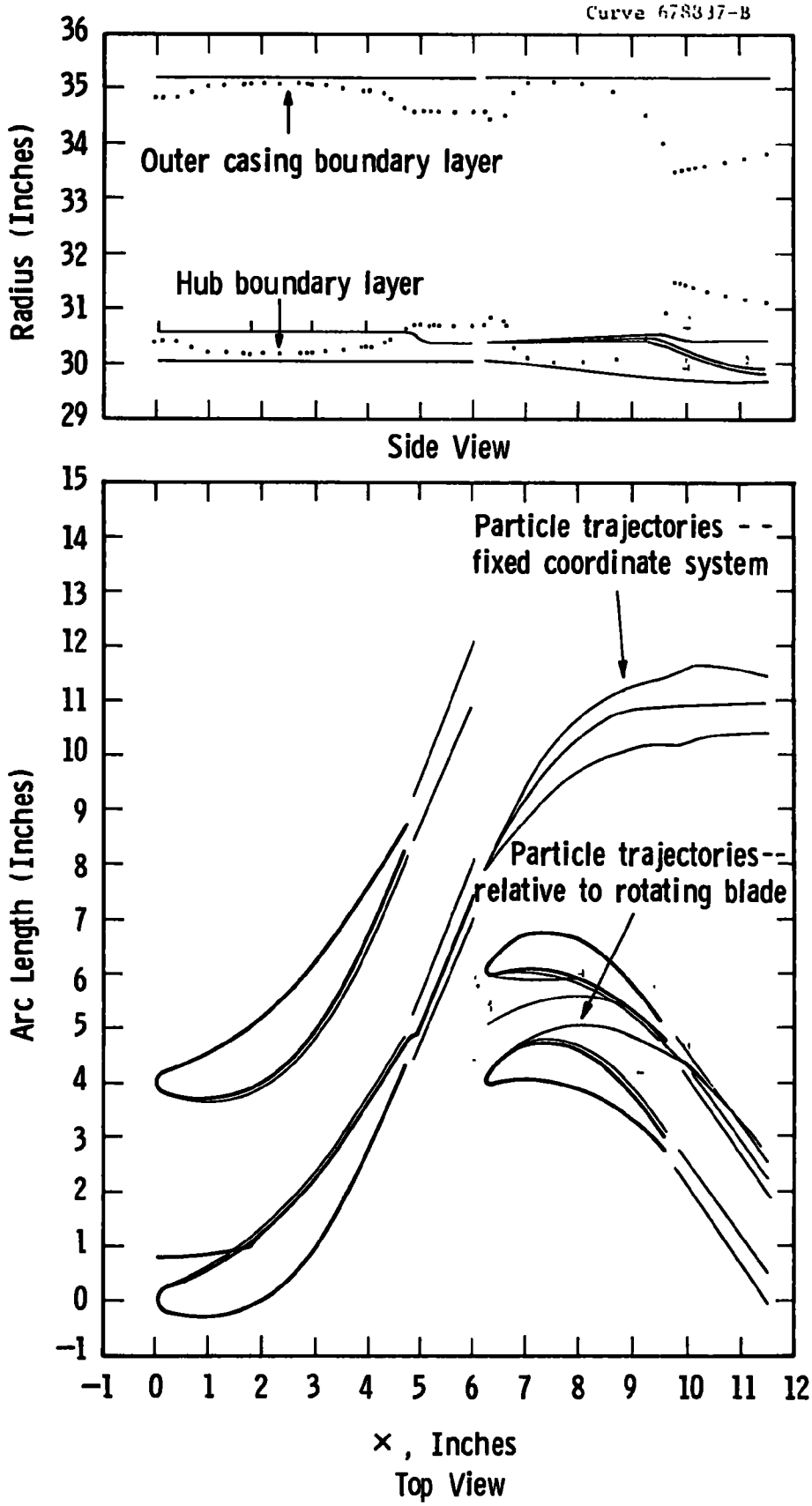

Figure J-12—Trajectory of a 6 μm particle through the first-turbine stage

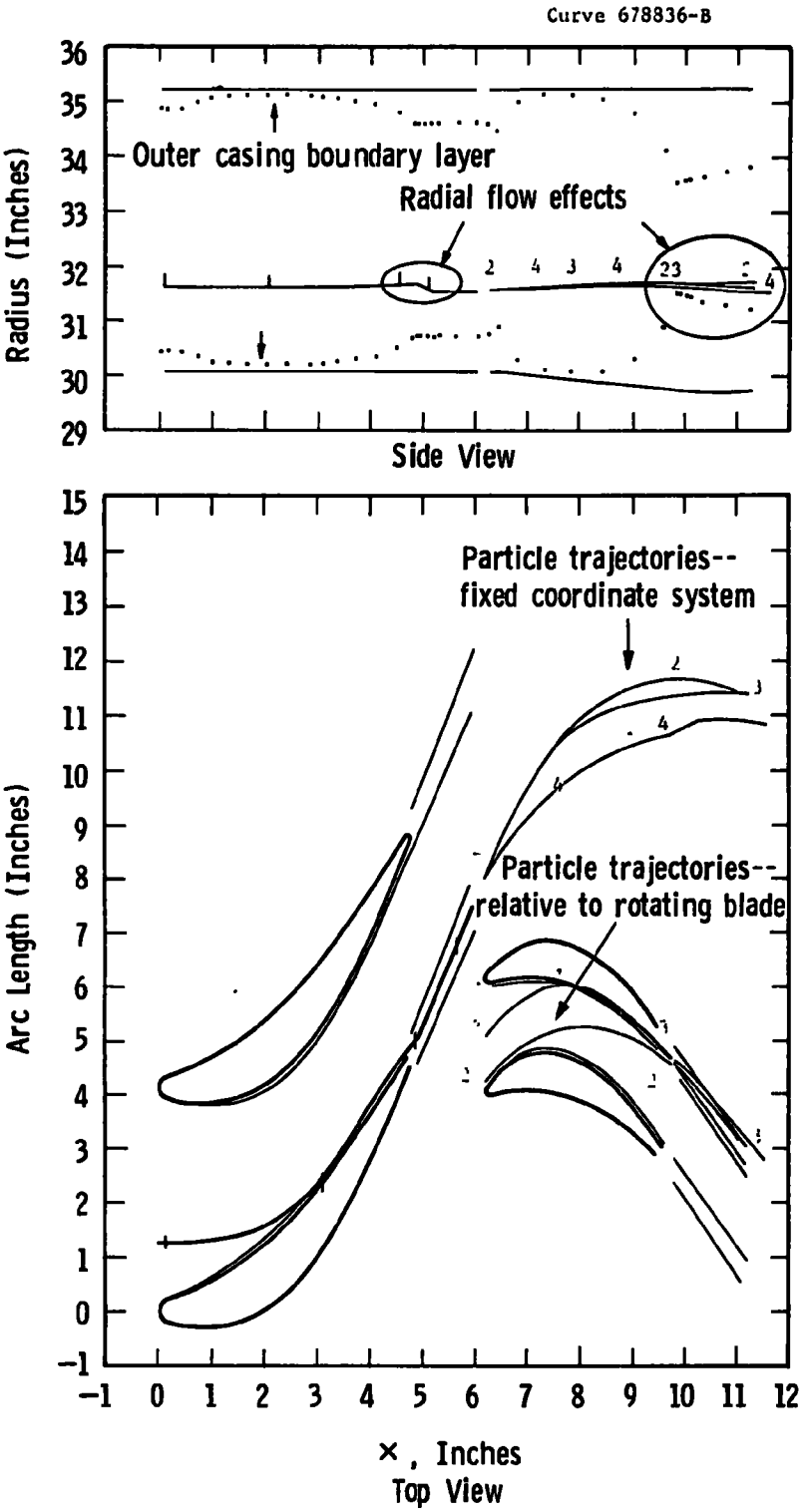

Figure J-13—Trajectory of a 6 μm particle injected nearer to mid-span and mid-pitch of the blade passage. Note the decreased effect of the radial flow at the trailing edges of both the stator vane and blade on the radial displacement of the particle as it leaves.

two high-pressure connections to the turbine. These installations have generally delivered hot gas at turbine inlet temperatures between 700 and 760°C (1300 and 1400°F),in other words, about 300°C (500°F) below the turbine inlet temperatures currently used in Westinghouse industrial gas turbines. Westinghouse Gas Turbine Division engineers have prepared a preliminary design using external manifolding to distribute hot gases around the annulus of our W501 (60 MW electric) turbine.[3,4] This design had the objective of avoiding distortion of the turbine casing by nonuniform temperature distributions which they feared would be associated with a single hot-gas distributor.

Further design work to assess the technical problems associated with these designs, improving them, and developing reliability and economic estimates of alternative constructions are required. The initial and advanced designs will then require tests on an integrated combustor-turbine system.

Past experience[5-7] with gas turbines expanding dust-containing gases indicate design modifications that may be helpful in avoiding life-limiting erosion of turbine hardware. Of special concern are design features in the turbine which may cause localized concentrations of the dust in regions susceptible to erosion attack. A turbine design is needed that:

- Provides for uniform distribution of the dust-laden gas over the inlet flow channel
- Directs particle flows in blade and vane wakes to avoid raising the erosion potential of dust at blade and vane roots
- Uses stepped sidewalls, carbide wear-resisting inserts, and/or cooling air injection as appropriate to protect blade and vane roots from erosion damage
- Appropriately thickens and hard-faces blade tips to resist erosion damage

- Incorporates spray systems and drains, and provides for injection and removal of milled nut shells for washing and cleaning of blade and vane surfaces without the need to open the turbine
- Lowers velocity of gases in the turbine, if required, to achieve satisfactory erosion life.

In order to realize the full potential of pressurized fluidized bed combustion systems, work must continue to:

- Develop commercial gas-turbine designs
- Carry out analytical and laboratory tests to understand turbine tolerance to corrosion, erosion, and deposition
- Obtain data on large-scale integrated fluidized bed combustor, particulate control, and turbine test systems.

REFERENCES

1. Interdepartmental Steering Committee. The Coal-Burning Gas Turbine Project. Department of Minerals and Energy. Aeronautical Research Laboratories. Department of Supply. Australian Government Printing Service. Canberra, Australia. 1973.

2. Grant,G.,and W. Tabakoff. Erosion Prediction in Turbomachinery Due to Environmental Solid Particles. AIAA Paper No. 74-16. AIAA 12th Aerospace Sciences Meeting. Washington, D. C. January 1974.

3. Archer, D. H., et al. Evaluation of the Fluidized Bed Combustion Process. Office of Air Programs. Westinghouse Research Laboratories. Pittsburgh, Pa. November 1971. NTIS PB 211-494, 212-916, 213-152.

4. Keairns, D. L., J. R. Hamm, and D. H. Archer. Design of a Pressurized Fluidized Bed Boiler Power Plant. AIChE Symposium. Series 126, 68: (1972).

5. Smith, J., R. W. Cargill, D. C. Strimbeck, W. M. Nabors, and J. P. McGee. Bureau of Mines Coal-Fired Gas Trubine Research Project - Test of New Turbine Blade Design. Bureau of Mines. U. S. Department of Interior. RI 6920. 1967.

6. Stettenbenz, L. M. Minimizing Erosion and Afterburn in the Power Recovery Gas Turbine. Oil and Gas Journal. 68:65-70, 1970.

7. Atkin, M. L. Australian Coal-Burning Unit. Gas Turbine International. September-October 1969. pp. 32-36.

APPENDIX K

GAS TURBINE CORROSION/EROSION PILOT-PLANT TEST PROGRAM

APPENDIX K

GAS TURBINE CORROSION/EROSION PILOT-PLANT TEST PROGRAM

INTRODUCTION

Exxon Research and Engineering is under contract to EPA for the design, construction, and operation of a small-scale, high-pressure, fluidized-bed boiler, 0.63 MW-equivalent miniplant to obtain information for the design of a high-pressure fluidized bed boiler demonstration plant. Westinghouse was responsible for designing and constructing an erosion/corrosion test rig for installation in the discharge line from the miniplant. The test rig was shipped in October 1973; minor modifications have been made at Exxon. In addition, Westinghouse is responsible for formulating a plan for the erosion/corrosion rig tests.

This appendix

- Discusses the technical basis for the design of the erosion/corrosion test rig
- Describes the test rig in detail
- Describes the apparatus and procedures for sampling particulates
- Presents a plan for tests to be conducted in the test rig
- Describes an analytical procedure for interpreting the test results.

BACKGROUND INFORMATION

The design conditions for the Exxon high-pressure fluidized bed boiler miniplant are as follows:

- Pressure - 1013 kPa (10 atm)
- Products temperature - 870 to 927°C (1600 to 1700°F)

- Airflow rate - 0.680 kg/s (1.5 lb/sec)
- Coal feed rate - 0.059 kg/s (0.13 lb/sec)
- Products flow rate - 0.739 kg/s (1.63 lb/sec)
- Gaseous products molecular weight - 29.0

Two stages of cyclone separators are located in the discharge line from the fluid bed combustion miniplant. Exxon has estimated that the concentration of fly ash in the product gases from the second-stage cyclone will be 0.0224 kg/m^3 (1.40×10^{-3} lb/ft^3) and that the size distribution of these particles will be as shown in Figure K-1.[1] No estimate has been made of the concentration or size distribution of the sorbent particles which will probably be present in the combustion products because of the attrition of the bed material.

The target for maximum solids concentration in the gas stream at the inlet to a Westinghouse gas turbine is as follows:[2]

Total Solids - 3.43 E-04 kg/sm^3 (< 0.15 gr/scf)

Particles > 2 μm - 2.88 E-05 kg/sm^3 (< 0.01 gr/scf)

Experience with erosion in gas turbines indicates that the erosion caused by particles with diameters less than 2 μm is negligible and that the allowable concentration of particles with diameters greater than 2 μm should be less than about 2.288×10^{-5} kg/sm^3 (0.01 gr/scf). At a pressure of 1013 kPa (10 atm) and a temperature of 870°C (1600°F), the above concentrations are equivalent to 0.881×10^{-3} kg/m^3 (0.055×10^{-3} lb/ft^3) total solids and 0.0593×10^{-3} kg/m^3 (0.0037×10^{-3} lb/ft^3) solids over 2 μm diameter.

For the high-pressure fluidized bed boiler system preliminary design presented in Reference 3, the estimated concentration of total solids in the gas-turbine inlet was 0.737×10^{-3} kg/m^3 (0.046×10^{-3} lb/ft^3) with the size distribution given in Figure K-1.[3] This gives a concentration of 0.0737×10^{-3} kg/m^3 (0.0046×10^{-3} lb/ft^3) solids over 2μm

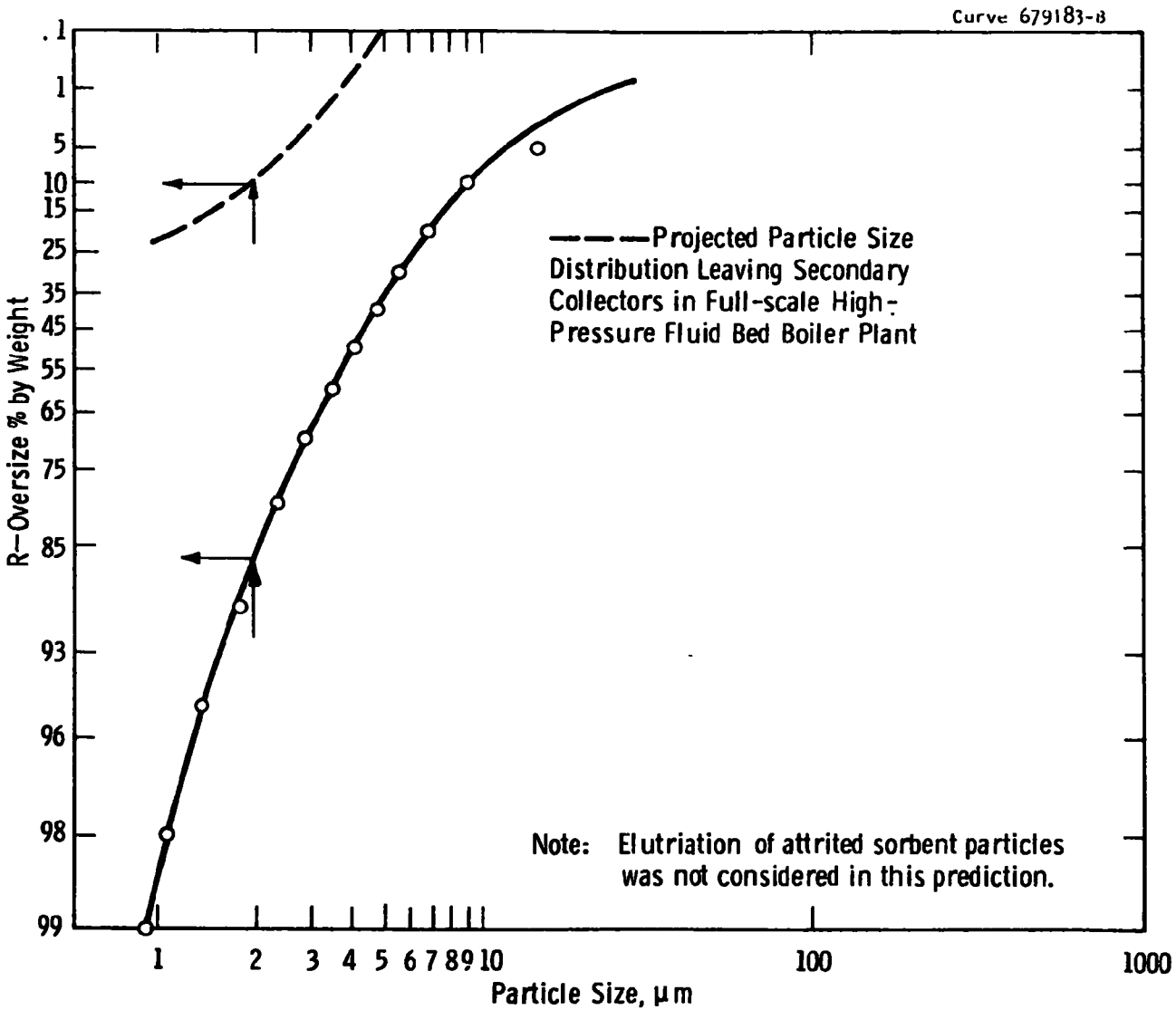

Figure K-1—Predicted size distribution of coal ash particles escaping from secondary cyclones in the Exxon miniplant

diameter. These values were subsequently revised to values approximately three times those originally estimated.[4]

Table K-1 compares the specified preliminary design and revised preliminary design concentrations with the predicted concentration of ash particles in the Exxon miniplant. The original predicted concentrations for the high-pressure fluidized bed boiler are essentially equal to the specified values, and the revised values are about three times the original. The estimated total ash concentration for the Exxon miniplant is about 25 times the specified level and 10 times the revised design level. For those particles greater than 2 μm in diameter the predicted concentration for the Exxon miniplant is over 300 times the specified value and almost 100 times the revised design value. The expected addition of attrited sorbent particles to the ash particles in the Exxon miniplant will increase these ratios to even higher values.

One possible method for reducing the solids concentrations in the Exxon miniplant is the addition of a third-stage separator. In order to reduce the total solids concentration to the revised system design value, this separator would have to have an efficiency of 90 percent. A 96 percent efficient third-stage separator would be required to reduce the concentration to the specification level.

A second possible method of reducing the solids concentration in the gas stream going to the erosion test rig is by diluting it with products of combustion of a clean fuel at the same temperature level.

The use of a sorbent for in-bed sulfur removal in the fluidized bed combustion of coal limits the temperature of the bed to 927 to 982°C (1700 to 1800°F). With bed temperatures of this level in the high-pressure boiler, the temperature of the products of combustion going to the gas turbine will be in the range of 871 to 927°C (1600 to 1700°F). This temperature level coincides with the maximum temperature for uncooled first-stage turbine vanes. In this application, therefore, the first-stage turbine vanes would most likely be uncooled, and the vane and blade materials would both be operating at near gas-stream temperatures.

With the conditions which prevail at the discharge of the miniplant (871°C/1600°F, > 15 percent excess air), all turbine vane and blade

Table K-1

COMPARISON OF PARTICULATE CONCENTRATIONS AT GAS-TURBINE INLET[a]

	Target for HPFBB[b]	HPFBB design[c]	Revised HPFBB design[d]	Exxon miniplant[e]
Total, kg/m^3 (lb/ft^3)	0.83×10^{-3} (0.055×10^{-3}) [1.0]	0.74×10^{-3} (0.046×10^{-3}) [0.83]	2.24×10^{-3} (0.14×10^{-3}) [2.5] [1.0]	22.4×10^{-3} (1.40×10^{-3}) [25.5] [10.1]
Particles > 2 μm, kg/m^3 (lb/ft^3)	0.059×10^{-3} (0.0037×10^{-3}) [1.0]	0.074×10^{-3} (0.0046×10^{-3}) [1.24]	0.22×10^{-3} (0.014×10^{-3}) [3.8] [1.0]	19.2×10^{-3} (1.20×10^{-3}) [325] [186]

[a] Conditions - 1013 kPa (10 atm) and 1127°C (2060°F).

[b] Evaluation of Fluidized Bed Combustion Process. Office of Research and Monitoring. Environmental Protection Agency. Westinghouse Research Laboratories. Pittsburgh, Pa. November 1971. Vol. II, p. 156.

[c] Ibid, p. 285.

[d] Yang, W. C., and D. L. Keairns. Particulate Removal Studies from High-Temperature, High-Pressure Gases. Westinghouse Laboratories. Pittsburgh, Pa. Report 73-9E3-COCLN-R1, April 25, 1975.

[e] Letter from M. S. Nutkis to J. R. Hamm dated August 8, 1973.

materials will be oxidized. If no corrosive contaminants are present in the gas stream and the velocity is low, a stable oxide film of 50 μm or more thickness will be formed in a period of about 50 hours, and the metal recession rate will approach zero. The metal oxidation rate is parabolic with time because of the diffusion characteristics of the oxide films.

If contaminants are present which cause the oxide film to spall, the oxide film will not stabilize and the recession of base metal will continue indefinitely. High-velocity gas streams can have similar effects on the oxide film. NASA-Lewis has conducted oxidation tests, wherein sonic jets of clean gas impinged on the metal surface, which showed that metal recession rates did not diminish with time.[5]

The presence of particulates in high-temperature gas streams will have a similar effect on the oxide films on turbine vanes and blade materials. If the erosion rate is high, so that the metal oxide is removed as soon as it is formed, erosion of the base metal will occur, and the metal recession will be due to the combined effects of the base metal oxidation rate and the particle erosion. If the erosion rate is low enough so that a minimal oxide film can be maintained, the film thickness will range between near zero and the stable film thickness. Metal recession will be due to oxidation, and erosion will take place in the oxide film rather than in the base metal. The rate of metal recession will be a function of the oxide film thickness under equilibrium conditions.

Erosion of solids by particulates in gas streams is primarily a function of the impact velocity and the physical characteristics of both the particles and the solid. The impact angle for maximum wear rate is a function of the target material type. Brittle materials have maximum rates at impact angles near 90 degrees and ductile materials at near 30 degrees. The turbine vane and blade materials which will be used in the erosion tests are typically ductile materials. The metal oxides which form on these materials are brittle at low temperatures. Their characteristics at operating temperatures, however, are not well known.

DESIGN OF THE EROSION/CORROSION TEST RIG

The initial concept of the static erosion test rig was patterned after the design used by the British Coal Utilization Research Association (BCURA) and is shown in Figure K-2. A cascade of turbine vanes is installed in a duct with typical vane inlet conditions. Targets are placed in the high-velocity gas stream downstream of the vane cascade which simulates the conditions at the leading edge of the turbine blades. These targets are placed normal to the vane axes so that a representative sample of the average conditions for the moving blades can be obtained. The use of multiple vanes and targets permits the simultaneous testing of several turbine vane and blade materials.

A test rig of this type was designed for the conditions in the Exxon miniplant (see Figure K-3). The complete drawing list for this rig is as follows:

- General assembly 4879D29
- Outlet assembly 256C008
- Outlet welding assembly 4879D32
- Outlet elbow assembly 255C987
- Inlet assembly 255C986
- Blade pack detail and assembly 4879D31
- Insert details 255C988
- Line details 4879D31

R. W. Hornbeck[6] made studies of particle dynamics in a turbine stage, which showed that the size of turbine vanes and blades has a substantial effect on the trajectory of particles within the turbine stage and, therefore, would affect the factors which control erosion. A cascade of the type shown in Figure K-3 with four free-standing vanes has vanes which are considerably smaller than those in current utility-type gas turbines when designed for Exxon test conditions. Even if the number of free-standing vanes were reduced to one or zero, the vane size would be unrealistically small.

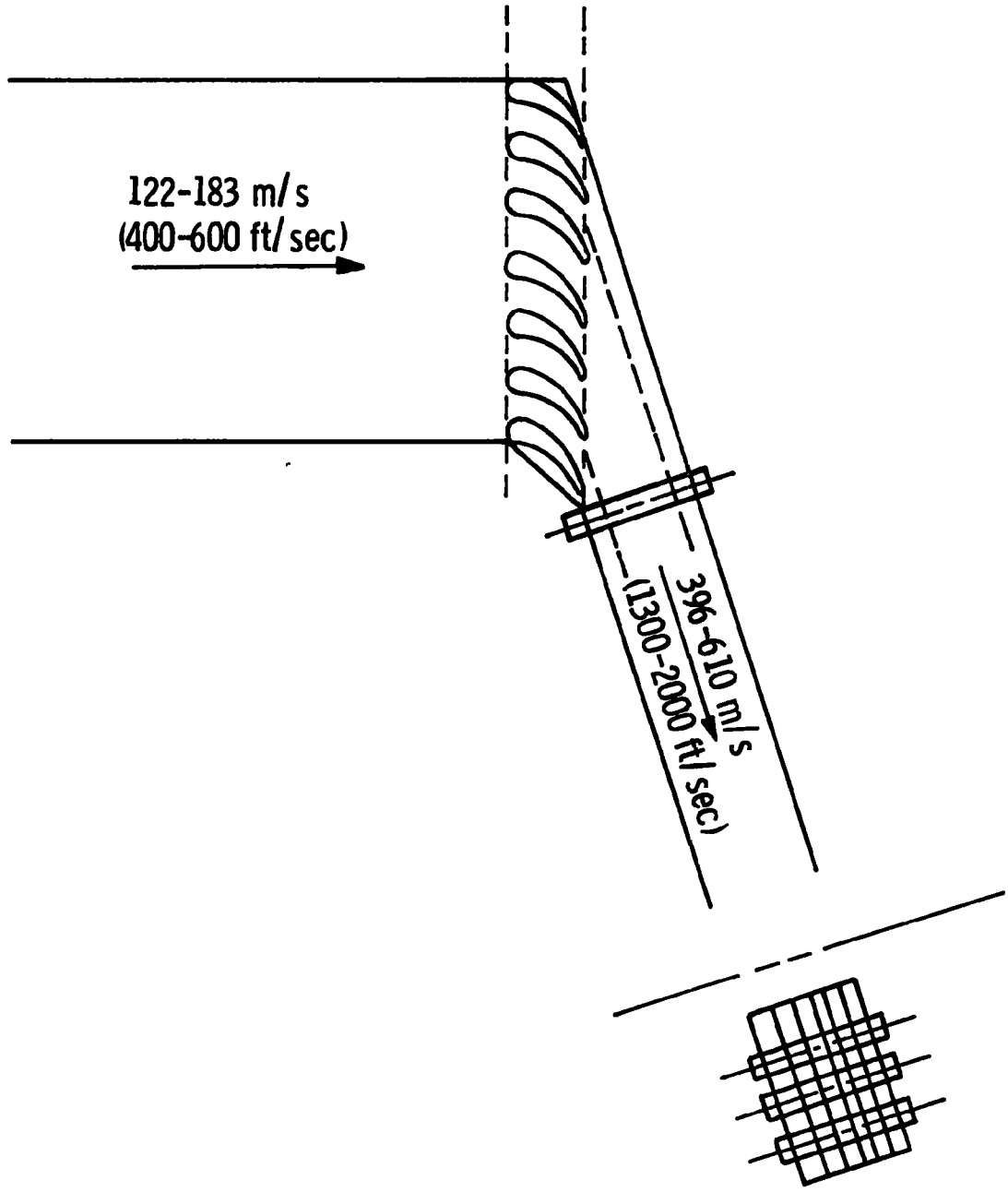

Figure K-2- Cascade type erosion test rig

PAGE NOT

AVAILABLE

DIGITALLY

The minimum practical diameter for a cylindrical target is considered to be about 6.35 mm (1/4 in). With four free-standing vanes only one target of this diameter can be used without causing choking at the target; with no free-standing vanes two 6.35 mm (1/4 in) targets could be used.

Since the results obtained on a cascade rig for the Exxon miniplant would be of questionable value because of the reduced scale, and simultaneous testing of several vane and blade materials would not be possible, it was concluded that a cascade-type erosion test rig was not feasible for this application. A straight-through erosion/corrosion test rig, therefore, was designed for the Exxon miniplant conditions (see Figure K-4). The complete list of drawings for this test rig is as follows:

	Dwg. No.	Figure No.
• Test section assembly	256C112	K-4
• Test rig assembly	256C111	K-5
• Inlet elbow assembly	256C113	K-6
• Outlet elbow assembly	256C114	K-7
• Straight run assembly	724B684	K-8
• Liner details	4880D54	K-9
• Liner details	4879D31	K-10
• Cylindrical target detail	6208A13	K-11
• Wedge target detail	6213A46	K-12
• Cooled target detail	6213A44	K-13

The straight-through erosion test rig consists of a bell-mouth nozzle followed by a length of straight duct to provide adequate time for the particles to accelerate to near gas-stream velocity ahead of the target. Here, again, a 6.35 mm (1/4 in) diameter cylinder is considered to be the minimum practical size for the erosion target. A 6.35 mm (1/4 in) diameter target located in the straight section would limit the velocity to less than 457 m/s (1500 ft/sec) because of choking in the plane of the target. Since this velocity is too low, the erosion target

PAGE NOT

AVAILABLE

DIGITALLY

PAGE NOT

AVAILABLE

DIGITALLY

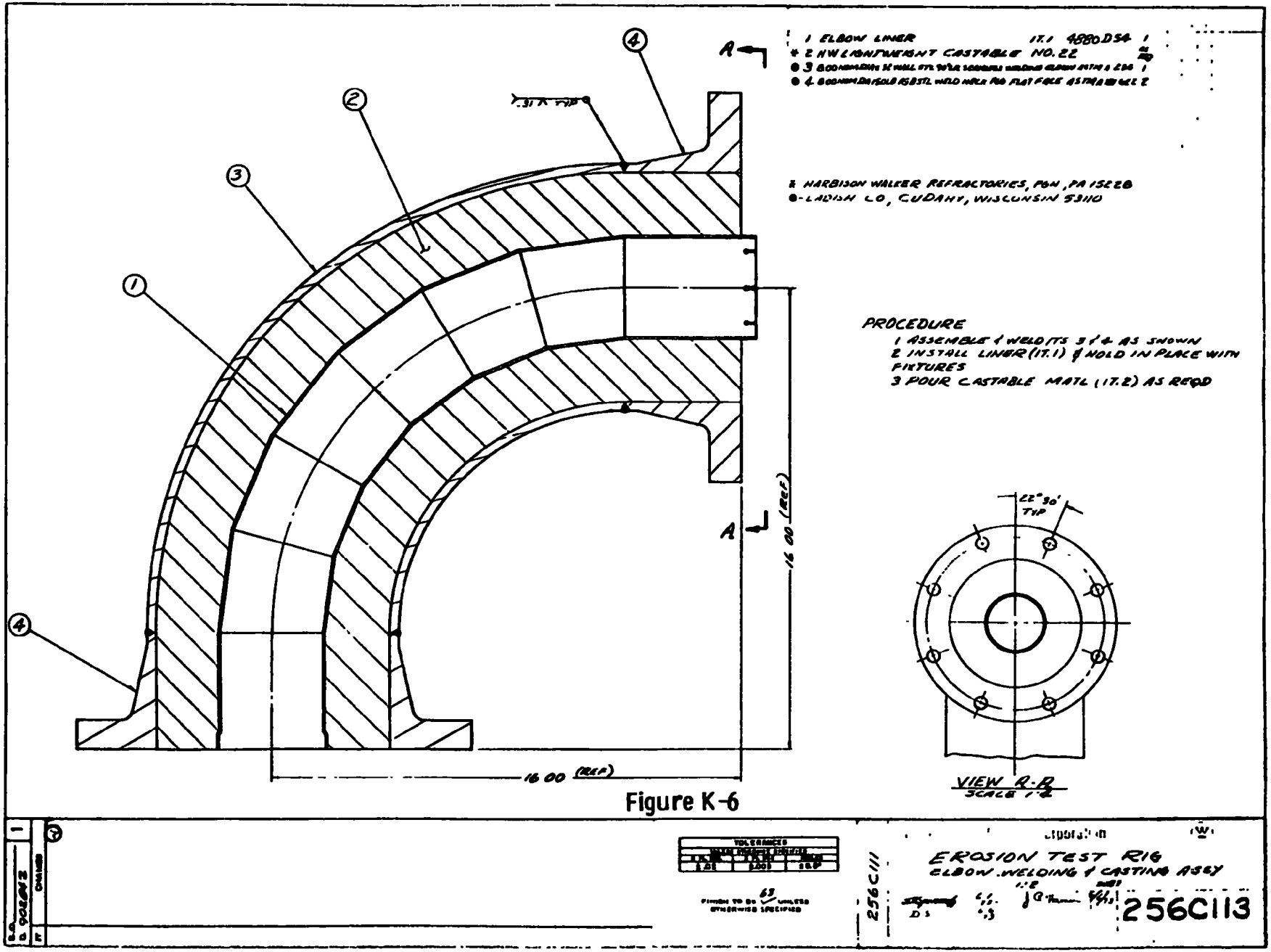
1 ELBOW LINER
2 HW LIGHTWEIGHT CASTABLE NO. 22
3
4
HARBISON WALKER REFRACTORIES, PGH, PA 15228
LADISH CO, CUDAHY, WISCONSIN 53110
PROCEDURE
1 ASSEMBLE & WELD ITS 3 & 4 AS SHOWN
2 INSTALL LINER (IT. 1) & HOLD IN PLACE WITH FIXTURES
3 POUR CASTABLE MATL (IT. 2) AS REQD
16.00 (REF)
16.00 (REF)
VIEW R-R
SCALE 1:2
EROSION TEST RIG
ELBOW WELDING & CASTING ASSY
256C113

Figure K-6

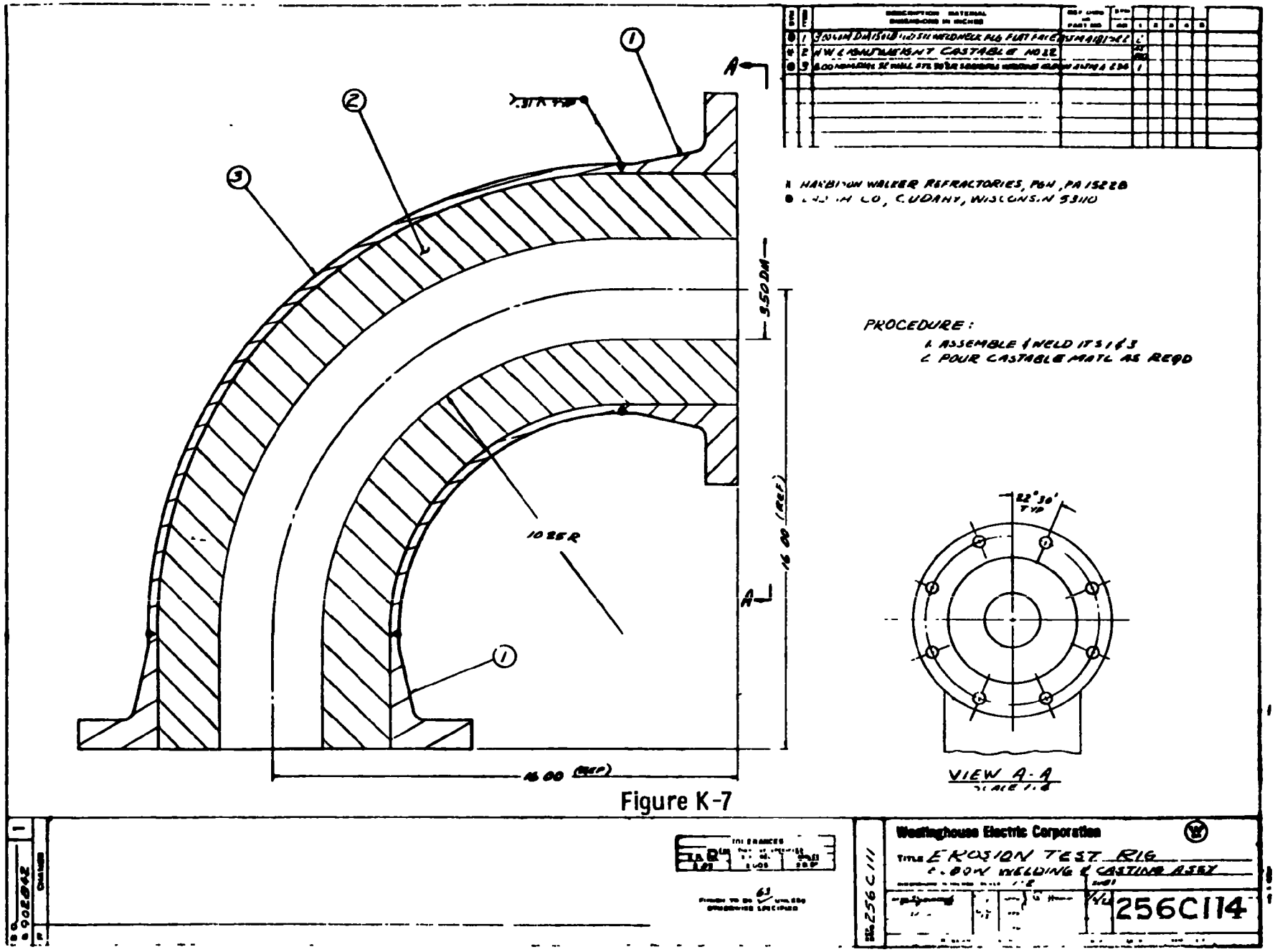
A
A
1
2
3
10.25 R
9.50 DIM
16.00 (REF)
46.00 (REF)
PROCEDURE :
1. ASSEMBLE & WELD ITS 1 & 3
2. POUR CASTABLE MATL AS REQD
82°30' TYP
VIEW A-A
Westinghouse Electric Corporation
256C114

Figure K-7

PAGE NOT

AVAILABLE

DIGITALLY

PAGE NOT

AVAILABLE

DIGITALLY

PAGE NOT

AVAILABLE

DIGITALLY

SUB.	S.O.
1	D. 2128412

Westinghouse Electric Corporation RESEARCH LABORATORIES CHURCHILL BORO PITTSBURGH, PA 15235, U.S.A.

TITLE EROSION TEST RIG
TEST SPECIMEN DET

SYM	ITEM	DESCRIPTION – MATERIAL DIMENSIONS IN INCHES	REF DWG OR PART NO.	SYM GR	1	2	3	4	5
	1	MATL TO BE SPECIFIED BY ENGR			1				

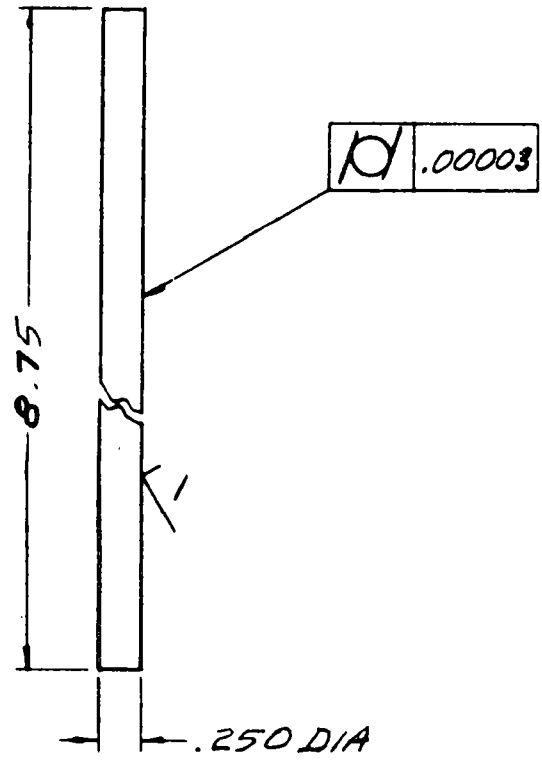

Figure K-11

REF DWG	TOLERANCES UNLESS OTHERWISE SPECIFIED			FINISH TO BE 63 UNLESS OTHERWISE SPECIFIED	
	2 PL DEC	3 PL DEC	ANGLES		
4879D29	.02	.005	± 0.5°		6208A13

SUB.	S.O.
1	D 902842

Westinghouse Electric Corporation RESEARCH LABORATORIES CHURCHILL BORO. PITTSBURGH PA 15235 U.S.A.

TITLE EROSION TEST RIG
TEST SPECIMEN

SYM	ITEM	DESCRIPTION -- MATERIAL DIMENSIONS IN INCHES	REF DWG OR PART NO.	SYM GR	1	2	3	4	5
	1	MATL TO BE SPECIFIED BY ENGR			1				

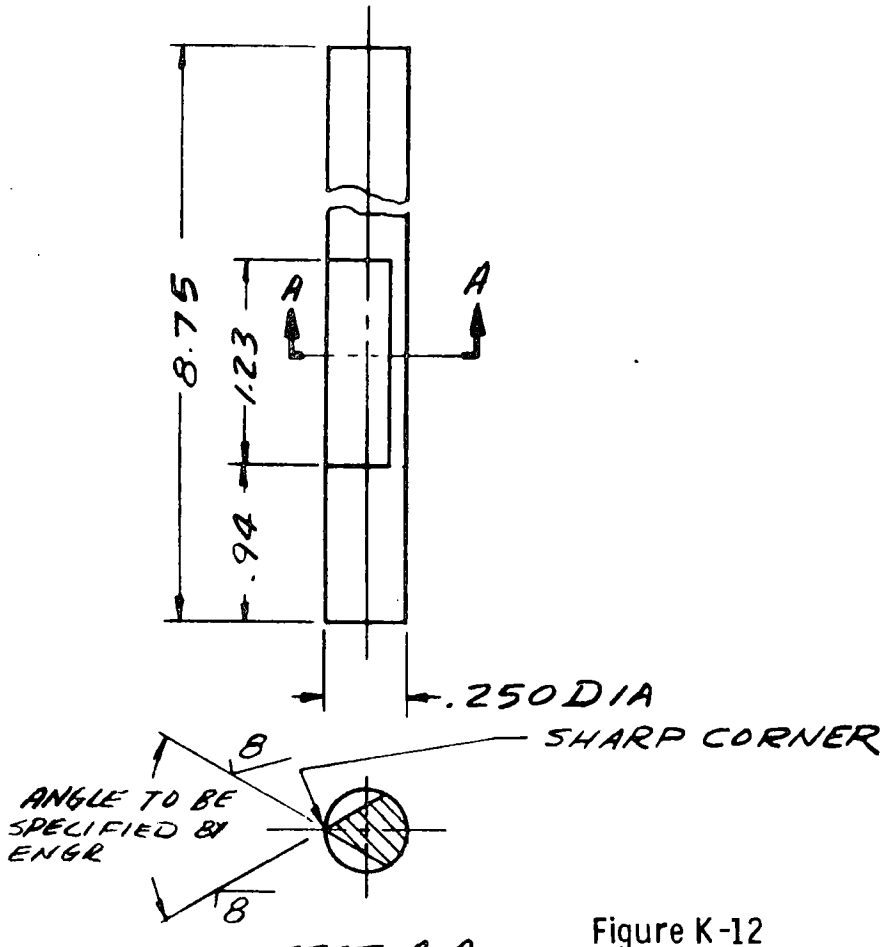

SECT A-A

Figure K-12

REF DWG	TOLERANCES (UNLESS OTHERWISE SPECIFIED)			FINISH TO BE 63 ✓ UNLESS OTHERWISE SPECIFIED	
	2 PL. DEC.	3 PL. DEC.	ANGLES		
256C111	± .02	± .005	± 0.5°		6213A46

SUB. SO		
1	D 702 242	6-24-73 D. Stewart

Westinghouse Electric Corporation RESEARCH LABORATORIES CHURCHILL BORO PITTSBURGH PA 15235 U.S.A.

TITLE EROSION TEST RIG

TEST SPECIMEN ASSY

SYM	ITEM	DESCRIPTION – MATERIAL DIMENSIONS IN INCHES	REF DWG OR PART NO	SYM GR	1	2	3	4	5
	1	MATL TO BE SPECIFIED BY ENGR			1				
*	2	6.62 OF .12 OD x 016 WALL SST TUBE TYPE 316			1				

* - TUBESALES, 456 NORDHOFF PLACE, ENGLEWOOD, N.J 07631

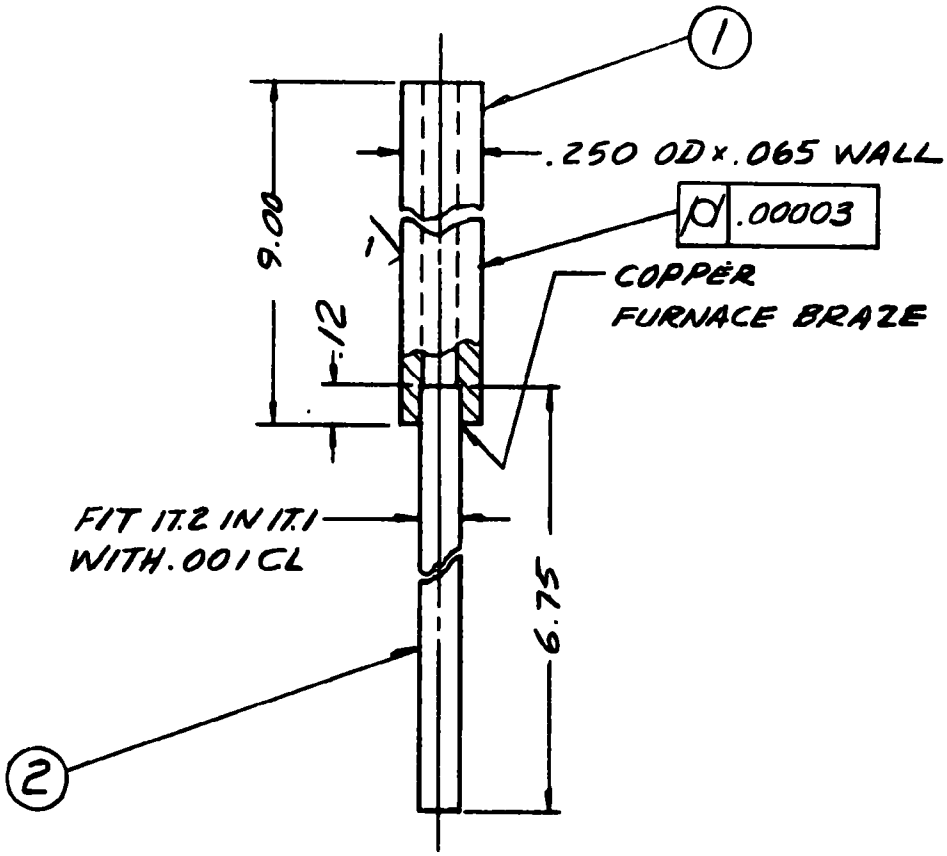

Figure K-13

REF DWG 256C111	TOLERANCES UNLESS OTHERWISE SPECIFIED			FINISH TO BE 63 ✓ UNLESS OTHERWISE SPECIFIED	6213A44
	2 PL DEC	3 PL DEC	ANGLES		
	.02	± .005	± 0.5°		

is located in the diffuser section where the gas stream velocity will reach about 579 m/s (1900 ft/sec) at the design conditions for the Exxon miniplant.

The piping between the exit of the second-stage separator and the test section, and the test section itself, is lined with oxidation-resistant material to prevent particles of refractory lining from getting into the gas stream.

The maximum allowable material recession for the turbine vanes and blades in the large Westinghouse utility-type gas turbines is about 0.762 mm (0.030 in). For a 25,000-hour target turbine life, the allowable metal recession rate is therefore 0.0305 μm/hr (1.2μ in/hr). A study has been carried out to learn what combination of erosion target design and metal recession measuring technique will determine whether the above metal recession rate is exceeded in the least possible test time.

Two types of erosion targets were considered—the cylindrical rod (Figure K-11) and the wedge target (Figure K-12). The cylindrical target has the advantage, theoretically, of giving erosion as a function of impact angle over a full spectrum of impact angles (from 0 to 90 degrees), whereas the wedge-type target will give erosion data for a relatively narrow range of impact angles. This is particularly significant since it is anticipated that erosion will be taking place in the oxide layer, and there is no information available on the impact angle for the maximum erosion rate of the oxide layer.

With the wedge-type probe, tests with a minimum of three angles would be necessary to determine the impact angle for the maximum erosion rate. An advantage of the wedge target is that it would give a more precise measurement of the erosion rate at the impact angle of maximum erosion rate.

Three techniques for measurement of erosion effects were considered. These are:

- Profilometer
- Optical comparator
- Weight loss.

The lubrication laboratory of Westinghouse Research Laboratories has a Gould Model 360 Surfanalyzer (profilometer). This instrument can measure surface roughness and profile on flat or cylindrical surfaces down to a minimum of 0.0254 μm (1 μ in) per chart division. A datum surface, however, is required in order to measure material removal. It is not possible to maintain a datum surface on a wedge-type target. The use of a profilometer, therefore, is not feasible with this type of target.

Two simulated wear tests have been conducted to determine the resolution possible with the profilometer on a cylindrical erosion target. Sample targets were prepared with a surface finish of 0.025 to 0.075 μm (1 to 3 μ in), and a cylindricity of about 1 μm (40 μ in). An attempt was made to simulate from 0.25 to 0.75 μm (10 to 30 μ in) of erosion over a 180 degree arc by liquid honing. It was found that a minimum application resulted in the removal of about 9 μm (350 μ in) of material. A second sample target had a nominal erosion of 0.75 μm (30 μ in) simulated by electroetching. Before and after profiles taken on these two sample targets indicate that 1.5 $\pm$ 0.3 μm (60^{+12} μ in) of metal removal can be measured with a 95 percent confidence level by this technique. At the maximum allowable metal recession rate, this amount of material would be removed in about 50 hours of operation.

The metallurgical laboratory of the Westinghouse Research Laboratories has an optical comparator which they use to measure metal recession of corrosion specimens from the corrosion test rig in the combustion laboratory. This instrument has a resolution of about 0.025 mm (0.001 in). Use of this technique requires sectioning the specimen. At the maximum allowable metal recession rate, this amount of material would be removed in about 800 hours of operation.

Precision balances are available with capacities adequate for measuring 6.35 mm (1/4 in) erosion targets with a resolution of 1 mg or better. Since weighing gives a measurement of total weight change, this technique is only applicable to the wedge-type target where the weight change would be roughly uniform over the exposed surface area. A resolution of 1 mg is equivalent to a metal recession of 0.4 to 0.5 μm (15 to 20 μ in).

At the maximum allowable metal recession rate, this amount of material would be removed in about 15 hours of operation.

As stated earlier the predicted concentration of ash particles in the exit gases from the second-stage cyclone separator of the Exxon miniplant is about 25 times the estimated concentration of total particulates in the full-scale, high-pressure fluidized bed boiler plant. In addition, the predicted size distribution of the particles in the miniplant exhaust is substantially larger than that projected for the commercial-scale plant. Because of the higher impaction factor of the larger ash particles on the target, the ratio of ash erosion effects will be greater than the concentration ratio. When the probable effect of attrited sorbent particles is added in, it is indicated that the erosion tests in the miniplant will be accelerated by a factor substantially greater than 25. In view of this, significant erosion effects would probably be obtainable with the cylindrical targets in test times of several hours. With the wedge-type target, test periods required for significant results would be of the order of one hour.

Test periods of several hours are substantially less than those required for a stable oxide film to form on the high-temperature turbine vane and blade materials. Because of the characteristic hyperbolic oxidation rate, however, the amount of oxidation which will occur during test periods of this magnitude is significant. This will result in a weight gain over the unexposed (to erosion) surface of the wedge-type target and a change in elevation of the unexposed surface of the cylindrical-type target. To prevent these changes, the unexposed surfaces of both types of targets will be coated with a thin layer (minimum of 1×10^{-3} μm) of oxidation-resistant material such as platinum.

The coals which will be used in the Exxon miniplant tests will contain corrosive contaminants such as sulfur, alkali metals, and chlorine. Some of these contaminants will be present in the combustion products as condensible vapors. Therefore, the amount of these contaminants which will be deposited on the erosion/corrosion targets by condensation is a function of the target temperature. An analysis of the heat transfer along the target shank (see Figure K-11) showed that the exposed surfaces of the target will be at near gas-stream temperature. In cases where the turbine vanes and/or

blades are cooled, the metal surface temperatures are, of course, below the gas-stream temperature. Tests of cooled cylindrical targets can be carried out in the erosion test rig by the use of the tubular target design shown in Figure K-13.

The ultimate measure of vane and blade life is the metal recession rate. Measurements of both the wedge- and cylindrical-type probes will be made, therefore, after removal of the oxide scale. The condition of the oxide surface, however, will also be of interest, so measurements will be made prior to descaling.

As noted earlier, the metal recession rate is dependent upon the combined effects of erosion and corrosion. Therefore, tests in which the erosion is accelerated by increased particulate concentration (as will be the case in the Exxon miniplant) may not give realistic metal recession rates. In view of this, tests should also be made with targets which have been preoxidized in order to provide some insight into the situation where the erosion effect is relatively small and a nearly stable oxide film exists.

HIGH-PRESSURE HIGH-TEMPERATURE PARTICULATE SAMPLING SYSTEM

Westinghouse has designed and constructed a high-pressure, high-temperature particulate sampling system for use in the Exxon miniplant erosion/corrosion tests.

Probe Assembly

A sampling probe -- 6.35 mm (1/4 in) OD, 4.57 mm (0.18 in) ID Inconel 600 tube -- is to be located in the straight pipe section which follows the secondary cyclones of the Exxon miniplant.

The probe subassembly will be mounted on a blank flange attached to a 76 mm (3 in) nipple, as shown in Figure K-14. The probe is held by a fitting which allows it to be retracted and rotated as required. Connected to the probe is a tee to provide a pressure tap; a heat exchanger to quench the gas sample; and an isolating ball valve.

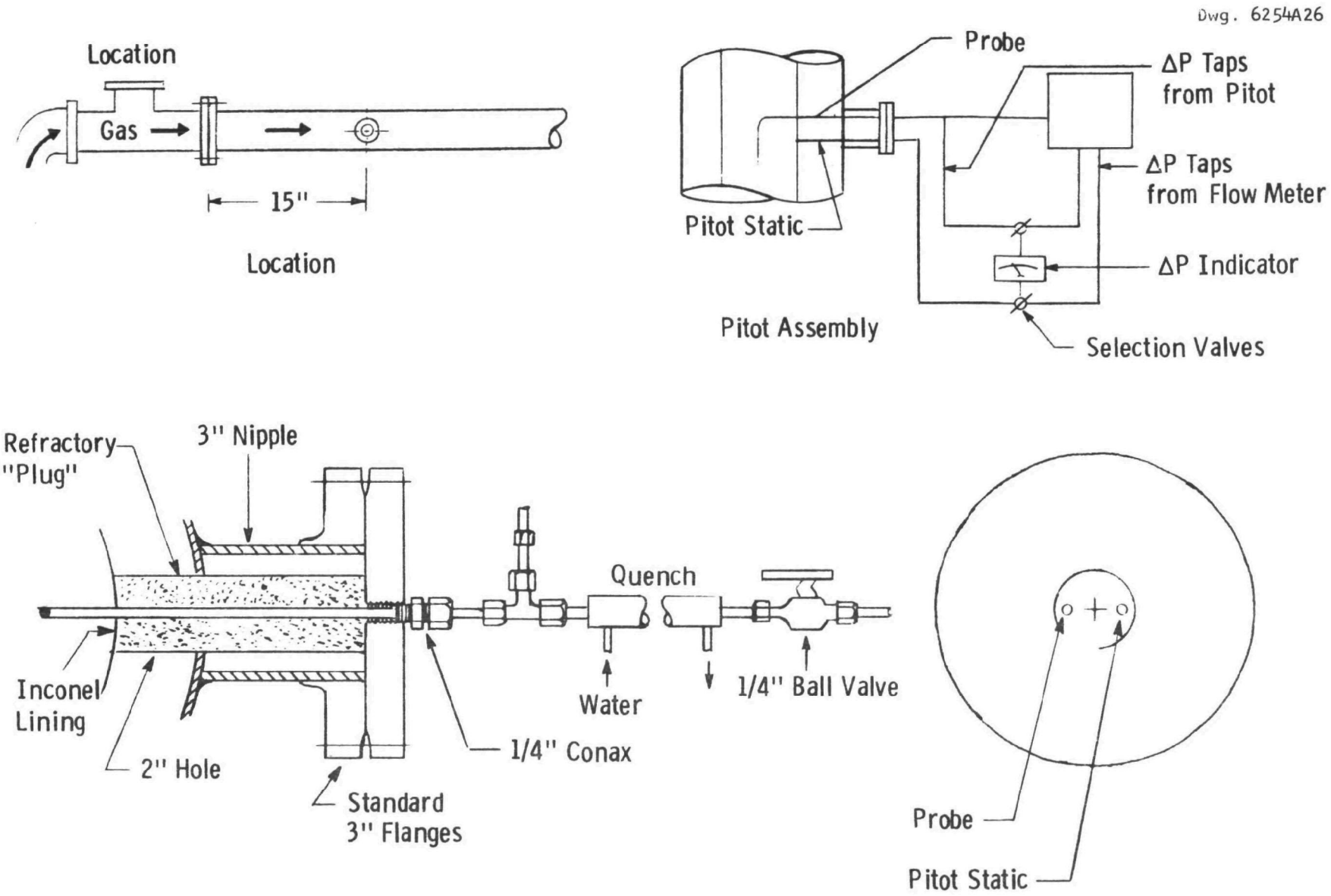

Figure K-14—Probe arrangement

A second port is provided in the flange for a static pressure probe which can be used in conjunction with the sampling probe to determine gas velocity and, thus, allow isokinetic conditions to be established.

High Flow Rate Sampling System

When the high flow rate Andersen impactor is used, the total sampling time available is of the order of 30 seconds. For accuracy it is thus necessary to preset the sampling flow carefully before sending it to the impactor. Serious errors would result if flow adjustments were made during the brief sampling period.

The sampling system thus incorporates two flow loops of equivalent pressure drops: one used when setting the sampling flow to isokinetic conditions, the other used while sampling. The arrangement of these circuits is shown in Figure K-15.

The sampling system incorporates a flat bottomed "scalping" cyclone which will collect essentially all particles above 20μm (preventing them from interfering with impactor operation). This is followed by a pressurized Anderson impactor, a flow meter, and a flow control valve. The alternative loop comprises a pressure drop equivalent to that of the sampling equipment and is connected to the flow meter and control valve which are common to both circuits.

Low Flow Rate Sampling System

The low flow rate Brink impactor assembly is shown schematically in Figure K-16. The gas stream from the sampling probe passes through a scalping cyclone and then splits into two streams. One stream is sent to the impactor, its flow rate controlled by a critical orifice; the other passes through a flow meter and control valve which are used to establish isokinetic conditions.

The impactor used in this assembly has been modified from the standard Brink design. Stages 4 and 5 (which classify submicron particles

Dwg. 6254A25

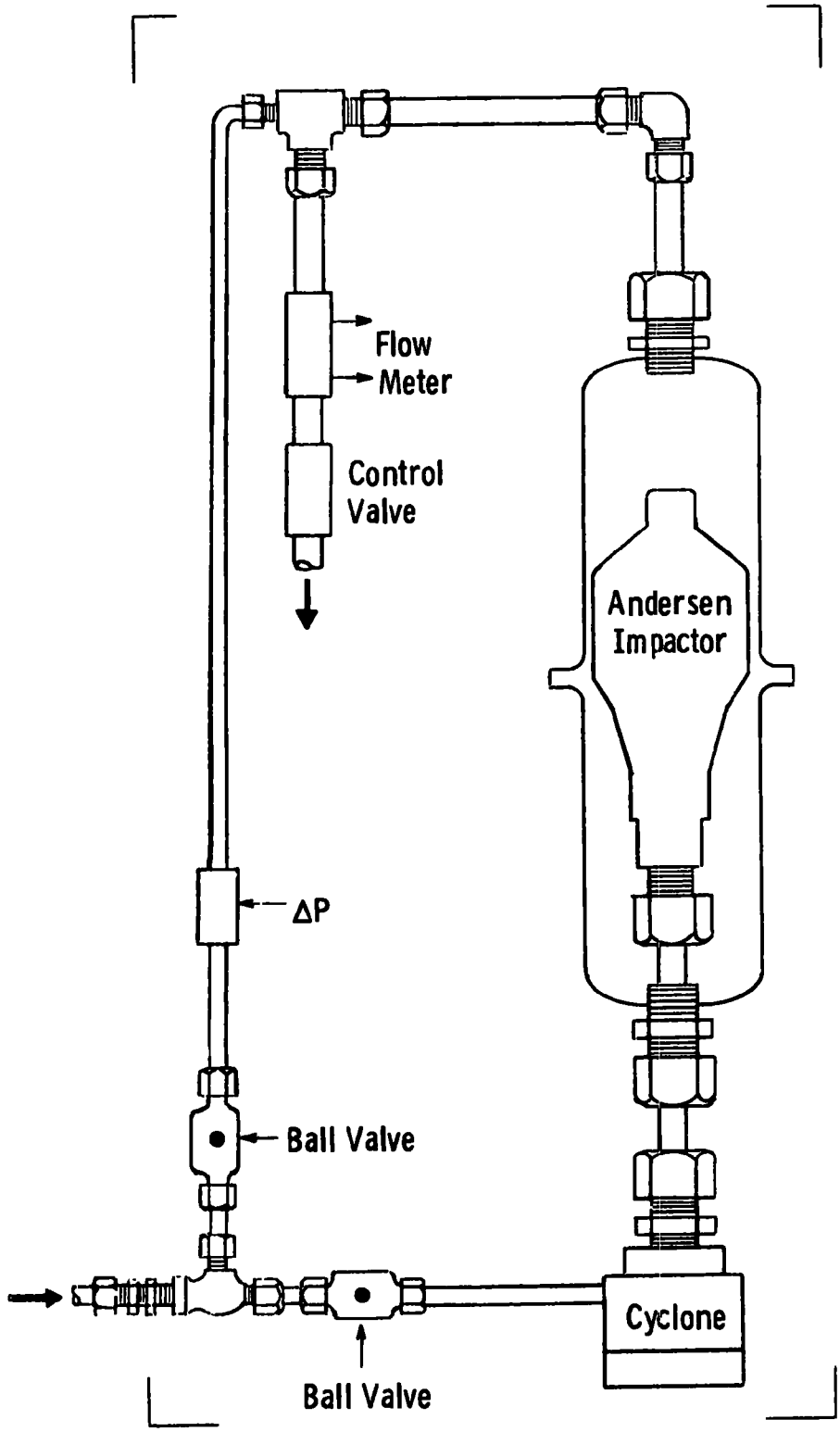

Figure K-15—Andersen impactor assembly

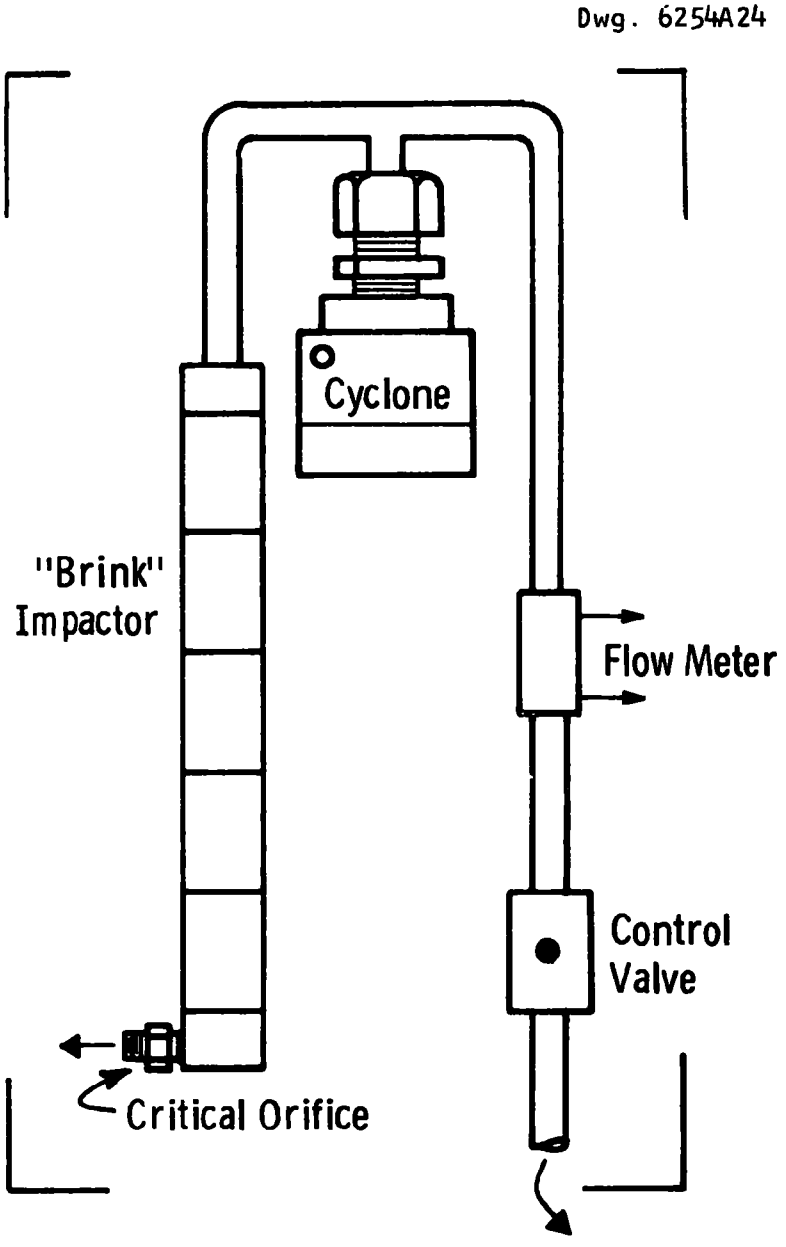

Figure K-16—Brink impactor assembly

under normal operation) have been removed and two additional steps added which extend the size range of the instrument into the 5-to-10 μm range.

Experience with High Flow Rate Impactors

Cascade impactors have been selected for sampling and sizing particulate dispersion, as they give a more direct measurement of size distribution than instruments which rely on collection-redispersion techniques.

The initial work on particle size determination was carried out with Andersen cascade impactors. To overcome problems associated with particle "bounce" from collection plate surfaces, the plates were covered with specially slotted glass fiber filters to retain impacted deposits. Experience showed that significant weight losses were encountered when these filters were handled. The exact cause of the weight loss was not determined but was probably due to loss of filter material where the filters were cut by the Andersen interplate gaskets. In subsequent experiments Andersen instruments were used without the glass collection mats. Results were unsatisfactory.

A comparative study of particle size determinations, using both Andersen and Sierra impactors, showed that the Sierra instrument consistently gave a coarser distribution than did the Andersen. In addition, the Sierra distribution corresponded closely to the particle size distribution of the initial test dust.

Scanning electron microscope examination of dust deposits on the collection stages of both instruments indicated that the Sierra impactor was measuring close to the real size distribution, whereas the Andersen impactor was indicating a distribution finer than that of the test dust.

TEST PLAN FOR EROSION/CORROSION TEST RIG IN EXXON MINIPLANT

The following test plan is proposed for the erosion/corrosion tests in the Exxon miniplant.

1. Target Preparation (Westinghouse Research Laboratories)

   a. Cylindrical target

      Diameter - $6.35^{\pm 0.025}$ mm ($0.25^{\pm 0.001}$ in)

      Surface finish - 0.025 μm (1μ in) rms

      Cylindricity - 0.75 μm (30μ in)

      Plate unexposed surfaces with oxidation resistance material ∿ 1.3 μm (50μ in) thick.

      Make profile measurements at three stations.

      Weigh.

      Preoxidize.*

      Make profile measurements at three stations.*

      Weigh.*

   b. Wedge target

      Diameter - $6.35^{\pm 0.025}$ mm ($0.25^{\pm 0.001}$ in)

      Surface finish - 0.13 μm (5μ in) rms

      Cylindricity - 1.3 μm (50μ in)

      Plate with oxidation resistance material ∿ 1.3 μm (50μ in) thick.

      Grind flats at specific angle to 0.2 μm (8μ in) rms finish.

      Weigh.

      Preoxidize.*

      Weigh.*

2. Nominal Test Conditions

   Pressure - 1013 kPa (10 atm)

   Temperature - 871°C (1600°F)

   Gas flow rate 0.739 kg/s (1.63 lb/sec).

In the event that operation at 1013 kPa (10 atm) is not possible, the flow rate should be adjusted to maintain a constant value of $W_g\sqrt{T}/P$.

*Only for preoxidized specimen.

3. Gas Stream Measurements

The dust concentrations in the gas stream leading to the test section shall be determined by procedures outlined in ASME Power Test Code 27-1957 or the equivalent. The sodium vapor and chlorine content of the gas stream should also be determined.

4. Properties of Particulate Matter

The size distribution of the particulate matter collected from the gas stream at the inlet to the test section shall be determined by procedures outlined in Section 5 of ASME Power Test Code 28-1965 or the equivalent.

5. Test Procedure

a. Install test target in passage so that target does not extend into gas stream, and secure pressure fitting.
b. Start up fluid bed combustor and operate at near atmospheric pressure until conditions are stabilized.
c. Loosen compression fitting(s) and move target into gas stream until stop is reached. Align probe accurately and tighten compression fitting. Increase pressure level as rapidly as practicable.
d. Take sample of particulates from gas stream.
e. Operate at steady-state conditions for three hours with cylindrical targets (both uncooled and cooled) and for one hour with wedge-type target.
f. Take sample of particulates from gas stream.
g. Reduce system pressure quickly to 101.3 kPa (1 atm).
h. Loosen compression fitting(s) and retract exposed section of target into well. Secure compression fittings.
i. Shut down fluidized bed boiler so that target can be removed from passage. (In removing target from passage, compression fitting should be dissembled so that target can be removed without damage to exposed section.)

6. Target Measurements (to be made at Westinghouse Research Laboratories)

   a. Cylindrical targets

      Weigh.

      Make profile measurements at three stations.

      Descale specimen.

      Make profile measurements at three stations.

      Weigh.

   b. Wedge targets

      Weigh.

      Descale specimen.

      Weigh.

7. Test Runs

Run	Material	Base	Target
1	X-45	Co	Uncooled cylinder
2	"	"	Uncooled cylinder preoxidized
3	"	"	Cooled cylinder
4	"	"	Wedge*
5	MARM-509	"	Uncooled cylinder
6	"	"	Wedge*
7	U710	Ni	Uncooled cylinder
8	"	"	Uncooled cylinder preoxidized
9	"	"	Cooled cylinder
10	"	"	Wedge*
11	IN738	"	Uncooled cylinder
12	"	"	Wedge*

*Wedge angles will be determined from tests on cylindrical targets. Wedge targets may or may not be preoxidized.

ANALYTICAL PROCEDURE FOR EROSION TEST RESULTS FROM EXXON MINIPLANT

The erosion test rig which has been fabricated for use with the Exxon fluidized bed boiler miniplant consists of a 28.19 mm (1.11 in) diameter passage with a 6.35 mm (1/4 in) diameter target placed normal to the direction of flow. After each erosion test, the amount of material removed from the upstream surface of the cylindrical target will be measured by a profilometer. A procedure has been developed for analyzing the results of these erosion tests in the Exxon miniplant.

The rate of erosion of a target placed in a flowing gas stream with entrained particles is a function of the following factors:

- The concentration of particles in the stream
- The size distribution of the particles
- The angle of impingement of the particles on the surface of the target
- The velocity of the particles at impact
- The physical properties of the particles
- The physical properties of the target material.

C. E. Smeltzer et al. have shown that, for a given angle of impingement and for impact velocities greater than the threshold values, the amount of material removed from a target is proportional to the mass of the particle and independent of the particle size. Figure K-17 shows a plot of the threshold energies MV^2 as a function of particle size based on test results from Reference 7.

The range of gas-stream velocity which will be used in the miniplant erosion tests extends well beyond the threshold levels shown in Figure K-17. The erosion effect, therefore, can be assumed to be independent of particle size for a given impingement angle. The trajectory of entrained particles in a gas stream flowing around a cylinder, however, is a function of particle size. Thus, the impingement angles and particle concentrations at specific points over the upstream surface of the cylindrical target will be a function of the particle size distribution in the free stream.

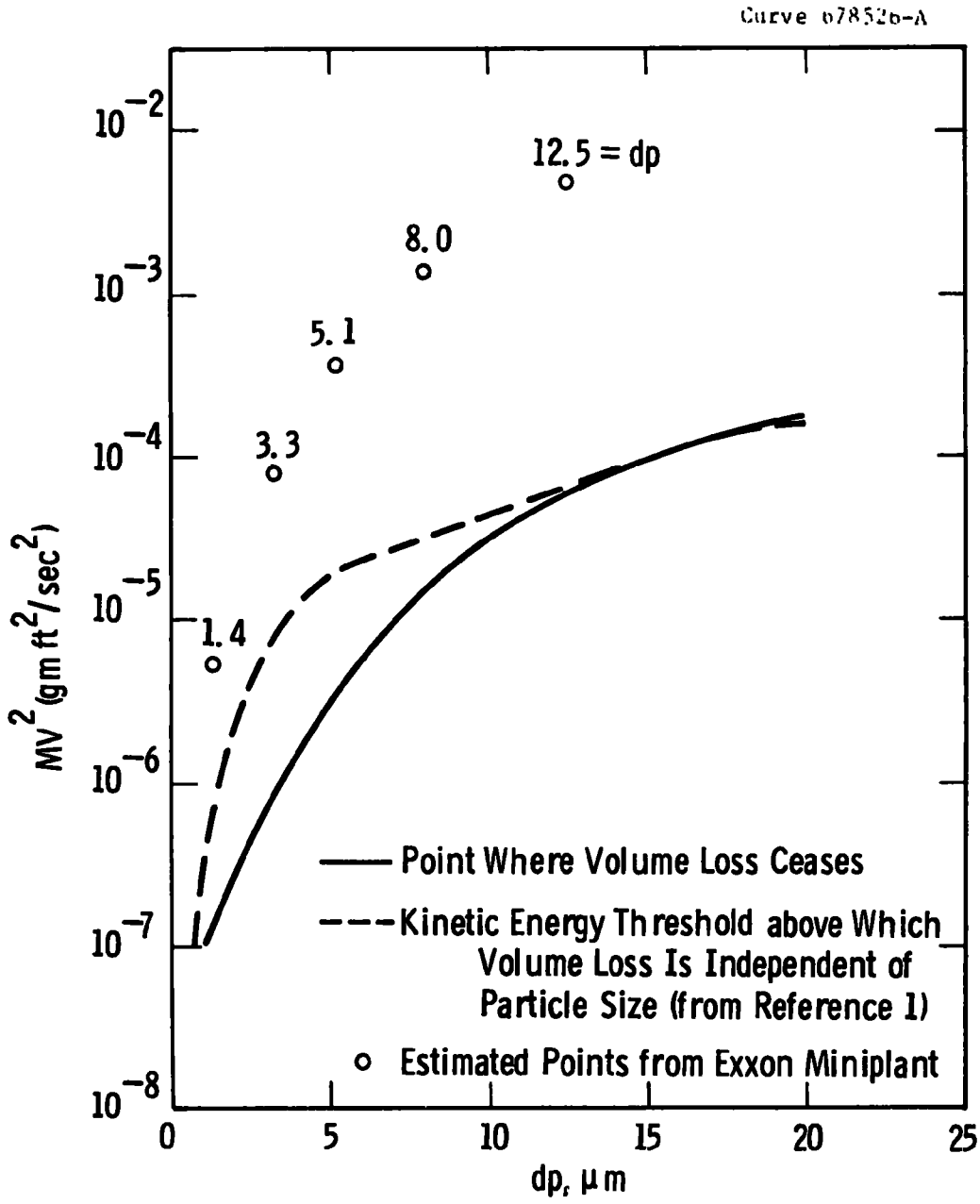

Figure K-17–Threshold kinetic energy vs particle size

The procedure which has been developed for analyzing the erosion test results from the miniplant includes:

- A program designed to calculate particle trajectories
- A preliminary model for calculation of a weighted average angle of impact with respect to a polar coordinate β (to designate a point on the target surface).
- A preliminary model for calculation of the total mass striking a unit area per unit time with respect to β.

This procedure has been applied to the ash particle size distribution and concentration at the discharge from the miniplant as estimated by Exxon (See Figure K-18). This estimate does not consider particles of attrited sorbent which will be present.

Particle Trajectories

A particle carried by a stream of gas will tend to cross stream lines when approaching a cylinder normal to the flow. The extent to which this occurs is, for a given velocity, a function of the size of the particle. For instance, a small particle will be deflected more than a large particle, given the same point of origin in the free stream.

Using the size distribution given in Figure K-18, ten average sizes were selected at the midpoint of each ten percent of the total mass of particles in the flow. A point of origin was chosen at a distance of five cylinder radii upstream of the center of the target. Here, the flow can be assumed to be undisturbed by the cylinder (See Figure K-19).

For each particle size, a number of free stream positions were chosen on the y-axis. A trajectory was computed for each particle size at these positions. If the particle struck the target surface, the point of impact and the angle of impact (with respect to the x-axis) was computed. By varying the value of (r/r_o) it was possible to determine for each particle size the point in the free stream outside of which the particle would pass by the cylinder.

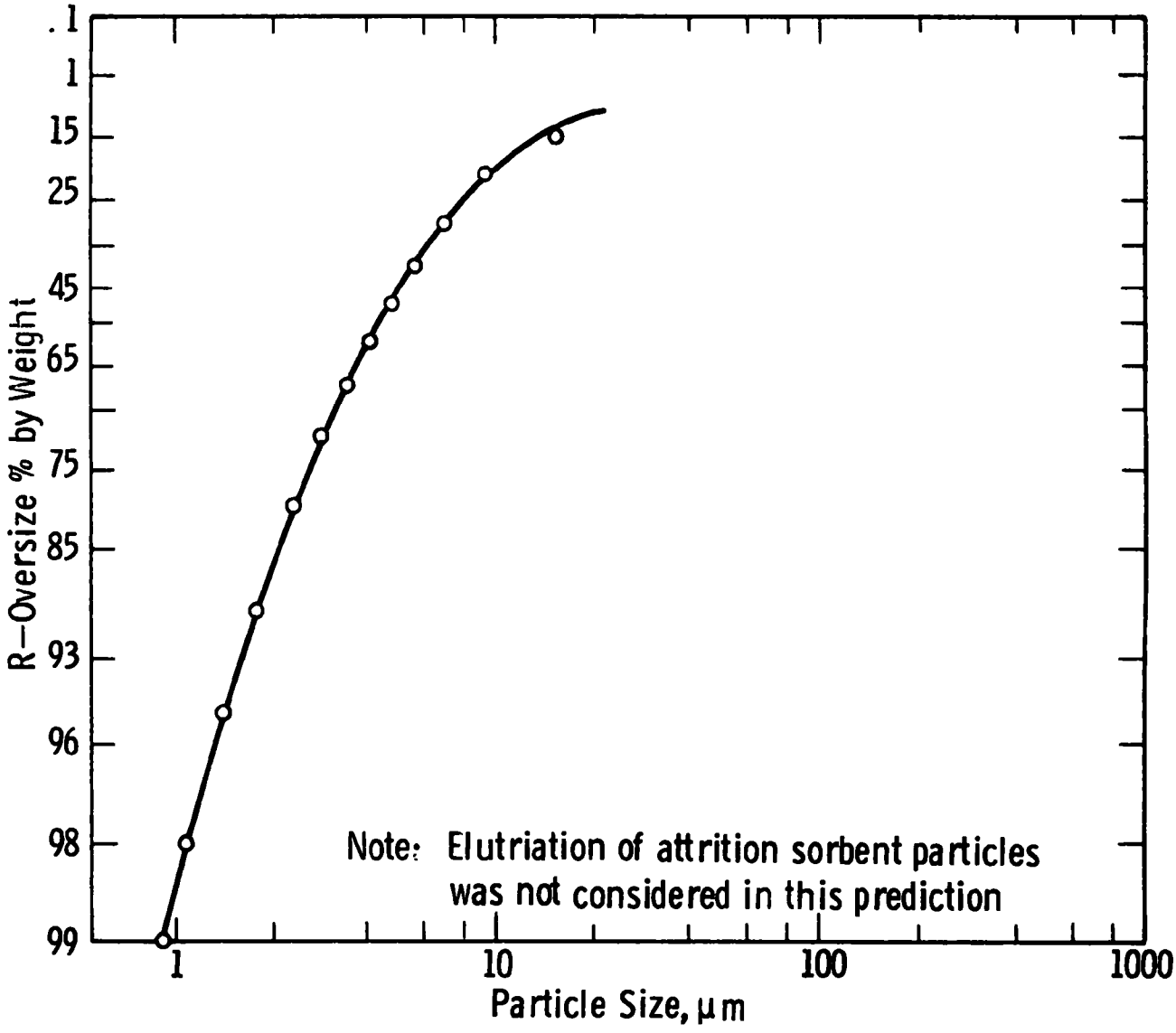

Figure K-18- Predicted size distribution of coal ash particles escaping from secondary cyclones in Exxon miniplant

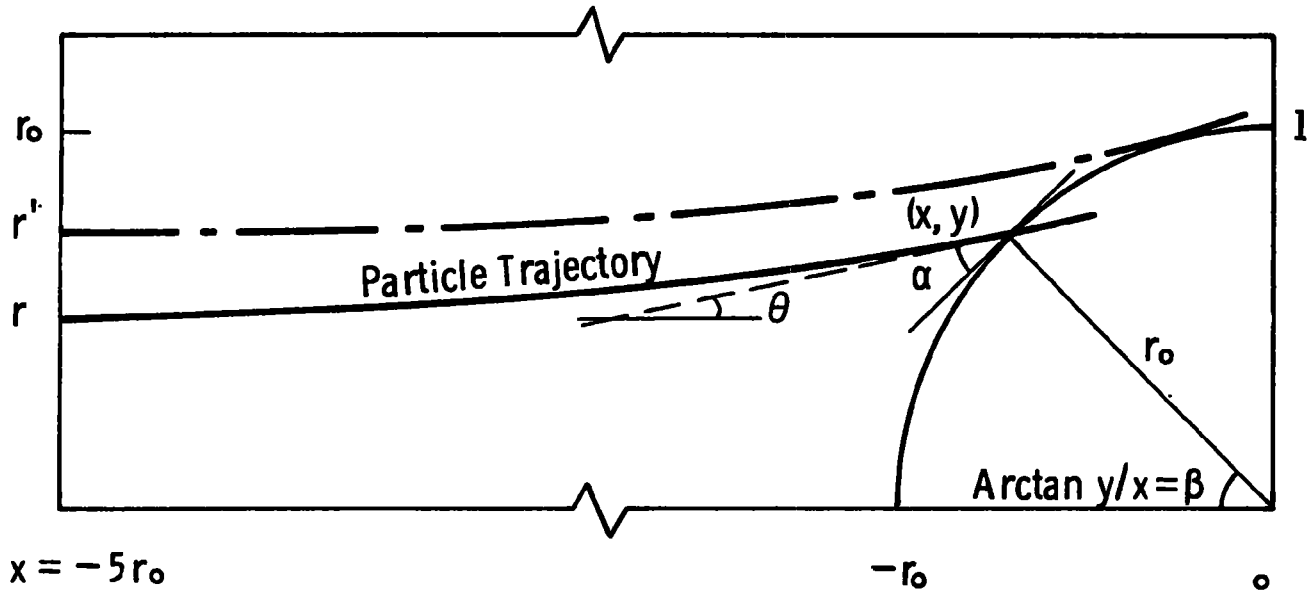

Figure K-19 —Analytical model for particle impaction

Table K-2

IMPINGEMENT CRITERIA

Particle Size (μm)	(r'/r_o) = criterical point of origin
1.4	0.125
2.1	0.280
2.7	0.390
3.3	0.485
3.7	0.535
4.4	0.605
5.1	0.660
6.3	0.725
8.0	0.795
12.5	0.880

Within these limits, a plot of the point of impact for each particle size as a function of the free-stream point of origin was made. (See Figure K-20.) On this plot the arrow designates both the limit in the free stream beyond which the particles will miss the target and the point on the target surface beyond which no particle of that size will strike. This occurs where the angle of impact approaches zero.

Concentration of Particles

The estimated concentration of particles in the gas stream at the outlet of the secondary cyclone in the Exxon miniplant is 1.40×10^{-3} kg/kg (1.40×10^{-3} lb/lb) gas. The total free stream mass flux through a plane at x = -5 is 2.53 kg/m^2 (0.519 lb/ft^2)/s. This is used to determine the mass of particles actually striking the target surface per unit time. This is an important parameter in the determination of erosion loss.

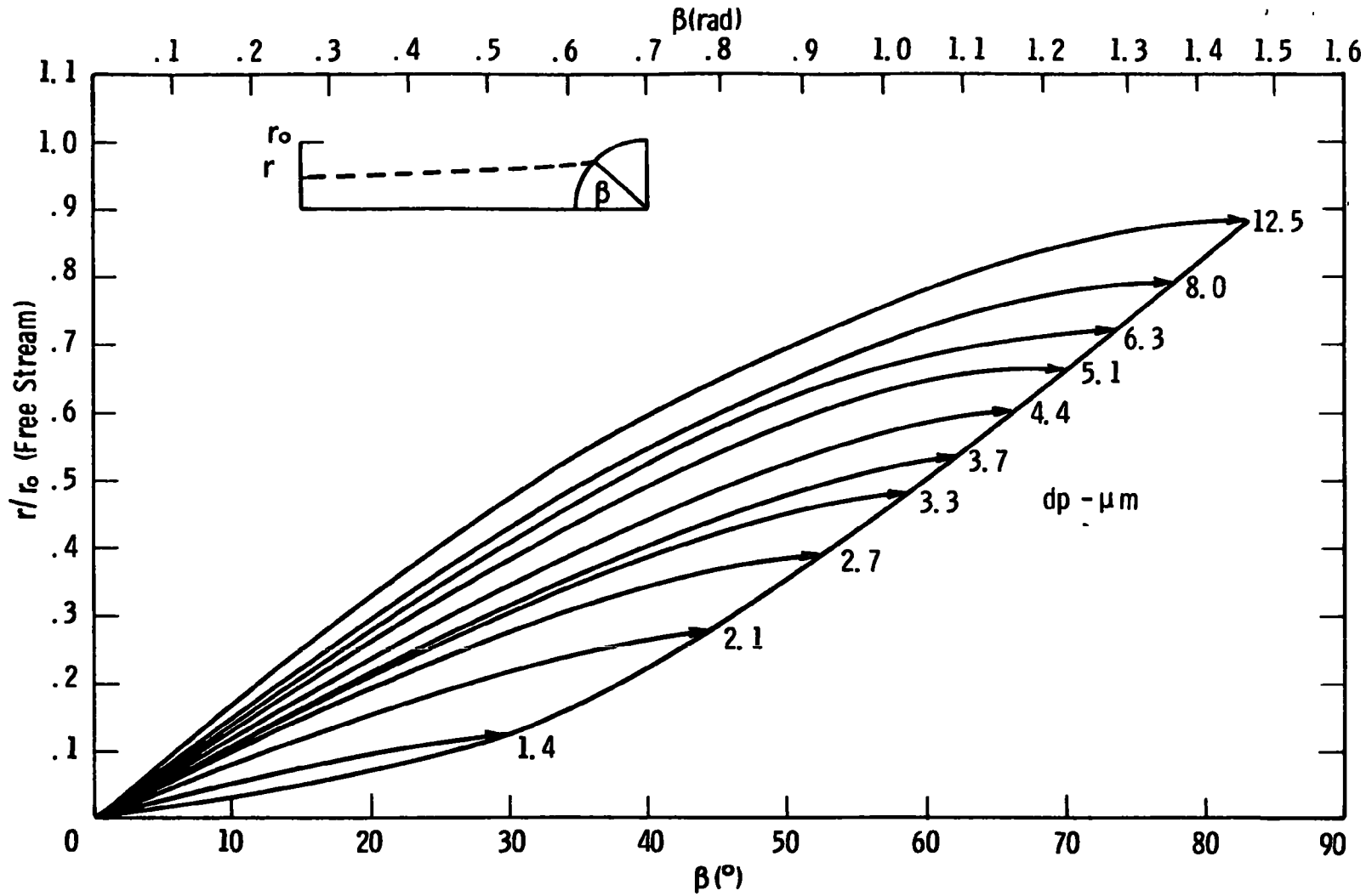

Figure K-20–Free stream position of particle vs point of impact

Angle of Impact Distribution

The data provided by the computer program include:

- The trajectory of the particle with respect to time
- The particle velocity (x- + y-components) with respect to time
- In the event of impact, the coordinates of the impact point (x,y) and the angle θ of the particle's trajectory with respect to the x-axis. (See Figure K-19.)

Although these quantities define the event of impact, they do not represent the simplest means of dealing with the phenomenon of erosion. Erosion is a function of the angle of impact. In this model this is the angle α, or the angle from the tangent line at the point of impact, at which the particle strikes. It is also more convenient to define the point of impact by the polar coordinate $\beta = \arctan y/x$. Therefore, α is given by $\alpha = 90 - \theta - \beta$ and can easily be computed.

For each increment of surface on the cylinder, there will be a range of particle sizes striking at angles dependent upon the size and point of origin. It should be possible, therefore, to compute an average angle of impact for each point on the cylinder surface (defined by β). Since the distribution of impacts over the surface from $\beta = 0°$ to $\beta = 90°$ is not the same for every particle size, the average must be weighted by some factor related to size.

Since each particle size used in the computation represents ten percent of the total mass flow of particles, the free-stream concentration for each size is equal: $C_{o_i} = C_o/10$.

The concentration at the surface of the cylinder is lower than the free-stream concentration by a factor of r'/r_o, the critical point of origin for a particular particle size. Small particles will fan out more than large particles. A weighting factor was derived which took into account this expansion. The free-stream interval from $y = 0$ to $y = r'/r_o$ was divided into ten equal segments. The concentration of particles was assumed to decrease by a factor of r'/r_o as it moved to the target surface. The weighting factor was calculated for each $\Delta\beta$ where $\Delta\beta_i$ is the segment of the cylinder surface corresponding to the i^{th} free-stream interval.

The weighting factor is given by:

$$W_{fi} = \frac{C_i}{C_o} = \frac{18\ (r'/r_o)i^2}{\pi \Delta \beta_i}$$

These factors were computed for $0<\beta<90$ and plotted, assigning W_f for each surface interval to a βm_i at the midpoint of ΔB_i. This developed a curve, with particle size as a parameter, of W_f versus β. (See Figure K-21.) The weighted average angle of impact was then computed by the formula

$$\bar{\alpha} = \sum_{i=1}^{10} \frac{W_{fi}\alpha_i}{\Sigma W_{fi}}$$

for ten points on the surface of the cylinder. This, in turn, generated a plot of $\bar{\alpha}$ versus β. (See Figure K-22.)

Concentration Distribution

The mass striking the cylinder per unit time is another factor in erosion and is easily calculated. The mass flow of each particle size has been shown to be ten percent of the total particle concentration. Since $W_{fi} = C_i/C_{o_i}$, the mass flow at the surface is given by

$$C_i = W_{fi}\ C_{o_i}$$

where $C_{o_i} = C_o/10$.
Thus, the total mass striking at a certain point is given by

$$\dot{M}_I \left(\frac{lb}{ft^2 sec}\right) = \sum_{i=1}^{10} W_{fi}\ \dot{M}_{Ii} = \dot{M}_{Ii} \sum_{i=1}^{10} W_{fi}$$

where

$$\dot{M}_{Ii} = 0.10\ (2.53\ kg/m^2 sec)(0.10\ (0.519)\ lb/ft^2 sec)$$
$$= .253\ kg/m^2 sec)(0.0519\ lb/ft^2 sec)$$

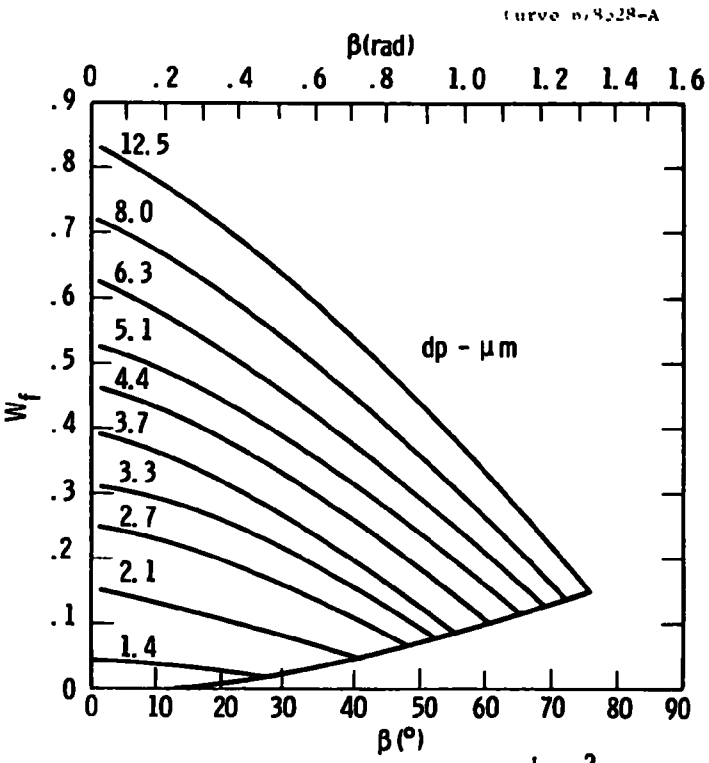

Figure K-21–Weighting factor $W_f = \frac{18(r'/r_o)^2}{\pi \Delta \beta}$ vs β

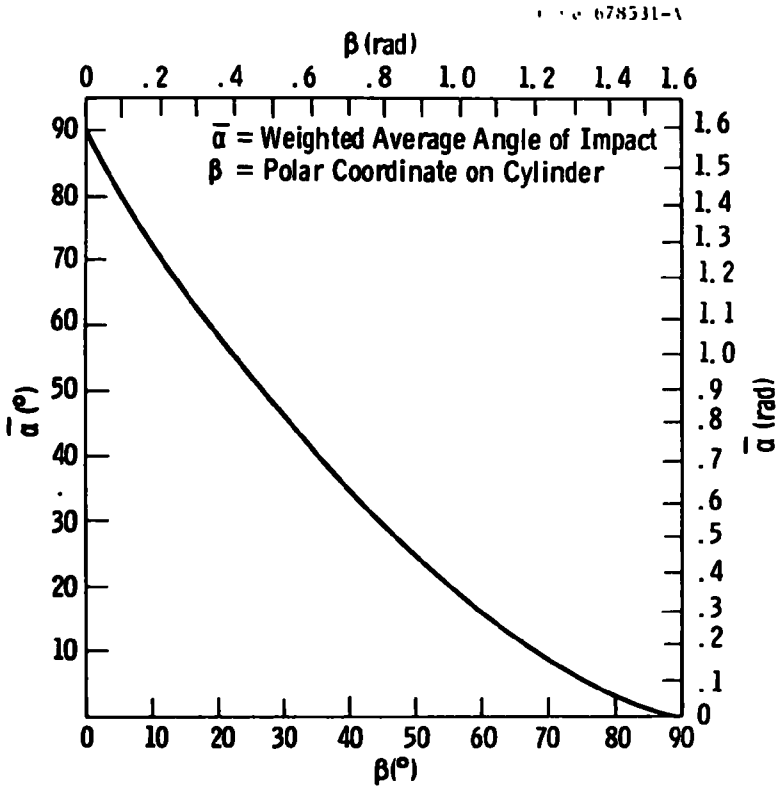

Figure K-22–Average angle of impact $\bar{\alpha}$ vs β

This generates a plot of $\dot{M}_I$ $\left(\frac{lb}{ft^2\ sec}\right)$ versus β. See Figure K-23.

This concentration distribution factor will be used to normalize the metal recession quantities measured on the erosion targets after a test run on the basis of particle mass concentration per unit of surface area. This will then permit a correlation of normalized metal recession as a function of $\bar{\alpha}$.

Except for the trajectory computations, all of the procedures described were carried through by hand and are thus subject to inaccuracies. The next phase will involve a modification of the trajectory computations to produce more convenient quantities and the writing of a program that will arrive at a more accurate analysis of the model.

CONCLUSIONS

The straight-through erosion/corrosion test rig designed for installation in the Exxon Research and Engineering high-pressure fluidized bed boiler miniplant will simulate the most severe conditions of impact velocity, impact angle, and temperature to be found in a gas turbine in the first generation high-pressure fluidized bed boiler. However, the predicted volumetric concentration of particulates in the discharge stream from the miniplant may be more than 25 times greater than the level anticipated in the full-scale plant with the present two stages of particle collection. In addition, the particle sizes in the miniplant may be substantially greater than those expected in a commercial plant. The addition of a third-stage unit to investigate fine particle removal should minimize the dust concentration.

The high concentration and large size of the particulates in the miniplant may pose a problem in the interpretation of the erosion/corrosion test results because of the unrealistic time relationship between erosion and corrosion. Consideration may have to be given to modification of the miniplant to attain particulate concentration and sizes which are more representative of those values expected in the commercial-scale plants.

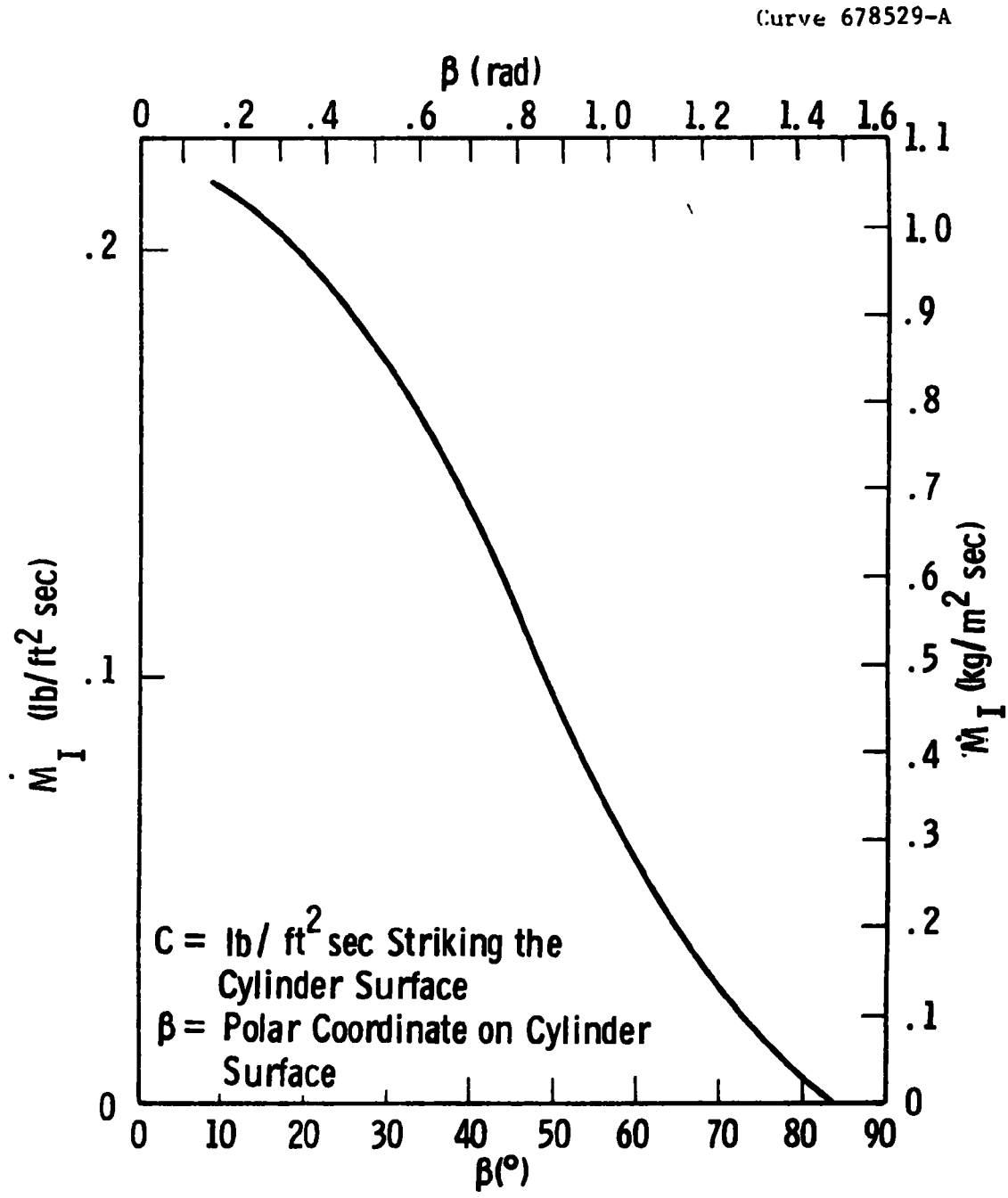

Figure K-23- Mass impacting per unit area per unit time vs β

REFERENCES

1. Letter from M. S. Nutkis to J. R. Hamm dated August 8, 1973.
2. Archer, D. H., et al. Evaluation of Fluidized Bed Combustion Process. Office of Research and Monitoring. Environmental Protection Agency. Westinghouse Research Laboratories. Pittsburgh, Pa. November 1971. NTIS PB 212 916. Vol. II. p. 156.
3. Ibid. p. 285.
4. Yang, W. C., and D. L. Keairns. Particulate Removal Studies from High-Temperature, High-Pressure Gases. Issued as part of Contract report to Office of Coal Research. Clean Power Generation from Coal. Contract OCR-14-32-0001-1223. Westinghouse Research Laboratories. Pittsburgh, PA. Report 73-9E3-COCLN-R1, NTIS PB-234 188. April 25, 1973.
5. Information obtained by W. E. Young during visit to NASA-Lewis Laboratories.
6. Analysis done under OCR Contract 14-32-0001-1514 and reported in monthly progress reports.
7. C. E. Smeltzer et al. Mechanisms of Metal Removal by Impacting Dust Particles. Journal of Basic Engineering. Sept. 1970.

APPENDIX L

POTENTIAL FOR ADVANCED STEAM CONDITIONS WITH FLUIDIZED BED COMBUSTION BOILERS

APPENDIX L

POTENTIAL FOR ADVANCED STEAM CONDITIONS WITH FLUIDIZED BED COMBUSTION BOILERS

Fluidized bed combustion boiler power plants can potentially increase overall power plant efficiency by increasing the steam temperature and pressure. The effect of higher steam temperatures on the performance of the plant has been reported previously.[1,2] An increase of 38°C (100°F) in both superheat and reheat temperatures will give a reduction of about 422 kJ/kWh (400 Btu/kWh) in plant heat rate. The use of advanced steam conditions may be attractive should the potential reduction in boiler tube material corrosion/deposition be realized. The commercial realization of advanced steam conditions in a fluidized bed combustion system will depend on the trade-offs between increased cycle performance, fuel costs, increased component costs, and plant reliability.

STEAM-TURBINE DESIGN AND OPERATION

Currently, the most prevalent design steam conditions for conventional steam plants are 16,548 kPa/538°C/538°C (2400 psig/1000°F/1000°F) and 24,130 kPa/538°C/538°C (3500 psig/1000°F/1000°F). In the past, 566°C (1050°F) and 593°C (1100°F) steam temperatures were common, but experience to date has shown that the economics of steam plants with steam temperatures greater than 538°C (1000°F) are not competitive with those at 538°C (1000°F).

The plants in the United States which were designed with supercritical cycles and steam temperatures above 593°C (1100°F) are now being operated at reduced steam conditions. The Eddystone No. 1 unit[3,4] was designed for 34,475 kPa/649°C/566°C/566°C (5000 psig/1200°F/1050°F/1050°F) and is now being run with a pressure somewhat less than 34,475 kPa (5000 psig) and a superheat temperature of 613°C (1135°F). American

Electric Power's Philo No. 6 was designed for 31,028 kPa/621°C (4500 psig/1150°F) and is now operating at 31,028 kPa/566°C (4500 psig/1050°F). Avon 8, Cleveland Electric Illuminating Company, was designed for inlet conditions of 24,133 kPa/593°C (3500 psig/1100°F) and is now operating at 24,133 kPa/566°C (3500 psig/1050°F).

The primary technical limitations on operating steam turbines at steam temperatures above 593°C (1100°F) are:

- High-temperature creep of steam turbine rotating and stationary parts. The use of austenitic materials in place of ferritic materials can extend the steam temperature range above 566°C (1050°F), but these materials have the undesirable characteristics of low yield point, low thermal conductivity, and large thermal expansion coefficient. These have led to thermal distortion of turbine housings.
- Low-cycle thermal fatigue of steam-turbine parts. The use of the heavier sections associated with high-pressure/high-temperature equipment tends to increase the severity of this problem. Also, the expected change from base-load to intermediate-load operation for fossil-fired steam plants as nuclear plants become more numerous will increase the degree of temperature cycling. Low reliability compounds this problem because of the increased number of shutdowns.

A steam power plant workshop sponsored by the Electric Power Research Institute (EPRI) in 1974 reached the following conclusions regarding the most advanced, highly reliable plant which could be built without research and development:

- A reliable 1000 MW single reheat unit could be built with steam conditions of 24,133 kPa/538°C/538°C (3500 psig/1000°F/1000°F).

- A reliable double reheat unit could be built for steam conditions of either 24,133 kPa/538°C/552°C/566°C (3500 psig/1000°F/1025°F/1050°F) or 24,133 kPa/566°C/566°C/566°C (3500 psig/1050°F/1050°F/1050°F) in maximum sizes ranging from 750 to 1000 MW.
- A reliable 24,133 kPa/566°C/593°C (3500 psig/1050°F/1100°F) unit could be built with a rating in the 600-to-800 MW range.

The limit on maximum unit size for the above steam conditions is imposed by the unavailability of forging equipment for the higher strength materials.

The consensus of those attending the EPRI workshop was that although the technology exists for construction of reliable plants at the above listed steam conditions, the increased costs of the steam generators and steam turbine for these higher steam conditions balance out the fuel savings associated with the lower heat rates. There is thus no economic advantage to using the higher steam conditions.

BOILER TUBE MATERIALS

The technical limit on operating the boiler at steam conditions above 593°C (1100°F) is the superheater and reheater tube wastage due to liquid-phase ash corrosion. In conventional pulverized coal-fired boilers this problem increases in severity as the steam temperature increases above 538°C (1000°F).

The use of fluidized bed boilers with in-bed desulfurization can potentially overcome this constraint on advanced steam conditions.[1,5-8] The ash corrosion problem for the boiler superheater and reheater tubes is substantially less in the fluidized bed boiler with in-bed desulfurization than in the conventional pulverized coal-fired boiler. In addition, the increased hot-side heat transfer coefficient in the fluidized bed boiler results in a substantial reduction in the boiler tube surface requirements, which will tend to make the use of steam temperatures in the 538-to-593°C (1000-to-1100°F) range economically viable.

This is particularly true for the pressurized fluidized bed combustion boiler-combined cycle power plant, where the heat transfer surface is reduced 60 to 70 percent over that of a conventional pulverized-fuel boiler.

ASSESSMENT

Short-term experimental data have been obtained on boiler tubes in fluidized beds of limestone and dolomite burning various coals. These data indicate that the boiler tube material limitations may be overcome by utilizing fluidized bed combustion boilers. Long duration tests—2000 hours or longer—are required to confirm these data. Additional materials tests are required to investigate advanced steam conditions with alternate materials.

Large expenditures on materials research and development programs also are required in order to attain the technology necessary for the design and construction of reliable steam turbines with steam temperatures in excess of 649°C (1200°F) with or without fluidized bed combustion.

Alternative steam cycles and apparatus should also be investigated. For example, the temperature limitation on boiler tube material may be reduced if boiler tubes unstressed because of balanced pressure are used (the super-reheat concept, Appendix A). Trade-offs between cycle performance, power plant component costs, fuel costs, and component reliability must be identified and assessed. Energy costs must be projected, operating characteristics reviewed, and control requirements identified to provide a basis for comparison with other advanced power generation concepts.

REFERENCES

1. Keairns, D. L., D. H. Archer, R. A. Newby, E. P. O'Neill, and E. J. Vidt. Evaluation of the Fluidized Bed Combustion Process. Volume I. Environmental Protection Agency. Westinghouse Research Laboratories. Pittsburgh, Pennsylvania. EPA-650-2-73-048a NTIS PB-231 162/9. December 1973.
2. Elliott, D. E.,and E. M. Healey. Some Economic Aspects of High Temperature Steam Cycles. NTIS 214 750. EPA AP-109. (Proceedings of Second International Conference on Fluidized Bed Combustion. 1970.)
3. Campbell, C. B., C. C. Frank, Sr., and J. C. Spahr. The Eddystone Superpressure Unit. Westinghouse Electric Corporation. Lester, Pennsylvania. 1957.
4. Williamson, R. B. Turbine Generator Unit Leads Heat-Rate Parade. Electrical World. March 11, 1963.
5. Archer, D. H., et al. Evaluation of the Fluidized Bed Combustion Process. Office of Air Programs. Westinghouse Research Laboratories. Pittsburgh, Pennsylvania. Contract 70-7, NTIS PB 211-494, PB 212-916, PB 213-152. November 1971.
6. Reduction of Atmospheric Pollution. Volumes 1, 2, and 3. Environmental Protection Agency. National Coal Board. London, England. Contract CPA 70-97. NTIS 210-673, 210-674, 210-675. September 1971.
7. Pressurized Fluidized Bed Combustion. R&D Report No. 85. Interim No. 1. Office of Coal Research. National Research Development Corporation. London, England. Contract No. 14-32-0001-1511. NTIS PB 235-591. 1974.
8. Dainton, A. D.,and D. E. Elliott. (Presented at Seventh World Power Conference. Moscow. 1968.)

APPENDIX M

FLUIDIZED BED COMBUSTION TEST FACILITY

APPENDIX M

FLUIDIZED BED COMBUSTION TEST FACILITY

INTRODUCTION

A pressurized fluid bed boiler development plant was conceived to demonstrate pressurized fluidized bed boiler operation under a previous contract to the Environmental Protection Agency (EPA). Preliminary designs, cost estimates, experimental program, schedule, and program alternatives have been reported.[1] The development plant design incorporated the pressurized fluidized bed boiler design concept proposed for commercial plants.[2] The plant objectives were to provide the capability for studying fluid bed combustion and heat transfer, steam generation, solids feed and handling, particulate removal, gas-turbine performance, boiler control, and sulfur dioxide and nitrogen oxide emission control.

EPA extended the concept for the development plant during 1974 to incorporate greater flexibility. Goals for the test facility included provision of:

- Complete environmental data on fluidized bed combustion processes — including conditions with first-and second-generation concepts
- Necessary environmental data on an experimental scale such that data can be directly applied to demonstration and commercial plants
- Necessary data on a schedule compatible with commercialization of fluidized bed combustion technology
- Direct dissemination of information to U.S. industry, government, and other interested institutions involved or interested in developing fluidized bed combustion technology.

Westinghouse was invited to submit a proposal for a program to design, construct and operate a multipurpose, environmental test facility. A proposal was submitted in November 1974. While this work was not carried out as part of the Westinghouse-EPA contract, it is related. The essence of the proposed work is included to provide perspective and to document some of the thinking subsequent to the development plant design reported in December 1973.

SCOPE

The test facility would have the ability to investigate

- Fluidized bed combustor designs — fluidized bed boiler, recirculating bed boiler, and adiabatic combustor concepts
- Sulfur removal systems — high utilization once-through limestone/dolomite, regenerative limestone/dolomite processes, alternative sorbent processes
- Particulate removal systems — cyclonic devices, granular bed filters
- Auxiliary equipment — solids feed systems, instrumentation
- Gas-turbine performance — corrosion, erosion, deposition tolerance
- Alternative fuels — coals, coal chars, low-grade petroleum fractions, refuse
- Advanced cycle concepts — supercritical steam cycles, liquid metal-topping cycles.

To meet these objectives, a test facility was proposed which includes the systems indicated in Figure M-1.

Two fundamental design philosophies should be considered for the flexible test facility during the conceptual design study:

- The utilization of a single pressurized fluidized bed combustor module capable of investigating fluidized bed

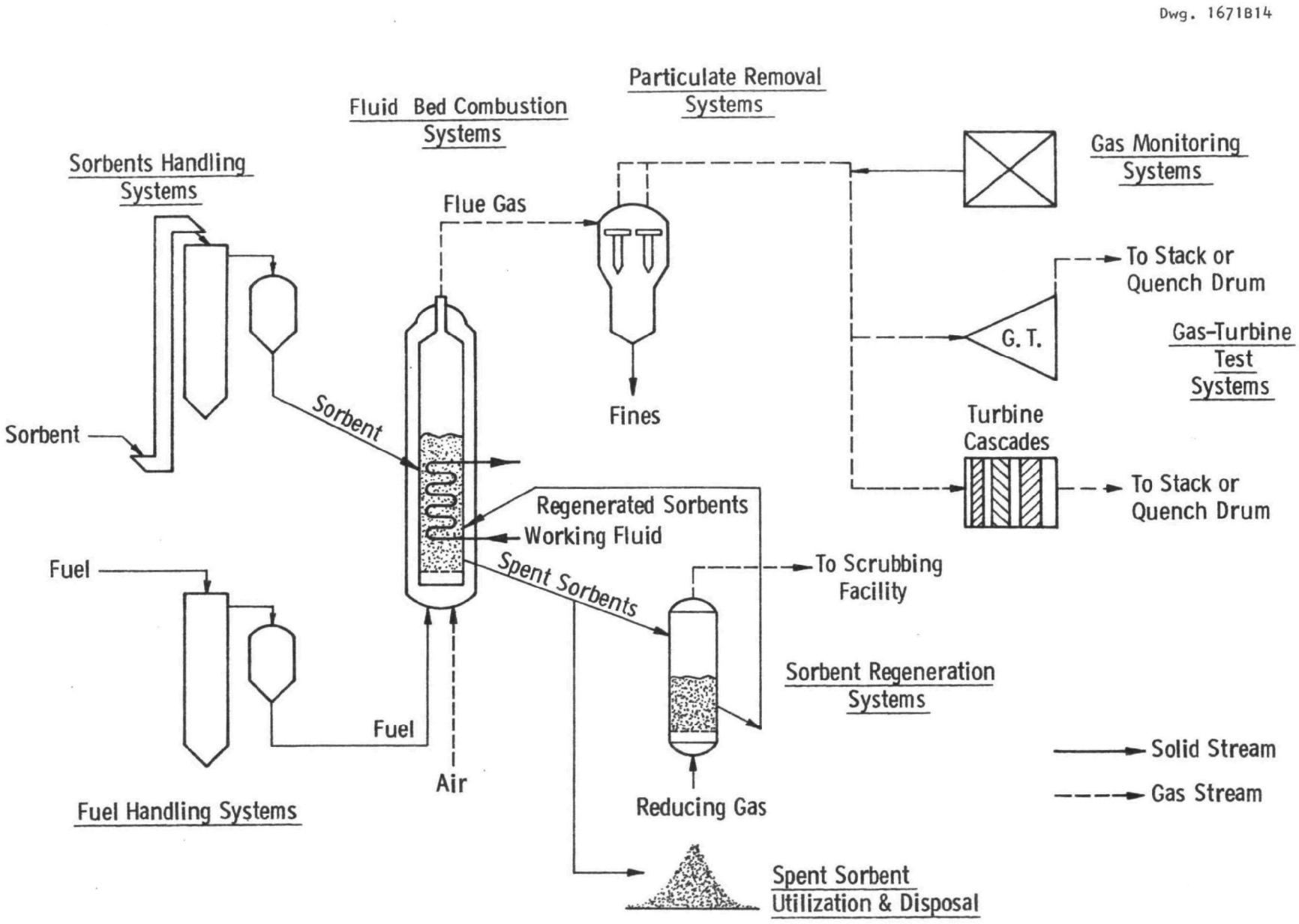

Figure M-1 — Overall schematic of the flexible test facility

boiler, recirculating bed boiler, and adiabatic combustor concepts

- The utilization of two pressurized fluidized bed combustor modules served by one common set of auxiliaries — one vessel designed as a fluidized bed boiler and the second designed as a recirculating bed boiler that is capable of conversion to an adiabatic combustor. The utilization of two modules with a common set of auxiliaries has the advantages of
  - Increasing the real-time test capability of the facility with only an incremental increase in plant cost
  - Providing the added capability of simulating multibed operation.

Since the two-module design provides greater flexibility, it was selected for the conceptual design which follows.

CONCEPTUAL DESIGN

Fluidized Bed Combustion Systems

A two-module test facility would consist primarily of two pressurized vessels nominally with an inside diameter of 3.7 m (12 ft). Vessel 1 is 23.8 m (78 ft) high and is designed as a fluidized bed boiler. Vessel 2 is 12.2 m (40 ft) high and is designed as a recirculating bed boiler, with the capability of subsequent conversion to an adiabatic combustor. Addition of the second vessel without the internals is estimated to cost approximately $150,000, or about 1 percent of the projected plant cost. With the internals for the recirculating bed boiler, the cost will increase to about 5 percent of the plant cost; this, however, doubles the real-time test capability. The three boiler design concepts initially considered are discussed in the paragraphs that follow.

The facilities would be designed for maximum flexibility of operation. The two vessels would be sited adjacent to one another and served by a common set of auxiliaries. Upstream would be units for receiving, handling, and feeding fuels and dolomite (or an alternative sorbent) to the vessels, and a compressor for supplying air for combustion and fluidization. Downstream would be a spent dolomite treatment and disposal system, a particulate removal system for cleaning the vessel fuel gas, and a gas-turbine test facility and by-pass dump quench drain for handling the product gas.

Fluidized Bed Boiler

Conceptual designs for fluidized bed steam generators for electric power generation using a combined cycle plant have been carried out for 320 and 635 MW stations.[2] These each consist of four sets of fluidized bed boilers, and each set contains four stacked fluidized beds as illustrated in Figure M-2. The beds are in parallel with respect to the airflow and in series with respect to the steam/water flow, and are contained in an unlined pressure vessel. The walls of the beds are water cooled, and banks of boiler tubes are immersed in the beds. The four beds carry out the functions of preevaporator, first superheater, second superheater, and reheater respectively.

Vessel 1 in the test facility would be capable of simulating the operation of any one of these fluidized bed boiler units at the actual size envisaged for the 320 MW station. In the 3.7 m (12 ft) inside diameter pressure shell there would be one 1.5 by 2.1 m (5 by 7 ft) fluidized bed unit similar to the previous Westinghouse-Foster Wheeler test plant design shown in Figure M-3. The range of operating parameters which could be accommodated are outlined in Table M-1. The operating conditions in the 320 MW commercial design are presented in Table M-2 for comparison. The 24 m (78 ft) vessel height allows for fluidized bed depths up to 9.1 m (30 ft) which is twice the maximum bed depth allowed for in the conceptual commercial design.

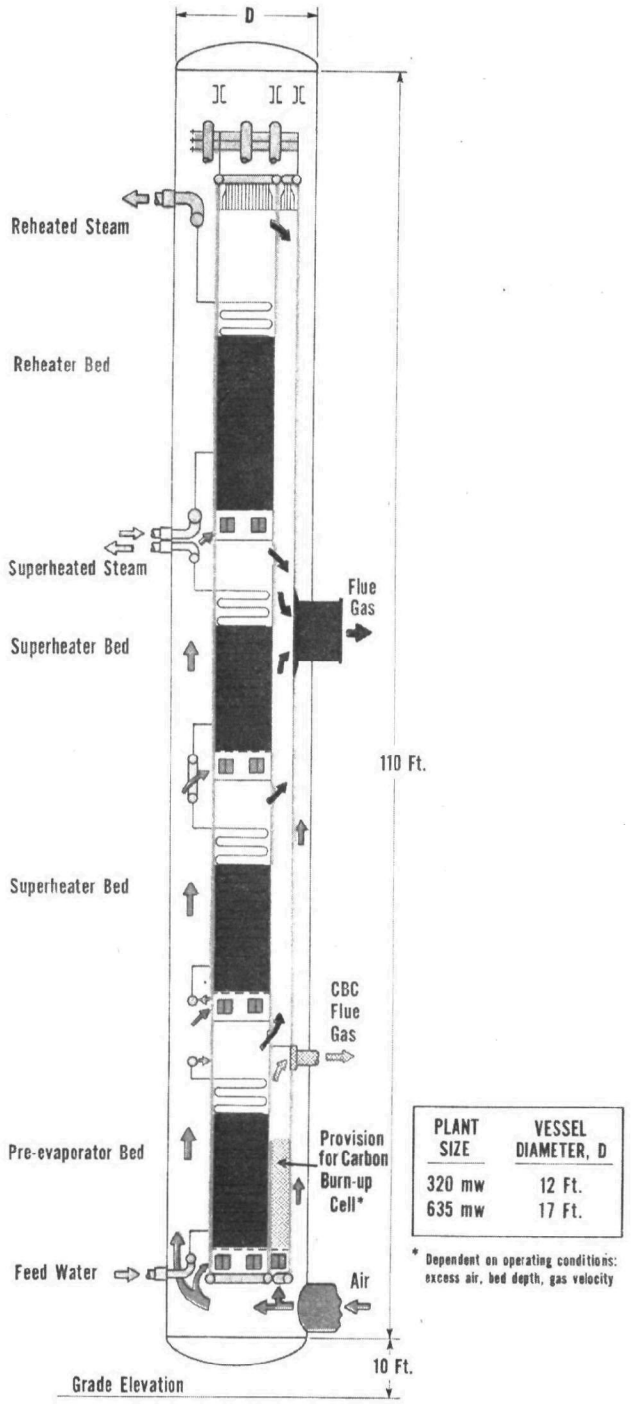

Figure M-2—Pressurized fluidized bed steam generator for combined cycle plant

Table M-1

DESIGN BASIS FOR PRESSURIZED FLUIDIZED BED BOILER

Pressure	101.3-2026 kPa (1-20 atm)
Temperature	816-1093°C (1500-2000°F)
Gas Velocity	1.8-4.6 m/s (6-15 f/s)
Bed Area	∿3.25 m^2 (∿35 ft^2)
Bed Depth	1.22-9.15 m (4-30 ft)
Ca/S	1-6 for once-through 2-10 for regeneration
Heat Transfer Coefficient	285 $W/m^2/°K$ (50 Btu/hr-ft^2-°F)
Particulate Carry-over	22.9-68.7 gm/m^3 (10-30 gr/scf)
Particle Size Coal	-6.35 mm x 0 (-1/4 in x 0)
Particle Size Dolomite	-6.35 mm x 0 or 6.35 mm x 0.6 mm (-1/4 in x 0, or 1/4 in x 30 mesh)
Site	Existing power plant
Air supply	Separate air compressor, motor drive
Excess air	>160% capability
Air preheat	To 316-454°C (600-850°F)
Feedwater temperature	To 110-260°C (230-500°F)
Heat transfer surface	Capability for testing water walls, preheat, evaporation, and superheat tube bundles
Coal feed	Up to 9979 kg (22,000 lb)/hr
Sorbent feed	Up to 16,194 kg (35,700 lb)/hr

Table M-2

FLUID BED OPERATING CONDITIONS IN 320 MW COMMERCIAL DESIGN

	Fuel flow, kg (lb)/min	Airflow kg (lb)/min	Flue gas, kg (lb)/min	Superficial velocity, mm/sec (ft/sec)	Bed depth, m (ft)	Bed temp., °C (°F)
Preevaporator	8,020 (17,680)	87,137 (192,100)	93,532 (206,200)	2.74 (9.0)	3.90 (12.8)	954 (1750)
First superheater	5,942 (13,100)	64,729 (142,700)	69,718 (153,700)	2.07 (6.8)	3.35 (11.0)	954 (1750)
Second superheater	4,872 (10,740)	53,026 (116,900)	57,108 (125,900)	1.71 (5.6)	3.35 (11.0)	954 (1750)
Reheater	5,620 (12,390)	61,145 (134,800)	65,863 (145,200)	1.95 (6.4)	4.36 (14.3)	954 (1750)

PAGE NOT

AVAILABLE

DIGITALLY

The simplified process flow diagram and material balance for the fluidized bed boiler, Vessel 1, in the test facility are given in Figure M-4 and Table M-3. The same auxiliaries will be used for operation of Vessel 2.

Commercial boiler design operating conditions (Table M-2) require that the bed be operated at higher gas velocity, higher bed pressure, higher temperature, and with a deeper bed than the test facilities currently available(for example, the British Coal Utilization Research Association (BCURA) unit[4-7] and the Exxon miniplant[8,9]). A comparison of the parameters of the commercial design and those of the existing pressurized pilot-scale experimental units is presented in Table M-4. In addition to the difference in physical size, some design parameters, such as bed height/bed diameter ratio and bed area/coal-feeding nozzle, are difficult to duplicate in small-scale combustors. There are also differences in the experimental results obtained from the small-scale combustors. For example, Exxon found a large temperature gradient in the order of 167°C/m (300°F/ft) bed depth in their initial bed design, but BCURA observed only a 17°C (30°F) temperature difference in their 1.37 m (4.5 ft) bed. All the design parameters listed in Table M-4 may contribute to this discrepancy. This points to the importance of providing a large-scale test facility to investigate the design, construction, and performance of the proposed commercial boiler plant,at the proposed operating conditions,so that commercial feasibility may be assessed. The flexibility features provided in Vessel 1 are:

- Capability of operating the fluidized bed boiler up to a 9.1 m (30 ft) bed depth. This changes the bed height/diameter ratio.
- Capability of changing the number of coal-feeding nozzles. This alters the variable bed area/coal-feeding nozzle.
- Capability of varying the coal feed rate, which changes the heat release rate per unit bed area and the heat release rate per unit bed volume.

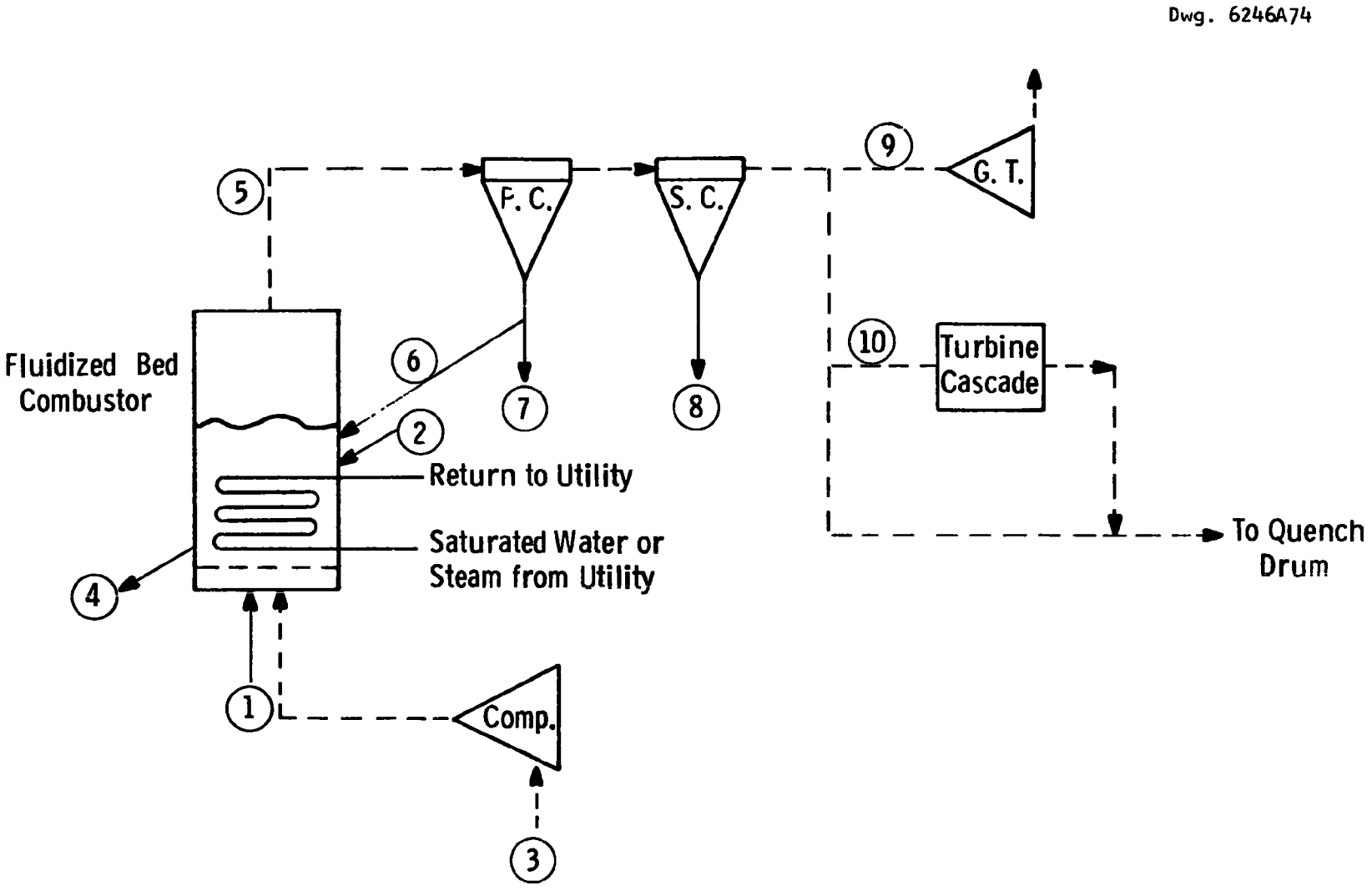

Figure M-4 – Material balance for the fluidized bed combustion boiler

Table M-3

MATERIAL BALANCE FOR THE FLUIDIZED BED COMBUSTION BOILER

Stream no.	Component	Flow rate, kg/hr (lb/hr)	Approx. temp. °C (°F)	Approx. pressure, kPa (psia)
1	Coal	9,979 (22,000)	Ambient	1216.3 (176.4) minimum
2	Dolomite	16,207 (35,730)	Ambient	1216.3 (176.4) minimum
3	Air	108,410 (239,000)	260 (500)	1206 (175)
4	Spent dolomite	9,526 (21,000)	871 (1600)	1206 (175)
5	Flue gas	124,286 (274,000)	871 (1600)	1137 (165)
6	Fines recycled	1,315 (2,900)	871 (1600)	1137 (165)
7	Fines	649 (1,430)	871 (1600)	1137 (165)
8	Fines	254 (560)	871 (1600)	1137 (165)
9	Gas to gas turbine	27,216 (60,000)	871 (1600)	1137 (165)
10	Gas to turbine cascade	68,584 (151,200)	871 (1600)	1137 (165)

Table M-4

COMPARISON OF DESIGN PARAMETERS BETWEEN THE BASIC DESIGN AND THE PILOT-SCALE EXPERIMENTAL UNITS

	Basic design[b]	BCURA unit	Exxon miniplant
Bed Cross-Section	1.52 m x 2.13 m (3.25 m^2) (5 ft x 7 ft [35 ft^2])	0.61 m x 0.91 m (0.56 m^2) (2 ft x 3 ft [6 ft^2])	0.3175 m I.D. (0.08 m^2) (12.5 in I.D. [0.85 ft^2])
Bed Height	3.35 m-4.27 m (11-14 ft)	1.37 m (4.5 ft)	3.05 m-4.6 m (10-15 ft)
Bed Height/Diameter Ratio[a]	2-2.5	2	9.5-14.5
Tube Packing, % bed cross-section	21.5-28.5	17	28
% bed volume	17-22.5	8	9
Heat Release Rate/Bed Area	1.2-2.0 x 10^7 J/m^2-sec (3.8-6.3 x 10^6 Btu/ft^2-hr)	3.2 x 10^6 J/m^2-sec (1.0 x 10^6 Btu/ft^2-hr)	1.46 x 10^7 J/m^2-sec (4.6 x 10^6 Btu/ft^2-hr)
Volume Heat Release Rate	3.6-4.7 x 10^6 J/m^3-sec (3.5-4.5 x 10^5 Btu/ft^3-hr)	2.3 x 10^6 J/m^3-sec (2.2 x 10^5 Btu/ft^3-hr)	3.7 x 10^6 J/m^3-sec (3.6 x 10^5 Btu/ft^3-hr)
Bed Area/Coal Feeding Nozzle	0.81 m^2 (8.75 ft^2)	0.14 m^2 (1.5 ft^2)	0.08 m^2 (0.85 ft^2)

[a] For beds of rectangular cross-section, the hydraulic diameters are used.

[b] Basic design has four fluidized beds of slightly different designs per module for preevaporation, superheating, and reheating.

- Capability of changing the heat transfer surface configuration — for example, horizontal tube versus vertical tube configurations. This alters the pattern of solid circulation, gas bubble size, and bed-tube heat transfer coefficient.
- Capability of changing the boiler tube material, which allows studies of corrosion/erosion of boiler tubes at different steam conditions.

Recirculating Fluidized Bed Boiler

Fluidized bed combustion technology can be applied with many different configurations and can be utilized in many different steam and power cycles, as has been discussed elsewhere.[2,3] Two alternative pressurized fluid bed combustion concepts can be studied:

- A recirculating bed boiler concept
- An adiabatic combustor combined-cycle plant which represents a modification of the base power cycle.

Conceptual designs, performance, and economics for these two concepts were projected and compared favorably with the pressurized fluid bed boiler combined-cycle plant.[3]

The concept of a deep recirculating fluidized bed boiler is illustrated in Figure M-5. Primary air, along with coal or low-grade liquid fuels, is fed to the boiler at the base of an open draft tube. The draft tube may be metallic or ceramic with water cooling and/or steam generation. The superficial velocity of the air and combustion gases flowing up the riser is 3.1 to 18.3 m/sec (10 to 60 ft/sec) at the operating temperature and pressure of 704 to 1093°C (1300 to 2000°F) and 405 to 2026 kPa (4 to 20 atm). The solids and gases emerging from the riser pass into a bed of expanded cross-section and decreased superficial gas velocity. The heat transfer surface may be located in the bed section and in the downcomer region for steam generation. The

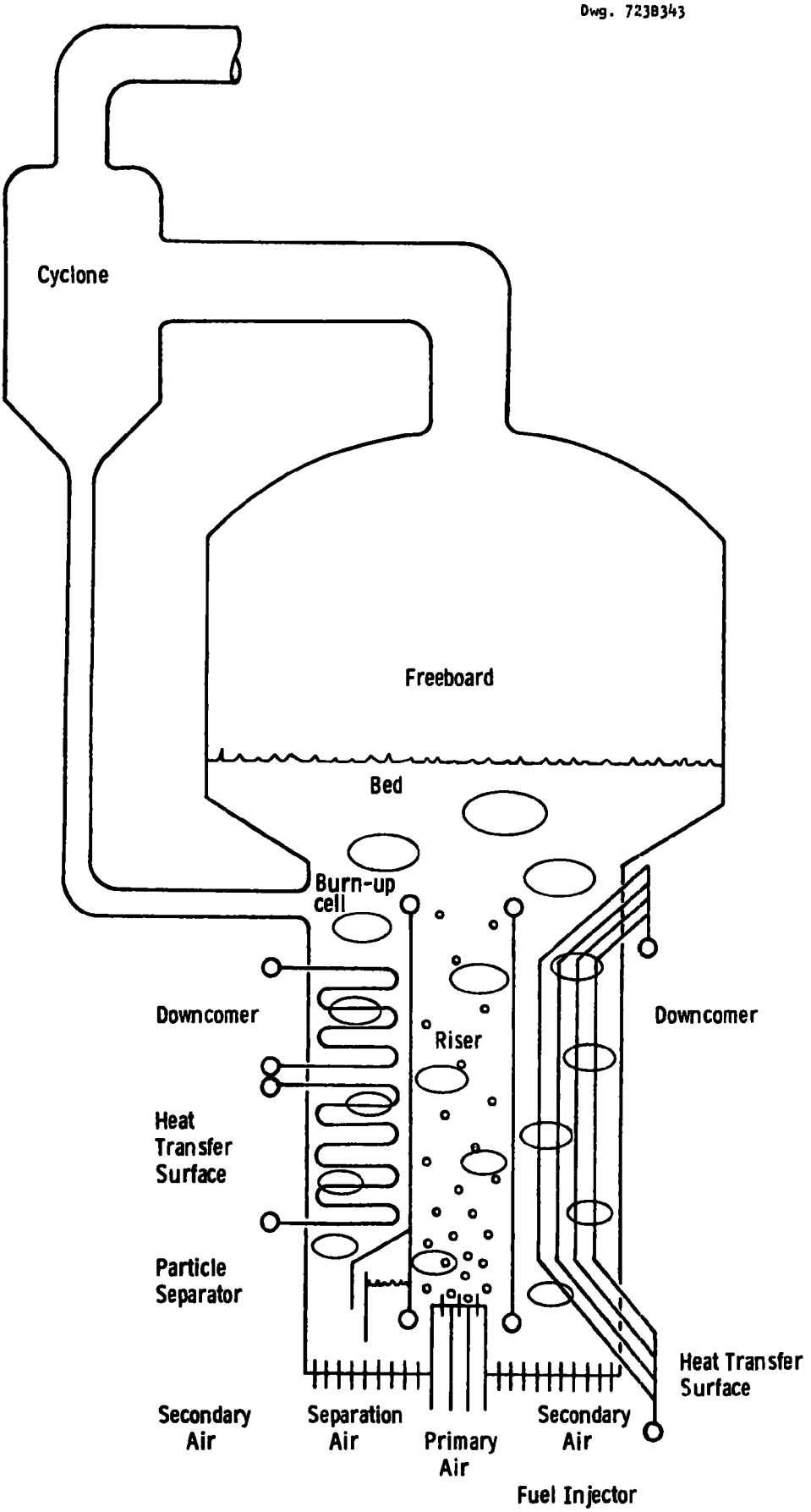

Figure M-5— Deep recirculating fluidized bed boiler

gas velocity in the bed is in the range of 0.31 to 4.6 m (1 to 15 ft)/sec. Sorbents may be added along with the fuel for sulfur removal. Secondary air is introduced at the base of the downcomer at a rate necessary to permit the downward free flow of the solids. Flow of the solids in the downcomer can be reduced or halted by reducing or cutting off the secondary air. This capability makes it possible to adjust independently the heat removal and heat production in the boiler.

A conceptual recirculating bed boiler design was prepared on the basis of the boiler plant design developed by Westinghouse under contract to EPA.[3] The design selected for a 320 MW recirculating bed boiler consisted of six individual modules of 3.7 m (12 ft) inside diameter with one module for preheater, two modules for evaporator, two modules for superheater, and one module for reheater. This design was selected to permit standard shop-fabrication of each vessel.

Vessel 2 can be used to study the recirculating bed concept with the upstream and downstream facility common with that for Vessel 1. This two-vessel facility with common upstream and downstream auxiliaries will substantially increase the availability of the facility. Both concepts can be evaluated in parallel. When one unit is shut down for modification, the other unit can be operated. The material balance for Vessel 2 operated as a preevaporator in the recirculating bed concept is presented in Figure M-6 and Table M-5.

Adiabatic Combustor

The pressurized fluidized bed boiler concepts operate at excess air values from 10 to 100 percent, with up to 70 percent of the heat released in burning the fuel with air transferred to the water/steam in the tubes surrounding and submerged in the bed. Increasing the design point excess air with constant bed temperature will decrease the total heat transfer surface in the fluid bed until no boiler tube surface will be required at an excess air of approximately 360 percent. In this case, the power system is a combined-cycle plant with the gas to the turbine expanders supplied from a coal-fired, adiabatic combustor.[3] Combined-

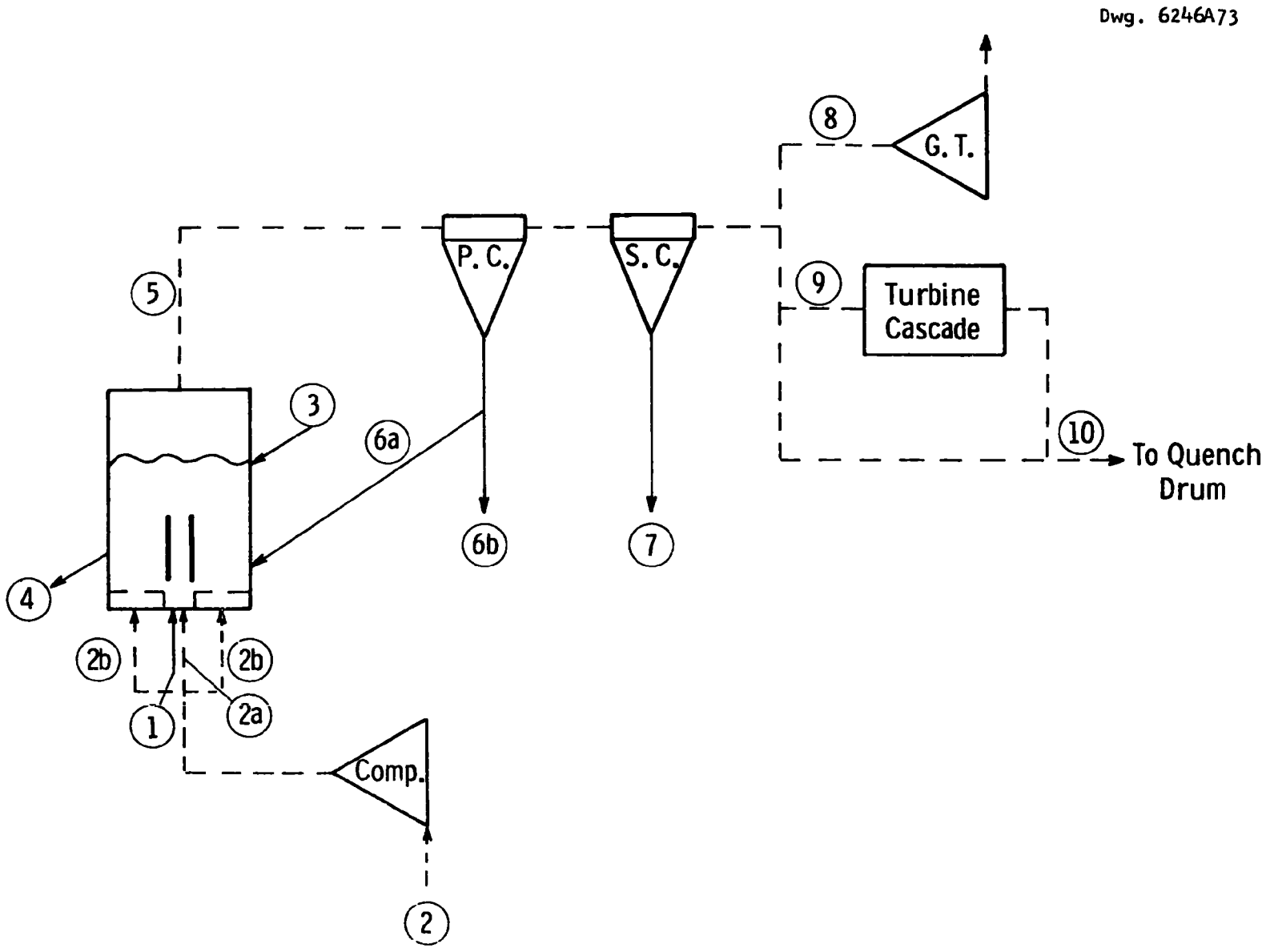

Figure M-6— Material balance for the recirculating bed concept (preevaporator)

Table M-5

MATERIAL BALANCE FOR THE RECIRCULATING BED CONCEPT

Stream no.	Component	Flow rate, kg/hr (lb/hr)	Approx. temp. °C (°F)	Approx. pressure, kPa (psia)
1	Coal	9,163 (20,200)	Ambient	1216.3 (176.4) minimum
2	Air	100,699 (222,000)	260 (500)	1207 (175)
2a	Air	85,277 (188,000)	260 (500)	1207 (175)
2b	Air	15,422 (34,000)	260 (500)	1207 (175)
3	Dolomite	10,478 (23,100)	Ambient	1216.3 (176.4) minimum
4	Spent dolomite (30% utilization)	6,804 (15,000)	871 (1600)	1216.3 (176.4)
5	Flue gas	109,771 (242,000)	871 (1600)	1138 (165)
6a	Fines recycled	1,216 (2,680)	871 (1600)	1138 (165)
6b	Fines	522 (1,150)	871 (1600)	1138 (165)
7	Fines	225 (495)	871 (1600)	1138 (165)
8	Gas to gas turbine	68,584 (151,200)	871 (1600)	1138 (165)
9	Gas to turbine cascade	27,307 (60,200)	871 (1600)	1138 (165)
10	Gas to quench drum	41,278 (91,000)	871 (1600)	1138 (165)

cycle plants of this type, which burn natural gas and/or heavy distillates, are now being marketed to electrical utilities for intermediate-and base-load applications. One embodiment of such a plant is the Westinghouse Power at Combined Efficiencies (PACE) plant.

A preliminary evaluation was made of the adiabatic combustor fuel processing system. Two design concepts — a single fluid bed module and a stacked fluid bed module — were considered, as illustrated in Figure M-7. A summary of the respective design features is presented in Table M-6. Vessel 2 can be modified to simulate a single-bed operation in the stacked-bed design. The same auxiliaries existing for the fluidized bed boiler can also be used here. Due to the compressor rating, the bed will operate at about 90 percent capacity. The material balance is summarized in Figure M-8 and Table M-7. Data obtained in this unit are projected to be applicable for any adiabatic combustor larger than 3.7 m (12 ft) in diameter.

Design Features

Vessel is a 3.7 m (12 ft) inside diameter unlined pressure vessel which contains the fluidized bed boiler module as described previously. This vessel will have an equivalent rating of 30 MW and will represent the full-size operation of individual fluidized beds in a multifluidized bed, 320 MW station. By operating the vessel in each of three boiler modes in turn, piecemeal simulation of the total commercial plant will be achieved.

Vessel 2 is designed as a recirculating bed boiler, with the capability of being subsequently modified for operation as an adiabatic combustor. It has refractory-lined walls of 12 ft inside diameter and a central draft tube around which circulation of the bed material takes place. This vessel also represents one full-size fluidized bed unit in a 320 MW multiunit plant and could be operated in any one of the four boiler modes. Vessel 2 uses the same auxiliaries as Vessel 1, and the vessels can initially be operated one at a time.

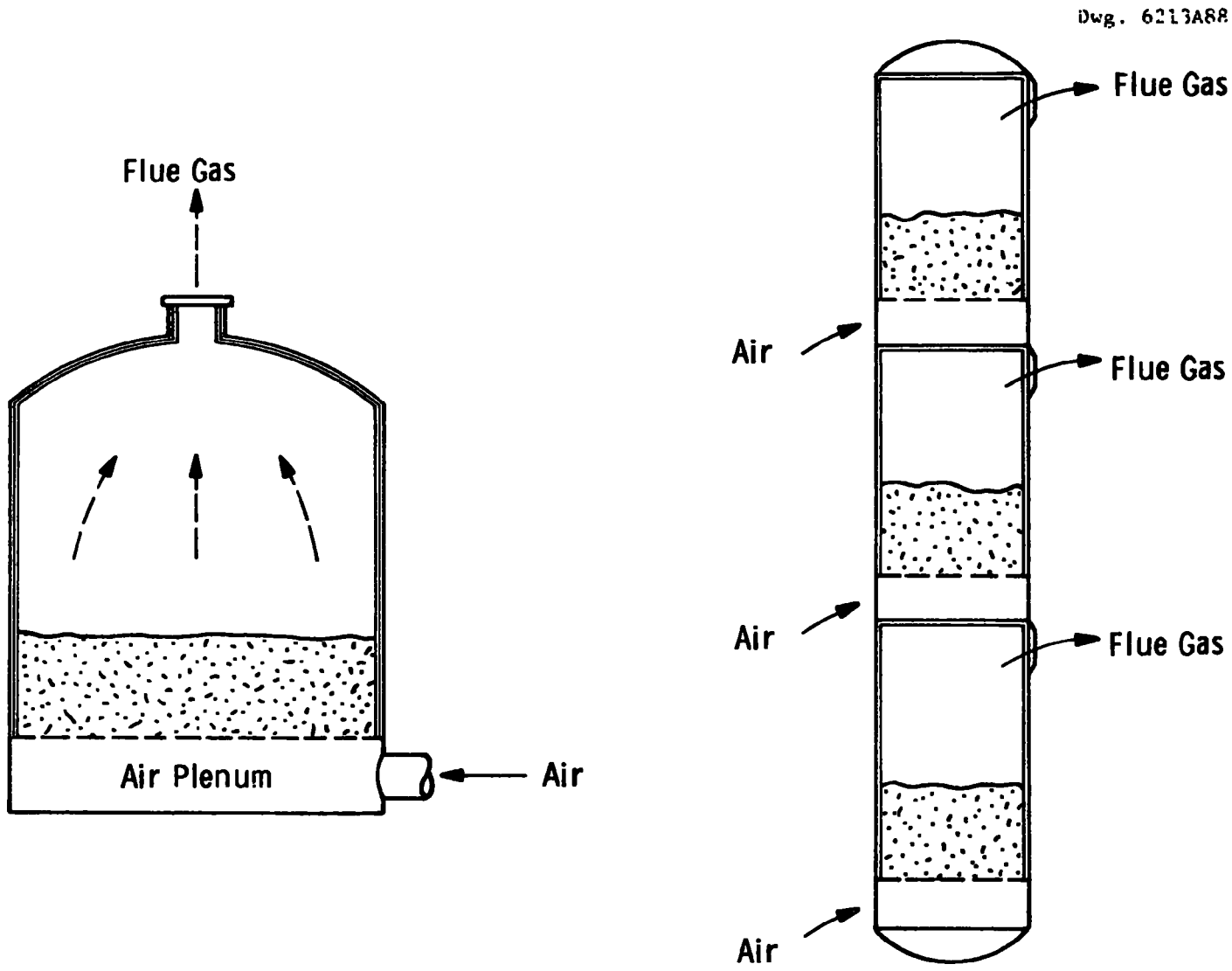

Figure M-7—Adiabatic combustor designs-Westinghouse/Foster Wheeler Design

Table M-6

ADIABATIC COMBUSTOR DESIGNS

	Single bed designs		Stacked bed designs	
	I	II	I	II
Number of modules	4	2	4	2
Number of beds per module	1	1	3	6
Module diameter, m(ft)	6.4(21)	9.1(30)	3.7(12)	3.7(12)
Module height, m(ft)	4.9(16)	4.9(16)	15.2(50)	152.4(500)
Bed depth, m(ft)	2.0(6.5)	2.0(6.5)	2.0(6.6)	2.0(6.6)
Bed area, $m^2(ft^2)$	32.3(347)	64.6(695)	10.5(113)	10.5(113)
Fluidizing velocity, m/sec(ft/sec)	1.8(6)	1.8(6)	1.9(6.2)	1.9(6.2)

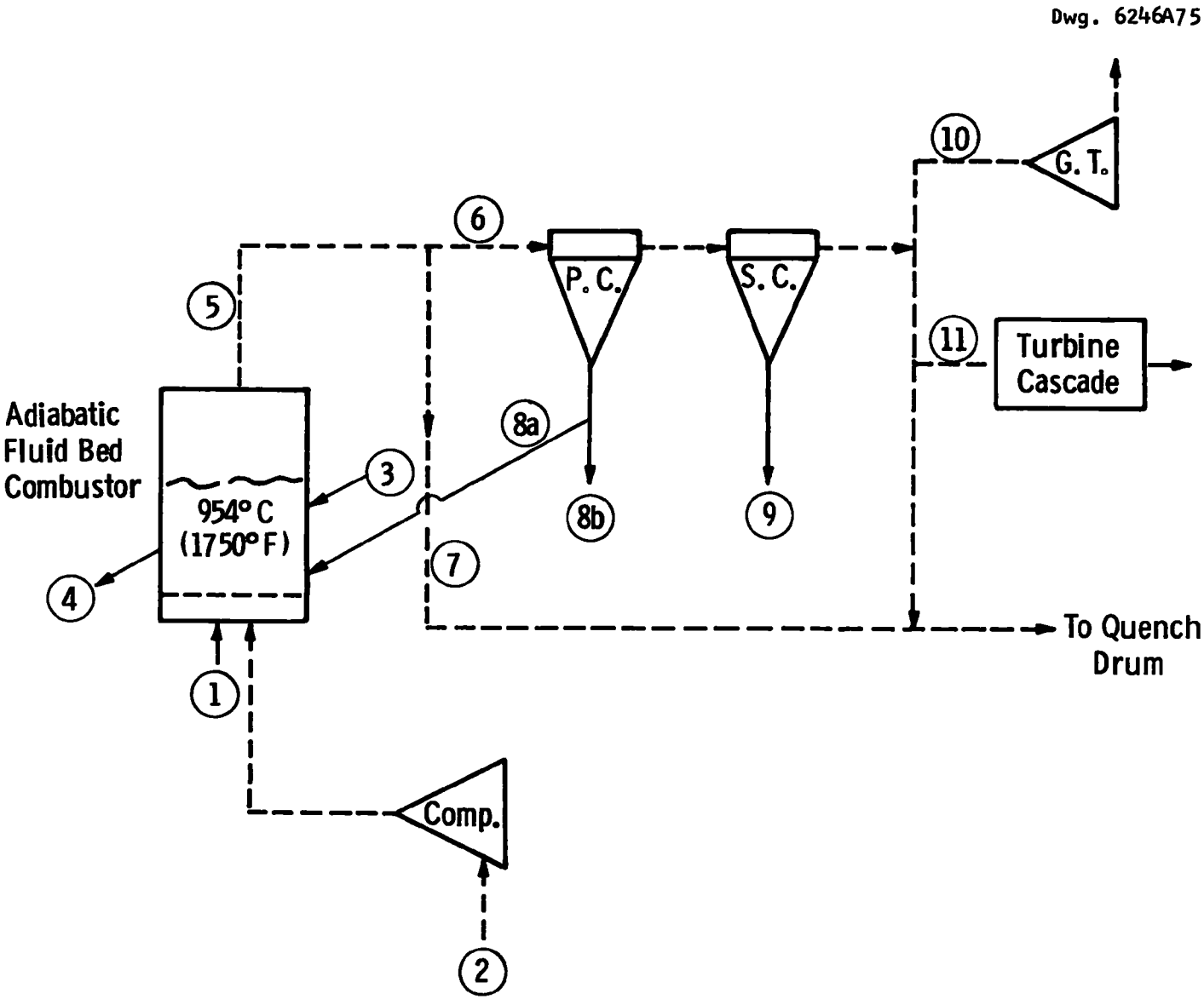

Figure M-8 – Material balance for the adiabatic fluid bed combustor

Table M-7

MATERIAL BALANCE FOR THE ADIABATIC FLUID-BED COMBUSTOR

Stream no.	Component	Flow rate, kg/hr (lb/hr)	Approx. temp. °C (°F)	Approx. pressure, kPa (psia)
1	Coal	4,808 (10,600)	Ambient	1,021 (148) minimum
2	Air	175,997 (388,000)	323 (614)	1,010 (146.5)
3	Dolomite	5,489 (12,100)	Ambient	1,021 (148) minimum
4	Spent dolomite	3,565 (7,860)	871 (1600)	1,021 (148)
5	Flue gas	180,805 (398,600)	871 (1600)	993 (144)
6	Flue gas to cyclones	124,286 (274,000)	871 (1600)	993 (144)
7	Flue gas to quench drum	56,519 (124,600)	871 (1600)	993 (144)
8a	Fines recycled	1,315 (2,900)	871 (1600)	993 (144)
8b	Fines	649 (1,430)	871 (1600)	993 (144)
9	Fines	254 (560)	871 (1600)	993 (144)
10	Gas to gas turbine	68,584 (151,200)	871 (1600)	993 (144)
11	Gas to turbine cascade	27,307 (60,200)	871 (1600)	993 (144)

Since the air compressor is 60 percent oversized for either vessel, the two vessels can be operated in parallel with the airflow to each at 80 percent maximum. In this way multibed operation as in the commercial unit can be simulated, which is particularly useful for developing start-up, shut-down, and control techniques. Vessel 1 would operate as a fluidized bed boiler and Vessel 2 as a recirculating bed boiler, as before. Any consecutive pair of boiler modes could be simulated with steam flowing in series from one vessel to the other.

A refractory-lined pressure vessel is formed by removing the draft tube and boiler tubes from Vessel 2 and modifying the air inlet distributor plate. This may be operated as an adiabatic combustor. In this mode the heat of combustion is removed from the vessel as sensible heat in the off-gas,and about 300 percent excess air is required. With coal as the fuel, the air requirement and the product gas volume are both twice that of either the fluidized bed boiler or the recirculating bed boiler. Operating the air compressor at full capacity will therefore enable the adiabatic combustor to operate at around 90 percent of its maximum rating. The 3.7 m (12 ft)inside diameter adiabatic combustor represents one full-size bed in a 300 MW plant, which consists of 12 such beds.

The tube bundles in the fluidized bed boiler are designed for easy alteration, the number of tube banks can be altered, or banks of vertical tubes can be substituted for horizontal tubes.[1] Appraisal of such tube configuration can be substituted for horizontal tubes. Appraisal of such tube configuration could most effectively be carried out in Vessel 1.

The recirculating bed boiler is designed with vertical tubes originating from headers positioned above the level of the fluidized bed; this arrangement facilitates complete removal of steam-raising equipment, and since the walls are refractory lined, Vessel 2 is most easily converted to an adiabatic combustor.

Vessel 1 may also be operated as an atmospheric-pressure boiler. In this case the bed depth must be kept low to minimize bed pressure drop, and the flue gas is no longer capable of driving a gas turbine. The same auxiliary systems would again be utilized; the compressor would be run at reduced pressure differential and increased throughput. All boiler tubes except those in the bed would be removed.

Vessel 1 could also be used to assess the application of fluidized bed boilers for use with advanced power cycles. The fluidized bed temperature is limited to about 1000°C (1832°F) by dolomite sulphur removal properties, but higher gas outlet tmperatures may be attained, for example, by burning fines in the freeboard area with secondary air injection. Also, the present heat transfer tube designs will allow for higher steam temperature and pressure.[3]

Additionally, Vessel 1 could be used to investigate the concept of the potassium vapor cycle,[10] in which liquid potassium replaces steam/water in the boiler tubes and the dry saturated vapor is delivered to a potassium vapor turbine for power generation. Such tests would involve changing the material of the boiler tubes.

In summary, the proposed fluidized bed combustion systems combine the characteristics of flexibility and full size simulation of fluidized bed boilers and combustors.

This flexibility is illustrated by the following summary of test capabilities to:

- Operate Vessel 1 as a fluidized bed boiler.
- Operate Vessel 2 as a recirculating bed boiler.
- Operate Vessels 1 and 2 in parallel to simulate multibed operation.
- Operate Vessel 2 as an adiabatic combustor.
- Test different tube bundle configurations in Vessel 1.
- Operate Vessel 1 as an atmospheric boiler.

- Operate Vessel 1 as a fluidized bed boiler with advanced power generation cycles.

It is always difficult to decide the size for a test facility. The basis for the size in this case was the selection of a commercial-scale unit. In reaching this decision, several criteria were considered:

- Objectives
  - Scope (e.g., first or second generation, alternative concepts)
  - Environmental control
  - Component development
  - Commercial scale demonstration
- Scale-up — scale-up of data to commercial operation: What is the minimum scalable size for each component?
- Operation — continuous
  - Integrated/discrete
  - Time required/experiment
  - Modification time
- Cost — capital
  - Operating
- Construction time.

A comparison of design parameters for commercial units and for two test units is summarized in Tables M-8 and M-9. The two test units identified in the tables can be assessed on the basis of the above criteria. In particular,

- Objectives — Maximum process information can be obtained with the minimum-scale plant; the larger plant, however, is required to develop commercial-scale operating credibility.

Table M-8

EVALUATION OF TEST FACILITY SIZE

Equipment	Design parameters in commercial design	Projected minimum scalable size	Suggested minimum size test unit			Recommended test unit size		
			Design parameters	Scale-up factor to commercial size	Equivalent capacity	Design parameters	Scale-up factor to commercial size	Equivalent capacity
Fluidized Bed Combustor				~1:2	15 MW		1:1	30 MW
Pressure vessel size, m(ft)	3.7(12) ID 3.3(1.5 x 2.1)	2.4(8) ID 1.9(1.5 x 1.2)	2.4(8) ID 1.9(1.5 x 1.2)			3.7(12) ID 3.3(1.5 x 2.1)		
Bed area, $m^2(ft^2)$	[35(5 x 7 ft)]	[20(5 x 4 ft)]	[20(5 x 4 ft)]			[20(5 x 7 ft)]		
Bed height/diameter ratio*	2-2.5	(Based on bed height/diameter ratio consideration)	2-6.5			2-2.5		
Tube packing,% bed cross section	21.5-28.5		10-30			10-30		
Tube packing,% bed volume	17-22.5		10-30			10-30		
Heat release rate/bed area, $W/m^2(Btu/ft^2-hr)$	$11.98-19.86 \times 10^6$ $(3.8-6.3 \times 10^6)$		$7.88-23.64 \times 10^6$ $(2.5-7.5 \times 10^6)$			$7.88-23.64 \times 10^6$ $(2.5-7.5 \times 10^6)$		
Heat release rate/bed volume, $W/m^2(Btu/ft^3-hr)$	$11.03-14.18 \times 10^5$ $(3.5-4.5 \times 10^5)$		$7.88-23.64 \times 10^5$ $(2.5-7.5 \times 10^5)$			$7.88-23.64 \times 10^5$ $(2.5-7.5 \times 10^5)$		
Bed area/coal-feeding nozzle, $m^2(ft^2)$	0.8(8.75)		0.5-0.9(5-10)			0.5-0.9(5-10)		
Water walls	Yes		Yes			Yes		
Regenerator				1:20-36			1:9-16	
Pressure vessel size, m(ft)	2.7-3.7(9-12) ID	0.9(3) ID	0.6(2) ID			0.9(3) ID		
Bed area, $m^2(ft^2)$	5.9-13.4(64-144)		0.3(3)			0.7(7)		
Bed height, m(ft)	1.5-3.0(5-10)		1.5-3.0(5-10)			1.5-3.0(5-10)		
Bed height/diameter ratio	0.5-1.0		2.5-5.0			1.5-3.0		
Particulate Removal Sys.								
Primary	Conv. design	Conv. design	Conv. design			Conv. design		
Secondary, ACMM(ACFM)	566-1132 (20,000-40,000)		382 (13,500)	~1:2		693 (24,500)	1:1 to 1:2	
Tertiary	?		382 (13,500)			693 (24,500)		
Gas Turbine	>30 MW	3 MW	3 MW	>10		3 MW	>10	
Turbine Cascade		7.26 kg/sec gas (16 lb/sec)	7.26 kg/sec gas (16 lb/sec)			7.26 kg/sec gas (16 lb/sec)		

*Hydraulic diameter is used when the bed is in rectangular shape.

Table M-9

EVALUATION OF TEST FACILITY SIZE

Equipment	Design parameters in commercial design	Projected minimum scalable size	Suggested minimum size test unit			Recommended test unit size		
			Design parameters	Scale-up factor to commercial size	Equivalent capacity	Design parameters	Scale-up factor to commercial size	Equivalent capacity
Recirculating Bed Combustor				~1:2	15-25 MW		1:1	30-50 MW
Pressure vessel size, m(ft)	3.7(12) ID	1.8(6) ID	2.4(8) ID			3.7(12) ID		
Bed area, $m^2(ft^2)$	10.5(113)		4.6(50)			10.5(113)		
Bed height, m(ft)	4.6-6.1(15-20)		4.6-6.1(15-20)			4.6-6.1(15-20)		
Draft tube ID, m(ft)	0.85(2.8)		0.67(2.2)			0.85(2.8)		
Draft tube height, m(ft)	3.0(10)		3.0(10)			3.0(10)		
Tube packing,% bed cross section	20-25		20-25			20-25		
Tube packing,% bed volume	20-25		20-25			20-25		
Coal-feeding nozzle	1		1			1		
Water walls	No		No			No		
Adiabatic Combustor				~1:2	7.5 MW		1:1	17 MW
Pressure vessel size, m(ft)	3.7(12) ID	1.2(4) ID	2.4(8) ID			3.7(12) ID		
Bed area, $m^2(ft^2)$	10.5(113)		4.6(50)			10.5(113)		
Bed height, m(ft)	2.0(6.6)		2.0(6.6)			2.0(6.6)		
Bed height/diameter ratio	0.5		0.8			0.5		
Bed area/coal-feeding nozzle, $m(ft^2)$	0.93(10)		0.46-0.93(5-10)			0.46-0.93(5-10)		
Water walls	No		No			No		

- Scale-up — Both plant sizes are specified to permit scale-up. The larger size minimizes risk since no further scale-up in size is required for the combustor. For example, tube support requirements to avoid excessive tube vibration and temperature distribution in the bed cannot be confidently projected from a small-scale test unit. The larger size also assumes the critical problem(s) are being investigated, since the same problem may not occur in a smaller unit.
- Operation — Both plants provide continuous, integrated operation. The time required for each experiment and the time required to make modifications are projected to be the same for each plant. The minimum size plant is not designed to operate the rotating turbine and test cascade simultaneously. Thus, more experiments would be required with the small unit to obtain the same information on turbine-blade corrosion/erosion.
- Cost — Capital cost for the large plant (base design) is estimated to be around $20 million. Cost for the minimum-scale plant is estimated to be $14 to 15 million. A demonstration plant is projected to cost in the order of $100 million. Manpower requirements to operate the plants will essentially be the same. Fuel and limestone costs will be lower for the minimum-size plant.
- Construction time — The time required for operating plant is expected to be the same for either plant size. The time will be limited by long lead-time equipment which will be the same for either plant.

On the basis of these comments, the only advantage of the smaller plant is the capital cost savings (~$5 million) and the savings in fuel and sorbent ($1 to 2 million over three years). The advantage of the larger plant is the minimization of risk in going to demonstration

plants. The projected savings represents about $6 to 7 million. A demonstration plant may cost $100 million or more. Potential savings in the demonstration plant capital and operating cost could be significant if results from the test system avoids a problem, a savings which could easily exceed the $6 to 7 million cost addition for the larger test system program.

Based on these considerations, a commercial-size test system is believed to offer the greatest return of technical and economic information needed to develop and commercialize pressurized fluidized bed combustion systems. Data from such a system will also provide the greatest confidence for a demonstration plant program.

Sulfur Removal Systems

On the basis of the available pilot plant data, sulfur removal to meet emission standards can be achieved. Once-through systems with high sorbent utilization have not been demonstrated on a large scale, however, and economically attractive regeneration processes have not been identified for limestone or dolomite sorbents. Alternative sorbents are known, but again their potential has not been assessed. Schemes to utilize waste sorbents in by-product functions or to convert them to environmentally acceptable products are being evaluated but have not been tested on any significant scale. The test facility would be capable of addressing these important areas. The test facility provides for tests on commercial-scale regenerative processes, once-through processes, and waste sorbent processing for by-product utilization or disposal with limestone/dolomite sorbents or alternative sorbents with new processing schemes or reaction schemes.

The process conceptual design and operation studies carried out in support programs will identify and characterize processing schemes and the associated process and equipment options in the design, installation, and operation of the test facility. Basic operating variables (temperature, pressure, concentration, and so on), temperature control options, waste heat utilization options, process turndown, and start-up options, would be considered for study. In addition, processing components common to many processes can be examined in order to identify and characterize

gas-cleaning system options and costs. These components include the following:

- Pneumatic transport processes for sorbent circulation
- Process-gas generation systems (for example, gasification systems for reducing gas generation, carbon dioxide recovery processes)
- Sulfur recovery processes (for sulfur dioxide or hydrogen sulfide processing; for sulfuric acid production, and so forth)
- Fluid bed reactors
- Other process components, such as high-temperature valves, particle pulverizers, waste heat boilers, and process

Particulate Control Systems

Provision is made to test equipment for primary, secondary, and tertiary particulate collection. The three-stage system would be capable of operating with both fluidized bed combustor test modules. It is clear that several different dust collection systems must be thoroughly evaluated and tested for the fluid bed combustion development program. Specific examples are cited at this point to illustrate the approach.

Primary collectors are considered to be conventional, state-of-the-art cyclones which will not require further investigation.

Secondary collectors will probably be cyclone collectors. Since broad choices are available — conventional multicyclone designs, or specialized designs which employ clean secondary gas flows — at this point it appears that the provision of a clean secondary gas flow may result in a more complex and less efficient gas-turbine plant. Thus, the secondary collector is considered to be a multicyclone unit of conventional design.

Tertiary collectors may be required to meet stringent dust collection efficiencies, which will limit the choice to the various

filter systems. Both porous ceramic and porous metal filters require back flushing with clean gas flows during the cleanup cycle. Granular bed filters may be designed to operate without back flushing or with cleanup by short bursts of high-pressure gas acting against the main flow. The granular beds will be simpler to incorporate into a complete system, and thus a unit of this type is considered attractive for the tertiary collection stage.

Turbine Test Facilities

A test facility consisting of a rotating, multistage turbine and several stationary test passages is recommended for the plant. This test facility, used in conjunction with analytical studies, will allow assessment of turbine blade erosion or deposition due to particulate matter and hot corrosion and/or deposition initiated by alkali-metal compounds in the gas stream. Table M-10 summarizes recommended components for the program. The multistage test turbine will provide information on the effects on erosion and deposition resulting from particle concentrations within the turbine flow path due to passage vortex development, radial pressure gradients, local flows due to stage-to-stage interactions, and particulate-blading interactions. One stationary test passage, designed with long particulate acceleration nozzles to obtain the high-particle-impact velocities that will be typical of an electrical utility gas turbine, will be used to correlate test-turbine erosion to full-scale turbine erosion. An additional full-scale first-stage turbine nozzle cascade will assess damage to this highest temperature component. A full annular cascade passage will provide information on the effect of the inlet design in patterning the particulates over the flow path in such a way as to prevent localized concentrations and, hence, prevent excessive deposition and/or erosion damage.

The turbine test facility must allow operating conditions in a large electrical utility gas turbine to be duplicated. The potential for condensation of volatile alkali-metal compounds — sodium and potassium chlorides and hydroxides and subsequent reaction to sulfate or molten

Table M-10

TURBINE TEST PROGRAM COMPONENTS

Component	Function
High-pressure, High-Temperature, Full-Scale Turbine Vane Cascade	Measures vane erosion/deposition with ability to evaluate film cooling deposition control options
High-Pressure, High-Temperature, Full Annular Stationary Cascade	Assesses particulate patterning
High-Pressure, High-Temperature Particle Accelerator Nozzle Impactor with Wedge Targets	Measures erosion/deposition rates at realistic impact velocities and angles
Rotating Hot Gas Multistage Turbine	Verifies particle concentration analytic model

sulfate-chloride mixtures — can be studied if similar gas temperatures and metal temperatures at points of corresponding pressure are duplicated and similarity of flow conditions are established over appropriate targets. Blading must be of hot-corrosion resistant materials so hot-corrosion attack of the test turbine will be comparable to attack of the large turbine. Erosion damage will be comparable if the velocities of particulate impact with turbine components are comparable in both magnitude and impact angle.

Rotating, Multistage Test Turbine

The recuperative version of the Solar Centaur industrial gas turbine appears attractive for the multistage rotating test vehicle. This machine is of the right scale for pilot-plant operation. Its gas flow requirement — 19 kg/sec (42 lb/sec) — is less than the bed output — 34.5 kg/sec (76 lb/sec) — but is sufficiently large to be useful as a demonstration of the viability of the overall concept. The inlet temperature of 871°C (1600°F) is acceptable for use on the fluidized bed combustion system, and the turbine can accept the required 1013 kPa (10 atm) inlet pressure.

Corrosion resistance of the first two stages of the Solar Turbine is roughly comparable to that of a modern electric utility gas turbine. The third-stage stator nozzles and blades should be replaced with those made of more hot-corrosion resistant materials such as alloys having at least the corrosion resistance of MAR 421.

The regenerative configuration of the machine provides both compressor outlet and hot-gas feed in locations that are immediately accessible.* The recuperative Centaur is virtually identical in all important characteristics to the present production model of the Centaur (except for the compressor outlet and hot-gas inlet) and should be reliable.

---

*In designing this facility, the turbine inlet design must be carefully examined to control dust concentrations presented to the first-stage vanes.

First-stage stationary vane erosion/deposition can be measured in a stationary cascade, provided that full-scale vanes are used in the passage. Such a cascade would require about 5 kg/sec (16 lb/sec) of gas for each nozzle passage used in the cascade. The effect of cooling airflows on deposition and erosion could be effectively studied in this facility.

A scaled full annular stationary cascade will allow experimental verification of the effectiveness of inlet manifolding design on controlling particulate concentrations over the inlet of the turbine.

This combination of test facilities allows all of the significant deposit forming/erosion mechanisms to be studied and related to the performance of full-scale commercial turbines at a fraction of the cost of operating a large machine.

Operation and Control

The test facility can be used to evaluate high-pressure fluidized bed combustion processes with particular emphasis on emissions control, component development, efficiency enhancement, and systems development. It also provides means for testing proposed commercial plant operation and control procedures. These tests could demonstrate that fluidized bed combustion power plants can meet electrical utility operating requirements such as 2:1 turndown per module, which will permit 8:1 turndown of a four-boiler plant and be capable of changing load at the rate of 5 percent per minute, while meeting environmental standards.

Auxiliaries

The test facility would also provide opportunities to test alternative coal and sorbent feed systems, gas-monitoring equipment proposed for control of particulates and trace element release, and alternative working fluids for the boiler.

Gas velocities relative to blading approach those of a large electrical utility gas turbine (similar to the Westinghouse 501) at the rotor trailing edges and at the exit to the third-stage stator. At other locations in the turbine, however, the gas velocities are considerably lower, typically reaching only about 50 percent of the Westinghouse 501 gas velocities at blade and vane leading edges.

If the particle velocities were to follow exactly the gas velocities, the erosion rate of the Solar blading at the rotor trailing edges and at the exit to the third-stage stator should be comparable to that in the Westinghouse 501, while the erosion rates at the leading edges of stator vanes and rotor blades may be as low as 6 percent of those at comparable locations in the full-size machine. Because of the rapid acceleration of the gas passing through the stator vanes and the deacceleration in the rotor blading, particles as small as 2 μm in diameter may have too much inertia to follow the gas flow. An analysis of this effect in a full-scale electric utility turbine showed that the variations in particle velocities lagged the variations in gas velocity. This effect increased with increasing particle size and resulted in particulate velocities leaving the rotors that were significantly higher than the gas velocity. A similar analysis of the test turbine flow path must be made to allow the erosion data to be interpreted properly.

Stationary Test Passages

The fact that impact velocities cannot be duplicated in the rotating test facility is the reason that the stationary passage erosion tests mentioned earlier are required. Particle acceleration nozzles of sufficient length (about 1.2 m [4 ft] with nozzles whose flow areas decrease linearly with length) must be used to provide sufficient time for particles to reach gas velocity before impacting the erosion targets. Erosion targets must be carefully designed so that the impact angle as well as the velocity are accurately known at the locations where erosion rates are measured.

By monitoring particulate levels in the gas stream before it enters the expansion turbine, three potentially hazardous situations can be detected and action taken to prevent turbine damage:

- Gross failure of dust collectors resulting in very high dust loading
- Dust loadings greater than the design values,which will result in turbine erosion if allowed to persist over an extended time period
- Gradual increase in loadings,which indicates that the dust collectors are not functioning correctly and require maintenance.

In addition, to get maximum information about the reactions and transport of trace elements in a fluidized bed combustion system, the test facility should be equipped with monitoring equipment. There is a particular need for monitoring the trace elements which are known to be capable of forming corrosive deposits on gas-turbine hardware, notably sodium and potassium, as well as environmentally important trace elements.

ESTIMATE OF TEST FACILITY COST

A preliminary cost estimate was prepared for the test facility installed at an existing power plant. The major subsystem costs for the base plant are summarized in Table M-11. The basic pressurized fluidized bed combustion plant includes the air supply systems; fuel-handling and feed system; sorbent-handling and feed system; two pressurized fluidized bed combustor test units; a single-train, three-stage particulate removal system; and a four-element gas-turbine test system. The installed cost (December 1974) complete with all necessary labor and materials for auxiliaries (piping, instrumentation, electrical, foundations, structures, and so forth), is estimated to be $21 million.

Cost estimates were also prepared for a representative regeneration system. A one-step regeneration system was selected and

Table M-11

INVESTMENT ESTIMATE FOR TEST FACILITY[a]

Component	Cost, $-million (12/74)
Air Supply Systems	4.7
Coal/Limestone-Handling Systems	6.0
Fluidized Bed Boiler	4.4
Adiabatic Combustor System	0.75
Recirculating Fluidized Bed Boiler Internals	0.25
Particulate Removal System	1.9
Turboexpander Test Systems	1.6
Auxiliary Equipment	1.4
Total Installed Systems Cost	21.0

[a]Installed subsystem costs complete with all necessary labor and materials for auxiliaries: piping, instrumentation, electrical, foundations, structurals, and so on.

estimated on the basis of available design projections.[3] The regeneration system is estimated to cost $5 million. This includes solids circulation, a fluidized bed regenerator, a gas producer, and sulfur recovery.

The cost estimates are based on the preliminary design and cost estimate for a pressurized fluidized bed boiler development plant, subsequent conceptual design modifications to the plant, and recent fuel-processing plant design and cost estimates developed by Westinghouse.[3,11-13]

REFERENCES

1. Keairns, D. L. et al. Evaluation of the Fluidized Bed Combustion Process. Vol. III. Pressurized Fluidized Bed Boiler Development Plant Design. Environmental Protection Agency. Westinghouse Research Laboratories. Pittsburgh, Pennsylvania. December 1973. EPA 650/2-73-048C. NTIS PB 232 439/3.

2. Archer, D. H. et al. Evaluation of the Fluidized Bed Combustion Process. Vols. I-III. Environmental Protection Agency. Westinghouse Research Laboratories. Pittsburgh, Pennsylvania. November 1971. NTIS PB 211 494; 211 960/9; 213 152/2.

3. Keairns, D. L. et al. Evaluation of the Fluidized Bed Combustion Process — Vols. I and II: Pressurized Fluidized Bed Combustion Process Development and Evaluation, and Vol. III: Pressurized Fluidized Bed Boiler Development Plant Design. Environmental Protection Agency. Westinghouse Research Laboratories. Pittsburgh, Pennsylvania. December 1973. EPA-650/2-73-048a, b, and c. NTIS PB 231 162/9, 231 163/7, 232 439/3.

4. Pressurized Fluidized Bed Combustion. Office of Coal Research. National Research Development Corporation, England. 1974. R&D Report No. 85. Interim No. 1.

5. Monthly Progress Reports. Multi-cell Fluidized-Bed Boiler. Office of Coal Research. Pope, Evans and Robbins Inc. Contract 14-32-0001-1237.

6. Annual Report. Reduction of Atmospheric Pollution by the Application of Fluidized Bed Combustion and Reduction of Sulfur-Containing Additives. Environmental Protection Agency. Argonne National Laboratory. June 1973. Publication No. EPA-R2-73-253. Interagency Agreement EPA-IAG-0020.

7. Reduction of Atmospheric Pollution. Final Report (Volume 1-3). Office of Air Programs. National Coal Board. London, England. September 1971. PB210 673, PB210 674, PB210 675.

8. Nutkis, M. S.,and A. Skopp. Design of Fluidized Bed Miniplant. Proceedings of the Third International Conference on Fluidized Bed Combustion. Hueston Woods, Ohio. 1972.

9. Exxon R&D Program. (Presented at FBC Contractors Meeting, Argonne National Laboratories, September 11-12, 1974.)

10. Fraas, A. P. Potassium-Steam Binary Vapor Cycle with Fluidized-Bed Combustion. (Presented at annual AIChE meeting, New York, November 1972.)

11. Initial Design Study for 50 MW Fluidized Bed Oil Gasification Demonstration Plant. Environmental Protection Agency. Westinghouse Research Laboratories. Pittsburgh, Pennsylvania. Contract No. 68-02-0605. March 1974.

12. Forty-Sixth Monthly Progress Report. Environmental Protection Agency. Westinghouse Research Laboratories. Pittsburgh, Pennsylvania. Contract No. 68-02-0605. February 1974.

13. Personnel Communications. Westinghouse Coal Gasification Plant Cost Study.

TECHNICAL REPORT DATA (Please read Instructions on the reverse before completing)		
1 REPORT NO. EPA-650/2-75-027-c	2	3 RECIPIENT'S ACCESSION NO.
4 TITLE AND SUBTITLE Fluidized Bed Combustion Process Evaluation Phase II--Pressurized Fluidized Bed Coal Combustion Development		5 REPORT DATE September 1975 6. PERFORMING ORGANIZATION CODE
7 AUTHOR(S) D. L. Keairns et al.		8 PERFORMING ORGANIZATION REPORT NO.
9 PERFORMING ORGANIZATION NAME AND ADDRESS Westinghouse Research Laboratories Beulah Road, Churchill Borough Pittsburgh, PA 15235		10 PROGRAM ELEMENT NO. 1AB013; ROAP 21ADB-009 11 CONTRACT/GRANT NO. 68-02-0605
12 SPONSORING AGENCY NAME AND ADDRESS EPA, Office of Research and Development Industrial Environmental Research Laboratory Research Triangle Park, NC 27711		13. TYPE OF REPORT AND PERIOD COVERED Phase II Final; 6/73-12/74 14. SPONSORING AGENCY CODE
15. SUPPLEMENTARY NOTES		

16. ABSTRACT The report gives results of a program to evaluate and develop pressurized fluidized-bed coal combustion. The historical, technical, and economic aspects of fluidized bed combustion (FBC) systems have been reviewed, systems analyses performed, commercial plant design and cost estimates prepared, and experimental data on the sulfur removal system obtained. Two pressurized FBC power plant systems have provided the basis for the work on system design, performance, economics, and development. The basic design and performance parameters for these two systems are presented. The present work extends the previous work to include collection and analysis of data on critical system parameters (e.g., sulfur removal, spent sorbent disposition, and trace element release); development of process options (e.g., particulate control); and assessment of power plant cycles and component designs (e.g., use of low-temperature gas cleaning, alternative cycles, and gas turbine corrosion/erosion test rig design and construction). The report includes an extensive bibliography.

17. KEY WORDS AND DOCUMENT ANALYSIS			
a DESCRIPTORS		b. IDENTIFIERS/OPEN ENDED TERMS	c. COSATI Field/Group
Air Pollution	Desulfurization	Air Pollution Control	13B 07D
Coal	Sorbents	Stationary Sources	21D 11G
Combustion	Trace Elements	Particulates	21B
Fluidized Bed	Test Equipment		14B
Processing	Bibliographies		13H, 07A 05B
Pressurizing	Gas Turbines		13G
18 DISTRIBUTION STATEMENT Unlimited		19 SECURITY CLASS (This Report) Unclassified 20 SECURITY CLASS (This page) Unclassified	21 NO. OF PAGES 489 22. PRICE